DOCKET NO. 50-171

Formal File 9.
Exam. w/ltr. of 7/31
as part of amend. No. 2

BEFORE THE

UNITED STATES ATOMIC ENERGY COMMISSION

APPLICATION OF

PHILADELPHIA ELECTRIC COMPANY

FOR

Construction Permit and Class 104 License

PART B

Preliminary Hazards Summary Report

Peach Bottom Atomic Power Station

VOLUME I — PLANT DESCRIPTION AND SAFEGUARDS ANALYSIS

A-172

August, 1961

TABLE OF CONTENTS

	Page
I. INTRODUCTION	
A. Purpose of the Report	I - 1
B. General Description of the Plant	I - 1
II. NUCLEAR STEAM SUPPLY SYSTEM	
A. Core Design	II - 1
B. Design Features of Reactor Components	II - 47
C. Fission Product Control, Traps and Helium Purification	II - 104
D. Primary Coolant System	II - 121
E. Helium Handling and Storage System	II - 135
F. Afterheat Removal and Emergency Cooling Systems	II - 139
G. Nuclear Steam Supply Instruments and Control Systems	II - 141
H. Fuel Handling System	II - 166
I. Shielding	II - 180
J. Research and Development	II - 181
III. CONVENTIONAL PLANT AND SERVICES	
A. General	III - 1
B. Main Turbine	III - 1
C. Condensing System	III - 1
D. Condensate and Feedwater System	III - 1
E. Circulating Water System	III - 2

III. (Cont'd)	Page
F. Service and Closed Loop Cooling Water System	III - 2
G. Water Storage	III - 4
H. Electrical System	III - 4
I. Fire Protection System	III - 6
J. Normal Heating and Ventilation	III - 7
K. Emergency Ventilation of Containment Atmosphere	III - 8
L. Containment Atmosphere Supply System	III - 8
M. Spent Fuel Pit Building Ventilation	III - 9
IV. CONTAINMENT	
A. General Description	IV - 1
B. Specifications	IV - 1
C. Penetrations, Access and Appurtenances	IV - 1
D. Testing	IV - 2
E. Containment Pressure Calculation	IV - 2
V. PLANT OPERATION	
A. Power Operation and Control	V - 1
B. Pre-Operational Testing	V - 5
C. Maintenance	V - 5
D. Plant Personnel	V - 7
VI. RADIOACTIVE EFFLUENTS	
A. Objectives	VI - 1
B. Gaseous Effluents Under Normal Operating Conditions	VI - 1

October, 1961

		Page
VI.	(Cont'd)	
	C. Liquid Effluents	VI - 4
	D. Solid Wastes	VI - 7
VII.	PLANT SAFETY ANALYSIS	
	A. Introduction and Summary	VII - 1
	B. Incidents Involving the Reactor	VII - 2
	C. Incidents Involving the Fission Product Trapping System	VII - 20
	D. Safety Considerations Relating to Fuel Handling	VII - 31
	E. Plant Behavior Under Abnormal Conditions Arising External to the Plant	VII - 37
	F. Environmental Consequences of Accidents	VII - 40

APPENDIX A - Figures

APPENDIX B - Radioactive Inventories

APPENDIX C - Calculations of Core Heat-Up Following Loss of Normal Cooling

APPENDIX D - Steam Generator Tube Rupture Calculations

APPENDIX E - Reactor Pressure Vessel

LIST OF TABLES

TABLE NO.	TITLE	PAGE
1	Fuel Element Characteristics	II - 3
2	Effects of Steam Leaks on Sleeve Permeability	II - 8
3	Physics Characteristics of HTGR	II - 10
4	Shutdown Reactivity for Control Rods and Emergency Rods at the Beginning of Life	II - 14
5	Nuclides Followed Explicitly in Lifetime Calculations	II - 19
6	Summary of Doppler Measurements	II - 23
7	Kinetics Parameters	II - 29
8	Average Core Outlet Temperature Required to Maintain Constant Plenum Outlet Temperature of 1354 F	II - 50
9	Fission Product Concentrations in Fuel Element Purge Stream	II - 109
10	Activities and Radiation Heat Loads in the Purification System	II - 111
11	Normal Concentration of Chemical Impurities in Reactor Helium	II - 117
12	Approximate Compressor Operating Conditions	II - 119
13	HTGR Capsule Irradiation Schedule	II - 182
14	Irradiation Data on Graphites	II - 184
15	Permeability of Irradiated Graphites	II - 190
16	Tensile Strengths of Low Permeability Graphite	II - 192
17	Modulus of Rupture of Graphites	II - 193

LIST OF TABLES (Cont'd)

TABLE NO.	TITLE	PAGE
18	Mechanical Strength Tests on Fuel Elements	II - 195
19	Results of Thermal Stress Tests	II - 196
20	Irradiation Effects in Graphite Base Fuel Bodies	II - 200
21	Dimensional Changes of Control Rod Material Due to Radiation	II - 203
22	Fission Product Element Yields and Characteristics	II - 208
23	Fiberglass Filter Effectiveness	II - 212
24	Kr and Xe Release Data	II - 214
25	Kr and Xe Release Data	II - 215
26	Kr and Xe Release Data	II - 216
27	Reactor Equivalent Delay for Iodine (Uncoated Charcoals)	II - 223
28	Reactor Equivalent Delay for Iodine (Coated Charcoals)	II - 223
29	Results of Trapping Tests on Tellurium	II - 225
30	Results of Tests Employing Modified Internal Fission Product Trapping Conditions	II - 225
31	Xenon Dynamic Equilibrium Adsorption Coefficient	II - 229
32	Krypton Dynamic Equilibrium Adsorption Coefficient	II - 230
33	Charcoal Grade Comparison at 25 C	II - 231
34	Typical Loop Operating Parameters	II - 232

LIST OF TABLES (Cont'd)

TABLE NO.	TITLE	PAGE
35	In-Pile Loop Sampling	II - 244
36	Irradiation Tests on Control Material	II - 261
37	Thermal Stability of Control Material	II - 263
38	Estimated Site Boundary Concentrations for Gaseous Effluents	VI - 3
39	Reactivity Losses from Volatile Poisons	VII - 3
40	Summary of Rod Withdrawal Accidents	VII - 8
41	Summary of Startup Accidents	VII - 9
42	Summary of Rod Fall Accident	VII - 10
43	Radioactivity Release due to Backflow	VII - 13
44	Fission Products Grouped According to High Temperature Retention by Uncoated Particle Fuel Compacts	VII - 14
45	Release of Fission Products from the Core to Secondary Containment during Emergency Cooling and with Ruptured Main Coolant System	VII - 17
46	Effect of Fuel Particle Coatings on Retention of Selected Fission Products in Fuel Compacts	VII - 18
47	Maximum Gas Temperatures from the Delay Beds following Sudden Depressurization	VII - 24
48	Primary Coolant Activity due to Release from Trapping System following Sudden Depressurization	VII - 25
49	Primary Coolant System Equilibrium Activities following Loss of Refrigeration	VII - 26

LIST OF TABLES (Cont'd)

TABLE NO.	TITLE	PAGE
50	Activity Release due to Fission Product Purge Line Rupture	VII - 28
51	Gaseous Fission Product Leaching Experimental Study	VII - 33
52	Volatile Radioactivity Inventory in the Highest Power Fuel Element in Spent Fuel Storage Pit and Activity Released from a Leaking Fuel Element Can in the Spent Fuel Storage Pit	VII - 34
53	Maximum Total Radioactivity Inventory in One Fuel Element in Spent Fuel Storage Pit 48 Hours after Reactor Shutdown	VII - 35
54	Summary of Accidents with Significant Radioactive Releases to the Containment	VII - 43
55	Dosages from Primary System Depressurization (Case A)	VII - 44
56	Dosages from Primary System Rupture with No Backflow From External Fission Product Traps (Case B-1)	VII - 45
57	Dosages from Primary System Rupture with Backflow from First Three External Fission Products Traps (Case B-2)	VII - 46
58	Dosages from Primary System Rupture and Loss of Normal Cooling with No Backflow from External Fission Product Traps (Case C-1)	VII - 47
59	Dosages from Primary System Rupture and Loss of Normal Cooling with Backflow from First Three External Fission Product Traps (Case C-2)	VII - 48
60	Dosages from Rupture of Fission Product Purge Line (Case D)	VII - 50

LIST OF TABLES (Cont'd)

TABLE NO.	TITLE	PAGE
61	Release of Volatile Fission Products from One Fuel Element in Spent-Fuel Storage Pool (Case E)	VII - 50
62	Relative Atmospheric Dilution for Accidents	VII - 51
63	Thyroid Dose from Inhalation of Iodine Isotopes	VII - 51
B - 1	Design Activity in Fuel	B - 3
B - 2	Design Activity in Internal Traps	B - 3
B - 3	Gaseous Activities in the Primary Coolant	B - 3
B - 4	Design Activities in External Fission Product Traps	B - 9
B - 5	Decay Heat Loads in External Fission Product Traps Based on Design Activities	B - 10
B - 6	Calculated Beginning of Life Activities in External Fission Product Traps	B - 13
B - 7	Decay Heat Loads in External Fission Product Traps Based on Calculated Beginning of Life Activities	B - 14
B - 8	Fission Products Released to the Plant Container after a Primary System Duct Rupture	B - 18

August, 1961

APPENDIX A

FIGURES

Figure 1 - Plant Perspective

Figure 2 - Reactor Cutaway

Figure 3 - HTGR Fuel Element

Figure 4 - Proposed HTGR Control Rod Arrangement

Figure 5 - Reactivity Inserted by Removal of Center Control Rod

Figure 6 - Reactivity vs. Time and Rate of Change of Reactivity vs. Time for Withdrawal of Inner Control Rod

Figure 7 - Scram Reactivity Input for 36 Rods; 1200 K; End of Life; Zenon and Samarium Present

Figure 8 - Scram Reactivity vs. Time for 36 Rod Scram; End of Life

Figure 9 - Multiplication Constant vs. Time of Operation

Figure 10 - Comparison of Values of the Neutron Flux in a Poisoned Graphite Block with Calculated Spectra Using a Free Gas Model and the Parks Crystal Model

Figure 11 - Comparison of Values of the Neutron Flux in a Poisoned Graphite Block with Calculated Spectra Using a Free Gas Model and the Parks Crystal Model

Figure 12 - Comparison of the Free Gas Model with the Parks Crystal Model for an HTGR Lattice

Figure 13 - Values of (1/I) (I/ T) vs. Temperature for TH-232

Figure 14 - Reactivity Change with Heating

Figure 15 - Doppler Coefficient $(\frac{1}{I})(\frac{\partial I}{\partial T})$

Figure 16 - Variation of Over-All Temperature Coefficient vs. Temperature at End of Life with Xenon Present

APPENDIX A (Cont'd)

FIGURES

Figure 17 - Values of $(1/P\ (\partial P/\partial T)$ vs. Temperature For TH-232 at Carbon-To-Thorium Ratios Indicated

Figure 18 - Variation of Over-All Temperature Coefficient vs. Temperature at End of Life

Figure 19 - Peak Fuel Compact Temperatures Following Ramp Insertions Corresponding to Maximum Rod Removal Rate (0.06 ft/sec) For Various Delay Times; End of Life; No Xenon Present; Normal Operating Power. Scram at 140% Normal Power

Figure 20 - Peak Fuel Compact Temperatures vs. Scram Delay Time; 1.0g Rod Drop; Normal Operating Power; Scram at 140% Normal Power

Figure 21 - Reactivity Added by Rod Fall vs. Time and Rate of Change of Reactivity vs. Time for 1.0g Rod Fall; Normalized to $.01\Delta k$

Figure 22 - Prompt Temperature Coefficient at End of Life; With Equilibrium Xenon and Samarium and Added Rhodium

Figure 23 - Peak Fuel Compact Temperatures Following 1.0g Rod Fall; End of Life; Xenon Present; Normal Operating Power, Scram at 140% Normal Power

Figure 24 - Peak Fuel Compact Temperatures vs. Magnitude of Prompt Temperature Coefficient Following 1.0g Rod Fall. Normal Operating Power; Scram at 140% Normal Power

Figure 25 - Peak Fuel Compact Temperatures vs. Scram Trip Level for a 1.0g Rod Fall; Normal Operating Power

Figure 26 - Peak Fuel Compact Temperatures vs. Neutron Lifetime for a 1.0g Rod Fall; Normal Operating Power; Scram at 140% Normal Power

Figure 27 - Simplified Flow Diagram Showing Reactor Flow Paths

Figure 28 - Per Cent of Fuel Compact Material Whose Temperature is Above a Given Temperature T. T is the Radial Average Temperature of the Fuel Compact

APPENDIX A (Cont'd)

FIGURES

Figure 29 - Per Cent of Sleeve Material Whose Temperature is Above a Given Temperature T. T is the Radial Average Temperature of the Sleeve

Figure 30 - Per Cent of the Total Fuel Element Surface Area Whose Temperature is Above a Given Temperature

Figure 31 - Radial Temperature Profiles - "Average" Fuel Element

Figure 32 - Radial Temperature Profiles - "Hottest" Fuel Element

Figure 33 - Variation in Fuel Temperature with Thermal Conductivity of the Sleeve and Fuel Material

Figure 34 - Variation in Fuel Temperature with Width of Gap Between Compact and Sleeve

Figure 35 - Axial Variation of Diametral Temperature Difference in a Fuel Element Next to a Fully Inserted Control Rod and in a Fuel Element at the Edge of the Core

Figure 36 - Hypothetical Deflections of Asymmetrically Heated Fuel Elements.

Figure 37 - Main Coolant Activity Increase (Exclusive of Kr^{85}) vs. Time for Continued Reactor Operation with One, Two, or Three Badly Fractured Fuel Elements

Figure 38 - Cleanup of Main Coolant Activity (Exclusive of Kr^{85}) With No Production and Continued External Trap Operation

Figure 39 - Cross Section of Vessel Internals

Figure 40 - Critical Radius of Hot Spot vs. Heat Transfer Coefficient for an Allowable Stress of 8000 PSI

Figure 41 - Refueling Nozzle and Removable Shield Plug

Figure 42 - Heat Generation Rates in Reactor Vessel Wall (Wall Thickness 2 - 1/2")

APPENDIX A (Cont'd)

FIGURES

Figure 43 - Effect of Amount of Thermal Shielding on Stress and Temperature in Pressure Vessel (2 - 1/2 inch Wall, 100% Coolant Flow). For Heating Rates Given in Figure 42 and Adjusted for Peak to Average of 1.6

Figure 44 - Maximum Thermal Stress in Vessel Wall Due to a Step Change in Fluid Temperature for a 2 - 1/2" Wall of A212

Figure 45 - Time for Transient to Raise Average Wall Temperature 25 F for 2 - 1/2" Carbon Steel Wall and a Heat Transfer Coefficient of 200 Btu/hr - ft^2 -°F

Figure 46 - Irradiation Temperature for a 100 F Rise in Impact Transition Temperature vs. Neutron Dose

Figure 47 - HTGR Control Rod

Figure 48 - Schematic of Control Rod and Drive

Figure 49 - Control Rod Drive Hydraulic Circuit

Figure 50 - Emergency Shutdown Rod Drive

Figure 51 - Thermally Released Emergency Shutdown Absorber as Installed in Emergency Shutdown Rod Guide Tube

Figure 52 - Thermally Released Emergency Shutdown Absorber as Installed in a Control Rod Guide Tube

Figure 53 - Fuel Element Vibration Test; Cross Section of Test Chamber

Figure 54 - Summary of Radioactivity Distribution - Design Activity Levels

Figure 55 - Summary of Radioactivity Distribution - Calculated Beginning of Life Activity Levels - Based on Experimental Release Data for Coated Particle Fuel

Figure 56 - External Fission Product Trapping System

Figure 57 - Steam Generator Purge Purification System

APPENDIX A (Cont'd)

FIGURES

Figure 58 - Main Coolant System Process Flow Diagram Showing Steady State Operating Conditions for 100% Power Output with Fouled and Plugged Boilers

Figure 59 - Helium Compressor Cross Section

Figure 60 - Concentric Pipe Construction

Figure 61 - Reactor Outlet Valve

Figure 62 - Compressor Inlet and Outlet Valves

Figure 63 - Piping Arrangement for Main Coolant Bypass Filter

Figure 64 - HTGR Steam Generator Circuit

Figure 65 - Recirculation Pump

Figure 66 - Non-Purified Helium Handling System - Process Flow Diagram

Figure 67 - Purified Helium Handling System Process Flow Diagram

Figure 68 - Helium Handling System Transfer Compressor

Figure 69 - Emergency Cooling Coil System

Figure 70 - Reactor Instruments

Figure 71 - Approximate HTGR Nuclear Instrument Ranges

Figure 72 - Control Rod Drive System Control and Instrument Diagram

Figure 73 - Over-All Plant Control and Instrument Diagram

Figure 74 - Simplified HTGR Scram System

Figure 75 - HTGR Fuel Handling Equipment

Figure 76 - Fuel Transfer Machine Inside Pressure Vessel

APPENDIX A (Cont'd)

FIGURES

Figure 77 - Fuel Transfer Machine Schematic

Figure 78 - Fuel Transfer Machine

Figure 79 - Charge Machine

Figure 80 - Fuel Element Canning Machine

Figure 81 - Fuel Handling Purge System Flow Diagram

Figure 82 - Steam-Graphite Reaction Furnace

Figure 83 - Change in Helium Permeability vs. Change in Weight for Two Great Lakes Carbon Co. Graphites After Exposure to Helium with 3% Water at 1000 C; Permeability Measured at a Pressure Difference of 1 Atm

Figure 84 - Schematic of Thermal Stress Apparatus

Figure 85 - Steady State Kr Release, Uncoated Carbide Particle Graphite Matrix Fuel Bodies

Figure 86 - Design Basis Steady-State Release of Fission Products from Uncoated Fuel

Figure 87 - Xe-133 Release From Fuel Compact Prepared From Uncoated Fuel Particles Following a Simulated Excursion to 2280 C, (Th:U) C, $(Th:U)C_2 \cdot 2.19/1.0$

Figure 88 - Xenon-133 Release From Coated Particles Due to an Excursion to 3000 C for 38 Minutes

Figure 89 - Cesium Sorption Apparatus

Figure 90 - Cesium Sorption by Activated Charcoal (Fischer Charcoal)

Figure 91 - Cesium Sorption on Activated Charcoal (Columbia Charcoal)

Figure 92 - Free Energy Change of Sorption for Cesium-Charcoal System

Figure 93 - Internal Fission Product Trap Evaluation System

APPENDIX A (Cont'd)

FIGURES

Figure 94 - Typical Sharp Boundaries Obtained in Iodine and Tellurium Vapor-Helium Chromatograms of Trapping Reagents.

Figure 95 - Dynamic Sorption Apparatus

Figure 96 - Adsorption Isobars for Iodine on Charcoal

Figure 97 - Iodine Adsorption Isobars on Activated Charcoal

Figure 98 - Static Sorption Apparatus

Figure 99 - Free Energy of Adsorption for Iodine on Charcoal

Figure 100 - Apparatus for Charcoal Trap Adsorption Tests

Figure 101 - Typical Ionization Chamber Current Traces for (a) Pulse Injection and (b) Constant Rate Injection of Tracer Gas Into Charcoal Trap Test Apparatus

Figure 102 - Experimental Dynamic Adsorption Coefficient vs. Reciprocal Temperature

Figure 103 - Transfer Unit Height vs. Particle Reynolds Number for Barnebey-Cheney 107 6/10 Mesh Charcoal

Figure 104 - Comparison of a Theoretical Effluent Curve with Experimental Results

Figure 105 - General Arrangement - Half-Linear-Scale Flow Model

Figure 106 - Probe Locations - Half-Linear-Scale Flow Model

Figure 107 - Static Pressure Distribution - Half-Linear-Scale Flow Model

Figure 108 - Local Velocities and Projected Regions of Equal Mass Flow Based on the 16 Points Shown.

Figure 109 - Outer Jacket Heat Transfer Coefficient For Air

Figure 110 - Local Velocities and Projected Regions of Equal Mass Flow Based on the 16 Points Shown.

APPENDIX A (Cont'd)

FIGURES

Figure 111 - Flow Paths in Upper Head, Outer Gap for Different Orifice Positions

Figure 112 - View of Fuel Element Vibration Test Chamber

Figure 113 - Comparison of Fanning Friction Factors Measured in Flow Through Tricuspid Channel with Literature Values for Commercial Pipe and Smooth Tubes

Figure 114 - Velocity Profile for Tricuspid Flow Channels

Figure 115 - Measured Over-All Heat-Transfer Rates from the Rod Surface to Air as a Function of Reynolds Number

Figure 116 - Peripheral Variation of the Measured Heat Transfer Rates

Figure 117 - Plant Layout, Ground Floor

Figure 118 - Plant Layout, Intermediate Plan

Figure 119 - Plant Layout, Operating Floor

Figure 120 - Plant Layout, Longitudinal Section A - A

Figure 121 - Plant Layout, Cross-Section B - B

Figure 122 - Plot Plan

Figure 123 - Condensate and Feedwater Flow Diagram

Figure 124 - Raw Water Flow Diagram

Figure 125 - Shield Cooling and Spent Fuel Pit Cooling Water Systems

Figure 126 - Containment Equipment Cooling Water System

Figure 127 - Electrical Single Line Diagram

Figure 128 - Containment Ventilation and Gaseous Waste Disposal Flow Diagram

APPENDIX A (Cont'd)

FIGURES

Figure 129 - Liquid Waste Flow Diagram

Figure 130 - Decontamination Flow Diagram

Figure 131 - Fuel Compact and Helium Outlet Temperatures Following Withdrawal of one Control Rod

Figure 132 - Fuel Compact and Helium Outlet Temperatures Following Fall

Figure 133 - Steam, Coolant, and Fuel Temperatures Following Instantaneous Loss of Pressure and One Helium Loop

Figure 134 - Activity in Containment During Emergency Cooling With Primary System Rupture and Backflow From First Three Fission Product Traps

Figure 135 - Temperature Rise in Delay Bed A-302 Following Complete Loss of Purge Flow at Time = 0

Figure 136 - Temperature Rise in Delay Bed A-304 Following Complete Loss of Purge Flow at Time = 0

* Figure C-1 - Initial Reactor Temperatures

* Figure C-2 - Reactor Temperatures After Loss of Coolant Circulation Accident

* Figure C-3 - Transient Temperature of Key Nodes After Loss of Coolant Circulation Accident Condition

* Figure C-4 - Transient Temperature of Key Nodes After Loss of Coolant Circulation Accident Condition

* Figure C-5 - Transient Temperature of Key Nodes After Loss of Coolant Circulation Accident Condition.

* Figure C-6 - Percent of Core Exceeding Various Temperatures vs. Time After Shutdown for loss of Coolant Circulation Accident

* Figure C-7 - Average Core Temperature vs. Time After Shutdown

* Located in Appendix C

APPENDIX A (Cont'd)

FIGURES

*Figure D-1 - Effect of Steam Addition on an Isolated Helium Coolant Loop and Dump Tank System

*Figure D-2 - Effect of Steam Addition on Unisolated Helium Coolant Loop and Dump Tank System

*Figure D-3 - Transient Steam and Water Quantities Following Rupture of Helium Coolant System and One Steam Tube

**Figure E-1 - Reference Points for Nuclear Heating and Fast Flux in Reactor Pressure Vessel

**Figure E-2 - Nuclear Heating Rates in the HTGR Reactor Pressure Vessel Wall

**Figure E-3 - Piping Loads on Inlet Nozzle

**Figure E-4 - Inlet Gas Temperature

**Figure E-5 - System Transients Considered

**Figure E-6 - Fast Flux at Upper Points Shown on Figure E-1. Energy $>$1.0 Mev.

**Figure E-7 - Fast Flux at Upper Points Shown on Figure E-1. Energy $>$0.1 Mev.

**Figure E-8 - Fast Flux at Lower Points Shown on Figure E-1. Energy $>$1.0 Mev.

**Figure E-9 - Fast Flux at Lower Points Shown on Figure E-1. Energy $>$0.1 Mev.

**Figure E-10 - Ductile-to-Brittle Transition Temperature Shifts with Integrated Neutron Dosage at Different Irradiation Temperatures

**Figure E-11 - Effects of Annealing of Steels Following Irradiation

* Located in Appendix D

** Located in Appendix E

August, 1961

1. INTRODUCTION

A. Purpose of the Report

The purpose of Part B of this Application, the Preliminary Hazards Summary Report, is to provide a basis for evaluating the safety of the Peach Bottom Atomic Power Station.

Volume I, Plant Description and Safeguards Analysis, presents the features of the design, construction, and operation of the nuclear power plant that are pertinent to its safety at the Peach Bottom site, and includes analyses of postulated accidents and their consequences.

Design features set forth in this report provide an adequate basis for the evaluation of plant safety. The design of the nuclear steam supply system is based on research and development work performed by General Atomic Division of General Dynamics Corporation under contract with the Atomic Energy Commission, as indicated in Part A, as a part of the Power Reactor Demonstration Program.

Volume II, Site and Environmental Information, presents the results of detailed investigations of the characteristics of the Peach Bottom site and a discussion of analytical procedures developed to evaluate the environmental consequences of the accidental situations postulated in Volume I.

Additional information pertaining to the final design of the plant and to the plant site will be provided in the form of a Final Hazards Summary Report to be filed approximately October, 1963.

B. General Description of the Plant

An arrangement of the plant and a cutaway view of the reactor are shown in Figures 1 and 2. The Reactor system is of the solid fuel homogeneous type, employing graphite as moderator and helium as coolant. The fuel (U^{235}) and fertile material (Th^{232}) are in the form of carbides homogeneously dispersed in a portion of the moderator and enclosed in a low permeability graphite cladding. The design outlet gas temperature from the reactor will be approximately 1380 F at 350 psia with steam system conditions of 1000 F at 1450 psi. Such high helium temperatures are possible because of the excellent high temperature properties of the graphite fuel elements. The steam cycle is typical of conventional power plants. The plant will have a nominal net electrical capacity of 40,000 kw.

At one time it had been contemplated that the first loading of fuel for the reactor would possibly consist of metal-clad elements in order to meet the schedule for the plant.

It has now been determined that graphite-clad fuel elements will be used as the first core for the reactor. Therefore, only the graphite-clad core is presented on this report.

August, 1961

II. NUCLEAR STEAM SUPPLY SYSTEM

A. Core Design

1. Mechanical Design of Fuel Elements

a. Description

The 804 fuel elements for the High Temperature Gas Cooled Reactor (HTGR) are of a solid semi-homogeneous type in which graphite serves as the moderator, fuel matrix, and cladding material. This fuel element, shown in Figure 3 consists of an upper reflector section, a fuel-bearing middle section and a bottom reflector section. A graphite sleeve made of low permeability graphite extends from the upper reflector section to the bottom of the fuel element, and contains the fuel bodies, a portion of the bottom reflector, and an internal fission product trap. In this graphite clad fuel element, the approach is not to attempt hermetic containment of fission products within the fuel elements, but rather to control the escape of these fission products and retain them in traps in such a way that the activity in the primary circuit is maintained at a satisfactorily low level.

Outwardly, an HTGR fuel element has the appearance of a solid graphite cylinder 3.5 inches in diameter by 144 inches long, with a grappling knob at the top for handling. Within the reactor each fuel element is supported by the core grid plate at its lower end and is restrained laterally near the upper end by the contact of six surrounding fuel elements. This contact is made at a spacer ring located immediately above the active fuel region of each fuel element. Additional spacer rings, not touching when fuel elements are perfectly straight, are located at two levels within the active core region. These serve to limit the amount of bowing possible during reactor operation.

The graphite sleeve is approximately 10 feet long and is joined to the upper reflector at one end and to a bottom connector fitting at the other end. The joint at the upper end is a screwed and cemented type while the lower graphite-to-graphite joint is a screwed and brazed type. The bottom connector fitting is made of the same type low permeability graphite as the sleeve. A female sealing surface within the bottom connector slips over a metal standoff pin which is anchored to the core grid plate. The standoff serves to maintain the pitch location and provides a means for drawing off a small amount of helium from each fuel element to purge the fission products which leave the fuel compacts.

Within the fuel element, annular fuel compact sections are stacked on a cylindrical graphite spine. The 1.5-in.-long compacts, 2.75 in. OD by 1.75 in. ID, contain a mixture of graphite, fissile, and fertile materials. Concentrating the fuel material in an annular ring helps to lower the maximum fuel temperature from that of a cylindrical compact with uniform fuel distribution. The graphite spine serves as a location for burnable poison in some of the fuel elements. The overall length of the spine and fuel compact assembly is 90 inches. A fuel

cap made of low permeability graphite rests upon the top fuel compact. This fuel cap reduces back diffusion of fission products and provides thermal shielding for the bonded joint between the sleeve and the upper reflector.

The uranium and thorium within the fuel compacts is in the form of carbides, uniformly dispersed as particles in a graphite matrix. The size of the carbide particles is from 100 to 400 microns in diameter. Each particle is pyrolitically coated with a 50 to 60 micron thickness of dense carbon. This coating protects the fuel material from oxidation reactions during fuel fabrication and serves to significantly increase the retention time of fission products during reactor operation.

An internal fission product trap is located in the lower reflector region of the element. The trap consists, mainly, of a graphite cylinder having 1/8-inch-wide by 13/16-inch-deep slots machined lengthwise on the outer surface. These slots are filled with silver coated charcoal reagent material in granular form. The internal trap is approximately 12 inches long.

In the reactor core, the primary helium coolant flows outside the fuel elements in an upward direction. From this primary coolant, 900 lb/hr of helium is drawn into the 804 fuel elements, thus providing the purge flow which sweeps fission products from the core of the reactor. This purge flow rate amounts to 1.1 lb/hr per element. In addition to the purge streams passing through the fuel elements, an inleakage of helium around the standoff connectors may contribute a maximum of 100 lb/hr to the total purge flow rate. Therefore, the total helium flow rate in the purge line leading to the external traps is about 1000 lb/hr.

The purge gas enters each fuel element through the relatively porous upper reflector piece. The gas is filtered as it passes radially through this reflector. The gas then flows downward around the fuel compacts, sweeping fission products out of the space between the fuel compacts and the graphite sleeve. Grooves molded in the outer surface of the fuel bodies provide additional flow area for the purge gas. After sweeping fission products from the active core zone, the purge gas flows through the internal trap where some of the fission products are adsorbed. The heat of decay of these adsorbed fission products and the sensible heat of the helium purge gas is carried radially through the graphite sleeve to the primary helium coolant. At the bottom end of the internal trap the gas stream is filtered through a porous graphite cylinder. Volatile fission products leaving each internal trap enter the standoff pin and are drawn through a purge line leading to the external fission product traps.

b. Performance Characteristics of Fuel Elements

In this report the design life of the HTGR fuel elements has been assumed to be three years at 80% load factor. It should be recognized that the actual life of the core however, may be different when the most favorable fuel cycle finally is chosen. The fuel elements for the HTGR are designed to generate 112.5 MW thermal, which together with 2.8 MW produced by nuclear heating in other reactor internals, gives a total thermal power of 115.3 MW. The power generated in an average fuel element is approximately 150 KW. The peak power generated in a hottest fuel element is approximately 200 KW. The fuel elements are designed to restrict the leakage of fission products sufficiently well so that the primary coolant activity does not exceed the Calculated Beginning of Life Activity (Calculated BOL) given in Appendix B. when all fuel elements are functioning properly. Higher coolant gaseous activity may be tolerated during continued reactor operation as described in the discussion of "Design" Coolant Gaseous Activity in Appendix B. I.

The fuel elements are designed so that they will be removable from the core by a fuel transfer machine. Allowances for dimensional changes of components are made so that a fuel element in any core location will be removable at the end of core life.

Changes in some of the characteristics of fuel elements are expected over the design life of the core. Table I below indicates the beginning and expected end of life characteristics which are of importance.

TABLE I
FUEL ELEMENT CHARACTERISTICS

	Beginning of Life	After 3 Yrs.
Over-all length at room temperature, inches	144.0 ± .1	142.5 minimum
Outside diameter at room temperature, inches	3.485 ± .005	3.450 min.
Diametric clearance between fuel and sleeve, at room temperature, inch	.009 ± .002	0 to .009
Clearance between spacer rings, at operating temperature, inch	0 to .010	0 to .030
Helium permeability of sleeve, cm^2/sec	1×10^{-6}	1×10^{-5}
Tensile strength of sleeve, minimum, psi	2500	2500
Flexural strength of sleeve, minimum, psi	3500	3500
Tilting Reflector restraining force, average lb/element	700	700

TABLE I. (Cont'd)

Maximum force between warped elements, lb.	0	375
Purge gas flow rate per element, lb/hr.	1.1 ± .2	1.1 ± .3
Stand-off seal leakage per element, maximum lb/hr.	.1	.1

The degree of change in each characteristic over the life of the core is predicted from tests on representative materials, and in no case does the change constitute a limiting condition. The major effort in the Materials Research and Development Program has been aimed at determining experimentally the maximum amounts of changes in characteristics of fuel element materials under conditions simulating actual reactor conditions. A summary of experimental results on graphite materials is presented in Section II.J.1. The effects on reactor performance of dimensional changes from irradiation, permeability changes, and purge gas flow changes are discussed more fully in Sections II.A.1.d, II.A.1.f, and II.A.4.

c. Arrangement of Fuel Elements in the Core

The base of each fuel element rests upon the grid support plate, and the upper end of each element is restrained by lateral contact forces from adjacent fuel elements. Contact forces on the outer ring of fuel elements are applied by side reflectors which pivot at the base of the core and which are forced against the fuel elements at the upper end. The force acting on the fuel elements by the side reflectors is equivalent to about 700 lb per fuel element and results from the helium coolant pressure differential across the tilting side reflectors. There is no upper grid plate or other mechanical supporting structure within the reactor core.

The pitch location of the fuel elements is maintained by the stand-off pins at the bottom and by the enlarged diameters of the fuel elements at the upper spacer level. The core configuration is prevented from twisting or tilting circumferentially by means of two design features. First, the 12-inch-thick restraining side reflectors are contoured to engage the full length of the outer ring of fuel elements. The side reflectors are anchored at the grid support plate in such a manner that they may tilt only in radial directions toward or away from the vertical centerline of the core. The amount of travel of each tilting reflector segment is limited to a total arc of approximately 2-1/2 inches at the upper end.

The second design feature which maintains the shape of the reactor core is the standoff pin supporting each fuel element. The length of the fuel element which slips over the standoff pin is 10 inches. The strength of this connection is sufficient for a single fuel element to stand vertically by itself within the core. At shutdown temperature conditions, the clearance between the graphite fuel element bottom connector and the metal stand-off allows the fuel element to tilt through an angle of approximately 0.1 degree.

d. Distortion due to Irradiation

Changes in dimensions of fuel elements are expected, to some degree, over the life of the core. The changes which could occur in HTGR fuel elements are (1) changes in over-all length, (2) changes in outside diameter, (3) changes in the gaps between fuel compacts and the sleeves, or (4) bowing of fuel elements from asymmetric contractions. Capsule irradiation experiments performed by General Atomic and Hanford have indicated that contraction rather than expansion occurs in graphite irradiated at high temperatures. Experimental data on graphite properties are presented in Section II. J. 1. The contraction of graphite per unit length is observed to be a function of the total integrated fast flux at any given irradiation temperature. The amount of deformation of HTGR fuel elements can be predicted over the core life, within at least a factor of two, on the basis of data obtained in high-flux test reactors.

Uniform changes in fuel element length or outside diameter do not pose serious problems, even when applying the more pessimistic of the experimental data available. For example, a 1% uniform contraction in the length or in the outside diameter would not require shutdown of the plant and would not cause hazardous operating conditions. Fuel removal would not be impaired in this case because the fuel transfer machine is not limited in its vertical travel.

Contraction conditions of more concern are the closing of gaps between fuel compacts and sleeves and the bowing of fuel elements in regions where a fast flux gradient exists across the sleeve diameter. The gap between fuel bodies and the sleeve exists because of assembly requirements and facilitates the sweeping of fission products from around the fuel compacts during reactor operation. It is desirable to keep the gaps small so that radial temperature drops through the fuel element are minimized. The design value for diametric clearance between fuel compacts and sleeves is 0.009 inch cold and 0.011 inch hot. The opening of the gap in going from shutdown to operating conditions is caused by the difference in the coefficients of thermal expansion of the fuel compacts and the sleeve.

Although the fuel material and the sleeve are both expected to contract to some extent from irradiation effects, the experimental data obtained to date indicate that the sleeve will contract more than the fuel compact. A contraction of 0.3% could occur before the gap at cold conditions would disappear. An additional 0.15% contraction could develop before hoop stresses in the sleeve would approach rupture values. Therefore, a total of 0.45% contraction of the sleeve relative to the fuel compacts could occur between nominally dimensioned components before any adverse operating effects would develop. The allowable total contraction would be somewhat lower, about 0.3%, for any fuel element in which fuel compacts on the high end of fabrication tolerances happened to be matched with a sleeve of minimum tolerance. If the allowable contraction were exceeded, the

most severe damage possible is a crack in the surface of the sleeve. The most-likely effect would be a crack developing at the time the stressed element was cooled down from operating temperatures. The plant operator may either continue operating with a few cracked fuel elements or he may remove them, depending upon the activity levels in the main coolant. The effects of cracked fuel elements on coolant activities are described in Section II.A.4. and Appendix B, I.

The experimental data in Section II.J.1 indicate that the contraction of the sleeve diameter could very possibly exceed 0.3% and that values on the order of 1% in 2×10^{21} nvt have been observed in low permeability graphites at 1100 to 1400 C. The maximum fast flux exposure (>.1 mev) for the HTGR fuel elements is approximately 4×10^{21} nvt. Current development work is aimed at selecting materials, particularly the base coke and binder of the sleeves, which will result in approximately the same contraction rates for the fuel compacts and the sleeves. An alternative approach under consideration is to slit the annular fuel compact vertically at one circumferential location, thereby allowing for a diametric deflection from the application of compressive forces. Laboratory experiments have shown that this is a feasible method for keeping sleeve hoop stress values at low levels.

Analysis of fuel element bowing conditions indicates that the region where it will be the greatest is the outer ring of fuel elements adjacent to the side reflectors. The fast neutron flux (above 0.1 mev) in this region decreases from 4.0×10^{13} to 2.5×10^{13} n/cm^2-sec across the fuel element diameter. Bowing from this flux gradient will cause mid-core spacer pads on these fuel elements to touch their neighbors and the side reflectors. The forces and stresses which could develop have been calculated for representative contraction values. A contraction rate varying linearly from 1% per 2×10^{21} nvt at 1450 C to 0.1% per 2×10^{21} nvt at 700 C was used in the analysis. The results indicate that the maximum flexural stress in the sleeve at the end of core life is 1800 psi. This stress value is safely below the minimum flexural strength value of 3500 psi spacified for the sleeve material. Measured values for representative graphites are between 3250 and 7260 psi as shown in Section II.J.1. Effects of creep are not included in this analysis, but such effects could be expected to beneficially reduce the stress below the 1800 psi value.

The bottom connector of the fuel element, which fits closely over the standoff support, is expected to maintain its dimensions throughout the core life. This component operates at a temperature of 700 F within a region of the bottom reflector where the fast flux is reduced to 5×10^{11} n/cm^2 sec. The total contraction of the bottom connector would be less than 0.1% in three years. A 0.1% contraction would reduce the radial gap between the connector and the standoff by 0.0002 inch. This reduction would cause no adverse effects on the connector.

e. Creep

Any creep in the HTGR fuel elements would tend to reduce stresses developed from irradiation contraction described in Section d., above. Although no credit has been taken for stress relief by creep or plastic deformation in the analysis, the stresses developed in the HTGR fuel elements are expected to be reduced somewhat by this effect.

f. Permeability

The production specification on permeability of the graphite sleeves is $1 \times 10^{-6} cm^2/sec$ as measured by helium leakage at room temperature. The plant may be operable for limited periods of time with a mean core helium permeability of $5 \times 10^{-4} cm^2/sec$.

The Calculated Beginning of Life Coolant Gaseous Activity, based on the helium permeability value of $1 \times 10^{-5} cm^2/sec$. is given in Appendix B.1. Permeability measurements on irradiated specimens of low permeability graphite have indicated small changes from irradiation. No significant permeability change is expected from irradiation effects since the graphite will have stabilized by heat treating at graphitization temperatures. Experimental data on this effect are shown in Section II. J.1.

Permeability changes may result from reactions between helium impurities and the graphite. In the HTGR system, the water side of the steam generator is at a higher pressure than the helium coolant side. A leak or a tube rupture in the steam generator would admit steam into the main helium coolant and thus to the reactor vessel where chemical reactions would occur in the hot graphite of the reactor core. These chemical reactions could selectively remove material from the low permeability graphite fuel element sleeves, causing them to become more porous.

Work is in progress, as described in Section II. J.1, to determine the change in permeability of the low permeability graphite sleeves versus weight removal by the steam reaction at various sleeve temperatures. Some preliminary results have been obtained on graphites more permeable than those which will be used in HTGR. Using these results, a conservative estimate can be made of the effect on the permeability at HTGR conditions. Table 2 presents these estimates for several leak conditions.

The "Small Continuous Leak" corresponds to a leak

at about the minimum detectable level (about 0.01 lb/hr), which could continue for the full three-year life of the core. Such a leak is guarded against by the steam generator purge stream which continuously draws helium from a chamber enclosing the tube-to-tube-sheet welds in the steam generator. Small steam leaks at the minimum detectable level are most likely to occur at these welds rather than along straight pipe sections. A flow rate of 200 lb/hr from the two steam generators is maintained in the steam generator purging stream, and this gas is pumped to the helium purification system.

A "Tube Rupture" assumes a complete shear of a steam generator tube. The reactor will immediately be scrammed for this condition and automatic controls will attempt to isolate the defective loop from the reactor. The final column of the table presents the ratio of the final permeability to the initial permeability of the sleeve.

TABLE 2
EFFECTS OF STEAM LEAKS ON SLEEVE PERMEABILITY

Type of Steam Leak	Leak Rate	Carbon Removed (lb)	Ratio of Final Perm. to Initial Perm.
Small Continuous Leak (for 3 years)	.01 lb/hr	167	10
Tube Rupture			
a. Valve isolation - The isolation valve closes 8 seconds after break, allowing 4 seconds time for steam to escape past the isolation valve. The reactor is scrammed after the break. System pressure is 350 psi.	10 lb/sec	26.5	1.5
b. No valve isolation - The isolation valve does not close, but the reactor is scrammed after break. System pressure is 350 psi.	10 lb/sec	40	2.5

2. Nuclear Design

a. Summary

The characteristics of the reactor design are summarized in Table 3.

In this section reactor control, power distribution, temperature coefficient and kinetics will be reviewed. The discussion of this information will form the basis for the analysis of potential reactivity accidents described in Section VII on Plant Safety Analysis.

The control of the reactor depends on the following design features:

(1) Thirty-six independently operated control rods which can be scrammed by appropriate signals.

(2) Nineteen backup shutdown rods which will have the strength and power so that they can be driven into the core even though the core may be damaged or crushed.

(3) Fuse operated poison rods which will drop by gravity into the core if a severe temperature excursion occurs.

(4) A strong over-all negative temperature coefficient at all times during reactor life and for all attainable core temperatures.

The effectiveness of each of these mechanisms is discussed in detail in Section II. A. 2. b. on Reactor Control.

In order to extract the maximum amount of power from the core within the limitations of a specified peak fuel temperature, it is, of course, desirable to maintain a power distribution which is as flat as possible. It has been the objective of the physics program to limit the over-all peak to average power distribution to approximately 1.5 at all times throughout reactor life. The use of non-uniform fuel distribution, partial length burnable poisons and control rod programming has made it possible to meet this objective. The details of the program to achieve a relatively flat power distribution throughout core life are described in Section II. A. 2. c. on Power Distributions.

As was expected on the basis of reactor physics considerations, there is considerable flexibility for achieving a strong negative temperature coefficient without serious penalty to fuel cycle economics. By using a heavier thorium load in the fuel elements and a small amount of rhodium poison, it has been found that a strong prompt and over-all negative temperature coefficient can be assured at all times throughout the core life and for temperatures throughout the normal operating range and, indeed, for all abnormal temperatures which might be postulated as the result of accident conditions. Doppler coefficient experiments in the critical assembly and neutron thermalization experiments using the General Atomic Linear Accelerator provide experimental confirmation for the basic data used in the analysis of the reactor temperature coefficients. This information is discussed in Section II. A. 2. d. on Temperature Coefficients.

TABLE 3

PHYSICS CHARACTERISTICS OF HTGR

Reactor Power (Thermal Output of Fuel Elements)	112.5 Mw(th)
Nuclear heating of reactor internals	2.8 Mw(th)
Total	115.3 Mw(th)
Effective core diameter	9.16 ft
Active core height	7.5 ft
Number of fuel elements	804
Number of control rods	36
Number of elec. driven emergency shutdown rods	19
Initial fuel loading	184.8 kg enriched uranium 173.3 kg U-235
Initial thorium loading	1987 kg
Initial boron burnable poison loading	0.950 kg
Initial rhodium loading	5 kg

Table 3 (Continued)

C/Th/U atom ratio	
696 fuel elements with	2126/9.57/1.0
108 fuel elements (outside ring) with	3511/24.46/1.0
Average moderator temperature	993 C
Average fuel compact temperature	1085 C
Maximum fuel compact temperature	1500 C
Initial thermal neutron flux	4.01×10^{13}
Initial fast flux (> .098 Mev)	4.38×10^{13}
Initial total neutron flux	16.55×10^{13}
Initial conversion ratio	0.48
Average conversion ratio	0.55
Final conversion ratio	0.61
Fuel life at full power	900 days

Because of the limited excess reactivity available and because of the large negative temperature coefficient, the calculated temperature excursions resulting from postulated credible reactivity insertions are not excessive, even for the case where no scram is assumed. A general discussion of the results of kinetic calculations is summarized in Section II. A. 2. e. on Kinetics. The detailed discussion of various specific reactivity accidents is contained in Section VII on Plant Safety Analysis.

b. Reactor Control

The following control objectives have been established for the HTGR:

(1) Thirty-six control rods will be used for normal control. These control rods will be driven downward to increase reactivity and will scram upwards.

(2) The core will be loaded initially with fuel elements containing fuel, thorium, burnable poison and rhodium

poison such that the k_{eff} with the core at operating temperature and all control rods removed will be approximately 1.08. This allows some margin above requirements for xenon and samarium to compensate for possible uncertainties in the calculations. With equilibrium xenon and samarium k_{eff} will be approximately 1.05 at the beginning of life.

(3) The reactor control system will be designed such that only three control rods will be in partially inserted positions at any time. All other control rods will be completely in or completely out. In the inner two rings, it will not be possible to drive more than one rod at a time manually, although in the outer two rings rods may be moved together in groups of three. These outer rings will normally be completely withdrawn during full power operation. Of the three partially inserted inner rods, one will normally be an automatic rod and one will be driven manually. Hence, during operation at full power, only two rods including the automatic rod can be in a partially withdrawn position at a time.

(4) The k_{eff} with all 36 control rods in and the core at its shutdown temperature will always be less than 0.95. Calculations for the reference design reactor indicate that the shutdown reactivity is substantially smaller than this objective (<0.93 at 300 K).

(5) The k_{eff} with any one control rod removed in the shutdown condition will always be less than 0.97. Calculations indicate that this objective can be met with some margin.

(6) Lumped boron burnable poison will be used to achieve a reactivity variation throughout life which is as uniform as possible within practical limitations. (In addition, rhodium will be used to insure a strong negative temperature coefficient. Although some of the rhodium will be removed by neutron absorption during the reactor lifetime, its purpose is not that of a burnable poison.)

(7) Nineteen backup shutdown poison rods will be available for emergency shutdown, which, together with the

rods inserted at operating conditions, will always be able to reduce the reactivity to less than unity even with the core at room temperature.

(8) A minimum of 19 fuse-operated poison rods will be suspended in the top reflector region of the reactor inside control rod guide tubes. These rods will be released on an interruption of coolant flow which causes excessively high temperature.

The planned locations of the control rods and backup poison rods in the reactor core are shown in Figure 4. The arrangement shown in the diagram is designed to effectively meet the requirements of normal shutdown margin, emergency shutdown margin and control rod programming flexibility. Although the relative numbers and arrangement of control rods and backup shutdown rods might change slightly, these possible modifications would be consistent with the over-all control objectives.

The reactivities for the various shutdown conditions have been calculated by means of two-dimensional XY and RZ calculations, and the results are summarized in Table 4. The calculated control effectiveness of the HTGR control rod has been checked by critical assembly measurements. As can be seen from the table, the maximum available reactivity at the beginning of life with no xenon poison in the core is 1.08 k with all control rods removed. After steady state xenon and samarium have been established, the maximum available reactivity is 1.05 k. With the 36 control rods inserted with the reactor at room temperature, i.e., 27 C, and with no Xe^{135} in the core, the shutdown reactivity is 0.93 at the beginning of life. In order to insure this shutdown margin, even though the calculated absolute reactivities may have an uncertainty of, perhaps, $\pm .03\Delta k$, some extra fuel rods containing lumped boron burnable poison will be available during loading operations so that the beginning of life reactivity can be increased or decreased by utilizing a smaller or larger number of burnable poison rods than specified. The worth of a burnable poison rod is approximately $-.004\Delta k$.

Although it is difficult to postulate any reasonable accident which could disable a multiple number of control rods simultaneously or disarrange the reactor core to an extent that several control rods could not be driven in, an Electrically Driven Emergency Shutdown System consisting of 19 high-force, high strength control rods will be provided which will permit shutdown to refueling temperature (about 200 C) even for the case where all the withdrawn control rods fail completely, a condition that is believed to be far beyond credibility. At the

TABLE 4

SHUTDOWN REACTIVITY FOR CONTROL RODS AND EMERGENCY RODS AT THE BEGINNING OF LIFE

Condition	k_{eff} (300°K)	k_{eff} (500°K)	k_{eff} (1200°K)
All control rods out All shutdown rods out No Xe or Sm	1.19		1.08
All control rods out All shutdown rods out Equilibrium Xe and Sm	1.16*		1.05
36 control rods in All shutdown rods out No Xe or Sm	<0.93	0.91	<0.85
No control rods in 19 shutdown rods in No Xe or Sm	1.02	1.0	0.92
6 control rods in No shutdown rods in Equilibrium Xe and Sm	1.11*		1.00
6 control rods in 19 shutdown rods in Equilibrium Xe and Sm	0.95*		0.85
6 control rods in 19 shutdown rods in No Xe or Sm	0.98*	0.96	0.88

*Estimated values based on extensions of calculated numbers. A small correction has been added to the derived shutdown numbers to allow for control rod shadow effects.

beginning of life when the reactor has an available $k_{eff} = 1.08$ with all rods withdrawn and the reactor hot, several control rods would normally be in the core to cover this excess reactivity. After equilibrium xenon and samarium buildup, the maximum available reactivity would become $1.05 \Delta k$, and the number of control rods in the core would be approximately six. If it is postulated that only the emergency shutdown rods could be inserted at this time, the reactivity would be reduced to about $0.85 \Delta k$ for the hot condition, allowing for some control rod shadowing effect. After the Xe^{135} has decayed this shutdown reactivity would increase about $0.03 \Delta k$, and with the reactor cooled to room temperature, the shutdown reactivity would be about $0.98 \Delta k$, again allowing for some control rod shadowing. Detailed shutdown calculations for the emergency rods have been made only for the beginning of life, since calculations for the regular control rods show that the control effectiveness increases throughout the reactor life.

A third shutdown system consisting of poison rods will be located in the top reflector inside the control rod guide tubes and held in their suspended positions by means of fuses which will melt during any extended interruption of the primary coolant flow. The detailed design of these fuse-operated rods is described in Section II.B.8. It is contemplated that a sufficient number of these rods (between 19 and 55) will be used to provide a reactivity worth at least adequate to cover the reactivity increase which could arise from Xe^{135} decay.

The control effectiveness of an inner control rod as a function of rod insertion is shown in Figure 5. Figure 6 shows that at a rod speed of 0.06 ft/sec, the average rate of reactivity change is about $0.8 \times 10^{-4} \Delta k$/sec., while the maximum rate is approximately $1.1 \times 10^{-4} \Delta k$/sec. The maximum number of control rods which can be driven out simultaneously will be limited to three in the outer two rings and two in the inner rings, including the automatic rod. Although the automatic rod and the manual rod would not usually move out simultaneously, the maximum reactivity addition even for this abnormal situation would be limited to about $2.2 \times 10^{-4} \Delta k$/sec. Because of the smaller effectiveness of rods in the outside two rings, the maximum rate of reactivity addition possible for withdrawal of these rods is not expected to be significantly larger than $2.2 \times 10^{-4} \Delta k$/sec.

The control effectiveness of the 36 control rods inserted as a rod bank has been calculated by a windowshade technique and normalized to the XY and RZ calculations for complete rod insertion and withdrawal. The results are shown in Figure 7 where control rod worth as a function of bank position is plotted. Figure 8 shows the shutdown

reactivity as a function of time for a scram condition, assuming the scram motion specified for the drive mechanisms.

A large part of the reactor physics analysis has been directed toward the study of reactivity changes and control effectiveness at various time steps throughout the reactor life. These calculations have been done primarily by four group one-dimensional burnup calculations using the FEVER diffusion theory code which was written at General Atomic. This code calculates the reactivities for the cold shutdown core and the hot poisoned and unrodded core at 100-day intervals throughout the reactor life. The control rod configuration is automatically determined at each time step to achieve a reactivity of k = 1, and the power distribution and group dependent neutron fluxes are obtained at each time step. On the basis of the calculated fluxes, the various isotopic changes during the next time step are calculated and the new isotopic compositions are obtained. The burnup calculations continue until the reactor falls below unity with all control rods removed, which is, then, the end of the reactor life.

Figure 9 shows the variation of the hot, poisoned and unrodded reactivity and the cold, shutdown reactivity as a function of reactor lifetime. It can be seen that the unrodded reactivity is very close to constant throughout most of the reactor life. It also can be seen that the control rod worth improves as the fuel is depleted.

c. Power Distributions

In order to maintain a relatively flat radial power distribution, it is planned that the U-235 concentration in the outside ring of fuel elements will be diluted to 60% of the fuel concentration in the rest of the fuel elements, and the thorium load will be increased to about 130% in this ring. The decrease in fuel concentration at the edge of the core removes the power peak which would normally occur at the core reflector interface due to the large absorption in U-235 of cold neutrons which are returned to the core by the reflector.

In order to minimize power tilts in the axial direction, it has been found that the control rods should be all in or all out of the reactor as much as possible. It is, therefore, planned to maintain at all times all but three rods in their completely inserted or completely removed position. The axial power distribution can be further improved by the use of a limited amount of boron poison in the top reflector and the use of partial length burnable poison in the core.

By experimenting with various sequences of control rod removal using the FEVER Burnup Code, a control rod program has been selected which will minimize variations in the radial power distribution throughout the reactor life. One promising control rod program studied calls for the initial removal of all the ring 4 and ring 5 control rods (Figure 4), half of the ring 2 control rods, and an appropriate number of control rods in ring 3 to achieve an operating condition. The reactor is then controlled by additional removals of control rods in ring 3 and, finally, the remaining control rods in ring 2.

By means of these experiments, the maximum peak-to-average power ratio is maintained at approximately 1.5 to 1 throughout the reactor life.

A discussion of the temperature distributions resulting from the calculated power distributions is included in the discussion of the thermal design.

d. Temperature Coefficient

The contributions to the temperature coefficient can be described quite easily by differentiating the four-factor formula:

$$k = \eta f p \epsilon P_F P_{Th}$$

where k = multiplication constant
η = the average number of neutrons produced per neutron absorbed in the fuel
f = thermal utilization
p = resonance escape probability
ϵ = fast fission effect

and P_F and P_{Th} are the fast and thermal non-leakage probabilities.

Hence,

$$\frac{1}{k}\frac{dk}{dT} = \frac{1}{\eta}\frac{\partial \eta}{\partial T} + \frac{1}{f}\frac{\partial f}{\partial T} + \frac{1}{p}\frac{\partial p}{\partial T} + \frac{1}{\epsilon}\frac{\partial \epsilon}{\partial T} + \frac{1}{P_F}\frac{\partial P_F}{\partial T} + \frac{1}{P_{Th}}\frac{\partial P_{Th}}{\partial T}$$

Since the changes in reactor size and graphite density resulting from temperature changes are relatively small, only the changes in η, f, p, ϵ and the thermal leakage contribute significantly to the temperature coefficient.

Because of the relatively high moderator temperatures in the HTGR, the cutoff energy for the thermal neutron group has been chosen at 2.1 ev. This choice allows substantially all of the neutrons

in thermal equilibrium with the moderator to be included in the thermal group. The choice of 2.1 ev for the cutoff energy also has the advantage that the effect of isotopes having low-lying resonances, particularly Xe-135, Sm-149, Rh-103, Pu-240, and U-233, on thermal energy reaction rates, can be calculated explicitly and included in the thermal energy group. It is found from the multigroup calculations for the HTGR that a significant number -- greater than 20% -- of the fissions occur above 2.1 ev. Hence, the factor η refers to the average number of neutrons produced per neutron absorbed in the fuel, U-233, U-235, etc., below 2.1 ev., while f represents the fractional absorption in the fuel below the 2.1 ev cutoff energy. The fast effect, ϵ, is the ratio of the total fissions to the fissions resulting from neutrons having energies below 2.1 ev. The temperature dependence of the fast effect arises from gross redistribution of the lethargy flux. The resonance escape probability, p, is the fraction of source neutrons that do not leak from the system as fast neutrons (>2.1 ev) which escape capture in all materials during the slowing down process. The temperature dependence of the resonance escape probability results primarily from Doppler broadening of the resonances in the fertile material, thorium. Contributions from other resonance poisons or fuels to the temperature dependence of p are small because of insufficient concentration and broad resonances, respectively.

The two largest contributions to the temperature coefficient in HTGR arise from the temperature dependence of both f and p. The change in thermal utilization with moderator temperature reflects the change in the neutron absorption rates in the fuels relative to the neutron absorption rates in the various poisons. Isotopes which have strong non 1/v cross section variations below 2.1 ev contribute strongly to the thermal utilization component of the temperature coefficient. In order to calculate the contribution from $(1/f)(\partial f/\partial T)$ accurately, it is necessary to have a good knowledge of the atom densities of the important absorber isotopes, their cross section behavior below 2.1 ev, and the thermal neutron spectrum as a function of temperature.

The atom densities of the various materials at the beginning of the reactor life are, of course, known with very good precision. However, as fuel burnup proceeds, substantial changes occur due to the depletion of U-235, the buildup of U-233, the growth of heavy isotopes such as Pu-239 and Pu-240 from the U-238 impurity in the fuel, and, finally, the accumulation and partial burnup of strongly absorbing fission product poisons. The buildup and burnup of all the important isotopes have been studied very carefully by means of the one-dimensional, four-group burnup code, FEVER, which follows in detail

TABLE 5

NUCLIDES FOLLOWED EXPLICITLY IN LIFETIME CALCULATIONS

	Nuclide	End of life loading, gm	Δk due to complete removal, %
1.	Lumped burn. poison (Boron-10)	1.354×10^{0}	0.14
2.	Thorium 232	1.907×10^{6}	54.36
3.	Protoactinium 233	4.094×10^{3}	0.61
4.	Uranium 233	4.345×10^{4}	-28.97
5.	Uranium 234	3.742×10^{3}	0.73
6.	Uranium 235	6.327×10^{4}	-17.89
7.	Uranium 236	2.107×10^{4}	1.08
8.	Uranium 238	1.096×10^{4}	0.55
9.	Neptunium 239	1.959×10^{1}	0
10.	Plutonium 239	2.927×10^{2}	-0.42
11.	Plutonium 240	1.077×10^{2}	0.42
12.	Plutonium 241	1.558×10^{2}	-0.25
13.	Plutonium 242	7.245×10^{1}	0.02
14.	Rhodium 103	3.208×10^{3}	4.56
15.	Cadmium 112	6.027×10^{-2}	0.01
16.	Xenon 135	7.079×10^{-1}	3.20
17.	Samarium 149	5.808×10^{0}	0.82
18.	Samarium 151	3.361×10^{1}	0.75
19.	Europium 153	6.006×10^{1}	0.09
20.	Gadolinium 155	6.956×10^{-1}	0.02
21.	Gadolinium 157	4.339×10^{-2}	0.01

all of the heavy isotopes and up to ten fission product poison isotopes throughout the reactor burnup history. The inventory of important isotopes at the end of life as calculated by FEVER is shown in Table 5, expressed in terms of their reactivity contributions.

Excellent differential cross section data are now available for all of the important heavy element and fission product isotopes for the energy range of interest;[1] in addition, the fission product yields of interest are well known. Hence, both atom densities and cross sections of all the important isotopes can be determined with considerable precision.

The calculated reaction rates require, in addition to the atom densities and cross sections, a good knowledge of the thermal neutron spectrum and its variation with temperature. It was recognized early in the HTGR physics program that the most severe limitation on the calculation of the thermal utilization contribution to the temperature coefficient might arise from the lack of knowledge regarding the thermal neutron spectra in poisoned graphite lattices. As a result, strong theoretical and experimental physics programs were initiated to provide adequate thermal spectrum information in time to assure good calculations of thermal reaction rates and their temperature dependence. The theoretical studies have shown that for moderator temperatures equal to and above 1200 K, a free gas representation of the neutron thermalization process is adequate as was expected. Recent work by Parks[2] has resulted in a theoretical model which describes the crystal binding effect in graphite exceedingly well as is evidenced by the data in Figures 10 and 11. The points indicate measured values of the neutron flux in a poisoned graphite block while the curves indicate calculated spectra using a free gas model and the Parks crystal model. The experimental work was done by Beyster[3] and his associates using the GA Linear Accelerator as a pulsed source of neutrons and time-of-flight equipment. Some recent neutron chopper spectrum measurements on the ZENITH critical assembly in England by Poole and his associates have yielded spectra data in excellent agreement with Beyster's results. It is, therefore, concluded that the Parks model for calculating neutron spectra is entirely satisfactory.

Figure 12 shows a comparison of the free gas model and the Parks crystal model for an HTGR lattice at 1200 K. As can be seen from the figure, the free gas model yields satisfactory results for temperatures at and above the normal HTGR operating temperature. On the basis of this kind of information, it was decided to use the free gas model for spectrum calculations at and above normal operating temperatures. Most of the HTGR work done to date at temperatures below the

operating temperature has used the Schofield crystal model which is not as accurate as the Parks model, but which will not have any significant effect on the hazards evaluation.

The evaluation of the temperature coefficient contribution from the change in resonance escape probability with temperature requires good information on the thorium resonance integral and its logarithmic change with temperature, i.e., the Doppler coefficient. Again, the importance of good information on the variation of the thorium resonance integral with temperature was recognized early in the project physics program and strong theoretical and experimental programs were planned to supply the necessary data. Nordheim's[4] procedures have been used to calculate resonance integrals using cross section information from Columbia University and the Neutron Cross Section Evaluation Center at Brookhaven National Laboratory. Measurements of the Doppler coefficient have been made in the HTGR critical assembly for fuel compacts having several different concentrations of thorium.

The following characteristics of thorium resonance capture in HTGR give some insight into the Doppler effect in this application. The system is essentially homogeneous with scattering contributed by graphite atoms in which thorium is dispersed having a marked influence, particularly on the lower energy levels. There is less self-shielding (minimum self-shielding factor about 0.3) of the lower levels than in the heterogeneous case. The "volume" effect dominates for all resonances, contributing about two-thirds of the resonance capture and a somewhat larger fraction of the Doppler effect in a typical case.

Nordheim has pointed out that calculations of $(1/I)\ (\partial I/\partial T)$ should be quite good in this situation. A more rigorous test of his methods of calculation is the determination of resonance integrals of metal or oxide rods. Calculations for these heterogeneous cases agree well with reliable measurements. This agreement gives considerable confidence in the calculation of $(1/I)\ (\partial I/\partial T)$ for HTGR. Figure 13 shows calculated values of the Doppler coefficient, $(1/I)\ (\partial I/\partial T)$, as a function of fuel element temperature for several thorium concentrations.

In order to evaluate the Doppler coefficient experimentally for HTGR fuel elements, a pile oscillator experiment was designed and constructed in the HTGR critical assembly to compare the reactivity of a hot and a cold fuel element[5]. The central region of the critical assembly was loaded with fuel elements having the same composition and dimensions as the HTGR fuel elements in order to establish a neutron spectrum very nearly the same as that in HTGR. Two identical fuel elements, located end to end, were then moved in and out of the test lattice region so that either of the two fuel elements could be

positioned in the lattice during some fixed interval of time. The dwell time in the lattice was 29 seconds compared to 1 second to exchange fuel elements. The fuel element on one side was withdrawn into an oven in its out position while the other fuel element was cooled by room air in its out position. The difference in reactivity between the two fuel elements was compensated by a calibrated control rod driven by a servomechanism which responded to an error signal from a neutron ion chamber and a fixed current source. The sensitivity of the pile oscillator was about .01 cent compared to a maximum reactivity difference of approximately 3.0 cents between a hot and cold fuel element.

By oscillating some fuel-bearing compacts with boron to replace the 1/v component of thorium (the thorium was removed for this test), the thermal base effect arising from changes in the moderator temperature was evaluated and subtracted from the reactivity swings for the thorium-loaded fuel elements. The results for a typical series of experiments are illustrated in Figure 14. The reactivity change with temperature, after the correction for the thermal base effect, is proportional to $\partial I/\partial T$. The Doppler coefficient $(1/I)(\partial I/\partial T)$ is, then, just $(1/\rho)(\partial\rho/\partial T)$ where ρ is the resonance component of the reactivity contribution of the thorium in the fuel element. This value of ρ is obtained from the difference of reactivity measurements between a fuel element containing thorium, and a fuel element without thorium but with an amount of boron such that the neutron absorption in the boron matches the 1/v absorption in the thorium. Hence, the Doppler coefficient is determined quite easily from reactivity measurements.

Figure 15 shows the measured values of the Doppler coefficient for a typical HTGR fuel element. The points represent the measured values while the solid line is the calculated Doppler coefficient, using the data and methods previously discussed. The experimental points for small temperature swings are subject to rather large errors since the incremental reactivity changes are small relative to the experimental errors. In general, the calculated and measured Doppler coefficients are in excellent agreement. As can be seen from the results in Table 6, results for other thorium loadings also show good agreement between calculation and experiment as well as good consistency between different experiments.

On the basis of the relative ease in handling the theoretical problem for this type of reactor and in view of the excellent agreement between calculation and experiment, it is concluded that the Doppler coefficients calculated for the HTGR have an uncertainty no greater than ±10%.

The temperature coefficients for the HTGR were calculated for both the beginning of life and the end of life using a one-dimensional four energy group code. The slowing down spectrum and the group-averaged cross sections for the epithermal energy groups were calculated by GAM-1, a P-1 multigroup code[6]. Resonance integrals are calculated in the GAM-1 code by the methods developed by Adler, Hinman and Nordheim[7]. Thermal neutron spectra were calculated from spectrum codes making use of the free-gas scattering kernels for moderator temperatures at 1200 K and above, and crystal model scattering kernels for temperatures below 1200 K. The thermal group average cross sections were then calculated by a spectrum-averaging program.

TABLE 6

SUMMARY OF DOPPLER MEASUREMENTS

C:Th Ratio of Sample	C:Th Ratio of Test Lattice	Average $1/I\ (\partial I/\partial T)$ (300 - 700 K)	
		Measured	Calculated
233	263	$-3.58 \times 10^{-4}/^{o}C$	$-3.40 \times 10^{-4}/^{o}C$
161	263	$-3.59 \times 10^{-4}/^{o}C$	$-3.40 \times 10^{-4}/^{o}C$
233	233	$-3.70 \times 10^{-4}/^{o}C$	$-3.52 \times 10^{-4}/^{o}C$
161	233	$-3.90 \times 10^{-4}/^{o}C$	$-3.52 \times 10^{-4}/^{o}C$

Using reactor composition data appropriate for the beginning of life or the end of life core, and the group-averaged cross section data appropriate for different moderator and fuel temperatures, the reactivities for various reactor temperatures were calculated. On the basis of the incremental reactivity changes for corresponding temperature changes, the over-all temperature coefficient was calculated as a function of the average core temperature. The results are shown in Figure 16 for the end of life. It can be seen that the over-all temperature coefficient is strongly negative at operating temperature and remains negative for all temperatures up to the vaporization temperature of graphite. The temperature coefficients reported here are strongly negative because of an increase in the thorium load, a lower fuel compact temperature, and better calculations for the end of life

reactor condition. Still more improvement is possible by introducing rhodium in the core. These improvements will be discussed in greater detail in succeeding paragraphs.

For a fast reactivity insertion followed by a rapid power increase, the added heat energy does not have time to diffuse from the fuel compact, so the prompt temperature coefficient depends only on the temperature rise of the thorium plus the fraction of graphite contained in the fuel body. The characteristic time for the heat to diffuse into the graphite spine and the graphite sleeve of the fuel element is of the order of 3 minutes so that reactivity insertions occurring in times of the order of seconds must depend only on the prompt temperature coefficient for control in the absence of corrective control rod action.

It has been found, as was expected, that both the prompt and over-all temperature coefficients can be adjusted by changes in reactor composition without seriously affecting other reactor characteristics including the fuel economics. One rather simple expedient for enhancing the prompt temperature coefficient is the possibility of increasing the thorium concentration in the fuel compacts. Since the temperature coefficient contribution from the resonance escape probability is related to the Doppler coefficient by

$$\frac{1}{p}\frac{\partial p}{\partial T} = (\ln p)\,\frac{1}{I}\frac{\partial I}{\partial T} ,$$

an increase in thorium concentration results in an increase in ln p (as well as a small increase in the Doppler coefficient) which, therefore, increases the magnitude of the temperature coefficient contribution. Figure 17 shows the variation of $(1/p)(\partial p/\partial T)$ with fuel temperature for different thorium concentrations in the fuel elements. It can be seen that an increase in thorium concentration from a C:Th = 325:1 to 220:1 results in an improvement of about 50% in the temperature coefficient contribution from the Doppler coefficient. Furthermore, a decrease in the average fuel element temperature of 300 C results in another increase of about 25% in the magnitude of $(1/p)(\partial p/\partial T)$. As a result of increasing the HTGR thorium loading from 1287 kg to 1987 kg and using a single-wall fuel element, thereby reducing the fuel compact temperature, the magnitude of the prompt negative temperature coefficient has been increased by about $1.5 \times 10^{-5}/^{o}C$. In addition, some improvement has also resulted from a negative moderator contribution, as will be discussed.

It was pointed out earlier that the analysis of the more heavily thorium-loaded reactor indicate a rather strong over-all negative temperature coefficient. The improvement in temperature coefficient results from the following changes:

(1) The increased Doppler coefficient due to the heavier thorium load.

(2) The increased Doppler coefficient due to the lower average fuel compact temperature.

(3) The increased ratio of U-235 to U-233 at the end of the reactor life.

(4) Improvements in the calculation of neutron leakage effects and contributions from individual fission product and heavy element isotopes.

In view of the relatively large contribution from the fission product isotope, Rh-103, particularly at abnormally high reactor temperatures, it was decided to spike the core with 5 kg of rhodium at the beginning of life. Although almost half of the rhodium burns out during the reactor life, the remaining fraction at end of life contributes very strongly to the over-all (and to some extent the prompt) temperature coefficient. Figure 18 shows a comparison of the end of life temperature coefficient as a function of moderator temperature, with and without the rhodium spike.

It is apparent from the experimental and analytical work which has been done in the HTGR project that both the prompt and over-all temperature coefficients will be strongly negative for all temperatures obtainable throughout the life of the reactor. For temperatures below the operating temperature, the contribution from the Doppler broadening of the thorium resonances predominates, while above the normal operating temperature, the contribution from rhodium predominates. On the basis of the Doppler coefficient experiments, it is estimated that the accuracy of these results is ±10%. Likewise, on the basis of the excellent agreement between theory and experiment for thermal neutron spectra, the good information now available on cross sections below 2.1 ev, and the careful analysis of isotopic concentrations from reactor burnup calculations, it is believed that the temperature coefficient contribution from changes in thermal utilization can also be calculated with about the same accuracy. Since the two contributions (plus the smaller ones) are additive and since the resultant

temperature coefficient is strongly negative, it is concluded that the reactor will be very stable.

e. Kinetics

Kinetic calculations based on approximate analytic solutions of the reactor kinetic equations have been supplemented by numerical solutions which allow for a more detailed description of the initial reactivity insertion and the shutdown worth.

A digital computer program (BLOOST) has been written for the IBM 7090 which combines a lumped parameter kinetics code (BLUP-3) with a time-dependent heat transfer code (RZTEMP), and calculates the behavior of an average fuel element during a reactivity transient. The following details can be supplied as input in the problems:

(1) An arbitrary reactivity change with time can be specified as the beginning of a hypothetical accident.

(2) An arbitrary reactivity change with time can be specified for the scram.

(3) The power level for scram initiation and the scram delay time can be specified.

(4) The temperature coefficient can have any desired variation with the moderator compact temperatures.

(5) The neutron lifetime, the delayed neutron fractions, and their precursor decay constants can be specified as part of the problem input.

The output of the BLOOST code provides in tabular form the average temperatures of the fuel compact and the entire fuel element, the power level, the net reactivity, and the contributions to the reactivity of the accident, the scram, and the temperature coefficient. At frequent intervals, a two-dimensional temperature map of the entire fuel element is printed, which includes the helium coolant temperatures. The average fuel compact temperatures and the average moderator temperature obtained at the end of each time step are used as feedback quantities to determine the temperature coefficient components arising from the Doppler coefficient and the thermal base effect respectively for the next time step.

The values for the neutron lifetime, delayed neutron fraction, prompt temperature coefficient and over-all temperature coefficient at normal operating conditions for the reactor at the beginning-of-life and the end of life are summarized in Table 7. On the basis of this information, the sensitivity of some postulated accidents to various conditions has been examined.

Figure 19 shows the peak fuel temperatures which would result from a ramp reactivity insertion of .01, .015 and .02Δk. For these accidents the following assumptions have been made:

(1) The ramp is inserted at a rate corresponding to the maximum rod removal rate (.06 ft/sec) until a total reactivity insertion indicated by the abscissa has been reached.

(2) The insertion begins from normal operating power, i.e., 112.5 MW.

(3) A scram is initiated when the power has reached 140% normal power.

(4) The scram delay time is as indicated.

(5) The temperature coefficient, delayed neutron fraction and neutron lifetime have values corresponding to the end-of-life condition.

(6) Helium cooling is maintained at full flow.

It can be seen from the curves in Figure 19 that a relatively long interval of time is available to scram the reactor before excessive fuel element temperatures are reached. Indeed, the maximum fuel element temperature even for the case of no scram is only 2331° C which is lower than the melting temperature for the carbides (2500 C) and well below the vaporization temperature of the graphite (4000 C).

Figure 20 shows similar data for a reactivity insertion corresponding to the free fall of a control rod out of the reactor core. Except for the mode of reactivity insertion, the assumptions are the same as for the previous case. The reactivity insertion and the rate of reactivity insertion, normalized to a total insertion of .01Δk, are shown in Figure 21. The maximum rate of change in reactivity is

.031Δk/sec, which is considerably greater than the previously discussed ramp insertion. As would be expected, the temperature excursions are substantially higher for this type of accident, although the maximum fuel temperature, even for an insertion of .02Δk, resulting from 2 rods dropping out simultaneously and no scram, is less than the graphite vaporization temperature.

In order to examine the importance of the scram trip level, the scram delay time, the temperature coefficient and the neutron lifetime on the severity of an accident, the maximum fuel element temperature has been calculated for a postulated reactivity insertion under a variety of assumed values for the aforementioned parameters. The postulated accident assumes the following:

(1) A free fall reactivity insertion having a maximum value of .01Δk.

(2) A negative scram reactivity insertion based on control drive specifications and present test results.

(3) A delayed neutron fraction of β = .00467 corresponding to the end of life condition.

(4) A neutron lifetime of 2.9×10^{-4} sec, unless specified otherwise.

(5) A scram trip level of 140% full power, unless specified otherwise.

(6) A scram delay time of 75 msec, unless specified otherwise.

(7) A prompt temperature coefficient of $-2.35 \times 10^{-5}/^{\circ}C$ at operating temperature and the characteristics indicated in Figure 22, unless specified otherwise. For other values, the variation with temperature is scaled up or down to have the same trend.

The results of these studies are summarized in Figures 23, 24, 25, and 26. In general, it can be seen that the maximum fuel element temperature is not critically sensitive to variations in the parameters, within the limits of probable error in meeting the specified values, or the uncertainties in calculating or measuring the physical characteristics.

It is again emphasized that the accidents chosen for these kinetic studies were not chosen on the basis of credibility, but simply to serve as a basis for illustrating the effect of various parameters on the magnitude of the fuel temperature excursion for two types of reactivity insertion. The studies demonstrate, however, the high degree of stability of this reactor to relatively large reactivity insertions. This stability arises primarily from the large prompt and over-all negative temperature coefficients.

TABLE 7

KINETICS PARAMETERS

Characteristic	Beginning-of-life	End-of-life
Neutron lifetime	1.8×10^{-4} sec.	2.9×10^{-4} sec.
Delayed neutron fraction, β	.00651	.00467
Prompt temperature coefficient for fuel compact at operating temp. (1358 K)		
No xenon	$-6.21 \times 10^{-5}/^{o}C$	$-3.65 \times 10^{-5}/^{o}C$
Equilibrium xenon	$-4.91 \times 10^{-5}/^{o}C$	$-2.35 \times 10^{-5}/^{o}C$
Over-all temperature coefficient for fuel element at operating temp. (1266 K)		
No xenon	$-6.46 \times 10^{-5}/^{o}C$	$-4.50 \times 10^{-5}/^{o}C$
Equilibrium xenon	$-5.16 \times 10^{-5}/^{o}C$	$-3.35 \times 10^{-5}/^{o}C$

REFERENCES

1. Wikner, N.F., and Jaye, S., "Thermal Cross Sections for the Heavy Elements and Fission Products Energy Dependent and Spectral Averaged for Several Temperatures and C/U-235 Ratios," GA-2113, March 1961.

2. Parks, D.E., to be published in The Physical Review.

3. Beyster, J.R., et al, to be published in Nuclear Science and Engineering. Also, see Trans. of the American Nuclear Society, Vol. 4, No. 1, paper 26-8 June 1961.

4. Nordheim, L.W., "The Theory of Resonance Absorption," Proceedings of Symposia in Applied Mathematics, Vol. XI, American Mathematical Society, pp. 58-88 (1961).

5. Brown, J.R., and Sampson, J.B., "Reactivity Oscillation Measurements of the Thorium Doppler Coefficient in the HTGR Critical Facility," GA-2313, June 1961.

6. Joanou, G.D., and Dudek, J.S., "GAM-1, A Consistent P-1 Multigroup Code for the Calculation of the Fast Neutron Spectrum and Multigroup Constants," GA-1850, June 1961.

7. Adler, F.T., Hinman, G.W., and Nordheim, L.W., "Effective Resonance Integrals: A Systematic Evaluation for All Temperatures and Geometries of Practical Interest," Proceedings United Nations Second International Conference on Peaceful Uses of Atomic Energy, United Nations, Geneva, Vol. 2, p. 1988 (1958).

3. Thermal And Fluid Flow Design

a. Summary

In this section is presented a discussion of the thermal design of the HTGR core, specifically as related to temperature gradients and thermal stresses. Also covered, as a subtopic, is the coolant flow through the core, as it influences strongly the rate of heat removal and, hence, the temperatures in various parts of the core.

Temperatures, in particular interior fuel element temperatures, are of interest from the point of view of core physics, materials stability, and fuel chemistry. The fission product retention properties of the fuel compacts, for instance, depend strongly on the operating temperature of the compacts. Temperature gradients are of interest indirectly as most of these gradients result in thermal stresses which must be controlled within the limits imposed by the mechanical properties of the fuel element graphite.

It is shown that during all normal modes of operation, temperatures, temperature gradients, and stresses resulting therefrom are well within safe limits.

The primary system of the HTGR must generate about 117.1 MW for an electrical net plant output of 40 MW. This 117.1 MW gross output is composed of the following:

Reactor power:	
Heat generated in fuel elements	112.5 MW
Nuclear heating in reactor internals surrounding core	2.8 MW
Power added by circulators	1.8 MW

In the discussions following, only the first quantity is of interest. It is the heat generated in the fuel elements by the nuclear reactions and by gamma heating. It determines, therefore, the operating temperatures and temperature gradients in the fuel elements.

The other most significant over-all design parameters of the core are summarized here for convenience:

Active core diameter	9.16 ft.
Active core height	7.5 ft.
Reflector thickness (all sides)	2.0 ft.

Shape of fuel elements	cylindrical
Number of fuel elements	804
Number of control rods	36
No. of elec. driven safety rods	19
Total number of fuel--and control--element locations	859
Number of coolant channels	1722
Cross-sectional voidage area of core	12.8%

Average coolant temperatures:

Core inlet	654 F
Core outlet	1380 F
Mixed mean above core	1358 F
Plenum outlet	1354 F

b. Coolant Flow Requirements

At full-power operation, the nominal coolant flow rate into the reactor is about 440,000 lb/hr.. Of this, 418,450 lb/hr. enter the core coolant channels. The remainder bypasses the core through various flow passages, i.e., as coolant flow through the control rods, as leakage past the dummy elements surrounding the core, as upward leakage between the segments of the side reflector and as leakage through the plenum-to-reflector seal. Within the core, 1,000 lb/hr. are diverted into the fuel elements as purge flow. This flow goes directly to the fission product trapping system. Its heat content is, therefore, unavailable to the primary loop. The net flow carrying useful yet out of the core is then 417,450 lb/hr. This flow must leave the core at an average temperature of 1380 F for a plenum outlet temperature of 1354 F, since it is being diluted by the several cooler bypass flows

The flow paths within the reactor are shown schematically in Figure 27. Some regeneration occurs across the walls of the plenum. Regeneration and gamma heating account for the temperature rise between points 1 and 3. They raise the helium temperature from 634 F at the reactor inlet to 654 F at the core inlet. Similarly, regeneration accounts for the 4 F drop between the "mixed mean" temperature of all flows above the core, and the reactor outlet temperature.

The temperature of the gas stream entering a particular coolant channel at the bottom of the core will be close to the average

core inlet temperature of 654 F. The temperature rise in each individual coolant stream, however, depends on the amount of heat generated at that particular location in the core. Consequently, the outlet temperatures of various channels differ appreciably. The hottest channel outlet temperature is 1791 F; that of the coldest channel is 874 F. By comparison, the average core outlet temperature is 1380 F.

Adjacent fuel elements do not touch each other except at the spacer pads. Hence, adjacent coolant flow channels intercommunicate essentially along their entire length, and cross flow from one channel to the next can and does take place. The effect of this cross flow has been taken into account in the calculation of core outlet temperatures.

During all normal modes of operation, helium flow will be controlled so that the average temperature at the plenum exit will be essentially at or below 1354 F. Average helium outlet temperature will also be maintained at or below 1354 F during startup, scheduled shutdown, and shutdown after reactor scram with both cooling loops operative.

Helium outlet temperature can exceed 1354 F in certain emergency cases, as discussed in Section VII . B.

c. Core Temperature Distribution

In order to be conservative, the core power distribution corresponding to the beginning of core life was used for the temperature calculation, since at this time the peak-to-average power ratio is highest. At the beginning of life, the number of control rods inserted into the hot operating core is also a maximum. Consequently, the power generation is depressed in the largest number of fuel elements adjacent to control rods.

A brief summary of the most significant core temperature information is presented in Figures 28 to 30. The figures are "temperature-percentage" curves. For instance, Figure 28 indicates what percentage of the fuel material is above a certain temperature. Figure, 29, is a similar curve for the sleeve material, and Figure 30 shows the statistical distribution of fuel element surface temperatures in the core. The fuel element spine temperatures, not shown, are just slightly higher than the fuel temperatures. They are, therefore, in effect represented by Figure 28.

For the sake of conservatism, most of the discussion in the remainder of this section on the thermal design centers around the so-called "hottest fuel element", that is, the maximum temperatures shown on Figures 28 to 30.

d. Temperature and Stresses in Fuel Elements During Normal Operation

The core temperatures discussed in the preceding section are the composit results of a large number of calculations, carried out for various representative fuel elements in the core. These individual fuel element studies are the topic of the present section, the first part of which deals with temperatures and stresses in the nominal fuel element (the hypothetical element built exactly to its specifications). In the second part of the section follows an evaluation of the various ways in which the actual fuel elements differ from the nominal concept.

(1) Nominal Fuel Element

Figures 31 and 32 are plots of radial temperature profiles in the fuel elements, at rated steady-state operating conditions. Temperatures are shown for three axial stations along the element: at the lower edge of the active core; at the midpoint of the core; and at the upper edge of the core. Figure 31 represents the "average" fuel element, i.e., the hypothetical element which produces 1/804th of nominal power. Figure 32 is a similar temperature plot for the hottest element in the core, i. e., the actual element which produces the highest power, which, therefore, is subjected to the highest temperatures, as well as the most severe temperature gradients. The most critical temperatures from Figure 32 (the highest temperatures in the hottest element), are summarized below:

Temperatures at hottest station in hottest fuel element	
Average spine temperature	2730 F
Average fuel compact temperature	2670 F
Average sleeve temperature	2060 F
Radial temperature drop in spine	Negligible

Radial temperature drop through compact	230 F
Radial temperature drop through sleeve	277 F
Temperature drop across gap between compact and sleeve	340 F
Temperature drop between outer surface of sleeve and coolant	570 F

The hottest station referred to here is somewhat above the center point of the active length of the hottest fuel element.

The "average" spine, fuel, and sleeve temperatures are the radial average values at the axial station being considered. An axially symmetric temperature distribution is assumed. The absolute maximum fuel temperature (ignoring the factors discussed later in this section) occurs at the inside surface of the hottest fuel compact in the hottest fuel element. It is essentially equal to the spine temperature at that point. The maximum fuel temperature is 2730 F, i.e., about 60 F higher than the 2670 F "average temperature in hottest compact" listed above. Hereafter, the 2730 F value will be referred to as the "maximum nominal fuel temperature".

(2) Deviations from Nominal Design

(i) Effect of Thermal Conductivity of Graphite and Fuel Compact

In the temperature calculations discussed so far, a graphite thermal conductivity of 15 Btu/hr-ft-°F was used, and was assumed to be independent of temperature and irradiation effects.

Experimental indications are that actual thermal conductivities of both compact and sleeve material, will be in the vicinity of 20 Btu/hr-ft-°F. Tests have shown the variation of thermal conductivity with temperature to be small, on the order of 10 to 20%. Tests have also shown (see Section II. J. 1) that irradiation at elevated temperatures to an integrated thermal flux of 10^{21} nvt has no appreciable effect on the thermal conductivity (at reactor temperatures) of HTGR type graphite.

It may be concluded that the radial thermal conductivity of the HTGR graphite will at all times be above 15 Btu/hr-ft-°F.

In Figure 33 is plotted, as a function of graphite thermal conductivity, the fuel temperature in that part of the core where a change in graphite thermal conductivity has the most pronounced effect on fuel temperatures (the fuel temperatures at this point are slightly lower than the maximum fuel temperature).

It is apparent from the figure, that the graphite thermal conductivity could be significantly below 15 Btu/hr-ft-°F without adversely affecting core performance.

(ii) Dimensional Changes

Irradiation- or temperature-induced growth or shrinkage of the fuel element sleeve and of the fuel compact diameters will have negligible effect on the heat transfer characteristics and, hence, temperatures, as long as these changes are all in the same direction in the various parts, i.e., as long as a growth (shrinkage) of the fuel element sleeve is accompanied by a proportional growth (shrinkage) of the fuel compact.

If the dimensional change in the compact differs appreciably from that of the sleeve, then the fuel element temperature can change as a result of the change in gap. This is illustrated in Figure 34, where the fuel temperature in the hottest element is plotted as a function of gap width. The curve is for the gap between the hottest compact and the surrounding sleeve, i.e., for that spot in the core where a change in gap width has the most pronounced effect.

(iii) Tolerances

Sleeve wall thickness tolerances or compact wall thickness tolerances have negligible influence on temperature. However, differential deviations from nominal dimensions (diameters) due to manufacturing tolerances will have the same effect as the differential dimension changes discussed above. For each mil of additional gap between fuel and sleeve, the fuel temperature increases by some 34 F. In the extreme case of a minimum compact OD combined with maximum sleeve ID, gap width increases from .0045 inch to .007 inch. Consequently, fuel temperatures increase by approximately 100 F.

Since uniform gap width between fuel and sleeve is not maintained around the circumference, the compact will tend to

shift to one side, resulting in a minimum gap at one point and a maximum gap 180 degrees from that point. Calculations were made for the extreme case where the compact touches the sleeve at the "minimum gap point". Maximum gap width was assumed in addition to maximum eccentricity, in order to be conservative. The resultant temperature asymmetry amounted to less than 20 F. The effect of circumferential variations in the convection film coefficient on the outer surface of the element was included in this calculation (see item (v) below).

The effect of straightness tolerances is identical to that of irradiation-induced bowing, and is, therefore, discussed under the topic following.

(iv) Bowing

Fuel element bowing could exist because of several causes:

(a) Deviation from straightness manufactured into the element.

(b) Irradiation-induced dimensional changes, nonsymmetric with respect to the fuel element.

(c) Diametral temperature gradients, as consequence of power gradients across the fuel element.

In all cases, a bowed fuel element runs hotter on the convex side. Since the hot side of the element bows into the adjacent coolant channel and thereby decreases the coolant flow through the channel, the temperatures on the hot side of the bowed element are increased further. To minimize this tendency, each fuel element is equipped with two spacer rings in the active core zone. The pads are equally spaced (approximately) between the bottom end of the element and the spacer at the upper reflector. They limit the amount of bowing to that allowed by the .01 inch clearance between the spacers on adjacent fuel elements.

The effect of the limiting amount of bowing on the maximum fuel temperatures is calculated to be 54 F (see section vi, "Hot Spot", below).

Power gradients cause diametral temperature variations in two instances: where the over-all core power level exhibits an appreciable gradient, and in the immediate vicinity of a control rod. The most severe control-rod-induced gradient would be next to a fully inserted control rod in the central region of the core. The edge-of-core fuel element also experiences a significant diametral temperature gradient. In addition, it will exhibit the most pronounced irradiation-induced bowing tendencies. However, the two bows counteract each other with the result that their combined effect is much lower than the bow in the element next to a control rod.

If a control rod in the central part of the core were fully inserted with the core operating at full power, an adjacent fuel element would experience a temperature difference across its diameter as shown in Figure 35. The side closest to the control rod would be coldest; the side 180 degrees from it, hottest. The corresponding temperature difference in the fuel element at the edge of the core is also shown in the figure. The temperature differences shown in Figure 35 are higher than actual, since they are based on calculations in which the alleviating effect of circumferential heat conduction in sleeve and compact was ignored.

It will be seen that the maximum temperature difference between two opposite points occurs at the upper end of the active section of the fuel element next to a control rod, and is 310 F. On the average, the temperature difference across the sleeve is on the order of 225 F. If the fuel element were restrained only at its lower end, the diametral temperature gradient would cause the upper end of the fuel element to bow away from the control rod, in the manner illustrated in Figure 36. Curve 1 in this figure is the hypothetical deflection which the fuel element next to a control rod would undergo if it were not restrained and only resting on its standoff. A similar deflection curve has been presented for the fuel element at the edge of the core. This curve is the composite unrestrained deflection which would occur as a consequence of both dimetral temperature gradient, and irradiation-induced bow. Actually, the spacing pads restrict the lateral displacement of the element of the very nominal values determined by the clearance between the spacers.

(v) Other Factors

~~Local Power Deviations~~

All temperature calculations are based on the nominal power distribution in the core. The actual local flux will differ from the nominal flux for a number of reasons: inaccuracies in fuel loading, local perturbations in the rate of fission product release from the fuel particles, inaccuracies in the power calculations, and so on. Experience in the production of prototype fuel compacts has established that fuel loading accuracy can be held to about 2.5 percent. It is difficult to assess realistically the significance of the other variants which affect local nuclear power levels. A total power deviation factor (including the effect of fuel loading) of 5 percent, i.e., twice the loading factor, has, therefore, been selected arbitrarily. All indications to date are that this is a reasonable, and somewhat conservative figure.

Circumferential Variation of Film Coefficient

The local convection film coefficient for heat transfer from the fuel element to the tricuspid coolant flow channel varies appreciably around the periphery. It ranges from a minimum value at the point of closest approach between two fuel elements to a maximum value at the point of the fuel element surface which is nearest the center of the tricuspid. The minimum is 50 percent, the maximum 130 percent of the average value. The average value was used in all calculations. Calculations have shown that this simplification introduces only very small errors. The combination of maximum eccentricity (which maximum clearance between compact and sleeve permits) plus minimum film coefficients raises local temperatures less than 20°F.

Calculational Inaccuracies

Both power calculations and temperature calculations for the core used IBM codes which assumed cylindrical symmetry. Control rods were, therefore, replaced by "equivalent control rings". This simplification was made in such a manner as to result in higher-than-actual calculated temperatures, the difference probably being somewhere below 50°F.

The inaccuracies involved in the actual calculation of temperature are, in most cases, the least significant factor involved. Convergence and other characteristics of the calculational

methods are such that conservative estimates have placed the upper probably numerical error limit at ± 10°F.

(vi) "Hot-Spot"

In the preceding discussions were presented the temperature variations in the core as a whole and in the individual fuel elements which result from the basic nuclear and mechanical design of the core. These calculations yielded a maximum nominal fuel temperature of 2730°F.

In parts (i) to (v) of this section, the influence on temperatures of various imperfections or secondary effects (flux disturbances, manufacturing tolerances, dimensional changes, etc.) were considered.

If the very conservative assumption is made that all those secondary effects which raise fuel temperatures and can physically occur at the hottest point of the hottest fuel element actually do occur simultaneously, then one obtains a maximum theoretical "hot-spot" temperature (in a core with a graphite thermal conductivity of 15 Btu/hr-ft-°F) composed of the following:

Maximum nominal fuel temperature, i.e., highest temperature in hottest compact	2730 F
Irradiation-induced dimension changes	70 F
Worst possible combination of radial tolerances	94 F
Circumferential variations in film coefficient and maximum internal eccentricity	20 F
Bow in fuel element	54 F
Power deviation factor	51 F
Inaccuracy of temperature calculations	10 F
Maximum theoretical "hot-spot" temperature	3029 F

The temperature allowance for diametral temperature gradients has not been included in the tabulation. The deletion is readily justified since such gradients will not exist in any appreciable magnitude at the point of maximum power.

It should be emphasized that the "hot spot" is not a realistic temperature, but one which results from pyramiding several unrelated conservative assumptions. The most important of these is the assumption that all "hot spot" contributors not only occur together, but that they occur together within the hottest fuel element. The above summation is also conservative in another respect. It assumes that the temperature difference resulting from the simultaneous occurrence of the various "hot spot" factors is equal to the sum of the temperature differences of the "hot spot" factors (each calculated independently). In reality, the combined effect of all these factors is appreciably less than the arithmetic sum of the individual temperature differences, due to the non-linear variation of radiant heat transfer with temperature.

Even if the improbable combination of circumstances on which the "hot spot" concept is based actually did occur, it would only cause a localized, moderate, increase in fission product migration. Since only a very small part of the core would be involved, the effect on the radioactive inventory of the primary system and the fission product trapping system would be insignificant--if not imperceptible.

As mentioned previously, the "hot spot" calculations were based on a graphite thermal conductivity of 15 Btu/hr-ft- F. Actually, thermal conductivity will in all probability be 30 percent higher than the assumed 15 Btu/hr-ft- F, and the corresponding "Hot spot" would be at least 110 F less than the value quoted above.

(3) Thermal Stresses During Normal Operation

The temperature gradients discussed above are of significance largely because they result in thermal stresses. In the following, such thermal stresses are evaluated. Specifically, it is shown that during all normal modes of operation, thermal stresses are well within acceptable limits.

Graphite is a strongly anisotropic material. Calculations, which take anisotropy into account, tend to become difficult and unwieldy. For this reason, all stresses quoted in this section were calculated on the basis of elastic, isotropic theory. Values for

mechanical properties were chosen in such a manner as to ensure that calculated stresses would be conservatively high.

Within the cylindrical structure of the element, two basic types of temperature gradients warrant consideration: radial temperature gradients, resulting in radial, axial, and hoop stresses; and "diametral" temperature gradients resulting in axial bending stresses. The two other stress-producing types of temperature variations are: circumferential gradients, resulting in hoop bending stresses; and the nonlinear component of axial gradients, resulting in axial bending stresses. The last two categories produce only insignificant stresses. For instance, a conservative estimate showed that circumferential temperature variations due to eccentricity and the local film coefficient must be less than 20 F. The corresponding hoop bending stress--again based on conservative assumptions--is less than 10 psi. The worst nonlinear component of the axial temperature gradients produces bending stresses of even smaller magnitude.

(i) Steady-State Stresses

The maximum radial temperature gradient occurs in the upper half of the hottest fuel element sleeve: a 300 F drop through a 3/8 inch wall, i.e., a gradient of 800 F/inch. The hoop- and axial surface stresses resulting from this temperature drop are: inner surface, 600 psi compression; outer surface, 500 psi tension. As mentioned above, these calculated stresses are based on conservative values of mechanical properties, and are therefore higher than the stresses expected in the element.

These stresses are inversely proportional to graphite thermal conductivity. Thus, if the conductivity were 20 instead of 15, the stresses would be 450 psi compression and 375 psi tension, for the inner and outer surface, respectively.

The maximum stresses, resulting from diametral temperature gradients, i.e., from bowing of a fuel element (see part (2) of this section) are: axial bending $\pm$ 800 psi. These stresses occur in the outer surface of the fuel element. They are experienced only by a fuel element adjacent to a fully inserted control rod. This fuel element does not produce full power, because of the proximity of the control rod; hence, it cannot be the hottest element. Furthermore, the axial position of the maximum stress due to bowing are not the same. It is therefore quite impossible for the two maximum stresses to be superimposed.

Consequently, the highest stresses expected in the fuel element during normal operation are considerably less than the graphite modulus of rupture which has been measured consistently above 3250 psi, with some values as high as 4700 psi, as given in Section II. J. 1.

Radial stresses are very much lower than either axial or hoop stresses and therefore need not be considered here.

A test program was carried out to verify the ability of the fuel element sleeve to withstand the worst temperature gradients it may be subjected to. A detailed description of the tests can be found in Section II. J. 1.

Short cylinders of sleeve material were subjected to a very high radially outward heat flux. The severity of the flux was increased until either the maximum capacity of the apparatus was reached or until defects developed in the graphite. All graphites representative of the type to be used in HTGR withstood temperature differentials across the 0.375-inch wall in excess of 1000 F, at a mean wall temperature of around 2000°F, without incurring any damage. This gradient, more than three times the maximum expected in the reactor, corresponds to a tensile stress in the outer surface of the tube of about 1700 psi. Because of limitations of the test apparatus (specifically, the rapid deterioration of the electric heating element at these very large heat fluxes) the high gradient could be maintained only for a limited time, i.e., a few hours. In other tests, however, temperature gradients of about 640°F, at an average temperature of 1700 F, were held for 160 hours. No structural damage to the specimens resulted, and termination was caused by heater failure.

(ii) Transient Stresses

During a power decrease, (be it a normal operational power decrease, a shutdown operation, or a scram in case of an accident) the temperature profile in the fuel element always becomes flatter than the full-power profile. Consequently, the thermal stresses during a power-decrease transient are no problem, if the steady-state stresses are acceptable.

The same is very nearly true for most power increase conditions. During normal load-following, core helium outlet temperature rises at a maximum rate of 20 F/min. During such a temperature rise, the temperature difference across the sleeve is only 4 F higher than the 300 F maximum temperature difference

across the sleeve wall. By comparison with the latter value, the increase in temperature difference is insignificant, and the thermal stresses associated with this increase are negligible.

Transient stresses during reactivity accidents are discussed in Section VII.B.1.

4. FUEL ELEMENT MALFUNCTIONS

a. Cracked Elements

The nominal diametric clearance between the fuel compacts and the sleeve is 0.009 inch. It is conceivable that after a long irradiation exposure this clearance could become smaller. A conservative analysis has been performed to determine the effects on fuel element integrity of a sudden thermal expansion of the fuel compacts at the time the diametric clearance has closed completely.

A fuel compact initially in contact with the sleeve can be heated rapidly through a calculated step increase of 1550 F before fracture of the sleeve occurs from diametric interference of the two components. Each radial gap increment of 0.001 inch allows an additional 550 F increase in the step change. The temperature increase from the accidents involving sudden increases in reactivity are discussed in Section VII. Such a fracture would occur in the hottest portion of the fuel element. This fracture would not cause a sudden high level burst of activity in the main coolant because the partial pressure of volatile fission products are on the order of 10^{-7} atmospheres within the fuel element purge gas passages. Continued reactor operation with a completely fractured fuel element sleeve results in the coolant system activity increasing to a value 7.5 times the Calculated Beginning of Life coolant gaseous activity (Appendix B I). This condition applies to all gaseous fission products except Kr^{85}, which is normally the major contributor to the gaseous activity. The increase in Kr^{85} is negligible following a fuel element fracture. The reason for the small increase is that the Kr^{85} recycled to the main coolant from the external trapping system is large in comparison to the amount escaping directly to the coolant from the fuel elements. Figure 37 indicates the relatively slow buildup in main coolant activity as a function of time following fracture of one, two, and three fuel elements.

The size of a circumferential crack which could be considered to cause a fuel element to fail completely is calculated to be 0.002 inch, occurring at the base of the fuel element. A smaller crack occurring at the bottom or a crack occurring at a higher location on the sleeve would result in a smaller activity increase than from the complete fracture at the base of the element. A large crack at the top end of the sleeve would cause no increase in activity released to the main coolant.

If the reactor is shut down following a fuel element fracture, the main coolant activity will decrease very significantly within a few hours. This decrease, which results from recycle of coolant through the external trap, is shown graphically in Figure 38 Even in a case in which all of the fuel elements in the core are arbitrarily assumed to be suddenly fractured completely, there would be no fast increase of activity in the main coolant stream. The main coolant could only build up significantly after a period of several hours of continued full-power operation. However, the reactor would be shut down before the activity could build up and the compacts would cool and terminate the fission product release. Within approximately five hours after shutdown, the recycle of coolant through the fission product trapping system would reduce the main coolant gaseous activity to the level of the Calculated Beginning of Life Activity as listed in Appendix B. I.

b. Closing of Gaps Between Fuel Compacts and Sleeves

During normal operation there is a small gap between the fuel compacts and the fuel element sleeve to facilitate the circumferential diffusion of fission products to the closely spaced purge grooves on the fuel compacts. After long irradiation there is some possibility that the sleeve will contract, closing off this annular gap and forcing the fission products to diffuse through the body of the compact to reach the purge grooves.

A conservative calculation indicates that for a fuel element in which this annular gap is sealed off along its whole core length, the increased fission product leakage rate of this element will be 11.5 times its normal leak rate. In the highly unlikely event of the annular gaps closing off in one-third of the fuel elements in the core, the coolant activity would increase to 4.5 times the Calculated Beginning of Life Activity as listed in Appendix B. I. A closing of the annular gaps in all of the fuel elements in the core would result in a main coolant activity increase of 11.5 times the Calculated

Beginning of Life Activity. Since these activities are still less than the Design activity, the reactor could continue to be operated.

c. Loss of Purge

A complete stoppage of the purge system will, of course, necessitate shutting down the reactor system. However, minor stoppages of the purge flow will not necessarily require shutdown. For instance, a total stoppage of the purge flow through one of the fuel elements can only increase the coolant activity to a value somewhat less than the factor of 7.5 quoted under part a above, and will therefore not require reactor shutdown. Similarly, a modest increase in the flow resistance of all of the fuel elements will not require shutdown since the purge system will behave as a constant volume flow device. Therefore, an increase in the flow resistance of the fuel elements will only increase the fraction of the purge gas which bypasses the fuel elements by leaking inward at the standoff connector. The fuel elements are designed so that the pressure drop of purge gas in the annular gaps and grooves is small in comparison with the drop through the gas inlet within the upper reflector. Variations in gap thicknesses do not have significant effects on purge gas pressure drop.

d. Change in Graphite Permeability

The main coolant gaseous activity is directly proportional to the graphite sleeve permeability value. Therefore, an increase in permeability results in an increase in coolant activity. The Calculated Beginning of Life coolant gaseous activity (Appendix B. I.) is based on a helium permeability of 1×10^{-5} cm^2/sec. This value could increase to 5×10^{-4} cm^2/sec in the complete reactor core before the Design Coolant Gaseous Activity would be reached. The operating conditions which could cause changes in permeability are described in Section II. A. 1.

B. DESIGN FEATURES OF REACTOR COMPONENTS

1. General Description

The reactor components described in Section II. B consist of the reactor pressure vessel, reflectors, reflector seals, fuel element standoff pins,, core support plate, thermal shield, plenum shroud, control rods and drives, and emergency shutdown systems. Figure 2 is a cutaway view of the pressure vessel.

Helium coolant at 350 psia, and 634 F enters the reactor vessel from the outer annulus of the concentric pipe circuit. By using the thermal shields and plenum shroud as baffles to direct the incoming gas along the vessel wall, the incoming gas removes both the nuclear heat generated in the vessel wall and the heat lost from the plenum shroud to the vessel, and keeps the vessel wall at a temperature less than 700 F.

The incoming coolant flow is split as it enters the vessel, approximately 50 percent flowing upward and 50 percent flowing downward. The upward flow travels up along the vessel wall to the fuel handling equipment nozzles in the top head. At these nozzles, it turns down into the two annular spaces between the thermal shields and plenum shroud. After flowing down these annular spaces, the helium passes down between the reflector blocks.

The other 50 percent flows downward from the inlet nozzles along the vessel wall, then between the lower thermal shield and the vessel wall, and so into the space below the core support plate. A small portion of this flow is passed through cooling holes in the support plate and then into the core. The remainder passes up and around the periphery of the core support plate. At the periphery of the plate the flow joins the gas coming down through the reflector. The combined flow passes into the core and then up into a plenum above the core. From the plenum the gas passes into the inner concentric pipe and then on to the steam generators.

2. Reflectors

The core is surrounded on the side by a graphite neutron reflector approximately 2 feet thick extending the full length of the fuel elements. A cross section of the core and reflector is shown in Figure 39. The inner 3.5 inches of the reflector are made up of

dummy hexagonal elements. The remainder of the reflector consists of two concentric graphite rings, each approximately 10 inches thick. Both rings are segmented circumferentially. The gaps between the reflector blocks in the inner ring are staggered from the gaps in the outer ring to minimize concentrated neutron streaming. The inner ring of segments is movable, each segment being pivoted at the bottom in such a manner that it can move radially inward. This movement allows the reflector to provide lateral support to the fuel elements near their upper ends. The force providing this lateral support results from the differential coolant pressure existing between the outer faces and the inner faces of the tiltable reflector segments. This force provides a firm yet thermally expandable restraint for the core. The inner faces of the inner reflector segments are machined to fit up against the dummy reflector elements so as to maintain the triangular pitch arrangement of the core.

A radial thermal gradient exists in the inner graphite reflector blocks. The temperature difference across the thickness varies from 600 F at the top of the reflector to 0 F at the bottom of the reflector. This temperature difference tends to bow the top of the blocks outward. The pressure loading on the top portion of the reflector tends to cause the blocks to bend inward. The pressure loading causes a maximum bending stress in the reflector of 180 psi. The thermal gradient is not linear and thus will result in an additional stress of 120 psi tension. Since the modulus of rupture for the graphite concerned is greater than 2100 psi, the probability of failure of the inner reflector blocks is very low.

A low temperature gradient exists in the outer blocks, but this is sufficiently small so that the blocks will remain very nearly straight and will not tend to block any coolant flow passages. The fast neutron flux in these blocks is low enough so that bowing due to differential contraction effects will also be very small.

The fast flux over 0.1 Mev varies from 2×10^{13} neutrons/cm^2-sec at the interface between the inner reflector and the core, and 2×10^{12} neutrons/cm^2-sec at the outside of the inner reflector. With this flux gradient, approximately 1/2 percent greater contraction of the inside of the reflector block than on the outside may occur due to irradiation effects over a thirty year period. This will result in a bow of the block of about one inch, if the bow is not restrained. Flexure of the reflector under its pressure loading will decrease this maximum bow by a small amount. The bow has some tendency to block the coolant flow and result in a change in pressure drop; however, the

inside faces of the outer reflectors will be grooved vertically (or the equivalent) so that no amount of reflector bow can excessively block the coolant flow.

If an inner reflector block should crack, for some reason, it can still function satisfactorily. This is because it is fully confined on four sides and thus cannot shift significantly out of place. Leakage through any crack will be kept at a minimum by the ring of hexagonal dummy reflector elements which will block the leak path to the core.

Provisions are being made for the removal of the reflector blocks and dummy graphite elements from the reactor. The hexagonal dummy graphite elements are approximately the same length and diameter as the fuel elements and have grappling knobs on top so that they can easily be removed by the fuel handling equipment. The larger blocks can be removed through the large center nozzle in the top of the reactor. These measures minimize the need for continued operation with a radiation damaged reflector should the damage be greater than predicted.

3. Reflector Seals

Since gaps exist between the reflector segments, and the reflector is not rigidly attached to the plenum shroud, seals are provided to prevent the coolant from bypassing the core. The bypassing is prevented by two systems of seals as shown in Figure 39. These are the vertical seals and the top seal.

The vertical gaps between the reflector blocks are sealed by a system of vertical bars of graphite. The bars are made of interlocking pieces to allow them to be replaced. These bars are inserted in vertical grooves and bridge the gap between reflectors.

The top reflector seal is located between the top of the reflector blocks and the bottom of the plenum shroud. This seal is essentially a circular ring of graphite with a 2-inch-square cross section. Because the steel seal retainer has a different thermal coefficient of expansion than the graphite seal, the retainer tends to expand to a larger diameter than the graphite seal. For this reason, the seal is segmented to allow it to maintain the same diameter as the retainer. The seal ring consists of 30 segments of graphite, one segment resting on each reflector block. Each block overlaps the other

so that no straight leak path exists across the seal.

The sealing surface, namely the top surface of the inner reflector, is kept level by the teeter-totter action of the reflector supports. The reflector supports are rocker arms with the weight of the inner reflector on the inner ends of the arms and the weight of the outer reflector on the outer ends. The weight of the outer reflector is thus used to hold the inner reflector blocks up against stops so that all the inner reflector block top surfaces are kept level with one another. To insure that friction against the stops does not restrain the inner reflector blocks from applying inward loads to the core, rollers placed between the reflector blocks and the seal retainer attached to the bottom of the plenum shroud resist the upward loads from the blocks.

The thermal stresses in the vertical seals are small because the temperature gradients through the blocks are low. The top seal will not have a high gradient because it will be shielded by an extension of the insulation or thermal baffle on the plenum shroud.

The plenum shroud is extended downward, as shown in Figure 39, almost into contact with the inner reflector. This extension forms a partial backup seal which limits the coolant bypass flow in the unlikely event of gross seal malfunction.

The leak rate between graphite interfaces, such as the interface between the top of an inner reflector block and the top seal has been checked by test. The calculated leak rate of the whole top seal based on the result of this test is less than 0.35 percent of the total helium circulated. The total leak rate through all the reflector seals is not expected to exceed 1 percent of the total coolant flow during normal operation; however, if this value should be exceeded, small increases of average core outlet gas temperature would result as shown in Table 8.

TABLE 8

AVERAGE CORE OUTLET TEMPERATURE REQUIRED TO MAINTAIN CONSTANT PLENUM OUTLET TEMPERATURE OF 1354 F

Reflector Seal Leakage, % of Total Mass Flow	Temperature, F
1.0	1380 F
2.0	1387 F
5.0	1408 F

Even if one entire seal block disintegrates, the resultant extra leakage would be roughly 3 percent. Average core outlet temperature would increase to 1394 F, and a similar temperature increase (21 F) would occur in the fuel elements. Maximum fuel temperature would remain within tolerable limits and the plant would continue to operate at rated power.

4. Core Support Plate

The core support plate is made from a solid slab of carbon steel about 5 inches thick into which the fuel element standoff pins are threaded. The standoff pins fix the locations of the fuel elements and serve as bases for the fuel elements. Passages in the grid plate, connecting all the standoff locations, serve as a manifold for collecting the purge gases leaving the fuel elements via the metal standoffs, and conveying them to two closed channels at the periphery of the grid plate. The hole passages are drilled so that a space below each standoff pin will act as a dirt leg to catch any large particles of solid fission products coming out of the fuel elements. The purge gas stream is piped from the core support plate to external fission product traps located outside of the reactor pressure vessel. The connections from the core support plate to the outlet pipes are made by means of expansion bends. There are two fission product take-off pipes in parallel. The connections can be plugged at the grid plate.

To prevent significant lateral motion of the grid plate relative to the reactor vessel for any reason, however unlikely, a system of steel spacer blocks will be provided.

The weights of the core, core support plate, and reflectors are carried into the lower head of the pressure vessel as shown in Figure 39 . The support consists of vertical bars welded into the vessel and to a ring. The weights are carried on this ring. This support has been designed to resist the loads mentioned as well as loads due to normal operation thermal expansions plus earthquake loads with a seismic factor of 0.1g. Sleeves around the control rod guide tubes have been provided to act as auxiliary supports of the core support plate should the core support plate become hot enough to sag slightly during emergency cooling following loss of normal coolant flow.

5. Thermal Shields and Plenum Shroud

a. Lower Thermal Shield

A thermal shield of carbon steel 3 inches thick is located between the graphite side reflectors and the reactor vessel. This shield extends from the top of the side reflectors down into the bottom head. The lower thermal shield is supported at the bottom and allowed to grow vertically. This shield is subject to circumferentially uniform thermal and fast neutron fluxes, gamma heating and thermal effects.

The shield is centered but floating inside the reactor vessel. To improve the flow distribution, the top of the shield has an elementary seal to take care of warping and misalignment at the joint between the lower thermal shield and the upper thermal shield. The seal is a 1/8-inch sheet-metal strip attached to the upper thermal shield and lapping over the bottom thermal shield. It is a non-critical component, partial failure of which will not cause excessive maldistribution of temperatures.

b. Upper Thermal Shields and Plenum

A hot helium plenum chamber is formed above the reactor core by the plenum shroud which is essentially a thermal shield made of 3/4-inch steel. This is to be lined with stainless steel reflective insulation or thermal baffles. The inner hot pipes of the concentric piping connect to this plenum shroud. High temperature long-time tests on possible materials to be used for the plenum shroud are being made to determine which is the most suitable. Between the upper plenum shroud and the pressure vessel are located two thermal shields - each one inch thick as shown in Figure 39. The spacing between these upper thermal shields is approximately four inches. They are also 4 inches away from the vessel and the plenum shroud.

The weight of the upper thermal shields and plenum shroud is carried into the vessel at the main flange. Since the vessel wall and the outer thermal shield are at almost the same temperature and thus have the same thermal expansion, the location of the outlet nozzle has been tied to the outer thermal shield.

Stagnant areas on both sides of the plenum shroud are being investigated in the flow model. This flow model is described in detail in Section II. J. 3. The testing is being done to assure that no hot spot of excessive size will exist. The permissible size of a

hot spot as a function of heat transfer coefficient over the surface of the spot is shown in Figure 40. From this figure it can be seen that a 3 foot diameter portion of the vessel wall can be completely uncooled without raising the stress in the vessel above the allowable stress.

The plenum shroud is designed to take a 300 psi internal pressure and a 50 psi external pressure, both for a short time. The shroud is thus strong enough to withstand sudden differential pressure arising from large ruptures of the helium ducting. The normal external pressure on the plenum is approximately 5 psi.

c. Plenum Shroud Seal Plugs

Five penetrations are provided in the top of the plenum shroud for the fuel handling equipment. To prevent flow of the inlet cooling gas from entering the plenum and bypassing the core, seal plugs are placed in these penetrations as shown in Figure 41. The seals will limit the bypass to flows less than 0.01 percent of total helium flow.

The plenum shroud seal plugs are removable for reactor refueling. They are seated by a spring load and the differential pressure between the inlet and the plenum. The seal plug spring load allows the plug to be seated even though the location of the plug seat in the plenum shroud moves more radially due to thermal expansion than does the fuel handling nozzle in the vessel.

In the remote case of a top nozzle breaking and allowing the helium in the vessel to escape, the plugs will arise from their seats allowing the helium to leave the plenum through the plug seat, thus preventing a large differential pressure buildup across the plenum shroud. The gas on the outside of the plenum shroud can relieve itself directly up the nozzle so that a large external pressure difference across the plenum shroud and core cannot occur. This prevents collapsing of the plenum shroud under external pressure.

6. Reactor Pressure Vessel

a. Description

The reactor pressure vessel is a vertical, 14-foot-ID cylinder with elliptical heads. The height is 35 feet 6-1/2 inches overall, including the heads. The upper head is flanged, and is removable for insertion of the reactor internals. The flange connec-

tion is seal-welded to prevent leakage during reactor operation. Penetrations in the pressure vessel are required in the upper head for fuel handling; in the lower head for the control rod drive and emergency shutdown drive mechanisms, instrumentation, and purge-gas lines; and at two locations in the cylindrical wall where the concentric primary coolant pipes are joined to the vessel.

During full-power reactor operation the pressure vessel is cooled by coolant returning from the steam generators at approximately 634 F, the coolant pressure being maintained at 350 psia. The reactor pressure vessel is being designed for 450 psig pressure at 725 F. The vessel will conform to appropriate ASME and Pennsylvania State Codes and to the latest nuclear case rulings. The vessel is thermally insulated externally to minimize heat losses to surrounding structures. However, the insulation is not attached to the vessel but is attached to the outside face of an emergency cooling jacket. This cooling jacket cools the vessel if the normal coolant flow fails for some unlikely reason. (See Section II.F.2)

The vessel is made of ASTM A212 Gr B carbon steel and is nominally 2-1/2 inches thick. The shell at the level of the inlet nozzle is about 4-1/2 inches thick. This 4-1/2 inch-thick-band acts as reinforcement of the inlet nozzles and uniformly distributes the vessel support load into the shell. Support is provided by a skirt around the vessel. The support rests upon a step in the reinforced concrete biological shield surrounding the pressure vessel.

Five penetrations are provided in the top head of the vessel. These serve as access ports for fuel handling equipment. These ports are arranged with one 22-inch-diameter port located centrally, and three 10-inch-diameter ports and one 6-inch-diameter fuel charging port all located on a 59-inch radius.

Fifty-five housings with an inside diameter of about 4 inches penetrate the bottom head of the vessel. These housings are for 36 control rods and 19 emergency shutdown rods. In addition, 4 penetrations of 4-inch diameter or less are provided in the bottom head for fission product trapping lines and for instrumentation leads. Structural support will provide firm lateral restraint of the bottom of the vessel so that significant horizontal relative motion between the vessel and the lower biological shield cannot occur.

The two nozzle penetrations in the side of the pressure vessel are each 42 inches OD at the plane where they are joined to the main coolant piping.

b. Thermal stresses During Normal Operation

The coolant flow in the vessel maintains the vessel wall temperature at less than 700 °F. Thermal stresses in the vessel wall due to gamma heating are not large because the gamma heating in the vessel wall is low. Figure 42 shows the effects of various amounts of thermal shielding on the heating rate in the vessel wall. The corresponding thermal stresses in the vessel wall level with the core area, at 100% coolant flow, are given in Figure 43. The expected wall temperatures for various thermal shield thicknesses are also shown in Figure 43. The effect of increased wall temperature is to decrease the allowable stress of the material. The conclusion from these graphs is that at normal operating pressure and temperature, thermal stresses are not a problem, and that with 3 inches of thermal shielding the vessel wall temperature will be 672 °F.

The effect of cyclic thermal stresses is similar to that of cyclic mechanical stresses. In both cases, the number of cycles that a part can endure under a cyclic load is expressed by $N\sigma^n = k$.

where σ = stress
n = number of cycles
N and k = constants for the type of material used

For a specific variation in temperature, one can determine from thermal fatigue data a permissible temperature variation for a given number of cycles. Values of cyclic thermal stress which will allow the application of infinite numbers of thermal cycles have been tabulated in the "Tentative Structural Design Basis for Reactor Pressure Vessels and Directly Associated Components, (Pressurized, Water-Cooled Systems)", December 1, 1958 Revision. For A212 grade B steel, the allowable alternating thermal stress permitting an essentially infinite number of cycles at 700 °F is 21,000 psi. This allowable thermal stress can be converted to an allowable temperature rise of the cooling fluid for a specific heat transfer film coefficient. This has been done and shown in Figure 44. The heat transfer coefficient in this reactor vessel has been shown by calculation and experiment to be no greater than 200 Btu/(hr) (ft^2) (°F). Figure 44 shows that coefficients for less than 200 Btu/(hr) (ft^2) (°F), thermal stresses will not be more than 21,000 psi for step changes of tempera-

ture as high as 200 F.

A plot of the time for a change of the helium temperature to penetrate the wall and cause a rise of 25 F in average wall temperature and thus reduce the allowable strength is shown on Figure 45. It shows the effect of both a ramp change and a step change. In a ramp change, fluid temperature change occurs over a period of time. In this case the period of time equals the time for the wall temperature to rise 25 F. The step change is an instantaneous change of fluid temperature. These are the two extremes in thermal transients considered. From Figure 45, it is seen that for either change a considerable length of time will pass before the vessel wall changes temperature. A 25 F step change in fluid temperature theoretically takes an infinite time to cause the wall temperature to rise 25 F. Controls on the fluid temperature are such that this will be the maximum fluid temperature change in the system. Thus, the addition of 25 F to the normal wall temperature to arrive at the design temperature guarantees that the wall operating temperature will not exceed the design temperature in normal operation.

c. Thermal Stress Due to Abnormal Variations in Operating Temperatures

Any conditions which produce variations in temperature greater than 25 F have been classified as abnormal. The extent of these abnormal variations and the number of cycles that are expected to occur have been determined, and the vessel supplier will design to meet these conditions. The vessel will therefore safely withstand these changes in temperature.

d. Code Considerations and Effect on Design Pressure

For a 450 psig design pressure the ASME Boiler and Pressure Vessel Code allows the pressure to build up during safety valve operation to 477 psig for Section I and 495 psig for Section VIII. In ordinary vessels this is not considered a problem; however, a more conservative approach has been thought to be desirable for this reactor vessel. The reactor relief valves are therefore set at 437 psig and are oversized to give full relieving capacity with 3 percent pressure accumulation in the primary coolant system. Thus, the maximum pressure in the vessel at any time will be no greater than 450 psig.

e. Reliability and Pressure Integrity

1. Materials

All of the carbon steels listed in Section II of the ASME Code are subject to embrittlement due to neutron irradiation and thus brittle fracture has been considered. Based on the best metallurgical information, this embrittling effect is highly temperature dependent, reaching a maximum effect at around 450 F irradiation temperature and then decreasing until 600 F where sufficient annealing occurs so that some ductility is maintained in the material. Further information covering the ductility of A212 materials is covered in paragraph f.

2. Stress Analysis

The specification for the reactor vessel calls for a detailed analysis of all steady-state conditions, shutdown and startup, power change, and emergency cooling conditions. These calculations will be guided by the Naval Reactor Design Handbook. All stress levels will be evaluated on a fatigue basis.

3. Quality Control

The reactor vessel specification requires that all welding in the vessel, including nozzle penetrations, is to be fully x-rayed and magnafluxed. All plate material is to be bought ultrasonically tested for laminations and transverse defects. Charpy impact testing is called for at five stages of production in order to insure ductility of the metal. Hydrostatic and mass spectrometer leak tests will be performed on the vessel before it leaves the manufacturer's shop.

f. Brittle Fracture Prevention

Neutrons with energies down to 500 ev can cause structural damage to steel. Most of the damage will be done by neutrons with energies of 0.1 Mev or greater. The extent of damage varies with the temperature or irradiation.

Radiation damage data for A212-Grade B steel indicate that there is a reasonable probability that the radiation damage incurred during the life of the vessel will not be severe enough to require annealing. However, because of uncertainties in these data, provisions are being

made so that an annealing system can be installed if it should later prove to be necessary. The provision which is being made is the inclusion of blind flanges on both sides of the compressor discharge valves. The flanges can be removed and an electrical heating system can be located between the flanges. By use of this heating system, the gas temperature can be raised from 633 F (compressor discharge temperature) to approximately 850 F. The piping layout and the clearances between the pressure vessel and the shielding are being designed to accommodate thermal expansions consistent with an 850 F annealing temperature.

Coupons from the steel plate used in making the pressure vessel will be located within the vessel and removed periodically to provide an early check on radiation damage. Should these coupons indicate a faster trend toward embrittlement of the vessel than expected, then the vessel can be annealed before a dangerous situation develops.

The criterion for prevention of embrittlement of the vessel steel is to limit the rise in transition temperature to 100 F by setting a minimum temperature for the vessel wall during operation. The minimum wall temperatures during reactor operation required to satisfy this criterion are shown in Figure 46.

g. Additional Information

Additional detailed information concerning the design criteria, material considerations, quality control and inspection procedures, and other information relative to the pressure vessel and the pressure vessel support is given in Appendix E.

7. Control Rods and Drives

a. Introduction and Summary

The 40 MW HTGR will normally be controlled by 36 control rods each worth about .006Δk reactivity on the average, the maximum rod worth being about .010Δk. Each control rod will be driven by a control rod drive which, for scram purposes, will be a self-contained system not dependent on any external equipment other than the supply of a scram signal in the form of interruption of an electric current.

The control rod absorbers will be made of a refractory material, boron-carbide-loaded graphite, supported on a gas-cooled metal support tube.

The control rod drives are to be located outside the primary biological shield in a region of low temperature (less than 200 F) and relatively low radiation flux (of the order of 1 r/hr). The location of the drives should make maintenance operations after reactor shutdown reasonably easy to perform since the environment is not such as to demand the use of seal welds. Careful application of conventional gaskets and/or O ring seals made of conventional materials is expected to provide satisfactory sealing. The environment in which the control rod drives are located is also one in which conventional lubricants can be used as a contribution towards maintaining a high standard of operational reliability. The control rod drives will not be accessible during reactor operation.

The type of drive adopted is one in which a hydraulic motor turns a ballnut screw for both regulating and scram motions. A nut engaged with the ballnut screw causes the control rod to move up or down as required. The control rod drive is located below the reactor. Scram motion of the control rods is in the upward direction.

An electrical circuit will monitor any kind of disconnection of a control rod from its drive. A positive mechanical lock will prevent inadvertent fall of a fully inserted control rod.

A primary aim in the choice of control rod drive design has been to make the easily detachable part of the drive a fully self-contained system in the sense of containing its own scram energy source, the motive power unit, all control devices, and all instrumentation transducers. This assists not only in ease of maintenance, but also in ensuring a really high standard of reliability since a complete performance and reliability check can be made on most of the important parts of the system on the bench, remote from the reactor.

Component selection has been based on the use of heavy duty industrial type units that have a history of successful operation for long periods with no maintenance, e.g., the industrial-type valves selected have a normal life expectancy of ten million to twenty million cycles of operation even though this far exceeds the duty to which the valves will be subjected in this application. All components have been selected to operate well below their normal continuous duty ratings. Components have been selected, modified, or designed where necessary, to provide minimum leakage and the best of fail-safe characteristics.

Hydraulic systems have been developed over the years into extremely reliable and versatile systems that have found applica-

tion in practically every field requiring some form of power transmission. Hydraulics have been chosen because of their high power-to-size ratio, high flexibility and high power-to-signal response capabilities. Hydraulic rotary output drives have acquired a reputation of long and reliable life in mobile equipment such as earth movers, tractors, military vehicles, etc. where operating environment and servicing conditions have been less than desirable. Industrial applications, such as machine tools have required extremely long life, far in excess of the duty life required of the control rod drives. High power output precision control requirements have been met by hydraulics, such as aircraft and missile control systems; sea, ground and airborne radar antenna and gun laying systems; and the more recent machine tool applications using programmed automatic control. Components and systems have been developed to meet near zero leakage requirements, and these are now commonplace.

Fluid selection has been based on its suitability for use in this hydraulic system, particularly its low vapor pressure property. Vapor pressure of the order of one-tenth of a micron of mercury at operating temperature is considered desirable in order to keep diffusion into the buffer helium at an acceptable level. The fluid chosen, a hydrocarbon turbine oil of relatively high viscosity, meets the necessary requirements and also possesses very satisfactory lubricity.

Grease type lubricants meeting similar requirements in regard to vapor pressure are to be used in bearings, clutches, etc., located in the power unit region.

The control rods and drives are the subject of a substantial research and development program. This program is described in Section II. J. 4.

b. Specification of Performance and Life Requirements

The specified performance and duty life requirements for the control rod drive are as follows:

Total rod stroke	7' - 6"
Emergency Insertion (Scram)	
Initial upward acceleration	100 ft/sec^2
Maximum deceleration	less than 32 ft/sec^2

Maximum rod velocity	10 ft/sec
Maximum time for first two feet of insertion, including delay time	0.36 second
Maximum time for first six feet of insertion, including delay time	0.88 second
Maximum response delay time*	0.075 second

It shall be possible to initiate a scram from any point in the rod stroke.

Regulating Motion

Maximum downward acceleration and upward deceleration	32 ft/sec^2
Maximum velocity (up or down)	0.060 ft/sec**
Maximum response delay time	0.20 second
Linear positioning accuracy	$\pm$ 1/4 inch

Duty Life

Number of revolutions in each direction (of motor and ballscrew)	1×10^6
Number of starts	5×10^6
Number of scrams	5×10^3

* This is the time between interruption of scram valve current and first detectable movement of rod.

** This rate of motion is equivalent to a maximum rate of reactivity change of about 1.6×10^{-4} Δ k/sec for the most valuable rod.

c. Description

(1) Control Rods

The reference design is shown in Figure 47. The neutron absorber portion consists of 5 cylindrical sections in a tandem arrangement separated by spacers and supported on a tubular support. Below the absorber sections is located a geometrically similar cylindrical reflector section made of graphite.

The poison sections are made of graphite loaded with boron carbide. They are approximately 17 inches long with an outside diameter of 2.25 inches and an inside diameter of 1.25 inches. The total length of the absorbers and spacers is about 7.5 feet.

The spacers consist of a collar brazed to the central support tube and a series of flexible discs stacked one upon another. The differential thermal expansions between the refractory and metal parts of the control rod are compensated for by these low-stressed disc springs. The entire rod assembly is preloaded by these discs at cold conditions to a value that will ensure a prescribed minimum compression load on the refractory sections at reactor operating temperature despite expected axial shrinkage of the refractory sections due to irradiation effects. The material selected at the present time for the disc springs is a wrought, high temperature, high cobalt alloy, namely Haynes Alloy No. 25.

The tubular support is made of type 304 stainless steel. The upper end of the support tube terminates in the form of a lifting knob for the fuel handling machine. The lower end, directly below the bottom reflector section, terminates in the form of a mechanical latch. These upper and lower tube fittings, in addition to being brazed and welded, are mechanically locked to the tubular support by the flared end configuration of the support tube.

Incorporated into the control rod is the conductor of a rod continuity monitoring electrical circuit. This is in the form of a high temperature metal-clad conductor consisting of a metal wire surrounded by magnesium oxide insulation in turn surrounded by an austenitic stainless steel tube, the whole forming a tightly swaged assembly somewhat similar to the more substantial types of available clad thermocouple wire.

The conductor will be connected to two single-pin connectors located at the base of the control rod and will be routed in the form of a loop up through the rod and securely anchored at the top as shown in Figures 47 and 48. Thus, no portion of the metal structure of the control rod or of the neutron absorbers can move a significant distance vertically relative to the connectors in the base of the control rod without the conductor being broken. Breakage of the conductor will result in an open-circuit signal being sent to the control room or else a signal indicating contact between the conductor and its tubular metal cladding sheath. Either type of signal will result in an alarm indicating to the reactor operator the possibility of some kind of a structural failure or separation of the control rod, although no rod movement will be initiated automatically by the rod disconnection signal.

The control rod slides inside a graphite tube approximately 12 feet long with an outside diameter of 3-1/2 inches and an inside diameter of 2-1/2 inches. The graphite tube is securely anchored at the bottom to the core support plate and terminates at the top at a level approximately in line with the top of the core.

The poison sections of the control rod do not actually rub against the inside surface of the graphite guide tube. An annular clearance of about 1/8 inch exists between the outside diameter of the control rod absorber and the inside diameter of the guide tube. The rod is guided by split ceramic rings located at each spacer, riding against the inside wall of the guide tube. Differential thermal expansion in the radial direction between the steel spacers and the graphite guide tube is absorbed by built-in clearance between the spacer and rider ring. The rings are made of a material that will not excessively abrade the graphite surface of the guide tube and will have low surface shear properties for low breakaway friction. The radial clearance between a ceramic ring and the graphite guide tube will be about 0.005 inch.

The control rod is moved up and down by the bottom-mounted drive unit through the agency of two push rods locked together and to the control rod by ball type latches. These items are described in the following sections covering the control rod drive mechanism.

Cooling of the control rods is accomplished by diverting a small portion (about 3%) of the helium coolant flowing through the core into the control rod guide tubes. The coolant enters a guide tube through holes in the metal control rod guide sleeve in the

region below the core grid plate and enters the control rod support tube just above the upper latch connection. Here the coolant divides into two paths. Through slots in the lower end of the support tube a portion of the coolant is directed upward into the annular space between the outside of the support tube and the inside of the absorber sections. The remaining, and major portion of the coolant continues on up through the inside of the support tube. Both coolant flows discharge into the plenum chamber above the core. Figure 47 shows the coolant flow pattern when the control rod is fully inserted.

The combination of a small diameter metal support tube and the radial clearances between the ceramic rings and the metal spacers over which they are fitted lends the control rod sufficient flexibility in bending that it can easily and smoothly negotiate a credibly bowed and inclined guide tube. The rod is nevertheless sufficiently stiff that it can stand up vertically without lateral support.

The yield strength of the control rod in tension or compression at operating temperature will be approximately 4000 pounds, its ultimate strength in tension about 11,000 pounds. The weight of the control rod, including the poison sections, will be approximately 45 pounds.

(2) Push Rods

The control rod is connected to the screw actuator portion of the drive by a series of two push rods. From the control rod downwards these are the solid push rod and the hollow push rod. The latter is attached to the ballnut which is engaged with the ballnut screw.

The solid push rod operates within the lower biological shield and maintains integrity of the shielding. This push rod is provided with multiple-ball latches at both ends whereby firm mechanical connection is made to the hollow push rod and the control rod. These latches are each provided with three 5/8 inch steel balls. Breakage of one or two balls will not allow disengagement of the two halves of a latch.

As will be seen from Figure 48, the balls in each latch are controlled by a circumferentially grooved rod. If the grooved rod is positioned so that the groove is aligned with the balls, then the balls are free to move radially inwards so that the two halves of the latch can be engaged or disengaged. Downward motion of the

grooved rod pushes the balls outwards into a latching groove in the female part of the joint. Dimensions of the latch assembly are such that both radial and axial backlash in the joint are maintained below about .002 inch. The grooved rods in the upper and lower latches in the solid push rod are connected together by a rod in such a manner that the two latches can be operated independently by appropriate motions of the rod. The latching rod will be operated by a long tool inserted through the bottom part of the drive. It will be kept in the down (latches closed) position by means of a spring. There will be no tendency for the latching rod to rise towards the unlatching position during control rod operation, even in the unlikely event of failure of the spring. Since the rods and latches will not be subjected to any tension during normal operation of a control rod, because the rod deceleration following scram will be less than 1g, the small available axial backlash in a latched joint will not give rise to any relative axial motion between the latched components.

During the unlatching process, the first step of upward movement of the latching rod releases the latch between the control rod and the solid push rod. The graphite guide tube and the control rod may now be removed by means of the fuel transfer machine. A second step of upward movement of the latching rod is required to release the latch between the solid push rod and the hollow push rod. The screw actuator and hollow push rod may now be removed downwards, the solid push rod being prevented from falling by a shoulder at the bottom of the lower push rod guide sleeve.

Following removal of the screw actuator and hollow push rod, the solid push rod is raised until it too can be removed by means of the fuel transfer machine. A long rod, of such a diameter as to maintain shielding effectiveness, is used to raise the solid push rod.

Re-installation of the push rods and engagement of the latches is accomplished by reversing the above procedure.

The final choice of using the ball type of latch was based on the basic premise that reliability follows simplicity. Many types of latches including pneumatic, solenoid, and manually remotely powered types, were considered. In conjunction with test models, it was concluded that multiple-ball type connectors would offer (1) the most reliability (failure of one or two balls will not sever connections) (2) the most ready connection (the self-seeking or self-aligning feature of the sphere would ensure easier engagement despite slight misalignment of the rather long and flexible latched components).

Both solid and hollow push rods are guided by two push rod guide sleeves connected together by a long-overlap joint which allows relative vertical motion due to thermal expansions but maintains alignment of the sleeves. The upper guide sleeve is attached to the core support grid plate. The bottom end of the lower sleeve is attached to the top of the control rod drive housing.

As a precaution against excessive friction developing between the push rods and their metal guide sleeves as a result of possible galling or similar effects, it is planned to nitride the inside surfaces of the guide sleeves and the important outside surfaces of the solid and hollow push rods.

Housed in both solid and hollow push rods are two metal-clad conductors forming part of the rod-continuity-monitoring circuit. Electrical connections for these conductors are made at each latch by two shielded single-pin connectors. Opening of a latch or breakage of a push rod will result in signals being sent to the control room of the same type as in the case of breakage or separation of some part of the control rod structure and absorber.

(3) Drives

The control rod drive utilizes an axial piston type hydraulic motor as the prime mover for both regulating and scram functions. Figure 48 illustrates schematically the mechanical arrangement and hydraulic circuitry of the drive.

The drive is composed of the following major sections: an outer containment or pressure shell, a screw actuator mechanism, and a hydraulic motor power unit.

The outer pressure containment is essentially one continuous tubular member welded to the bottom of the reactor vessel, with the power unit attached to the lower end by means of a mechanically sealed service disconnect, all of which forms a completely sealed unit. In the biological shield region the outer containment is surrounded by bolted-on sleeves. These sleeves provide a step configuration to the gap between the control rod drive containment and the concrete shield clearance hole for the purpose of reducing neutron streaming through this void.

(a) Screw Actuator Mechanism

The screw actuator portion of the drive is supported and packaged within a tubular member, fitting within the outer pressure shell. The purpose of this arrangement is to provide a convenient means of removing and servicing the mechanism without disturbing the outer drive containment. The ballnut and leadscrew are located within this support tube. The screw is retained and supported by a combination of radial and thrust bearings at its lower end. The recirculating ballnut is attached to the lower end of the hollow push rod. This push rod is grooved and prevented from rotating relative to the support tube by means of a ballspline. Rotation of the screw thus causes the ballnut to translate in an axial direction, raising or lowering the hollow push rod.

A positive lock is provided in a pocket in the side of the pressure shell. The lock is located approximately four inches below a flange on the ballnut when the ballnut is in its fully up position. The function of this lock is to prevent a fully inserted control rod from falling out of the core due to any kind of structural failure or malfunction of the mechanical, electrical, or hydraulic components of the drive. The lock actuator will have to be energized in order to retract the lock prior to withdrawing the control rod in question. Energization of the lock actuator will not continue after withdrawal of the rod. De-energization of the lock actuator will result in automatic protrusion of the lock. Scram or upward regulating motion of the rod can only be impeded by lock malfunction over the last four inches of upward rod travel where the speed of rod motion is low and the worth of the rod is small. The lock will automatically jump back into place below the flange on the ballnut after the flange has moved up past the lock. Microswitches operated by the locks will generate signals resulting in appropriate indication in the control room in the event that a lock fails to protrude following de-energization. It will not be possible to withdraw a lock if it is supporting a significant fraction of the weight of a control rod and associated push rods.

The four inches of rod travel available between the rod up position and the position where downward motion of the rod is prevented by the lock can be used, if desired, for ensuring normal rod behavior prior to withdrawal of the lock. The lock control circuits will be arranged so that not more than three locks can be withdrawn at a time.

Located within the screw actuator mechanism, just below the ballnut, in a region of ambient temperature (less than 200 F), is an extensible coil consisting of two metal-clad conductors whose cladding sheaths are brazed together. This coil forms the connection between the rod continuity monitoring circuit located in the vertically moving push rods and control rod and the stationary portion of the circuit leading to the outside of the drive containment.

Normally, the entire drive containment, including the hydraulic power unit, is pressurized with helium to a pressure slightly above reactor pressure by means of a supply of purge helium derived from the helium purification system. During removal of the hydraulic power unit for servicing, the atmosphere in the actuator containment region is retained by means of a rotary differential-pressure face-seal between the screw and support tube, and a static seal arrangement between the support tube and outer shell. During normal operation, the rotary seal is very lightly loaded. During servicing, when sealing is required, the seal becomes highly loaded either by differential pressure or by the introduction of buffer helium pressure into the volume between the two components which comprise the seal. It should be noted that the seal is static during high loading and consequently, no significant wear is expected. Should there occur a substantial pressure drop in the power unit housing due to gasket leakage or other unlikely cause, the rotary seal will automatically become effective and prevent excessive leakage of purge helium into the subpile room through the leakage path.

The helium purge flow is injected into the control rod drive at a point slightly above the face-seal and flows upwards through the substantial gaps between the push rods and the push rod guide sleeves. The main function of this flow is to prevent migration of fission products or finely powdered material down into the drive.

(b) Hydraulic Power Unit

A hydraulic power unit is attached to the lower end of the outer pressure shell. Connection is made by a gas-tight mechanical joint that is readily separated for servicing. The power unit consists of an outer pressure shell containing a hydraulic motor, a deceleration valve, a mechanism arrangement to actuate the deceleration valve, an emergency deceleration device, a clutch-brake assembly and a gear drive to actuate a position transmitter and limit switches. Position is transmitted by means of a synchro transmitter turning approximately 180° for full rod stroke. Two limit switches are incor-

porated for full-up and full-down position indication. The synchro transmitter and the cams operating the limit switches are driven by the hydraulic motor output shaft through the medium of a gear train.

A clutch-brake assembly is located immediately below the position indicator gear train. It consists of a friction brake and an over-running clutch, the latter being a device that will transmit torque from its hub to its outer housing in one direction but not in the opposite direction. The output shaft of the drive unit is splined to the hub of the over-running clutch. The outer case of the over-running clutch is connected to the motor housing via the spring-loaded friction brake. During rod insertion, torque from the hydraulic motor is transmitted unrestricted to the ballnut screw. However, torque generated from the screw end, due to the weight of the control rods and push rods, or torque from the hydraulic motor in the rod withdrawal direction, is resisted by the brake to which the torque is transmitted by the clutch. The purpose of this device is to prevent the control rod from drifting downwards due to slight internal leakages when rod position is to be held with the regulating valve in the null position, and also in the case of failure of a hydraulic motor or of all hydraulic pressure. The brake torque is set at a value of 1.75 to 2.5 times the torque due to the vertically-acting dead weight.

The torque which the hydraulic motor can exert during regulating motion is restricted to about 2.75 times the torque due to the vertically-acting dead weight, i.e., only a little more than the brake torque that resists downward rod motion. The maximum tensile force which the drive can apply to the bottom of the control rod during normal downward regulating movement is thus limited to a value of approximately 400 pounds, i.e., about one tenth of the force required to cause yielding of the weakest section of the control rod at maximum operating temperature.

Below and external to the pressure shell, but part of the hydraulic power unit, is an integral valve and manifold assembly. Attached to this are an accumulator, check valves, a directional regulating control valve, two pilot-operated scram control valves, and various subsidiary items. Flow connections between valves are accomplished through a drilled manifold on which the valves are mounted. Replaceable static seals between valve and manifold mounting faces effectively eliminate fluid leakage.

A noteworthy feature of the hydraulic power unit packaging is the emphasis on porting and interconnecting the hydraulic components via drilled passages and the embedding of check valves,

filters, etc., inside the manifold. The elimination of external pipes and protuberances was considered desirable from the standpoints of elimination of leakage and added reliability.

The basic hydraulic circuit, its principle of operation and associated components are schematically illustrated in Figure 48, the hydraulic circuit itself being shown in greater detail in Figure 49. The hydraulic motor is of the axial piston type. Fluid leakage from the motor is prevented by the fact that the inside of the motor casing is vented directly to the external oil reservoir so that the motor casing is not subjected to any pressure difference (See Section II. B. 7. c. (4)). The motor shaft is connected to the bottom end of the screw actuator by means of a splined coupling. The position transmitter and limit switches are driven by gears connecting to the motor shaft. The deceleration valve is driven by means of a nut engaged with a threaded sleeve mounted on splines on the motor output shaft.

The hydraulic motor provides two modes of control rod operation: normal controlled regulation at a relatively low speed, and rapid insertion at high or scram velocity. This is accomplished by running the motor at two different flow rates. Regulating motion is accomplished by use of a low oil pressure controlled by restricted, low volume, delivery ports and externally controlled directional valving. Scram is accomplished by use of a high oil pressure controlled by large, high volume delivery ports, one-directional control valves and a deceleration valve. The oil pressure for scram is supplied from the inert-gas pressurized hydraulic accumulator. Pilot pressure for the scram valves comes from the accumulator also.

Dual pressures are used in order to limit acceleration during regulating motion to less than 32 ft/sec^2 and also to allow orifices of reasonable diameters to be used for controlling the speed of the regulating motion. Regulating pressure is about 1,000 psi. Initial acceleration during scram will be of the order of 100 ft/sec^2, and this requires a pressure of approximately 3,000 psi. The low pressure system is routed through the regulating valve only, and the high pressure system is routed to the accumulator and thence to the scram valves. The provision of dual pressures results in the useful feature that, if for some unlikely reason frictional effects in a rod and drive increase greatly with time, regulating movement of the rod will be prevented long before scram motion is substantially impeded. Thus the reactor operator will obtain early warning of excessive friction.

The deceleration valve throttles the flow of oil leaving the hydraulic motor during the last two feet of rod insertion travel. The mechanical drive between the motor and this valve progressively closes the motor fluid exhaust orifice, i.e., the deceleration valve, so that the rod velocity is brought down to zero with less than 1 g deceleration.

The combination of hydraulic motor, transmission and deceleration valve has been designed so that if the deceleration valve fails to close due to seizure of the valve or its drive, then the kinetic energy of the hydraulic motor, ballnut screw, control rod, etc., will be absorbed in a mechanical energy absorber built into the deceleration valve drive. The resultant abnormally high, but controlled, deceleration of the system will not give rise to forces great enough to break or distort any part of the rod and drive. Operation of the emergency mechanical energy absorber will become apparent to the reactor operator because withdrawal of the rod subsequent to operation of the emergency deceleration device will be prevented mechanically by a jamming action. The drive will have to be dismantled for rectification before it can be put into service again.

In the extremely unlikely event of seizure of the spool of the deceleration valve, the emergency snubbing device would come into operation automatically as follows. If the spool actuator nut becomes stalled in the axial direction, for any reason, it will cause the sleeve to which it is threaded to translate in the downward direction. This will cause the threaded sleeve to engage a thread-cutting tool at its lower and outer periphery. The energy that must be absorbed to decelerate the drive in a non-destructive manner will then be effectively absorbed by the process of cutting metal. The metal cuttings will be removed when the drive is dismantled for investigation of the cause of malfunctioning of the normal means of deceleration and for replacement of the emergency energy absorber.

Since normal deceleration of the rod following scram is less than 1 g, disconnection of the rod from the drive presents no hazard from the deceleration point of view. In fact, the rod itself and its push rods are always decelerated by gravity alone, the deceleration device only being needed to decelerate the hydraulic motor, ballnut screw and other rotating parts.

Regulating is accomplished by a two-direction, three-position control valve. In the de-energized or null position the supply port is blocked. Valve position will be determined by electric solenoid actuation.

Scram will be controlled by two spring-offset two-position pilot-operated valves connected in series. During normal operation the main valves are held closed by hydraulic pressure supplied from the energized pilot valves. De-energization of the solenoids of the pilot valves results in the spools of these valves shifting so as to allow hydraulic pressure to shift the main valve spools to the open (scram) position so that hydraulic pressure from the accumulator is channeled to the hydraulic motor. The spools of the main valves are spring-loaded towards the open position.

Two scram valves are employed in order to allow exercising and testing these critical components at intervals without the necessity of performing an actual scram. This is accomplished by opening in turn each of the scram valves while the other is left closed. Ability to scram is not jeopardized by this process. The valves are instrumented to provide a signal at a remote location indicating full travel of the valve spool.

An adequate reserve of energy for performing the scram function is stored in the form of the inert gas in the hydraulic accumulator. A piston type accumulator is used in order to allow monitoring of the stored fluid supply volume by instrumentation indicating the position of the piston. In addition, the fluid pressure in the pressure supply system will be monitored, as well as the presence of fluid in the accumulator gas volume region.

Rod withdrawal at scram speed is inherently impossible. Referring to Figure 48 , it will be noted that the scram fluid porting is such that scram fluid can only enter the motor port that will cause linear travel of the rod in the upward direction. The fluid porting through the regulating valve is so much smaller than the scram fluid porting that only a very small fraction of the scram fluid volume could be bypassed to the reservoir through the regulating valve during scram, whatever the position of the regulating valve spool.

In the unlikely event of complete jamming of a control rod in its guide tube, the maximum steady up load which the drive can exert on the control rod is approximately 2500 pounds. This force is large compared with the weight of a control rod (45 lb) and anticipated frictional resistances, and yet is substantially less than the yield loads of the individual control rod and drive components.

It should be noted that the accumulator oil and gas charging systems are equipped with safety valves, set at about

1-1/4 times the normal maximum system operating pressure, in order to protect the drive accumulators from overpressurization.

(4) Auxiliary Equipment

The external or auxiliary equipment will consist of a fluid pressure supply system, a fluid return or reservoir system and pressure regulating control circuits. The pressure supply will be provided by two parallel electric-motor-driven pump units. In each pump unit a double-ended electric motor drives a high pressure pump at one end and a low pressure pump at the other end. One pump unit will provide sufficient capacity for normal regulating control and accumulator recharging. The other pump unit will act as a standby and will be switched on automatically if the system pressure should fall below about 90 percent of normal; or, it can be driven in parallel if greater capacity should be needed. With one pump unit, the re-charging time for all accumulators together after a scram will be about 1-1/2 minutes.

The fluid return or reservoir system is maintained pressurized at essentially the same pressure as the drive containments. The main reason for this is to prevent the possibility of a sudden leakage of contaminated helium into the hydraulic system. Another reason for pressurizing the reservoir is to prevent possible frothing of the hydraulic fluid due to release of absorbed gas if the oil is subjected to a sudden reduction of pressure from drive containment pressure to atmospheric pressure.

Gas pressure supply for the accumulators is in the form of bottled inert gas and will be available at a pressure higher than system fluid pressure. During initial charging of the accumulators with fluid pumps off, gas pressure will be supplied at about 50 percent of normal fluid system pressure prior to filling the accumulators by means of the fluid pressure pumps. During reactor operation, with system fluid pumps operating normally, instrumentation indication that an accumulator piston is too low would mean an escape of accumulator gas. For this condition, gas would be available at above normal system pressure to bring the piston slowly back to the correct position. Normally, gas pressure will not be maintained in the gas supply lines after charging the accumulators.

Auxiliaries to the control rod drive system which may require inspection or maintenance during reactor operation will be

located out of the sub-pile room and will be made available for limited maintenance purposes by locating them in an air-filled room within the secondary containment.

Located within the sub-pile room will be the necessary fluid pressure and fluid return headers to which the control rod drives will be connected by flexible lines. Fixed piping will connect these headers with the pumping units and pressurized reservoir in the air-filled room.

(5) Instrumentation and Interlocks

(a) Drive Unit

The general condition of the drive unit will be indicated by instruments located external to the reactor containment. These instruments will indicate the following information from various sensing devices.

a. Excessive hydraulic fluid in the pressure containment of the drive unit; a switched signal from a float-actuated liquid-level sensing device.

b. Excessive hydraulic fluid in the gas region of the hydraulic accumulator; a switched signal from a float-actuated liquid-level sensing device.

c. Accumulator piston position; a variable voltage signal from a magnetically coupled moving traveller that shunts out a resistive bridge across which a meter is connected.

d. Excessive hydraulic fluid filter resistances; switched signals from differential-pressure-sensitive switches.

e. Freedom of scram valves; switched signals from spool-actuated limit switches.

With this information, the operator will know at all times that adequate energy is available for scram and the general operating condition of the drive hydraulic circuit.

Position information will be supplied from each drive unit by a synchro transmitter and two limit switches.

Other instruments, located in the control room, will indicate the positions of the rods at all times, except for the first two to five seconds after scram. This small lag is due to the fact that the planned high resolution position indicator cannot keep pace with the drive during scram. The indicator will show correct rod position after the two to five second lag. Actuation of the switches of items a, b and d will result in an alarm in the control room. An alarm will also sound in the control room if any accumulator piston position monitor indicates too low a piston position, i.e., inadequate accumulator gas volume, or too high a position prior to rod withdrawal, i.e., inadequate accumulator oil volume.

(b) Auxiliary Equipment

The hydraulic power supply controls and instrumentation will be located in the auxiliary equipment compartment. They will consist of a panel arrangement mounted with shut-off valves, pressure regulators, pressure gages, fluid temperature indicators, fluid level indicators, alarms, etc.

The operation and condition of the auxiliary equipment will be monitored by instruments located external to the reactor containment region. These instruments will indicate the following information from various sensing devices:

a. System fluid pressures too low; switched signals from pressure switches.

b. Fluid temperature too high; a switched signal from a temperature sensitive device.

c. Insufficient fluid volume in reservoir; a switched signal from a float-actuated liquid-level sensing device.

d. Insufficient back pressure in reservoir; a switched signal from a differential-pressure switch.

e. Excessive fluid filter resistances, switched signals from differential-pressure-sensitive switches.

In addition, the operator station will have the necessary pump start-up manual controls and automatic switchover controls which will start up the standby pump unit when necessary.

An interlock sensitive to the pressure in the high pressure supply header in the sub-pile room will cause all drives to scram if the pressure in the high pressure supply head falls below about 85% of normal. The existence of this interlock prevents safe operation of the reactor from being dependent on correct functioning of the hydraulic equipment in the auxiliary equipment compartment.

d. Normal Operation

The operating principle of the drive system is as follows. The drive and mechanism region inside the outer pressure shell is pressurized with purge helium to a pressure slightly above reactor pressure. This provides a means of preventing fission products from the reactor entering the drive region by maintaining a flow of helium from the drive containment to the reactor vessel.

Figure 48 illustrates the basic hydraulic equipment of the drive unit. Fluid pressure for normal regulating movement of the rod is supplied by auxiliary equipment external to the sub-pile room and not shown in the figure. The external pump system also maintains the scram accumulators at proper pressure by means of the separate high pressure circuit. Upward and downward movement is determined by the spool position of the regulating control valve. The present plan is to use not more than three rods at a time for regulating purposes. Any three of the innermost twelve control rods may be assigned the function of being regulating rods. These rods will be actuated by automatic and/or manual control, while the remainder will be operated by manual control only. Rod control circuits will be arranged so that not more than one of the regulating rods can be moved outwards at a time by automatic control or manual control. The reactor will be operated so that all rods will be either fully inserted or fully withdrawn except for the three being used for regulating purposes. For further details of rod programming for startup and normal operation see Section II, G. 5. c.

During normal operation, the scram control valves are held energized, blocking the ports between the accumulator and the motor. An emergency insertion or scram will call for a shut-off signal. In other words, all solenoid coils of the scram valves will be de-energized. Accumulator discharge will then provide the high volume

flow to accelerate and drive the hydraulic motor at scram velocity. Deceleration is normally accomplished during the last two feet of rod travel by the mechanically driven deceleration valve assembly located above the hydraulic motor. If the deceleration valve were to seize in the open position, although such failure is extremely unlikely, the deceleration valve transmission would smoothly stall the motor through the previously described metal cutting mechanism. (See Section II. B. 7. c. (3)(b)). The extremities of the rod travel are to be cushioned by high rate, low displacement springs to absorb residual energy resulting from end-of-stroke rod creep due to hydraulic motor slippage (in up-direction) or continued regulating movement into contact with the stops.

Valves are constructed and connected so as to prevent pressure buildup in the motor ports from internal valve leakage which could conceivably cause the motor to drift with the system in the static condition. In addition, porting of the valves, especially the scram valves, is such that inadvertent external action or component failure will make rapid or scram velocity withdrawal of the rod impossible.

Non-return check valves will prevent rapid decay of accumulator oil pressure in the unlikely event of failure of the external pressure lines or pumps, thus maintaining the capability for all drives to scram even if there were a loss of pressure in the high pressure oil supply system. A significant loss of pressure in the pressure supply system would automatically cause a scram (See Section II. B. 7. c. (5)(b)).

The helium purge line is equipped with a non-return type of check valve to prevent a pressure loss in the drive containment in the case of rupture of the helium purge line. The orifice size of the purge helium port is of such small size that, even if the check valve failed to close, the pressure drop in the drive containment and reactor would be so gradual that non-emergency action could be taken to cool the core, shut the plant down and pump as much helium as possible into the dump tanks. The initial rate of loss of coolant inventory from one broken line would be not more than 1% per hour. Cooling the reactor down promptly and reducing the coolant pressure would, of course, reduce the rate of loss.

The credible malfunctions which can occur in the hydraulic circuit are minor and will not require an automatically initiated scram. These situations will normally be taken care of by appropriate corrective action by the plant operators. The only potentially serious

situation that would initiate an automatic scram would be the case where the high pressure system oil pressure dropped below a chosen level. In this case, scram would be automatic in order to utilize accumulator pressure before it is dissipated into the system by valve leakage.

A standard checking procedure will be adopted during certain shutdown periods where each rod will be withdrawn individually and scrammed. This will assure that accumulator pistons are free and functioning normally. The previously described method of exercising the scram valves will also be part of a scheduled preventative malfunction checking procedure.

e. Pre-Operational Testing

After installation of control rods, control rod drives and associated systems at Peach Bottom, the whole system will be exercised for a time in order to transport any residual dirt in the system into the filters, and in order to detect normal startup "bugs". Following this the filters will be cleaned and each rod will be put through at least 100 cycles of withdrawal at regulating speed followed by scram, both for system-cold and system-hot conditions. For the system-hot condition, the reactor will be heated by operation of the coolant circulators without heat removal via the boilers.

During these checkouts, the performance capabilities of individual rod drives will be monitored and unusual accelerations, impeded motion, vibrations, and shocks looked for.

Following these tests, at least 50 further withdraw-scram cycles will be performed, all rods scramming simultaneously in this case. This operation, of course, will be carried out prior to the loading of fuel.

f. Periodic Examination

Periodically, control rod drives will be removed, disassembled, inspected, and reassembled. During this process, all organic seals and any badly worn parts will be replaced. Dry lubricant will be replaced if necessary. Following reassembly, each drive will be functionally checked in order to detect assembly faults, if any.

Control rods will be replaced periodically as required, by new control rods. During this process the graphite guide tubes

will be inspected and reinserted, any badly worn or distorted parts being replaced by new or rectified ones.

The frequency of removal of drive mechanisms and control rods will depend upon the operating history of the system.

g. Possible Malfunctions of Control Rod

(1) Fracture of Poison Sections

The control rod has been designed to preclude fracture of the poison elements during normal reactor operation. As described previously under Section II.B.7.c.(1), the refractory type poison elements are supported in a cushioned manner that allows only axial compression loading due to either differential thermal expansion and/or acceleration loads from the drive mechanism. If the control rod were to be subjected to some kind of vertical impact, and assuming the worst condition where the center support tube had negligible deflection upon impact, the poison elements would then individually bottom out on the disc spring/spacer assemblies. The discs have been designed with a load/deflection rate that will effectively absorb this impact condition, without damage to the poison elements. Should a poison element fracture through some unaccountable thermal or mechanical shock, the fracture would be localized to the relatively short length of the poison element in question. Fragments from the fracture would be retained in the region between the spacers, resulting in very minor deviation in relative rod worth. Sufficient strength in the rod structure is available to dislodge a rod due to any likely jamming effect between the fractured poison fragments and the graphite guide tube; however, the hydraulic motor would stall if the resistance to rod motion exceeded about 2500 pounds, and so the metal structure of the rod would not be overloaded (See Section II.B.7.c.(1)). It does not appear that a poison element fracture is possible, nor would it constitute a hazard if it were to occur.

(2) Fracture of Structural or Connecting Rod (Including Separation of Rod Elements from Drive)

This event will actuate the rod continuity monitor for the drive in question as described in Section II.B.7.c.(1). The reactor operator will stop withdrawal of the rod in question. If the indication cannot be proved due to an instrumentation fault, the rod concerned

will not be used as a regulating rod, nor will it be withdrawn any further for the remainder of the current period of reactor operation, unless flux distribution considerations make further withdrawal desirable. In this case, the rod concerned will be withdrawn in small increments until it is fully withdrawn, another rod, of similar worth being incrementally inserted into the core to maintain constant reactivity in order to monitor for satisfactory withdrawal of the suspect absorber. Of course, the suspect rod could be inserted fully if preferred, and another rod withdrawn in its place. Fracture of the structural member would probably not prevent scram motion of the rod.

To minimize the possibility of a rod becoming broken or detached and subsequently stuck, a great deal of emphasis has been placed on providing the maximum structural integrity of the rods and their connecting fittings. The proper procedure in performing the rod latching operation as explained in Section II. B. 7. c. (2), assures that such separation of rods could only occur from actual structural failure. Although the hydraulic motor drive can apply substantial forces, the rod components have been designed with a large strength margin in excess of this. (See Section II. B. 7. c. (1) and (3) (b).

(3) Fracture of Graphite Guide Tube

Fracture of the graphite guide tube due to forces externally generated by the control rod drives is not likely. The most critical normal loading of the guide tube would be in the tension direction when the drive unit is scramming the rod upward. The guide tube is anchored to the core grid plate by a breech type of connection. Calculations and tests (See Section II. J. 4) have indicated that the strength of this connection is more than a factor of 2 in excess of the force capability of the drive unit. The drive thus would stall well below the breaking point of the guide tube breech connection. If a guide tube were fractured due to other unforeseen external or metallurgical causes and pieces were still in cylindrical forms, upward and downward rod motion would most likely be unaffected.

(4) Over-Temperature of Structural Members

In the event of complete loss of cooling, the control rod structural member may be damaged by over-temperature. If coolant flow is not restored, the control rod structural member may melt. The control rod would be held in the core by its push rod but

the metal spacers between the poison compacts may melt. The melting of the spacers could effectively shorten the control rods a few inches, but this would have only a small effect on rod worth. The absorber sections will still be positively supported from below. The temperature of the grid plate, push rod, guide sleeves, etc., will be maintained at safe values through the agency of the emergency cooling system (See Section II. F. 2).

Control rods which are partially or fully withdrawn at the time of the accident postulated can be inserted by normal scram action since no part of the rods located at or below grid plate level at the time will be damaged by over-temperature. This is true however long the scram is initiated after the accident. Scram will occur automatically as soon as a loss of coolant flow occurs. (See Section II. G. 6)

Any melting of any metal part of a control rod will be accompanied by melting and disintegration of the adjacent part of the rod continuity monitoring circuit conductor, and hence a rod disconnection indication in the control room.

(5) Rod Behavior Due to Pipe Rupture

If it is postulated that a clean separation could occur in the primary coolant outlet circuit, downstream of the heat exchanger, where the ducting reverts to conventional single walled piping (as opposed to the double walled co-axial arrangement upstream of the heat exchangers), a temporary excessive pressure drop would occur in the plenum chamber above the core. A break in the pipe at this location causes the maximum transient levitation force across the core. (See Section II. B. 9. c) Preliminary calculations have shown that the transient pressure drop across the reactor core would peak at about 8 psi. In order to consider this accident as possibly contributing towards hazardous rod behavior one would also have to postulate that a control rod became detached from its drive mechanism at the same time. This in itself does not appear credible. However, if these conditions were to be considered, the control rod could not be lifted out of the core since its weight is in excess of the piston force that can be developed from a pressure drop of the stated magnitude.

h. Possible Malfunctions of Drive

It should be noted that each control rod drive unit has its own accumulator to provide the energy to power a scram. The fact that any one drive unit was prevented from scramming by a malfunction of that unit would not remove the ability to shut down the

reactor by means of either the remaining control rods or the backup shutdown rods. In the following sections various malfunctions of the individual drive units are discussed.

(1) Jammed Scram Valve

Duplicate scram valves in series are provided (See Figure 48). As often as desired, possibly once per shift, and without causing a scram, each valve can be opened in turn while the other is left closed in order to ensure that the valves are free to move. Limit switches operated by the main valve spools will result in positive indication in the control room of whether the valve spools have shifted fully or not. This system of frequent monitoring will ensure a suitably small probability of failure to scram due to scram valve jamming. Determination of the probability of malfunction of the scram valves is one of the objectives of the test of the complete prototype control rod and drive (See Section II. J. 4).

The drive is still capable of inserting the control rod into the core at regulating speed if both scram valves were jammed closed.

(2) Seizure of Hydraulic Motor

When hydraulic motors are operated with clean oils of suitable lubricity and are not subjected to excessive temperatures or speeds seizure is extremely unlikely.

(3) Seizure of Ballnut Screw

This can only happen if a considerable amount of material is transferred to or from the balls and either the screw or the nut or both. One of the objectives of the research and development program is a thorough check of the extent of such metal transfer in a very pure helium atmosphere. There is considerable evidence that with hard surfaced materials this problem is not significant in the temperature range of interest here (less than 200 F). The test of the prototype control rod and drive is described in Section II. J. 4.

(4) Seizure of Push Rod in its Guide Sleeve

The critical surfaces of both the push rod and its guide sleeves are nitrided. The push rod is coated with an inorganic type of dry lubricant as well. Data concerning the probability of

seizure will be obtained from the wear and friction tests and the test of the complete prototype control rod and drive which form part of the research and development program.

(5) Accumulator Piston Seizure

The accumulator is a standard proven design, using conventional materials, that has been used extensively. Further experience of operation of the accumulator will be obtained in the tests of the prototype control rod drive.

A monitoring procedure can be used to ensure at suitable intervals that the accumulator pistons are free to move. A suitable check during reactor operation is to reduce the system oil pressure by a small amount, say 10%, and check that all drive accumulator piston position monitors indicate a small piston movement after a short period of time. (See Section II. G. 2. c. (2))

A more positive check can be made during reactor shutdown by withdrawing the control rods one at a time and then scramming them while the appropriate accumulator piston position monitors are watched.

In the event of piston seizure, the drive affected could still scram at reduced speed, the speed being governed by the rate at which oil is supplied by the external pumping system. In this case, the total time to insert the affected rod would be about 3 seconds, while the remaining rods would move at normal scram speed.

(6) Seizure (Closed) of Outlet Check Valve

The type of check valve chosen for this application is one of such construction that this kind of failure is virtually incredible since no small clearances between sliding components are involved and lubrication is virtually perfect. Extensive experience on the operation of this valve will be obtained in the test of the complete prototype control rod and drive.

(7) Excessive Friction

If for some unlikely reason frictional effects in a rod and drive increase greatly with time, regulating movement of the rod will be prevented long before scram motion is substantially impeded. This results from the use of a low hydraulic pressure for regulating motion and a high pressure for scram. Thus the reactor

operator should obtain early warning of excessive friction. The force available for inserting a control rod during scram is about 2500 lb.

(8) Loss of Inert Gas from Accumulator

The loss of gas can conceivably occur in two ways. In the first way, the gas is lost through a leak to the atmosphere. The accumulator piston position monitor for the drive in question will tell the operator by an alarm signal that gas has been lost.

In the second way, the gas somehow gets past the accumulator piston into the drive's hydraulic system. A fall in accumulator gas volume will then occur and this will be apparent to the operator as before, or else oil leaks past the piston into the gas space to replace the gas lost and this becomes apparent to the reactor operator via the drive accumulator's oil leakage monitor, a float switch in the base of the accumulator.

In either case, even if all gas is lost the rod drive can still scram at reduced speed, the speed being governed by the rate at which oil is supplied by the external pumping system. In these cases, the total time to insert the rod would be about 3 seconds. In the more likely case of a slow gas leak to the atmosphere, or back through the gas check valve, the gas pressure can be restored to its proper value by manually letting a little gas into the accumulator from an available high pressure source while the accumulator piston position monitor is watched.

In the case of gas leakage past the accumulator piston into the drive's hydraulic system, substantial accumulation of gas in the drive will be prevented by the normal small oil leakage past the valve spools and through the hydraulic motor.

(9) Malfunction of Clutch

In the most unlikely event of seizure or jamming of the over-running clutch, the multi-disc brake on which it is mounted would slip and allow the drive to insert the control rod normally except for a relatively small reduction in scram speed. The construction and lubrication of the clutch are such that this type of malfunction is regarded as incredible. The clutch will be lubricated by the low-vapor-pressure oil in the hydraulic drive unit. Seizure of the clutch will be detectable by the reactor operator since the oil pressure available for regulating motion is not great enough for the hydraulic motor to be

able to insert the control rod into the core against the resistance from the brake under regulating conditions.

(10) Dirt in the Hydraulic System

The hydraulic system operates pressurized so that the lowest pressure in the system (in the reservoir) is equal to reactor gas pressure. Therefore dirt can get in only when the reactor is shut down and depressurized or when one of the duplicate pumping units is being replaced.

Not only is the pumping system provided with fine filtration equipment on the output side, but each drive is equipped with pressure-drop-indicating 10-micron filters at the oil pressure supply inlets to the drive. Each pressure-drop indicator will send a signal to the auxiliary equipment room in the event that sufficient dirt collects in the associate filter to cause an abnormally high pressure difference to be generated across it. An alarm will be sent to the control room if any pressure-drop indicator is actuated.

Clogging of the filters will not affect scram performance since control rods will not be withdrawn from the core unless all drive accumulators are fully charged (shown by piston position monitors). A secondary indication of filter clogging will also be available in the form of an abnormally long time for accumulator recharging by the pumping system following scram, or unusually low regulating speed.

(11) Breakage of Helium Purge Line

The purge helium, which is purified helium supplied from the reactor's helium handling system, is inserted into the drive through a check valve rigidly attached to the drive housing in series with a very small hole drilled through the housing. Breakage of the helium purge line will not normally result in significant leakage of reactor coolant since flow will be stopped by the check valve.

In the extremely unlikely event of simultaneous breakage of the purge line and failure of the check valve, the rate of loss of reactor coolant will be kept to a small value by the small size of the hole through the drive housing. The initial rate of loss of coolant would be of the order of 10 lb/hr. The rate of loss would drop with time. (See Section II. B. 7. d)

(12) Leakage from Hydraulic Motor

Any leakage of the hydraulic motor, from its fluid connections, through its body, past its shaft seal or from its deceleration valve, will collect in the pressure housing surrounding the motor and eventually, when enough fluid has collected, will actuate the fluid leakage monitoring float switch there.

(13) Gas Leakage from Hydraulic Unit Pressure Housing

Since the purge helium flow is inserted into the drive above the pressure housing, a small leak in the latter will result in leakage of purified helium. This purified helium will contain small quantities of the radioactive isotopes xenon and krypton. A monitor will give warning of leakage.

In the extremely unlikely event of a large hole appearing in the pressure housing, or a blown gasket, the rotary face seal located in the drive at the bottom end of the ballnut screw will limit the rate of leakage of reactor coolant to a low value since, in the case of a relatively large leak, a pressure difference will cause the seal to seat firmly.

(14) Vibrations of Ballnut Screw

The first critical speed of the screw is less than the maximum speed. Therefore the possibility of screw vibration exists as the screw accelerates and decelerates through its critical speed. Tests carried out to investigate this phenomenon indicate that, because of the rapid rate at which the actual speed passes through the critical speed, no significant vibrations occur.

(15) Excessive Rate of Wear of Ballnut Screw and Ballspline

It can be postulated that the ballnut screw and nut grooves may get wider and wider, and the balls smaller and smaller until finally satisfactory engagement of the balls with the grooves no longer occurs. Information on this point will be obtained from the complete prototype control rod and drive test which forms part of the research and development program. (See Section II. J. 4) The postulated malfunction is regarded as incredible.

(16) Deceleration Valve Seized Open

The emergency mechanical energy absorber will bring the rod and drive safely to rest as outlined in Section II. B. 7. c. (3)(b). This statement will be checked by simulating seizure of the deceleration valve during tests of the prototype control rod and drive and recording the consequences of the simulated failure.

(17) Regulating Valve Seized Open

At least one regulating rod will, of course, execute a compensating movement if the regulating rods are under automatic control at the time. In addition, or as an alternative, the operator will be able to manually effect a compensating movement of another control rod.

If the regulating valve is seized in the rod withdrawal position, and the operator takes no corrective action, scram will occur when the reactor power reaches 140% of normal maximum power. For further discussion of this case see Section VII.

The amount of fluid that can be wasted during scram by flow through a regulating valve, whatever its position, is not enough to affect scram performance significantly.

(18) Breakage of Flexible Lines

The inlet check valves will prevent inability to scram on the part of any drive. Breakage of a high pressure oil supply line will result in reduction of pressure in the external high pressure supply system and consequently a scram through the agency of the "Rod Pressure Low" scram circuit. The reduced oxygen atmosphere will prevent fire in the event of a break or leak in any oil supply line.

Breakage of a low pressure oil supply line will merely result in loss of regulating motion on the drive in question. The reservoir low level and low regulating pressure alarms will operate soon after the line breakage. If the operator does not take corrective action before the contents of the reservoir have been pumped out of the broken line, a scram will be initiated automatically by the "Rod Pressure Low" scram circuit as soon as the high pressure system oil pressure starts to fall.

Breakage of a return oil line will not prevent scram of the drive affected. After a relatively long time, or after a

substantial amount of regulating or scram movement, enough oil will have been lost from the system for the reservoir low level alarm to be actuated. If the operator does not take corrective action before the contents of the reservoir have been exhausted, a scram will be initiated by the "Rod Pressure Low" scram circuit as soon as the high pressure system oil pressure starts to fail.

Breakage of a flexible hydraulic line is regarded as a most unlikely event. The flexible oil lines to be used will be the braided-steel wire covered type. Their bursting pressures will be at least a factor of three greater than the pressures contained in them. They will not flex significantly during normal operation. They will not be subjected to more than about 2000 cycles of pressure application and removal.

Breakage of the accumulator gas supply line is not critical since it is used during reactor operation only to restore accumulator pressure in case of accumulator leakage. This line is normally not pressurized. The gas charge is retained in the accumulator by a check valve located in the accumulator.

(19) Loss of System Pressures

An alarm will result if the high pressure supply system pressure falls to about 90% of the normal value. The "Rod Pressure Low" scram circuit will cause a scram if the pressure in the high pressure supply falls below about 85% of the normal value.

Loss of pressure in the low pressure system will cause an alarm. The operator can manually scram the control rods if the reactor condition departs excessively from the desired condition before the low pressure supply is restored.

Restoration of pressures will normally be automatic since the stand-in pumping unit will start automatically if either system pressure drops by more than about 10%.

(20) Burst Accumulator

In the remote event that an accumulator bursts, the drive will be prevented from withdrawing its associated control rod at substantial speed on opening of the scram valves by the outlet check valve which will prevent hydraulic fluid at reservoir pressure from flowing back into the drive. In the case of fully inserted control rods, the lock described in Section II. B. 7. c. (3)(a) would also be available

to prevent drive withdrawal. The operator would be aware of the malfunction from his drive accumulator instrumentation display. The accumulators are protected from over-pressurization by safety valves in the inert gas and oil pressure supply systems.

(21) Foaming of Oil

As explained in Section II. B. 7. c. (4), significant foaming of the hydraulic oil will not occur in the pressurized hydraulic system. The oil will be saturated with helium at reservoir pressure, which is essentially equal to reactor coolant pressure. There will be a continuous leakage flow from the reservoir, through the pumps and drives, back into the reservoir of a few gallons per minute.

(22) Excessive Oil Leakage

Excessive oil leakage within the drive casing is monitored by two oil leakage float switches located in the only internal spaces where oil can collect. Excessive external leakage of oil from the auxiliary system will be indicated by the reservoir low level alarm.

(23) Malfunction of Clutch-Brake

The postulated malfunction here is one which will result in the control rod not being prevented from dropping by the clutch-brake.

Fully inserted rods will be prevented from dropping by the lock described in Section II. B. 7. c. (3)(a). Thus only partially withdrawn rods will be available to drop and these will be only three in number - the regulating rods.

In the most unlikely event of this malfunction actually occurring, the rod will drop at about normal regulating speed, i. e., 1 to 2 inches per second, governed in speed by the hydraulic motor pumping oil in a closed circuit through two orifices. This motion of the rod will give the operator warning of the clutch-brake failure. The operator can then raise the rod by normal upward regulating motion until the rod is retained in the up position by the lock mentioned above. Of course, the operator could insert all rods by scram action if he preferred.

The above rod behavior due to clutch-brake failure will be verified by appropriate test of the prototype control rod and drive.

(24) Disconnection of Rod from Drive

The fuel transfer machine will be used to ensure that the control rods are securely latched to the drives immediately after closure of the latches.

If a rod should become detached from its drive due to the occurrence of some remote eventuality, the rod continuity monitoring circuit will cause a rod disconnection indication in the control room as described in Sections II. B. 7. c. (1) and (2). The indication will appear before significant separation of the rod from the drive occurs. The reactor operator will stop withdrawal of the rod in question. If the indication cannot be proved due to an instrumentation fault, the rod concerned will not be withdrawn any further for the remainder of the current period of reactor operation.

If the operator were to ignore the rod disconnection indication, and the control rod were subsequently to fall freely out of the core after full withdrawal of the drive, no public hazard would result even for the case where none of the remaining rods scrammed following the resultant power excursion.

i. Other Events Conceivably Interfering with Control Rod Motion

(1) Fire or Explosion in Subpile Room

Appropriate fire protection against fire and explosion hazards will be provided in the sub-pile room for protection for those times when the containment vessel is not filled with nitrogen.

(2) Lateral Shift of Vessel Relative to Lower Biological Shield

Steel structural members will preclude significant relative lateral motion between the vessel and the shield.

(3) Lateral Shift of Grid Plate Relative to Vessel

Steel blocks interposed between the grid plate and the vessel (See Section II. B. 4) will preclude any significant lateral motion which can be accommodated by the flexibilities of the control rod push rods and guide sleeves and equivalent components of the emergency shutdown rods.

(4) Lateral Shift of Core Relative to Grid Plate

Each of the 859 core components is attached to the grid plate in such a manner that it can withstand a lateral load of at least 4000 pounds. Lateral shift of the base of the whole core relative to the grid plate is consequently regarded as incredible, however, should it happen, the electrically driven emergency shutdown rod drives have a sufficiently large force capability to be able to insert the emergency shutdown rods despite a shift of the core.

All components of the core, including the control rod guide tubes, possess sufficient flexibility that only modest stresses in the components will result from lateral motion of the top of the core to the full extent permitted by the available clearances between the side reflectors and between the outer side reflector and the thermal shield.

8. Emergency Shutdown Systems

a. Introduction and Summary

In addition to the normal complement of control rods and drives capable of both slow regulating motion and rapid insertion during scram, there will be 19 electrically driven emergency shutdown rods under the control of the reactor operator and a number of thermally released, gravity operated shutdown absorbers which will not be under the control of the reactor operator but will be released into the core on any occasion when the coolant flow is not adequate to maintain core temperatures at safe levels.

The purposes of the electrically driven emergency shutdown rods are two-fold. They are:

(i) To provide additional shutdown capacity to cover the remote possibility that enough control rods fail to be inserted into the core during scram so that the core is only shut down hot and not cold. This additional shutdown margin would be used in the unlikely case of failures of four or five control rod drives. In this case, the operator can fully insert the emergency shutdown rods in a period of the order of 20 seconds.

(ii) To enable the reactor to be shut down in the extremely remote event of some kind of crushing, lateral movement or other kind of disarrangement of the core which might result in no open guide tubes being available for the insertion of the normal control rods. In this

case, the operator can still insert the emergency shutdown rods. Their drives possess the necessary force capability to insert the rods into the core even if fuel elements or debris of guide tubes have to be forced upwards by the rods out of the top of the core. The time required to fully insert the rods will be about one minute if insertion is resisted by a force of 10,000 pounds per rod.

The reason for inclusion of the thermally released absorbers is to cover the extremely unlikely event that not enough control rods and emergency shutdown rods can be inserted to keep the core shut down hot following xenon decay or if the core for some remote reason becomes hot enough to lose substantial amounts of poisons by evaporation.

The electrically driven emergency shutdown rod drives will be simple, rugged electric-motor-driven devices, containing their own energy sources in the form of storage batteries, and capable of test operation at any time, preferably during reactor shutdown. The total worth of the emergency shutdown rods, for various cases, is indicated in Table 4 of Section II. A. 2.

The thermally released last-ditch shutdown absorbers will consist of short absorber rods normally held within the top reflector by a metal tie bar and fusible link. Loss of coolant flow when the core is at normal operating temperature, or gross over-temperature of the core together with inadequate coolant flow, will result in melting of the fusible links and release of the absorbers into the core. The number and total worth of these absorbers will be decided later.

As a minimum, the total worth of the thermally released absorbers will be large enough to compensate for the decay of xenon.

Both the emergency shutdown systems will be of very simple construction and of the highest standard of reliability. Both will use a refractory poison material.

Extensive testing of a prototype electrically driven emergency shutdown rod and drive will be undertaken in order to prove the reliability of this device. Tests will also be run to establish the reliability of operation of the thermally released shutdown absorbers.

b. Electrically Driven Emergency Shutdown Rods and Drives

(1) Description

The prime function of the emergency shutdown rods is to provide a back-up system available to the operator for shutting the reactor down in the extremely remote event that the minimum required number of control rods do not all respond to a scram signal. These emergency shutdown rods will be inserted into graphite guide tubes similar to those used for the control rods. They will be distributed fairly uniformly through the core as shown in Figure 4 of Section II. A. 2. The total worth of these rods is indicated in Table 4 of Section II. A. 2.

Figure 50 is a schematic illustration of the secondary shutdown drive. The mechanisms of this drive will be relatively simple and of extra rugged design. The principle of actuation will be based on a linear motion from a conventional screw and nut mechanism. Withdrawal will be in the downward direction. The pitch of the screw will be small enough to ensure irreversibility, i. e., a downward load applied to the shutdown rod will not cause the screw to turn and hence allow the rod to descend.

The main components of the linear actuator portion will be: a graphite guide tube similar to the control rod guide tubes, a shutdown rod made in the form of a stiff metal tubular member filled with compacts made of refractory poison material, a tubular push rod, its upper end latched to the bottom of the shutdown rod and its lower end terminating in the form of an Acme thread type nut; an Acme threaded screw extending up inside the push rod with its lower end supported by a thrust-radial bearing assembly; a guide tube arrangement extending down from the grid plate which provides alignment and support for the sliding members and an external pressure shell in the form of a nozzle extension of the reactor vessel which encloses the mechanisms and reacts against the full thrust of the actuator. Also included in this portion of the drive are two rotary differential-pressure face seals of the same type and fulfilling the same functions as in the case of the control rod drive. (See Section II. B. 7. c. (3)(a)).

The lower end of the actuator pressure shell is in the form of a bolted flange connection. Attached to this flange is a drive unit consisting of an electric motor and gear reduction drive with self-contained energy storage in the form of a battery whose

output is controlled by a heavy-duty solenoid switch. Based on an insertion time of approximately one minute for a stroke of 8 feet, the chosen direct current electric motor, with appropriate speed reduction gears, will provide the specified thrust with a high degree of reliability.

Ample short-time energy delivery capacity is achievable in a battery of moderate size. Figure 50 shows a storage type battery of the cadmium-nickel type in which the cells are continuously immersed in the electrolyte and which is continuously floating on a charging system.

To check mechanical continuity between the shutdown rod and its drive, the rod/drive assembly will be monitored by an electrical continuity circuit of the same type as that used in the control rods and drives (See Section II. B. 7. c.). Separation at the latch or breakage of a critical component during withdrawal of the rod will instantly result in an alarm being sounded in the control room.

To prevent migration of fission products and fine powders down into the emergency shutdown drives, a flow of purge helium will be injected into the drives at a point just above the face seals as in the case of the control rod drives (See Section II. B. 7. c. (3)(a)).

These rods and drives will be capable of exerting a thrust of approximately 10,000 pounds each. A force of this magnitude will be readily capable of forcing a shutdown rod into the core, regardless of the amount of interference or distortion of the core. If necessary, the emergency shutdown rod will force any obstructing fuel element or guide tube debris up out of the core. Thus, continued insertion of all emergency shutdown rods appears to be certain once the insertion process has begun. The time required for full insertion of the rods will be approximately one minute if insertion is resisted by forces of 10,000 pounds per rod, or about 20 seconds if unresisted.

A small percentage (about 2 percent) of the reactor coolant will be normally diverted into the emergency shutdown rod guide tubes to maintain the metal structures of the rods at safe temperatures in case the rods are inserted into a normally operating core. In the event of loss of coolant simultaneous with an accident requiring insertion of the emergency shutdown rods, the resulting high temperature may cause the metal structure of the rods to melt after insertion. As in the case of the control rods, this will not constitute an added hazard as the refractory ceramic poison elements will remain

whole and stay in the core, supported by the still solid actuator rod located in the relatively cool region below. (See Section II. B. 7. g. (4))

The upper end of the screw has excess thread for absorbing over-travel of the rod. In addition, the thread at the upper end of the screw finally runs out to a relief diameter smaller than the root diameter of the thread. This last feature positively stops the upward travel of the actuator, in case of limit switch failure during an emergency insertion, by allowing the nut to run off the screw thread and subsequently allowing the screw to free-wheel until the battery runs out. Rotation of the nut and hollow push rod are prevented by a key and keyway arrangement.

The latch between the shutdown rod and the hollow push rod is released by turning the screw so as to raise the shutdown rod beyond its normal fully-up position and disengage the nut from the screw thread. The balls in the latch will then be aligned with a groove in the graphite guide tube and thus free to move radially outwards out of engagement with a groove in a part of the hollow push rod. Both shutdown rod and hollow push rod are then free to be removed upwards. When the rod is in its normal fully-up position the latch balls will be below the top of the metal guide tube.

Appropriate surface treatment, in addition to the use of a film of dry lubricant, will be used to prevent seizure or substantial galling between the screw and nut. All bearings and the reduction gear will be grease-lubricated.

A nickel-cadmium type battery has been selected because this type is capable of very high discharge rates, can be sealed for a long trouble-free life, and requires no attention over very long intervals other than monitoring of its output.

(2) Instrumentation and Control

Instrumentation within the drive will be limited to simple limit switches controlling and indicating the upper and lower limits of the rod stroke, and the rod continuity monitoring circuit mentioned above. The limit switches will be housed in the drive unit containment and driven by an instrument type gear-cam arrangement.

The energy stored in the storage battery will be used for rod insertion but external auxiliary circuits will be used to supply power to the motor for rod withdrawal. Rod insertion will be initiated by de-energizing the solenoid switch so that its contacts close and connect the battery output to the electric motor.

(3) Auxiliary Equipment

The auxiliary equipment will consist of the requisite direct current charging system.

(4) Normal Operation

Prior to withdrawal of any of the regular control rods, the emergency shutdown rods will be withdrawn downward completely out of the fueled region of the core. They will remain in this position throughout normal operation of the reactor.

The rods and drives will be periodically exercised to make sure that the actuator parts and motors are in normal functioning order. The storage battery output voltages will be checked at frequent intervals. Periodically the batteries will be subject to a rapid-discharge output-voltage test.

It should be noted that no harm will be done to any reactor components by inadvertent insertion of the emergency shutdown rods.

(5) Safety and Reliability

Since the emergency shutdown rods will be fully withdrawn prior to withdrawal of any control rods, and since these rods will be provided with rod continuity monitoring circuits indicating possible disconnection of a rod from its drive, it is believed that there are no potential hazards ascribable to these devices themselves.

c. Thermally-Released Shutdown Absorbers

(1) Description

These will consist of a minimum of 19 units as shown in Figure 51 mounted in the tops of the 19 emergency shutdown rod guide tubes, and possibly up to 36 additional units as shown in Figure 52, mounted in the tops of control rod guide tubes.

As shown in Figures 51 and 52, each of the thermally-released shutdown absorbers consists of a neutron absorber section suspended in an extension of the guide tube in which it is mounted. The suspension system is a stainless steel rod with a collar brazed on the lower end which takes the weight of the tubular absorber as transmitted through a stack of metal shock absorber washers and a positioning plate. The neutron absorber will be made of a stack of graphite compacts loaded with refractory poison.

The brazed joint and the metal parts of the unit are cooled by the rod cooling gas which will have a nominal maximum temperature of 1000 F. If this cooling gas flow should fail when the core is hot, the brazed joint temperature will rise to about 1800 F and cause the brazing material to melt. The heat required to raise the temperature of the brazed joint to the level stated will be derived by conduction from hot fuel compacts in adjacent fuel elements.

On fusion of the brazed joint, the neutron absorber and position assembly drops off the suspension rod into the guide tube. It drops until it is stopped either by the top of a rod absorber or by means which will stop the falling absorber at the most reactive location. One method for achieving the latter is the use of a system of lugs and grooves as shown in Figures 51 and 52.

The shock of the fall of the emergency absorber compact is cushioned by the collapse of the shock absorber washers.

It will be seen that this gravity drop system is still effective if, even for some remote reason, the hydraulically driven control rod system and the electrically driven emergency shutdown rod system have both failed to operate, but the guide tubes are reasonably intact.

Its operation is completely independent of all electrical or mechanical systems and uninfluenced by any accident external to the reactor vessel which leaves the core relatively undisturbed.

The satisfactory operation of the thermal release will depend only on the choice and stability of the braze fusion temperature and freedom of motion of the falling parts, while inadvertent operation will be prevented by conservative joint design and good creep properties of the alloy. The clearances between the absorber sections and the guide tubes will be made as large as is feasible.

9. Evaluation of Core Arrangement and Restraint

a. Lateral Stability

The arrangement of the fuel elements, rod guide tubes, and dummy reflector elements in the core is set by the locations of the standoff pins and rod guide tube seats in the core support plate. Each of these core components is held at core support plate level by means which rigidly maintain the center-lines of the components in a vertical position at their lower ends. Lateral motion of the tops of these components, then, can only occur by virtue of flexure, and all 969 components must flex together. The core thus experiences a fairly large restoring force tending to keep it upright if the top of it is somehow deflected sideways.

The maximum possible sideways deflection is limited by the fact that the total movement available to the inner side reflector is restricted by fairly small clearances between the inner and outer side reflectors. It is also small enough so that the maximum possible sideways movement of the tops of the core components is not great enough for the latter to be broken by the resulting flexure.

The mechanical properties of the complete core structure are further described in Section II. A. 1. c. Details of the standoff pins can be found in Section II. C. 3. The reflector is described in Section II. B. 2.

All core components will individually stand up vertically. When the coolant blowers are started, a pressure differential is established across the inner reflector blocks so that the latter apply radially inward forces to the core components

at a level about 2 feet below their tops. This pressure differential results from the pressure drop experienced by the reactor coolant as it flows down between the reflectors and up through the core. As the blower speed is increased, the pressure differential across the inner reflector increases until, at full power operation, the load applied to the core by the inner reflector exceeds one ton per reflector segment. Sideways deflection of the top of the core is now prevented by the large available frictional forces between core components since, if sideways deflection is to occur, relative sliding motion must take place between all core components. It can be shown by calculation that with the expected coefficient of friction between adjacent components of 0.5, sideways movement of the top of the core will not occur unless one side of the core experiences a force about twice as great as the opposite side experiences. The net side force required to tilt the core sideways during full power operation is of the order of 10 tons. There is no conceivable way that external forces of this magnitude could be brought to bear on the core.

The lateral stability of the core during an earthquake has been analyzed. The support of the core support plates has been designed to resist a 0.1g horizontal seismic acceleration. Also, steel blocks will be interposed between the core support plate and the vessel in order to limit possible lateral motion of the grid plate and thus the bottom of the core relative to the pressure vessel to an inconsequential value (See Section II. B. 4).

b. Helium Flow Disturbances

(1) Pulsations During Normal Operation

Minor disturbances in the flow may be generated in the helium circuit outside the vessel during normal operation. These disturbances will enter the vessel via the inlet nozzle. The flow splits as it enters the nozzle and the flow affecting the reflector must first pass up along the vessel wall. This upward flow then goes through the opening in the top of the thermal shields and then into the annulus between the thermal shields and also into the annulus between the inner thermal shield and plenum shroud. As the flow travels from the reactor inlet to these two annuli, the velocity of the gas drops from 158 ft/sec to 26 ft/sec. The lower velocity is approximately that of the average velocity in the plenum. This reduction in velocity plus

the turns and restrictions at the top of the vessel will act as a very effective damper on any pulsations in the flow generated outside the vessel.

The gas flows in the annuli above the reflector have only two large obstructions. These two obstructions are the outlet nozzle pipes which connect the plenum to the inner concentric ducts. The ratio of hydraulic diameter of the annulus to the length of flow path from the duct to the top of the reflector is 1:15. This results in the turbulence from the pipe being largely damped out.

(2) Effects of Depressurization Accidents

A pulsation which could affect the core restraint is that which results from a rupture in the primary coolant system. A rupture which causes a rapid increase in flow through the core from bottom to top will result in an increase in restraining force applied by the reflectors to the core, and thus no lateral core motions. This case is covered in paragraph II. B. 9. c. on core levitation.

For the case of a rupture which causes reverse flow down through the core, the reflector will be pushed back as much as 2". Because the reflectors will move back, the top of the core will not be restrained and thus the fuel elements will be free to spread apart somewhat at the top of the core. However, the amount of movement available to the tops of the fuel elements and rod guide tubes will not be great enough for excessive stresses to be generated in them as a result of flexure. Integrity of the fuel elements and control rod guide tubes thus will be maintained.

c. Core Levitation

The HTGR system employs a concentric duct design whereby the returning cool helium completely surrounds the hot helium in the passages between the reactor core and the steam generators, as described in Section II. D. Therefore, any rupture of the outer concentric pipe will cause a reverse flow of helium through the reactor core and will not cause core levitation. Similarly, a rupture of both the inner and outer walls of a concentric pipe will allow the vessel to blow down at about equal rates in both directions and will not develop a large enough pressure drop to lift the core. Thus, the only accident conditions which could cause core lifting forces are a rupture of the cold helium pipe at the outlet of the steam generator or a rupture of one of the fuel handling nozzles.

Each fuel handling nozzle contains a shield plug to the bottom end of which is attached a seal plug (See Section II. B. 5. c). The function of the seal plug is to close the corresponding fuel handling port in the plenum shroud. Each fuel handling nozzle is restrained at about operating floor level to prevent it from lifting high enough to allow complete removal of the seal plug from the port in the plenum shroud in case the nozzle should fracture. Lifting of the seal plug allows the coolant to communicate between the flow channels above the plenum shroud and the interior of the plenum shroud via the ports mentioned. If a nozzle should fracture for some very unlikely reason, the flow through the fracture will consist predominantly of coolant from the flow channels above the plenum shroud (which communicate with the bottom of the core) and only a small amount from inside the plenum shroud. The resulting lifting forces are not sufficient to cause levitation.

The other rupture condition which could cause an upward force on the core is a complete coolant pipe separation at the outlet of the steam generator. Of all possible rupture locations, this condition presents the minimum resistance to flow in the forward direction and the maximum resistance to flow in the reverse direction because of the presence of the helium compressors in this circuit. Conservative calculations have been performed for various rupture conditions and the results indicate that the core rise for this worst condition is less than one inch if the core is completely unrestrained. This limit in levitation results from the very short time interval over which lifting occurs. However, the core will be held down by friction between the core and the tilting reflectors and at the standoff supports. The tilting reflectors are forced against the core by the pressure differential existing across the reflectors during normal operation. Any increase in the pressure differential across the core due to increased upward flow through it will also increase the holding effect of these reflectors. Therefore, it is highly unlikely that any motion of the core would result from this worst rupture condition.

d. Oscillatory Movements

(1) Of the Core as a Whole

Vibration or oscillatory movement of the core as a whole with the reflectors will be precluded by the powerful damping provided by the frictional effects mentioned in Section II. B. 9. a.

Visual observation in the half-scale flow model, described in Section II. J. 3 has shown no oscillatory movement of the core or reflectors, nor have any visible movements been detected resulting from switching the model air flow on and off.

(2) Of Fuel Elements

Tests were made with a full scale cluster of 19 elements. Initially, metallic dummy elements were used. These dummy elements were dynamically equivalent to the actual fuel element, but, being made of metal, lacked the internal damping inherent in graphite. In later tests, the central group of 7 metal dummies was replaced by actual, prototype fuel elements (containing no fuel). The rod clusters were subjected to air flow at Reynolds numbers covering the entire flow range expected in the reactor and extending beyond that range. The mounting of the rods was identical to the manner in which the fuel elements will be mounted in the reactor, except that the metallic dummies had no intermediate spacers. The only effect not duplicated was the heat transfer which would take place in the reactor. Several elements were instrumented. The instrumentation was sensitive enough to clearly record vibrations with amplitudes as low as .001 inch and frequencies up to 100 cps. A detailed description of the test set up, and the procedures followed, is given in Section II. J. 3.

Figure 53 is a schematic cross section of the test chamber used for the vibration experiment. The elements represented by heavy circles were instrumented. The central element was equipped with an internally mounted exciter.

The results of the tests can be summarized as follows:

1. Under no condition of flow did the fuel elements (either metallic dummies or prototypes) start to vibrate.

2. When excited with a single-impact pulse, the resulting vibrations at the natural frequency of the elements (around 20 cps) decayed rapidly. The decay was accelerated by the gas flow, i.e., the flow had a definite damping effect.

3. When the central fuel element was forced to vibrate continuously at its natural frequency, by the internally mounted exciter, the amplitude of the forced vibration decreased markedly with increasing gas flow. Going from zero flow to full flow reduced the amplitude approximately to 1/2 of the no-flow value.

4. When the central element was forced to vibrate very violently, the surrounding gas transmitted enough energy to the adjacent elements to induce very slight vibrations in them. These induced vibrations were of barely perceptible magnitude when the forced excursions of the central element were as large as was possible without having the element actually strike its neighbors.

The conclusion drawn from the outcome of the tests was that there is no mechanism in the coolant flow which could cause fuel elements to vibrate. Rather, the flow has a stabilizing effect and tends to reduce vibrations caused by some extraneous effect.

C. Fission Product Control, Traps, and Helium Purification

1. General Considerations Regarding Fission Product Control

Several mechanisms are used to limit the level of radioactive fission products in the reactor primary cooling system. First, release of volatile fission products from the fuel compacts is delayed until the short-lived products have decayed. Extensive experiments (Section II. J. 2) have demonstrated a moderate delay with uncoated fuel particles and a long delay with coated fuel particles, the latter to be used in the Peach Bottom reactor. Second, most of the condensible fission products which do escape from the fuel compacts will be removed in the cold end of the fuel element by an internal trap. Third, the noble gas and halogen fission products which do not decay within the fuel element are carried by a helium purge stream to charcoal traps external to the reactor pressure vessel. This external purification system is also used to remove chemical impurities from the helium coolant. Fourth, the sleeve of the graphite fuel element is made of a low permeability graphite. This serves to reduce to a very small value the fraction of the fission products which are actually released into the primary coolant.

Although fuel compacts made with coated fuel particles will be used in the reactor, the analysis of the main coolant system activity and the external trapping system activity and heat load are conservatively based on the use of uncoated fuel particles. The reason for this conservatism is that long burnup experiments duplicating end-of-life characteristics have not yet been completed for coated particles. At worst, coated particles would behave as uncoated particles at the end of core life. The experimental values of fission product release rate from uncoated fuel have furthermore been increased by a safety factor of 3 in arriving at the Design Activity (See Appendix B) and the corresponding decay heat generation.

Figure 54 is a schematic of the primary coolant system and the fission product trapping system which summarizes the Design Activity levels within these systems. For comparison, a similar schematic is presented in Figure 55 showing the Calculated Beginning of Life (BOL) Activity levels within these systems. These Calculated BOL Activity levels are based on fission product release from coated particle fuel (see Section II. J. 2 for experimental data on release rates). Appendix B presents detailed information on Design Activities as well as Calculated BOL Activities in the primary system, fuel elements, internal traps, and external traps.

2. Fission Product Control Within Fuel Elements

The fuel elements of the HTGR may be considered to offer four barriers to limit the escape of fission products to the main helium coolant. These barriers are (1) the coated fuel particles, (2) the fuel compact matrix, (3) the purge gas stream, and (4) the low permeability graphite sleeve.

The Research and Development results on fuel compacts containing coated fuel particles presented in Section II. J. 2 indicate that a significant fraction of volatile fission products are held up within the fuel particles themselves. In particular, the GE-309 irradiation capsule data described in Section II. J. 2 indicate that an isotope with a 100-hour halflife, for example, is held up sufficiently long for approximately 97 percent of the decay to ovvur within the fuel compact. Shorter half life fission products show an even higher holdup fraction.

Credit is taken only for fission product holdup of uncoated fuel particles in a graphite matrix, although the more retentive coated particles are expected to be used in the HTGR fuel elements. The holdup from particle coatings may be considered an additional safety factor in the fission product control characteristics from the point of view of normal release of activity to the main helium coolant. This safety factor is significant. The data on the GA-309-5 purged capsule after a burnup equivalent to more than 50 percent of the HTGR end-of-life value show that the main coolant activity in HTGR would be reduced by a factor of 2.5 with the coated particle fuel compacts as compared with uncoated particle fuel compacts.

Fission products which do escape from the fuel compacts immediately encounter the helium purge stream flowing down in the gap and channels between the fuel compacts and the sleeve. This purge stream carries the fission products to the internal trap and finally to the external traps located outside the reactor vessel. Since the graphite sleeve surrounding the fuel compacts is not completely impervious to fission products, some activity escapes through the sleeve into the primary system helium. The primary mechanism for

escape of gaseous fission products through the sleeve is by Knudsen flow. Therefore, the rate of fission product leakage through the sleeve is proportional to the product of the permeability coefficient of the sleeve graphite and the concentration difference across the sleeve. Since the concentration difference is inversely proportional to the purge flow rate, the use of a purge flow in combination with low permeability graphite serves to control the release of activity to the primary system.

The average flow rate of the purge stream is 1.1 lb/hr per fuel element. Analysis shows that if one-half of the fuel elements were being purged at a rate 30 percent above this value and one-half at a rate 30 percent below this value, the over-all leakage of fission products to the main coolant would increase by only 10 percent. The effect of complete loss of purge in a fuel element is described in Section II.A.4.

The low permeability graphite sleeve serves as the outer barrier for limiting escape of fission products from the fuel elements. The helium permeability of this sleeve is 1×10^{-5} cm^2/sec or better. As an example of the retention qualities of this sleeve, only about two parts in 10^4 of any gaseous fission product present within the space between the fuel compacts and the sleeve escapes to the main coolant. The effects on system activities due to cracked sleeves or permeability changes are discussed in Section II.A.4.

The fission products are carried from the active fuel region to the internal trap located in the bottom of the fuel element. The tellurium, cesium, barium, strontium, antimony, and rubidium fission products which reach the internal trap are retained completely and the iodine and bromine fission products are held up for at least 32 days. Krypton and xenon fission products, along with delayed iodine and bromine, are carried on to the external trapping system. The hold-up characteristics of internal traps have been investigated extensively as part of the HTGR R and D program. These experiments are described in Section II.J.2. The internal trap is a cartridge fitted within the fuel element sleeve, and it consists of a graphite cylinder 2.75 inches in diameter by 12 inches long holding reagent material. A total of 16 slots, each 1/8 inch by 13/16 inch by 11 inches long, are machined on the outer circumference of the trap body and serve to hold the reagent material. The reagent is silver-coated charcoal which holds fission products by means of condensation, adsorption, and reaction with silver. Heat generated in the trap by local fission product decay and gamma heating from the core is removed by radial conduction to the outer surface of the sleeve. At this point,

the heat is removed by the relatively cool incoming main coolant. The inventory of fission products in the internal trap is presented in Appendix B.I.

3. Standoff Pins

The standoff pins are hollow stainless steel cylindrical members which are screwed into the core support plate. They serve to locate the fuel elements and to conduct the fission products from the fuel elements to the purge manifold system inside the grid plate. The junction between standoff and grid plate is a simple conical seal, while the junction between standoff and fuel element is effected by having the standoff pin fit closely inside the low permeability bottom connection of the fuel element. The difference in the coefficients of expansion of the stainless steel and graphite will allow a relatively loose fit at fuel loading temperatures and a much tighter fit at operating temperatures. Since the pressure inside the standoff pin is at least 3 psi less than the pressure of the surrounding main coolant stream, any leakage of helium at the standoff pin will be in an inward direction. Calculations indicate that the diffusion of fission products out of either seal will be negligible in comparison with the normal leakage of the fuel elements, even with the highly conservative assumption of diffusion through a stagnant gas rather than back diffusion against an inflowing gas. Therefore, the main function of the seals is to limit the amount of inleakage of purge gas which has, in effect, bypassed the fuel elements. With a design inleakage fraction of 10 percent of the total purge flow through the fuel elements, this requirement presents no difficulties.

A standoff pin could possibly become damaged during refueling operations, or become clogged, or otherwise damaged during normal operation. Therefore, the standoff pins are designed to be removable by a tool operated by the fuel transfer machine. In the unlikely event of a standoff pin being non-removable, the standoff pin will be plugged and the fuel element replaced with a non-fueled graphite element.

The central hole in the standoff is sized to limit the amount of flow through an uncovered standoff pine, thereby allowing for purge system operation during fuel changing and during operations with broken fuel elements.

4. Purging Manifold

The carbon steel core support plate contains a system of cross holes connecting all the standoff locations. These holes

carry the purge gas from the fuel elements to two closed channels welded around the periphery of the grid plate. A pipe connected to each peripheral channel then carries the purge stream out of the reactor vessel to the external traps.

The purge manifold normally operates at least 3 psi below the pressure of the surrounding main coolant stream. Therefore, any leakage of helium will be into the purge manifold, and fission products must diffuse against an inflowing stream of helium to escape from the purge manifold. Consequently, any small leaks in the manifold system should not allow enough fission products to escape to raise significantly the activity of the main coolant stream. If a large leak occurred in one of the pipes leading from the core support plate, the failed line can be isolated and operation of the reactor can continue with the full purge stream passing through the remaining purge line.

5. Purge Line

Because of the high concentration of radioactivity in the two parallel purge lines between the reactor pressure vessel and the fission product trapping system these lines will be doubly contained, i.e., they will consist of a pipe within a pipe. The outer annulus will contain helium at a slightly higher pressure than the reactor system pressure, in order to insure that leakage will be inleakage if any small leak should occur within the inner pipe. A suitable excess-flow shutoff will be provided to insure that a gross failure of the inner pipe will not result in appreciable quantitles of helium at a higher pressure being introduced into the reactor coolant helium system.

6. External Fission Product Trapping System

a. General Description

The fission product concentration in the purge line is given in Table 9. These activities are based on experimentally determined fission product release characteristics of uncoated particle fuel compacts, and the fission product retention characteristics of the internal traps, as discussed in Section II. J. and Section II. C. 2. Since coated particle fuel will be used in the reactor, use of fission product release data for uncoated particles is a convervative design basis. In addition, these data on fission product release rates have

TABLE 9

FISSION PRODUCT CONCENTRATIONS
IN FUEL ELEMENT PURGE STREAM

Isotope	Half-life	ppm (by volume)	Design Activity Curies/lb of He
Br^{81}	stable	3.3×10^{-4}	-
Kr^{83m}	112m	3.3×10^{-4}	6.3×10^{1}
Kr^{83}	stable	1.6×10^{-2}	-
Kr^{84}	stable	2.8×10^{-2}	-
Kr^{85m}	4.4h	5.4×10^{-4}	4.4×10^{1}
Kr^{85}	10.3y	8.0×10^{-3}	3.1×10^{-2}
Kr^{86}	stable	5.1×10^{-2}	-
Kr^{87}	78m	5.2×10^{-4}	1.4×10^{2}
Kr^{88}	2.8h	9.3×10^{-4}	1.2×10^{2}
Kr^{89}	3.2m	1.6×10^{-4}	1.1×10^{3}
Kr^{90}	33s	5.0×10^{-5}	1.9×10^{3}
I^{127}	stable	6.4×10^{-4}	-
I^{129}	stable	2.6×10^{-3}	-
I^{131}	8.05d	1.9×10^{-3}	3.5
Xe^{131m}	12d	3.2×10^{-5}	3.9×10^{-2}
Xe^{131}	stable	6.1×10^{-2}	-
Xe^{132}	stable	9.1×10^{-2}	-
I^{133}	20.9h	1.6×10^{-5}	2.7×10^{-1}
Xe^{133m}	2.3d	1.8×10^{-4}	1.2
Xe^{133}	5.65d	9.1×10^{-3}	2.4×10^{1}
Xe^{134}	stable	1.5×10^{-1}	-
Xe^{135m}	15.3m	7.0×10^{-4}	9.8×10^{2}
Xe^{135}	9.13h	3.4×10^{-3}	1.3×10^{2}
Xe^{136}	stable	1.3×10^{-1}	-
Xe^{137}	3.9m	2.5×10^{-4}	1.4×10^{3}
Xe^{138}	17m	4.9×10^{-4}	6.1×10^{2}
Xe^{139}	41s	6.9×10^{-5}	2.2×10^{3}
Xe^{140}	16s	1.8×10^{-5}	1.4×10^{3}

been increased by a safety factor of 3 over the experimentally determined values, and the iodine delay in the internal traps has been taken as 7 days (compared to the expected holdup of 32 days). These further safety factors have been applied in order to insure that the heat removal capacity of the external purification system will be capable of accommodating perturbations in fission product release from the fuel elements. Table 10 gives the total fission product activity in the fission product removal system and also the radiation heat loads. The tabulation of radiation heat loads differentiates between beta and gamma heating.

The isotopes Kr^{85}, Sr^{90}, Y^{90}, Cs^{137}, and Ba^{137m} are either quite long-lived or are the daughter products of long-lived isotopes. In the case of Sr^{90}, Cs^{137}, Y^{90}, and Ba^{137m}, the maximum possible accumulation is that for the design life of the reactor plant; the values corresponding to this period of operation are given in Table 10. Kr^{85} will be removed periodically from a liquid nitrogen refrigerated system. The activity inventory and heating rate given in Table 10 for Kr^{85} are based upon an assumed six-month accumulation.

The activities and heat loads given in Tables 9 and 10 represent the design basis for the fission product trapping system. For purposes of comparison, the activities and heat loads which might actually be expected in the trapping system, based on recent experimental results for coated-particle fuel, are presented in Appendix B.II. These activities and heat loads are approximately a factor of 7 lower than the corresponding design values.

TABLE 10

ACTIVITIES AND RADIATION HEAT LOADS
IN THE PURIFICATION SYSTEM

Isotope	Half-life	Design Activity (10^6 Curies)	Beta Heat (Btu/hr)	Gamma Heat (Btu/hr)
Kr^{83m}	112m	0.17	140	3
Kr^{85m}	4.4h	0.28	1,400	900
Kr^{85}	10.3y	0.019	92	1
Kr^{87}	78m	0.27	7,300	5,800
Kr^{88}	2.8h	0.48	3,900	19,900
Rb^{88}	17.8m	0.48	20,200	10,500
Kr^{89}	3.2m	0.087	2,500	4,200
Rb^{89}	15.4m	0.087	1,100	4,300
Sr^{89}	50.4d	0.087	970	-
Kr^{90}	33s	0.024	670	-
Rb^{90}	2.7m	0.024	340	2,600
Sr^{90}	28y	0.011	40	-
Y^{90}	64.3h	0.011	200	-
I^{131}	8.05d	0.96	3,700	7,800
Xe^{131m}	12d	0.024	78	3
I^{133}	20.9h	0.008	79	90
Xe^{133m}	2.3d	0.090	360	66
Xe^{133}	5.65d	4.68	15,100	2,800
Xe^{135m}	15.3m	0.36	540	3,400
Xe^{135}	9.13h	2.19	14,600	11,100
Xe^{137}	3.9m	0.13	2,600	3,200
Cs^{137}	30y	0.055	210	-
Ba^{137m}	2.57m	0.051	70	590
Xe^{138}	17m	0.25	2,900	7,900
Cs^{138}	32.2m	0.25	5,400	10,900
Xe^{139}	41s	0.036	1,200	-
Cs^{139}	9.5m	0.036	1,100	550
Ba^{139}	82.9m	0.036	550	280
Xe^{140}	16s	0.009	240	-
Cs^{140}	66s	0.009	350	260
Ba^{140}	12.8d	0.009	54	36
La^{140}	40.3h	0.009	93	450
		TOTAL	88,000	98,000

A process flow sheet of the external fission product removal system is shown in Figure 56. Iodine and bromine are removed by adsorption on charcoal at near room temperature; since adsorption of the halogens on charcoal at this temperature is very strong, the charcoal bed can operate for many years without breakthrough occurring. Radioactive xenon and krypton are removed by a series of charcoal adsorption beds which are run at saturation. The noble gas fission products (except Kr^{85}) are removed from the helium by delaying them within these adsorption beds, thus permitting the fission products to decay within the trapping system. Seven charcoal delay beds are provided in the system for removal of xenon and krypton.

A side stream is taken through a liquid-nitrogen-cooled adsorption system (also shown on Figure 56), which is used to remove Kr^{85}, the only noble gas fission product whose half life is too long to permit its removal by a system of delay beds. This liquid-nitrogen-cooled system also removes chemical impurities, in particular, nitrogen, argon, and carbon monoxide.

Leaving the reactor through the purge lines the helium enters a watercooled heat exchanger E-301, which removes the sensible heat from the gas. A complete spare E-302, in parallel, is furnished for this heat exchanger. The cool gas then enters a water knockout drum T-301 which is used to remove liquid water which may have condensed out following a major steam leak. The process helium then passes into a water-cooled condensibles trap A-301 which is used to remove iodine and other non-noble gas fission products which might be present. This unit A-301 is, in effect, an installed safety factor. The experimental evidence discussed in Section II.J.2 clearly indicates that the release from the fuel elements and the holdup of non-volatile fission products in the internal trap is such that iodine is the only significant condensible present at this point, and the following adsorption beds could readily be designed to accommodate the iodine release. However, this direct-cooled trap is furnished in order to insure that a mechanism is available to remove any unanticipated release of condensible fission products, due to accident conditions, in such a manner that the resultant heat load can be accommodated readily without compromising the efficiency of the krypton-xenon trapping system. (Upon completion of the current experimental program on fission product release under all reactor operation conditions, the need for A-301 will be re-evaluated. It may be eliminated at that time.)

The helium stream then enters a precooler E-303 which cools the gas entering the first charcoal delay bed A-302. No direct cooling is provided for A-302, i.e., the cool process gas is used to remove fission product decay heat generated within this delay bed. This is done primarily to make it possible to construct the delay bed in a very simple manner and thus insure the reliability of this unit in service. Leaving A-302 the process helium enters an exactly identical combination precooler and delay bed E-304 and A-303.

Leaving delay bed A-303, the process gas then enters a regenerative feed-effluent heat exchanger E-305, which is used to precool the gas before it enters a series of five low temperature charcoal delay beds A-304, A-305, A-306, A-307 and A-308. A complete spare E-306 is furnished in parallel with E-305 to be used in the event of icing of heat transfer surfaces; E-306 is not normally in operation. This low temperature portion of the delay bed system also consists of separate heat exchangers and delay beds, again in order to make possible simplicity of construction and consequent increased reliability of operation of the delay beds.

The cooling water system for the fuel element purge helium cooler E-301, the condensibles trap A-301, the first and second water-cooled precoolers, and the emergency trap cooling system (see Figure 56), is designed with a storage tank of cool water in the cooling system which can provide normal cooling without any operator action or reliance on outside power for a period of approximately one hour after complete loss of electrical power. Water fed from the storage tank to these heat exchangers is by gravity feed. A second storage tank of sufficient capacity to receive the one hour's flow of cooling water is provided. In the unlikely event that electrical power is not restored and the emergency diesel cannot be brought on line within one hour, an alternate supply of cooling water will be available from a diesel-driven fire pump. [illegible]

Temperatures, flow rates, heat loads, and delay times of both xenon and krypton in the fission product trapping system are shown on the process flow sheet, Figure 56.

A computer program has been used to predict the steady-state performance of the krypton-xenon delay beds (A-302, A-303, A-304, A-305, A-306, A-307 and A-308). In this program, the adsorbent in each trap is divided into a number of small segments, typically 100 to 1000 segments per trap. The following calculational steps are used for each segment: (1) an estimate of the average

temperature of the segment is made; (2) the krypton and xenon delay times in the segment are calculated, using the exponential dependence on inverse temperature which is observed experimentally for the dynamic adsorption coefficients (See Section II.J.2); (3) the activity of each krypton and xenon isotope in the segment is calculated from the delay times; (4) decay heat generation rates are calculated for each krypton and xenon isotope and its daughter products, and the heat generation rates are summed; (5) temperature rise of helium through the segment is calculated from the decay heat load; (6) average temperature of the segment is calculated and compared with the original estimate. If the estimated and calculated temperatures do not agree within 0.5° F, the procedure is repeated using the calculated temperature as a new estimate. Successive segments are analyzed in this manner. The characteristics of the physical situation are such as to preclude the possibility of cumulative errors in temperature. Temperature reduction of helium in the heat exchangers is calculated using coolant temperature, heat transfer coefficient, and surface area of each heat exchanger. A special iterative procedure is used to analyze performance of the regenerative feed-effluent exchanger.

Output of the computer program includes: (1) activities in each trap, (2) helium temperature leaving each trap, (3) krypton and xenon delay in each trap, (4) krypton and xenon activities leaving the system, and (5) resulting primary system activities. Detailed distributions of both design and expected activities and decay heat loads in the system during normal operation are presented in Appendix B.II Besides predicting normal operating performance of the fission product trapping system, the program has been used to analyze certain abnormal conditions where the assumption that steady-state conditions exist is acceptable.

The experimental data on which the calculated holdup in the trapping system has been based are summarized in Section II.J.

The side stream which is used to remove Kr^{85} takes partial flow to a liquid-nitrogen-cooled adsorption bed A-309. This bed is not operated as a delay bed, i.e., it is not saturated. The flow rate to this Kr^{85} removal trap has been selected sufficiently high to maintain the level of Kr^{85} activity in the primary coolant system below the specified limit of 50 curies. Thus, it is possible to run with this liquid-nitrogen-cooled system off-line for long periods of time without exceeding allowable levels of Kr^{85}. For this reason no spare heat exchangers or traps are provided within this system.

Kr^{85} is generated at the rate of approximately 77 curies per day. Accumulated Kr^{85} will be periodically removed from the liquid-nitrogen-cooled trap by valving off this unit, permitting it to heat up, and removing the desorbed Kr^{85}. The Kr^{85} will normally be shipped offsite for disposal.

Filters are provided in the helium purification system for removal of graphite dust and aerosols.

During normal operation, the effluent from the fission product removal system enters a purified helium tank. Clean helium from the purified helium tank is supplied to the main helium compressors and to the reactor control rods as purge gas. (A portion of the purge gas supplied to the main helium circulators is returned to the helium purification system, while the remainder enters the primary system by leakage through the shaft seal. All of the purge gas supplied to the control rods passes into the primary system.) A portion of the flow from the purified helium tank passes directly to the primary system. Purified helium is also used for purging of fuel handling equipment furing refueling, and to actuate primary system valves under emergency conditions, but these functions do not require any helium flow during normal operation.

b. Handling, Storage, and Disposal of Trapped Fission Products

It is anticipated that the traps will be able to operate for the entire life of the reactor plant without replacement. However, it is recognized that a mechanical failure or a decrease in performance due to interference effects resulting from chemical contaminants may require replacement of a delay bed. Therefore, the fission product removal system is being designed and laid out on the assumption that each trap must be removable.

Where necessary, radiation shielding for traps is provided to permit personnel access five days after reactor shutdown. Vent lines are provided to permit venting each component prior to removal. In addition, purge connections are also provided so that a trap can be purged with clean helium, if necessary, prior to removal.

In the event that replacement of a trap is necessary the reactor will be shut down and purge flow continued for a waiting

period. At the end of this waiting period, personnel can enter the compartment, vent the trap to the low pressure helium tank, cut the piping, and seal off the open pipe. If necessary, the trap can first be purged with helium from the purified helium tank to remove any gas-borne activity present in the tank; the purge effluent will be taken to the low pressure tank. The trap can then be removed from the compartment. In the event that the component containing fission products is to be used as a shipping container, it will be designed so as to meet all pertinent regulations.

7. Steam Generator Purge Purification System

The primary chemical contaminants in the main helium are expected to be nitrogen, argon, hydrogen, carbon monoxide, and water vapor. The sources of these contaminants are unpurged air during the helium filling operation and from maintenance operations, degasification products from the core graphite and metal surfaces, and moisture in-leakage from the steam generator. Nitrogen and argon will come primarily from air contamination. The degasification products of graphite are primarily hydrogen, carbon monoxide, and water. A chemical impurity cleanup system is furnished as part of the helium purification system. This system is capable of maintaining the concentration of chemical impurities at an acceptable level during reactor operation.

A purge stream is taken from each steam generator through the chemical impurity removal system. A flow sheet is given in Figure 57. The helium in the dump tanks and the low pressure tank can also be processed through this system, which consists of an oxidizer A-311 in which CO and H_2 are converted to CO_2 and H_2O, a condenser which removes the bulk of the water, and two molecular-sieve beds in parallel, in which the remaining H_2O and most of the CO_2 are removed. The plate-out trap A-314 is used to reduce plate-out of condensible activity in this system. Additional chemical purification is accomplished by the low temperature liquid nitrogen traps, which form part of the fission product removal system. The effluent from the chemical cleanup system is taken through a portion of the fission product removal system, in order to remove any residual fission product activity before the gas enters the purified helium tank.

Table 11 lists the significant helium contaminants together with the normal levels.

TABLE 11

NORMAL CONCENTRATION OF CHEMICAL IMPURITIES IN REACTOR HELIUM

Impurity	Concentration (ppm by volume)
Hydrogen	10
Carbon Monoxide	10
Carbon Dioxide	1
Water	1
Methane	1
Nitrogen	10
Argon	0.25
A^{41} (1.82-hour)	5×10^{-10}
H^3 (12.3-year)	1.4×10^{-4}
Oil	0.002

Hydrogen will be removed by a copper oxide bed A-311 in the steam generator purge stream, where it is converted to water vapor. The copper oxide bed will be designed for one year's operation under normal conditions without regeneration, and for the conversion of all of the hydrogen produced as a result of a major steam leak. The copper oxide bed is regenerated by taking if off line and passing oxygen through it. The water produced in the oxidizer during operation is removed by cooling the carrier helium in a heat exchanger E-317 and removing the condensate by means of a water knockout drum T-302. The remaining water present in the helium is removed in either of two molecular sieve adsorbers in parallel, A-312 and A-313. These adsorbers are alternately in use so that regeneration may be carried out as required.

The adsorber beds are regenerated periodically with heater purified helium sweep gas which subsequently passes through a condenser, water knockout drum and caustic scrubber unit which removes the carbon dioxide. The effluent helium from the scrubber unit then joins the steam generator purge gas and is taken through the condenser; E-317 and knockout drum, T-302.

After a major steam leak some water may enter the fuel element purge stream. Most of this water is removed by the knockout drum T-301, shown in Figure 56. The remainder of the water entering the external fission product trapping system is removed by

diverting the flow through the steam generator purge purification system. The effect of water on the purification system following a steam leak is further discussed in Section III. C. 4. c.

The major portion of carbon monoxide will be removed by the copper oxide bed referred to above for the removal of hydrogen. The carbon dioxide produced from carbon monoxide in the oxidizer during operation is removed in either of the same two molecular sieve adsorbers used for the removal of water produced in the oxidizer. A significant portion of the carbon monoxide will also be removed in the liquid-nitrogen-cooled adsorber section of the fission product trapping system.

Carbon dioxide in the reactor helium will be removed by either of the two molecular sieve adsorbers referred to above. A very small quantity of the carbon dioxide may be removed in the liquid-nitrogen-cooled section of the fission product trapping system.

Methane, nitrogen and argon will be removed in the liuqid-nitrogen-cooled section of the fission product trapping system. This section consists of two adsorber beds in series. The first adsorber bed A-309 will contain Kr^{85}, methane, carbon monoxide, nitrogen, and argon; the second adsorber A-310 will contain carbon monoxide, nitrogen and argon only.

Most of the oil will be condensed from the purified-helium-compressor effluent stream by means of a water-cooled heat exchanger E-320 followed by a demister unit. Removal of the trace quantity of oil remaining can be accomplished by passing the helium through an oil removal filter containing molecular sieve pellets of charcoal at room temperature.

8. Purified Helium Compressors

Two helium gas pressure-boosting compressors are provided in the helium purification system (Units C-301 and C-302 in Figure 56); one of the two compressors will be in service and the other on standby duty. The compressors boost the pressure of the helium to the pressure of the purified helium tank from which it can be distributed to the various circuits requiring purified helium. The compressor operating conditions are summarized in Table 12.

TABLE 12

APPROXIMATE COMPRESSOR OPERATING CONDITIONS

Fluid	Helium
Suction Pressure	295 psia
Suction Temperature	100 F
Discharge Pressure	535 psia
Flow Rate	1380 lb/hr (max)

The compressors are presently planned to be of the rotary positive displacement type, hermetically sealed or with shaft seals that permit no leakage of helium. Oil lubrication will be utilized.

These compressors normally handle helium with very low activity. Under some transient conditions, the helium may contain moderately high levels of xenon and krypton, but no plate-out of activity will result. Therefore, normal maintenance techniques can be used on these compressors.

If the compressor in service should fail, the standby unit will be used to maintain purge flow while the reactor is being shut down and during repair of the defective compressor.

9. Minor Malfunctions

Major malfunctions of the trapping system and helium purification system are discussed in detail in Section VII. C. Several minor malfunctions are possible which are either tolerable for extended periods of time, or which can be guarded against and corrective action taken immediately by conventional instrumentation and control systems. The following are typical minor malfunctions:

a. Loss of Liquid Nitrogen Cooling System

The liquid-nitrogen-cooled system is used to remove Kr^{85}. The flow rate through this system has been selected such that the equilibrium concentration of Kr^{85} in the primary coolant is below the specified maximum level. It is anticipated that the Kr^{85} inventory in the main helium system will normally be maintained at approximately 25 curies. If the liquid nitrogen system requires shutdown due to a malfunction, the primary system Kr^{85} level will not reach the 50 curie design value for ten weeks. Thus, it is possible for the purification system to operate with the liquid-nitrogen-cooled trap out of service for long periods of time without exceeding the permissible levels of radioactivity in the helium system. The liquid-nitrogen refrigeration

system will be located so as to be readily accessible for maintenance or repair. If circumstances delay repair of this unit, bulk liquid nitrogen can be used.

b. Carry-over of Water and Carbon Dioxide from the Molecular-Sieve Beds

The mode of operation of molecular-sieve beds A-312 and A-313 (see Figure) is for one of the pair to be on the adsorption cycle for removal of water and carbon dioxide while the other is either being regenerated or standing by after being regenerated. During the regeneration cycle the majority of the desorbed water is removed by a condenser and water knockout drum while the remaining desorbed water and CO_2 enters a caustic scrubber unit in which the CO_2 is removed. The sweep gas is then taken through the condenser, E-317, and knockout drum, T-302, and then enters the other molecular sieve bed which is on the adsorption cycle. The caustic solution will be replaced at approximately 6-month intervals. The regeneration cycle of the beds will be short relative to the breakthrough time of water and CO_2, but it is possible that breakthrough might occur through maloperation. The exit helium from the molecular sieve beds will be monitored for water and CO_2; upon detection of either water or CO_2, regeneration will be initiated.

In the unlikely event of water or carbon dioxide carry over from these beds, the purification system design permits this carryover to be purged from components following the molecular-sieve beds. Water carryover will be frozen in passing through the feed effluent exchanger, E-305, and most of the ice formed will remain here. This exchanger has a spare, E-306, which can be put in operation while the water is removed from E-305 by a warming and helium purging operation. Any carbon dioxide carried over together with any ice which may have blown through E-305 will enter the first low temperature delay bed, A-304. The carbon dioxide will be adsorbed by the charcoal as a vapor while the ice will remain in the solid phase. A bypass around A-304 will permit removal of water and carbon dioxide from A-304 by a warming and helium purging operation.

D. Primary Coolant System

1. Helium Circuit

a. General Description

The primary coolant system consists of the reactor, two steam generators, two helium compressors and their related piping and auxiliaries. The steam generators and helium compressors are arranged to form two parallel loops for circulation of the helium coolant, with each loop designed for half the total coolant flow rate of 439,600 lb/hr. Helium flow through the reactor core is common to both loops as shown in Figure 58.

Helium leaving the reactor core divides into two streams, each of which supplies one of the circulating loops. For each loop, heliuim at 1354°F leaving the reactor vessel flows through the inner passage of a concentric pipe; the annulus between pipes serving as the cold helium return to the reactor.

Hot helium enters the steam generator at the side of the vessel and passes horizontally across the superheater, evaporator and economizer tubes generating high-temperature, high-pressure steam. The cooled helium then flows through the annulus between the generator shell and an internal shroud, exiting from the generator at 622°F at full load.

The cool helium leaves the generator and flows through a non-concentric pipe to a helium compressor. From the compressor, the helium flows through a non-concentric pipe to the annulus formed by the concentric pipes and on to the reactor vessel. Compression and regenerative heating in the concentric piping raises the helium temperature approximately 12°F before arrival at the reactor inlet. Shutoff valves at the steam generator inlet and at the compressor inlet and outlet can isolate each steam generator and helium compressor from the reactor.

Each coolant loop contains a bypass filter which is located in parallel with the helium compressor. Approximately one per cent of the total recirculating helium stream from the compressors is bypassed through the filter circuits.

After entering the reactor vessel, the helium flow divides. Part of the flow enters the annular spaces between the thermal shields, cooling them and the inside surface of the reactor vessel, and

the remainder of the flow passes down through the reflector. Both streams mix below the core grid plate and then pass up through the core. The helium is heated while passing through the core and leaves the reactor from the hot gas plenum through the internal pipe of the concentric nozzle, completing the loop.

Within the reactor, approximately 1000 lb/hr of the main helium stream is withdrawn from the main coolant system through the fuel elements. This purge stream goes to the helium purification system for fission product trapping and chemical removal. The resulting purified helium is returned to the main coolant system in three major streams: the buffer helium to the helium compressors, buffer helium to the control rod drives, and the pressure control helium.

The main coolant system operates normally at a constant pressure of 335 psig at the compressor discharge. The control system admits helium as described under Control Systems, Section II. G. 5. In the event of an overpressure, a combination of several safety devices protects the system. At 390 psig, back-pressure-operated dump valves open to blow helium to the dump tanks in the helium handling system. These dump valves are tight-seating valves located in the cold helium downstream of each steam generator. They serve to protect the boiler-compressor-pipe system from overpressures due to a steam leak into the helium.

Should these valves fail to operate and the pressure continue to rise in the piping loops, ASME Code relief valves will relieve to the secondary containment. These valves are arranged in three sets, each with a full-sized spare, for the reactor and for each steam generator.

The plant safety system is so designed that only a steam leak can cause the relief valve system to open, and this will only occur if several other automatic dump and isolation actions do not take place correctly. The Plant Protective System is described in detail in Section II. G. 6.

b. Equipment Description

(1) Helium Compressors

Two horizontal, single-stage, centrifugal compressors circulate helium through the main coolant loops. Each compressor is designed to circulate 33, 800 cfm of helium at 325 psig and

628 F inlet with a pressure rise of 10 psi. Design speed is 3500 rpm. A cross-sectional drawing of the design being used is shown in Figure 59.

Each compressor is driven by an electric motor through a variable speed fluid coupling. The fluid coupling provides speed control for regulation of the main coolant flow. An auxiliary drive motor is included in the design to operate each compressor from the emergency diesel-generator set to ensure shutdown cooling in the event of a failure of all normal power.

A helium-buffered, oil-flooded, floating bushing shaft seal is used to seal the compressor shaft. The compressor is designed with an overhung impeller requiring only one shaft seal. Purified helium from the Helium Purification System is injected to internal shaft labyrinths to provide buffer helium between the main coolant helium and the seal oil. A static shutdown seal is included in the design.

A separate seal oil system for each compressor supplies seal oil for the shaft seal. The system includes filters, coolers, instruments and controls to regulate pressures and flows of seal oil and buffer helium. Degasifiers separate the seal oil and buffer helium for reuse.

Each seal oil system has two electric motor driven pumps. One pump serves as a standby pump and is automatically started on loss of the main pump or the inability of the main pump to supply sufficient oil to the system. The standby pump is powered from an emergency power source to insure seal oil supply in the event of loss of plant power.

A common pressure lubrication system is provided in each loop for the compressor and drive motor. Each lubrication system includes two electric-motor-driven pumps. One pump serves as a standby pump and is automatically started on loss of the operating pump or the inability of this pump to supply sufficient oil to the system. The standby pump is powered from an emergency power source to insure lube oil supply in the event of loss of plant power.

Each fluid coupling is provided with its own combined hydraulic and lubricating oil system. Each system includes a shaft driven oil pump and a separate electric-motor-driven oil pump. The electric motor driven pump is automatically started if the shaft driven pump fails to maintain adequate oil pressure.

Supervisory instrumentation, alarms, and interlocks are provided to properly monitor and protect the compressor and drive components. In addition to these major alarms and interlocks, the supervisory instrumentation indicates all necessary pressures, temperatures, flows, motor current, and vibration to properly monitor the unit operation.

A compressor will be automatically shut down by high motor current, isolation of one coolant loop, and low lube oil pressure or seal oil supply. Alarm warnings will permit manual shutdown of a compressor to prevent damage. The outage of a compressor will require shutdown of the reactor.

(2) Concentric Piping and Internal Insulation

The piping and valves are designed to the requirements of the ASA Code for Pressure Piping B31.1, Section I, Power Piping systems, and all nuclear case rulings. In addition to all code requirements, the piping and valves will meet rigorous welding, ultrasonic testing, stress analysis, and leak tightness specifications.

The piping for the reactor inlet and outlet helium flow consists of two concentric pipes; 30-inch nominal inner pipes for the hot helium and 42-inch nominal outer pipes. See Figure 60. The cool inlet gas is carried through the annular passages between the inner and outer pipes. The inner pipes are carbon steel pipes lined with a stainless steel thermal barrier. The thermal barrier consists of closely spaced layers of corrugated or dimpled stainless steel with a stainless steel inner liner. The barrier is installed in sections arranged to permit thermal expansion and to vent the spaces in the barrier when pressurizing and depressurizing the system. The performance of this type of thermal barrier has been well established experimentally. Thermocouples are provided to monitor the inner pipe temperature. The barrier will maintain the pipe wall under 700 F during normal operation and accident conditions. The inner pipe is designed to withstand internal and external pressure differentials imposed by operating or accident conditions. The external pipes are also carbon steel, designed to Code requirements for 725 F design temperature and 450 psig design pressure. The outer pipes are externally insulated to limit heat losses.

(3) Non-concentric Piping

The piping for the cooled helium between the steam generators and compressors and concentric pipe is 30-inch-diameter carbon steel, designed to code requirements for 700 F design temperature and 450 psig design pressure. The pipes are externally insulated to limit heat losses.

Thermal expansion of the coolant system is absorbed by bends and loops in the 30-inch-diameter piping. The size and complexity of the loops are determined by the limited loads and moments which may be put on the compressor nozzles.

(4) Isolation Valves

Isolation valves are provided in the hot gas pipes between the reactor and steam generators, and in the cooler pipes at the compressor suction and discharge.

(a) Reactor Outlet Valves

The valve for the hot gas line, as shown in Figure 61, is installed in the concentric piping and is essentially a pipe-line conduit gate valve with a stainless steel thermal barrier provided on all surfaces exposed to the hot helium stream and an outer jacket body for the reactor inlet gas. The valve discs close only the inner pipe carrying reactor outlet gas. The reactor inlet gas passes around and cools the inner valve body. The pressure-containing parts of the valve, the gate seats, and moving parts, are maintained at relatively low temperatures by the effect of the thermal barrier, the conduit bridge which isolates the flowing hot gas in the open position, and the flow of cooler helium over the chamber surrounding the valve body and gate. In addition, a small flow of cooler helium is established through the chamber and into the hot helium stream by way of the gap between the conduit bridge and valve seat. Thermal analysis of the valve shows that under normal operating conditions the maximum temperature at the seats, disc and flow barrel will be less than 900 F, and the inner and outer bodies less than 700 F. The maximum temperatures at any part during the pressure loss accident will be under 1000 F. When one valve is closed and the other loop is operating for afterheat removal, the maximum temperature at any part in the inner pipe, valve body, or valve disc will be under 1000 F.

The isolation valves in the hot lines serve the following operating and maintenance functions:

1. To isolate a rupture in the helium system.

2. To isolate a steam leak in one of the boilers.

3. To permit maintenance on the boiler and piping in one of the loops while the other loop is operating at sub-atmospheric pressure for afterheat removal.

4. To permit isolation of the boiler for startup and maintenance testing.

The valves are designed to close in three seconds. The time for steam leak detection and for transmission of an actuation signal is less than five seconds, which allows a leaking steam generator to be isolated in eight seconds or less. Closing the valves following a steam leak will minimize the steam graphite reaction damage to the core.

(b) Compresssor Inlet and Outlet Valves

Valves in the cold lines at the compressor suction and discharge, see Figure 62, permit isolation of the compressors for maintenance and decontamination. The compressors will require bearing and seal inspection and possible maintenance at not greater than annual intervals. The design of the bearings and seals is such that circulator decontamination is not required before maintenance. However, decontamination connections will be provided on the circulator casing for use in decontaminating the circulator in the event the impeller has to be removed.

In addition to providing isolation of the compressor, the valve at the compressor suction is used to isolate the steam generator for maintenance and to throttle for flow control during plant startup or other low load operations. The compressor discharge valve is used for emergency reactor isolation in addition to compressor isolation.

(c) Safety Considerations

The control of the valves for emergency loo isolation is discussed in Section II. G.6.

All valves have the special features of hermetically sealing all leakage paths to the atmosphere by welding. All valves are actuated by identical double-acting helium cylinders which are mounted at the top of the valve bodies by seal-welded flanges. The disc on all valves is below the valve port in the open position, providing a gravity fail-open feature to prevent loss of reactor coolant flow. The valve actuation helium is normally supplied from the purified helium storage tank. An emergency bottled helium supply automatically cuts in if the pressure from the purified helium storage tank falls.

The hot valve design incorporates features so that loss of the internal insulation will not result in failure of the pressure-containing parts.

(5) Bypass Filters

The main coolant bypass filters are located in the compressor bypass of the main helium coolant piping to collect graphite dust and other particulate matter, some of which will be radioactive. See Figure 63.

The bypass streams in which the filters are located carry a flow of helium equal to one percent of the maximum total flow at normal operating conditions. The filters separate from this flow 92 percent of all graphite dust and other particulate matter over 5 micron size.

The filters are of the dust collector type which are designed to use centrifugal force to effect a positive separation of solids. The solids-bearing gas enters the side of the vessel tangentially thus importing a centrifugal motion to the gas. The solid particles are thrown outward and downward, while the clean gas rises and leaves through the top of the vessel.

The filters are of welded construction in strict accordance with all applicable codes. They are tested with a mass spectrometer for helium leak tightness and all welds are radiographed.

The filters will be located behind shielding. There are two dust outlet valves on each collector. These valves are located below the floor of the filter room; Figure 63 illustrates the layout.

By monitoring the radioactivity and dust level in the spool piece between the valves, it will be possible to determine when to dispose of the accumulated dust.

The dust is dumped to the shielded container. When required it will be removed and hauled offsite for disposal.

2. Steam Circuit

a. General Description

Two helium circuits, each containing one forced recirculation type steam generator, cool the helium from 1352 F to 622 F and generate a total of 365,500 lb/hr of superheated steam at 1544 psig and 1005 F. See Figure 58.

Each steam generator is a vertical shell and tube type unit and contains separate economizer, evaporator and superheater sections in a single shell. For each loop a separate piping system interconnects each steam generator, steam drum and recirculation pump. The separate tube banks are enclosed by an internally insulated cylindrical shroud of stainless steel. Hot helium enters the steam generator through a concentric inlet nozzle and passes in cross flow through the tube banks. The cooled effluent helium then flows between the internal shroud and external shell before being discharged from the steam generator. This arrangement blankets the external pressure-containing shell with cool helium and permits the use of carbon steel of moderate wall thickness.

Each vertical, constant-speed, recirculation pump is designed for a 4 to 1 recirculation ratio at full design load. The pump is located in the steam drum downcomer and is supported by its inlet and discharge piping. The pump recirculates the 604 F water over the full range of operation at a constant flow rate.

To provide natural recirculation following loss of the recirculation pump due to power or mechanical failure, the steam drum liquid level is maintained 35 feet above the top of the main steam generator tubesheet. During emergency shutdown a heat removal rate of 0 to about 50 percent of design load can be maintained with stable natural recirculation boiling.

Feedwater enters the economizer section of the steam generator about 1587 psig and 425 F at full load. After heating in the economizer, the feedwater enters the steam drum where it is mixed with the recirculating bulk water. The mixture flows through the downcomer and is pumped to the evaporator section where about one-fourth of the water flow is evaporated. The steam-water mixture then enters the steam drum through the riser.

The steam separated from the water passes through the steam purification equipment in the drum and then passes through the superheater section. After leaving the superheater the steam from each generator flows through the control desuperheaters to the plant turbine generator, in separate steam headers.

Control of feedwater flow, steam pressure, and temperature is covered under II. G. 5, Control Systems. Basically, superheater outlet temperature is controlled by means of helium temperature. Steam pressure is controlled by means of helium flow. Feedwater flow is regulated by a conventional three-element control system, spray type desuperheaters are used in the superheater outlet piping. On a sudden decrease in load, such as a turbine trip, these will be required to keep the final steam temperature from rising above 1005 F.

The steam generators are each supplied with conventional steam safety valves as required by the ASME Power Boiler Code. The two drum safety valves and the superheater outlet safety valve all discharge into the containment. A back-pressure-operated steam dump valve, set at a lower pressure, is provided for each steam generator to prevent the steam discharge into the containment by dumping steam outside the containment. As described under Plant Protective Systems (see section II. G. 6), when a tube leak occurs a moisture-actuated loop isolation requires the steam pressure to be reduced rapidly, thus decreasing the total water inleakage and the resultant pressure rise in the helium side of the steam generator loop.

b. Equipment Description

(1) Steam Generators

The shell-and-tube-type steam generator is shown in Figure 64. Each section is composed of a bank of U-tubes. The economizer tubes are manufactured from SA-179 carbon steel, and the evaporator tubes are made of type

SA-192 carbon steel. The superheater tubes are made of type SA-213-type 304H stainless steel.

Hot helium discharged from the reactor and entering the superheater section strikes an impingement baffle which distributes the flow and prevents erosion of the superheater tubes. Normal helium temperature leaving the superheater section is 1129 F. Steam enters the superheater section at 604 F and leaves at 1005 F. Steam flow through the superheater section is parallel to the helium flow. This means that the hot helium flows first across the cold leg of the steam tubes and then across the hot leg. The parallel flow design provides the lowest superheater tube metal temperatures and is less affected by high temperature helium transients. However, these tubes are designed for higher than normal steam temperatures during transients. This section contains 212 U-tubes. Tubes are 3/4-inch O.D., 11 gauge. Steam pressure at the superheater outlet is normally 1544 psig. The superheater is designed for 1750 psig at 1150 F.

Helium leaving the superheater enters the evaporator at 1129 F and leaves at 749 F. Boiling takes place in the evaporator tubes at 604 F and 1578 psig. The evaporator consists of 361 U-tubes. Each tube has an O.D. of 3/4-inch with a 14 gauge wall. Tubes are placed on a 60° pitch. Recirculation water to the evaporator section is supplied from the steam drum by means of a recirculation pump. A recirculation rate of 4 to 1 at full load was established to provide stable boiling under all load conditions. Economizer and evaporator tubes are designed for 1750 psig at 700 F.

Hot helium enters the economizer section at 749 F and leaves at 620 F. Feedwater enters the economizer at 425 F at full load, leaves the economizer at 588 F, and is piped to the steam drum. The water from the economizer is then mixed with the recirculation water and the resulting water temperature is about 600 F.

a. Generator Shell

The steam generator shell is fabricated from grade SA-212-Grade B steel. Carbon steel can be used for the shell by virtue of the inner plenum design. A shroud made of type SA-167-type 304, 16 gauge steel is placed within the shell in a manner that eliminates contact between hot helium and the steam generator shell. The steam generator shroud is insulated from the hot gas by sheets of dimpled 304 SS. The cooled helium leaving the economizer section flows through the annular space formed by the shroud and the shell wall. The helium flow keeps the shell cool but in the process of so doing is itself heated about 3 F due to heat transfer through the shroud.

b. Shell Nozzles

The helium outlet nozzle to the helium compressor is of conventional design. The hot helium from the reactor enters the steam generator shell through the center portion of a concentric type pipe nozzle. Cooled helium from the compressor discharge enters the annular portion of the nozzle and returns to the reactor through the outer pipe. A welded obstruction in the annular portion of the nozzle prevents the cooled helium from re-entering the steam generator. An 18-inch manhole is provided for maintenance accessiblity through the steam generator shell.

c. Channel Head

The channel head is welded to the top of the steam generator shell. A tubesheet isolates the helium side of the steam generator from the channel head (steam side). The physical shape of the channel head resembles a segmented sphere with flat portions on top and bottom. All U-tubes in each section, that is the economizer, evaporator, and superheater, are rolled and welded into the tubesheet. All sections are completely isolated from each other by means of channel plates which form individual headers. The tubesheet material for the economizer and evaporator sections is SA-105-II. The tubesheet at the superheater inlet is SA-105-II with an SS-304 overlay. The return leg of each superheater U-tube connects into the lowered portion of the tubesheet. This portion of the tubesheet is fabricated from SA-182-F-304. The tubesheet is lowered to eliminate excessive thermal stresses that would develop under normal operating conditions. Saturated steam from the steam drum enters the channel head through the annular portion of a concentric pipe nozzle. The saturated steam fills the channel head and then passes through the superheater. Separate inlet and outlet nozzles are provided for the economizer and evaporator channel headers. The top portion of the channel head is provided with a removable cover. The cover is bolted in place and made leak tight with a seal-welded diaphragm.

d. Baffle

One requirement of the design and construction of the steam generating unit is that there be essentially no leakage of water or steam into the helium coolant. Specifications require stringent helium leak testing requirements. These tests will detect any leakage between the water side and helium side of the steam generator at the time of fabrication. However, it is possible that leaks

at the tubesheet may develop after the unit has been thermal cycled during operation. The most probable source of water in-leakage is at the tube-to-tubesheet welds. A baffle running parallel to the main tubesheet but some small distance below it will be installed to enable a continuous helium purge flow to flush out the steam in-leakage. The steam generator tubes will pass through the baffle with a small clearance between the baffle and tubes. Helium will be drawn up through the tube-baffle spaces at a rate of 100 lb/hr per baffle. The water-contaminated helium will have the water removed in the helium purification system.

e. Steam Drum

The steam drum is a spherical pressure vessel designed for mounting separately from the steam generator shell. The steam drum serves two main functions. First the drum contains steam separation equipment whch maintains the steam quality leaving the drum to not less than 0.995 and the solids carryover to 1 ppm or less. The installed steam separation equipment is constructed so as to provide maximum practical accessibility for examination, cleaning and repair. The second function of the drum is to provide sufficient water holdup for the evaporator. The drum design utilizing a vortex breaker prevents the entry of steam into the downcomer pipe feeding the recirculation pump. This avoids erosion of the recirculation pump impeller. The drum is fabricated from SA-212-Grade B carbon steel and is designed for a pressure of 1750 psig at 650 F.

F Welding, Inspection and Quality Control

All welding procedures, qualifications and inspection will be in accordance with applicable code requirements, and additional tests will be performed such as weld sectioning and examination: visual, dye penetrant and 100 percent radiographic inspection.

All pressure-containing parts including interconnecting piping and generator tubes will be subjected to ultrasonic inspection, in accordance with MIL-STD-271-A. Steam generator tubes will be rigorously examined for irregularities and imperfections.

The steam generator will be subjected to hydrostatic testing in accordance with the requirements of all applicable codes. In addition, the steam generator will be subjected to a helium leak test on both the shell and tube sides.

g. Safety Considerations

The steam generator unit has several safety features built into it. In the event the steam generator recirculation pump fails, about 50 percent of the normal heat load can be removed by natural recirculation. If a steam or water tube break occurs, water flow is restricted to a maximum of 10 lb/sec per tube. The steam-helium mixture is relieved to the dump tanks.

In the event the exit temperature of the superheated steam gets too high the temperature will be automatically reduced by a desuperheater in the superheater outlet piping from the steam generator.

Morpholine for pH control and hydrazine for oxygen scavenging will be injected into the steam generator feedwater to assure satisfactory boiler feedwater conditions.

h. Instrumentation

Adequate instrumentation and controls as required by applicable codes will be provided. The following instruments are provided.

Two safety valves on the steam drum and one on the superheater outlet are provided. The combined safety valve capacity exceeds the maximum steaming rate of the steam generator at 110 per cent of rated duty. The superheater safety valve is set so that it will reach maximum capacity without causing the steam drum safety valves to pop.

A pressure gauge suitable for remote viewing is provided on the steam drum.

The steam drum is provided with an alloy steel, high-pressure, high-temperature gauge glass complete with block and drain valves. The gauge glass provides continuous visibility over the normal controlled water level range. Several remote reading level indicators are also provided.

Temperature indication is provided by means of high-speed steam thermocouple assemblies. The assembly consists of a screwed stainless steel well with number 14 gauge iron constantan thermocouple wire. Thermocouples are placed at the recirculation pump discharge, the economizer outlet, evaporator outlet and the steam drum outlet.

(2) Recirculation Pumps

One recirculation pump is provided for each steam generator. Each of the two pumps will be located below its associated steam drum. Water flows from the steam drum downcomer into the pump suction and is pumped into the evaporator section of the steam generator. Each pump is rated for 2400 gpm at 605 F and a discharge pressure of 1625 psig.

The pump is a vertically mounted, bottom suction, single-stage centrifugal pump designed for the above conditions and supported by the piping. See Figure 65. The pump impeller is of the single-suction enclosed type. The casing is a one-piece, special high quality steel casting with end suction and side discharge. Pump efficiency is approximately 83 percent. Motor driver is mounted on and supported by the pump.

Below are listed the possible manfunctions and imposed hazard conditions to which the pump can be subjected.

In the event that steam is dumped from the steam drum there would be a tendency for steam and water to backflow through the pump. To prevent this occurrence a check valve is placed in the pump discharge line.

If for some reason the recirculation pump fails, 0 to about 50 percent cooling is effected by natural circulation.

If the pump loses suction and runs dry no damage is incurred. This is due to the fact that the pump wear ring clearances are large enough to prevent excessive wear.

If the seal water supply is lost, the seal water in the seals can be automatically locked into the system to prevent drum water from flashing through the seals. Even if the seal water is lost and the "lock-in" system is inoperative the pump can be run for a nominal period without damage. Packing and rings will wear but will remain serviceable.

E. HELIUM HANDLING AND STORAGE SYSTEM

The helium handling and storage system is divided into two sections. One section handles non-purified helium and the other purified helium. The two systems are shown in Figures 66 and 67.

1. Non-purified System

a. General Description

The salient components of this system are three transfer compressors, two helium dump tanks, and a low pressure helium tank. The system is joined to the main coolant system and the helium purification system to perform the following functions:

(1) Provide storage of helium when the main coolant system pressure is reduced to slightly subatmospheric (during maintenance and fuel handling, for example).

(2) Serve as a dump system during accident conditions

(3) Maintain a low pressure sink for vent lines, sample lines, and relief valves.

The preceding functions all involve the transfer of helium from one point in the system to another. The transfer from low pressure to higher pressures is accomplished by the transfer compressors. All three compressors are of identical diaphragm type design and connected to a common manifold system. The maximum number of compressors required at any time is two; thus there is a single common spare to allow for compressor maintenance without interrupting service.

During the system pumpdown operation the helium is removed from the main coolant loop by first equalizing helium pressure between the main coolant loop and the dump tanks through the plate-out activity adsorber. The plate-out activity adsorber is a water-cooled charcoal bed filter. The function of the adsorber is to minimize the accumulation of plate-out activity in the helium handling system which would complicate maintenance operations, principally diaphragm replacement on the transfer compressors. After equaliztion, helium is transferred from the main coolant loop to the dump tanks with either one or two transfer compressors. It will require approximately six hours to pump down the main coolant loop to atmospheric pressure with two transfer compressors.

To repressurize the main coolant loop the reverse operation will be carried out except the return flow will go directly to the main coolant loop and not back through the plate-out activity adsorber.

In case of a severe steam leak accident condition, in which the pressure in the main coolant loop rises high enough to actuate the dump valves, a helium-steam mixture would be relieved to the dump tanks from the steam generator side of the reactor outlet valves. This mixture will then be transferred to the purification system for clean up.

A low pressure storage is always provided in the low pressure helium tank by removing in-flowing helium to the purification system. The tank pressure is normally maintained at from 0 psig to 2 psig by one transfer compressor on automatic stop-start control. The compressor start is initiated when the low pressure tank pressure rises to 2 psig and the compressor will stop when the tank pressure falls to 0 psig. The low pressure storage tank must be continuously maintained at low pressure and this will require that one transfer compressor always be available for this duty. The main feed streams to the low pressure tank are as follows:

(a) Main coolant rupture disc leak-off vents.

(b) Main coolant analyzer sample returns.

(c) Helium purification system relief valves.

(d) Main coolant block valve actuators.

(e) Equipment vents.

b. Equipment Description

(1) Transfer Compressors

The compressors are vertical, reciprocating, two-stage diaphragm machines, with integrally mounted motors, precoolers, intercoolers, aftercoolers, and interconnecting piping. All three compressors are of identical design. See Figure 68.

Three diaphragms are used to separate the helium gas and the compressor pulsing oil. The gas side diaphragm is welded to the gas side head to eliminate helium out-leakage.

Each compressor is fitted with a ruptured diaphragm detector, oil relief valves, low oil pressure shutdown switch, and moisture detectors. The oil relief valves are used to control the maximum discharge pressure of the compressor. To prevent damage to the transfer compressors from entrained water a moisture collection sump, trap, and moisture detector are provided with the compressor precooler, intercooler, and aftercooler.

The precooler, intercooler, and aftercooler are designed in accordance with applicable codes. Tube-to-tubesheet attachments are of a rolled and seal welded design.

(2) Dump Tanks

The two identical dump tanks are designed in accordance with applicable codes. Each tank is fitted with a relief valve, remote liquid level indicator, and drain valve. The level indicators are to signal the accumulation of condensate which may form when steam is dumped to the dump tanks. The total dump tank volume is 5000 ft^3.

(3) Low Pressure Tank

The low pressure tank is designed in accordance with applicable codes, and is equipped with a safety valve, remote liquid level indicator, and drain valve. The low pressure tank volume is 1000 ft^3.

2. Purified System

a. General Description

The purified helium handling and storage system consists of a purified helium tank, helium make-up bottles, and interconnecting piping. The system has the following functions to perform:

(1) Provide storage for helium used to maintain a constant pressure in the main coolant loop during load changing.

(2) Distribute purified helium received from the purification system to the various feed streams.

(3) Provide a limited surge capacity to feed the purified helium users in the event of a purified helium compressor failure.

(4) Supply the plant with make-up helium.

Purified helium is supplied to the system by a compressor in the helium purification system. Operation and description of the above purified helium compressor is covered in Section II C.

The helium required for load change and the surge supply are provided by maintaining the purified helium tank above loop pressure. The surge capacity provides a supply of helium for a limited time to purified helium users to permit starting the standby unit in the event of a purified helium compressor failure.

Helium distribution and make-up is handled through appropriate headers and valving.

b. Purified Helium Tank

The purified helium tank is designed in accordance with applicable codes. The tank is equipped with a safety valve and drain valve. The volume of the purified helium tank is about 2500 ft^3.

F. Afterheat Removal and Emergency Cooling Systems

1. Steam Generator Shutdown Cooling System

During extended periods of plant shutdown (>1 hour), decay heat generation in the core and helium temperature from the reactor are low enough so that steam generation for heat removal is no longer necessary. Instead, water circulating through the evaporator section of the steam generators will be cooled in a sub-boiling heat exchanger installed inside the containment using plant service water as the coolant. The sub-boiling exchanger is sized to remove 7,000,000 Btu/hr from the water.

The discharge of each of the steam generator recirculation pumps is connected to the sub-boiling exchanger through a bypass line. Thus, either of the main coolant loops can be used for shutdown cooling. The amount of recirculating water routed through the exchanger is varied to insure that the cold helium returned to the reactor is maintained at the proper temperature.

2. Reactor Vessel Emergency Cooling System

a. Cooling Jacket

The Reactor Vessel Emergency Cooling System is to be used when the normal means of cooling the reactor cannot operate. It is assumed that the reactor has been shut down by means of the control rods or the emergency shutdown systems so that the emergency cooling system is required to remove the decay heat in the core in addition to eventually reducing the general temperature level of the core.

The emergency cooling jacket consists of a steel plate shroud surrounding the pressure vessel and a series of coils welded to the shroud. A piping system to supply cooling water to the coils is provided. The shroud and jacket are shown in Figure 69. The piping system is described in Section III F.

The temperatures of the core, pressure vessel, and internals during emergency cooling are given in Appendix C.

Heat is lost from the reactor and internals by radiation and convection, mainly the former. This heat is absorbed and removed from the reactor cavity by the emergency cooling system.

The coils consist of tubing spaced on 4-inch centers. These tubes are welded or brazed to a steel plate shroud. Outside the shroud will be placed about 4 inches of insulation to assist maintenance of the vessel above neutron embrittling temperatures and prevent excessive heat loss from the vessel to the concrete shield. Coils are placed on the outside of the shroud in order to minimize the possibility of water accidentally coming in contact with the vessel.

b. Reliability

To insure reliability of the coils, they will be composed of several separate parallel circuits. Each circuit will enter and leave the containment separately and will be valved off outside the containment.

G. Nuclear Steam Supply System Instruments and Control Systems

1. Control Room

The HTGR control room contains all the normal and emergency operating instruments and controls for the entire power plant. These are connected to the primary measurement and final control devices in the containment by means of electrical connections only. Connections from the control room to auxiliary systems outside the containment may be by pneumatic as well as electric lines. Also centralized in this control room are voice communications with the containment and auxiliary plant systems.

a. Control Boards

The main control room boards are free-standing panels arranged in two ranks in front of the central operating console. All nuclear indicators, rod position indicators, main helium and steam process instrumentation, turbine-generator supervisory instruments, auxiliary electrical system instruments and controls and annunciators are located on the front rank of panels. The secondary rank holds the nuclear measurement and control rod control circuitry, radiation monitoring instruments, helium purification and handling instruments, and electrical relays.

b. Console

A central reactor operator's console is provided in front of the main control boards. Most of the major plant variables are indicated here, such as: neutron flux level and rate of change; automatic control rod position; helium flows, pressures, and temperatures; compressor speeds; steam flows, pressures, and temperatures; drum levels; and main valve positions. All these indications are in parallel with control-board-mounted receivers, giving additional protection against failure of indication or recording instruments. (Failure of transmitters is protected against by redundant measurement of critical variables.)

In addition to indicating plant variables, the console serves to contain the important manual controls that are vital to the reactor's operation and safety. These manual controls include: control rod group and rod selectors for automatic or manual rod control; manual scram switch; compressor speed control; all main coolant valve controls including the helium dump valves; manual feedwater valve control; steam generator dump valves control; and the main turbine generator loading

control. Many of these controls are normally in automatic mode but may be taken over manually by the reactor operator as required.

In addition to the main control board annunciators which alert the operators to malfunctions and off-normal operation, the console has many parallel alarm lights and indicating lights. These give the control room operators two checks on the operation of the more important auxiliaries. Failure of these lights or alarms is further precluded by the operator's test button which allows periodic check of all lights and alarms on the controlboards and console.

2. Reactor Instruments

a. Flux Instruments

The nuclear instrumentation provided for monitoring neutron flux is composed of nine channels: three count rate, two log N and four linear power level as shown on Figure 70. These instruments provide flux measurements from source level to above full power as shown in Figure 71 and their outputs are indicated and recorded in the control room. The nuclear instrumentation provides signals to the plant protective system in addition to providing reactor control signals during power operation. The neutron detectors are mounted in water-cooled thimbles located in the concrete biological shield adjacent to the reactor vessel. The detectors used for the count rate channels measure source level activity at startup and require neutron shielding during high flux operation. Movable cadmium shields are used and are automatically lowered into shielding position at approximately 0.01 percent power.

(1) Count Rate Channels

Three count rate channels, using Boron-10 proportional counters, are employed during startup to furnish the operator with neutron flux level information. Rod withdrawal is prohibited below a set minimum count rate, thus insuring that the operator has neutron flux information to allow a safe startup. Two of the three channels provide low level rate of change information and alarm circuits. A log count rate recorder and rate of change meter are provided on the reactor operator's console.

(2) Log N Channels

Two compensated ion chambers are used in providing log N and rate of change information over seven decades. More than

one full decade of overlap with adjacent channels is provided at each end of the range as shown on Figure 71. The log N channels are used to bypass the count rate channels, actuate the proportional counter shield drive mechanisms, and also to initiate a low power scram during initial startup. The rate of change circuits initiate a scram trip. A log N recorder and rate of change meter are provided on the reactor operator's console.

3. Power Level Channels

Four power level channels, utilizing uncompensated ion chambers, are provided to give accurate linear flux measurement in the upper two decades of power operation. Signals from these channels are used to initiate scram and also to provide signals to the automatic flux control loop. Spatial distribution of the detectors around the reactor allows the additional use of these channels in indicating gross flux tilts. A power meter is provided on the reactor operator's console to display any one of the four channels, the four channel average or the highest reading channel. The four channels are recorded on a panelboard recorder and the total full power hours are computed.

4. Safety Features

Fail-safeness is an important criterion for all the nuclear instrumentation. For example, a loss of power will cause all the affected trip circuits to assume their scram or alarm output. All similar channel outputs are continuously cross-compared and any deviations annunciated. This serves not only to detect gross malfunction but also to indicate areas of possible malfunction by calling attention to equipment drift. The instrumentation is of advanced solid-state design to enhance ease of operation and trouble-free use. Each trip is annunciated and a local indicator light is provided to show the condition of each trip circuit. All channels are electrically isolated and driven from the proper power source as dictated by the protective system logic. The use of different power sources and dual scram valves allows comprehensive operational testing of the instruments. At any time, including full power operation, a channel can be functionally tested from input to the releasing of one scram coil. This testing does not cause a false scram nor does it prohibit a necessary safety action.

b. Control Rod Drive System

All the thirty-six control rods and nineteen emergency shutdown rods are fully instrumented for safe operation from the main control room (see Figure 72). Monitoring instruments for mainten-

ance and local operation
during maintenance of the rod drives and auxiliaries are located in the rod drive auxiliary room inside the air-filled portion of the containment. The details of the control rods and drives are covered under Section II. B 7 of this report.

(1) Position Instruments

Each control rod contains a synchro-transmitter which gives continuous rod position indication on a panel in the control room. This same signal is wired into the reactor operator's console where any rod position may be placed on a precise digital indicator. Rods selected for automatic control and partially withdrawn rods will be normally displayed on the console position indicators. Each rod also has two position limit switches mounted in the drive mechanism. These are connected to individual indicating lights mounted on the rod drive panel in the control room, providing backup indication for each continuous rod position indicator. The lights indicate when the rod has reached its full travel limits.

A limit switch is mounted on each scram valve spool of each control rod mechanism. When its associated valve is completely open, a signal light is energized in the main control room. This indicates to the operator the position of all scram valves during scram and scram testing. Each scram valve coil is individually fused. Blown fuse indicators bring to the operator's attention any malfunction of scram coils.

Each control rod accumulator piston position is continuously indicated in the control rod drive auxiliary room. This same signal is used to operate a light mounted on the rod drive panel in the control room. When the light indicates the piston has reached a low position, helium may be admitted into the accumulator from the auxiliary room panel where the position indicator and charge valves are located.

All control rods have holding locks that must be energized in order to withdraw the rod from the fully inserted position. Rod control circuits provide that no more than three rods and their locks can be moved simultaneously. Whenever a lock is open, a common light notifies the control room operator. Local lights in the auxiliary room permit identifying the open lock, should a fault occur.

2. Pressure Instruments

Continuous indication of the pressure in the low and high pressure hydraulic supply lines is provided to the main control room. Three switches actuated by low pressure located in the high pressure header connect into the scram circuit. These give scram protection when the pressure in the high pressure supply drops to 85 percent of its normal value, insuring the use of the scram energy stored in each accumulator. Any two of the three pressure switches actuating will scram all rods immediately. Hydraulic supply pressures are regulated by self-actuated valves in the pump discharges. The spare pump set is started by low pressure in either the high or low discharge line, and the pump start is annunciated in the control room. A spare high pressure regulating valve may be switched in from the control room. This is set so that a check may be run on the accumulator piston motion, as well as serving as a backup for the on-line regulator.

The hydraulic storage tank pressure is kept near reactor pressure by maintaining a helium blanket above the hydraulic fluid. A large differential between reactor and storage tank pressure sounds an alarm in the main control room. In addition, all filters and strainers in the supply system and in each rod have high differential-pressure switches which sound common alarms in the main control room. Clogging of an individual rod filter is signaled in the air room to allow for identification and repair.

3. Rod Continuity Instruments

Each control rod is provided with an electrical monitoring circuit to detect separation or disconnection of any part of the rod assembly. The circuit within the rod is constructed of a stainless-steel-sheathed single-conductor cable which traverses from the recirculating ball nut to the top of the rod and back again in a continuous loop. Rod separation causes a loss of continuity in the central conductor which will be monitored and alarmed in the air room. A common alarm in the central control room warns the operator to stop all rod withdrawal until the cause is identified in the air room monitoring circuits. Additional details of the circuit within the rod are discussed in Section II.B.7.

Two monitoring circuits are provided. One detects loss of continuity (open circuits) of the central conductor of the sheathed cable, which indicated possible rod breakage of separation at one of the two mechanical latches. The other monitor detects possible shorts between the sheath and central conductor. The detectors will be constructed to warn the operator in the event of detector failure.

4. Miscellaneous Instrumentation

Additional instruments and controls are provided to ensure the safety and integrity of the control rod drive system. Fluid leak detectors (level switches) are located in each rod drive housing and in each accumulator gas space. These sound a common alarm in the main control room for all rods and individual alarms in the rod drive auxiliary room. Defective rods can be driven in at the operator's option.

Buffer helium flow to each rod drive is manually set in the auxiliary room by means of purge rotameter flow indicators. Each rotameter has a low flow alarm switch which sounds a common alarm in the main control room. Individual alarms are located in the auxiliary room where the flow adjustment valves are available.

The hydraulic fluid storage tank and heat exchanger provide surge and cooling for the hydraulic supply system. Pressure, temperature and level are signaled to the control room. Since the equipment is in the air-filled auxiliary room, local pressure gages, thermometers and gage glasses provide for direct inspection, repair and replacement. Relief valves and the main pressure regulating valves are also available to the operator in this room, providing complete protection against overpressure.

c. Emergency Shutdown Rods

The electrically driven emergency shutdown rods are actuated manually by the reactor operator, by means of a master switch located within the control room. Actuation of the one switch causes all 19 rods to be forced into the core. Limit switches are provided to allow the operator to assess their position before and after actuation. Local instrumentation in the rod drive auxiliary room monitors the rod continuity detectors and the condition of the drive batteries. Common alarm signals in the main control room alert the operator to service needs in the auxiliary room.

3. Helium Loop Instruments

a. Pressure Instruments and Connections

Pressure and differential pressure transmitters are located inside the plant containment, in low radioactive areas to minimize radiation damage to the instruments and to provide easier access for calibration and maintenance during shutdown. The connection from the

measuring point to the instrument is heavy wall tubing or pipe to minimize the chance of line breakage. Excess-flow check valves are located in the instrument connection line close to the main process line. All instrument components in contact with helium will be leak-checked to insure that their leakage is less than the design amount. All-welded, bellows sealed valves are used in instrument connection lines. These valves are backseating and have a secondary packing to provide secondary containment in the event of bellows failure.

All welded diaphragm-sealed liquid-filled systems are used to measure pressures and differential pressures in highly radioactive helium services, such as portions of the Helium Purification System. The diaphragm seal is located close to the process line and the pressure is transmitted by the fill fluid to the transmitting instrument located outside the radiation shield. This scheme minimizes the piping of highly radioactive gases and the diaphragm seal inherently offers double containment of the process fluid. The all-welded seals are the full-pressure safety type.

Electrical transmission of signals to the main control room has been selected over pneumatic transmission to eliminate the introduction of many leakage paths for containment gases to enter the control room. Pressure transmitters are generally of the bourdon type or metal bellows type. These relatively thin-walled devices are made helium leak-tight and enclosed within gasketed metal cases to minimize outleakage in case of failure of the primary element. The use of heavy wall pipe, excess-flow check valves, leak-tight hand shut-off valves, and leak-tight elements provides the integrity required. Where measurements are required for operation of vital control or protective systems, they are made by complete multiple systems.

b. Differential Pressure and Flow

Differential pressure devices (transmitters and switches) are similar to pressure instruments in construction and installation. Where a bellows measuring element is used, the bellows is generally liquid-filled with the process helium gas external to the bellows. The pressure housing external to this is helium leak-tight and pressure-proof.

Where differential pressure is used for flow measurement, the differential producer (orifice, venturi, etc.), is welded into the pipe line and all connections are as described under Section II. G. 3. a. Pressure Instruments and Connections. The main coolant flow meters consist

of modified venturi tubes with low over-all head loss construction. These are used in the main compressor discharges to indicate mass flow for plant performance calculations, to assist in identifying the helium loop which has ruptured and to warn of unbalanced compressor operation. Small flow rates in the helium systems are measured by hermetically sealed, leak-tight rotameters wherever feasible. Orifice meters and differential pressure transmitters are used on larger flow lines.

c. Temperature

In general, temperature measuring elements in the helium systems are thermocouples installed in solid barstock thermowells made of stainless steel. Duplex elements are used in vital control and protective systems with both pairs of leads run to the control room. One element will be connected and the other element is used as an installed spare which is also available for check purposes. These elements are replaceable.

The hot helium from the reactor outlet pipes requires fast response measurement which must be completely reliable. These temperatures are used for reactor control and for scram action. Multiple instrumentation is used.

Other temperature measurements in the cooler helium from the steam generators, from the main compressors and in the helium handling and purification systems, will be handled by conventional thermocouple assemblies. All thermowells are individually leak-checked and welded into the pipe or vessels being measured. The temperature elements may be removed from these wells for repair only after plant shutdown. Temperature measurements inside the reactor and inside the concentric piping are made by using metal-sheathed, ceramic-insulated, helium-leak-tight thermocouples.

d. Radiation Monitoring

A radiation monitoring system is used to measure the main coolant activity to indicate possible fuel element failures and changes in the normal fission product release rates of the fuel elements. The system monitors the activity of the circulating coolant with a collimated dector located in the main helium pipe. A lead shield colimator is utilized so that the detector sees a large volume of coolant and only a small section of the pipe wall. This reduces the background signal from any fission product plate-out in the loop. The display instrumentation is

located in the control room with associated alarm circuitry. Gamma energy discrimination, possible with the use of scintillation detectors, is used to optimize the response of the system to changes in coolant activity.

e. Helium Leak Detection

Two leak detection systems are used for the indication of helium leakage from plant systems which are important to the reactor operator. The first system detects small helium leaks which require location to enable maintenance crews to locate the source and make the necessary repairs after a reactor shutdown. A central leak detection system detects small helium leaks in the main loops and auxiliary systems. Air samples from the various containment compartments are monitored by helium mass spectrometers and radiation detectors for abnormal concentrations of helium and radioactivity. This system allows for a normal manual shutdown before a major loss of coolant occurs or before the resultant radioactivity release contaminates the apparatus within the containment vessel. An alarm signals the compartment from which the higher concentration of helium or radioactivity originates and the monitors indicate the relative magnitude of the fault.

The second type of failure is a large fault where loss of coolant and system pressure are the prime considerations. For large leak rates, the location of the fault is accomplished by beta radiation detectors placed in the coolant loop compartments.

The use of two separate systems provides additional safety so that a wide range of helium leak rates can be detected with a minimum time delay.

f. Moisture Monitors and Gas Analyzers

Because of the effect of moisture on the graphite core, provision is made for rapid detection of moisture in the helium coolant. The most probable cause of moisture inleakage results from a steam generator tube leak at the tube sheet. Moisture detectors continuously sample the main coolant helium stream at each steam generator. Two successive trip levels are provided for each detector output: one for alarm and one for plant shutdown. Utilization of three detectors at each boiler prevents the failure of one instrument from (1) inhibiting an actual high moisture shutdown signal, or (2) causing a spurious plant shutdown. High velocities in the sample system to the moisture

detectors provide for detection of a high moisture level within five seconds after a tube failure. The instrument selected for moisture detection is an electrolytic hygrometer which has been well proven.

Detection of very small steam leaks below the range of the electrolytic hygrometers is achieved by measurement of the carbon monoxide produced by the steam-graphite reaction. An infrared analyzer continuously monitors for the presence of CO. If the integrated steam inleakage indicates possible core damage, the plant can be manually shut down in order to effect repairs on the defective steam generator.

An additional moisture monitor (electrolytic hygrometer) is installed in each steam generator purge stream. This will continuously monitor for leaks at the tube sheet and alert the operator to look for water and CO buildup in the main coolant helium. This is another back-up which should make instrument failure a very unlikely cause for operating the main coolant system with undesirable water leaks.

Main coolant helium is intermittently sampled for trace impurities such as CO, O_2, N_2, CO_2, CH_4 and argon. A sample system is provided to concentrate the level of impurities in the helium sample. The concentrated sample is injected into a gas-chromatograph for determination of each impurity level.

The helium handling system transfer compressors are another potential source of water which could be carried into the reactor. Each of the three compressors has three water-cooled exchangers for reducing helium temperature. Tube leak in any exchanger might add significant amounts of water to the main coolant system. An electrolytic hygrometer is used in the discharge header to shut down the compressor at a preset moisture level.

In the helium purification system, the effluent from the oxidizer is continuously monitored for unreacted CO and excess oxygen. Trace levels of oil are also measured in the purified helium effluent to detect abnormal leaks from compressor seal and lube oil systems or malfunction of the oil removal unit.

4. Steam Loop Instruments

Pressure, differential pressure, flow, temperature and level conditions of the steam and feedwater systems in the containment are

measured by conventional steam plant instruments and are transmitted electrically to controls, alarms and indicators located in the main control room. Instruments utilized for automatic safety protection of the plant are installed in multiple. Heavy wall piping and line class instrument valves are used to insure reliability. Those instruments not accessible during operation, are installed outside radioactive areas for ease of servicing during shutdown.

a. Pressure and Differential Pressure

Bourdon tube and bellows or diaphragm transmitters are used for all measurements. No special construction is required on steam instruments. Differential pressure across the steam generator recirculation pumps is sensed by three differential pressure transmitters whose signal is utilized for loop isolation on flow stoppage. Steam drum pressure is utilized for automatic control of the steam dump valves. Backup protection of the steam drum against overpressure is provided by standard safety valves. Steam pressure is also sensed in each superheater outlet line, upstream of the desuperheater. This signal is utilized in the three-element feedwater control system and provides an additional check on the drum pressure indication. The main steam pressure controller and the turbine bypass controller are both actuated by pressure measurements in the main steam header outside the containment. Failure of these instruments is covered under Control Systems, II. G. 5.

b. Flow

All feedwater and steam flows are sensed by differential pressure transmitters across orifices or nozzles. The measuring elements are welded into high pressure lines and connecting piping is line class up to the instrument isolation valve. A signal from each feedwater line transmits information into the three-element feedwater controller, Main steam flow is measured and is used in the feedwater controller.

c. Temperature

All critical temperature sensors in the steam and feedwater systems inside the containment consist of duplex thermocouple assemblies whose output leads are brought to the control room, one element to be used as an active element, the other to be used as an installed spare. These double elements are mounted in individual stainless steel wells, which are welded into the line. The

control and safety elements may have additional duplex elements installed for use in event of operating equipment malfunction. All elements are accessible for repair and replacement after plant shutdown. The main superheater outlet thermocouples are used for helium temperature control, compressor speed trimming and for flowmeter compensation. These must be fast response elements with high reliability. Commercially available high speed steam thermocouples are installed in multiple for this application and for the desuperheater control thermocouples. These latter elements are installed in the superheated steam lines downstream of the spray nozzles in each loop. They are used for control of the desuperheater water control valve. High temperature alarms in the main turbine inlet lines back up a failure of these thermocouples. The temperature of the lines downstream of the relief valves on the steam generators alarm at high temperature to give warning of relief valve operation or seat leakage. These temperatures are sensed from the outside of the line by a single element. Many additional steam and water temperature measurements are monitored to provide operating data and to warn of less critical equipment malfunctions throughout the plant.

d. Level

Steam drum level is measured for use in the three-element feedwater control system and the plant protective system which requires isolation of a boiler that has lost water level. The steam drums are located inside the nitrogen-filled containment and thus reliance must be placed on remote level instrumentation. Provisions are made to remotely view the drum gauge glass, either by periscope or television. Additionally, compensated manometric level indicators are installed in the containment air room. These are used to verify the readings from the three-element controller transmitter and to provide the low level trips required.

e. Feedwater and Condensate Analyzers

Feedwater samples are taken of condensate and blowdown and steam from each boiler. These samples are analyzed for solids, pH, conductivity and dissolved oxygen. This instrumentation is backed up by sampling and laboratory analysis techniques to verify the adequacy of analysis and treatment, and to insure acceptable water conditions.

5. Control Systems

a. Over-all Plant Control

The Peach Bottom Atomic Power Station is primarily a manually-loaded generating station which has automatic capabilities to follow the turbine generator loading. Constant steam conditions are automatically maintained at the turbine inlet throughout the normal load changes at the design rate of 3 percent per minute. Automatic control loops vary helium coolant flow rate to hold steam pressure, and vary reactor power to hold steam temperature. Turbine auxiliary controls for abnormal conditions include an overpressure-actuated turbine bypass to the condenser and an initial-pressure regulator to maintain a minimum throttle pressure. Feedwater control and helium temperature controls are secondary loops that operate as required by the over-all plant control system. Manual operation of all automatic control loops is available as a backup for controller failure. See Figure 73 for a simplified over-all plant control diagram.

b. Reactor Control

For any given steam load, a proper combination of helium flow rate and helium temperature is required. Helium temperature is controlled by reactor power as determined by control rod movement. Rod movement in automatic operation is determined by three cascaded controllers. Steam temperature actuates a proportional plus reset controller. The output of this steam temperature controller adjusts the setpoint of the reactor helium outlet temperature controller. This second controller generates proportional and rate action. The output of this controller adjusts the setpoint of the neutron flux controller. This is a three-zone contactor controller with adjustable deadband which operates the regulating solenoid valve of the control rod through the regulating rod selector switch. The solenoid valve may be positioned to drive the rod in or out or to hold the rod stationary.

Two types of controller malfunctions can be hypothesized. One would be a failure that caused a sudden change in a setpoint or measured variable. Deviation alarms are provided to indicate when the measured variable and setpoint are apart by a preset amount. The alarm also can be made to transfer automatically to manual, giving the reactor operator control. A second type of failure could cause a slow drift in setpoint which would bring the controlled variable into a danger zone. The helium temperature and flux controllers each have high and low setpoint limits beyond which the master controllers cannot

drive them. And, as detailed under the plant protective system, there are several levels of alarm and scram for these variables should they exceed normal limits.

c. Rod Control

Of the 36 control rods in the reactor, only the inner 12 rods are used for regulating purposes. All 36 are identical and may be inserted or withdrawn by remote manual controls. These controls direct hydraulic fluid through a reversible hydraulic motor to move the rod at normal speed. At any time, all rods may be scrammed into the reactor regardless of the demand of the automatic or manual controls.

During startup, and in the intermediate range, manual control only is used. The outer 24 rods may be manually moved in groups of 3 to reduce the time required for startup. Group operation also allows for more symmetrical flux distribution. Group operation does not exceed limits set on the rate of reactivity insertion. Manual controls for the inner rods are limited to moving only one rod at a time. Automatic control is used in the power range, but only one rod at a time may be moved by the rod controller. Other regulating rods are manually shimmed during automatic control, but only one rod at a time is moved outward. No more than 3 regulating rods will be in an intermediate position during power operation.

Selector switches are used to select manual or automatic rod operation. An unlikely failure in the switching operation is a short between two electrical lines feeding solenoids. Actuation of a rod or group of rods under this condition could result in two rods or two groups of rods moving. However, inadvertent rod motion is unlikely since the selector switches are separate from the rod actuation switches and both require operator action and supervision. Automatic flux control and scrams further prevent this malfunction from becoming a hazard.

d. Helium Loop Control

(1) Pressure

The main helium coolant loop is maintained at 335 psig constant pressure during normal plant operation. This is accomplished by admitting purified helium to the loop from a storage tank fed from the helium purification system. This stream must make up the difference between the fuel element purge outflow and the inflow from the buffer seals and purge lines at the control rods and main helium

compressors. Pressure in the main loop is measured and a control valve is automatically controlled during all normal load swings to keep this pressure constant. Additional pressure measurements in the loop sound alarms on high or low pressure. A low pressure scram action occurs at the selected low pressure limit.

Misoperation or failures that can cause overpressures are protected against by the helium dump and relief valve systems. At 390 psig, back-pressure-operated dump valves open to release helium to the dump tanks in the helium handling system. These dump valves are tight-seating valves located in the helium piping downstream of each steam generator. They serve to protect the boiler-compressor-pipe system from overpressures due to a steam leak into the helium. These valves can be remotely operated both automatically and manually.

Should these valves fail to operate and the pressure continue to rise in the piping loops, ASME Code relief valves set at 450 psig will relieve to the containment atmosphere. These valves are arranged in three sets, each with a full-sized spare, for the reactor and for each steam generator. All relief valves have an upstream rupture disk with a tell-tale leakoff chamber between it and the relief valve. Each pair of relief valves is provided with interlocked manual shutoff valves which permit taking one assembly out of service but not both. The reactor relief valve setting is 437 psig.

The plant safety system is so designed that only a steam leak can cause the rupture disk and relief valve system to open, and this will only occur if several other automatic dump and isolation actions do not take place correctly. See II. G. 6. The manual shutoff valves allow for regular testing of relief valves. Repair and replacement of leaky disks can be effected during plant shutdowns. The number of valves provided makes their simultaneous failure incredible and the interlocked block valves prevent isolating the loop from its required relieving capacity.

Pressures in the dump tanks, low pressure tanks and purified helium tanks, etc., are all controlled by simple pressure switch pumpup or pumpdown controls that operate the associated compressors. These are all backed up by remote reading transmitters, pressure switch alarms, relief valves, and remote manual compressor controls, which ensure safe operations.

(2) Flow

Flow of helium in the main coolant loop is controlled by the variable speed compressor-driver train. Generally, the speed of both compressors will be the same as they are controlled by the main steam pressure at the turbine throttle. To allow for small differences in the two helium-steam loops, superheater outlet temperature is used to trim each compressor speed to achieve equal superheat. The flow measurement signals, previously described, are used for high flow ratio alarm, warning of a possible compressor surge condition should compressor speeds differ greatly. Low compressor flows and speeds are also alarmed and used in safety circuits as described below.

Helium flow in the helium handling purification systems is basically controlled by the purified helium compressors. These operate to maintain the fuel element purge flow from the reactor, discharging the gas into a storage tank. From there it enters the main coolant system through several streams. Differential pressure controls insure flow through the main compressor buffer seals and the control rod purge streams. The main loop pressure control supplies the makeup helium to the loop. Consequences of a failure of a purified helium compressor are minimized by automatic opening of a low-flow-bypass from the helium purification system to the helium dump tanks. This insures several minutes of purge flow while the spare purified helium compressor is being started.

(3) Temperature

Main loop helium temperature is continuously controlled at the two reactor outlet pipes. The two temperatures are transmitted to an auctioneer circuit which selects the highest temperature and uses it for the measured variable. The controller output and setpoint are described under Reactor Control. Use of the high auctioneer allows for small differences in the two coolant loops. Both temperatures are indicated continuously and a high difference alarm is provided to indicate malfunction of the measuring devices. Additional temperature measurements are provided with redundant combinations being connected into the safety system to actuate a high temperature scram. These may be used as check measurements for the controller.

Elsewhere in the helium systems, helium temperature is controlled by direct heat exchange. Temperatures are monitored, recorded and alarmed where faults might cause operating hazards.

e. Steam Loop Control

(1) Pressure

Steam flow, pressure and temperature are the major controlled variables in the plant. As described in Section II. G. 5. a, steam flow is set by manual loading of the turbine throttle valves. Steam pressure is controlled by varying the helium flow through the compressors. Failure of this control loop is backed up by additional measurements and controls. Steam drum pressures are indicated and used to control steam overpressure dump valves. High pressure at the turbine throttle opens up the turbine bypass pressure control. Relief valves on the drums and superheater outlets give additional protection. Protection against low pressure in the main steam lines is provided by the turbine initial-pressure regulator system. This regulator moves the throttle valves to maintain steam pressure at a point that is safe for the turbine.

(2) Temperature

Superheater outlet steam temperature control is effected by controlling the hot helium temperature, as described previously. The two superheater temperatures are auctioneered and the higher temperature is used by the controller for resetting the hot helium temperature controller. Both temperatures are also compared in a temperature difference controller which operates to trim the main compressor speeds to achieve equal superheat in both loops. As a backup, for use during fast load decreases, each steam generator has a water spray desuperheater to prevent final steam temperature from exceeding design values. Check thermocouples for additional indication, recording, and alarm purposes are provided throughout the steam generator circuits to alert and assist the operator during manual control following a control failure. All critical thermocouples are duplex type in fast response assemblies.

(3) Level

Steam drum level is controlled by means of a conventional three-element feedwater control system. Steam flow is compared to feedwater flow and kept in balance except as sustained changes of drum level require further trimming of feedwater. Additional level measurements are made which actuate alarms and safety system action as the level exceeds prescribed limits. Level gages are installed in accordance with the ASME Power Boiler Code to ensure means of checking the calibration of the feedwater level instruments.

Manual control of the feedwater valve is available to the control room operator when required by controller failure. Feedwater line stop valves are also available for remote operation from the control room as a backup to the main feedwater valve.

6. Plant Protective System

The plant protective system has been designed to provide protection against a wide variety of accidents. Variables have been chosen that give clear-cut indication for each accident. Trip circuits and logic functions have been assembled to take the required protective action. The protective system has a builtin program for automatically taking action in case of major accidents and manual inputs for minor incidents. Additional bypass circuits and interlocks have been included to enable safe startup and maintenance procedures.

Three basic types of logic are used:

Single trip with backup is provided by back-pressure-operated dump valves. The backup is a reliable Code relief valve.

Two-out-of-three logic is provided for reliable trip from a measured variable. Maximum reliability is attained when three separate instrument channels measuring the same variable are fed from three independent power sources. Single channel indications of failure (correct or not) neither cause improper safety actions nor prevent proper ones.

Two-out-of-four logic with fail-safe design is provided for highly critical variables, such as reactor flux. Four independent channels measure the same variable. Two channels and one set of logic are fed from one of the two independent power supplies. Safety action occurs on simultaneous trip of any two channels but not on the same power supply. Failure of one power supply does not cause scram action, nor will it prevent proper scram action from occurring upon loss of the other electrical supply or measurement channel.

a. Scram

A scram is implemented by inserting all 36 control rods into the reactor at the maximum rate. Each rod is released by opening two solenoid-operated hydraulic valves and inserted by energy stored in the rod drive mechanism accumulator as described in Section II. B. 7. The coils of the solenoid operators in turn are controlled by the decisions of two identical sets of scram logic. The release of both coils

and the opening of both valves is required to initiate a scram. The logic and control actions required for scram are implemented by solid state devices except for the final electromechanical contactors. The logic circuits utilize redundancy at both the component and functional levels to increase reliability. The logic is composed of two independent sections operating from separate power supplies. Each section controls one release coil on each rod. The final control elements for each group of scram coils will be redundant solid-state relays followed by rugged, derated, electromechanical contactors. See Figure 74.

(1) Accidents or Conditions Causing Scram

A scram will be initiated by a high flux excursion upon coincidence of correct two-out-of-four power level trips.

Scram will be initiated on high reactor outlet temperature. Two temperature measuring channels are provided in each coolant loop with each channel fed from a different power source. Correct two-out-of-four logic is used.

Three moisture detectors are provided for each main coolant loop for a total of six channels. Scram is initiated by high moisture trips in two out of the three units in either loop.

Scram on low main coolant (helium) pressure is caused on coincidence of two-out-of-three low pressure indications. Pressure is measured in the isolatable portion of each coolant loop and also in the reactor portion of the coolant system. This scram can be bypassed during initial criticality and low power runs.

A low pressure condition in the control rod high pressure oil header will cause scram and also uses two-out-of-three coincidence.

During startup a high rate of change trip in both log N channels will cause a scram. This function is bypassed automatically by the linear power channels during power operation.

During initial criticality and for low power testing, a scram can be initiated by a flux level trip in either log N channel. During normal startups and normal power operation this scram is deactivated.

Since it is not intended that the plant be able to continue operation with only one helium coolant loop, scram is arranged to

accompany every automatic loop isolation. See Section II. G. 6. b. As an additional precaution, a manual scram can be initiated by the reactor operator.

(2) Logic Failures

The scram logic and associated instruments are arranged so that a failure of any single source of instrument AC power will not adversely affect plant operation or safety. The power failure will initiate a "half-scram" (release of one of the two solenoid coils in each rod) and will disable one set of logic. The other set of logic will still be available for initiating a scram if the process requires it. Single instrument channel failures will not adversely affect performance because of the coincidence and redundancy provided. Should one channel trip erroneously, one or more of the remaining channels is required to cause a scram. Failure of one log N rate of change channel does not cause false scram. Linear power level scram provides backup in this case.

The reliability of the logic circuit elements will be an order of magnitude higher than the instrument channel reliability. With diode resistor logic, circuits are so arranged that individual component failures do not cause scram nor prevent scram. At worst, failure of one component is equivalent to trip of an individual channel.

b. Loop Isolation

Either helium coolant loop can be isolated from the reactor by actuating the helium isolation valves. All three isolation valves in one loop are simultaneously closed by the loop isolation logic circuits on detection of certain accidents, and the helium compressor is tripped. Limit switch interlocks insure that only one loop may be automatically isolated at a time by requiring that the isolation valves be at their open limit before the opposite loop can be isolated. At the same time as helium loop isolation, the corresponding steam loop will be automatically isolated from the common feedwater supply by closing the feedwater stop valve. A reactor scram will accompany each loop isolation to help limit high temperature transients.

Since isolation of both loops has to be avoided, it is not practical to arrange the instrumentation to isolate on loss of power. However, individual instruments are arranged to fail safe (tripped condition) on loss of power to the instrument. All instruments and logic circuits will be fed from the most reliable power sources and solid state circuitry will be used for reliability. Redundant detecting

instruments and logic circuitry will be used to avoid unnecessary loop isolation and yet be able to isolate when needed.

Logic output elements will employ redundant relays. The hot helium isolation valves are provided with redundant pilot valves each controlled independently. Either one will admit high pressure helium to the main valve actuator, in order to close the valve.

(1) Accidents or Conditions Causing Loop Isolation

Loss of one main helium compressor leads to flow reversal in the affected loop and drastic reduction in coolant flow through the reactor core. Automatic loop isolation of the corresponding loop is arranged on detection of low shaft speed of the defective compressor. A centrifugal switch is attached to the compressor shaft and redundant trips are fed speed signals from the tachometer generators in the compressor speed control circuits. Two-out-of-three indications of low speed are required to isolate the loop.

Loss of feedwater to one boiler can occur through ruptures or stoppages in lines external to the boiler. Low steam drum level or recirculation flow stoppage will be detected depending on the location of the failure. Three independent instruments are provided for measuring water level in each steam drum, and three differential pressure devices are connected across the pump in the recirculation line. The closure of the pump discharge valve produces a high differential trip. Automatic loop isolation is arranged on two-out-of-three coincidence of trips from either set of instruments.

A tube rupture in either boiler can put large amounts of steam into the main helium coolant. Three moisture detectors are placed near the helium outlet from each steam generator. On coincidence of two detectors in one loop, the helium and steam loops associated with the failed steam generator are isolated. Steam pressure is then automatically reduced by dumping steam to the outside atmosphere from the isolated steam generator. See Section II. G. 6. c.

Ruptures or leaks in the main coolant loops can lead to loss of system pressure and release of radioactive material to the secondary containment. The compartmentation system associated with each loop is ventilated separately. A series of beta ray scintillation detectors are placed to detect radioactive gases leaking into the compartment with the helium. These detectors will assist in determining which coolant loop has the leak and will signal for closure of the loop isolation valves.

(2) Isolation Failures

Since only one loop may be safely isolated at a time, isolation valves are arranged to remain in their normal position on loss of electrical or pneumatic power. Helium isolation valves remain open on loss of compressed helium supply. The feedwater isolation valve will remain as is on loss of instrument air while the steam blowdown valve will remain closed. The control circuits require electrical power in order to effect a loop isolation. Single instrument failures will not adversely affect performance because of the coincidence and redundancy provided in two-out-of-three channel logic. Should one channel be unable to trip, the other two will operate. Should one channel trip erroneously, trip on one more channel is required before loop isolation. Simultaneous failure of more than one instrument is extremely unlikely considering the reliability of each channel. The reliability of the logic circuit elements will be an order of magnitude higher than the instrument channel reliability. With diode resistor solid state logic gates, circuits are so arranged that individual component failures do not cause loop isolation nor prevent loop isolation. At worst, failure of one component is equivalent to trip of an individual channel.

Failure of one isolation valve to operate when required must be considered. Simultaneous failure of more than one valve is extremely unlikely. Failure of the cold isolation valve at the helium compressor suction does not affect loop isolation. Failure of the cold isolation valve at the helium compressor outlet means inability to isolate ruptures within the circulator but does not affect protection against other accidents. Failure of the hot helium isolation valve has more serious consequences. Ruptures anywhere in the loop cannot be isolated except for those in the helium circulator. Moisture leaking from the steam generator will be flashed into the main coolant and carried to the reactor core. The attendant rise in pressure will be relieved to the helium dump tanks but with operation of the steam dump valve, release of helium to the containment will be avoided. Failure of one pilot valve will not prevent closure of the main valve.

Failure of the feedwater isolation valve should not affect loop isolation because it is backed up with another valve - the main feedwater regulating valve.

c. Other Coolant System Safety Actions

(1) Load Reduction

Loss of one boiler recirculation pump reduces flow to the natural convection rate. The control system reduces plant load to approximately 50%, the natural recirculation level. Coincident low trips on two-out-of-three pump differential pressure measurement channels are required.

(2) Steam Dump

After loop isolation upon detection of moisture in the helium coolant, steam pressure is automatically reduced by dumping superheated steam from the affected boiler to the atmosphere outside the secondary containment. This is done by utilizing the steam dump valves which are normally used for overpressure protection, to minimize safety valve operation. These valves are set at approximately 1660 psig and are actuated by remotely set automatic back-pressure controllers. In the steam leak case, the valve on the affected boiler is opened and steam pressure is bled down to about 50 psi above the helium pressure in the affected loop. The valve closes automatically to prevent backflow of helium. In this manner, the maximum amount of steam is released and a steam tube rupture is accommodated without release of helium to the containment or to the atmosphere. The pressure in the helium loop is vented to the helium dump tanks as described in II. G. 5. d.

In the event of a low coolant pressure scram, the same steam dump valves are automatically opened to reduce steam pressure in both boilers. This serves to lessen the steam generator tube stress during the subsequent temperature transient. Should a steam tube rupture also occur, lower steam leak rates result. In this unlikely event, the plant safety system stops the recirculation pump and closes the recirculation pump discharge valve, to further reduce water inleakage. Drum water is also blown down to a tank in the containment. Thus, the total amount of water which can enter the reactor core is kept within safe limits.

The steam dump valves can be manually operated and checked periodically for freedom to operate. Their measuring anc control circuits are available in the control room for the operator to scan as required. Additional backup is provided by the steam turbine

bypass to the condenser which will accept full capacity of both steam generators.

d. Overpressure Protection

As required by the ASME Code, standard relief and safety valves are provided on all portions of the helium and steam circuits within the secondary containment. Since these valves would discharge helium and steam inside the containment, where it would be retained by the pressure-tight design of the secondary containment, presenting an undesirable problem, several additional means of overpressure protection have been provided.

In addition to the steam generator safety valves, described under Primary Coolant System, II. D., steam dump control valves are provided to discharge steam from the superheater outlet lines to the atmosphere outside the containment. They are set to operate at a lower pressure than the safety valves and are sized to pass full steam generator capacity. Except when this dump line is closed by containment isolation, or the dump controller fails, the safety valves should never discharge steam into the secondary containment. The steam dump line is closed automatically only if radioactivity is detected in the line itself. This is precluded when steam is dumped during a steam tube leak by keeping steam pressure always at least 50 psi above helium pressure until dumping is completed. The dump line would not be closed during an overpressure or helium leak dump since no connection exists between the helium and steam circuits.

The main coolant system helium relief valves are also backed up by two sets of dump valves which are also set below relief valve popping pressure. The helium dump valves discharge helium to dump tanks in the helium handling system. These dump tanks can accommodate all helium pressure excursions in the main loop except that which may occur should the steam dump fail during a steam generator tube leak. As described above, the steam generator is automatically isolated and steam pressure is dumped through the aforementioned steam dump valve. When this occurs, the helium dump valves open and the isolated main coolant loop equalizes with the helium dump tanks at a pressure well below the helium relief valve popping pressure, thus effectively preventing a discharge to the containment. Should these actions not occur, the helium loop relief valves will discharge but this

will consist of steam with only traces of helium as the steam will have purged most of the helium into the helium dump tanks.

Throughout the helium handling and purification systems, helium relief valves are provided as required on helium compressors and on tanks that can be overpressured by loss of cooling. These valves discharge to the low pressure helium tank in the helium handling system which is kept at a few pounds pressure by pumping to the helium purification system. This tank, if overpressured, will relieve to the containment which is the last pressure container. Wherever possible, leak-tight assemblies of rupture disks and relief valves are used to minimize relief valve leakage to the containment and all installations are in accordance with the applicable codes.

e. Annunciators

Alarms throughout the plant are indicated on a main alarm annunciator to warn the reactor operator that an abnormal condition requiring his attention exists or that an automatic protective action has taken place. The circuits feeding each alarm point are arranged to alarm on loss of electrical power. The critical annunciators are fed from the most reliable power source.

A separate annunciator is supplied to indicate scram. It will indicate the trip that caused a scram so that positive identification may be made of the trouble source. This annunciator is fed from the most reliable power source.

H. Fuel Handling System

1. General Information

Batch loading of fuel will be used for the Peach Bottom Atomic Power Station. Because of the relatively long core life expected, fuel handling should normally be necessary only on very infrequent occasions.

The fuel handling equipment includes a fuel transfer machine, a charge machine, a fuel element canning machine, a pickup cell and a viewing system. A gas purge system is used for filling the fuel handling equipment with clean helium and for removing contaminated helium from the machines. Parking holes in the side reflector are used to facilitate the transfer of fuel elements within the reactor. A storage pit and associated equipment are provided for the storage of spent fuel. Access to the core is obtained through ports in the top of the pressure vessel. During reactor operation these ports contain shield plugs and are sealed with blind flanges.

The function of the transfer machine is to move control rods and fuel and reflector elements from any position within the reactor core to one of several parking holes. New fuel elements are picked up from the parking hole directly under the fuel charge access port and moved by the transfer machine to a position previously vacated by a discharged element.

The charge machine transfers fuel elements between a position over the fuel charge access port, a position over the canning machine, and a position over the pickup cell. Spent elements are picked up from the parking hole and transferred to the canning machine. On its return trip the charge machine stops over the pickup cell, picks up a new fuel element, moves over to the fuel charge access port, and deposits the element into the parking hole in the side reflector.

The viewing device is used to provide general information during fuel changes. It is not necessary to depend upon the viewing device for precise information since the transfer machine and charge machine have built-in self-alignment features.

New fuel in sealed cans is received at the Peach Bottom Station completely assembled and ready for insertion into the reactor. After arrival, the fuel element and can is placed in a storage area until required for recharging, at which time it is moved to an area adjacent to the pickup cell.

To change fuel, the reactor is shut down, the core cooled, and the coolant pressure reduced to slightly below atmospheric to ensure that any leakage will be inward, into the reactor during fuel handling. The blind flanges covering the access ports in the top of the reactor vessel are removed and replaced by shielded gate valves. Shield plugs in the access ports are lifted into a shielded cask and removed. The fuel transfer machine is then secured to the isolation valve flange, the valve is opened, and the machine is lowered into the pressure vessel through the centrally located port. A single spent fuel element is lifted up out of the core and transferred to a parking hole. The fuel element is then lifted vertically upward into the charge machine by means of a cable-operated grappler. The charge machine travels to a position over the canning machine and the spent fuel element is lowered into a canister previously placed therein. The canister has a welded bottom, and a cap is brazed in the top by remote control to hermetically seal the spent fuel element within the canister. The canister is then leak-tested before being lowered out of the plant container to the bottom of the spent fuel storage pit by the elevator. A winch mounted on a movable platform picks up the canister, moves it underwater, and places it in a storage rack.

The charge machine on its return trip to the access port stops over the pickup cell. A new fuel element previously placed therein is raised into the charge machine. The machine is then moved over to the access port above the reactor and the element is lowered into the parking hole. It is then transferred by the fuel transfer machine to the previously vacated position in the core, and the next fuel element is then removed from the core by the transfer machine to repeat the cycle.

Between each operation in the fuel reloading cycle, when equipment is to be attached to or disengaged from the reactor vessel or other pieces of equipment, all spaces which are opened to the containment atmosphere are purged of helium and refilled with air.

The following table summarizes the principal operations for the fuel handling procedure and the equipment used to perform the operation.

a. Preparation for Refueling

Operation	Major Equipment Used
Purge space beneath access port blind flanges	Purge system
Remove blind flanges	Hand tools
Install isolation valves	Building crane and hand tools

Purge space below valves	Purge system
Remove shield plugs	Plug removal cask
Install transfer machine	Building crane and hand tools
Install viewing device	Building crane and hand tools

b. Spent Fuel Removal

Operation	Major Equipment Used
Transfer fuel element from core to charge port parking hole.	Transfer machine
Raise fuel from parking hole. Carry to canning machine. Lower into canning machine.	Charge machine
Seal fuel element into canister	Canning machine
Leak check	Leak detector
Lower canister into spent fuel storage pit.	Fuel elevator
Place canister in storage rack.	Fuel storage pit bridge

c. New Fuel Insertion

Operation	Major Equipment Used
Transfer new fuel from storage room to reactor operating floor.	Building cranes and transfer dollies.
Transfer fuel element from shipping canister to pickup cell.	Lightweight hoist
Lift fuel from pickup cell. Carry to reactor. Lower into reactor through charge port.	Charge machine
Transfer fuel element from parking hole to core position.	Transfer machine

d. Spent Fuel Shipping

Operation	Major Equipment Used
Place fuel in shipping cask.	Fuel storage pit crane
Ship to process plant.	Shipping cask

e. New Fuel Shipping

Operation	Major Equipment Used
Ship to plant	Shipping container
Store fuel at plant	Cranes and storage racks

2. Fuel Handling Equipment

Figure 121 is an over-all plant layout including part of the fuel handling equipment, while Figure 75 shows the transfer equipment in greater detail. The lower end of the fuel transfer machine with its pickup mechanism may also be seen in Figure 76.

a. Access Ports

Before a fuel element can be removed from the core, access must be gained to the primary system by way of the refueling ports located in the top of the pressure vessel. There are five of these ports: a central port of approximately 20 inches minimum diameter, through which the transfer machine is inserted; a charge machine access port of 6 inches minimum diameter; and three 10 inch diameter access ports for the viewing system and salvage equipment. During normal operation, each of these ports is sealed by means of a bolted blind flange. Shielding is provided by means of an internal shield plug located within each access tube. Leakage into or from the primary system is prevented when the blind flanges are removed by "O" ring seals incorporated in the shield plug. Manually operated valves in the access port flanges used to connect the space between the blind flange and the nozzle plug with the purge system are sealed tight during reactor operation. These seals are removed and flexible pipes are used to connect the valves on the nozzle with the automatic purge system control valves when the reactor is to be recharged with fuel. An "O" ring gasket provides a gas tight seal between mating flanges on the isolation valve and the access port after the blind flange has been removed for the refueling operation. Once an isolation valve is attached to an access port and the plug is removed, the valve is never opened directly to the atmosphere, but is opened only when the appropriate machine is attached.

When removed from the reactor, the access port plugs are stored in a shielded storage facility. Since these plugs may have picked up some surface contamination, the lower section will be

encased in a plastic bag after its removal from the nozzle. Storage and decontamination facilities are provided for the fuel handling equipment.

b. Fuel Transfer Machine

The transfer machine, shown schematically in Figures 77 and 78, operates within the reactor pressure vessel and serves to transfer fuel elements between any core location and the parking space directly under the charge machine access port. It consists of a fuel element grappler head, a hoist mechanism for raising and lowering the head, a rack-operated linkage mechanism that maintains the head at constant height during change of radial position, and a rotating mechanism that rotates the head to an azimuth position. All machine positions are remotely indicated and controlled. Once the grappler head is within a 1-1/2 inch diameter circle of the proper location over the fuel element, it can align itself directly over the fuel element with precision since the sensing mechanism in the grappler head locates the position of a fuel element by making contact with one or more of the six adjacent fuel elements. This is accomplished by means of a free-floating grappler head. Another safety feature incorporated into the head is a device which enables the operator to determine the force with which he is pulling or pushing on a fuel element. All elements of the mechanism and the fuel handling system are suitably interlocked with each other to prevent malfunctioning of the system.

The machine is designed for operation at 450 F, and it will be removed from the pressure vessel during reactor operation.

c. Viewing System

A viewing device will be inserted into the reactor during fuel changes to view the top of the reactor core and view a fuel or control element during the refueling operation. The transfer machine and charge machines have built-in self-aligning features making it unnecessary to use the viewing machine for precise information.

d. Charge Machine

The charge machine (shown in Figure 79) consists of a movable shielded cask mounted on rails. It travels between a position over the fuel charging access port of the reactor pressure vessel, a position over a pickup cell in the floor, and a position over a canning machine which is located above an elevator that connects with

the spent-fuel pit. A direct current variable speed motor is used to propel the charge machine. A winch mounted in the upper end of the charge machine serves to lift fuel elements into the cask from the pickup cell or from the reactor by means of a grappler which is supported by two steel tapes; a third tape between these two actuates the grappler jaws. All three tapes lie in one plane and pass through a tape seal assembly consisting of rubber discs which can be squeezed onto the tapes by means of external gas pressure. The seal assembly will permit emergency maintenance work on the hoist mechanism while the machine is over the reactor.

All tapes pass over independently mounted idler pulleys and then onto tape drums. To actuate the grappler jaws, the idler for the grappler-actuating tape is raised and lowered by means of a plate cam. The two other idler pulleys for the main-load-carrying tapes are supported by strain gage load cells which will permit the operator to know the total load and the load on each tape; a zero load indication for one tape may indicate a broken tape.

A pneumatically-operated piston and seal device provides the sealing between the charge machine and the various components that the machine serves. When the device is operated and the valves of the various pieces of equipment are opened, the seal connects the machine and reactor into a continuous tube for the passage of reactor core components.

Purging of the space between the valves at the bottom of the charge machine and the nozzle access port minimizes the release of fission products to the containment building during fuel changing operations.

e. Fuel Element Canning Machine

The canning machine, shown in Figure 80, is located at operating floor level in the reactor biological shield. The upper end, encased in concrete, houses the pneumatically operated isolation valves and the canister capping mechanism. A steel tube filled with water encloses the canister positioning device and the elevator for lowering the canister into the storage pit. The canister is 4-1/2 inches in outside diameter and approximately 13 feet long. Its bottom end is sealed tight and is fitted with a groove to hold the canister in position when placed in the water filled tube. A pneumatically-operated torus seal surrounds the canister and provides the lower seal for the housing during the canning operation. Each canister is manually placed before the charging machine moves horizontally to its position over the canning

machine. A previously placed cap is automatically moved into the canister and brazed under a helium atmosphere by a remotely operated induction brazing machine to hermetically seal the spent element within the can. Before the canister is conveyed to the storage pit, it is tested with a leak detector for helium or activity.

The canning machine has the capability of decanning an element. Thus, the cap can be removed from a leaky can, the element pulled back into the charge machine, and then the element recanned by the procedure described above. In a similar manner an irradiated element can be decanned and recharged into the reactor.

f. Spent-Fuel Elevator

The spent-fuel elevator is designed to assure the safe transfer of spent fuel elements to and from the spent fuel pit and the canning machine located on the operating floor level of the containment structure. The spent-fuel transfer tube and elevator are shown in Figure 118. During operation, the elevator will be sealed to maintain containment leak tightness and integrity.

The elevator operates within a shielded tube connecting the canning machine with the spent-fuel pit. It consists of a carriage mounted on rails within the tube and powered by a cable-winch arrangement. The winch and elevator controls are located on the operating floor level inside the containment.

The upper transfer station is integral with the canning machine canister guide tube. While the elevator is in operation, a continuous supply of water from the spent-fuel pit is pumped into the upper station to cool the canned fuel element until it reaches the spent-fuel-pit water level in the elevator tube. Overflow from the fuel transfer tube will drain by gravity to the spent-fuel pit.

The transfer operation is as follows:

(1) An empty canister is placed in the canning machine guide tube.
(2) After the charge machine has placed the fuel element in the canister and after the canister has been sealed and tested, the canister is released from the canning position and locked in the elevator transfer position.
(3) The can is permitted to descend by gravity, the rate of descent being controlled by the hoist controls.

(4) Upon reaching the lower parking position, the water flow to the upper station is stopped, the element is released from the elevator carriage, picked up by the spent-fuel-pit traveling hoist and transferred to its designated position in the spent-fuel-pit.
(5) The elevator is raised to its starting position.
(6) The above cycle is reversible for situations in which it is desired to transfer fuel temporarily stored in the spent-fuel pit, back to the reactor core.

g. Pickup Cell

The pickup cell, shown in Figure 75, consists of a 9-inch outside diameter circular pipe 13 feet long encased in the biological shield. The upper end is flanged to receive the support section which is a closed end tube 5-1/2 inch diameter by 12 feet long. It includes a valve at the upper end which is flush with the floor. Each new fuel element is lifted from its shipping canister by means of a lightweight hoist and placed in the pickup cell. The valve is closed and the cell is evacuated of air and filled with helium. The valve is opened again when the charge machine stops over the pickup cell to receive the new element.

h. Fuel Handling Purge System

The fuel handling purge system for the HTGR has been designed so that essentially all helium used in the operation will be contained within the helium handling and main coolant systems (Figure 81.) Purified helium is used for filling the fuel handling machines; the helium evacuated from these machines is returned to the low pressure tank in the helium handling system. This arrangement retains within the plant about 99 percent of the total activity released to the fuel handling equipment during a complete core change. The only activity escaping to the atmosphere will result from the residual activity which is swept out in the evacuation of each machine after a helium purge operation. The activity released, based on maximum primary system activities, is estimated to be 0.16 curies total for one complete fuel change or an average of 0.01 curies per day during the refueling operation. This activity is filtered and discharged to the stack through the waste gas system.

The machines to be serviced by the purge system can be divided into two groups. The first group of machines is purged

only at the start and upon conclusion of a normal fuel recharge cycle or search for failed fuel elements. These machines are:

(1) Transfer Machine
(2) Plug Removal Cask
(3) Viewing System
(4) Failed Fuel Element Locator

The second group of machines is purged of air and helium during the charge or discharge of each fuel element as well as at the start and conclusion of the recharge cycle. The machines in this group are:

(1) Charge Machine
(2) Pickup Cell
(3) Fuel Element Canning Machine

Before starting the fuel handling operation, the helium purification system will be continued in operation at rated volume flow rate for one day while the reactor pressure and temperatures are being reduced following reactor shutdown. The main coolant system will then be depressurized to slightly below atmospheric pressure. The inlet valve of the fuel handling purge helium surge tank is opened at this time to build up surge capacity for the first helium fill.

During fuel handling, the manual valves at the individual machines are kept open. Only the purge valves on the appropriate fill or evacuation lines from the machine headers are operated. Purified helium or air for purging is supplied through the fill header and resultant contaminated helium or air is removed through the evacuation header. The contaminated fluid is passed through an "absolute" filter.

Separate vacuum pumps for helium and for air evacuate the particular machine being purged in the fuel handling cycle. In passing through the vacuum pump, helium will pick up a small amount of oil. This oil contamination is removed in an oil trap by an adsorption type cleanup unit.

Air is evacuated from the machines, filtered, and discharged to the stack through the waste gas system. Helium is evacuated to the low pressure helium tank. From this tank, the helium is transferred to the dump tanks, from which it can be reinjected into the main coolant system.

i. Spent-Fuel Pit and Equipment

The spent-fuel pit is located outside the containment and connected to the canning machine inside the containment by the spent-fuel elevator previously described in this section. The spent-fuel pit has been designed to prevent any leakage from the pit to ground water. This will be achieved by the following provisions incorporated into the pit design:

(1) The structure consists of two reinforced-concrete water-tight tanks, one inside of the other, each designed to resist full hydrostatic loading.
(2) The two tanks are separated by a drain barrier which provides additional protection against any leakage into or out of the spent-fuel pit. Such leakage will go directly to a sump from which it will be pumped to radwaste for subsequent handling.
(3) The exterior surface of the outer tank will be completely covered with a waterproof membrane.
(4) The interior surface of the inner tank will be coated with a watertight and decontaminable phenolic coating.
(5) Continuous water stops will be provided at all construction joints on both tanks.

The canned elements are removed from the elevator carriage at its lower parking position by the spent-fuel-pit traveling hoist and placed in the spent-fuel storage rack in the pit. All transfer operations in the spent-fuel-pit are performed under water for shielding purposes.

In addition to providing storage space for 130% of reactor load in a non-critical array; the spent-fuel-pit can be used for storage of limited quantities of contaminated equipment. Storage-pit water will be monitored for radioactivity. Also, it can be circulated to the radioactive liquid waste water demineralizer for cleanup.

Makeup to the system will be from the condensate system. The spent-fuel-pit cooling system (shown in Figure 125) will be a closed system, cooled by the spent-fuel-pit heat exchanger.

3. New Fuel Handling

a. Receiving and Inspection

New fuel elements will be shipped from the fabrication plant to the Peach Bottom site within individual metal canisters. A blanket gas will surround the fuel elements in the canisters. Shipping racks will be used to prevent criticality by ensuring that the elements maintain a 5.5-inch pitch.

Fuel elements will be adequately inspected to assure they are in an acceptable condition prior to placing them in the reactor.

b. Storage

New fuel will be stored in the sealed canisters used for shipping. No special environmental conditions are therefore required in the new fuel storage room. The elements will be stored in a non-critical array in storage racks 2 ft-6 in. square, each containing 25 elements. When the reactor is to be reloaded, the storage rack will be transferred by a crane to a dolly, then moved through the containment equipment door. The containment equipment crane will lift the racks to the operating floor, and place them in the vicinity of the pickup cell. The racks will be used for temporary storage while placing the individual canisters into the pickup cell.

4. Criticality

Calculations of possible critical configurations for the fresh and spent fuel storage areas show that one hundred fresh fuel elements, compactly arranged in a right circular cylinder are needed to form a critical configuration. Approximately 60 elements would form a critical system if reflected. One thousand fresh fuel elements sealed in individual canisters are safe if arranged on a 5.25-inch square pitch even when moderated by total immersion in water.

5. Damaged Fuel Element Removal and Equipment

Consideration has been given to the following postulated situations during fuel handling operations:

(1) A reflector dummy element broken off at the discharge hole prior to the removal of any others from the core.
(2) A spent fuel element in the unloading hole and so damaged that it cannot be removed by the usual grappler.
(3) A new or spent fuel element, or section of element, dropped so that one end is on top of the core and another leaning against the shroud.
(4) A new or spent fuel element lying across the core top in one or more pieces.
(5) A fuel element that has disintegrated at any point after its removal from the core.
(6) A fuel element in a core position and broken off just below the lifting knob.
(7) A fuel element, in a core position, and broken in several pieces some of which may be small.
(8) A fuel element which is stuck on its standoff support.
(9) The examination of standoffs in place.
(10) The refinishing or deburring of a standoff.
(11) The replacement of a badly damaged standoff.

Simple tools and attachments for machines normally used in the fuel handling cycle will be used for the above situations. The same basic types of equipment can be employed for recovering control rod absorber sections and sleeves.

6. Failed Fuel Element Locator

The Failed Fuel Element Locator hereafter referred to as FFEL, provides a means for finding an element that is releasing an excessive amount of fission products. Positive indication of the occurrence of a fault in a fuel element or its standoff is provided by the coolant monitoring system which continuously monitors the primary coolant activity. After a fault is know to exist, the FFEL is employed to locate the source of abnormal fission product release. It may also be used to measure the temperature and flow distribution of the coolant in the plenum chamber.

The FFEL consists of three components: the sampling and positioning mechanism, sample monitor, and the control console.

The sampling mechanism is a sniffing device which is inserted into the central access port at the top of the reactor. The reactor is shut down for insertion and then started up at reduced power and full system pressure for the sniffing operation. The drive units and seals are at the top, outside the biological shielding for easy access. All the drives are encased in a helium pressurized housing. The pressure in this housing will be substantially above reactor pressure so that all leakage will be into the reactor and all drive mechanisms will remain uncontaminated.

The lower end of the FFEL sampling mechanism consists of a Russel straight line linkage which guides the sampling probe radially from 3 inches to 63 inches in radius. The entire mechanism can be rotated through one turn; continuous rotation is not possible. Also the probe can be raised and lowered through a 7 inch stroke from 2 inches above to 5 inches below the tops of the fuel elements.

The sampling mechanism is lowered into the reactor from, or withdrawn into, a plug removal cask which is bolted to the access port isolation valve during transfer operations. The cask will be purged of air before the mechanism is lowered into the reactor and purged of radioactive gases before being disconnected from the isolation valve.

While the sampling mechanism is expected to be used only occasionally and for short periods of a day or less, the parts subject to high temperature and radiation will be designed for the eventuality of being left in the reactor continuously. Thus, high temperature and neutron activation properties will govern the materials selection.

The sample monitor is enclosed in a leak-tight container which is connected to the sampling mechanism. A helium purge system is used to remove any activity which might leak into the container and to flush all sample lines after operation. The primary components of the monitoring assembly are: a small charcoal fission product trap to remove all fission products other than Kr and Xe; a pump to maintain sample flow; and scintillation counter assemblies to monitor the remaining gaseous Kr and Xe activity. Solenoid valves

are used for remote control and close on loss of system pressure to prevent excess leakage to the container. The measured sample is returned directly to the reactor through the sampling mechanism. The sampling operation requires from four to ten hours to locate the fault, depending upon its magnitude.

The control console for the FFEL system is outside the reduced oxygen containment to allow full operator access during operation of the FFEL system. Automatic and manual control of the sampling mechanism and sample monitor is accomplished from this console. The position of the faulty element is indicated by the higher levels of Kr and Xe activity of a coolant sample taken from the coolant channels adjacent to the failed element. The channel coolant activity is recorded and compared to the over-all coolant activity as measured by the coolant monitoring system. Provisions are included for background subtraction and cancellation of normal coolant activity buildup. Gamma energy discrimination available with the use of scintillation detectors increases the ability of the system to locate failures. Reduced coolant flow as a result of reduced power operation of the reactor further increases the response of the system at full system pressure and decreases the coolant activity with existing failed elements.

Failure of the sample monitor during failed fuel element location constitutes no public hazard. After an orderly shutdown and decontamination of the sample monitor, it can be repaired and replaced for further scanning operations.

I. Shielding Criteria

The plant will be separated into a number of individual areas for the purpose of meeting the various accessibility and/or isolation requirements.

1. Radiation Levels

The radiation dose rates selected for the purpose of design are based on a maximum accumulated dose of 3.0 rem per calendar quarter, a total lifetime accumulation of 5(N-18)rem, where N = the age of the individual employee. Based on the above values, an adequate arrangement of the plant and local shielding will be made. The following criteria will be used in the design for establishing limiting values of radiation exposure in the various zones.

Zone I - Unlimited access: not more than 1.0 mrem/hr

Zone II - Limited access: not more than 2.5 mrem/hr

Zone III - Controlled access: not more than 40 mrem/hr

Zone IV - Area inaccessible during normal plant operation: over 40 mrem/hr

2. Abnormal Operating Conditions

Sufficient shielding will be provided to prevent excessive exposure as a result of abnormal conditions which could reasonably occur during the lifetime of the plant and for maintenance to correct the abnormal conditions.

In addition, the control room and personnel decontamination room will be arranged so that exposure of the operators performing necessary functions in the plant following the major accidents as well as exposure during evacuation of the area after a reasonable delay time, will be limited to less than once in a lifetime dose. Operating procedures, which will be developed as the plant design progresses, will stipulate that all plant personnel, except on-shift operators, gather in the shielded personnel decontamination room following an incident. Operators will remain in the shielded control room.

J. Research and Development Program

1. Graphite Integrity

a. Introduction

General Atomic has a research and development program to establish long-term integrity of graphite components for the Peach Bottom reactor. These components are graphite tubes of low permeability, fuel compacts, control materials, and reflector materials. The program involves the investigation of the effects of irradiation, temperature, and chemical impurities on the mechanical and physical properties, as well as on the dimensional stability of all graphite materials in the reactor. For the low permeability graphite components, the effects of environment on permeability are also being investigated.

In the following pages, a brief description of the research and development program, with the results to date, is presented. Most of the results presented herein were obtained from the research and development program carried out by General Atomic for the Peach Bottom reactor. However, some data from other sources, particularly Hanford data on CSF and similar graphites, are included. A part of the General Atomic research and development program involved capsule irradiations of graphite materials in the General Electric Test Reactor. A brief description of the capsules is presented in the following paragraphs, and a summary of the test conditions and a schedule of the irradiations are given in Table 13.

Capsule program GA-308

This program is designed to test primarily the dimensional stability and physical integrity of fuel bodies and fuel particles as a function of fuel particle size, temperature, fuel concentration and exposure. Results were also obtained on metal-graphite compatibility in a simulated HTGR environment, and strength and dimensional changes of graphite specimens at design temperature but low fast neutron exposure. Six capsules make up this series.

Capsule program GA-309

This program is designed to obtain gaseous fission product data on the in situ release rates and delay times of various fuel body-graphite can combinations. Helium is swept over the specimen

TABLE 13

HTGR CAPSULE IRRADIATION SCHEDULE

Capsule Designation	Type of Capsule	Fuel Temp, C	Graphite Temp, C	Exposure		Scheduled into GA Hot Cell	Status of Post-Irrad. Examination
				Burnup, %U	nvt fast, (>0.1 Mev)		
308-1	Fuel compacts	760-955	370-680	2	---	---	Complete
308-2	Fuel compacts	845-1205	570-840	16.7	---	---	95%
308-3	Fuel compacts	1095-1480	650-925	18	---	---	95%
308-4	Fuel compacts	1095-1480	650-925	18	---	---	95%
308-5A	Fuel compacts	1650-1925	1095-1425	Failed	---	---	Complete
308-5B	Fuel compacts	1650-1925	1095-1425	Failed	---	---	85%
309-1,2,3	Sweep gas fuel bodies	1095-1915	760-1480	11	---	---	75%
309-4,5,6	Sweep gas fuel bodies	1205-1815	870-1315	In reactor	---	September 15, 1961	---
309-7,8,9	Sweep gas fuel bodies	1095-1815	870-1315	In reactor	---	October 15, 1961	---
310-1	Control Matl's	---	590-790	---	10^{19}	---	Complete
310-2	Control Matl's	---	540-675	---	4.9×10^{18}	---	Complete
311-1	Graphite	---	315-650	---	$\sim 10^{21}$	---	Complete
311-2	Graphite	---	1370	---	2×10^{21}	---	95%
313-1	Fuel bodies	80	---	7-8	---	---	Complete
310.5-1,3	Control Matl and graphite	---	360-650	---	0.5×10^{21}	June, 15, 1961	---
310.5-2,4	Control Matl and graphite	---	360-650	---	2.1×10^{21}	Nov. 15, 1961	---
311-3,5	Graphite	---	1100-1425	---	0.5×10^{21}	June 15, 1961	---
311-4,6	Graphite	---	1100-1425	---	1.4×10^{21}	Sept. 15, 1961	---
313-2-8	Fuel bodies	80	---	7.8	---	June 15, 1961	---
311-7,8	Graphite	---	650-1000	---	2×10^{21}	Dec. 1, 1961	---

periodically and the sweep stream is analyzed qualitatively and quantitatively for typical fission product gases. A secondary objective is to study the behavior of advanced fuel types which were not tested in the GA-308 program. The properties of interest are dimensional and physical stability, and fuel particle integrity. Nine capsules make up this series.

Capsule program GA-310

This irradiation program was designed to study the dimensional stability of control rod materials at HTGR temperatures and exposures. Re-evaluation of this program has resulted in the 310.5 program. Two capsules make up this series.

Capsule program GA-310.5

This program was initiated to accelerate the control rod irradiation program (GA-310) by exposing the samples in a core to a neutron density higher by about a factor of six. Concurrently the samples would receive a fast neutron dose equal to, or in excess of, that expected in HTGR. Low permeability graphite specimens are included to supplement the data from the GA-311 program over a lower temperature range, 371 to 648 C. Twenty, thirty, and forty weight percent boron as B_4C in graphite are being irradiated in each of four capsules in the program.

Capsule program GA-311

The GA-311 series of capsules is designed to investigate the changes in permeability, thermal conductivity, dimension, and crushing strength of low permeability graphites. The graphite specimens are irradiated in uninstrumented capsules to an exposure range of 7×10^{20} to 2.2×10^{21} nvt fast, at temperatures of 315 to 1427 C. Eight capsules compose the series. Capsules GA-311-3 through GA-311-6 contain identical specimens.

Capsule program GA-313

The objective of this irradiation program is to study the end-of-life behavior of fuel particles in which fission has occurred in 7 to 8 percent of the U^{235}. Post-irradiation annealing will be performed to determine the fission product release rate as a function of annealing temperature.

TABLE 14

IRRADIATION DATA ON GRAPHITES

GA Capsule or Source of Data	Source of Graphite	Type of Graphite	Irrad. Temp, C	Exposure, nvt (>0.1 Mev)	Dim. Changes, % ΔD	ΔL	Remarks
Impregnated Graphites							
308-2[a]	NCC	RXLP-2, impregnated (imp.)	690	$\sim 10^{19}$	-0.05	-0.03	
308-2[a]	NCC	RXLP-2, imp.	845	$\sim 10^{19}$	-0.06	-0.02	
308-2[a]	NCC	CEY, hot formed, imp.	690	$\sim 10^{19}$	-0.03	-0.18	
308-2[a]	NCC	CEY, hot formed, imp.	760	$\sim 10^{19}$	-0.12	-0.09	All samples were machined but not heat treated prior to irrad.
308-2[a]	NCC	CEY, hot formed, imp.	815	$\sim 10^{19}$	-0.11	-0.03	
308-2[a]	NCC	CEY, hot formed, imp.	800	$\sim 10^{19}$	-0.10	-0.07	
308-2[a]	HS	HS-142, imp.	760	$\sim 10^{19}$	-0.06	-0.03	
308-2[a]	HS	HS-142, imp.	800	$\sim 10^{19}$	-0.06	-0.03	
308-2[a]	HS	HS-4, imp.	815	$\sim 10^{19}$	-0.02	-0.03	
311-1[a]	NCC	RXLP-2, imp.	326/670	$\sim 10^{21}$	0.0/-0.10	---	Cyl. 1/2"OD
311-1[a]	NCC	CEY, hot formed, imp.	326/670	$\sim 10^{21}$	0.0/-0.15	---	Cyl. 1" OD
311-1[a]	HS	HS-145, imp.	326/670	$\sim 10^{21}$	-0.4/-0.6	---	Cyl. 1/2" OD
311-2[e]	NCC[b]	AGW, imp.	1100/1400[h]	2×10^{21}	-1.0	-0.76	Sample cut parallel to the extrusion force
311-2[e]	NCC[b]	AGW, imp.	1100/1400[h]	2×10^{21}	-1.2	-1.06	
311-2[e]	NCC[b]	AGW, imp.	1100/1400[h]	2×10^{21}	-0.5/-0.8	---	Sample cut perpendicular to the extrusion force
311-2[e]	NCC[b]	AGW, imp.	1100/1400[h]	2×10^{21}	-0.2/-0.7	---	
311.2[e]	NCC[b]	AGW, imp.	1100/1400[h]	2×10^{21}	-0.4/-0.8	---	
311-2[e]	Morgan[b]	EYX-60, GA imp.	1100/1400[h]	2×10^{21}	-0.6/-0.8	-2.04/-2.44	Small disc.
311-2[e]	Speer[b]	Carbon, GA imp.	1100/1400[h]	2×10^{21}	-1.6/-2.0	-1.2/-2.0	Small disc.
311-2	Hawker-Siddeley	Morgan H/S Imp.	1100-1400[h]	2×10^{21}	-1.2 -1.6	-1.6 -1.6	Both samples from same tube
311-2	General Elec. Co. Ltd.	Sugar Impregnated Discs	1100-1400[h]	2×10^{21}	-0.7	-2.4	Sample 42
					-0.8	-1.2	Sample 47

TABLE 14 (cont'd.)

GA Capsule or Source of Data	Source of Graphite	Type of Graphite	Irrad. Temp, C	Exposure, nvt (>0.1 Mev)	Dim. Changes, % ΔD	ΔL	Remarks
Impregnated Graphites							
311-3[g]	NCC	AGW, Imp.	780/960	$5x10^{20}$	-0.55/-.60	-0.60	
311-3[g]	GLCC	HC-26, Imp.	780/960	$5x10^{20}$	-0.75/-.84	-0.94	
311-3[g]	Speer	901-S, Imp. at GA	780/960	$5x10^{20}$	-0.37/-0.56	-0.90	
311-3	NCC	AGOT	780/960	$5x10^{20}$	-0.09		
311-5[g]	NCC	AGW, Imp.	~1450	$5x10^{20}$	-1./-1.36	-1.04	
311-5[g]	GLCC	HC-26, Imp.	~1450	$5x10^{20}$	-0.75/-1.10	-1.40	
311-5[g]	Speer	901-S, Imp. at GA	~1450	$5x10^{20}$	-0.75/-1.39	-1.04	
311-5	NCC	AGOT	~1450	$5x10^{20}$	-0.20		
310.5-1[g]	NCC	AGW, Imp.	330/420	$5x10^{20}$	-0.12/-0.31	-0.10	
310.5-1[g]	GLCC	HC-26, Imp.	330/420	$5x10^{20}$	-0.20/-2.4	-0.30	
310.5-1[g]	Speer	901-S, Imp. at GA	330/420	$5x10^{20}$	-0.08/-0.24	-0.22	
310.5-1	NCC	AGOT	330/420	$5x10^{20}$	+0.14		
310.5-3	NCC	AGW, Imp.	610/650	$5x10^{20}$	-.20/-0.25	-0.14	
310.5-3	GLCC	HC-26, Imp.	610/650	$5x10^{20}$	-.16/-0.30	-0.08	
310.5-3	Speer	901-S, Imp. at GA	610/650	$5x10^{20}$	-0.10/-0.36	-0.20	
310.5-3	NCC	AGOT	610/650	$5x10^{20}$	-0.01		
Graphite Base-Stock for Impregnation							
311-2	GLCC	HC-26, not Imp.	1100/1400[h]	$2x10^{21}$	-0.1/-0.4	-0.93	Sample cut para. to the extrusion force.
311-2	GLCC	HC-26, not Imp.	1100/1400[h]	$2x10^{21}$	-1.2/-1.5	-1.2	
311-2	GLCC	HC-26, not Imp.	1100/1400[h]	$2x10^{21}$	-0.7/-1.1	---	

NOTE: Accuracy of dimensional measurements is ± 0.1%. The temperature for capsule 311-2 was between

TABLE 14 (cont'd.)

GA Capsule or Source of Data	Source of Graphite	Type of Graphite	Irrad. Temp, C	Exposure, nvt (>0.1 Mev)	Dim. Changes, % ΔD	ΔL	Remarks
Nuclear Grade Graphites							
Ref. 1*	NCC	TSGBF, graphitized at 2450 C	750	1.8×10^{20}	---	-0.06	
Ref. 1	NCC	TSGBF, graphitized at 2450 C	750	1.0×10^{20}	---	-0.32	
Ref. 1	NCC	TSGBF, graphitized at 2450 C	975	2.6×10^{20}	---	-1.11	Fast Flux >1 Mev.
Ref. 1	NCC	TSGBF, graphitized at 2450 C	975	1.9×10^{20}	---	-0.13	
Ref. 1	NCC	TSGBF, graphitized at 2450 C	1050	2.0×10^{20}	---	-0.49	
Ref. 2	NCC	Needle Coke graphite	450	1×10^{21}	-0.049	-0.116	
Ref. 2	NCC	Needle coke graphite	500	1×10^{21}	-0.036	-0.097	
Ref. 2	NCC	Needle coke graphite	600	1×10^{21}	-0.021	-0.069	
Ref. 2	NCC	Needle coke graphite	700	1×10^{21}	-0.014	-0.054	
Ref. 2	NCC	Needle coke graphite	800	1×10^{21}	-0.012	-0.050	
Ref. 2	NCC	Needle coke graphite	900	1×10^{21}	-0.013	---	Diameter is perpendicular to C-axis Length is parallel to C-axis. Fast Flux > 0.18 Mev.
Ref. 2	NCC	Needle coke graphite	1000	1×10^{21}	-0.019	---	
Ref. 2	NCC	Needle coke graphite	1100	1×10^{21}	-0.035	---	
Ref. 2	NCC	Needle coke graphite	1200	1×10^{21}	-0.070	---	
Ref. 2	NCC	CSF graphite	450	1×10^{21}	-0.070	-0.116	
Ref. 2	NCC	CSF graphite	500	1×10^{21}	-0.057	-0.097	
Ref. 2	NCC	CSF graphite	600	1×10^{21}	-0.040	-0.069	
Ref. 2	NCC	CSF graphite	700	1×10^{21}	-0.028	-0.054	
Ref. 2	NCC	CSG graphite	800	1×10^{21}	-0.023	-0.050	
Ref. 2	NCC	CSF graphite	900	1×10^{21}	-0.026	---	
Ref. 2	NCC	CSF graphite	1000	1×10^{21}	-0.036	---	
Ref. 2	NCC	CSF graphite	1100	1×10^{21}	-0.061	---	
Ref. 2	NCC	CSF graphite	1200	1×10^{21}	-0.112	---	

*See Page II - 204.

TABLE 14 (cont'd.)

GA Capsule or Source of Data	Source of Graphite	Type of Graphite	Irrad. Temp, C	Exposure, nvt (>0.1 Mev)	Dim. Changes-% ΔD	ΔL	Remarks
Nuclear Grade Graphites							
Ref. 2	NCC	CSF graphite	1200	$3x10^{21}$	-0.35	---	
Ref. 2	Morgan	EYX-60	550/700	$0.8/1.5x10^{21}$	-0.33/-0.46	---	
Ref. 2	Dragon	H-10, pitch bonded	550/700	$0.8/1.5x10^{21}$	-0.1/-0.16	---	
Ref. 2	Dragon	H-12, furfuryl alcohol bonded	550/700	$0.8/1.5x10^{21}$	-0.17	---	
Ref. 2	NCC	TSF graphite	550/700	$1.3/1.7x10^{21}$	-0.04/-0.14	---	

Footnotes to Table 14

a. The samples in capsules 308-2 and 311-1 were laboratory materials obtained early in the program.

b. The five NCC low-permeability samples of AGW stock were all cut from the same piece; therefore, they are duplicate samples. This material contains 15/20% impregnant coke.

c. The GLCC base stock HC-26 consists of petroleum coke and carbon black (>10% as filler bonded with coal tar pitch which had been heated above 2500 C during manufacture. The three samples were cut from the same piece.

d. The Speer and Morgan materials were impregnated 3 times with carbonization of the impregnant after each impregnation. The 3rd carbonization was followed by graphitization at 2650 C. This was followed by an additional impregnation and carbonization at 1000 C.

e. All samples in Capsule 311-2 were heat treated for one hour at 2650 C after machining.

f. The graphites in References 1 and 2 were irradiated by Dr. D. R. de Halas of Hanford at MTR and GETR.

g. The diameter changes represent a combination of the dimensions both parrallel and perpendicular to the extrusion force. The length changes represent the dimension parallel to the extrusion force.

h. This temperature range is probably close to 1380 - 1430 C.

b. The Effects of Radiation on Low Permeability Graphites

(1) Dimensional changes in graphite sleeve materials

Table 14 presents information obtained as a result of General Atomic's research and development program, as well as information from other sources, as cited in the references. It will be observed from these data that all graphites contract when irradiated at elevated temperatures. The amount of contraction measured is dependent upon the temperature of irradiation and total fast neutron exposure (compare capsules 308-2 and 311-1 with capsule 311-2), and the type of graphite. The current program, discussed below, is designed to elucidate the effect of these variables on the contraction of graphite.

With respect to current work underway, two 311 type capsules and two 310.5 type capsules were removed from the General Electric Test Reactor (GETR) in June and the preliminary results are presented in Table 14. Analysis of the samples included in these capsules indicates that they add to the available data on the effect of radiation on a variety of low permeability graphites, base stocks, and heat treatments. However, these graphites, except for one type, contain either lampblack as an additive to the filler or a non-graphitizing impregnant coke, or both, and the final heat treatment temperature after carbonization was not high enough to fully graphitize the impregnant coke.

Two 311 capsules and two 310.5 capsules, containing the same types of graphites as described above, will be removed from the reactor in September and November.

In addition, two capsules, designated as 311-7 and 311-8, were inserted into GETR early in June. These capsules contain GLCC base stock (HLM-85) impregnated at GA, NCC low permeability graphite, and graphite fuel matrix material. Temperatures of irradiation are 660 and 1100 C. The exposure of these capsules will be $\sim 2 \times 10^{21}$ nvt (> 0.1 Mev). The General Atomic In-Pile Loop element is made of HLM-85 base stock impregnated at General Atomic. This irradiation will be conducted in the GETR loop. Operation of the loop is scheduled to begin during the second half of 1961.

A cooperative program with Hanford has been defined; two capsules will be irradiated in MTR or ETR. These capsules will contain Great Lakes HLM-85 base stock, and needle coke base stock chosen by Hanford, both impregnated at General Atomic. Dr. D. R. de Halas of Hanford will monitor these capsules and will evaluate the results. The purpose of these irradiations is to define the role of impregnant and the

final heat treatment temperature on the contraction of graphite with respect to crystallite changes and dimensional stability under irradiation. The results will be available later this year.

The results from all of these irradiations will assist in the choice of the type of low permeability graphite to be specified for the Peach Bottom core. These results will be available during the first half of 1962 when the particular type of graphite to be used will be selected.

(2) Effect of radiation on the permeability of graphite sleeve materials

An important property to be evaluated is the change in permeability of the graphite sleeve during irradiation. To determine this effect, permeability data measured at room temperature and one atmosphere of helium pressure were obtained on two groups of samples before and after irradiation (Table 15). These data indicate that the increase in permeability of the graphite as a result of irradiation is less than a factor of ten. (A change of $\pm$ 2 times in the permeability is within the experimental error.) Additional permeability data will be obtained from the 311 and 310.5 capsules at present in the test reactor or the GA hot cell (Table 13).

(3) Effect of radiation on the thermal conductivity of graphite sleeve materials

An extruded CEY graphite tube (capsule 311-2) was irradiated at 1380 to 1430 C to an exposure of 2×10^{21} nvt (>0.1 Mev). Thermal conductivity measurements were made before and after irradiation at temperatures from 1100 to 2000 C. Although a scatter in the data was observed ($\pm$ 1 Btu/hr/ft°F). the reduction in thermal conductivity due to radiation was approximately 15% when measured in the temperature range of 1100 to 1400 C. Also, an extruded CEY graphite tube was irradiated at 326 to 670 C to an exposure of approximately 10^{21} nvt (>0.1 Mev). The radiation effect, if any, could not be detected due to a large scatter in the thermal conductivity values ($\pm$ 25%), when measured in the temperature range of 900 to 1200 C.

(4) Effect of radiation on the strength of graphite

Radiation increases the strength of graphite. Woods[3] et al have shown that the compressive strength of graphite increases by approximately 125% when irradiated at 30 C to 10^{21} nvt (thermal). Davidson and Losty[4] report increases in the tensile strength of 50 to 100%, when irradiated at 80 C to 8×10^{19} nvt (thermal). General

TABLE 15

Permeability of Irradiated Graphites

Sample No.	Capsule No.	Temp. of Irrad., C	Exposure, nvt Total Fast Flux (>0.1 Mev)	Source and Type of Graphite	Permeability, cm^2/sec Pre-Irrad.	Post-Irrad.
1	311-2	1100-1400	$2x10^{21}$	GLCC, base stock	$7.9x10^{-2}$	$3x10^{-2}$
2	311-2	1100-1400	$2x10^{21}$	NCC, impregnated	$1.9x10^{-4}$	$4.5x10^{-4}$
3	311-2	1100-1400	$2x10^{21}$	NCC, impregnated	$6x10^{-6}$	$4.6x10^{-5}$
4	311-2	1100-1400	$2x10^{21}$	NCC, impregnated	$1.9x10^{-5}$	$7x10^{-4}$
5	311-2	1100-1400*	$2x10^{21}$	HS, impregnated	$1.6x10^{-4}$	$1.6x10^{-4}$
6	311-2	1100-1400*	$2x10^{21}$	HS, impregnated	$1.3x10^{-4}$	$2x10^{-4}$
7	311-2	1100-1400*	$2x10^{21}$	GEC, Sugar impreg.	$8x10^{-5}$	$6x10^{-5}$
8	311-2	1100-1400*	$2x10^{21}$	GEC, Sugar impreg.	$1.5x10^{-4}$	$3x10^{-4}$
1	311-1	326-670	$\sim 10^{21}$	NCC-CEY	$4x10^{-7}$	$4x10^{-7}$
2	311-1	326-670	$\sim 10^{21}$	NCC-CEY	$2x10^{-6}$	$6x10^{-6}$
3	311-1	326-670	$\sim 10^{21}$	NCC, impregnated	$2x10^{-10}$	$3x10^{-10}$
4	311-1	326-670	$\sim 10^{21}$	NCC, impregnated	$9x10^{-9}$	$3x10^{-9}$
5	311-1	326-670	$\sim 10^{21}$	HS, impregnated	$3x10^{-7}$	$5x10^{-10}$

* This temperature range is close to 1380-1430 C

Atomic compressive strength data reveal increases of 100% or more, when irradiated at 1100/1400 C to 2×10^{21} nvt (>0.1 Mev).

c. Out-of-Pile Tests on Graphites

(1) Thermal dimensional stability

Several experiments have been conducted to separate thermally induced dimensional changes under operating conditions from the irradiation changes. A variety of impregnated graphites and base stocks was heated in helium for 1000 hours at 1300 C. No measurable dimensional changes within experimental error of $\pm$ 0.2% were observed.

(2) Tensile strength and modulus of rupture

The tensile strengths of low permeability graphites at elevated temperatures are given in Table 16. The values compare favorably with commercial graphites manufactured from petroleum coke bonded with pitch. The strength of all low permeability graphites tested to date is adequate for HTGR operation. The modulus of rupture data are presented in Table 17. These values exceed HTGR design requirements.

(3) The integrity of graphite joints

The 10-foot-long sleeve of the fuel element is joined to the upper reflector at one end and to the bottom connector at the other end. Each of these joints is a screwed and bonded type in which the screw thread carries the structural loads imposed upon the joint. The bonding material is different in each case. The upper joint is bonded by means of a carbonaceous cement, and the flow resistance to helium through this joint must be equal to or greater than the flow resistance through the relatively porous material in the upper reflector.

The flow resistance to helium for the lower joint must be equal to or greater than the flow resistance through the low permeability graphite sleeve; therefore, a metallic braze is utilized in the bottom location. The effective helium permeability of this joint, including a 1/2-inch width of graphite on each side of the braze, is specified to be less than 1×10^{-4} cm^2/sec. This joint operates in a relatively cool region of the core, at a temperature of approximately 700 F. Techniques for making brazed joints have been developed using silicon, zirconium or molybdenum disilicide as a brazing material.

TABLE 16

TENSILE STRENGTHS OF LOW PERMEABILITY GRAPHITE

Sample No.[a]	Permeability,[b] cm^2/sec	Testing Temp., °C	Failure Stress, psi	Youngs Modulus, 10^6 psi
GLI-S6-1[d]	2.1×10^{-5}	366	2560	1.65
2		650	1870 (3)	1.63
3		650	2710	1.64
4		1100	2880	1.65
NCI-S1-4	6.2×10^{-4}	366	3290	2.48
3		366	3750	2.48
2		650	4110	2.65
1		1100	4390	2.66
GA imp 1	7.9×10^{-5}	93	4220	2.11
HLM85 2		650	4220	1.96
3		1100	3230	1.96
HLM85 1		371	2700	1.52
Base 2		648	2050	1.51
Stock 3		1093	2730 (c)	1.87 (c)
4		1483	3200 (c)	4.14 (c)
Speer 1		371	2500	1.18
Stock 2		1093	2350 (c)	1.57

(a) Represents typical material available for HTGR sleeve.

(b) Measured at General Atomic

(c) Specimen parted at shoulder, not at test section

(d) GLCC base stock contains carbon black (HC-27)

TABLE 17

MODULUS OF RUPTURE OF GRAPHITES

Type of Graphite			Modulus of Rupture, psi 25 C	Modulus of Rupture, psi 1400 C	Direction of bending with respect to extension axis
GLCC	HC-27	Impreg.	4350	---	Transverse
			4770	---	Transverse
			4150	---	Longitudinal
			3250	---	Longitudinal
GLCC	HLM-85	Not Impreg.	4600	---	Transverse
Speer	901-S	Not Impreg.	5700	---	Transverse
Morgan	EYX-60	Not Impreg.	5500	---	Transverse
NCC	Type N	Impreg.	4,460 (a)	8,435 (a)	Longitudinal
			7,260 (b)	10,180 (b)	Longitudinal
			7,420 (b)	10,450 (b)	Transverse

(a) HTGR sleeve stock

(b) HTGR can stock

One of the requirements of the joint is that it be able to withstand some thermal cycling and long time exposure to relatively high temperatures in a helium atmosphere containing impurities (CO, CO_2, H_2, and H_2O). A total of 25 jointed specimens, cemented and brazed, has been subjected to thermal cycling between 316-950 C in such an atmosphere. The effective helium leak rate of these joints as measured at room temperature and one atmosphere of pressure before cycling ranged from 7×10^{-4} cm^2/sec to 2.5×10^{-6} cm^2/sec. The test was designed to subject the joints to one thermal cycle per day and a maximum number of hours of exposure at the higher temperature. In this way, a 100-day test yields data on the effects of 100 cycles and exposures at high temperatures for longer than 1000 hours. These tests are still in progress. Examination at several intermediate numbers of cycles indicates that the leak rate of the joints increased by about a factor of 10 in the first 10 cycles and further testing through 50 cycles has evidenced no additional degradation of the joints.

Joints using silicon as the brazing material have proved to be the best in the above tests. Based on these data, silicon joints are being tested in the in-pile loop experimental fuel element.

(4) Mechanical tests on fuel elements

A number of mechanical strength tests have been performed on full size fuel element components fabricated from reactor-grade graphite. Table 18 indicates the results of these tests in which components were purposely loaded to failure.

(5) Change in permeability of graphite to reaction with steam

Steam leaking into the helium stream can be expected to react with the graphite sleeve. Under normal operating conditions, essentially all of the water leaking in will react before it is drawn off as CO and H_2 through the purge stream. Thus a steam leak of 0.01 lb/hr for the life of the core corresponds to 1 percent loss of the sleeve. In order to establish the effect of such a loss of graphite on the permeability of sleeve material, three-inch sections of sleeve material have been exposed to steam with periodic measurements of the room temperature helium permeability.

A schematic of the furnace used for heating the specimen is shown in Figure 82. Water vapor was added to the inlet helium stream by bubbling the helium through water. The

TABLE 18

MECHANICAL STRENGTH TESTS ON FUEL ELEMENTS

Fuel Element Component	Type of Loading	Graphite Type	Load at Rupture
Upper reflector fitting	Tensile	AGOT	1750 lb
Upper reflector fitting	Tensile	AGOT	1785 lb
Upper reflector fitting	Tensile	ATJ	1600 lb
Upper reflector fitting	Tensile	ATJ	1650 lb
Grappler knob	Bending	AGOT	1165 in-lb
Grappler knob	Bending	Speer 901s	1305 in-lb
Grappler knob	Torque	AGOT	120 in-lb
Grappler knob	Torque	Speer 901s	186 in-lb
Complete element (without fuel compacts)	Tensile	AGOT	1410 lb (Grappler knob failed)
Complete element (without fuel compacts)	Cantilevered, with load applied at grappler knob	AGOT	25 lb (3 in. of deflection occurred, and the failure was at the bottom connector)
Complete element (without fuel compacts)	Bending, with the bottom end on standoff, a restraint at the upper spacer, and the load applied to middle spacers.	AGOT	165 lb (0.42 inches of deflection occurred, and the sleeve failed 60 in. up from the bottom)

temperature controls the vapor pressure of water. Extent of oxidation of the graphite was measured by weighing the specimen before and after exposure to steam. Helium permeability measurements were made at room temperature by making the graphite specimen be a barrier between two vessels - one evacuated and one held at 1 atmosphere of helium pressure. The helium permeability was then calculated from the pressure rise in the evacuated vessel.

Preliminary tests on relatively permeable graphite indicated that there was a larger change of permeability with weight of carbon lost at 1000° C than at 1200° C. At 900 °C the results appeared to be approximately the same as at 1000 C; however, the rate of reaction was sufficiently slow so that it appeared most practical to make the majority of measurements at 1000 C.

Results of tests at 1000°C on two pieces of Great Lakes graphite are shown in Figure 83. In these tests, the water concentration was held at 3 percent and the helium flow rate was 400 cc/min. At these conditions approximately 50% of the water was reacted. No accurate reaction rate measurements were made in these tests. On the tighter sleeve with an initial permeability of 7×10^{-6} cm^2/sec, an increase in permeability of approximately a factor of 10 for a 1 percent loss of graphite was observed.

(6) Resistance to thermal stress

Tests were made to determine whether structural damage could occur in fuel element sleeves subjected to temperature drops as large as, or larger than, those expected in the reactor. The highest radial temperature drops across a fuel element sleeve will be about 300° F during normal operation. Short sections of low permeability graphite sleeves 3/8 inch thick were subjected to temperature drops of 640° F. for as long as 160 hours, and to drops of 1000°F for several hours without consequent damage. Average temperatures of the graphite specimens were between 1700°F and 2000°F. No damage occurred in any of the graphites typical of HTGR material.

The tests were carried out on graphite specimens of 3-1/2 inch OD, 2-7/8 inch ID, and 4-1/2 inch length. The samples were heated with a graphite resistance heater whose centerline coincided with that of the specimen. A water cooling jacket was placed around the specimens to remove the heat. The average specimen temperature and the wall temperature gradient were adjusted by varying the gap between the specimen and the cooling jacket and by varying

power input. Thermal shields were placed above and below the sample to prevent axial heat losses and keep the ends of the chamber cool. The sample was held in place by two retainers which were fixed in position by the cooling jacket. The entire assembly of heater, specimen, and cooling jacket was placed into a chamber, which could be filled with helium. Figure 84 is a schematic of the basic test apparatus.

The outer surface temperature of the specimen was measured pyrometrically. Thermocouples were cemented to the sample at four locations to measure the outer wall temperature, when optical pyrometer readings could not be obtained.

The chamber was evacuated and filled with helium three times prior to operation to remove as much air as possible. A positive helium pressure was then maintained in the chamber for the duration of the test. The sample, having been sonically tested for defects before installation, was brought up to the desired temperature gradient and maintained there until steady state conditions were reached. Outer surface temperature of the specimen and power consumption of the heater were then measured. The apparatus was cooled down and the sample again sonically tested for external and internal defects. Temperature gradients were calculated from the measured quantities and the known thermal conductivity and dimensions of the specimen.

Typical results are presented in Table 19. The third specimen was graphite of a type which will not be used as fuel element material, and was incompletely regraphitized. No imperfections developed in the other specimens.

d. Fuel Compact Stability Under Irradiation

As pointed out in the discussion on graphite stability, some contraction of the sleeve under irradiation may be encountered in the reactor. A series of capsules containing graphite matrix fuel bodies has been irradiated to determine the deformation which may occur to these bodies under irradiation.

With respect to fuel compact stability, Table 20 presents a compilation of pertinent irradiation data. The first capsule contained six fuel compacts, three of which were produced by National Carbon and three were made by General Atomic. The fuel content was present as $(Th, U)C_2$ converted from the oxide in situ. The U^{235} content was 3 w/o and the Th content was 7 w/o. The temperature of the

TABLE 19

RESULTS OF THERMAL STRESS TESTS

SAMPLE	O. D., in.	I. D., in.	Length, in.	Temp. Drop, * F	Approx. Mean Temp., F	RESULTS
CP-20,	3.50	2.75	4.5	421	550	No defects.
				671	1700	No defects.
				828	1800	No defects.
				1025	2000	No defects.
				1460	2600	No defects.
HSI-2	3.50	2.75	4.5	421	550	No defects.
				617	1650	No defects.
				828	1775	No defects.
				1025	1950	No defects
				1460	2550	Void formed.
GA-ΩK-4A	3.50	2.75	4.5	--	--	No defects
				515	1400	Defects started
				690	1650	Defects remained the same.
				855	1800	More defects present and sample spalled on inside.
				1034	2400	Defects grew to three times size from 855 F.
GLIS-63	3.50	2.732	4.5	254	1000	No defects.
				364	1250	No defects.
				636	1700	No defects after 160 hours, at this condition.

* across 3/8-inch wall.

graphite can containing these fuel compacts was measured, and varied from 575 C at one end of the capsule to 830 C at the other end; the fuel compact temperatures were estimated to be 260 C higher than the can temperatures. The maximum calculated burnup was 16.6% of U^{235}, which is equivalent to 4.25×10^{19} fissions per cm^3 (the average burnup in the reactor will be 10^{19} fissions per cm^3. On the disassembly of the first capsule, it was noted that the general physical appearance of all the fuel bodies was excellent. It will be noted in the table that the National Carbon bodies, whose fuel particle sizes were approximately 4 microns, had the greatest dimensional changes, i.e., contraction in a longitudinal and diametral direction. (The fuel particles in the General Atomic fuel bodies were 110 to 250μ in diameter). This contraction may therefore be attributed primarily to the fission recoil damage to the graphite, since the total fast neutron flux, >0.1 Mev, was only on the order of 10^{19}nvt. (Average range of fission fragments in graphite is about 20 microns.)

The fuel bodies for the second capsule, Table 20, were approximately of the same outer dimensions as for the first capsule; these fuel bodies were annular in shape and contained 22 w/o metal (6.5% U^{235}, 15.5% Th) as $(Th, U)C_2$. The burnup attained was 18% or 6.87×10^{19} fissions/cm^3. It will be noted that the diametral change of these bodies was one of contraction while the longitudinal dimension of the bodies increased. Furthermore, the largest variations occurred for fuel particle sizes of less than 50 microns. The results obtained from these capsules indicate that the minimum size of particles should be in the range of 110 to 250 microns in order to minimize the change in dimensions caused by fission fragment recoils during irradiation.

The cores of the fuel elements were made from graphite of nuclear purity and low permeability. These suffered no physical degradation. These graphite cores contained metal wires that indicated the temperature range up through the melting point of platinum (1774 C).

The fuel bodies used in the third capsule, Table 20, were approximately identical in composition and size to those in the second capsule, except that they were prepared from silicide fuels. Conversion of the silicide to dicarbide was accomplished by sintering. The exposure of these fuel bodies was 6×10^{19} fissions/cm^3. The calculated centerline temperature of these fuel bodies range up to 1480 C. These fuel bodies contained 22 w/o of combined uranium-thorium in a ratio of Th/U=2.5. The particle sizes range from <50

TABLE 20

IRRADIATION EFFECTS IN GRAPHITE BASE FUEL BODIES

Capsule No.	Fuel Compact No.	Manufacturer	Fuel Particle Size, μ	Max. Burnup, 10^{19} fissions per cc	Ave. Temp. of Graphite Can, °C	Fuel Body Centerline Temp, C (calc.)	Dimensional Change, % ΔD	ΔL	Remarks
1	1	NCC	4	4.25	575	840	-1.7	-0.7	Post Irrad.
1	1	NCC	4	4.25	690	955	-1.7	-0.7	Appearance Excellent
1	3	NCC	4	4.25	750	1150	-1.5	-1.4	3 w/o U_{235} and 7 w/o Th as solid solution dicarbide formed from oxide conversion in situ.
1	4	GA	110-250	4.25	815	1205	-0.2	0	
1	5	GA	110-250	4.25	830	1205	-0.1	-0.5	
1	6	GA	110-250	4.25	775	1040	0	0	
2	1	GA	250-500	6.87	650/750	1205	0	+0.2	
2	2	GA	110-250	6.87	730/840	1315	-0.2	+0.2	Appearance good
2	3	GA	<50	6.87	840/900	1400	-1.7	+2.2	6.5 w/o U_{235} and 15.5 w/o Th as solid solution dicarbide
2	4	GA	<50	6.87	900/925	1480	-2.2	+3.0	
2	5	GA	110-250	6.87	760/840	1210	-0.3	-0.1	
2	6	GA	250-500	6.87	705/790	1150	0	+0.1	
3	1	GA	<50	6.01	650/760	1095	-0.9	+3.0	Appearance good
3	1	GA	250-500	6.01	705/790	1290	0	+0.3	Appearance good
3	3	GA	<50	6.01	790/870	1370	-0.8	+0.8	Surface roughened
3	4	GA	110-250	6.01	870/925	1480	-0.1	+0.1	Appearance good
3	5	GA	250-500	6.01	790/840	1230	0	+0.1	Slight long. crack
3	6	GA	110-250	6.01	730/815	1175	0	+0.1	

Note: All group 3 bodies contained 22 w/o U, Th as dicarbides converted from silicide in the ratio of Th/U = 2.5.
Experimental error in measurements: $\pm$ 0.0001" or $\pm$ 0.01%.
Fast neutron exposure: approx. 10^{19} nvt (>0.1 Mev).

to 500 microns. Except for the surface roughening of compact number 3 and a crack in compact number 5, the appearance of the remaining compacts of this capsule is comparable to that prior to irradiation. The dimensional changes indicate the importance of particle size. In this capsule, one of the small particle size fuel bodies was placed in the cold region and another in a hot region. The contractive effect was still greater in both cases for the small particle fuel bodies than for the large particle fuel bodies. The fuel temperature for a fuel body at one end of the capsule was measured and was found to be at 1095 C. The temperatures of the other fuel bodies are not exactly known. However, it was established that a nickel wire in body number 4 had melted which places the temperature in the vicinity of 1480 C.

The data obtained from these capsules would indicate that, generally, the compacts are acceptable from a dimensional and physical integrity point of view. It should be mentioned, however, that the total fast neutron flux was approximately 10^{19} nvt >0.1 Mev. The dimensional stability can be affected by fuel particle size, although it seems to be somewhat temperature insensitive. The burnups for these capsules are in the range of 60 to 75% of that expected for the HTGR fuel. The starting material, whether oxide or silicide, performed satisfactorily.

In addition to the three capsules described above, three sweep gas capsules, (309 series) containing coated carbide fuel particles, have been operating in GETR satisfactorily for the past few months.

The total exposure to date is equivalent to two year's operation in HTGR. Three additional capsules, one with 10 to 15μ coating on the fuel particles and two with 50 to 60μ coating, were inserted in GETR early in May. These capsules are operating satisfactorily. The fuel bodies from these capsules will be examined in the GA Hot Cell later in 1961.

e. Control Materials Irradiation Tests

With respect to the effects of radiation on the control materials, one capsule was irradiated for two cycles in the GETR. It was operated at a temperature of 650 C, the maximum temperature that the HTGR rods would experience. By this comparatively short irradiation, it was hoped to obtain a preliminary evaluation as to whether alpha particles would have a deleterious effect on the graphite matrix. When it was removed from the reactor and examined in the

GA Hot Cell, it was noted that the appearance of all bodies was good, with the exception of one which showed spalling of the surface. It is believed that the defective surface was produced by a short circuit in the capsule heater, which failed during the in-pile operation. The dimensional variations of the capsule are given in Table 21. The degree of contraction shown is not more than expected for graphite subjected to a similar irradiation exposure, and the magnitude is approximately equal to the experimental limits of resolution. Preliminary data on materials in two additional capsules now undergoing examination in the General Atomic hot cell are also presented in Table 21.

A program has been initiated to increase both the amount of boron captures and the fast neutron effects on the control rod graphite matrix by placing samples of control material in the core of the GETR. The first irradiation will be for two cycles which would be equivalent to approximately one-third of the exposure lifetime of an HTGR control rod material. It will not have any temperature control or thermocouples attached. However, metal wires will be inserted in the capsule for the purpose of obtaining indications of the maximum temperature to which the samples were exposed. Additional capsules of this series will be irradiated for six reactor cycles, an exposure equivalent to that expected in HTGR. For information on additional control materials irradiations, refer to the Series 310.5 capsules in the irradiation schedule of Table 14.

TABLE 21

DIMENSIONAL CHANGES OF CONTROL ROD MATERIAL DUE TO RADIATION

(Capsule 310-1)

Temperature of Irradiation: 650 C; Total Fast Flux 0.1 Mev: 10^{19} nvt; Thermal Flux: 1×10^{20} nvt

Sample and Source	Percent Boron	Treatment	Change in Diameter[a], %	Change in Length[b], %
A (Speer)	4.5	Graphitized	-0.03	---
B (Speer)	0	Baked	-0.01	---
C (Speer)	0	Graphitized	-0.08	-0.07
D (Speer)	13	Graphitized	-0.10	+0.10
E (Carborundum)	20		-0.01	+0.13
F (Carborundum)	30			-0.03

(Capsule 310.5-1)

Temperature of Irradiation: 330/420 C; Total Fast Flux 0.1 Mev: 10^{20}nvt.

General Atomic	20	Warm pressed and sintered	-0.19	---
General Atomic	30	"	-0.20	---
General Atomic	40	"	+0.05	---

(Capsule 310.5-3)

Temperature of Irradiation: 610/650 C; Total Fast Flux 0.1 Mev: 10^{20}nvt.

General Atomic	20	Warm Pressed and sintered	-0.15	---
General Atomic	30	"	-0.15	---
General Atomic	40	"	-0.06	---

Error in measurement is $\pm$ 0.1%

(a) Diameter of samples: 310-1, 0.8"; 310.5-1, -3 1.0"

(b) Length of samples: 2.0"

REFERENCES

1. Nightingale, R. E., J. M. Davidson and W. A. Snyder, "Damage Effects to Graphite Irradiated up to 1000°C", Geneva Conference 15/P/614, June 1958.

2. de Halas, D. R., Hanford Labs., to be published.

3. Woods, W. K., Bupp, L. P., and Fletcher, J. F., "Irradiation Damage to Artificial Graphite," Geneva Conference, VII A/Conf. 8/P/746. (1956).

4. Davidson, H. W., and H. H. W. Losty, "The Effect of Neutron Irradiation on the Mechanical Properties of Graphite," Geneva Conference A/Conf. 15/P/28, June 1958.

2. Fission Product Control

a. Introduction

The control of radioactive fission products in the Peach Bottom reactor is based on the following steps:

(1) Delay in the release of volatile fission products from the fuel compacts until the short-lived products have decayed.

(2) Trapping of a large fraction of the condensible fission products in the cold end of the fuel element in an internal trap.

(3) Limitation on release of radioactive fission products to the primary coolant by fabrication of the outer sleeve of the graphite fuel element from low permeability graphite.

(4) Trapping of the most volatile fission product elements (the noble gases, halogens, and traces of a few other elements) from a purge stream passing through the fuel elements in charcoal traps external to the reactor pressure vessel.

The fundamental physical information on which the conceptual design of such a fission product system was based existed in the open literature or in the early results of the HTGR research and development program. The recent experimental work has been carried out to give quantitative information for detailed design purposes. The experiments bearing on the points enumerated above have been as follows:

(1) Experiments to measure the release of individual fission product elements from fuel compacts at elevated temperatures and after varying amounts of fuel burnup. These experiments have been of increasing complexity and have been of the following types:

(a) Tracer experiments in which lightly irradiated compacts have been heated in a furnace and the amount of fission product release as a function of time measured.

(b) Purge capsule experiments in which the steady state release of volatile fission products during irradiation of the fuel compact in a test reactor has been directly measured.

(c) Experiments to measure the change in release rate of volatile fission products from fuel compacts following accelerated

irradiation of the fuel compacts to full HTGR burnup.

(d) Measurements of the behavior of all of the fission product elements in an integral test of the whole system will be made using the In-pile Loop in the General Electric Test Reactor at Vallecitos. The loop is now scheduled to be in full operation during the fourth quarter of 1961.

(2) Quantitative measurements have been made of the efficiency of trapping condensible fission products by reagents which will be used in the internal fission product trap. These experiments have emphasized the important elements cesium, iodine, and tellurium and have demonstrated fully the effectiveness of a charcoal-silver reagent for use in the internal trap.

(3) The program to measure the properties of, and to develop a source for, low permeability graphite, has been described in Section II. J. 1. of this report.

(4) Experiments have been carried out to measure, with quite high precision, the capacity of activated charcoal to remove iodine, xenon and krypton from a helium gas stream as a function of temperature.

The body of this section presents in detail the experimental results which have been obtained in the course of this program.

b. Research and Development Results and Progress

(1) Background Technology

(a) Retention of Fission Products

The retention or delay of the fission products within the HTGR fuel compacts is determined by solid state diffusion. More specifically, the fraction of a particular fission product nuclide which escapes is a decreasing function of $\sqrt{\lambda\tau}$ where λ is the radioactive decay constant of the nucleus and τ is the characteristic diffusion time of the given element which is determined by the diffusion constant and dimensions of the material from which the nuclide escapes. In general, there can be several components and associated characteristic diffusion times which are required to specify the diffusional behavior. The fraction of a component escaping will be approximately 1 if $\tau \ll 1/\lambda$ and approximately 0 if $\tau \gg 1/\lambda$. The characteristic diffusion time τ has been measured for the important volatile fission product elements as

part of the research and development program.

The volatility characteristics of the thirty-five predominant fission product elements have been studied at General Atomic.[1] Seventeen of the thirty-five elements from germanium to dysprosium may be considered non-volatile at HTGR operating temperatures. These elements comprise volatility Category 3 in Table 22 . In addition, it should be noted that the following elements form carbides of moderate to great stability.*

Y	La	Pm
Zr	Ce	Gd
Nb	Pr	Tb
Mo	Nd	Dy

The formation of the fission product carbides significantly lowers the vapor pressure of the element. It is expected, therefore, that these elements will remain fixed in the fuel compacts, or at worst diffuse out only at extremely slow rates. Their disposition will be determined in the in-pile loop program discussed below.

The remaining fission products are either gases at reactor temperatures or have appreciable vapor pressures at the operating temperatures. These volatile fission product elements must be retained in the trapping systems.

The fission yields of elements given in Table 22 correspond to the sum of the yields of all mass chains ending with a stable nuclide of the element or a nuclide of the element with a half life greater than one year. This gives the distribution of the elements (the number of atoms produced is proportional to ΣY) corresponding to that obtained when the reactor has run for an extended period of time ($\geq$ one year).

In accordance with these volatility characteristics, the following fission product elements are expected to reach the internal fission product traps in significant quantities: Se, Br, Kr, Rb, Sr, Sb, Te, I, Xe, Cs, Ba, Sm, and Eu. These are elements in volatility categories 1 and 2 in Table 22 . Others in these categories which are unimportant because of low yields are: As, Cd, Ge, Ag, and In.

(b) Trapping of Iodine

Activated charcoal has been known for some time to have a high affinity for iodine and bromine. In 1935, Reyerson and

*Sr, Ba, Sm, and Eu also form carbides but the vapor pressures of the elements themselves are relatively high.

TABLE 22

FISSION PRODUCT ELEMENT YIELDS AND CHARACTERISTICS

Volatility Category of Element*	Element	Fission Yield of Element ΣY (%)	b. p. (^{o}K) of Element	Temp. (^{o}K) at which Carbide Vapor Pressure $<10^{-7}$ atm.
2	Ge	0.00232	3,100.	
1	As	0.0008	866.	
1	Se	0.485	958.	
1	Br	0.14	331.4	
1	Kr	5.86	119.75	
1	Rb	3.5	974.	
2	Sr	9.4	1,640.	
3	Y	4.8	(3,500.)	2000
3	Zr	31.0	4,650.	2500
3	Nb	0	5,200.	2500
3	Mo	24.5	5,100.	2500
3	Tc	6.1	4,900.	
3	Ru	11.29	(4,000.)	
3	Rh	3.0	(4,000.)	
3	Pd	1.173	3,400.	
2	Ag	0.03	2,450.	
1	Cd	0.097	1,038.	
2	In	0.011	2,320.	
3	Sn	0.095	2,960.	
2	Sb	0.058	1,910.	
1	Te	2.42	1,260.	
1	I	1.03	456.	
1	Xe	22.3	165.04	
1	Cs	18.0	958.	
2	Ba	5.7	1,910.	
3	La	6.2	3,640	2000
3	Ce	12.4	3,200.	1500
3	Pr	6.0	3,290.	1500
3	Nd	21.17	3,360.	1500
3	Pm	2.4	(3,000.)	1500
2	Sm	1.92	(1,860.)	
2	Eu	0.183	(1,700.)	
3	Gd	0.015	(3,000.)	1500
3	Tb	0.001	(2,800.)	1500
3	Dy	0.00005	2,600.	1500

*Volatility Category:

1. b.p. $< 1500^{o}K$
2. Intermediate between 1 and 3
3. v.p. of element or carbide $<10^{-7}$ atm at $1500^{o}K$

Cameron [2] reported studies that indicated activated adsorption is monomolecular in depth of the adsorbed layer. Adsorption isotherms were obtained which followed the Langmuir equation. More recently the effectiveness of charcoal in removing iodine from gas streams has been studied at Hanford and at Oak Ridge.

The removal of iodine from a helium stream by charcoal at room temperature was studied by Finnigan, et al. at Hanford. [3] They observed a decontamination factor of 10^7, i.e., a fractional iodine penetration of 10^{-7}. The iodine was all adsorbed in the first few millimeters of a 4-inch long charcoal bed, and the iodine showed essentially no movement in the bed after the bed was heated to 80 C.

Similar studies were performed by Adams and Browning at Oak Ridge, [4] using air rather than helium as the carrier gas. A removal efficienty of 99.95 per cent (5×10^{-4} fractional penetration) was observed for a 12-inch long charcoal bed at room temperature with an air velocity through the bed of 180 ft/min.

In more recent studies, [5] Adams and Browning compared the effectiveness of charcoal and silver-plated copper ribbon in removing iodine from room temperature air streams. Removal efficiency of the charcoal was found to be superior to that of the ribbon. Efficiencies of 99.63, 99.89, and 99.99+ percent were observed for three different charcoal mesh sizes operating at room temperature. Air velocities from 82 to 275 ft/min showed little effect on efficiency. Use of moist air at 80 per cent relative humidity had no significant effect on efficiency. Use of charcoal containing large amounts of dust reduced the efficiency, indicating some penetration of iodine adsorbed on dust particles.

A charcoal bed is currently being used to remove iodine from the off-gas of the radioactive lanthanum dissolver at the Chemical Processing Plant of the National Reactor Testing Station, Idaho Falls, Idaho. Off-gas from the dissolver is air containing I, Kr, and Xe. Total activity content for a single run includes about 30,000 curies of I^{131}, 35,000 curies of I^{132}, and 6,000 curies of I^{133}. The off-gas (16 to 20 cfm) is passed through a 16-inch-diameter, 6-foot-long bed of charcoal at room temperature to remove iodine.

Efficiency of the adsorber bed was measured by locating small test traps on bypass lines at the inlet and outlet of the adsorber. The test traps consisted of small charcoal beds followed by glass wool filters. Comparison of total activity in the two test traps indicated inlet to outlet activity ratios which ranged from 12/1 to 33/1. However, some of the activity in the outlet test trap was in the filter section, rather

than the charcoal, indicating that this activity passed through the adsorber in particulate form. Comparing the activities on the charcoal sections of the test traps gave inlet to outlet ratios greater than 1000/1, indicating that the adsorber bed was quite efficient for removing gaseous iodine.

The adsorber bed has been in operation for two years during which time about 20 runs have been carried out. The absorber has not required regeneration or replacement thus far, but provision has been made in the adsorber design to permit insertion of a "vacuum-cleaner" nozzle which would suck out the old charcoal and thus permit replacement with fresh adsorber.

(c) Trapping of Krypton and Xenon

Information on the removal of radioactive krypton and xenon from gas streams by adsorption has been developed in connection with the following three projects: The Homogeneous Reactor Test (HRT) at Oak Ridge National Laboratory, the dissolver off-gas system of the Idaho Chemical Processing Plant, and the AERE Dragon Project in Great Britain. Activated charcoal has been the adsorbent of primary interest in all three cases. Two different types of adsorption processes have been studied. In the first type, an adsorber bed operating at approximately 20 C is used to delay the passage of the fission gases and thus cause decay of the shorter-lived radioactive isotopes; in the second type, an adsorber bed operating near the boiling point of nitrogen (-320F) is used to provide complete retention of the fission gases.

Browning and his associates have carried out fission gas adsorption experiments over a fairly wide range of temperatures, adsorber materials, and carrier gases.[6] Two parallel adsorber beds, each containing 520 pounds of charcoal, are used on the HRT. These tests have shown[7] that these adsorbers provide a krypton holdup of more than 200 hours, with the xenon holdup being about ten times greater.

Experiments on the adsorption of krypton and xenon have also been performed at Harwell in Great Britain, in connection with the fission product trapping system for the Dragon Reactor. Dynamic experiments similar to those of Browning have been performed by Sangster,[8] using hydrogen as the carrier gas. Amphlett and Greenfield,[9] also at Harwell, obtained adsorption isotherms in a static system by direct pressure measurement (no carrier gas). Amphlett and Greenfield included measurements on irradiated charcoal; results showed either no change with irradiation or a moderate increase in adsorption after irradiation.

A charcoal bed operating at about -300 F has been used to separate krypton and xenon from the dissolver off-gas at the Chemical Processing Plant in Idaho. The off-gas stream (principally nitrogen) is passed through charcoal-filled tubes, the tubes being submerged in liquid nitrogen. Adsorption data used in the design of the off-gas facility were correlated by Holmes. [12] Holmes also presents data on the mass transfer rates in charcoal beds, expressed in terms of the "height of a transfer unit," which permit adsorber lifetime to be calculated as a function of the required adsorber efficiency. Adsorption isotherms for krypton and xenon on charcoal at low temperatures ($\sim$-300 F) have been measured by Burdick. [13]

(d) Filters

Methods of removing radioactive particulate matter from gas streams have been given considerable study at the Hanford Atomic Products Operation. The Hanford work has been summarized by Blasewitz and Judson [14]; they recommend the use of packed glass fiber filters. By arranging the filter in layers of successively finer fibers, relatively long service life can be obtained (filters of this type have operated for over 3 years at Hanford). Blasewitz and Judson have determined the filter characteristics for a superficial gas velocity of 20 ft/min as shown in Table 23. The filter efficiency is observed to increase as the filter becomes loaded. Quoted efficiencies are for particles in the size range of 0.2 to 0.7 micron. Particles of 0.1 to 1.0 micron diameter are generally the most difficult to remove by filtration. [15]

(2) Results and Continuing Program

(a) Fission Product Release Data

GA 309 Irradiation Capsule Tests

Fission product release data have been obtained through operation of General Atomic purge capsules in the GETR. These purge capsules contain approximately 2 grams each of 93% enriched uranium together with 2.25 times as much thorium. The fissile and fertile material are intimately mixed together in the form of solid solution ThC_2 - UC_2 particles and are coated with about 25 microns of pyrolytic carbon. The particles themselves are approximately 50-60 microns in diameter. These particles are imbedded in a graphite matrix and in turn are sealed in a graphite can with a zirconium braze. Three such capsules are assembled in separate compartments of a stainless steel facility tube, which is inserted into the reactor. Each capsule is provided with its own supply of sweep gas for sampling. Activity of the sampling gas is an indication of holdup capability of the capsules.

TABLE 23

FIBERGLASS FILTER EFFECTIVENESS

Layer	Type Fiberglass*	Mean Dia.	Packing Density (lb/cu. ft)	Bed Depth (in)	Initial Efficiency (%)	Initial Pressure Drop (in. of Water)
Bottom	115K	30	1.5	12	39	0.10
Second	115K	30	3.0	10	53	0.24
Third	115K	30	6.0	20	93	1.34
Clean-Up	AA	1.3	1.2	1	99.9	2.20
	Total			43	99.9	4.0

*Owens Corning designation

Such an assembly, with three purge capsules, has been under irradiation since November 16, 1960. These capsules have received roughly 50% of HTGR burnup as of May, 1961. The fractional release of krypton and xenon fission product activity shows an increase with fuel body temperature and a tendency to increase with total megawatt days exposure in the reactor. There is also some indication of a half-life ($T_{1/2}$) dependence - but with n less than 0.5 where release is taken as proportional to $(T_{1/2})^n$.

In general, the steady state release of xenon and krypton fission products at 1700 C is less than 1% for the short-lived Kr and Xe (<2.8 h) and up to about 3% for the longer-lived species (4.4 h Kr^{85m} and 5.3 d Xe^{133}). This, however, does not include Kr^{85} (10.3y). The rate of release relative to the rate of production for this isotope is in the range of 20%.

Fission product release data obtained on the 309-4, -5 and -6 capsules to date are given in Tables 24, 25 and 26.

GA-313 Irradiation Capsule Experiments

The 313 capsule program is primarily for investigating the effect of burnup and fission product accumulation on the integrity of pyrolytic carbon coatings. In preparing the fuel samples, approximately 1 mg of U^{235} as coated ThC_2-UC_2 particles was hot-pressed in a graphite matrix 1 inch in diameter by 1 inch long. An aluminum capsule was used to enclose the graphite capsule during irradiation. Each capsule was irradiated one reactor cycle (24 days) at 2×10^{14} n/cm^2-sec thermal neutron flux. This amount of irradiation produced 20% burnup of the U^{235} which corresponds to the end of life condition expected for HTGR fuel elements.

One capsule was irradiated in December 1960 and after about two months cooling the sample was annealed at 1700 C for approximately 60 hours. This annealing experiment showed a fairly rapid release rate until about 18% of the Xe^{133} and Kr^{85} was lost, then the release rate was very slow. The fast release showed a diffusion time of about 10 hours while the slow component was in excess of 10^4 hours.

The results of the experiment indicated a degradation of some of the particle coatings due to fission product buildup inside the particle while the bulk of the particles (82%) still retained excellent retentive properties. It should be pointed out that the particles examined had rather thin coatings (25μ).

TABLE 24

KR AND XE RELEASE DATA

309-4 CAPSULE

Sample Series	Date and Time	GETR Total MWD	Approximate HTGR Equivalent Burnup (%)	Fuel Body Temp (°C)	Percent Steady State Release						
					Xe^{138} 17m	Kr^{87} 78m	Kr^{88} 2.8h	Kr^{85m} 4.4h	Xe^{135} 9.1h	Xe^{133} 5.3d	Kr^{85} 10.3y
8	11/22/60 1945	191	4	960	-	0.002	0.004	0.006	0.0011	0.017	0.29
11	12/9/60 1009	518	12	1650	-	0.09	0.07	0.30	0.005	0.041	2.1
12A	1/12/60 1135	764	16	1471	-	0.13	0.15	0.23	0.015	0.12	-
14	1/18/61 0921	944	20	1588	≤0.06	0.10	0.19	0.26	0.028	0.28	2.4
17	1/25/61 0927	1111	25	1427	0.027	0.057	0.094	0.12	0.009	0.078	-
20	2/1/61 1402	1321	28	1535	-	0.09	0.15	0.23	0.014	0.20	1.9
23	3/23/61 0945	1495	33	-	-	0.13	0.10	0.20	0.015	0.028	-
28	4/5/61 1011	1824	40	1320	-	0.13	0.17	0.29	0.0095	0.058	-
31	4/10/61 0924	1973	43	1540	-	0.17	0.34	0.56	0.034	0.058	12.0
34	4/18/61 0923	2166	47	1420	-	0.12	0.19	0.33	0.017	0.22	7.9
38	4/26/61 1119	2389	52	1700	-	0.41	0.61	2.0	0.12	1.1	47
40	4/27/61 1024	2419	53	1460	-	-	-	1.2	0.090	0.85	-
41	4/28/61 1032	2449	53	1350	-	0.14	0.30	0.63	0.020	0.43	-

TABLE 25

KR AND XE RELEASE DATA

309-5 CAPSULE

Sample Series	Date and Time	GETR Total MWD	Approximate HTGR Equivalent Burnup (%)	Fuel Body Temp (C)	Percent Steady State Release						
					Xe^{138} 17m	Kr^{87} 78m	Kr^{88} 2.8h	Kr^{85m} 4.4h	Xe^{135} 9.1h	Xe^{133} 5.3d	Kr^{85} 10.3y
8	11/22/60 1604	191	4	1524	-	0.11	0.19	0.35	0.028	0.14	1.0
10	12/8/60 1035	494	11	1702	-	0.39	0.65	0.94	0.0049	0.78	7.2
13	1/13/61 1358	794	18	1760	-	0.37	0.49	0.76	0.047	0.53	-
15	1/19/61 0922	974	21	1799	-	0.79	0.62	0.92	0.072	0.79	-
18	1/26/61 0926	1141	25	1904	0.68	0.56	0.58	0.80	0.073	1.17	25
21	2/2/61 0923	1351	29	1751	-	0.11	0.19	0.36	0.016	0.27	5.4
24	3/24/61 0913	1525	33	-	-	0.27	0.31	0.70	0.027	0.18	-
29	4/6/61 0920	1854	40	1400	-	0.32	0.64	1.2	0.15	0.41	-
32	4/11/61 0946	2003	44	1580	-	0.69	0.81	0.69	0.029	1.2	-
35	4/19/61 0954	2196	48	1550	-	0.41	0.74	1.3	0.053	0.81	8.6
36	4/25/61 1125	2359	51	1650	-	0.91	1.4	1.7	0.19	3.3	64

TABLE 26

KR AND XE RELEASE DATA

309-6 CAPSULE

Sample Series	Date and Time	GETR Total MWD	Approximate HTGR Equivalent Burnup (%)	Fuel Body Temp (C)	Percent Steady State Release						
					Xe^{138} 17m	Kr^{87} 78m	Kr^{88} 2.8h	Kr^{85m} 4.4h	Xe^{135} 9.1h	Xe^{133} 5.3d	Kr^{85} 10.3y
8	11/22/60 1800	191	4	1549	-	-	0.12	0.18	0.010	0.17	0.75
9	12/7/60 1035	470	11	1865	-	0.28	0.37	0.51	0.031	0.64	7.0
16	1/20/61 0953	1004	22	1616	-	0.63	0.53	0.93	0.19	0.87	20
19	1/27/61 0916	1171	26	1746	-	1.4	1.8	2.7	0.16	2.2	-
22	2/3/61 1014	1381	30	1750	0.34	0.8	1.2	2.5	0.13	2.3	-
25	3/25/61 0934	1555	34	-	-	0.22	0.36	0.66	0.027	0.137	-
30	4/7/61 0945	1884	41	1320	-	0.15	0.31	0.61	0.012	0.35	8.2
33	4/12/61 1010	2028	44	1420	-	0.37	0.71	1.2	0.039	1.3	11
36	4/20/61 0938	2217	48	1440	-	0.38	0.74	1.4	0.016	0.44	-
39	4/27/61 1003	2419	52	1240	-	0.30	0.84	1.6	0.05	1.1	20

As of May 1961, additional capsules have been irradiated and will be evaluated in the near future to determine the effect of various parameters.

Post Irradiation (Tracer Level) Annealing Experiments with Uncoated Fuel Particles

Many experiments have been run using tracer activity of xenon in HTGR compacts with uncoated carbide fuel particles to determine the diffusion times at various temperatures. These compacts were prepared from UO_2-THO_2 solid solution particles which were sintered and converted to the dicarbides after being incorporated in a hot-pressed graphite matrix. Particle sizes included diameters ranging from 100 to 200 microns. Measurements taken on these compacts have been fairly consistent and are currently being used as a basis for calculating gross fission product release for emergency design purposes. The method used is to produce approximately 10^{13} fissions in the compact (where the U in the ThC_2-UC_2 is normal uranium) followed by a temperature anneal of 24 to 48 hours. Prior to the anneal, the activity of the compact was allowed to decay for about 5 days. This time is sufficient to allow all short-lived krypton and xenon to decay away except 5.27 day Xe^{133}. Kr^{85} (10.3 y) is not produced in sufficient quantity to be detected.

During the anneal the irradiated compact is purged with pure helium gas. The Xe^{133} in the effluent helium purge is trapped in a liquid N_2 charcoal bed and is monitored continuously using a single channel gamma-ray spectrometer. The resultant data give the integrated fractional release of Xe^{133} out of the compact as a function of time. Using a diffusion model based on the concept of having an assemblage of n types of "equivalent spheres" one can determine diffusion times which are proportional to the equivalent sphere radii squared and inversely proportional to the corresponding diffusion coefficients. Usually, the release function can be represented by two components (i.e., n=2); however, occasionally three are found.

Measurement of Steady-State Release of Xenon and Krypton under Irradiation using a Linear Accelerator

In connection with the tracer studies on uncoated particle compacts, a series of experiments has been completed on Kr-Xe steady state release rates using the linear accelerator facility. These experiments utilized the photofission process for steady state production of rare gas fission products. In this study use is made of the fact that

uranium and thorium stearates are known to release their rare gas fission products very rapidly, i.e., all krypton and xenon isotopes with half-lives greater than 1 sec are released 100%.

A comparison is made between release of specific Kr and Xe nuclides from the subject compact and from the uranium-thorium stearate standard. The compact is heated to the proper temperature during the fissioning process and all rare gases released are trapped in a charcoal bed at liquid nitrogen temperature. A 256 multichannel gamma-ray spectrometer is used to analyse the gamma spectra from both the compact and the standard. The ratio of activity of an isotope observed from the compact release to that observed from the standard, after correction for uranium and thorium weight difference, is the steady state release fraction for the isotope. The following isotopes have been evaluated in this manner over a temperature range of 900 C to 2000 C: Kr^{85m}(4.4 h), Kr^{87}(78 m), Kr^{88}(2.8 h), Kr^{89}(3.2 m), Xe^{138}(17 m), and Xe^{139}(41s). Data on steady state Kr release are shown in Figure 85 .

The fission product release curve shown in Figure 86 has been used to calculate design activities in the reactor system. This curve is based on steady-state release measurements from the linear accelerator, and on expected reactor fuel temperatures. The post-irradiation annealing experiments confirm this curve in that they agree quite well with linear accelerator measurements.

Post Irradiation (Tracer Level)Annealing
Experiments With Coated Fuel Particles

Many runs have been made on the Xe^{133} release from pyrolytic carbon coated particles. These measurements have been made by the post-irradiation anneal procedure as outlined above. The diffusion times have been measured as a function of temperature up to 2200 C and as a function of coating thickness from 25μ - 60μ .

From theoretical considerations and from past experiments such as the GA-313 capsule series, the small release observed is believed to be due to incompletely coated particles and not to diffusion through (permeation of) the coating.

Experiments at temperatures of 1900-2000 C, which are well above the maximum core temperature during full power operation, have shown deterioration of the particle coatings in 150 hours both in isothermal experiments and in experiments with a temperature gradient

of 100 -150 C through the fuel compact. Other experiments have been run with one-inch-diameter fuel compacts at approximately 1700 C (about 200 C above the maximum fuel temperature). These tests were run isothermally and with a 100 C thermal gradient. At the end of 150 hours, the test compacts were examined, and no measurable effect on the coating was observed. Tests of longer duration, up to 1500 hours, showed some reaction between carbide and coating. Half or more of the coating appeared unaffected in these longer tests. Very long-term tests are now in progress at 1500 C (i.e., at about the maximum nominal fuel temperature). These samples have logged 1800 hours to date, but it is expected that several thousands of hours will be required to show any detectible reaction between particle and coating.

Post-Irradiation Annealing Experiments at High Temperatures

Post-irradiation annealing experiments which simulate a temperature excursion in the reactor have also been carried out. In a test of this type performed on a fuel body made from uncoated fuel particles (see Figure 87), the temperature of the irradiated fuel was increased from 1400 C to 2280 C in less than one minute and held at 2280 C for five minutes. The temperature was then reduced to 1850 C and held there for about 16 hours. At the end of the 16-hour period, 46% of the original Xe^{133} was still retained in the fuel body. Following the 16-hour period at 1850 C, the temperature was raised to 2600 C (above the melting point of the carbide fuel). After two hours at 2600 C, essentially all of the remaining Xe^{133} had been released from the fuel body.

Results from a similar test using coated-particle fuel are shown in Figure 88. The temperature was increased from 1400 C to about 3000 C in several minutes, held at 3000 C for 30 minutes, and then reduced to room temperature. The amount of Xe^{133} released during the period at 3000 C was less than 20% of the total, but essentially all of the Xe^{133} was released following reduction to room temperature. These data suggest that cracks were produced in the fuel particle coatings, which opened up as the temperature was reduced.

(b) Internal Trap Experiments

In order to evaluate the performance of the internal trap, emphasis has been placed on its success in removing cesium, iodine, and tellurium. These three elements were chosen because of yield and ability to serve as indicators of trap removal of rubidium, bromine, and selenium respectively. Each also possesses isotopes

with relatively short half lives. With the exception of krypton and xenon, other elements which might reach the internal trap are either of small yield or of considerably reduced volatility.

Since the temperature of the internal trap renders it ineffective for rare gas adsorption, krypton and xenon were not included in this study. Cesium sorption and iodine-tellurium adsorption lend themselves to different experimental techniques and will be discussed separately.

Activated charcoal was chosen as the appropriate trapping material for cesium and an investigation undertaken to determine the specific sorption (gms Cs/gm C) of various charcoals as a function of temperature and cesium vapor pressure. The experimental approach was to use Cs^{137} tagged metal of known specific activity, and then to continuously monitor the amount of cesium sorbed on the charcoal by use of a calibrated scintillation crystal detector gamma ray spectrometer system. The apparatus is shown schematically in Figure 89 . The charcoal was sealed in the horizontal portion of the inverted L, , and after evacuation the cesium was sealed in the vertical portion of the tube. The charcoal temperature and the cesium vapor pressure were controlled by heaters on the respective portions of the tube.

The results indicate the sorption of cesium on activated charcoal can be represented by an expression of the form:

$$\log_{10} Q = A \Delta F + B \qquad (1)$$

where:

Q = specific sorption (gms Cs/gm C)
A, B = functions of only the particular charcoal and the sorption mechanism
ΔF = free energy change for the reaction:
Cs (liq) = Cs (sorbed)

$$\Delta F = RT \ln P/P_o$$

$$= RT \ln P + \Delta H_v^o - T \Delta S_v^o \qquad (2)$$

where:
R = 1.99 cal/mole ^oK
T = charcoal temperature (^oK)
P = P (Q, T) = equilibrium pressure of cesium over activated charcoal
$P_o = P_o(T)$ = vapor pressure of cesium over liquid cesium
ΔH_v^o = heat of vaporization of cesium
ΔS_v^o = entropy of vaporization

Figure 90 plots isotherms as a function of specific adsorption, Q. For Q below about 0.60 gms Cs/gm C the cesium is very tightly held. Figure 91 is a plot of representative isobars obtained for a second charcoal. The data conform very well to the predicted linear dependence of the log Q on temperature. However, an interesting effect is noted in that there is a break in the curve at about the temperature where one would expect the formation of CsC_8 in graphite.

Possibly at this breakpoint the cesium atoms, which are sorbed on the surface up to this point, actually penetrate the small crystallites in the charcoal and spread the carbon layers apart, thus changing the sorption characteristics. An effect that may be related to this has been observed in charcoal saturated with sodium or potassium. Such charcoal shows a marked increase over unsaturated charcoal in its ability to adsorb organic vapors.

Figure 92 shows the log Q plotted as a function of ΔF. The data fall on the straight lines. The break is also evidenced in this plot.

One useful consequence of this method of interpretation of the data is that the cesium sorption on various charcoals can easily be determined by evaluating Q at a minimum of points and then developing the various isotherms or isobars from the resulting equations.

For iodine and tellurium adsorption, a dynamic experimental apparatus simulating HTGR internal trap operating conditions was constructed. A schematic diagram of the system is shown in Figure 93.

It was observed that metal coated charcoal exhibits much better holdup characteristics than metal mesh or turnings alone. Very sharp boundaries were noted in the iodine and tellurium vapor-helium chromatograms of these reagents, and it appeared that the migration of silver and copper iodides through the trapping bed is suppressed significantly by the presence of charcoal (see Figure 94).

In order to evaluate the use of copper and silver as trapping agents, it was necessary to run tests at partial pressures of iodine similar to those expected in the actual fuel element purge system (5×10^{-6} atmosphere upper limit). Because the vapor pressure of AgI and CuI at trap temperature is of the same order of magnitude as the partial pressure of iodine, the role of the charcoal as a metal iodide

adsorber is of critical importance. There is a significant difference between the iodine delay characteristics exhibited by different varieties of charcoals, and the effect of temperature on the breakthrough times is most pronounced.

The capacity for delaying fission products is measured in terms of "Reactor Equivalent Delay" (in days). These "RED" values give an indication of how long a particular fission product atom entering one of the high temperature traps can be expected to remain (neglecting the decay factor). In the case of I^{131}, the most abundant iodine fission product, the half life is only 8.1 days. Thus, a delay of ten half-lives or 81 days would result in a decrease in iodine activity by a factor of 1024. This long a delay (equivalent to a RED value of 81) would therefore reduce the iodine concentration leaving the trap to less than 0.1% of its original value.

In the first series of experiments, thirty-five long-term radioiodine adsorption tests were completed. An average flow rate of 20.7 cc/minute (measured at 25° C and 1 atmosphere) was maintained and an iodine partial pressure of approximately 5×10^{-6} atmosphere was employed. Tests were run at several different temperatures. The results of these studies for uncoated charcoals are presented in Table 27, while the results of the metallic coated reagent evaluation tests are shown in Table 28. It can be seen from the first table that coconut charcoals exhibit greater delay characteristics for iodine than do charcoals of coke origin. This is apparently due to the very fine grain structure of coconut shells which permits the development of a maximum number of "micro-pores" when they are converted into activated charcoal. The resultant greatly increased internal surface area makes this material ideally suited for application in gas purification work.

The strong dependence of delay time on temperature is clearly shown in Table 28. It appears that no matter what the incoming iodine concentration, if there is excess unreacted metal in the trap, the exit iodine concentration (neglecting decay) will depend mainly on the vapor pressure and stability of the metal iodide formed. Thus copper, which forms a more volatile iodide than silver, offers less delay for iodine, whereas various densities of silver coating offer similar delay values since in all cases a considerable excess of silver metal is present. The methods employed in applying the metal coatings and the base materials used result in some variation in RED values, but by far the greatest effect is due to the vapor pressure and stability of the iodide within the trap.

Results have been obtained in tests of tellurium trapping employing Te^{121} which was produced specifically for this ap-

Table 27

REACTOR EQUIVALENT DELAY* FOR IODINE (UNCOATED CHARCOALS)

Trapping Reagent				Reactor Equivalent Delay (Days)	
Charcoal Designation	Type	Mesh Size	Manufacturer	Test Temperature 850 F	1000 F
BPL	Coke	12x28	Pittsburgh Chemical	6	-
HCC	Coke	12x28	National Carbon	16	5
L-5578-1	Coconut	12x20	Barnebey-Cheney	-	46
MI-1	Coconut	12x20	Barnebey-Cheney	137	51
PCB	Coconut	12x28	Pittsburgh Chemical	143	59

Table 28

REACTOR EQUIVALENT DELAY* FOR IODINE (COATED CHARCOALS)

Trapping Reagent			Reactor Equivalent Delay (Days)		
Charcoal	Mesh Size	Metallic Coating	Test Temperature 850 F	1000 F	1150 F
HCC	12x28	37 wt-% Cu	-	13	-
BPL	12x28	16 wt-% Ag	>200	59	-
HCC	12x28	37 wt-% Ag	>200	63	8
HCC	12x28	15 wt-% Ag	>200	70	-
1/4 HCC over 3/4 MI-1	12x28 12x20	37 wt-% Ag uncoated	>200	70	-

* RED values calculated on the basis of 24 channels per trap, each channel 11 inches in length and 1/4 inch in diameter.

Helium flow rate = 20.7 cc/min (equivalent to 0.25 lb/hr. per HTGR fuel element).

plication via neutron irradiation of enriched Te^{120} in the Oak Ridge Research Reactor. Both a 37 wt-% silver coated charcoal and a cesium impregnated charcoal reagent (1/4 g/g) were employed in these tests. These results, as well as those of a study employing a mixture of tagged iodine and tellurium, are presented in Table 29. After more than 600 equivalent days of reactor operation at 1000 F, no tellurium had been detected downstream of the silver charcoal trap. Based on the results presented in Table 29, it appears that there will be little difficulty in removing all significant tellurium activity from the purge stream at 1000 F. (The weighted average half life of the important long-lived fission product tellurium isotopes is approximately 5 days.)

The single wall fuel element results in a change of internal trap operating conditions from those of the double wall fuel element. For the single wall design, the purge gas flow is five times greater than the 1/4 pound per hour used with the double wall design. The new trap design allows a greater reagent cross section, however, and this results in only a 3.7-fold increase in flow velocity through the trap. It is also anticipated that the improved cooling effect to be achieved by the new design will allow the trap operating temperature to be reduced to 900 F. With the above modifications in mind, a new series of fission product trapping tests was undertaken. The results of these tests, which employed average helium flow rates of 76 cc/minute (measured at 25 C and 1 atmosphere) and an iodine partial pressure of 6×10^{-7} atmosphere, are presented in Table 30. Only commercially available material was evaluated. From the data presented in the table, it is again apparent that, above 15%, excess silver coating has little influence on the trapping efficiency, while the quality of the carbon base stock is of critical importance. The results obtained are quite reproducible and it appears that the loss of trapping efficiency caused by the increased flow rate has been more than compensated by increased efficiency due to the reduction in trap operating temperature.

c. Iodine Adsorption Data

The containment of iodine at temperatures expected

TABLE 29

RESULTS OF TRAPPING TESTS ON TELLURIUM

Material Under Test	Nuclide	Concentration (atm)	Trap Temp. (F)	RED Value* (days)
37 wt-% Ag coated coke base charcoal**	Te^{121}	5×10^{-6}	1000	> 600
37 wt-% Ag coated coke base charcoal**	I^{131} Te^{121}	5×10^{-6} 3×10^{-5}	1000	> 130
Cs impregnated (1/4 g/g) coconut charcoal***	Te^{121}	3×10^{-5}	1000	> 460

* RED valued calculated on the basis of 24 channels per trap, each channel being 11 inches in length and 1/4 inch in diameter. Helium flow rate = 20.7 cc/min (equivalent to 0.25 lb/hr per HTGR fuel element).

** National Carbon HCC 12X28 mesh.

*** Barnebey-Cheney MI-1 12X20 mesh.

TABLE 30

RESULTS OF TESTS EMPLOYING MODIFIED INTERNAL FISSION PRODUCT TRAPPING CONDITIONS

Test Number	Material Designation	Carbon Base	Mesh Size	Metallic Coating	Reactor Equivalent Delay ***(days)
45	AG-2B*	coconut blend	12x28	15 w/o Ag	97
41	AG-2A*	coconut blend	12x28	21 w/o Ag	60
42	AG-2A*	coconut blend	12x28	21 w/o Ag	59
43	PTB-104**	petroleum coke blend	12x28	26 w/o Ag	36
44	PTA-103**	petroleum coke blend	12x28	18 w/o Ag	21
46	PTA-103**	petroleum coke blend	12x28	18 w/o Ag	21

* Barnebey-Cheney Company, Columbus, Ohio

** Calsicat Company, Grove City, Pennsylvania

*** RED values calculated on the basis of 16 channels per trap, each channel being 0.1 square inch in cross sectional area and 12 inches in length. Helium flow rate = 76 cc/min (equivalent to 1.25 lb/hr per HTGR fuel element).

in an external trapping system has been studied at General Atomic. Activated charcoal is an effective reagent for the removal of iodine and certain other fission products at the low partial pressures (order of 10^{-6} atm where reduction to 10^{-11} or 10^{-13} atm is desired) in the HTGR. Finnegan et al. [3] have reported on activated charcoal adsorbers for removing iodine from gas streams, and Browning and co-workers [4,5,6] have shown the usefulness of activated charcoal for the removal from streams of krypton and xenon as well as iodine. Accordingly, experiments were initiated to determine the parameters necessary for the design of fission product traps which might run at temperatures from 0 to 400 C. Adsorption data for iodine at very low partial pressures were required since previously reported studies had been at higher pressures.[2]

Two methods were employed to obtained adsorption isobars and isotherms at low iodine partial pressures and low specific adsorption. Both methods made use of I^{131}-tagged iodine crystals of rather high specific activity.

The first method was dynamic system using helium gas to transport iodine vapor into a small heated charcoal bed. The system is shown schematically in Figure 95. By using rather slow flow rates (10 cc/min) of helium over a bed of iodine crystals maintained at constant temperature, equilibrium partial pressures of iodine can be obtained readily. Knowing the temperature of the iodine crystals one can compute equilibrium partial pressure.

A calibrated scintillation detector mounted directly under the charcoal bed monitors the deposition of iodine on the bed continuously. Knowing the counting efficiency of the detector and the specific activity of the iodine, one can then calculated the amount of iodine adsorbed in the charcoal bed at any time. The helium is allowed to flow in this manner until the scintillation detector indicates no further deposition of iodine on the bed. At this point, the pressure of iodine over the charcoal bed was equal to the incoming iodine partial pressure. Figure 96 shows a plot of several isobars obtained in this manner. The log of the specific adsorption of iodine (grams of iodine per gram charcoal) is plotted on the ordinate and charcoal bed temperature is plotted on the abscissa. Figure 97 compares an isobar obtained with two different charcoals. The data indicate that the logarithm of the specific adsorption is a linear function of the temperature in the range of iodine pressures shown and over a temperature range from 25 C to 350 C. There may be a slight flattening of the cruve at the lower temperatures due to a saturation of the pores. At the dew point temperature the curve

would, of course, rise straight up.

Since the vapor pressure data below 300° K used here had to be extrapolated from data in the literature, it was deemed necessary to check these by experiment. This was accomplished by the conventional transpiration method using radioactive tracer in the same manner as used in the adsorption experiment. Good agreement was obtained down to at least 3×10^{-6} atmospheres.

The second method for obtaining isobars involved the adsorption of iodine on charcoal in an evacuated static system where the iodine would presumably behave as a Knudsen gas at low vapor pressures. Figure 98 gives a schematic representation of this system. This experimental technique has an advantage over the dynamic system in that a steady state equilibrium can be obtained much more quickly at low partial pressures. The dynamic system ceased to be practical at the lower partial pressure ($<10^{-5}$ atm) due to the very small quantities of iodine transported.

With this apparatus isobars were obtained for pressures as low as 3×10^{-7} atmosphere and charcoal temperatures up to 400 C. The data obtained by these two experimental methods were in satisfactory agreement.

It was found that the adsorption of iodine by activated charcoal at low partial pressures could be represented by:

$$\log_{10} Q = A \Delta F + B \qquad (1)$$

where: Q = specific adsorption (gms iodine/gm charcoal)
A and B are constants, and
ΔF corresponds to change in free energy for the reaction:

$$I_2\,(s) \rightleftharpoons I_2\,(ads)$$

i.e, the ΔF for iodine going from the actual or hypothetical (above the melting point) solid state to the adsorbed state. Accordingly,

$$\Delta F = RT \ln P/P_o \qquad \text{(calories)}$$
$$= RT \ln P + \Delta H_v^o - T \Delta S_v^o \qquad (2)$$

where: $P = P\,(Q, T)$ = the equilibrium pressure of iodine (as I_2) over activated charcoal with a specific adsorption, Q
$P_o = P_o(T)$ = vapor pressure of iodine (as I_2) over solid iodine
ΔH_v^o = heat of sublimation of iodine
ΔS_v^o = entropy change for sublimation

A plot of free energy of adsorption vs. specific adsorption of iodine is shown in Figure 99 .

Since the temperature and pressure dependence of iodine adsorption on activated charcoal is given in equation (1), evaluation of a particular charcoal can be made by experimentally determining two points at any temperature and pressure. From these points, the A and B in equation (1) may be determined, and thus the adsorption characteristic of a particular charcoal over a range of temperatures and pressure can be readily estimated.

(d) Xenon and Krypton Adsorption Data

General Atomic has carried out an experimental research program on the performance of charcoal as a rare gas adsorber. Krypton and xenon equilibirum adsorption data have been obtained through dynamic adsorption experiments under conditions applicable to an external trapping system. Similar techniques have been used to determine rates of adsorption in charcoal beds. The performance of various charcoal grades has been compared and mechanical properties of suitable materials investigated.

The experimental apparatus can conveniently test charcoal traps of any reasonable dimensions at room temperature and of approximately 500 gram size at other temperatures from -80 °C to 100 C. System pressure may be varied from atmospheric to 400 psia; flow rates have ranged between 65 cc/min at 1 atmosphere to 900 cc/min at 350 psia.

As may be seen in the schematic diagram of the system, Figure 100, this is a closed loop in which recirculation of the tracer gas (Kr^{85} or Xe^{133}) is prevented by a small liquid-nitrogen-cooled charcoal trap. The tracer material may be introduced into the helium carrier gas at the test trap inlet as a pulse of short duration, or alternatively, injected at a constant rate in a manner similar to the actual purge stream case.

If the first technique is employed, a chart recording or ionization chamber current similar to that depicted in Figure 101a is obtained; the time after pulse injection at which maximum current occurs (corresponding to maximum effluent activity) is used in the expression developed by Browning [6], to obtain the dynamic adsorption coefficient, k, (equivalent to the slop of the equilibrium isotherm, cc/gm):

$$k = \frac{Ft}{m} \qquad (1)$$

there:

F = carrier gas volume flow rate (cc/min)
m = trap adsorber mass (gm)
t = time of maximum effluent activity after pulse injection (min)

If the second technique is used, the ionization chamber current trace appears as shown in Figure 101b, with effluent activity reaching inlet activity (for delay times short compared to tracer half-life). This method also provides the dynamic adsorption coefficient, when one substitutes for the time, t, in the Browning expression above, that time at which the trap effluent activity has reached 1/2 of its final value. Furthermore, this type of experiment produces adsorption rate data, allowing one to predict the percent of theoretical loading achieved at the time of breakthrough at some specified concentration. In either case, the tracer concentration of 0.1 to 1 ppm approximates the order of expected rare gas concentration.

If the adsorber is to serve as a delay bed, achieving fission product disposal by decay, the dynamic adsorption coefficient data are of primary significance since they provide a means of deriving delay as a function of bed mass and carrier gas flow rate through the expression $t = km/F$. Tables 31 and 32 present representative krypton and xenon dynamic adsorption data obtained at General Atomic. These values are incorporated in a plot of experimental dynamic adsorption coefficient vs. inverse temperature in Figure 102.

TABLE 31

XENON DYNAMIC EQUILIBRIUM ADSORPTION COEFFICIENT

TEST CONDITIONS				RESULTS
Bed Size (gm)	Flow Rate (cc/min)	Temperature (°C)	Pressure (psig)	Dynamic Adsorption Coefficient (cc/gm)
33	420	-45	345	40,500
21	469	-28	349	13,800
21	502	0	350	2,500
420	607	25	350	936
420	640	75	345	167
420	604	90	345	130

TABLE 32

KRYPTON DYNAMIC EQUILIBRIUM ADSORPTION COEFFICIENT

TEST CONDITIONS				RESULTS
Bed Size (gm)	Flow Rate (cc/min)	Temperature (°C)	Pressure (psig)	Dynamic Adsorption Coefficient (cc/gm)
392	500	-60	350	1250
392	500	-50	350	660
21	469	-28	349	324
503	490	-25	350	260
503	125	0	0	172
420	547	8	344	108
503	520	25	0	71.2
503	290	25	158	60.6
503	460	25	342	59.0
503	500	25	158	60.0
420	545	55	348	29.8
420	703	88	340	18.0
503	300	93	362	15.9

The body of data indicates no detectable effect of flow rate on the value of the dynamic adsorption coefficient. Below about 150 psi there is seen to be some increase in the coefficient with decreasing pressure.

Should it be desirable to employ the adsorber as an absolute trap, regenerating prior to breakthrough, adsorption rate data are essential. Such information answers the question of how long an initially clean bed may be operated before it begins to release activity at a prescribed level. It is derived from raw data and correlated in terms of the height of a transfer unit in the manner described by Hougen and Marshall[16]. Figure 103 is a plot of such values against particle Reynolds number. A curve such as this is useful in illustrating the ability of HTU measurements to discover the magnitude of fission product bypassing due to wall or interior corner effects. The smaller overall values of the height of a transfer unit for a 2-inch diameter charcoal test trap are indicative of less bypassing here than in a 1-inch diameter test trap. The insertion of a single internal fin with its attendant surface and corners is seen to increase the bypass effect to the extent that this 2-inch finned tube has the HTU equivalent of a 1-inch trap. Such data, used in conjunction with the theoretical expression relating effluent concentration, height of transfer unit, and delay time[16] enable one to specify bed dimensions required to obtain a certain operating cycle while holding penetration to the required low value. In essence, knowledge of the number of transfer units which a trap possesses permits prediction of the shape of the effluent curve; i.e., the form which a recorder trace such as that shown in Figure 101 will assume. The success of this method is illustrated in Figure 104 .

Concurrently with the previously described experiments, a program of evaluating charcoal grades recommended for this application by various manufacturers has been executed. The results of this study, performed at 25 °C, are tabulated in Table 33 . These values show about 10 per cent difference in dynamic adsorption coefficient separating the best 6 grades. The 3 grades possessing highest k values are natural (unreconstituted) coconut base charcoal materials.

TABLE 33
CHARCOAL GRADE COMPARISON AT 25 °C

Charcoal Grade	Mesh Size	Manufacturer	Dynamic Adsorption Coefficient (cc/gm)
HH-1	6/10	Barnebey - Cheney	49.5
L-5578-4	6/10	Barnebey - Cheney	54.2
Columbia CXC	6/8	National Carbon	56.4
Columbia NXC	6/8	National Carbon	57.3
AC-4	6/10	Barnebey - Cheney	57.5
Columbia G	8/14	National Carbon	60.5
107	6/10	Barnebey - Cheney	61.0
PCB	6/10	Pittsburgh Coke and Chemical	62.0

In order to determine what effect the base material has on mechanical properties, especially dust-producing breakdown, the two coconut base grades having highest k values and the petroleum base grade of best performance were subjected to a friability test imposing conditions considerably more extreme than a fixed bed should encounter. The samples were first standardized as to screen size, then abraded through vigorous agitation in the top screen of an assembly of standard screens. Both coconut base materials were less susceptible to breakdown than the reconstituted petroleum base product, and a 7.5 hour abrasion test of one of the coconut grades indicated a leveling off of breakdown rate after the first 30 minutes. Total fines after 30 minutes represented .3% of the sample; after 7.5 hours of abrasion, they comprised .5% of the total. For the reconstituted grade, 30 minutes of abrasion produced 2% fines passing a Number 48 Tyler screen.

A consideration of the interference effects of impurities on rare gas adsorption is in progress as of May 1961. While no deleterious effects have been found for normal concentrations of impurities, further research into the possibility and extent of interference under extreme conditions will be performed during 1961.

(e) In-Pile Loop Fission Product Release and Trapping Data

While other experimental programs have been established to provide the basic design data for HTGR, the in-pile loop at the General Electric Test Reactor will be used to obtain information of a confirmatory nature under simulated reactor conditions. In the in-pile loop, an element can be irradiated in a thermal neutron flux slightly higher than 10^{13} nv in an atmosphere of purified helium at 350 psia. The element can generate 76 kw of fission and gamma power resulting in a heat flux of about 150,000 Btu/hr-ft^2. The loop is designed to operate over a fairly wide range of temperatures, flows and pressures. Typical operating conditions are given in Table 34.

TABLE 34

TYPICAL LOOP OPERATING PARAMETERS

Fuel element diameter, in	3.50
Fuel element length, in	43
Fuel element active length, in	22.50
Fuel element loading of U (93% enriched), g	195
Fuel element loading of Th, g	425

Power generation, kw	76
Fuel element temperature, F	3060
Graphite surface temperature, F	2200
Entrance gas temperature, F	600
Exit gas temperature, F	1400
Helium flow rate, lbs/hr	260
Purge flow rate, lbs/hr	0.6
Helium pressure, psia	350

1. In-Pile Equipment

The experiment will be located in the pool of the General Electric Test Reactor adjacent to the reactor pressure vessel, that is, at the core-reflector interface. In order to thermally insulate the hot facility tube from the water in the pool, the entire in-pool portion is located within an aluminum vacuum chamber. A secondary function of the vacuum chamber is that it provides secondary containment for radioactive fission products in case of leakage from the in-pool portion of the loop. The disconnects for the lines connecting the facility tube to the remainder of the system are Marman-type flanges utilizing double seals. The space between the two seals on each flange is evacuated. The leakage, if any, is directed to a leakage collection system.

The facility tube assembly consists of a pressure vessel containing the fuel assembly and flow in thermal baffles, coolant inlet and outlet piping, tempering gas piping, purge gas piping, thermocouples, disconnect joints, and internal shielding. During normal loop operation, the facility tube is located in close proximity to the reactor vessel to take advantage of the high neutron flux. Means are provided, however, to retract the vacuum chamber in the core region up to five inches from the reactor vessel when it is desired to operate the reactor with the loop facility shut down. In the retracted position, a shutter consisting of lead, steel, and cadmium shields the fuel in the facility tube to minimize heat generation. During this time helium is provided in the vacuum chamber annulus assuring the necessary conductance for removal of the small amount of heat still being generated.

The fuel element assembly consists of the following: fifteen HTGR fuel compacts located within a graphite sleeve; graphite end plugs, heat insulators, connections and structure; an internal fission product trap; purge lines and thermocouples. Each of the fuel compacts consists of a central core of graphite and an annular cylinder of U^{235} and Th^{232} dispersed in graphite. Heat is

transferred to the helium coolant at the outer surface of the graphite sleeve. Helium purge gas enters at the top of the element and flows downward between the fuel compacts and the sleeve. At the lower end, the purge gas flows either through an internal fission product trap or through a trap bypass purge line. The two purge lines are connected to the external fission product trapping system in the main cubicle.

A baffle separates the downward and upward coolant flow and virtually eliminates radiative heat transfer between the graphite and the pressure vessel. Stagnant helium between the baffle walls minimizes heat transfer between the two flowing helium streams. The baffle consists of an outer wall of stainless steel and two walls of Nichrome V.

Provision is made to measure temperatures of the fuel compact internals and the helium at the test section inlet, fuel element inlet, and fuel element outlet. Steel shielding is provided in the upper region of the facility tube to minimize radiation in a vertical direction above the fuel.

2. Out-of-Pile Equipment

The out-of-pile portion of the primary system is located within a concrete cubicle on the second floor of the GETR. The cubicle is lined inside with steel plate which forms a secondary containment. The cubicle is divided into two levels with the fission product trapping system equipment located on the lower level and the primary loop and associated equipment located on the upper level. The upper level is divided into two compartments, the larger of which is open to the lower level and contains the major loop components, such as the circulators, heat exchanger, cooler, full flow filter, hot helium storage tank, leakage collection hold up tanks, depressurizer tank, cubicle cooling system, ventilation blower, main loop piping, and valves and instrumentation. The other compartment on the upper level is the pump room which contains the main transfer pump, leakage transfer pump, vacuum chamber pump, purge containment blower, fission product trapping system vacuum pump, and depressurizer compressor. The pump room is provided to permit access to the pumps for periodic inspection and maintenance. It is shielded from the components in the other compartment and is also surrounded by shielding. Local shielding is provided around the circulators, cooler, full flow filter, hot helium storage tanks, and leakage hold up tanks to minimize radiation to personnel entering the cubicle for inspection and maintenance during accessible periods. The cubicle normally operates under a slight negative pressure to minimize out-leakage.

The primary loop main cooler is a single wall gas-to-water type (approximately 7 ft x 1-1/2 ft x 6 ft). The purpose of the main cooler is to transfer heat from the hot helium gas to a closed demineralized secondary water system which in turn transfers heat to the GETR cooling tower water through a secondary heat exchanger. The cooler is designed to operate at 1400 F maximum helium inlet temperature without local boiling on the water side. The maximum capacity of the heat exchanger is 328,000 Btu/hr.

A full flow filter is located in the line upstream of the circulators. It will be used to remove graphite fragments from the main loop steam to protect the circulators in case of fuel element erosion. The main loop flow can be remotely directed through a filter bypass by valves controlled from the main loop panel.

Two circulators are installed to pump the helium coolant around the closed loop. One of the circulators is normally not operated but held as an in-line spare in the event of a circulator failure. The entire pumping system will be leak tested to an over-all loop leakage rate of 10^{-5} atm. cc/sec. The circulators are designed to meet the following performance conditions.

Inlet temperature	650 F
Inlet pressure	340 psia
Pressure rise	10 psi
Mass flow	>0.05 lb/sec

A system is provided to collect and contain leakage from points in the system most likely to leak radioactive gas.

The main evacuation pump serves several purposes. During normal operation, this pump is used to maintain a high vacuum on the vacuum chamber to minimize heat losses to the reactor pool water. The same pump also maintains a vacuum on the space between the seals of the facility tube disconnect flanges. Leakage, if any, into the vacuum chamber is directed through a moisture detector, cold trap and vacuum pump to the low pressure hold up tank. Leakage from the disconnect interseals is also directed to the tank through the same pump. A slight negative pressure is maintained on the purge line containment shell by the purge containment vacuum pump. The sample lines to the junior cave and sample blister are also evacuated by separate pumps to purge the lines of gas which may be radioactive. The gas from the interseals, sample lines and purge line containment discharges through a filter into the 10 cubic foot low pressure hold up tank. If and

when the pressure in this tank reaches 15 psia or over, a leakage transfer pump transfers the gas to the five cubic foot, high pressure holdup tank. The gas is stored here until it becomes necessary to relieve excess gas through an iodine trap and filter to the main cubicle ventilation exhaust. Radiation detectors are included on the system to monitor activity in the various lines. The main loop may also be evacuated by the main evacuation pump if required during shutdown.

The emergency helium cooling system provides a means of admitting helium to the vacuum annulus of the vacuum chamber which will increase heat loss from the fuel element to the pool. The system is put into operation in case of low coolant flow and/or low coolant pressure in the loop. A cylindrical tank in the system is kept charged with sufficient helium to feed this annular space upon demand. Double valves are used to increase reliability.

A 50-kw electric heater is located downstream of the circulators to control the return gas temperature. The heat output is automatically regulated by a saturable core reactor controlled by the helium temperature downstream of the heat exchanger on the main loop coolant return line to the fuel element. The control equipment for the heater is located outside the cubicle on the control mezzanine.

The fuel element inlet gas temperature conditions required for the experiment are higher than the maximum permissible operating temperature of the gas circulators. In order to minimize the loop heat losses, a regenerative heat exchanger is used.

Located within the cubicle is a ventilation system designed to maintain a negative pressure on the main cubicle, junior cave, sample blister, pump room and auxiliary equipment containment area; and to isolate the containment system in the event of high activity release from the loop. The ventilation system includes a mechanical blower located in the main cubicle, two high efficiency air filters, an iodine trap, radiation monitors, and associated piping.

The mechanical blower takes suction from the main cubicle through a high efficiency filter and discharges to the stack through an iodine trap and the second high efficiency filter. Air flow into the main cubicle is from the GETR containment through the auxiliary containment, junior cave, pump room and sample blister.

Valves, located on all inlets, will close on a signal of high radiation or high pressure in the main cubicle. The valves on the interconnecting lines between the various units being

ventilated will open in case the pressure in the units becomes higher than the main cubicle pressure.

3. Fission Product Trapping System

The external fission product trapping and helium purification system (FPTS) is provided to remove radioactive fission products and gaseous impurities from the fuel element purge stream and to return the essentially clean helium to the main coolant stream. It consists of a series of adsorbent beds and filters, operated at various temperatures, through which the purge stream is psssed. This equipment is located on the lower level of the main cubicle.

The main components are:

a. Charcoal Trap No. 1, water-cooled and contained in a lead cask about nine inches thick. This trap is designed to remove the volatile fission products other than the noble gases.

b. Charcoal Trap No. 2, whose purpose is to provide a holdup period for the noble gases, is freon-cooled to -40 F and shielded with six inches of lead.

c. A copper oxide bed with electric heater and lead brick shielding, to convert carbon monoxide in the coolant to CO_2 and hydrogen to H_2O.

d. A CO_2-H_2O trap to remove the CO_2 and H_2O formed; it is cooled by liquid nitrogen and shielded with lead bricks.

e. Charcoal Trap No. 3, cooled by liquid nitrogen to -320 F and shielded with six inches of lead. This trap is designed to retain the noble gases held up temporarily by Charcoal Trap No. 2.

f. Emergency Trap No. 1, which is used as a standby trap for Charcoal Trap No. 1. It is water-cooled and shielded with nine inches of lead.

g. Emergency Trap No. 2, which is liquid-nitrogen-cooled and shielded by six inches of lead. It will be used as a standby trap for Charcoal Traps No. 2 and No. 3.

Circulation of purge gas is accomplished by taking advantage of the pressure drop across the main loop. A booster pump is used only when the pressure differential is not sufficiently great to obtain the desired flow rate.

The purge lines between the pool penetration flange and Charcoal Trap No. 1 and Emergency Trap No. 1 are contained in a secondary containment shell to minimize the possibility of excessive leakage to the main cubicle. The purge lines are also connected to the junior cave trapping sampling systems. The water and freon cooling systems for the FPTS are located in the auxiliary containment cubicle.

4. Junior Cave

A Junior Cave is located outside the main cubicle on the second floor adjacent to the reactor biological shielding. The cave is a shielded containment vessel constructed with the same leak-tightness requirements as the main cubicle containment structure. Penetrations are provided on the cubicle face of the cave for sample connections from the purge lines and from sample points at the several locations in the fission product trapping system. To reduce the radiation field to within working limits, the structure is shielded with eight inches of steel plate placed on the top, left and front faces. The remaining faces of the case are shielded by the reactor biological shielding and the main cubicle shielding.

All of the required operations within the cave are performed by a claw-type manipulator. The control mechanism for the equipment is located on the outside front face of the cave and is easily accessible to one operator. The manipulator is designed to operate valves for control of gas flow and to handle and remove the test traps. Observation of operations within the cave is provided by a high-density lead-glass window.

Instrumentation within the cave will include provisions for measurement of local gamma activity in the purge line, and gross activity within the cave area.

5. Gas Sampling

a. Purge Gas

Within the junior cave, means are provided for sampling the purge gas stream both as it leaves the fuel

assembly and after it has passed through various traps within the FPTS. Two separate functions of purge gas sampling are performed within the cave.

The study of the efficiency of various trapping materials is accomplished by passing purge gas through small test traps and then removing the traps from the cave for analysis.

Analytical study of the purge gas stream at four different locations in the FPTS is carried out by intermittently sampling the gas stream and either analyzing the samples with a gas chromatograph installed in the cave or by external radiochemical means.

b. Primary Coolant

Primary loop samples are handled in a sample blister located adjacent to the main cubicle shield wall on the operating mezzanine. The blister contains stop valves on the piping leading to and from the system sample points, a gas chromatograph analyzer, a liquid-nitrogen-cooled charcoal trap, a connection point for a sampling container and miscellaneous piping and valves.

The blister is a steel enclosure normally kept under a slight negative pressure to insure in-leakage. A sealed viewing window and glove ports are provided to permit handling of equipment within the blister. A pass-through chamber is also provided which can be flushed to minimize the probability of internal air escaping to the GETR containment when samples or equipment are passed in and out of the blister.

The sampling equipment is connected to the helium loop at several sample take-off points and one sample return point. Samples can be passed through the gas chromatograph for direct reading of impurity content, or alternatively, samples can be removed from the system in a sample container. While loop gas is recirculating through the sample equipment to purge the sample system prior to taking a sample, the sample system is under loop pressure. After isolation of the system by closing the valves, the gas pressure is reduced to atmospheric by bleeding excess gas through the nitrogen-cooled cold trap where fission products, if any, are trapped. Samples are then removed with the system at atmospheric pressure. The sample container is normally evacuated before filling and therefore draws in a known volume of gas from the sample system.

The sampling system is connected to a clean helium supply and to a vacuum pump (which discharges to the leakage collection system). This system is used to purge the sampling system initially.

6. Gas Charging System

The charging system, which is located outside the main cubicle, is designed for manual operation and supplies high-purity helium for filling and purging of the main loop and subsequent main loop make-up requirements. Through suitable valving, including a backflow check valve, high-purity helium from this charging system can be supplied when required to the junior cave, sample blister, interseal disconnect chambers, and Charcoal Trap No. 1 of the fission product trapping system.

The helium purifier in the charging system consists of a 10-micron filter, a molecular sieve cartridge for water vapor removal and an oil vapor cartridge. This unit is designed to limit the impurities in the helium to the following values:

Water Vapor	less than 10 ppm/volume
Hydrocarbons	less than 10 ppm/weight
Solid particle size	less than 6 microns

7. Instrumentation

All instrumentation needed for the loop is centralized at a local control panel in the experiment area. Critical parameters are repeated and recorded in the reactor control room. An annunciator on the control room panel indicates loop troubles. Additional annunciators on the local panel indicate the source of the trouble. Critical parameters have two levels of action -- alarm and either scram or rundown of the reactor.

The loop is fully instrumented to measure required fuel element and coolant temperatures, flow rates, and pressures. All measurements of interest throughout the system will be transcribed on recorders, thus providing information for post-operational analyses. Suitable instrumentation is provided for reactor shutdown should a potentially serious condition be indicated. Reactor scram will be initiated by high exit gas temperature, high circulator intake gas temperature, low flow or pressure of main loop gas. In addition, a reactor rundown will be initiated by activity monitors located on the main loop and purge lines. Intermediate levels of these

parameters and other warning signals will be annunciated. The general system is laid out in such a way that all parameters concerned with the operation of the system and the contained experiments are under the direct control of the loop system operator. Should a transient occur, the operator will be able to make suitable system adjustments to return the system to equilibrium condition. Fast-acting transients involving temperature, pressure, or flow excursions will cause automatic reactor scram should these parameters exceed preset limits.

Primary heat exchanger water flow will be metered, and low flow will cause an alarm. Discharge water high temperature will also operate an annunciator.

A separate continuous monitoring system is provided to determine cubicle exhaust gas activity before release to the GETR stack.

The controls and instruments allow the reactor operator, in case of an emergency, to introduce emergency cooling which will increase the heat loss from the experiments, thereby reducing the gas and fuel assembly temperature. If the loop fails to respond, the gas coolant may be transferred to the hot helium storage tank, reducing the loop pressure and automatically causing a reactor scram.

8. Shielding

The shielding design assumptions are that a large percentage of fission products escape from the system to the main cubicle and that large quantities of fission products are plated out in various sections of the loop. Under normal operation, the majority of the fission products will be retained within the fuel element and/or the individually shielded fission product trapping system traps, which will reduce the dose rates calculated by several orders of magnitude.

The in-pool shielding was based on the maintenance requirements of the reactor and the requirements for direct work on the facility, under the set of assumed conditions listed below; for direct maintenance of the reactor, access to the top head is required 8 to 10 hours after reactor shutdown.

a. 0.05 curie/cm^3 activity in the main loop coolant.

parameters and other warning signals will be annunciated. The general system is laid out in such a way that all parameters concerned with the operation of the system and the contained experiments are under the direct control of the loop system operator. Should a transient occur, the operator will be able to make suitable system adjustments to return the system to equilibrium condition. Fast-acting transients involving temperature, pressure, or flow excursions will cause automatic reactor scram should these parameters exceed preset limits.

Primary heat exchanger water flow will be metered, and low flow will cause an alarm. Discharge water high temperature will also operate an annunciator.

A separate continuous monitoring system is provided to determine cubicle exhaust gas activity before release to the GETR stack.

The controls and instruments allow the reactor operator, in case of an emergency, to introduce emergency cooling which will increase the heat loss from the experiments, thereby reducing the gas and fuel assembly temperature. If the loop fails to respond, the gas coolant may be transferred to the hot helium storage tank, reducing the loop pressure and automatically causing a reactor scram.

8. Shielding

The shielding design assumptions are that a large percentage of fission products escape from the system to the main cubicle and that large quantities of fission products are plated out in various sections of the loop. Under normal operation, the majority of the fission products will be retained within the fuel element and/or the individually shielded fission product trapping system traps, which will reduce the dose rates calculated by several orders of magnitude.

The in-pool shielding was based on the maintenance requirements of the reactor and the requirements for direct work on the facility, under the set of assumed conditions listed below; for direct maintenance of the reactor, access to the top head is required 8 to 10 hours after reactor shutdown.

a. 0.05 curie/cm^3 activity in the main loop coolant.

b. 50 curie/cm^3 activity in the purge stream.

c. 0.2% of the potential loop plate-out occurs in the region of the joints ($\sim$190 curies) which region is adjacent to the reactor vessel head.

d. Direct beaming of radiation from the fuel element up the evacuated secondary containment.

e. Maximum dosage contribution from all loop components to a man on the reactor vessel head is 100 mr/hr.

The shielding required was calculated to be about 5 inches of lead in certain locations. A shielded radiation detector is located above the disconnect flanges and calibrated to indicate the dose level at shutdown. The contribution of plate-out to the radiation level indicated, will be estimated from decay curves obtained during reactor shutdown and by comparison with decay curves obtained from detectors located elsewhere in the system.

The cubicle shielding thickness requirements were based on a loop power of 100 kw for about three years operation. The resulting equilibrium fission product activity level for potential helium contaminants having half lives greater than 10 minutes would be about 1×10^5 curies.

Under normal operation, the fission products will be retained within the main loop piping and in the individually shielded FPTS traps.

For potential accident situations, shielding calculations for the lower level of the main cubicle assumed that 100% of all the equilibrium volatile fission products with half lives greater than 10 minutes are distributed uniformly in the cubicle. The dose rate through 1-1/2 feet of ferro-phosphorous concrete is about 300 mr/hr under this emergency condition.

9. System Leak-Tightness

Components of the loop which will be operated under helium pressure have been mass spectrometer leak-tested to a minimum sensitivity of 5×10^{-8} atmospheric cc/sec. During the shop fabrication phase, the out-of-pile portion of the main

loop was pre-assembled and operated at temperature and pressure to verify system performance and leak-tightness. The leakage of the system as measured by a mass spectrometer was less than the design objective of 10^{-5} atmospheric cc/sec.

10. Program

The construction and operation of the in-pile loop during 1961 and 1962 will furnish substantial information on operations of a fission product control system as follows:

a. The gross radioactivity of the purge line will be continuously measured upstream and downstream of the first charcoal trap in the Fission Product Trapping System. This will provide data on the release of activity from the fuel element as a function of time, and the over-all effectiveness of the trap for removing radioactive impurities.

b. The first trap, which consists of 5 tubes containing charcoal and one tube containing glass wool, has a detector mounted on it which can monitor each tube. Since the glass wool is present to remove aerosols formed, it is anticipated that data on the formation or lack of formation of aerosols will be obtained from this trap.

c. Sampling locations in the in-pile loop are listed in Table 35 with the frequency of testing and the tests presently planned. It should be noted that the isotopes to be selected for testing will be determined during operation of the in-pile loop.

d. The first charcoal trap, which was discussed previously, is water cooled. The effectiveness of all traps in removing fission products and/or chemical impurities can be measured by use of the sampling system described in Table 35.

e. The measurements of plate-out can be determined by the use of removable sections of pipe. These sections of pipe will be forwarded to the hot cells at General Atomic for chemical analysis and measurement of activity.

TABLE 35

IN-PILE LOOP SAMPLING

	Source	Frequency	Tests to be Performed: Radioactive	Tests to be Performed: Non Radioactive
1.	Between Heat Exchanger and Cooler - (Main Loop)	1/wk	all isotopes that can be identified	O_2, H_2, CO, CO_2, CH_4
2.	Return from Fission Product Trapping System	3/wk	selected isotopes for obtaining delay times	O_2, H_2, CO, CO_2, CH_4
		Biweekly	all that can be identified	----------
3.	Between Heat Exchanger and Test Section (Fuel Element)			continuous H_2O
4.	Between Test Section (Fuel Element) and Trap No. 1	1/wk w/bypass* 1/wk w/o bypass	all that can be identified	----------
		3/wk	selected isotopes for obtaining delay times	----------
5.	Between Charcoal Traps No. 1 and No. 2	3/wk	selected isotopes	H_2O
6.	Between Charcoal Traps	3/wk	selected isotopes	O_2, H_2, CO, CO_2, CH_4
7.	Between CuO Bed and H_2O-CO_2 Trap	To be established		continuous H_2O / O_2, H_2, CO, CO_2, CH_4

*Bypass internal trap

References:

1. L. R. Zumwalt, Fission Product Element Yields and Characteristics, GAMD 891 (July 29, 1959)

2. L. H. Reyerson and A. E. Cameron, "Studies of the Sorption of Halogens by Silica Gel and Charcoal", J. Phys. Chem. 39, p. 181 (1935)

3. J. W. Finnigan et al., HW-26113, "Removal of Iodine Vapor from Gas Streams by Sorption on Charcoal" (Nov. 4, 1952)

4. R. E. Adams and W. E. Browning, CF-58-5-59, "Proposed Method for Removal of Radio-Iodine Vapor from Experiment Off-Gas System of the ORR" (May 21, 1958)

5. R. E. Adams and W. E. Browning, ORNL-2872, "Removal of Radioiodine from Air Streams by Activated Charcoal" (April 1, 1960)

6. W. E. Browning, R. E. Adams, and R. D. Ackley, CF-59-6-47, "Removal of Fission Product Gases from Reactor Off-Gas Streams by Adsorption" (June 11, 1959)

7. R. E. Adams and W. E. Browning, CF-58-4-14, "Fission Gas Holdup Tests on HRT Charcoal Beds" (April 2, 1958)

8. D. F. Sangster, AERE-C/M-280, "The Isotherm for the Adsorption of Krypton on Charcoal" (June 1956)

9. C. B. Amphlett and B. F. Greenfield, AERE-C/R-2632, "Krypton and Xenon Adsorption Isotherms on Charcoal Irradiated with 1 Mev Electrons" (July 1958)

10. W. E. Browning and C. C. Bolta, ORNL-2116, "Measurement and Analysis of the Holdup of Gas Mixtures by Charcoal Adsorption Traps"

11. K. Peters and K. Weil, AEC-tr-2470, "Adsorption Experiments with Heavy Noble Gases" (1930). Translated from Z. physik, Chem. 148(A), 1-26(1930).

12. J. M. Holmes, CF-52-11-39, "Design of the Dissolver Off-Gas System for the Idaho Chemical Processing Plant" (November 5, 1952)

13. J. N. Burdick, ORO-118, "Adsorption of Krypton and Xenon" (November 5, 1952)

14. A. G. Blasewitz and B. F. Judson, Chemical Engineering Progress, 51, 1, p. 6-11 (January 1955)

15. U.S.A.E.C., Handbook on Aerosols (1950), p. 63

16. O. A. Hougen and W. R. Marshall, Jr., Chemical Engineering Progress, 43, 4, p. 197-208

17. B. M. W. Trapnell, "Chemisorption," Academic Press, New York (1955)

3. FLOW AND HEAT TRANSFER EXPERIMENTS

a. Flow Model

(1) Summary

A half-scale flow model of the HTGR reactor vessel has been operated since January 26, 1961. The Reynold Numbers of the maximum gas flows in the model are approximately one-half of those that will exist in the full scale reactor. Early operations were devoted to selection of exact instrumentation location. This was done by performance of smoke tests which revealed the areas in the model requiring detailed information.

The results to date show that:

(a) The reactor pressure drop is less than the calculated value of 4.5 psi.

(b) The tilting reflector is a workable concept, and it prevents vibration of the core.

(c) The heat transfer coefficients for the cylindrical section of the vessel wall are within the range predicted for normal reactor operation at power.

(2) Flow Model Test Facility - Description

The flow model test site as shown in Figure 105 contains a fully integrated facility for large scale tests of flow distribution, pressure drop, and convective heat transfer. The system is an open loop, using ambient air as the working fluid. The flow model vessel thermal shields, plenum shroud and reflectors are made from plexiglass. The core support plate and fuel elements are made of aluminum. Figure 106 shows a layout of the flow model and location of test probes.

Air is supplied to the model by a centrifugal blower operating at 16,800 cfm at 71" water vacuum and 70°F. The blower is driven by a 250 hp motor. The blower is connected to the outlet side of the model to avoid pressurizing the all-plexiglass flow model. Outlet flow monitoring is provided by a recording 2-pen pressure gauge. Flow metering is accomplished in each outlet duct by means of 18" venturi connected to a controller. The control elements are connected to 18" butterfly valves with pneumatic actuators. At full capacity, total flow controllability is within ±5% and repeatability within ±2%. Flow balance between the two outlet ducts is within ±5%.

Test instrumentation is installed for simultaneous indication of static pressures at up to 400 different points. Indication is on four banks of manometers with separate variable height reservoirs. Three boards are set up to read gauge pressures to ±69" water, while the fourth board reads gauge pressures to ±196" water. These boards are back-lighted for recording pressures by means of photographs.

Another panel contains 20 inclined manometers reading to ±2.00 inches of water and 20 manometers reading to ±0.500 inches of water. Each of these manometers is connected through a header to 3 test points, and each of these is also indicated on the vertical manometers for photographs. A total of 50 total-head probes are available for use with the inclined manometers.

Convective heat transfer coefficients are measured by inserting 1" diameter probes through the wall to the surface at the point of interest. These probes are small electric heaters, insulated to minimize heat transfer through the walls, and instrumented to indicate heat flux to the fluid and heater surface temperature. By measuring local fluid temperatures, it is possible to calculate approximate film coefficients. A total of 60 calibrated probes are available, with provisions for connecting 40 simultaneously to a portable instrument console for reading. The console has two potentiometers for use with surface and fluid thermocouples, two sets of dial indicators for heater power, and a battery power supply for the heaters.

The test facility is also equipped for flow visualization studies in transparent models, using a non-corrosive, non-plating grey smoke. Smoke bombs are set off in a hood assembly containing a small blower. Smoke is piped to a header in the test facility through a 5" elephant trunk, and from there to the test model through as many as ten smoke injection lines. Flow visualization test results are recorded by motion pictures.

(3) Purpose of Test Program

The objectives of the test are:

(a) To check the core restraining capabilities of the tilting reflector and the stability of the core.

(b) To determine the pressure drop characteristics of the reactor internal flow paths.

(c) To study the flow patterns in the gas coolant passages.

felt that the manufacturing tolerances would affect the film coefficients adversely and thus the spacers were accepted as a necessity.

Approximately three hours of motion picture films of smoke testing in the outer gap have been made. The flow patterns for the cylindrical gaps are shown in Figure 110 and for the upper head in Figure 111, obtained from the smoke tests. The motion pictures also show some apparently minor areas of stagnant flow and eddy capture in the upper heads for one-nozzle flow.

The effect of rotating the top nozzles with respect to the inlet nozzles has been investigated. Motion pictures of smoke tests have been completed. Results for flow distribution in the outer gap, top head, are shown in Figure 111. Measurements have also been made of pressure drop with the heads rotated 45° as a part of the general pressure drop testing.

The tilting reflector has remained tight to the core with no visible sign of vibrations. Quantitative tests are being planned to determine the holding force exerted on the core as a function of flow rate.

(6) Further Testing

The data from Phase I already collected is now being evaluated for possible design changes. Based on the results of the static pressure and film coefficient measurements, the test program has been re-evaluated, and the following work is expected to be completed by the end of 1961:

(a) Phase I

This program is to confirm existing data and include some new points now considered necessary. Spacer blocks affecting the flow in the outer gap were removed during the re-evaluation period.

1. Pressure Drop

Pressure drop measurements have been repeated without the spacers to confirm earlier results. The results show a slight decrease in Δp after removal of the blocks.

2. Heat Transfer Data

a. Tests will be run to simulate the HTGR reactor normal and emergency operating conditions and normal shutdown

(d) To measure how effectively the inlet gas cools the reactor vessel wall.

(e) To determine how effective the core reflector seals are.

(4) Test Program Completed

The first phase of the test program is complete. This phase was an investigation of the over-all effects of flow distribution on the cooling of the reactor vessel, the pressure drop, and the general working of the core restraint, with model flow rates of 100 percent to 30 percent and flow through both nozzles of the model.

The objectives of this test were:

(a) Measure and determine the over-all pressure drop through the model.

(b) Measure the pressure drop from the inlet nozzle to the upperhead, the thermal shields, reflector and outlet nozzle.

(c) Determine if any stagnant areas exist in the annular gap between the thermal shield and vessel wall.

(d) Determine the velocities in the annular gap between the thermal shield and reactor vessel, and the film coefficients on the inside surfaces of the vessel wall.

(e) Qualitatively determine the tightness of the fuel elements in the core and note any vibrations due to looseness of the core.

(5) Results to Date

The pressure drop from inlet to outlet is shown in Figure 107. This pressure drop has been measured with all reflector seals held shut by a rubber gasket around the core, pending studies of the efficiency of the reflector seal design.

Velocity traverses in the outer gaps have been made. The data superimposed on the electrical analog results of velocities and film coefficients for two-nozzle flow are shown in Figures 108 and 109. The data are for an arrangement of the model which had a number of gap spacers which affected the flow pattern. These gap spacers were installed by the vendor during manufacture of the model. It was

and startup procedures. Film coefficient data from these tests will be used by the vendor to calculate stresses in the reactor vessel.

b. In the upper head and the cylindrical part of the vessel, film coefficients are required (1) on vertical planes through the nozzles and midway between the nozzles, and (2) on a horizontal plane through the nozzles.

c. In the lower head, film coefficients are required in the vicinity of the core support structure to determine the efficiency of the cooling in this area.

3. Flow Rates Up and Down in the Outer Gap

These data will be used to determine the distribution of flow in the various coolant passages for the present nozzle dimensions in the upper head.

(b) Phase II

This phase of testing is to provide design data for the upper thermal shields and plenum. The information to be obtained is:

1. A check on the reliability of the calculations of Δp in the inner gaps.

2. Determine the quantitative effects of the top nozzle orifices on the Δp.

3. Estimate the amount of heat flowing through the plenum shroud in the full-scale reactor.

4. Heat Transfer Data

a. The film coefficients at four points on the inner and outer surfaces of the plenum shroud above an exit nozzle and four points below the exit.

b. Smoke patterns in the inner gap between the thermal shield and the plenum shroud at the exit nozzles.

5. Flow Rates

a. In the gaps between the thermal shields and the plenum shroud.

b. Across the core support plate.

(c) Phase III

This phase is to obtain design data for the design of the lower thermal shield, side reflector and reflector seals. The data to be obtained are:

1. The leak rate through the reflector seals.

2. The restraining load on the core exerted by the reflector during operation.

(d) Phase IV

This area of testing covers those items whose design may be or is now being changed. The items affected by these changes are:

a. The core support plate.

b. The vessel diameter and thermal shield diameter tolerances. As pointed out previously, this item has already been partially investigated. If tolerances prove to be a problem, data have to be obtained and evaluated to show where spacer pads can be safely installed to improve flow characteristics.

b. Fuel Element Vibration Tests

(1) Summary

The purposes of these tests, which have been completed, was to determine if the fuel elements in the HTGR could be induced to vibrate by the coolant flowing past them. A test chamber was built in which a cluster of 19 full-scale fuel elements was subjected to flow conditions equivalent to those in the reactor. The end support conditions of the fuel elements were simulated very closely, as were the flow channels. Both metallic dummy fuel rods and prototype graphite rods were tested. Gas flow was varied from 10 percent to 225 percent of the Reynolds numbers expected in the reactor. There was no tendency of the air flow to initiate or sustain fuel element vibration.

(2) Apparatus

A full-scale, rather than sub-scale, mockup was built to eliminate scaling factors and to facilitate instrumentation of the fuel element models. It was decided to test metallic models as well as graphite elements, in order to obtain conservative results. The metallic models lacked the damping properties inherent in graphite and, therefore, should have shown vibration tendencies much more readily than the graphite elements.

A hexagonal test chamber was built containing 19 fuel rods; Figure 53 is a schematic cross section of the test chamber. The chamber is shown in Figure 112, with one of the side panels and two dummy elements removed. Two half-rods were attached to each side of the chamber, and a 120 rod segment was installed in each corner, to make the test section a true duplicate of the core lattice. The lower end of the test section was spanned by a dummy grid plate, i.e., a small aluminum plate identical to its counterpart in the core support plate in every respect but material and thickness. Prototype steel standoffs were used. The test chamber was constructed such that the degree of fixity imposed on the upper end of the fuel elements could be adjusted to simulate approximately the type of restraint existing in the reactor. The test chamber contained 54 tricuspid flow channels with a combined area of 38.2 square inches. Plenum chambers were attached to the top and bottom of the test section which were large enough to permit reduction of the flow velocity to a very low value, in order to minimize pressure losses at the transition from the ducting to the test section. No provision was made to duplicate the heating effect which exists in the core.

Air flow was provided by the blower normally used for the HTGR half-scale air flow model. The vibration test chamber was mounted on a filter box which kept the entering air clean. The blower and associated ducting were of sufficient capacity to permit a maximum flow equivalent to 225 per cent of the maximum Reynolds number existing in the core. The minimum flow rate was determined by the sensitivity threshold of the manometer and venturi used to measure flow rates, which amounted to approximately 10 percent of the reactor flow.

The metallic dummy elements were made dynamically equivalent to real fuel elements. In order to simulate end conditions as closely as possible, they were equipped with graphite end sections. The graphite prototype fuel elements used for the latter part of the test program were representative of the fuel element, except that they contained no spine or fuel compacts. It is believed that these prototypes were a conservative model of the actual fuel elements, since they had a lower mass, and lacked dynamic vibration absorption inherent in the loosely-fitting fuel compacts. The metallic rods were equipped with a spacer ring at the upper end, but had no intermediate spacers. The graphite rods had three spacers, with the exception of the three instrumented rods. The intermediate spacers had to be removed from these in order to permit installation of strain gauge leads.

(3) Instrumentation for Vibration Measurements

For each test run, three rods in the center of the cluster (marked X in Figure 53) were instrumented with strain gauges as vibration pickups. Two strain gauge half-bridges were mounted at the center and halfway between the center and the top of each of the instrumented rods. Each half-bridge was made up of two strain gauges located opposite each other on the rod. The two half-bridges at one station were displaced 90° with respect to each other. The strain gauge outputs were fed into a high-speed Brush recorder capable of continuously recording oscillations with frequencies up to 125 cps. The strain gauges were calibrated against a dial indicator by manually deflecting the rods. The recorder gain was adjusted to give a 2 mm pen deflection for each mil of rod deflection.

(4) Exciter

For several of the test runs carried out with metallic dummies, it was decided to forcibly vibrate the central fuel element. For this purpose a small direct current electric motor was mounted inside the element at its mid-point. The shaft of this motor was fitted with an eccentric which consisted of a 2-gram weight mounted

1 cm from the axis of revolution. With the shaft running at a speed corresponding to the natural frequency of the element, the half-amplitude of the induced vibration was .01 inch.

(5) Flow Measurements

Air flow was measured across a venturi installed in the main air duct, by means of an inclined water manometer with a 10:1 slope. The threshold response of this manometer corresponded to an air flow of .2 lb/sec.

(6) Test Procedure and Results

Six types of test runs were made with equipment. The first four were carried out with 19 metallic dummies; the remaining two with a central group of 7 graphite rods surrounded by a ring of 12 metallic dummies.

During the first set of runs the instrumented rods were placed in the center position and two diametrically opposite positions next to the center. Air flow was increased in 28 equal steps from a .2 lb/sec. to 2.6 lb/sec. At each increment the flow rate was held constant for about half a minute. No vibration was observed.

The second set of runs duplicated the first, except that at each flow rate the chamber was struck with a rubber mallet. Each such blow caused a rapidly decaying vibration of the rods with an initial half-amplitude at the center of the rods of about .002 inch. The rate of decay and the initial amplitude of the vibration were unaffected by the air flow. The length of time it took for the oscillations to disappear was the same at full flow as it was at no flow.

The third set of tests were made with the exciter mounted inside the central element. For these tests the axis of the exciter was mounted horizontally. A number of runs were made with the axis of the exciter in different angular orientations. Air flow was varied as previously, while the motor was running at the natural frequency of the rod. Air flow was cycled up and down at varying rates. There was no reinforcement of the vibration by the air flow. If anything, the air flow had a slight damping effect on the forced vibration of the rod.

For the fourth test, the exciter was mounted in the central metallic rod with its axis parallel to that of the fuel rod. The air flow tests gave the same results as before.

With the fifth test, the central group of metallic dummies were replaced by graphite fuel elements. The instrumentation was placed as before. Air flow was varied, again in small increments from .2 lb/sec to 4.5 lb/sec.. The latter figure corresponds to 250 percent of the Reynolds number in the core at full flow. There was no vibration.

A final set of runs was made similar to the second set. At each flow increment the chamber was struck with a rubber mallet. The initial half-amplitude of the resulting transient vibration was .003 inch. Again, the damping of the oscillation was essentially unaffected by the air flow. Roughly the same flow range was covered as in test number 5.

(7) Discussion and Conclusions

Under no conditions of flow did the elements ever vibrate, at least not within the sensitivity of the instrumentation. This sensitivity was such that a half-amplitude of .0001 inch would have been detectable.

Vibrations forcibly imposed on the elements by an external or internal exciter (neither of these can reasonably be expected to exist in the HTGR core) are not amplified or reinforced by the gas flow. In fact, the gas flow has a very slight damping effect. In the case where one specific fuel element is being excited, sympathetic vibrations occur in the adjacent fuel elements. The half amplitude of these is of barely perceptible magnitude, i.e., slightly above .0001 inch.

As a corollary of the tests, the natural frequencies of the rods under various conditions of end fixity were determined. The natural frequency increases, of course, with the degree of end restraint. Specifically, natural frequency of the rod, as mounted in the reactor, is 30 per cent higher than the natural frequency of the rod when simply supported at the ends. The degree of end fixity also had no measurable influence on the existence or lack of vibrations.

c. Thermal and Flow Characteristics of Core Coolant Channels

The design of the HTGR core incorporates lengthwise coolant-flow passages formed by the spaces between the parallel cylindrical fuel rods arranged in a closely spaced equilateral array. The coolant channels there have a tricuspid cross section, and adjacent channels intercommunicate since the fuel elements do not touch each other (except at the spacer rings). The coolant shear stress distribution in these channels is quite different from that found in ordinary ducts and results in unusual heat-transfer rates and velocity profiles within the passages. Experimental measurements have been completed for the determination of these parameters.

(1) Description of Measurements

Two air-flow systems were used to make the measurements, the pressure drops and velocities being measured under isothermal conditions in a dual tricuspid flow channel and the constant-wall-temperature heat-transfer coefficients being measured in a seven-rod cluster.

(2) Velocity and Pressure-Drop Measurements

Air was delivered by a centrifugal blower through a rotameter and a plenum chamber to a dual-channel test passage from which the air was vented to the atmosphere. The test passage was formed by joining two 120° and two 60° circumferential segments of aluminum tubing. Static pressure taps were located 110 and 134 equivalent diameters downstream from the channel entrance. The stagnation probe penetrated the channel wall just upstream from the static pressure taps.

The static pressure losses were measured over a

Reynolds number range of 3,000 to 30,000 at 90 F. The stagnation pressures were measured at an entrance length of 105 equivalent diameters for a Reynolds number of 20,000 as functions of the distances from the channel wall and angular positions on the circumference of the rod. The measured Fanning friction factor and air velocity are shown in Figures 113 and 114 respectively.

(3) Heat Transfer Measurements

The heat-transfer system utilized the same blower as the velocity and pressure drop system, being connected to the inlet side of the blower. Air was drawn through the test lattice, was passed through a calibrated orifice, and was then vented to the atmosphere by means of valve arrangements.

The test lattice consisted of seven rods spaced in an equilateral cluster within a hexagonal chamber. Each rod was composed of three hollow aluminum cylinders mounted in series on the same center line: (1) a thin-walled, upstream flow development portion; (2) a thick-walled, heated portion; and (3) a thin-walled, downstream exit portion. The heated portion of each rod contained a tightly wound helical electrical resistance heater which passed, longitudinally, through the center of this thick-walled cylinder. Calibrated copper-constantan thermocouples were embedded in the rods to measure the rod surface temperatures. The central rod of the seven rod cluster contained additional calibrated surface thermocouples as well as a small temperature-controlled surface heater which was used to determine the rod circumferential heat flux variation. The average and the circumferential heat transfer coefficients were measured at 38, 57, and 74 equivalent diameter hydrodynamic entrance lengths and are shown in Figures 115 and 116 respectively.

(4) Applicability of Results to Reactor Design

The results of this investigation can be summarized for the HTGR reactor design as follows:

(a) Conventional correlations may be used to predict the average heat-transfer coefficients and pressure losses.

(b) The local heat-transfer coefficient varies by a factor of approximately three for a Reynolds number of 20,000, the factor becoming progressively less as the gas flow rate is increased.

4. Research and Development Program for Control Rods and Drives

a. Test of Prototype Control Rod and Drive

The main test simulates full scale reactor operation of one entire drive system complete with the prototype control rod. Reactor simulation includes pressurized helium of representative purity with expected temperatures, temperature gradients and various degrees of guide tube misalignment, but no radiation effects. Complete control and monitoring instrumentation proposed for the actual plant installation is essentially duplicated. Additional instrumentation is used to control and record variables essential to the system and the test.

The test will provide data on response, performance, life, rates of metal transfer, wear rates, friction and reliability of the system as a whole as well as of the individual components. It is planned to subject the rod/drive combination to at least 10^6 inches of essentially random motions at regulating speed, and at least 5,000 scram operations starting from various rod positions. The latter number is five times as many scrams as are expected to occur in the life of a control rod drive.

The test procedure also includes investigations of the consequences of various component malfunctions by simulation of the malfunction in question and recording the consequent behavior of the rod and drive.

Initial testing in air at normal temperature, to the extent of approximately 2000 full strokes of motion at regulating speed and 200 full-stroke scrams, the subsequent disassembly and inspection, has revealed no basic design problems or appreciable wear effects. No malfunctions of the hydraulic drive other than one oil leak, occurred in this testing. Problems encountered with other components were minor and of types normally encountered during development of new mechanisms. The measured delay time was between 0.040 and 0.050 second (see Section II. B.7.b).

b. Wear Tests on Material Combinations

Although it is planned to lubricate most critical parts of the mechanisms, there are certain points where it may be difficult to assure really good lubrication over long periods without frequent

inspection and maintenance. In these instances, it is intended to employ material combinations that offer minimum friction and maximum wear and galling resistance. This is particularly important where the operating environment is an inert and dry atmosphere such as helium.

The research and development program includes a series of friction-wear tests designed to provide information on the behavior of various material combinations operating in a helium atmosphere. The tests include checks of materials with various finishes and hardnesses running dry, and also include checks of the life or permanency of certain anti-friction coatings, such as dry-film type lubricants, which may be found to be necessary.

c. Ballnut and Screw Test.

A test setup was built to determine the dynamic behavior of various ballnut and screw configurations. The main object of the test was to run screws of representative length at various accelerations and speeds in air to determine stability and critical speed effects. Another objective was to run endurance tests on at least one screw in a vacuum, in lieu of pure helium, in order to acquire preliminary friction and wear data. The test rig used a hydraulic motor drive to provide the required accelerations and velocities, but did not simulate the hydraulic circuit proposed for the actual control rod drive.

Two ballnut screws were tested under this heading. The first was not representative of the final configuration chosen for the control rod drive, so testing of it was confined to studying its wear behavior in air during regulating motion.

The second screw, made of through-hardened SAE 4150 steel with a black oxide finish and provided with tungsten carbide balls, was subjected to 5000 full-stroke cycles of regulating motion plus 500 scrams in air, and then to 4000 full-stroke cycles of regulating motion plus 300 scrams in vacuum, all without lubrication. Fifty of the scrams performed in air were started from part-stroke positions. The peak angular speed of the screw reached during most scrams was somewhat higher than the speed to be used in the reference design control rod drive, but a range from 30% above to 20% below design angular speed was covered in various test runs. Untoward vibrations and screw motions associated with whirling effects were looked for during scram but were not discovered. At the end of the testing mentioned, the screw and balls were carefully inspected and found to be virtually unworn except that bare metal of the screw was visible in some places where the black oxide finish had been worn away.

d. Pressure Housing Joint Test

This was a cyclic loading test of a specimen representing the seal-welded screw joint between the control rod drive housing and the pressure vessel nozzle extension. The object of the test was to discover whether or not deformation of the screwed joint under cyclic loading will give rise to cracking of the seal weld.

The operating temperature of the joint will not exceed 200 F and so room temperature tests were regarded as representative.

This test has been completed. In it, the specimen was subjected to one pressure cycle of 0 to 1000 psig, the application of an axial load of 2000 lb together with internal pressure of 450 psig, 4000 pressure cycles ranging from 0 to 650 psig and one cycle from 0 to 2200 psig. No cracking of the seal weld occurred, no leak was discoverable by helium leak detector and virtually no permanent deformation could be detected even after the application of 2200 psig.

e. Irradiation of Control Material

The program of investigation of the effects of irradiation on boron carbide loaded graphite compacts consists of irradiation of four capsules containing such materials in in-core positions of the GETR reactor and irradiation of one capsule in a reflector position, together with subsequent post-irradiation inspection and evaluation of specimens in order to discover any changes of dimensions or integrity. The details of the capsules are given in Table 36.

TABLE 36

IRRADIATION TESTS ON CONTROL MATERIAL

Capsule	Irr. Temp.	Irr. Exposure	Equivalent HTGR Lifetimes
GA-310-1	1200 F	2 GETR Cycles (in reflector)	1 month
GA-310.5-1	700 F	2 GETR Cycles (in core)	1 year
-2	700 F	6 GETR Cycles " "	3 years
-3	1200 F	2 GETR Cycles " "	1 year
-4	1200 F	6 GETR Cycles " "	3 years

The test specimens in each capsule of GA-310.5 series were identical -- one each of 20, 30 and 40 w/o boron carbide dispersed in a graphite matrix. In addition, a control specimen of AGOT graphite was inserted in an attempt to differentiate the fast neutron effects from those produced by the boron-neutron reaction. Melt wires and a flux monitor were placed near the center of each capsule for post-irradiation determination of the irradiation exposure and temperature.

The four capsules in the GA-310.5 series were inserted in the GETR on March 20, 1961. The first two capsules (nos. GA-310.5-1 and -3) were discharged on June 4, 1961. Post irradiation examination is now underway. Preliminary results are given in Table 21 of Section 2.J.1.

Capsule GA-310-1 was irradiated and evaluated during 1960. No significant changes of integrity or dimensions could be discovered after irradiation. (See Section II. J.1)

f. Measurement of Coolant Pressure Drop Through Control Rod

The object of this test was to measure the pressure drop through the control rod at various simulated positions in the core at various coolant flow rates in order to verify calculated results. Calculations have indicated that the reference design rod configuration will allow a flow of helium of about 350 lb /hr with a pressure drop of less than 3 psi. This rate of flow will maintain the metal sections of the rod at a temperature below 1000 F at the hottest part of the core. These calculations have been confirmed by experiment.

g. Graphite Guide Tube Strength Test

This test has been performed using test specimens made of National Carbon's AGOT reactor grade graphite. The shear strength of the breech connection which anchors the graphite guide tube to the core grid plate was measured by application of axial load to the specimen to the point of failure. The loading was initially run up to 3000 pounds and then relaxed. The specimens were visually inspected with no sign of any detrimental effects observed. They were then gradually loaded until failure occurred. The minimum load at failure was 5750 pounds and the maximum load was 6080 pounds. The six load-carrying "threads" of the breech connection all sheared off cleanly at their roots. The maximum force which a control rod drive can apply to the control rod itself is about 2500 pounds. This represents the maximum axial load which the graphite guide tube could experience in either tension of compression.

h. Thermal Stability of Control Materials

Some measurements have been made of loss of boron from boron carbide loaded graphite compacts as a result of heating the compacts to various temperatures for various lengths of time in a helium atmosphere. The results are given in Table 37.

TABLE 37

THERMAL STABILITY OF CONTROL MATERIAL

Compact	Temperature, C	Time at Temp., hr	Boron Loss, %
1	1700	100	0
2	2160	16	1/2 ± 1/2
3	2300	6	1/2 ± 1/2
4	2500	6	2.7 ± 1/2

These results are in substantial agreement with theoretical predictions, and show that boron loss will not reach an unsafe value dueing the period when the core is at high temperatures following loss of all coolant flow immediately after full power operation of the reactor. (For Temperature/time history during this accident, see Appendix C). Very large losses of boron may, of course, be compensated by insertion of the electrically operated emergency shutdown rods. (See Section II.B.8.)

i. Thermal and Radiation Stability of Graphite Guide Tubes

The control rod guide tubes will be located in a region of about 1×10^{13} nv (>1 mev). Their wall temperatures will be in the range of 660-1400 F. Graphite tubes for this purpose will be procured as extruded commercial graphite manufactured from a petroleum coke filler bonded with coal tar pitch. The separate thermal and neutron induced changes during HTGR lifetime can be estimated for this type material based on some recent work.

Recent out-of-pile thermal stability evaluation of National Carbon and Carbide Corporation's AGOT nuclear graphite indicates no measurable dimensional change after 1000 hours at 2372 F.

Creep experiments at 2250 psi in tension at 1300 F indicate a creep rate or deformation rate of 10^{-9} in/in-sec for 300 hours and a strain of about 0.20%. No further deformation was evident in the next 300 hours. (See Section II.J.1).

Based on this result, a flattening of a control rod guide tube of the order of 0.010 inches in expected due to the radial loads applied to the guide tube by adjacent fuel elements for the worst case where only two diametrically opposed fuel elements bear against the guide tube. This flattening is of about the same magnitude as the flattening due to elastic deflection under the same condition.

For control rod guide tubes the neutron-induced contraction is most important in the diameter. The tubes also will contract longitudinally. Because of the particle and crystallite orientation caused by the extrusion forces during manufacture, the contraction is most severe in the longitudinal direction (the A. direction of the graphite crystal system).

A specimen of a CSF grade graphite which is quite similar to AGOT in manufacture, crystal structure, and purity has been irradiated in the temperature range 842-1562 F to an integrated fast flux of $\sim 10^{21}$ ($>$ 1 mev). Contraction in the diameter was 0.02 to 0.04% and in length 0.06 to 0.08%. Additional specimens are now being irradiated.

j. Status of Tests

Of those tests which have been itemized in this section, those described under (c), (d), (f) and (g) are complete; those described under (b), (e) and (h) are scheduled for completion by the end of 1961 and the remainder scheduled for completion by mid-1962.

5. RESEARCH AND DEVELOPMENT PROGRAM FOR EMERGENCY SHUTDOWN SYSTEMS

a. Electrically Driven Emergency Shutdown Rods and Drives

Much of the information developed in the research and development program devoted to the control rods and drives will be directly applicable to the emergency shutdown rods and drives. The applicable tests and investigations are items b, d, g, and i of Section II. J. 4, above.

A complete prototype emergency shutdown rod and drive will be tested in a helium environment as in the case of the prototype control rod and drive. In fact, the same test set-up will be used with the same kind of simulation of reactor conditions (See Section II. J. 4. item (a). In this test, the emergency shutdown rod and drive will be put through at least 5,000 cycles of full-stroke movement against no resistance, and at least 50 cycles of full-stroke operation against a resisting load of 10,000 pounds applied to the absorber rod. The numbers of operating cycles given are of the order of 50 times the numbers expected actually occur in the life of a drive.

The tests will provide data on response, performance, wear rates, friction and reliability of the system as a whole as well as of individual components.

Completion of these tests is scheduled for the middle of 1962.

b. Thermally Released Shutdown Absorbers

Creep and release tests are in progress on a brazed joint specimen with a view to finding a material and configuration having indefinite life at 1000 F, good short-term creep performance up to 1600 F, and a melting temperature below 1800 F. The first material in the evaluation schedule is a standard brazing alloy made up of 85% silver and 15% manganese.

Completion of this work is scheduled for the middle of 1962.

III. CONVENTIONAL PLANT AND SERVICES

A. General

The preliminary plans and sections of the Peach Bottom Atomic Power Station are shown in Figures 117, 118, 119, 120 and 121. The layout of the plant on the site is shown in Figure 122.

B. Main Turbine

The electric generating portion of the plant is an outdoor, single turbine-generator unit. The equipment will be of conventional design and of maximum reliability, consistent with an economical plant design.

The turbine-generator is a 3600 rpm tandem compound, double-flow, condensing unit capable of producing 40,000 kw net plant electrical output with 1450 psig, 1000 F steam at the throttle.

C. Condensing System

The main condenser performs the following functions:

(1) Condenses steam exhausted from the turbine to maintain the desired vacuum.

(2) Provides a heat sink for main steam flow during reactor startup or shutdown conditions, when steam will bypass the turbine and flow to the condenser via the bypass dump line.

The main condenser is a conventional welded steel, single-pass, divided water box type, with a hot well which will provide for several minutes condensate storage at design load. The condenser and associated equipment are capable of desuperheating, reducing in pressure and then condensing full throttle flow of 1450 psig, 1000 F steam.

D. Condensate and Feedwater Systems

The condensate and feedwater systems are shown schematically on Figure 123.

Two half capacity motor-driven, vertical condensate pumps are provided to pump condensate from the condenser through two low-pressure horizontal U-tube closed feedwater heaters in series to the

deaerating feedwater heater. Morpholine for pH control and hydrazine for oxygen scavenging will be injected in the condensate header in the deaerator outlet.

Two half capacity steam generator feed pumps will take suction from the deaerator storage tank and feed the steam generators through a high pressure feedwater heater. One pump will be driven by a 3600 rpm, 2300 volt, 3 phase, 60 cycle motor and the other by a 3600 rpm, 1450 psig, 1000 F mechanical drive steam turbine. One reduced capacity shutdown feed pump is furnished for startup and shutdown.

E. Circulating Water System

One full capacity, vertical, axial flow pump located in the pump house at the intake structure will pump pond water to the condenser. Floating debris is removed by passing the pond water through a bar screen and a traveling screen before reaching the suction of the pump. An intermittently operated chlorination system is provided. After passing through the condenser, the water discharges to a 60-inch discharge line which is carried below grade to the discharge structure.

F. Service and Closed Loop Cooling Water Systems

The service water systems, shown schematically in Figure 124, Raw Water Flow Diagram, will provide a continuous supply of strained pond water to a number of heat exchangers as shown on the diagram. Two service water loops are provided: main service water and critical service water. The critical service water will supply those heat exchangers which will require a continuous supply of service water after reactor scram and loss of all outside power. These include:

Turbine Building Cooling Water
Containment Equipment Cooling Water
Fission Product Traps Cooling Water
Emergency Diesel-Generator Cooling Water
Reactor Vessel Emergency Cooling System
Fission Product Traps Emergency Cooling System

Two full capacity critical service water pumps will be provided at the intake-discharge structure. One pump will be reserved for automatic standby service on loss of discharge pressure or loss of motor voltage of the running pump. Either pump may be supplied by the emergency diesel-generator.

The reactor vessel and fission product traps emergency cooling system will be used when the normal means of cooling the reactor or the traps are inoperative. The critical service water pumps will circulate cooling water through the reactor vessel and fission product traps emergency cooling system, discharging directly into the pond. Backup for the critical service water pumps will be provided by a cross-tie to the fire system which can utilize the diesel-engine-driven fire pump.

Two full capacity vertical main service pumps located at the intake-discharge structure will supply all services not considered critical. One pump will be reserved for automatic standby service on loss of discharge pressure or loss of motor voltage of the running pump. These pumps are normally tripped from the essential bus when supply is from the emergency source.

The following three closed cooling water systems are shown schematically in Figures 125 and 126: Spent Fuel Pit Cooling Water System, Shield Cooling Water System, and Containment Equipment Cooling Water System. A closed cooling system, shown in Figure 56 is also used for external fission product trap cooling.

In the first two systems, which are normally slightly radioactive, the cooling water is normally maintained at a pressure less than service water pressure. With this design the service water will not become contaminated even if the cooling water heat exchangers were to fail.

If any of the closed cooling water loops should become contaminated the water may be pumped out to the liquid waste handling system for cleanup or disposal.

Each closed cooling water loop will have two full capacity circulating pumps, one of which will be reserved for automatic standby service on loss of discharge pressure or loss of motor voltage of the running pump. Each pump on the containment equipment cooling water system will be supplied from the emergency diesel-generator when normal sources fail. Pumps on the first two systems are not on the essential bus, but, if necessary, each may be fed from the emergency source by manual switching.

Two full capacity service water heat exchangers are provided for each closed cooling water loop on the critical service water system.

G. Water Storage

Two large tanks are provided for storage of demineralized water and oxygen reduced condensate. In the event of loss of the main condenser, these tanks provide adequate water to shut down the plant and dissipate afterheat for an extended period by blowing steam to atmosphere. A third large well-water storage tank is also provided for domestic water.

H. Electrical System

1. Generation and Transmission

Generation will be at 13.8 kilovolts, 3 phase, 60 cycles. The generator will furnish power through a generator circuit breaker to a main transformer. The main transformer will supply power at 220 kilovolts through a high voltage oil circuit breaker to a solid tap from a high capacity transmission line. This line, which extends from the Philadelphia Electric Company Nottingham Substation to the Baltimore Gas and Electric Company Graceton Substation, is one of a number of high voltage, high capacity connections between five member companies of the Pennsylvania-New Jersey-Maryland interconnection.

Total capacity of the power pool represented by the interconnection is approximately 15,000 megawatts of which the Philadelphia Electric Company represents about 3500 megawatts and the Baltimore Gas and Electric Company about 1800 megawatts.

For startup and during periods when the generator may be inoperative, station auxiliary power will be supplied from the 220 kilovolt transmission line through the main transformer and an auxiliary transformer, the generator being disconnected from the system by the opening of the generator circuit breaker.

The plant electrical system arrangement is shown on the Electrical Single Line Diagram, Figure 127.

2. Auxiliary and Emergency Power

Power for plant auxiliaries will be supplied at 2400 volts for the large auxiliaries and 480 volts for smaller equipment. The auxiliary power system will be energized normally from two auxiliary power transformers, one of which is solidly connected to the generator side of the generator air circuit breaker and the second to the main transformer side of the generator air circuit breaker. The second auxiliary

transformer can receive power from the 220 kv system through the main transformer when the generator air circuit breaker is open and will normally supply power for startup and shutdown. Both auxiliary transformers may receive power from the generator when it is in operation and the generator air circuit breaker is closed. Two 2400 volt busses, each normally energized by one of the two auxiliary transformers, will supply the larger auxiliaries and the 480 volt load center transformers. A reserve transformer can energize the auxiliary system from a 33 kv power source under conditions when power may not be available from the 220 kv system or main generator. This reserve power source will have sufficient capability to operate essential plant auxiliaries required for orderly shutdown.

Equipment rated 440 volts and essential for emergencies and orderly plant shutdown will be connected to bus sections arranged for normal power supply from the station auxiliary system with automatic transfer to an emergency diesel-generator power source under abnormal conditions. The diesel-generator set will start automatically, initiated by an undervoltage relay connected to the emergency bus. Automatic transfer will occur at such time as the generator voltage has reached normal. The unit will be completely self-contained and will start and run independent of station auxiliary power sources. The cooling water supply for the emergency diesel-generator will be furnished by pumps supplied from the essential 480 volt busses.

A battery supplied d-c system and a critical power a-c system will provide highly reliable sources of power for control, instrumentation, and critical equipment. The battery supplied d-c system will be ungrounded operating at 125 volts nominal. The battery will be adequate to supply the peak power requirements of the connected load. A charger supplied from the 480 volt emergency bus will keep the battery in fully charged condition and will supply continuous load requirements.

The electrical power system is arranged so that no single equipment failure will result in an interruption of the power supply to essential plant auxiliaries. Further power source backup is provided for multiple failures as described below.

Faults resulting in tripping of the main turbine generator will trip the generator air circuit breaker and leave the auxiliary power system supplied by the 220 kv system through the main transformer and its associated auxiliary transformer.

Faults in the main transformer, its associated auxiliary transformer or loss of the 220 kv supply, will trip the generator air circuit breaker and leave only the auxiliary power system supplied by the main turbine generator through its associated auxiliary transformer. The turbine governor will, with high reliability, control the unit speed below the overspeed trip setting for this sudden reduction in load. Should, however, the turbine trip on overspeed, there is sufficient energy stored in the rotating masses of the turbine-generator to supply useable power to the auxiliary electrical system for a sufficient length of time to provide initial reactor cooling. Adequate excitation for the main generator during the coastdown period will be provided by an automatically switched emergency excitation storage battery. Further cooling will be accomplished by the helium compressors on their pony drivers, supplied by the emergency diesel generator or the 33 kv reserve source. Although cooling at the reduced rate will normally be initiated toward the end of the coastdown period, the initial cooling will have lowered reactor temperatures to the point where delay of further cooling can be tolerated for a considerable period without major damage to the core.

During the coastdown period the operator may manually reset the overspeed trip, re-admit steam and bring the unit back up to speed to furnish auxiliary load only for approximately one half hour.

Multiple equipment failures resulting in neither the 220 kv system nor the main turbine-generator being available as power sources will initiate an automatic transfer of approximately half the auxiliary load to the 33 kv reserve source and start of the diesel-generator.

The 33 kv reserve source as well as the emergency diesel-generator provides backup for shutdown in case the 220 kv source is lost during startup or shutdown when the main turbine-generator is not operating.

I. Fire Protection System

The fire protection water system will be an automatically controlled pressure system consisting of hydrants with hose shelters, hose stations located within enclosed portions of the plant, an accumulator, and two fire pumps. The fire pumps located at the intake structure will consist of a motor-driven, main fire pump and a diesel-engine-driven pump for standby service.

Pressure for the fire system accumulator will be maintained by a jockey fire pump supplied from the service water system. Pressure

drop in the fire loop will actuate a pressure switch and automatically start the main fire pump. The standby fire pump will be started manually. Control room alarms will indicate which pump is in operation.

Fire extinguishers will be placed strategically throughout the plant. Carbon dioxide fire protection will be provided for various electrical components, lube oil processing equipment, and in the subpile room.

J. Normal Heating and Ventilation

The containment ventilation system is shown schematically in Figure 128, Containment Ventilation and Gaseous Waste Disposal Flow Diagram. The normal ventilation system provides a completely contained recycle of the containment inert gas atmosphere and a fresh air makeup and exhaust for the air room. Facilities for purge and makeup of insert gas as necessary to maintain the system differential pressure balance are also provided. During shutdown periods, the containment is purged with fresh air to permit personnel access.

1. Containment Ventilation

Normal recirculation of the containment reduced oxygen atmosphere is accomplished by blowers which take suction from the control rod drive and auxiliary equipment areas and from the helium dump tank and purified helium storage tank areas. The gas is filtered through absolute filters, cooled for sensible heat removal and then returned to the containment by discharge at the operating floor elevation. The general containment volume will be maintained at a slight negative differential with respect to atmospheric pressure in order to restrict release of fission product activities from the general containment to the ventilation stack where such releases will be monitored and controlled as described in Section VI. The oxygen concentration in the recirculating gas stream will be monitored so that safe concentrations can be maintained.

2. Air Room Ventilation

In order to provide for equipment which may require frequent maintenance and must be located inside the containment because of process or radioactivity requirements, such as control rod drive auxiliaries, an air room is included within the containment. Fresh filtered air from the intake plenum is supplied to the air room by a supply fan and discharged to the ventilation stack by a separate exhaust fan. The air room pressure is controlled at about atmospheric pressure, and will preclude leakage from the containment to the air room. Exhaust ducting within the air room is arranged to take suction from the equipment cubicles and from other areas having the highest probability for radioactive contamination.

3. Equipment Cavities

Both primary loop cavities and the helium purification system cavity are provided with independent recirculation systems within the containment for sensible heat removal from the reduced oxygen blanketing gas.

4. Gaseous Waste Disposal System

The gaseous waste disposal system consists of a separate exhaust duct which collects purge gases from the various cavities mentioned above. Collected gases are drawn through an absolute filter and discharged to the containment ventilation stack.

K. Emergency Ventilation of Containment Atmosphere

The primary loop and helium purification system ventilation circulation systems (Section III. J above) may be continued in operation when the presence of radioactivity has necessitated closure of the general ventilation system containment isolation valves.

A 2000 cfm bypass absolute filter in the containment exhaust recirculation duct provides approximately four changes of the containment atmosphere per day for removal of Sr-90 airborne activity following an incident.

L. Containment Atmosphere Supply System

An oxygen burning system will provide nitrogen gas containing approximately 0.5 percent oxygen by volume (plus residual argon) to the containment. Prior to operation of the HTGR this system will be used to purge air from the containment. During operation the system will supply makeup quantities of gas, as required, to maintain the required containment atmosphere.

1. Containment Purge

The secondary containment vessel prior to initial operation of the HTGR and during reactor shutdown periods contains fresh air to permit personnel access. Before the HTGR is brought to full operating power level the air in the secondary containment, excluding the air room, is replaced with reduced oxygen gas from the supply system to provide an inert atmosphere during reactor operation. Thus, explosions or combustion of CO_2 and H_2 formed during certain accidents

cannot occur since the containment atmosphere contains less than 5 percent oxygen by volume.[1] Combustion of the core graphite in the event of a primary system rupture is also prevented by the reduced oxygen containment atmosphere.

2. Containment Makeup

A portion of the gas in the secondary containment will be bled off to the stack for the following reasons:

(a) To maintain the desired sub-atmospheric pressure in the containment.

(b) To maintain the safe low oxygen content in the containment by disposing of any oxygen inleakage from the air room.

The containment atmosphere supply system will provide makeup as required to replace the reduced oxygen gas in the containment.

3. Oxygen Burning Equipment

The oxygen burning system consists of a standard unit which burns a hydrocarbon fuel in air to complete combustion, converting the oxygen in the air to carbon dioxide and water. The water is removed by condensation. The resulting gas which contains about 0.5 percent oxygen (and residual argon) is then fed into the secondary containment vessel via the containment ventilation system.

M. Spent Fuel Pit Building Ventilation

The building over the spent fuel pit is designed to retain radioactive materials which may be released due to an accident in the spent fuel pit. In the event of abnormal emission of radioactive material, suitable radiation monitoring devices will sound audible alarms, and trip closed the leak-tight valves in the normal ventilation air inlet and discharge lines. Negative pressure developed by the cleanup exhaust system will assure that the building air contents will not leak out except through the stack.

The building clean-up ventilation system is designed on the basis of accident concurrent with a low velocity wind of unvarying direction and different conditions of possible atmospheric diffusion. Consideration of possible exposures off-site under the worst of these conditions has established a design rate of discharge from the building.

[1]Coward, H. F., and Jones, G. W., "Limits of Flammability of Gases and Vapors, "U.S. Bureau of Mines Bulletin 503, 1952

The building clean-up exhaust system has been proportioned to realease air from the building through the stack at or below this rate.

Operation of the clean-up exhaust system will cause a reduction of air pressure within the building when other building penetrations are closed. Admission of outside air will be controlled to hold the building pressure one quarter inch of water below ambient atmospheric pressure.

The rate of discharge from the clean-up exhaust system, 100% of the building volume per day, is adequate to compensate for pressure variations due to barometric and temperature changes. Under the condition of low wind velocity, the building will not be subjected to a net internal pressure and no exfiltration could occur.

IV. CONTAINMENT

A. General Description

The containment structure will consist of a vertical, capsule-shaped steel shell with dished top and bottom heads. The configuration of the containment structure is shown in Figure 120.

The containment will be constructed in two stages. Most of the concrete and all major equipment items will be installed between the first and second stage, the shell being completed after these have been installed. The pressure tests will be made after completion of the shell erection.

B. Specifications

Following are the design specifications for the containment structures:

(1)	Design internal pressure	8.0 psig
(2)	Design temperature	150 F
(3)	Design negative pressure	0.2 psig
(4)	Leakage at design pressure	0.2%/day, of the contained volume
(5)	Snow	30 lb/sq ft
(6)	Seismic	0.05 gravity
(7)	Wind	100 mph
(8)	Material	A-201 Carbon Steel made to A-300 specifications
(9)	Weld rods	Low hydrogen

The containment vessel will be designed and tested to conform to the applicable State of Pennsylvania, ASA, and/or ASME Codes.

C. Penetrations, Access and Appurtenances

Penetrations will be designed to be leaktight and will conform to the requirements of the codes referred to above. All normally

open penetrations including steam lines, feedwater lines and ventilation openings will have provision for closing either automatically or remote manually under appropriate conditions to insure that the specified containment leakage is not exceeded.

Access to the air room will be provided by means of an air-lock.

Additional personnel access to the containment during the shutdown condition will be provided by a fully gasketed autoclave door at operating floor elevation.

The personnel lock will have doors not less than 3 feet in diameter and will provide not less than 5 feet clear space. Doors will swing toward the inside of the containment and will be mechanically interlocked to prevent simultaneous opening of both doors.

Equipment access at ground floor elevation will be provided for use during shutdown. It will consist of an 8'-0" diameter fully gasketed, autoclave type door opening inward to the containment.

D. Testing

All seams will be soap bubble tested under nominal pressure or by means of a vacuum box. This will be done prior to making any portion of the shell inaccessible for testing or repair.

X-ray testing of the shell seams will be as required to conform to the codes referred to above.

Pressure testing will be performed after the containment structure is complete. The structure will be pneumatically tested for integrity in accordance with the applicable codes. Following the overpressure strength test, a leakage test at design pressure will be conducted to verify that the leakage is within the specified limits.

Provisions will be made to permit leak tests to verify periodically that the containment leakage specification is not exceeded.

E. Containment Pressure Calculation

The most severe accident which involves a single failure is the rupture of the primary coolant loop releasing 926 lb of circulating inventory helium at 790F. The calculated equilibrium containment pressure and temperature for this release is 3.8 psig at 155 F.

The most severe accident postulated involves a series of failures. They are 1) a primary system rupture, 2) rupture of one steam generator tube, 3) failure of helium loop valves to isolate the ruptured steam generator from the reactor, and 4) loss of all forced circulation cooling of the core. The consequences of these failures were calculated using the following conservative assumptions:

(1) Release of 926 lbs. of primary coolant loop helium at 790 F.

(2) Release of 2200 lbs. of water and steam from the faulty steam generator system. (See Appendix D)

(3) Total immediate chemical reaction of 1100 lbs. of the released water and steam with the reactor core graphite assuming its complete conversion to carbon monoxide and hydrogen which are then released at 660 F to the containment.

This is assumed to occur simultaneously with the release of the remaining 1100 lbs. of steam at 660 F to the containment atmosphere.

(4) Subsequent chemical reaction of the remaining water, steam, oxygen and carbon dioxide in the containment atmosphere with the core graphite at a rate dictated by natural convection of the containment gas mixture through the reactor vessel.

Up through the third assumption no credit was taken for heat absorption by the containment steel and concrete or heat rejection to the external environment. The containment pressure calculations assume adiabatic conditions and complete thermal and phase equilibrium between the released components.

During the additional process indicated in (4) above, heat losses, heat absorption and containment ventilation have been factored into the calculations.

The highest peak containment pressure resulting from this multiple accident, based upon these conservative assumptions, is 8.0 psig at 150 F. This has been used as the internal design pressure.

V. PLANT OPERATION

A. Power Operation and Control

1. General

This section describes briefly the normal operation of the nuclear power plant. A more detailed description will be submitted in the final Hazards Summary Report.

2. Preparation for Normal Reactor Startup

a. Pressurizing Main Coolant Helium System

Charging and evacuation of the gaseous coolant is by means of the helium handling and storage system and its associated equipment.

Repressurization of the main helium system preparatory to starting up the plant requires that the main helium loops and their associated equipment be valved to the helium dump tanks through an equalizing line. Pressure in the interconnected systems would be allowed to reach equilibrium after which the equalizing line would be closed. Helium transfer compressors would be placed in continuous operation and valved to pump down the helium dump tanks to their normal operating pressure and to increase the main primary coolant system pressure.

During depressurizing or repressurizing the main coolant helium system, steam-generator water-side pressures may vary and will normally be maintained above the maximum helium pressure. This water-side pressurization will be designed to preclude entrance of water to the superheater and to maintain normal drum water levels with reduced boiler temperatures.

b. Placing Helium Purification System in Operation

The steam generator purge purification system would be started and, when the desired purity level is attained in main coolant helium, the Freon refrigeration system and the low temperature traps would be placed in service. Normal flow of the fuel element purge stream would then be established through the helium purification system.

c. Establishing Helium Flow in Main Coolant System

Helium circulator auxiliary equipment such as lube oil and seal oil systems with cooling water supplies would be placed in service prior to establishing flow in the primary helium coolant system. Helium purge flow to the control rods would be established and the helium buffer seals would be started if previously shut down.

After all circulator auxiliary equipment is in service and has been determined to be capable of normal operation, the hot helium valves and the circulator bypass and discharge valves would be opened. The suction valves would remain closed until the appropriate point in the starting cycle.

Both circulators would be started on bypass flow and brought to the normal system warmup speed. After flow is essentially balanced between the two coolant loops, the suction valves for each circulator would be opened while the bypass valves were closing, and in this manner, helium flow through the reactor would be established.

d. Other Preparations for Normal Reactor Startup.

The auxiliary equipment including the following would be placed in service or checked in its normal operating condition:

(1) Instrumentation including: count rate channels, scram trip channels, scram annunciator, and primary loop instrumentation.

(2) All steam generator circulation loop block valves open.

(3) Proper water levels in steam drums.

(4) Control rod actuator hydraulic system in service and normal.

(5) Safety systems, such as fire protection and radiation monitors in normal condition.

(6) The electrically driven emergency shutdown rods.

3. Achieving Criticality

The increase of neutron flux from source level to power range of reactor operation is effected by manual control rod withdrawal.

The rate of control rod withdrawal is limited to a value such that a predetermined rate of reactivity increase will not be exceeded. During the initial stages of control rod withdrawal, neutron level information is provided by the count-rate channels of the nuclear instrumentation. After the neutron flux level has increased several decades above source level, an uninterrupted continuation of neutron flux monitoring is provided by Log N channel indicators. After achievement of criticality and the increase of neutron flux to a level within the range of the power level channels, (a minimum of approximately 5 percent of rated power) further rate of change in the neutron flux can be controlled either manually or automatically by the flux controller.

4. Equipment Warmup

When the reactor reaches the power range of operation, the neutron flux and its rate of increase are manually controlled as required to limit the increase in reactor and helium coolant loop equipment metal temperatures to a predetermined safe level.

As the coolant loop temperatures rise, the boiler pressure will increase and the steam lines would be vented through the pressure breakdown and desuperheating station to the main condenser.

When the steam lines are hot, warmup, starting, and synchronization of the turbine-generator would be accomplished following conventional practice.

Startup from the hot standby condition may be initiated for any condition in which the main coolant system and all main equipment components would be at elevated temperatures following a brief outage. Minimum conditions for the hot standby state are listed below. However, a hot restart may be initiated at any time prior to the occurrence of these minimum conditions. Such a restart from more favorable conditions would follow appropriate preliminary procedures. Equipment status and auxiliary system conditions for the hot standby state are as follows:

a. The reactor would be shut down with control rods inserted in the core.

b. Both coolant loops would be in operation with the helium circulators driven at reduced speed.

c. All plant auxiliary systems would be in their normal operating condition.

The initial requirement in preparation for a hot restart would be the re-establishment of normal pressure relationships in the coolant system. The rate of pressure increase would be controlled in such a manner that temperature transients in excess of a predetermined safe rate are avoided.

5. Power Range Operation

When an increase in power output is desired, the turbine admission valves are opened to increase steam flow through the turbine. A control signal proportional to the deviation of steam pressure from standard is transmitted to the helium circulator speed controller. The resultant increase in helium flow rate reduces the hot helium temperature. Regulating rod action subsequently increases the helium temperature and maintains steam temperature. Rod movement is in response to a control signal derived from the relation between steam temperature, hot helium temperatures, and the neutron flux. In this way, reactor temperature varies as required to maintain constant steam temperature under all normal loads. The normal maximum rate of load change for the plant would be 3% per minute.

6. Normal Shutdown

Upon the initiation of a plant shutdown, the turbine generator govenor would be adjusted downward at the maximum rate of 3% per minute to the minimum load point for the turbine generator. Down to approximately 30% of full load setting, the plant control system would automatically follow this load reduction by lowering helium circulator speed to hold desired steam pressure and by lowering reactor power level to provide the required reactor outlet helium temperature to maintain constant steam temperature. Below 30% load, the plant would be unloaded manually. Excess steam flow would be bypassed to the main condenser through the turbine-bypass desuperheating and pressure-reducing station and auxiliary load transferred to the 220 kv line.

After minimum load point is reached on the turbine-generator, the turbine stop valve would be tripped and the generator 13.8 kv air circuit breaker would be opened.

After the turbine is shut down, the reactor flux controller would be taken off automatic control, and the reactor control rods would be manually driven into the core at a controlled rate.

In order to remove stored heat from the reactor core, and to facilitate decay heat removal following shutdown of the turbine-generator and reactor, speed of the helium circulators would be gradually reduced, allowing steam temperature and pressure to decay.

Helium circulation during shutdown cooling will be provided by main motor drivers with control of flow rates accomplished by the fluid couplings. The mass flow rate of helium would be gradually decreased, and steam pressure would be reduced slowly at a controlled rate by manually resetting the control point on the turbine bypass pressure controller.

Shutdown cooling would be continued through the sub-boiling system during plant shutdown to remove all decay heat generated in the reactor core.

The helium purge flow will normally be maintained through the purification system during all periods of normal shutdown duration. This requirement will necessitate that all purification system equipment necessary to maintain flow through the purification loop be in operation.

B. Pre-Operational Testing

Prior to and following completion of construction of the plant and before fuel elements are loaded into the reactor, all plant components and systems will be thoroughly tested and checked out. Testing, then, will include: operation of the control rod drives at normal insertion and withdrawal speeds, as well as scram speeds; the operation of all components of the fuel handling equipment, of the main helium circulators, of auxiliary helium system equipment circulators, and of the helium purification system.

During this test period, before reactor power operation, the source of heat for the primary loop will be the work input of the main helium compressors. While the amount of power available in this manner is relatively small, it will permit bringing the main coolant system up to a temperature of about 600 F in two days. Since this temperature is approximately the same as the design temperature of the cooler portions of the main coolant system, much of the equipment installed can be tested under nearly operating conditions. System cleanup will be accomplished with non-nuclear operating conditions.

C. Maintenance

Certain nuclear steam supply system equipment will require maintenance. The maintenance procedures will be specifically directed to cope with the special problems introduced by fission product plate-out or other contamination. Following is an outline of some of the present maintenance concepts. A more detailed description will be submitted in the final Hazards Summary Report.

1. Fuel Handling Equipment

Fuel handling equipment is not present in the reactor vessel during operation, therefore, this equipment will not become activated by neutrons. A certain amount of activity is expected to exist on the surfaces of the fuel handling equipment as a result of fission product deposition. However, since fuel handling within the reactor vessel does not begin until approximately one day after shutdown, and until the core outlet gas temperature is reduced to approximately 450 F at sub-atmospheric pressure, the deposition of fission product activity on fuel handling equipment surfaces is not expected to be serious.

The transfer machine is the most complicated piece of equipment involved in fuel handling and might be expected, therefore, to require the most maintenance. Maintenance on this machine will be performed after the machine has been removed from the pressure vessel.

2. Control Rods and Drives

The auxiliaries to the control rod drive system --- the helium storage tanks, pumps, etc. --- will generally be located out of the sub-pile room but they may not be available for maintenance during reactor operation. After shutdown, the radiation level in the sub-pile room will be low enough to permit personnel limited access for maintenance purposes. Since the control rod drive mechanism will be sealed it is not intended to perform extensive maintenance operations on the drives in place. If required, a failed mechanism will be removed in its entirety from the sub-pile room and replaced with a spare. The drive mechanism requiring service may then be repaired outside the sub-pile room. During the process of changing a complete control rod drive, the system pressure will be sub-atmospheric so that leakage is inward. Some purging may be required.

The removal of a control rod and guide tube can be accomplished by means of the transfer machine. The transfer machine can remove the control rod and guide tube from the reactor in a manner similar to that used in removing a spent fuel element.

3. Primary Coolant System

Steam generator specifications provide excess tubes to allow full rated capacity with 5% of the tubes plugged. Steam drum and recirculation pump maintenance will follow conventional methods. Controls are located outside the shield walls. Leakage from the primary coolant system will be continually monitored.

4. Fission Product Traps and Helium Purification System

All traps in the purification system are designed to operate effectively for the life of the plant. Provisions will be made in the plant layout, however, to accomplish trap removal and replacement if this should ever become necessary.

5. Helium Handling and Storage System

During normal operation, the helium dump tanks and the purified helium storage tanks are not accessible for maintenance. The tanks can be repaired after a suitable decay period following shutdown. The clean helium equipment is always accessible for maintenance. The helium transfer and purfied helium compressors will normally be accessible for maintenance during operation.

6. Containment

Because of the necessity of maintaining the integrity of the containment during the lifetime of the plant, maintenance procedures will be instituted specifically for this purpose. Penetrations will be periodically inspected. Gaskets and seals around air locks or other penetrations will be inspected and replaced if necessary.

D. Plant Personnel

Preliminary estimates of the types and classification of personnel for the Peach Bottom Plant have been made and some key members of the staff have already been chosen.

Most of the plant personnel will be selected from present employees of the Philadelphia Electric Company. Those responsible for plant operations will have had considerable conventional power station operation experience and will be trained in the nuclear plant operation. Some new employees having special technical experience or training may be used to round out the organization.

Training of persons who will be part of the supervisory group began in 1959, and plans are presently being made for the selection and training of additional technical personnel. Basic nuclear technology courses will be given before off-site training facilities are utilized. Off-site training at AEC and other reactor facilities and the assignment of personnel to General Atomic will provide additional training. Thorough knowledge of health physics aspects by all supervisory personnel will be stressed.

It is expected that the off-site training program for supervisory employees will be completed by the end of 1962. At this time a plant operator training program will begin. This program, conducted by the plant supervisory personnel, will be similar but less detailed than their own training. The installation, testing and initial operation of plant equipment will be closely followed by all personnel so that they may become intimately familiar with their operation.

Equipment operating manuals and detailed operation procedures for both normal and emergency conditions will be prepared prior to preliminary operation of the plant. Safe procedures for removing equipment for service maintenance work will be established. These will include the steps necessary to insure safety to the personnel working on contaminated equipment or in an environment where higher than normal levels of radioactivity may be encountered.

All plant personnel will wear film badges while they are on the plant site. In addition, all personnel except those few whose duties would not take them near the containment vessel or other possibly contaminated area will be issued pocket dosimeters. Film badges will be read daily. Exposure records will be maintained by the plant Health Physicist for all plant employees as well as for others who may work at the plant on temporary assignments.

Area monitors will be located within the containment vessel and in other critical areas to continuously monitor the background activity at those locations. Any excessive activity will be indicated by an alarm in the control room at which time a prepared plan of action will be initiated. Periodic surveys will also be made to determine the activity levels throughout the plant. Records will be kept of the survey results.

While the plant design will be such that normal personnel exposure will be considerably less than the maximum tolerances, these limits may be reached during maintenance operations. Should an employee receive the maximum permissible dose, he will be assigned to other duties removed from any radiation activity for the required period of time.

The Company Medical Director will be kept informed of the radiation dose received by each employee and will be notified immediately should anyone receive greater than the permissible dose.

VI. RADIOACTIVE EFFLUENTS

A. Objectives

This plant is being designed so that there will be no radioactive effluents discharged to the environment that will constitute a public hazard. All applicable regulations will be complied with.

B. Gaseous Effluents Under Normal Operating Conditions

Possible sources of radioactive gases under normal operating conditions, including maintenance, are:

1. Leakage from the primary coolant system to the recirculating containment atmosphere and then to the stack with the small continual filtered bleed of the containment atmosphere.

2. Leakage from the helium purification system to the recirculating containment atmosphere and then to the stack with the small filtered bleed.

3. Neutron activation of the containment atmosphere.

4. Purging and flushing gases from maintenance and refueling operations.

A small amount of activity will leak from the radioactive systems, mix with the recirculating atmosphere, and eventually be carried up the stack with the bleed required to keep the containment at a negative pressure. The amount of activity discharged depends on the leakage experienced from the various systems as well as the activity present in them.

While the reactor is designed to limit the fission product activity in the primary system at the beginning of life to 109 curies, the design of the plant is based on the assumption that the primary system may contain as much as 4225 curies for limited periods. (See Appendix B.I). In addition to this fission product activity it is estimated that the system will contain only 1 curie of tritium from the He^3 (n, p) H^3 reaction and 0.1 curie of A^{41} from neutron activation. It is conservatively estimated that the average coolant activity for an annual period will be less than 1800 curies. The system activities will be measured during plant operations.

In Part B, Volume II, Section II, it is estimated that the annual average atmospheric dilution from the top of the stack to the site boundary will be 5×10^{-5} sec/m^3. Based on the maximum annual average of 1800 curies in the primary loop, the estimate of the total daily containment atmosphere purge, and 80% removal by the stack filters of the gross activity in the containment purge for all activity other than halogens and rare gases, the fractional primary loop leakage could be as high as 1.6×10^{-3}/day without exceeding the off-site tolerance of 1×10^{-10} μc/cc for unidentified isotopes at the site boundary. The design objective is for the primary system fractional leak rate to be 10^{-4}/day or less.

Special precautions are used to reduce the leakage from the helium purification system. Since the gaseous specific activity varies widely in this system, the high activity at the inlet of the system is doubly contained. The design objective is to obtain a leakage equal to or less than 500 μc/hr from this system during reactor operation before decay or filtration in the containment atmosphere. The stack discharge from this source after decay and filtration is estimated to be less than 95 μc/hr during plant operation.

A^{41} will be formed from neutron activation in the reduced oxygen atmosphere around the reactor vessel. Leakage from the reactor cavity to the containment atmosphere will be restricted to reduce thermal convection heat losses. Assuming a 100% per day interchange of gas between this cavity and the containment atmosphere and decay in the containment atmosphere before discharge to the stack, the A^{41} emission is estimated to be 0.6% of the allowable discharge for this isotope. It is estimated that the C^{14} production from the nitrogen in the reactor cavity will be 0.006 curie/day of plant operation.

Kr^{85} is removed from the helium coolant by an adsorber at liquid-nitrogen temperature in the purification system and will be shipped off-site for disposal.

The total gaseous radioactive release from the fuel handling equipment purging and flushing to change one core is estimated to be 0.16 curie.

The gaseous radioactive release from maintenance operations is estimated to be about 2.5 curies per year based on four purges a year of a volume equivalent to the gas volume of the steam generator with purified helium. If not contaminated with air, this purge helium would normally be pumped back to the primary loop rather than releasing it and its gaseous activity through the stack.

Calculations show that the total gaseous radioactive effluents from the plant will be less than the maximum permissible concentration at the site boundary, and will be well below the permissible concentration for plant personnel. Moreover, it is believed that in the aggregate, the design assumptions and objectives provide a considerable margin of safety in the estimates of activity to be discharged with the gaseous effluents.

Table 38 summarizes the stack effluents as described above.

TABLE 38

ESTIMATED SITE BOUNDARY CONCENTRATIONS FOR GASEOUS EFFLUENTS

Source	Annual Average Concentration at Site Boundary,[a] $\mu c/cc$	Maximum Permissible Concentration, $\mu c/cc$	Fraction of MPC
Primary Loop Leakage[b]	6.2×10^{-12}	10^{-10}	.062
Fission Product Trapping System Leakage	1.3×10^{-12}	10^{-10}	.013
A^{41}	2.3×10^{-10}	4×10^{-8}	.006
C^{14}	3.2×10^{-13}	10^{-10}[c]	.003
Refueling	2.5×10^{-13}	10^{-10}	.003
Maintenance	4×10^{-12}	10^{-10}	.040
			.127

(a) Based on annual average dilution from top of stack to site boundary of 5×10^{-5} sec/m^3.

(b) Based on 1800 curies in primary loop, 10^{-4}/day fractional leakage, 80% removal in stack filters of all fission products other than halogens and noble gases.

(c) Since this isotope will not be identified, unidentified MPC is used. 10 CFR Part 20 allows $1 \times 10^{-7} \mu c/cc$ for C^{14} on an identified basis.

The containment ventilation and gaseous waste disposal system, shown in Figure 128, includes equipment for carefully filtering, monitoring and controlling all activity which might become mixed with the containment atmosphere and exhausted up the stack.

The stack discharge is monitored continuously for gaseous activity. A continuous flow sample of stack gas is collected isokinetically at a level approximately one-third of the stack height by a gas sample system. The sample is passed through a filter which can be removed and checked periodically for particulate contamination. After filtering, the sample is monitored continuously for gamma activity.

The gamma activity of the sample is monitored with a dual channel gamma spectrometer that is employed so that one channel monitors the gross gamma activity and the other channel monitors a single energy or band of energies. Both channels are recorded continuously. The gross activity level is used to show significant changes in over-all stack discharge and the differential monitor is available to aid in determining discharge rates of specific isotopes.

The stack monitor will sound alarms in the control room and will also serve as a signal for the automatic closure of the containment ventilation valves. In critical areas of the containment and other portions of the plant, area monitors will be available to check local activity levels and will be equipped with suitable alarms.

A plant site environmental monitoring program, described in Part B, Volume II, has been instituted in advance of plant operation to obtain data on background radiation levels. The program will be continued when the plant goes into operation.

C. Liquid Effluents

1. General

Because Conowingo Pond is a valuable water resource many special features have been incorporated in the plant design to guard against the possibility of accidental release of any radioactive liquids from the plant.

The design features of this reactor system assure that very little radioactive liquids are generated in the course of normal operations. Radioactive liquids for routine disposal come from laundering the clothes worn by workmen in the plant, water from the chemical impurities removal system, and drips which will collect in the

various sumps and drains in the containment vessel or in related cooling systems. Liquids from the fission product trapping system will be specially handled as required. From time to time it may be necessary to drain the spent-fuel pit, the shield cooling loop or the cooling water from the fission product trap system, all of which normally operate as closed loops, and process these liquids through the liquid waste system for disposal. The liquid waste system is shown in Figure 129.

Provisions are made for collecting, processing, holding up, monitoring, and controlled discharging of potentially contaminated liquid wastes. All tanks in the liquid waste disposal system are contained in a concrete pit which will collect any leakage from the tanks. An automatic sump pump is provided at the bottom of the pit to pump any leakage back into the receiver tank in the radwaste system.

The liquid waste system consists of two containment liquid waste receiving tanks and filters, a mixed-bed demineralizer, two tanks for monitoring treated waste, and a laundry waste holdup tank. The activity of the water in the holdup tank will be monitored and the water will be recirculated through the demineralizer to the treated waste monitoring tank. If necessary, the water can be reprocessed in the demineralizer for further cleanup. When the activity of the water has been sufficiently reduced the water will be returned to the plant for reuse or will be pumped under a controlled discharge to the circulating water discharge line where it will mix with the 50,000 gallons per minute of condenser cooling water. A continuous sampling system will be placed in the circulating water discharge to monitor the activity level.

Radioactive waste solutions would result from decontamination of the refueling equipment. The decontamination system, shown in Figure 130 includes decontamination supply and drain piping, chemical mixing tanks, chemical and rinse drain tanks, circulating pumps, filters, and other miscellaneous items of equipment. The chemical and rinse drain tanks are sized to hold the drainage volume from the decontamination and rinse solutions and allow holdup so activities and spent chemicals may settle out as sludge which can be removed by filtration. Rinse waters will generally be treated in the radioactive waste demineralizer. Spent chemical solutions and sludges will be shipped off-site for disposal.

2. Laundry Wastes

The liquid laundry wastes would be routed to the laundry holdup and monitoring tank where the radioactivity in the liquid would be measured. If the activity is low enough to allow controlled release,

it would be pumped through the radioactive waste controlled discharge pump to the circulating water discharge line. It is very improbable, considering the source of this radioactivity, that the laundry waste will contain enough activity to prevent controlled release; however, if such were the case, it would be shipped off-site for disposal. The laundry holdup and monitoring tank will be located so that leakage from the tank will be collected in a sump and routed to the radioactive waste receiver tank. It is conservatively assumed that one load of clothes is washed per hour producing 50 gallons of water containing 10^{-4} microcurie per milliliter for a total of 19 microcuries. Even if the entire laundry waste with the activity estimated above were to be accidentally released to the circulating water over a ten-minute period, the activity at the point of discharge to Conowingo Pond would be within the permissible concentration.

3. Shield Cooling Water

The biological shields are cooled by a closed water loop which is described in Section III. F. Within the loop are approximately 1000 gallons of water in which the activity level might be as high as 10^{-4} microcurie per milliliter. Using the estimated quantities and activity in this system, the total radioactive inventory will be less than 400 microcuries. This entire system could be dumped into the circulating water over a three and one-half hour period and yet be within permissible limits at the discharge of the circulating water to Conowingo Pond.

4. Spent-Fuel-Pit Water

The spent-fuel pit is located outside the containment to allow access for fuel shipping during plant operation. The spent-fuel pit is described in Section II. H. All spent fuel elements will be canned in metal cans upon removal from the core. These cans are tested for leakage before being placed in the spent-fuel pit; thus the normal activity of the spent fuel water should remain at a very low level. As an extra precaution, the spent-fuel-pit cooling water can be bypassed through the radwaste demineralizer for cleanup. Accidents considering leakage from a fuel element can in the pit are described in Section VII. D.

5. Fission Product Trap System Cooling Water

This system is a closed coolant system completely housed in the containment vessel. If the coolant accidentally becomes contaminated it will be decontaminated as necessary by passing it

through the demineralizer in the liquid waste system. Any leakage of the closed loop will be collected in the containment sump.

6. Chemical Impurities Removal System Effluent

The chemical impurity removal section of the helium purification system removes hydrogen and carbon monoxide from the primary helium coolant by oxidation and subsequent adsorption of the resulting water and carbon dioxide in a molecular sieve bed. Regeneration of the beds will occur on a relatively short interval by desorption into a heated purified helium sweep gas at normal operating pressure. The water removed from the bed is then condensed from the sweep gas and drained to the liquid waste system for disposal; the CO_2 present is removed by means of a caustic scrubber unit. Most of the gaseous activity is returned to the helium system with the sweep gas and the remaining small fraction of the gaseous activity remains in the caustic liquid. Regeneration of the beds for CO_2 and water will occur approximately once a week. The caustic will be disposed of off-site approximately once every 6 months and will consist of about 75 gallons of caustic solution containing an activity of 6.5×10^{-2} curies of Kr^{85}.

7. Other Radioactive Liquid Wastes

Small amounts of liquid radioactive wastes may be generated in normal tool decontamination, from personnel showers, from the chemical laboratory, from the sumps and drains in the containment or in the liquid waste system, and from the fission product trap condensers. These wastes will normally be collected, monitored, and processed through the liquid waste system or if necessary shipped off-site for disposal.

D. Solid Wastes

The solid radioactive wastes consist of material from maintenance operations and laboratories, filters from the liquid systems, dust collected from the primary loop system, ventilation filters, and spent resins from demineralizers. The spent fuel elements are also solid wastes. There will be no disposal of these wastes on site; all radioactive solid wastes will be placed in shielded casks and shipped off-site.

Low level radioactive maintenance and operating waste materials such as paper, oil, clothes, small tools, or laboratory equipment are expected. Such materials will require a minimum of shielding and will be packaged for shipment off-site.

The filters from the ventilation systems and the liquid systems should require very little shielding and will be packaged and shipped off-site.

The resins from the demineralizers and the filters in the helium loop will be shipped in casks for off-site disposal.

The spent fuel, after a suitable decay and cooling period in the spent fuel pit, will be loaded under water into shipping casks which will conform to applicable regulations.

The main coolant bypass dust collectors will be located in side streams of the main helium lines and will remove graphite dust and other particulate matter, some of which will be radioactive. The dust will be collected in shielded disposal barrels which are seal welded to outlet valves at the bottom of the dust collectors during operation. When radioactivity in the barrels reaches a maximum for safe handling, the barrels are removed and shipped off-site for disposal.

All shipments of radioactive material for off-site disposal will be by licensed carriers and in conformity with applicable regulations.

VII. PLANT SAFETY ANALYSIS

A. Introduction and Summary

The preceding sections of this report describe the general plant design including features of the plant to prevent accidents. This design represents over two years of intensive research, engineering, analysis, and design effort for which plant safety is one of the foremost objectives. In the course of this design and analysis a number of accidents have been evaluated to determine the adequacy of the plant. It is the purpose of this section to summarize a broad spectrum of accidents, most of which are extremely difficult to visualize as having even a remote possibility of occurrence. The analyses of these accidents show that the many safety features incorporated in the plant design provide adequate protection to the health and safety of the public and are indicative of the upper limit of the potential hazard of this plant.

Section VII. B discusses the accidents involving the reactor (reactivity accidents, loss of integrity of fission product barriers and loss of forced circulation cooling), accidents involving the fission product trapping system are discussed in Section VII C, and Section VII D discusses fuel handling accidents. Plant behavior under abnormal conditions arising external to the plant is discussed in Section VII E. Environmental dosages from all accidents are contained in Section VII F.

The safety analysis shows that no credible reactivity accident results in a significant release of radioactive effluents from the plant.

The emergency cooling system assures that complete loss of normal cooling capability results in no significant release of radioactive effluents.

Only accidents which involve rupture of the primary loop, of the fission product trapping system, or of a spent fuel canister are capable of releasing quantities of radioactivity which warrant an environmental evaluation. This evaluation indicates that the safety features provided in the plant limit the resultant releases to the environment so that the health and safety of the public will not be endangered. For example, the accident involving the maximum off-site dosage results in a whole body gamma dosage of only 0.03 rem at the site boundary for the first two hours with an inversion. This accident requires coincident rupture of the primary system and loss of all normal coolant, with failure of the fission product purge line check valve to close, and loss of purge flow.

B. Incidents Involving the Reactor

1. Reactivity Accidents

The nuclear design of the reactor has been discussed in Section II where special attention was given to the physics evaluation of control effectiveness, prompt and overall temperature coefficients, and reactor kinetics. In this section possible sources of reactivity accidents are examined emphasizing the safeguards to prevent these accidents. The discussion also includes cases where postulated severe accidents are followed by failures in the safety system. Reactivity accidents might conceivably be initiated by any of the following:

(1) Excessive removal of control poison.
(2) Loss of fission product poisons.
(3) Rearrangement of core components.
(4) Introduction of steam into the core.
(5) Sudden decrease in reactor temperature.

The possibility and potential severity of each of these accidents will first be examined and on the basis of this examination, the potentially severe accidents will be presented in more detail.

a. Excessive Removal of Control Poison

Some malfunction of a control rod drive or a possible operational error might result in the unintentional removal of a control rod, thereby increasing the reactivity and consequently the power level beyond specified limits. In particular, three types of control rod accidents might be postulated, i.e.:

(1) An excessive control rod removal during operation,
(2) A rod fallout accident, and
(3) An excessive control rod removal during start up.

These accidents are discussed in detail in Section VII.B.1.f.

b. Loss of Fission Product Poisons

At the end of the reactor life, the total fission product inventory including Xe^{135} will be worth approximately 0.17 Δk, assuming no poisons have escaped from the fuel compacts. The reactivity contributions from the more volatile poisons are as shown

in Table 39.

TABLE 39

REACTIVITY LOSSES FROM VOLATILE POISONS

Isotopes with half lives greater than core life	$t_{1/2}$	Δk
Xe-131	stable	.0109
Cs-133	stable	.0105
Cs-135	3×10^6 y.	.0020
Sm-149	stable	.0082
Sm-151	73 y	.0075
Sm-152	stable	.0052
Total		.0443
Isotopes with short half lives relative to core life		
Xe-135	9 hr.	.0320

In addition to the above volatile materials, it is probable that some small fraction of the non-saturating fission product aggregate, having a total poison value of $.0331\Delta k$, may be volatile. Hence, it is possible that a total of about $.09\Delta k$ including Xe^{135} could be held up in reactivity by volatile poisons at the end of the reactor life.

On the basis of experiments discussed in Section II.J.2, it is concluded that the release of volatile fission product poisons, in intervals that are short relative to control rod and emergency rod shutdown times, is not possible. Thus, this type of reactivity insertion cannot lead to an accident condition.

c. Rearrangement of Core Components

The effects of rearrangement of core components on reactivity have been examined. The following geometry changes have been investigated:

(1) A large accumulation of graphite in the core coolant channels.

(2) A large shrinkage in the core volume.

(3) A levitation of the fuel elements, thereby moving the core away from the control rods.

Reactivity calculations show that 1300 pounds of graphite uniformly distributed in the core voids would be required to increase the reactivity by 0.01Δk. There is no plausible mechanism which could introduce such a large additional amount of graphite in the core.

Calculations show that a volume shrinkage of about 2 percent would be required to increase the reactivity by .01Δk. Even if all the standoff tubes were sheared off at the base of the fuel elements and the .035 inch spacers on the fuel rods were somehow crushed so that all fuel elements come in contact along their entire length, the total volume shrinkage would only be about 2 percent. Hence, it is concluded that a sudden large increase in reactivity resulting from a core shrinkage is not credible.

A sudden large pressure drop across the core could cause lifting forces to act on the fuel elements. This condition is described in Section II.B. The levitation might result from a rupture in the primary coolant system which would allow the primary coolant pressure to decrease at a more rapid rate at the core exit than at the core entrance. A careful analysis of this postulated condition shows that the maximum levitation which could occur would be less than one inch. A core displacement of one inch relative to the control rods would be equivalent to a one inch withdrawal of the control rods. For a typical operating condition where 24 control rods are completely inserted and 3 are inserted halfway, a one inch levitation of the entire core would result in a reactivity increase not exceeding .001Δk.

Therefore it is concluded that there is no credible mechanism whereby the reactor core could be accidentally rearranged in a way to constitute a serious reactivity hazard.

d. Introduction of Steam Into the Core

Calculations show that uniformly distributed water or steam in the core causes a reactivity increase of about $2.4 \times 10^{-4}\Delta k$ per pound of water introduced.

For the case where one steam generator tube breaks completely, and the isolation valves do not close, the maximum amount of steam which could be introduced assuming a pressure of 450 psi and a temperature of 1000 F, is 0.53 lb/ft^3 which would allow about 46 lb of water to be distributed in the core, thereby increasing the reactivity by about .01Δk. Hence, the introduction of steam into the primary loop does not constitute a serious reactivity hazard, even for the case where the loop is not isolated.

e. Sudden Decrease in Reactor Temperature

Because of the large temperature coefficient and high operating temperature of the reactor, a sudden decrease in temperature could result in a rather large reactivity increase. However, due to the large heat capacity of the reactor core materials and the relatively small heat capacity of the helium coolant, quick changes in the core temperature are not possible. Therefore, the cold coolant accident in this type of reactor does not constitute a reactivity hazard.

f. Accidents Involving Removal of Control Poison

On the basis of the preceding, it can be seen that the only significant reactivity accidents which warrant discussion are those involving malfunctions of the control rods; consequently the circumstances and consequences of these accidents listed in (a) above will be discussed in detail.

(1) Control Rod Withdrawal During Operation

Physics calculations for various possible control rod configurations indicate that the power distribution in the reactor core is sensitive to the control rod patterns. To avoid severe power tilts in the axial direction, it is advantageous to limit the number of control rods which are partially inserted to as small a number as possible. Hence, most of the rods will be fully withdrawn during full power operation, a few may be fully inserted and locked in position, while a maximum of three rods will be used for shim and automatic control. In order to minimize radial power tilts, it is planned to program the control rods during power operation so that symmetry will be maintained in 120° intervals. Accordingly, the three partially removed control rods will normally be at the same radius and separated by 120°. Although all three of the partially removed control rods will be used for power regulation, the control circuitry will allow the manual withdrawal of only one control rod at any time for rods in the inner two rings. In addition, one of the three available rods will normally be driven by an automatic control rod drive.

Malfunction in the control system could erroneously cause the automatically operated control rod to be driven at maximum speed to the completely withdrawn position. If the operator, through some error, drives a manually operated control rod at maximum speed to the completely withdrawn position, the automatic control

rod would normally compensate. Therefore, the only plausible rod withdrawal accident would be one which involved the malfunction of a single control rod.

Only the results of the rod withdrawal accident occuring at the end of reactor life will be described, since the accident would be more severe for this condition because:

(a) the delayed neutron fraction is smaller, therefore allowing shorter reactor periods for the same Δk accident;

(b) the control rods are worth more, and

(c) the negative temperature coefficient is smaller in magnitude.

It should be noted that at the end of the reactor life, practically no excess reactivity would normally be available after xenon has reached equilibrium; and, hence the rod withdrawal accident would be impossible for this condition. Therefore, rod withdrawal accidents will be considered as follows:

Case A. The reactor is at the end of the life and is operating at full power with no xenon and with the last three control rods fully inserted, whereupon, either the automatic control rod or a manually operated control rod is moved to its fully withdrawn position at maximum speed.

Case B. The reactor is not quite at the end of life and enough excess reactivity is available so that three control rods are normally in and equilibrium xenon is present. The automatic control rod or a manually operated control rod is moved to the fully withdrawn position at maximum speed. Although the temperature coefficient would be somewhat more strongly negative before the end of life, the end-of-life value has been used for the latter case, making the calculated temperature excursions pessimistically large.

The loading of the reactor and the control rod design are such that the effectiveness of the three most valuable rods will be about .030Δk for all three as a group. The effectiveness of a single rod withdrawn from group will be .010Δk.

The results of the postulated rod withdrawal accidents are shown in Figure. 131.

The data are based on calculations using the digital computer code, BLOOST, which was described in Section II. B. 2. The important results, summarized in Table 10, are as follows:

Case A If the reactor scrams at 140 percent full power, the hot spot fuel temperature would rise only from 1500 C to 1518 C and the helium outlet temperature would only increase less than 9 F. If the reactor failed to scram on the power level trip, a helium over-temperature scram would result in a shutdown which would limit the hot-spot fuel temperature to about 1665 C and the helium outlet temperature to 1472 F. Even for the implausible case where no scram occurs, the maximum fuel element temperature would be 1919 C and the maximum helium outlet temperature would be 1725 F, reached after 2.5 minutes. If corrective action is taken within a few minutes, there would be no severe damage to the plant.

Case B. Since the temperature coefficient is not as strongly negative for the equilibrium xenon case, the previous case was re-analyzed to examine the effect of the xenon on the accident excursion. It can be seen from the table that the maximum fuel element temperature is increased by less than 300 C and the maximum outlet helium by only about 63 F over that shown for Case A.

TABLE 40

SUMMARY OF ROD WITHDRAWAL ACCIDENTS

Assumed Action	Maximum Power, MW	Time, Sec.	Maximum Fuel Compact Temp., C			Maximum Helium Outlet Temp.	
			Average Element	Hottest Element	Time, Sec.	F	Time, Sec.
Case A:							
(a) Normal Scram	159.0	8.6	1095	1518	10.0		
(b) Helium Over-temp. Scram	295.0	28.0	1193	1665	30.0	1472	48.0
(c) Emergency Scram in 30 sec.	307.6	31.3	1249	1750	39.8	1515	57.1
(d) No Scram	307.9	32.0	1360	1919	120.0	1725	140.0
Case B:							
No Scram	420.0	28.0	1550	2204	110.0	1780	120.0

Hence, because of the large negative temperature coefficient, the large heat capacity of the reactor and the high temperature behavior of the fuel elements, plausible reactivity accidents resulting from excessive control rod withdrawals can be tolerated without serious damage to the fuel elements or the plant.

(2) Control Rod Removal During Startup

Startup accidents for the HTGR are insignificant because of the large negative temperature coefficient, particularly at low temperature, the large heat capacity of the core and the limited rate of reactivity insertion which is possible.

Prior to reactor startup, the emergency shutdown control rods are withdrawn, and the helium circulators are operating at partial flow. In addition to the normal power level scram which is set at 140% full power, the log level instruments will be capable of initiating a scram at a low power on the basis of an excessive rate of change in power. This rate scram will be effective in the power range of 5000 to 6000 kw thermal, approximately.

Control rods in the last ring followed by the next ring will be removed in groups of three at a time. The groups of three rods each will have a control effectiveness of approximately 0.02Δk per group and will increase the reactivity at a rate less than about $2.2 \times 10^{-4}\Delta k/sec$ for the maximum withdrawal speed. The reactor will normally achieve criticality in the cold, unpoisoned condition before the 24 control rods in the outside two rings have been completely removed. The startup instrumentation including the log level and rate-of-change instruments will limit the rate at which the power is increased. The reactor will be manually controlled to maintain some specified rate of power increase until the reactor power reaches some predetermined value. The reactor temperature will be allowed to increase at some controlled rate until system temperatures are stabilized at a predetermined level. The reactor will then be brought to full power by appropriate adjustment of the control rods and the helium flow.

It has been postulated for the startup accident that the reactor has reached criticality at 200 C before all of the 24 outer control rods have been withdrawn, and a group of three rods is then withdrawn at maximum speed. Hence, the reactivity increases at a rate of $2.2 \times 10^{-4}\Delta k/sec$, until the accident is terminated, either by a scram or by a reduction in reactivity as the result of a temperature rise. The results of the accident for various termination conditions are summarized in Table 41. Even in the unrealistic case of no scram at all after complete removal of the three rods, the hot spot temperature rise would be less than 250 C (due to the negative temperature coefficient) which would not result in any damage to the fuel compact.

TABLE 41

SUMMARY OF STARTUP ACCIDENTS

Accident	Δk	Maximum Power, MW	Time, Secs.	Max. Fuel Temp. Rise, C	Time, Secs.
(a) Rate of Change Scram	.02	<15 Kw.	11.5	no rise	
(b) Power level Scram	.02	251	13.0	29	13.0
(c) No Scram	.02	532	13.4	237	78.0

(3) Rod Fallout Accident

The control rod drives are located at the bottom of the pressure vessel, the reactivity is increased by withdrawing the control rods downward, and the control rods are scrammed upward into the reactor core. An electrical circuit will be used on each control rod to indicate the separation of the poison section from the control rod drive. In order to guard against the possibility that a control rod might accidentally coast down from its normally in position, all rods fully in the core will be mechanically locked in until it is desired to remove them as part of the control operation. Even though a rod fallout accident is considered to be very unlikely because of these precautions, the consequences of a rod fall accident have, nevertheless, been examined. It has been assumed for this study that the last three control rods have just been unlocked, so that they are still practically fully in, and one of these rods, for some unidentifiable reason, falls freely to its most reactive position. Conditions similar to those discussed in Case B in Section VII.B.1.f.(1), have been used for similar reasons and a total reactivity effectiveness of .010Δk has been used for a single control rod.

The temperature history for the hot spot, the average fuel element and the outlet helium during the excursion are shown in Figure 132. The essential results for this postulated accident are summarized in Table 42.

TABLE 42

SUMMARY OF ROD FALL ACCIDENT

Action	Δk	Maximum Fuel Compact Temp., C			Maximum Helium Outlet Temp.	
		Average Element	Hottest Element	Time Secs	F	Time, Secs
(a) Normal scram	.01	1085	1504	.589	1384	4.68
(b) Emergency scram in 30 sec	.01	1554	2207	2.9	1750	41.0
(c) No scram	.01	1554	2207	2.9	1781	96.6

For the case where the accident is followed by a normal scram which is initiated when the power reaches 140 percent of the normal operating power, the peak fuel element temperature increases only 4 C, which is insignificant in terms of fuel element damage. Likewise, the helium outlet temperature is not increased significantly.

In order to examine the effectiveness of the negative temperature coefficient in limiting the accident, a case has been studied where no scram occurs following the rod fall accident. Item c in the Table above shows the results. This no-scram condition predicates a combination of failures beyond credibility.

If the emergency shutdown rods are activated within 30 seconds after the accident, the hot spot reaches a maximum of 2207 C and remains above 1800 C for a time interval of 71 seconds. No gross release of fission products would occur in this short temperature transient and the fuel elements would not suffer any damage. The maximum thermal stress resulting from the described reactivity insertion occurs at the outer surface of the sleeve after about two seconds and amounts to 1900 psi. This stress is still below the minimum modulus of rupture of the sleeve material, therefore, the sleeve of even the hottest fuel element would probably be able to tolerate the excursion, and significant damage to other elements could not result. Under the conditions postulated for this accident, the helium outlet temperature rises from 750 C to 954 C (1750 F) within 40 seconds and remains above 900 C for a period of about 55 seconds. Even though the maximum stress in the superheater tubes would exceed the yield strength at maximum helium temperature, there would be no serious damage because the coolant outlet temperature remains at these high levels only for a limited duration.

2. Accidents Involving Fission Product Barriers

a. Fuel Element Malfunctions

Fuel element malfunctions have been discussed in Section II.A.4., where it was shown that no known malfunction of the fuel elements would cause a sudden large release of activity to the main coolant stream.

b. Effect of Steam Leaks on Fission Product Barriers

The amount of water leaking to the helium system from small tube-to-tube-sheet leaks is controlled by the baffle and helium purge flow from this area described in Section II.D.2.b(1)(d). Leakage outside of this vented area or leakage penetrating the vented area would cause an increase in the water content of the coolant as discussed in Section II.A.4.

In order to examine the effectiveness of the negative temperature coefficient in limiting the accident, a case has been studied where no scram occurs following the rod fall accident. Item c in the Table above shows the results. This no-scram condition predicates a combination of failures beyond credibility.

If the emergency shutdown rods are activated within 30 seconds after the accident, the hot spot reaches a maximum of 2207 C and remains above 1800 C for a time interval of 71 seconds. No gross release of fission products would occur in this short temperature transient and the fuel elements would not suffer any damage. The maximum thermal stress resulting from the described reactivity insertion occurs at the outer surface of the sleeve after about two seconds and amounts to 1900 psi. This stress is still below the minimum modulus of rupture of the sleeve material, therefore, the sleeve of even the hottest fuel element would probably be able to tolerate the excursion, and significant damage to other elements could not result. Under the conditions postulated for this accident, the helium outlet temperature rises from 750 C to 954 C (1750 F) within 40 seconds and remains above 900 C for a period of about 55 seconds. Even though the maximum stress in the superheater tubes would exceed the yield strength at maximum helium temperature, there would be no serious damage because the coolant outlet temperature remains at these high levels only for a limited duration.

2. Accidents Involving Fission Product Barriers

a. Fuel Element Malfunctions

Fuel element malfunctions have been discussed in Section II.A.4., where it was shown that no known malfunction of the fuel elements would cause a sudden large release of activity to the main coolant stream.

b. Effect of Steam Leaks on Fission Product Barriers

The amount of water leaking to the helium system from small tube-to-tube-sheet leaks is controlled by the baffle and helium purge flow from this area described in Section II.D.2.b(1)(d). Leakage outside of this vented area or leakage penetrating the vented area would cause an increase in the water content of the coolant as discussed in Section II.A.4.

Large steam leaks are discussed in Appendix D. This analysis shows that complete rupture of a steam generator tube would not result in venting of reaction products or the coolant activity through the relief valves to the containment.

c. Steam Leaks with simultaneous Rupture of Helium Coolant System

The containment will be filled with a reduced oxygen atmosphere in order 1) to preclude burning of the graphite fuel elements, and 2) to prevent oxidation of the H_2 and CO from the reaction of water with the graphite fuel elements.

The failed steam generator will normally be isolated by the cold and hot valves in the primary loop. In this case only a few pounds of steam and reaction products would reach the secondary containment. However, if the failed steam generator cannot be isolated a maximum of 2200 pounds of steam or resulting reaction products would reach the secondary containment. The containment vessel is designed to accommodate this pressure release as shown in Section IV. The fission product release for this accident would be essentially the same as that given in the next section for the primary coolant system rupture.

d. Primary Coolant System Ruptures

Should a small leak develop in the main coolant system there would be a gradual depressurization as the helium flowed to the secondary containment. Radiation detectors located in various compartments would aid in locating the leak. If the leak were in the steam generator, circulator, or adjacent piping, the loop would be isolated by automatic circuitry in order to minimize the release of helium and its associated gaseous activity. Small leakage from parts of the system which cannot be isolated can be minimized by dumping the helium to the dump tank and reducing the helium pressure in the primary loop. Further reductions in pressure would be achieved by pumping the helium into the helium dump tank.

Depending on the leak size and the degree of isolation possible, some fraction of the activity contained in the primary loop would be released to the secondary containment.

Reduction of helium pressure in the primary system would also reduce the pressure of the gases in the helium purification system. Since most of the traps in the purification system are cooled by the gas flow, the coolant of the traps would be reduced. This would result in a gradual increase in the primary loop activity to about 0.3 Megacurie (entirely Kr and Xe see Section VII. C. 2. b). The fraction of this activity which would reach the secondary containment depends on the size of the leak.

Larger leaks could cause a flow reversal in the fuel element purge flow and an additional release of gaseous activity from the fuel elements, internal traps, or even the external fission product traps. A check valve in the purge line just before the first external trap is designed to prevent backflow from the external traps. The activity release from this source has been estimated for two cases as given in Table 43.

TABLE 43

RADIOACTIVITY RELEASE DUE TO BACKFLOW

Purge line check valve operating.	0.54 Megacurie
Purge line check valve not operating.	2.0 Megacuries

The isotopic breakdown of this release is given in Appendix B. III. Dosages for these sources are given in Section VII. F. Section VII. F shows that the largest release considered in this section combined with an inversion produces a whole body gamma dosage less than 0.01 rem and a thyroid dose less than 0.4 rem during the first 24 hours at the site boundary.

If the primary system ruptured, the pressure would equilibrate with the containment to a pressure of about 4 psig. At this pressure, one circulator is capable of supplying approximately 3 percent of rated flow through the core. Figure 133 illustrates the temperature transients even if there is no delay in reaching equilibrium. The peak helium temperatures reach 1780 F. The piping and steam generators are designed to withstand this transient condition and the temperature attained in the core does not produce damage to the fuel elements.

3. Loss of Both Main Coolant Loops Following Rupture

a. General

Simultaneous unavailability of both primary coolant loops would make it necessary to utilize the emergency cooling system. This could occur if a rupture of a coolant loop makes one loop inoperative and if the circulator in the second loop subsequently fails during the period that the radioactivity released to the containment precludes access for an extended period of time.

Figure C-3 indicates the performance of the emergency cooling system where core center temperature is plotted as a function of time following the start of emergency cooling. For a detailed discussion of transient reactor temperatures for this case see Appendix C.

b. Release from Primary System

Calculations have been made of the timewise release of fission products from the reactor to the plant containment during emergency cooling if the primary loop is ruptured. Fission products were placed in four retention groups, depending on their ability to leave the fuel compacts at high temperatures, as listed in Table 44 The fourth group includes all those fission products which are not expected to escape from the fuel compacts at the higher than normal temperatures during emergency cooling (3600 F maximum). Each group was assigned a temperature dependent release rate conservatively based on uncoated particle fuel compact data. This information, together with temperature-time histories obtained from the emergency cooling analog calculations (Appendix C), permitted computation of the percent release of fission products from the fuel compacts with time.

TABLE 44

FISSION PRODUCTS GROUPED ACCORDING TO HIGH TEMPERATURE RETENTION BY UNCOATED PARTICLE FUEL COMPACTS

GROUP I	(lowest retention by compact at high temperature) Sr, Ba
GROUP II	(next lowest retention by compact at high temperature) Br, Kr, Sb, Te, I, Xe, Cs, Sm*
GROUP III	(slowly released from compact at high temperature) Y, Ru, La, Ce, Pr, Nd, Pm
GROUP IV	(not released from compacts) Zr, Nb, Mo, Tc, Rh, Sn

* The fission products, Se, Rb, and Br are also in Group II. However, they are too short-lived for significant amounts to escape.

For conservatism, no reduction or delay was assumed for the fission products as they permeated through the graphite sleeves surrounding the fuel compacts.

The cooler graphite surfaces of the reflector regions condense certain fission products escaping from the higher temperature fuel during emergency cooling, giving a significant reduction of activity that could escape to the plant containment atmosphere. The escaping elements experiencing a very large reduction due to condensation would be Sm, Y, Ru, Rh, La, Ce, Nd, Pr, and Pm. A lesser reduction would affect Sr and Ba, and no significant condensation in the reflector regions is expected of Cs, Br, I, Te, Sb, Kr, and Xe. Account has been taken of this condensation in calculating the minimum expected fractional release from the reflector.

The minimum expected condensation of fission products on the graphite surfaces of the top reflector was calculated considering three times the maximum calculated natural convection rate, and assuming the entire top reflector was 120 F above the temperature of any location in the top reflector during emergency cooling.

It appears that conditions favoring aerosol formation are not present in the core-reflector region, i.e., no sudden temperature drops, such as might occur after the hot vapors escape to the plant containment atmosphere. Therefore, no aerosol formation is assumed. Also no further condensation, fallout, or plateout is assumed to occur before the fission products reach the plant containment atmosphere.

The release of fission products to the containment during emergency cooling has been calculated by taking into account:

(1) Complete retention of all fission products in Group IV of Table 44.

(2) The slow release from uncoated particle fuel compacts of Group I, II, and III fission products (each group at a different rate).

(3) Radioactive decay during the slow release.

(4) Condensation on the top reflector of essentially all of each fission product in Group III.

(5) Total condensation on the top reflector of Sm from Group II, and no condensation of the remainder of fission products in Group II, and;

(6) Condensation of some of the Ba and Sr on the top reflector.

No additional methods for reduction of fission products entering the secondary containment were considered.

For conservatism the initial fission product inventory in the fuel was assumed to be 100 percent, as shown in Appendix B.I., i.e., no removal of fission products to the external trapping system. A compilation of the resulting escape of fission products to the containment during emergency cooling and with a ruptured main coolant system, appears in Table 45.

The fission products held up in coated fuel particles could be considered available for release during a severe temperature excursion. However, experiments have indicated that the release of stored fission products in coated particles is not rapid until a temperature near the melting temperature of uranium-thorium carbides (2500 C) is reached.

Table 46 shows the inventories of longer lived fission products stored within the fuel compacts at the end of core life for the coated particle and uncoated particle fuel.

It is evident from the table that there is not much difference between the two inventories, however, the rate of release of fission products from the coated particle fuel would be significantly lower.

TABLE 45

RELEASE OF FISSION PRODUCTS FROM THE CORE TO SECONDARY CONTAINMENT DURING EMERGENCY COOLING AND WITH RUPTURED MAIN COOLANT SYSTEM

Isotope	Retention Group	Half Life	24 hr Total		48 hr Total		120 hr Total	
			Fraction Released	Activity,* Megacuries	Fraction Released	Activity,* Megacuries	Fraction Released	Activity,* Megacuries
Sr^{89}	I	50d	.05	.25	.13	.65	.34	1.70
Sr^{90}	I	28y	.05	.02	.13	.04	.34	0.11
Sr^{91}	I	9.7h	.05	.30	.13	.79	.34	2.06
Sr^{92}	I	2.7h	.05	.31	.13	.82	.26	2.14
Ba^{140}	I	12.8d	.04	.27	.09	.60	.26	1.74
Br^{83}	II	2.3h	.42	.24	.56	.31	.70	.39
Kr^{83m}	II	112h	.42	.24	.56	.31	.70	.39
Kr^{85m}	II	4.4h	.42	.57	.56	.76	.70	.94
Kr^{85}	II	10y	.42	.02	.56	.02	.70	.03
Kr^{88}	II	2.8h	.42	1.56	.56	2.08	.70	2.60
Sb^{127}	II	88h	.42	.07	.56	.10	.70	0.12
Sb^{129}	II	4.6h	.42	.35	.56	.47	.70	.58
Te^{127m}	II	105d	.42	.02	.56	.02	.70	.03
Te^{127}	II	9.4h	.42	.07	.56	.10	.70	.12
Te^{129m}	II	33d	.42	.13	.56	.17	.70	.21
Te^{131m}	II	29h	.42	.19	.56	.26	.70	.32
Te^{132}	II	77h	.42	1.92	.56	2.56	.70	3.20
I^{131}	II	8d	.42	1.28	.56	1.71	.70	2.14
I^{132}	II	2.33h	.42	1.92	.56	2.56	.70	3.20
I^{133}	II	21h	.42	2.88	.56	3.84	.70	4.80
Xe^{131m}	II	12d	.42	.01	.56	.01	.70	.01
Xe^{133m}	II	2.3d	.42	.07	.56	.10	.70	.12
Xe^{133}	II	5.7d	.42	2.88	.56	3.84	.70	4.80
I^{135}	II	6.75h	.42	2.70	.56	3.52	.70	4.45
Xe^{135}	II	9.1h	.42	.58	.56	.77	.70	.97
Cs^{137}	II	30y	.42	.21	.56	.27	.70	.34
TOTAL ACTIVITY:				19.06 *		26.68 *		37.51 *

* (Based on time zero activities)

TABLE 46

EFFECT OF FUEL PARTICLE COATINGS ON RETENTION OF SELECTED FISSION PRODUCTS IN FUEL COMPACTS

Nuclide	Half-Life	End of Life Multiplication Change, %	Holdup Fraction in Fuel Compact	
			Uncoated Particles	Coated Particles
Neutron Poisons:				
Tc^{99}	2×10^5y	0.37	1.0	1.0
Cd^{112}	Stable	0.01	1.0	1.0
Rh^{103}	Stable	1.51	1.0	1.0
Xe^{131}	Stable	1.09	.10-.50	.10-.90
Xe^{135}	9.1 h	3.20	.94	.99
Cs^{133}	Stable	1.05	.10-.50	.10-.90
Cs^{135}	2×10^6y	0.20	.10-.50	.10-.90
Nd^{143}	Stable	2.00	1.0	1.0
Nd^{145}	Stable	0.69	1.0	1.0
Pm^{147}	2.6 y	1.71	1.0	1.0
Sm^{149}	Stable	0.82	1.0	1.0
Sm^{151}	90 y	0.75	1.0	1.0
Sm^{152}	Stable	0.52	1.0	1.0
Eu^{153}	Stable	0.09	1.0	1.0
Gd^{155}	Stable	0.02	1.0	1.0
Gd^{157}	Stable	0.01	1.0	1.0
Hazardous for Ingestion:				
Sr^{89}	50d		.73	.90-.98
Sr^{90}	28y		.10-.50	.10-.90
Y^{91}	58d		1.0	1.0
Zr^{95}	65d		1.0	1.0
Nb^{95}	35d		1.0	1.0
Ru^{103}	39.7d		1.0	1.0
Ru^{106}	1.02y		1.0	1.0
Te^{127}	9.4h		.94	.99
Te^{129m}	33d		.74	.90-.98
I^{131}	8d		.83	.93-.99
Cs^{137}	30y		.10-.50	.10-.90
Ba^{140}	12.8d		.81	.92-.99
La^{140}	40.3h		1.0	1.0
Ce^{141}	32.5d		1.0	1.0
Ce^{144}	285d		1.0	1.0
Pr^{143}	13.7d		1.0	1.0
Nd^{147}	11.1d		1.0	1.0
Pm^{147}	2.65y		1.0	1.0

c. Activity in Containment

Figure 134 shows the activity in the containment for the first two days after the accident. The activity in the containment rises to a maximum of about 5.2×10^6 curies at 16 hours and then drops slowly as a result of the continuing release from the reactor, radioactive decay, and removal by the emergency filtration system.

The relatively smaller initial outrush of gaseous activity during the initial blowdown, as previously mentioned in Section VII. B. 2., must be added to the above to obtain the total release during this accident.

d. Off-Site Dosages

Off-site dosages from this radioactive source in the containment are shown in Tables 58 and 59, Section VII. F. Whole body gamma dosages at the site boundary for the first 24 hours during an inversion is less than 0.4 rem; thyroid dosage with these same assumptions is less than 100 rem.

C. Incidents Involving the Fission Product Trapping System

1. General Considerations

Because of the relatively high levels of radioactivity which may be contained within the fission product trapping system, the system has been designed to minimize the probability of any accident which could release a significant quantity of radioactivity from the system. Detailed studies of abnormal and accident conditions, which are described in this section, show that even very serious failures in the fission product trapping system do not release a large fraction of the total radioactivity contained in the system.

All analyses of the fission product trapping system are based on the design fission product inventories and decay heat loads tabulated in Appendix B. II, which in turn are based on experimental release data from uncoated fuel particles, increased by a factor of three for upper limit design considerations. The lower release rates of coated fuel particles are expected to result in an actual inventory approximately a factor of seven less than the data employed for this analysis.

In order to bracket all accidents involving the fission product trapping system, irrespective of credibility, the total release of the entire fission product inventory of the trapping system into the secondary containment has also been evaluated herein to demonstrate that even this would not result in an undue public hazard. Release of the entire design inventory of 11.2×10^6 curies (Section II. C. 6) to the secondary containment, with the design containment leakage rate of 0.2 percent per day and coincident atmospheric inversion conditions, would result in the following integrated doses for a person standing at the site boundary during the first two hours following the accident:

0.1 rem whole-body gamma
16 rem thyroid

2. Loss of Full Cooling Capability

a. Loss of Purge Flow

Loss of purge flow through the fuel elements and fission product trapping system is considered unlikely due to the many design features permitting continuation of the flow which are described in

this and following sections. However, if purge flow should be lost, the reactor would be shut down immediately. Temperatures in the condensibles trap A-301 (see Figure 56) would not change, as this trap is cooled directly, but temperatures in the remaining fission product traps would rise since these traps are normally cooled by the purge gas itself.

Plots of average charcoal temperature are shown as a function of time after loss of flow in Figures 135 and 136 for the first delay bed A-302 and the first refrigerated delay bed A-304, respectively. The curves are based on the assumption that flow is lost during reactor operation and recognize that a large fraction of the gamma energy is adsorbed outside the charcoal; heat transfer between the charcoal and the vessel wall is neglected because of the very low thermal conductivity of charcoal. Temperature rise in the second delay bed A-303 would be less rapid than in the first delay bed A-302, and temperature rises in the last four refrigerated delay beds A-305, A-306, A-307, and A-308 would be less rapid than in the first refrigerated delay bed A-304. Charcoal temperatures at the inlet end of the delay beds will be higher than the average charcoal temperatures. However, high charcoal temperatures do not lead to any safety problems; because the charcoal is contained in an inert atmosphere (helium), no chemical reactions would occur.

Temperature rise of the vessel wall near the inlet to the bed, where gamma heating is greatest, has been calculated assuming no heat lost from the vessel and no heat conduction along the vessel wall. Maximum vessel wall temperatures following loss of purge flow are also plotted in Figures 135 and 136 for the first delay bed A-302 and the first refrigerated delay bed A-304, respectively. When any delay bed wall temperature reaches 300°F, the delay bed emergency water cooling system will be activated to prevent further temperature increase. The time at which emergency cooling would be initiated is shown in Figures 135 and 136. Also shown in Figures 135 and 136 is the wall temperature rise if emergency cooling is not initiated, and the point at which vessel failure would occur.

Failure of a delay bed would at worst lead to release of the contained activity (see Appendix B.II) to the secondary containment, but the release would in any case be less than that considered in Section VII.C.1.

If one or more of the fission product traps should be isolated and bypassed, temperature rises would be equal to or less than those given above for loss of purge flow. When a fission product

trap is isolated and bypassed, a pressure relief system prevents overpressure of the trap by venting to the low-pressure tank.

b. Loss of Purified Helium Compressors

The probability of coincident failure of both purified helium compressors is very low; a failure of either one of the compressors would be repaired so that the plant would not operate for any appreciable period of time with only one compressor operable. In the event of failure or loss of both purified helium compressors, however, reactor shutdown would be initiated and purge flow would be maintained by venting purified helium from a point just upstream of the purified helium compressors to the dump tank until one or both compressors can be repaired. During this period, the helium transfer compressors would be used to return helium from the dump tank to the primary system, thus maintaining the dump tank pressure below system pressure.

If both the purified helium compressors and transfer compressors are not available, purge flow would be continued by venting purified helium to the dump tanks at a rate of 100 lb/hr until the primary system and dump tank pressures had equalized (after approximately 6 hours), at which time the purge flow rate would go to zero. Cooling of the traps after loss of power is discussed in Section VII. C. 2d.

c. Primary System Depressurization

The primary system will be routinely depressurized for certain types of equipment maintenance or for reactor refueling. Depressurization may also occur due to a rupture in the helium system. Under depressurized conditions, the purified helium tank is bypassed and the purified helium compressors return purified purge gas directly to the primary system at approximately normal volume flow rate. The lower mass flow rate of purge gas will impair cooling capability for all fission product traps except the direct-cooled condensibles trap A-301 (Figure 56). Because depressurization is always accompanied by reactor shutdown, the reduced cooling capability will be at least partially offset by decay of fission products in the traps.

In order to evaluate the effects of depressurization, two cases have been considered: (1) routine depressurization in which the pressure is held at approximately 250 psia for 24 hours following shutdown, and then reduced to atmospheric pressure; and (2) an

assumed instantaneous reduction of pressure to about 19 psia, corresponding to a rupture of the primary system. It should be noted that this section deals only with the effects of a primary system rupture on the trapping system; a complete analysis of the effects of a primary system rupture is given in Section VII. B. 3.

In the routine depressurization case, trap temperatures remain roughly constant during the 24-hour period following shutdown. One day after shutdown, the primary system is depressurized to atmospheric pressure. Although some time is required to pump down the primary system, the depressurization has been taken as occurring instantaneously after the one-day waiting period and the traps are assumed to heat up instantaneously for purposes of analysis.

The change in primary coolant activity due to increased penetration of krypton and xenon through the trapping system is relatively small in this case. Approximately 15 curies of Kr^{85m} and 1000 curies of Kr^{85} will be added to the primary system, but these increases will be counterbalanced by reduced escape of fission products from the fuel elements to the primary system, and the total primary coolant activity will remain well below the design level. Negligible quantities of the remaining isotopes will enter the primary system from the trapping system.

The consequences of an accident resulting in instantaneous pressure reduction to about 19 psia have been analyzed in the same manner as the routine depressurization case, except that credit has been taken for the time required for the traps to heat up.

Decay heat generation in the liquid-nitrogen-cooled trap A-309 is so low that its performance will not be appreciably affected by loss of pressure.

Gaseous activities in the primary coolant due to increased penetration of the trapping system are given in Table 48. These activities do not include any release due to backflow through the fuel element, as this subject has been treated in Section VII. B. 3. The whole body gamma dosages from this source in the containment for the first 24 hours at the site boundary during an inversion is about 0.003 rem.

The activities given in Table 48 are average values for a 24-hour period following the depressurization; some fluctuations about these averages will occur due to transient effects in the trapping system and decay of the activity. Because penetration of activity

through the trapping system occurs some time after the loss of pressure, there will be no outflow of helium through a primary system rupture at the time when these activities enter the primary system. None of the fission products listed in Table 48 give rise to long-lived daughter products which would represent a plate-out problem.

Maximum gas temperatures from the delay beds following sudden depressurization are given in Table 47 along with normal operating values for comparison:

TABLE 47

MAXIMUM GAS TEMPERATURES FROM THE DELAY BEDS FOLLOWING SUDDEN DEPRESSURIZATION

	Exit Gas Temperature, F	
Trap	Normal Operation	Following Sudden Depressurization
A-302	108	130
A-303	71	124
A-304	- 48	116
A-305	- 83	102
A-306	-104	89
A-307	-110	169
A-308	-111	152

Vessel wall temperatures will be approximately equal to the exit gas temperatures. It can be seen that emergency cooling will not be required on any of the delay beds. Temperatures following the routine 24-hour depressurization will be lower than those given above.

TABLE 48

PRIMARY COOLANT ACTIVITY DUE TO RELEASE FROM TRAPPING SYSTEM FOLLOWING SUDDEN DEPRESSURIZATION *

Isotope	Activity (curies)
Kr^{83m}	4,200
Kr^{85m}	20,000
Kr^{85}	1,600
Kr^{87}	3,600
Kr^{88}	20,000
Rb^{88}	20,000
Xe^{131m}	1,300
Xe^{133m}	2,700
Xe^{133}	220,000
Xe^{135}	500

*Activity release from the fuel element due to backflow through the purge line is not included (see Appendix B).

The primary system may be routinely depressurized in less than 24 hours, depending on the circumstances requiring the depressurization. In any case, trapping system temperatures and primary system activities will be less than shown for the case of sudden depressurization.

d. Loss of Cooling Water

The emergency cooling water system is described in Section II. C. 6a. This system prevents immediate loss of cooling due to loss of power.

It is conceivable that a very major failure, such as a rupture in the shell which contains the cooling water around one of the traps, could cause complete draining of cooling water from that trap. This accident would not be serious if it occurred during normal operation, since the condensibles trap A-301 is the only trap normally cooled directly by water. Even this trap can be satisfactorily cooled by the purge gas itself. If such an accident occurred during a period when there was no purge flow, however, trap failure could occur due to overheating and a large fraction of the activity contained in the trap could be released to the containment vessel. Activity levels in each trap are shown in Appendix B, indicating the maximum release which could occur. In any case, the release would be less than that considered in Section VII. C. 1.

e. Loss of Refrigeration

The probability of loss of the refrigeration system which cools delay beds A-304, A-305, A-306, A-307, and A-308 (see Figure 56) will be minimized by providing spare refrigeration compressors and by locating them in an area which is accessible during reactor operation; if one compressor fails, it will be repaired while operation continues using the installed spare. In the unlikely event that complete loss of refrigeration does occur, a reactor shutdown will be initiated. In evaluating the possible consequences of this accident, it is assumed that the refrigeration system is lost for an indefinite period and that the liquid-nitrogen-cooled trap A-309, is isolated.

The total quantity of activity of the noble gas fission products in the primary coolant system will rise to the values given in Table 49, which are average values for a 24-hour period following loss of refrigeration. Some fluctuations about these averages will occur due to transient effects in the trapping system and decay of the activity. Those noble gas isotopes which do not change are not listed. It should be noted that the decay products of the isotopes listed are such that the effective plate-out of activity in the primary system does not change, because the daughters are either very short-lived or stable. Thus, radiation levels affecting maintenance of equipment are not changed.

TABLE 49

PRIMARY COOLANT SYSTEM EQUILIBRIUM ACTIVITIES FOLLOWING LOSS OF REFRIGERATION

Nuclide	Activity (curies)	Half-life	Daughter	Half-life of Daughter
Kr^{83m}	5,100	112 minutes	Kr^{83}	Stable
Kr^{85m}	23,000	4.4 hours	Kr^{85}	10.3 years
Kr^{85}	1,800	10.3 years	Rb^{85}	Stable
Kr^{87}	4,500	78 minutes	Rb^{87}	6.0×10^{10} years
Kr^{88}	23,000	2.8 hours	Rb^{88}	17.8 minutes
Rb^{88}	23,000	17.8 minutes	Sr^{88}	Stable
Xe^{131m}	1,400	12 days	Xe^{131}	Stable
Xe^{133m}	4,200	2.3 days	Xe^{133}	5.27 days
Xe^{133}	260,000	5.27 days	Cs^{133}	Stable
Xe^{135}	15,000	9.13 hours	Cs^{135}	2.0×10^{6} years
	361,000			

3. Loss of Fission Product Trapping System Integrity

Stop valves and check valves are provided at a number of places in the fission product trapping system. These valves allow parts of the system to be isolated in the event of a rupture in a trapping system component or associated piping, thereby minimizing the release of radioactivity to the containment vessel. In addition, the inlet end of the system, which contains the greatest quantity of radioactivity, is doubly contained in order to further guard against release of radioactivity.

In the event of a rupture in the fission product trapping system the amount of radioactivity released depends on the location and nature of the failure. For any break, the radioactivity contained in the helium in the pipes adjacent to the breaks will be released. In addition some of the radioactivity which had previously been adsorbed on the traps adjacent to the break may be desorbed and released. The amount of desorbed activity depends on the amount of helium available to flow through the trap following the break (that is, the amount of helium contained between the trap and the nearest closed valve).

Analyses have been made of the expected release from various assumed breaks in the fission product trapping system piping. These analyses indicated that less than 20 percent of the activity contained in the trapping system would be released by an accident involving a rupture in the trapping system. As an example of release from trapping system ruptures, Table 50 shows the activity release to the containment vessel following a rupture in the purge line. These activities are based on the assumption that a break occurs between the first check valve and the first trap. The second check valve following the second delay bed is assumed to close. Therefore the first three traps back flow from the downstream side of the break and the primary system helium inventory flows out from the upstream side of the break.

In determining the amount of helium and radioactivity released to the containment vessel following a rupture in the primary system or purge line it is conservatively assumed that the check valve in the purge line between the reactor vessel and trapping system (and also the stop valve) fail to close. Therefore the 26 lb of helium in the trapping system between the reactor vessel and the valve downstream of the second delay bed, A-303, as well as the 900 lb of helium in the primary system is released following a rupture in the primary system or purge line. The remainder of the helium in the trapping system is prevented from escaping to the containment by the valves downstream of A-303 and valves in the helium handling system.

TABLE 50

ACTIVITY RELEASE DUE TO FISSION PRODUCT PURGE LINE RUPTURE

Isotope	Activity Release (10^6 Curies)
Kr^{83m}	0.0255
Kr^{85m}	0.0180
Kr^{85}	0.0002
Kr^{87}	0.0565
Kr^{88}	0.0489
Kr^{89}	0.087
Kr^{90}	0.024
I^{131}	0.037
Xe^{131m}	0.00002
I^{133}	0.0031
Xe^{133m}	0.00059
Xe^{133}	0.0124
Xe^{135m}	0.360
Xe^{135}	0.0643
Xe^{137}	0.131
Xe^{138}	0.250
Xe^{139}	0.036
Xe^{140}	0.009
Total	1.16

4. Change in Feed

a. Increase in Fission Product Concentration

Design levels of radioactivity entering the fission product trapping system are based upon experimentally observed release rates of fission products from uncoated fuel, i.e., the retentive effects of pyrolytic carbon coatings have been neglected, and the experimental release fractions have been further increased by a safety factor of 3 (See Section II. J. 2 for a discussion of the experimental data on fission product release). Because of the conservatism included in these design levels, it is highly unlikely that they will be exceeded even under abnormal operating conditions. Furthermore, if temperature monitors within the fission product trapping system should indicate excessive heat generation, the reactor would be shut down and core temperatures reduced before performance of the trapping system had been significantly affected.

b. Increase in H_2O Concentration

High concentrations of water vapor will be present in the primary system helium in the event of a steam leak in one of the steam generators. Immediately following the steam leak, while the fuel elements are still at high temperature, essentially all water vapor drawn into the fuel element purge system will be converted to H_2 and CO. After the core has cooled, however, the purge gas entering the fission product trapping system may contain as much as 200,000 ppm of water if the hot valve fails to isolate the defective steam generator. The first heat exchanger in the trapping system, E-301, (See Figure 56) acts as a condenser and is followed by a knockout drum to collect condensate; the water concentration entering the condensibles trap, A-301, is reduced to 1500 ppm by this exchanger. Experiments by Adams and Browning* indicate that this concentration of water vapor will not affect iodine adsorption in the condensibles trap.

Purge flow rate will be reduced to 100 lb/hr shortly after the steam leak occurs (when the core temperature has fallen to the point where water passes through the fuel element purge channels without reacting with graphite). At 100 lb/hr, the concentration of 1500 ppm

* R. E. Adams and W. E. Browning, Jr.; ORNL-2872; "Removal of Radioiodine from Air Streams by Activated Charcoal"; April 1, 1960.

corresponds to a water throughput of 0.7 lb/hr. If operation is continued for an extended period of time, water will eventually penetrate and enter delay bed A-302. Based upon experimental work by Browning*, the noble gas delay time in the bed should be reduced by about 40 percent. Some activity carryover into the refrigerated delay beds may result, but this effect will be counterbalanced by decay following shutdown, and no serious change in the fission product trapping system performance will occur.

As soon as the purge flow rate is reduced to 100 lb/hr, the helium leaving delay bed A-303 can be diverted through the chemical cleanup system to avoid carryover of water into the refrigerated portion of the system.

c. Increase in Chemical Impurity Concentration

The most significant change in concentration of chemical impurities (other than water) would occur following a steam leak, when 60,000 ppm of H_2 and CO could result from the steam-graphite reaction. Some air inleakage might also occur during maintenance operations when the primary system is subatmospheric. The work of Browning, Adams, and Ackley cited above shows, however, that room temperature delay of krypton by charcoal is reduced only 25 percent when hydrogen, argon, nitrogen, oxygen, or dry air are substituted for helium as purge gas. Since CO is of about the same volatility as these gases, it should produce about the same interference effects. These data indicate that very high concentrations of H_2, CO, or air will not have a serious effect on trapping system performance.

* W. E. Browning, R. E. Adams, and R. D. Ackley; CF-59-6-47; "Removal of Fission Product Gases from Reactor Off-Gas Streams by Adsorption"; June 11, 1959.

D. Safety Considerations Related to Fuel Handling

In the description of the fuel handling system in Section II. H, it was pointed out that the storage, shipping, and handling racks and equipment are designed to prevent a critical mass from being assembled by control of geometry and to limit the number of fuel elements handled as a group. These objectives will be reinforced by administrative procedures and controls. For these reasons, the possibility of criticality occurring outside of the reactor vessel is not considered possible.

The possibility of release of gaseous fission products from spent fuel elements after being withdrawn from the reactor vessel, either before removal from the plant container or after submergence in the spent fuel storage pit, is discussed below.

1. Escape of Fission Products from a Leaking Spent Fuel Can

a. General

Spent fuel elements are remotely canned in heavy wall metal cans before placement in the spent-fuel pit. Caps for these cans are mechanically attached to the can as well as brazed. Each can is leak tested before placement in the spent-fuel pit in order to preclude release of activity to the spent-fuel pit.

During placement in the spent-fuel pit the cans are lifted by the can wall rather than the cap in order to minimize the possibility of causing a leak to develop.

If, in spite of the above provisions, a leak should develop while the can is in the spent-fuel pit, fission products may escape from the fuel compacts and can into the spent-fuel-pit water. Some of the more volatile fission products will subsequently escape from the water into the air above the spent-fuel pit.

The rate at which fission products escape from the can depends on the size of the hole in the can and the rate at which water enters the can. If the coated fuel particles are intact the fuel particles are protected from the water and most of the fission products

will remain in the fuel compacts. However, if the fuel particle coatings are not intact, the water will combine with the uranium and thorium carbides in the fuel particles causing disintegration of the compacts and accelerated release of the fission products. Most gaseous fission products which escape from the compacts will leak out of a hole in the can, through the water, and into the air above the pit. Soluble fission products will dissolve in the water within the can and slowly diffuse through the hole in the can to the spent-fuel-pit water. The spent fuel storage pit building design will permit the controlled release of gaseous activity to the ventilation stack as described in Section III. M.

The following paragraphs describe possible releases of gaseous and water-soluble fission products from a leaking spent-fuel can.

b. Gaseous Fission Product Release

A series of experiments was made at General Atomic to obtain quantitative information on the leaching of gaseous fission products from irradiated fuel during storage as a result of leakage of pool water into defective fuel element canisters. HTGR fuel compacts (made of uncoated fuel particles, for conservatism) were irradiated in the General Atomic TRIGA reactor to yield tracer levels of fission product activity and then exposed to flowing helium and various amounts of moisture ranging from dry helium to the compact being totally submerged. Temperatures were adjusted to match conservatively high calculated temperatures of a spent fuel element in a canister submerged in water. Testing conditions and results are shown in Table 51. These data have been used in predicting the release of activity to the air from a leaking can and the results are shown in Table 52.

The maximum gaseous activity release from the water surface of the fuel storage canal after rupture of a spent fuel can is 11,148 curies, distributed among isotopes as listed in column 4 of Table 52. Off-site consequences of this accident are described in Section VII-F in Table 61 . This release, if it occurred during an inversion, produces a dose of less than 0.1 rem at the site boundary.

c. Release of Activity to Water

At the time it is placed in the spent-fuel pit the most active fuel element will contain approximately 152,000 curies of mixed fission products as given in Table 53. If the leak is small the faulty can will be located and immediately recanned in an oversize container. The water will then be cleaned up with the liquid waste system demineralizer.

TABLE 51

GASEOUS FISSION PRODUCT LEACHING EXPERIMENTAL STUDY

Test No.	Treatment	Exposure Temp, F	Differential Exposure Time hr.	% of Total I^{131} Escaping in Helium Stream	% of Te^{132} Escaping in Helium Stream	Observation
FPL-1-A	Dry helium flowing over compact	205°	20	0	0	No damage readily apparent
1-B		410°	5	0	0	
FPL-2-A	Helium containing 30,000 ppm water flowing over compact	205°	65	0.2[b]	1.8[b]	Compact crumbled slowly during exposure. Activity released mainly in first 20 hours.
		205°	6.5	0.01	0.03	
		400°	16.5	0.05	0.5	
FPL-3	Helium bubbling over compact totally immersed in water	205°	22	0.013[a]	0.091[a]	Compact disintegration very noticeable after 2 hours. Disintegration complete by end of test.
FPL-4	Compact totally immersed in water. No helium	205°	22	79%* in water	** not measured	
FPL-5	"Control" submitted for I-131 analysis	not exposed	-	-	-	-

* Activity measured in filtered water after compact disintegration. Helium was not bubbled over compact.

** Analysis completed before Te^{132} identified as being a major contributor.

(a) and (b) The percentages marked (a) could be legitimately used as basis for calculation of gaseous iodine and tellurium activity released from the surface of the fuel storage pit to environment after leakage of a submerged spent fuel element canister. However, for conservatism, the percentages marked (b) are used as a basis for this calculation.

TABLE 52

VOLATILE RADIOACTIVITY INVENTORY* IN THE HIGHEST POWER FUEL ELEMENT IN SPENT FUEL STORAGE PIT AND ACTIVITY RELEASED FROM A LEAKING FUEL ELEMENT CAN IN THE SPENT FUEL STORAGE PIT

(48 hours after scram)

(Column 1) Releasable Gaseous Fission Products in Fuel Element (Significant at 48 hours)	(Column 2) Half Life	(Column 3) Maximum contained activity, curies	(Column 4) Gaseous activity released from a leaking can and escaping from surface of fuel storage pit to the building atmosphere curies
Kr^{85m}	4.4h	1	1.
Kr^{85}	10.6y	68	68.
Kr^{88}	2.8h	--	--
Te^{127m}	105d	62	1.12
Te^{127}	9.35h	171	3.1
Te^{129m}	33d	500	9.0
Te^{131m}	29h	258	4.6
I^{131}	8.05d	4440	8.9
Xe^{131m}	12d	34	34.
Te^{132}	77h	5130	92.
I^{132}	2.5h	5050	10.1
I^{133}	20.9h	2390	4.8
Xe^{133m}	2.3d	195	195.
Xe^{133}	5.3d	10,220	10,220.
I^{135}	6.75	73	0.15
Xe^{135}	9.2h	497	497.
	TOTAL CURIES:	29,089	11,148

*Assumes no fission product removal during reactor operation.

For larger leaks the soluble activity, approximately one fourth of the total, is the maximum that can be dissolved in the water. After appropriate decontamination of the water by the waste demineralizer, the faulty element will be recanned in an oversize container. As indicated in Section II. H., the spent-fuel pit is designed so that no activity can be released to Conowingo Pond.

2. Stuck Spent Fuel Element in Charge Machine

The fuel handling equipment provides a containment barrier between the spent fuel and the atmosphere at all times as discussed in Section II. H. Calculations indicate that a spent fuel element can remain in any part of the system for extended periods of time with only radiant cooling without overheating. It is not considered necessary to have the plant containment closed during fuel handling because of the protection afforded by the fuel handling equipment.

TABLE 53

MAXIMUM TOTAL RADIOACTIVITY INVENTORY IN ONE FUEL ELEMENT IN SPENT FUEL STORAGE PIT 48 HOURS AFTER REACTOR SHUTDOWN

Fission Products and Daughters	Activity, Curies	Fission Products and Daughters	Activity, Curies
Kr^{85m}	1	Te^{131m}	258
Kr^{85}	68	I^{131}	4440
Sr^{89}	8270	Xe^{131m}	34
Sr^{90}	560	Te^{132}	5130
Y^{90}	560	I^{132}	5050
Sr^{91}	335	I^{133}	2390
Y^{91m}	220	Xe^{133m}	195
Y^{91}	10100	Xe^{133}	10220
Y^{92}	4	I^{135}	73
Y^{93}	440	Xe^{135}	497
Zr^{95}	10800	Ce^{137}	832
Nb^{95m}	210	Ba^{140}	10200
Nb^{95}	11000	La^{140}	5580
Zr^{97}	1380	La^{141}	2
Mo^{99}	6500	Ce^{141}	10900
Te^{99m}	6340	Ce^{143}	3670

TABLE 53 (Cont'd.)

Fission Products and Daughters	Activity, Curies	Fission Products and Daughters	Activity, Curies
Ru^{103}	5130	Pr^{143}	10100
Ru^{105}	1	Ce^{144}	9470
Rh^{105}	730	Pr^{145}	27
Ru^{106}	680	Nd^{147}	4220
Sb^{127}	198	Pm^{147}	2220
Te^{127m}	62	Pm^{149}	950
Te^{127}	171	Pm^{151}	240
Sb^{129}	1	Sm^{151}	550
Te^{129m}	500	Sm^{153}	155
		TOTAL	151,664

E. Plant Behavior Under Abnormal Conditions Arising External to the Plant

1. Loss of Outside Power

Two transmission lines of the Philadelphia Electric Company will be brought into the plant. The line over which generated power will be transmitted and which will normally supply power for startup and shutdown, is rated at 220 kv and will be a tap, approximately 2000 feet in length from a high capacity, inter-system tie line to the north of the plant. This line will be of heavy duty construction on steel towers with lightning protection provided by overhead ground wires. The other transmission line will be an extension of an existing 33 kv line originating at the Philadelphia Electric Company Conowingo Hydro Generating Plant. Except for about 3 miles of common right of way, the 220 kv and 33 kv lines approach the plant over entirely separate routes. The 33 kv line is of adequate capacity to supply approximately half of the plant auxiliary load and could, in an emergency, start one of the main helium compressors. The 33 kv source will be used as an emergency standby source for situations when the main turbine generator is not in operation, such as during startup, shutdown or when multiple accidents involving coincident failures results in neither the 220 kv source nor the turbine generator being available as power sources, and as backup for the emergency diesel generator.

Complete loss of both the 220 kv and 33 kv outside power sources will not result in interruption to the plant auxiliary power system. As described in detail in Section III.H.2, auxiliary power will continue to be supplied by the main turbine-generator supplying at house load only. If, in addition to the loss of outside power, the turbine should unexpectedly trip on overspeed, the reactor would be scrammed. Auxiliary power will continue to be supplied to maintain essential loads for about six minutes by turbine-generator coastdown. Within less than one minute, the emergency diesel generator will have automatically started and taken over part of the essential load. After the six minute coastdown period the reactor will have been cooled to the point where continued cooling will be accomplished by means of the pony motor driven helium compressors supplied from the emergency diesel generator. Actually by this time the reactor has cooled down to the point where cooling could be interrupted for approximately one half hour without major damage to the core. This time is available to manually start the emergency diesel generator in the unlikely event it did not start automatically, or to restore either of the outside power sources, and resume cooling. Furthermore, during or subsequent to the coastdown period, the operator may reset the overspeed trip, re-admit steam to the turbine and continue to supply

all auxiliaries from the turbine-generator using post-scram heat from the reactor to generate steam. This has the further potential to cool the core down to the point where an interruption of cooling could be tolerated for several hours without damage to the core. In the extremely unlikely event that none of the above means are successful in providing reactor cooling, the reactor vessel emergency cooling system supplied by the diesel fire pump will prevent the occurrence of a public hazard.

2. Earthquakes

The plant site is located in a region of minor seismicity. An investigation concerning the seismic history of the Peach Bottom, Pennsylvania area indicates no report of any earthquakes having occurred in the area or immediate vicinity. (See Part B, Volume II, Section I)

Plant construction will be in accordance with the conventional design practice for nuclear facilities in such zones and the area is classified as Zone 1 in accordance with the Uniform Building Code, 1961 edition.

3. Floods

The finished grade of the plant will be at elevation 115 feet (Conowingo Dam Datum) which is above the maximum flood level expected at the site as indicated in Part B, Volume II, Section III.

The plant is designed such that any expected floods will not affect the safeguards analysis presented in this report.

4. Landslides

The site does not present any landslide hazard to the containment structure or other plant structures. Detailed information regarding geological conditions in the plant area and vicinity may be found in Part B, Volume II, Section IV.

5. Fire

Like most conventional power plants, the Peach Bottom Atomic Power Station will employ some flammable materials; fuel oils for the diesel-driven emergency generator, emergency fire pump, lubricating and seal oils, transformer and circuit breaker oils, hydraulic oil systems, and hydrogen coolant for the generator. In all such cases the fire protection measures will follow conventional practice, which are expected to prevent any fire from compounding major accidents.

6. Severe Weather

The meteorological conditions affecting the plant site are presented in Part B, Volume II, Section II.

All plant structures will be designed to withstand the wind and other potential loadings in accordance with standard code provisions and normal engineering practice.

The containment will be designed to withstand a wind velocity of 100 mph and 30 psf snow load.

F. Environmental Consequences of Accidents

1. Summary of Accidents Releasing Radioactivity to the Containment

All accidents which have been identified in Sections VII B and C as having significant radioactive releases to the containment are summarized in Table 54.

The accident which combines the primary system rupture with the purge line check valve not operating and loss of forced circulation in both primary coolant loops is the most severe accident analyzed.

2. Assumptions for Dosage Calculations

The effect on the plant environs from each of the accidents has been calculated using the assumptions described in this section. The results are presented in Tables 55 to 61.

The maximum specified leakage from the containment of 0.2%/day is conservatively assumed to apply throughout the course of each accident even though the calculated pressure in the containment is less than the design pressure. The filter on the recirculating system inside the containment will be operated after accidents primarily to reduce the long term Sr^{90} leakage. The filter will also reduce leakage of other particulate matter. It is conservatively assumed in the dosage calculations that this filter removes from the containment atmosphere 50% of the non-gaseous radioactivity contained in 2000 cubic feet each minute.

The consequences of any release of airborne radioactive material from the plant depends to a great extent on the atmospheric conditions which prevail at the time the leakage occurs. Appropriate atmospheric dilution factors for use in accident analyses are developed in Volume II, Section II, Part B. For convenience, Table 62 repeats the applicable atmospheric dilution factors for accident analyses.

Whole body gamma dosages from radioactive clouds are estimated assuming immersion in a semi-infinite medium. Thyroid dosages assume the dose per microcurie of iodine isotopes inhaled shown in Table 63. The bone dosages use the dosage relationship in T. J. Burnett's paper, "Hazards vs. Power Level."*

* Burnett, T. J.; "Hazards vs. Power Level"; Nuclear Science and Engineering; May, 1957

Radiation from fission products inside the containment are calculated using 50% self shielding which approximates the actual design for the various plant layout alternatives being considered. No credit for condensation of the less volatile fission products in shielded areas is included. The calculation is based on the work of Geller and Epstein, "A General Method for Evaluating Containment Shielding Under Normal and Emergency Conditions"* for the 1000 ft dosages. At greater distances a point source is assumed.

3. Discussion of Environmental Consequences of Accidents

The most severe accident involving a single failure in the reactor is a rupture in the primary loop of a size which gives a significant backflow of the purge gas inside the fuel elements to the coolant loop and through the rupture to the containment. The total activity released from this accident is 0.84×10^6 curies which includes the design coolant radioactive inventory, activity released by the backflow through the fuel elements, activity contained in the purge line, and the release as the external fission product trap radioactive effluent slowly increases due to the increased trap temperature caused by cooling with gas at atmospheric pressure. In this accident, the purge line check valve between the reactor and the first fission product trap, which is installed specifically to prevent backflow from the entire fission product trapping system, is assumed to operate. This accident, which is described in Section VII. B. 2. d, and Table 56 produces a whole body gamma dosage at the site boundary of about 0.005 rem during the first 24 hours with an inversion and a corresponding thyroid dose of 0.05 rem. The consequences of smaller primary system ruptures with no backflow of the purge gas inside the fuel elements are given in Case A of Table 55.

The most severe accident involving two failures in the reactor system is the rupture of the doubly contained fission product purge line between the first check valve and the first fission product trap. The second check valve (following trap A-303) is assumed to close, preventing backflow from the downstream traps. The potential dosages from this accident during an inversion for the first 24 hours at the site boundary are 0.01 rem for whole body gamma and 6 rem to the thyroid as shown in Table 60. A slightly less severe accident involving a double failure is rupture of the primary system with failure of the first purge line check valve and backflow from the first three

* Geller, L., and Epstein, R.; "A General Method of Evaluation of Containment Shielding Under Normal and Emergency Conditions"; Second Geneva Conference on the Peaceful Uses of Atomic Energy; Paper P/435.

fission product traps. The consequences of this accident are shown in Case B-2, Table 57.

The most severe accident postulated in this report involves a series of failures. They are a primary system rupture, simultaneous unavailability of both coolant loops, and failure of the purge line check valve to close. An initial radioactive release to the plant container corresponding to Tables 55-57 would result from a primary system rupture. As the core heats up to the peak temperature resulting from heat removal only by the emergency cooling system, additional fission products would be released from the compacts. Combining the primary system rupture with failure of purge line check valve and loss of normal cooling, the dosages for the first 24 hours at the site boundary during an inversion would be: whole body gamma 0.4 rem, thyroid 100 rem, and bone 20 rem as shown in Case C-2, Table 59. Table 58 shows the potential doses for the loss of normal cooling accident with primary system rupture but with no backflow from the external fission product traps.

The maximum dose at the site boundary from the leakage of the volatile fission products from the highest powered fuel element in the spent fuel pool, immediately after removal from the containment, during an inversion, is less than 0.1 rem (Case E). This release is less than 20% of the 0.5 rem annual off-site dose specified in 10 CFR Part 20 even with the most pessimistic assumptions.

Appropriate evacuation procedures will be developed and suitable communication facilities will be included in the plant to notify proper authorities and personnel near the site in case evacuation is necessary.

TABLE 54

SUMMARY OF ACCIDENTS WITH SIGNIFICANT RADIOACTIVE RELEASES TO THE CONTAINMENT

Case	Accident	Maximum Activity in Containment, Megacuries	Discussion Reference	Environment Consequences Reference
A.	Primary System Depressurization	.29	VII. B. 2. d	Table 55
B.	Primary System Rupture			
	1. No backflow from fission external product traps	.84	VII. B. 2. d	Table 56
	2. With backflow from first three external fission product traps	2.26	VII. B. 2. d	Table 57
C.	Loss of Normal Cooling with Primary System Rupture			
	1. No backflow from external fission product traps	5.2	VII. B. 3	Table 58
	2. With backflow from first three external fission product traps	5.2	VII. B. 3	Table 59
D.	Rupture of Fission Product Purge Line	1.16	VII. C. 3. a	Table 60
E.	Release of Volatile Fission Products from One Fuel Element in Spent Fuel Storage Pool	*	VII. D	Table 61

* Controlled release; a maximum of 11, 148 curies of noble gases through ventilation stack

TABLE 55

DOSAGES FROM PRIMARY SYSTEM DEPRESSURIZATION
(Case A)

Whole Body Gamma Dosage From Immersion, Rem

	Site Boundary		10 Miles	
	Inversion	Unstable Atmosphere	Inversion	Unstable Atmosphere
0-10 min.	$3x10^{-5}$	$1x10^{-6}$	$2x10^{-7}$	$6x10^{-9}$
0-1 hr.	$2x10^{-4}$	$7x10^{-6}$	$2x10^{-6}$	$4x10^{-8}$
0-2 hr.	$3x10^{-4}$	$1x10^{-5}$	$2x10^{-6}$	$6x10^{-8}$
0-8 hr.	$2x10^{-3}$	$4x10^{-5}$	$8x10^{-6}$	$3x10^{-7}$
0-24 hr.	$4x10^{-3}$	$1x10^{-4}$	$2x10^{-5}$	$7x10^{-7}$

TABLE 56

DOSAGES FROM PRIMARY SYSTEM RUPTURE WITH NO BACKFLOW FROM EXTERNAL FISSION PRODUCT TRAPS
(Case B-1)

Whole Body Gamma Dosage From Immersion, Rem

	Site Boundary		10 Miles	
	Inversion	Unstable Atmosphere	Inversion	Unstable Atmosphere
0-10 min.	$3x10^{-4}$	$9x10^{-6}$	$2x10^{-6}$	$6x10^{-8}$
0-1 hr.	$7x10^{-4}$	$3x10^{-5}$	$6x10^{-6}$	$2x10^{-7}$
0-2 hr.	$2x10^{-3}$	$4x10^{-5}$	$8x10^{-6}$	$3x10^{-7}$
0-8 hr.	$3x10^{-3}$	$8x10^{-5}$	$2x10^{-5}$	$5x10^{-7}$
0-24 hr.	$5x10^{-3}$	$2x10^{-4}$	$3x10^{-5}$	$1x10^{-6}$

Thyroid Dosage, Rem

	Site Boundary		10 Miles	
	Inversion	Unstable Atmosphere	Inversion	Unstable Atmosphere
0-10 min.	$2x10^{-3}$	$7x10^{-5}$	$2x10^{-5}$	$4x10^{-7}$
0-1 hr.	$1x10^{-2}$	$4x10^{-4}$	$7x10^{-5}$	$2x10^{-6}$
0-2 hr.	$2x10^{-2}$	$7x10^{-4}$	$1x10^{-4}$	$4x10^{-6}$
0-8 hr.	$3x10^{-2}$	$9x10^{-4}$	$2x10^{-4}$	$6x10^{-6}$
0-24 hr.	$5x10^{-2}$	$2x10^{-3}$	$3x10^{-4}$	$9x10^{-6}$

Bone Dosage, Rem

	Site Boundary		10 Miles	
	Inversion	Unstable Atmosphere	Inversion	Unstable Atmosphere
0-10 min.	$6x10^{-5}$	$2x10^{-6}$	$4x10^{-7}$	$1x10^{-8}$
0-1 hr.	$4x10^{-4}$	$1x10^{-5}$	$2x10^{-6}$	$7x10^{-8}$
0-2 hr.	$6x10^{-4}$	$2x10^{-5}$	$4x10^{-6}$	$2x10^{-7}$
0-8 hr.	$2x10^{-3}$	$7x10^{-5}$	$2x10^{-5}$	$4x10^{-7}$
0-24 hr.	$3x10^{-3}$	$7x10^{-4}$	$2x10^{-5}$	$6x10^{-7}$

TABLE 57

DOSAGES FROM PRIMARY SYSTEM RUPTURE WITH BACKFLOW FROM FIRST THREE EXTERNAL FISSION PRODUCTS TRAPS (Case B-2)

Whole Body Gamma Dosage From Immersion, Rem

	Site Boundary		10 Miles	
	Inversion	Unstable Atmosphere	Inversion	Unstable Atmosphere
0-10 min.	$1x10^{-3}$	$3x10^{-5}$	$1x10^{-5}$	$2x10^{-7}$
0-1 hr.	$3x10^{-3}$	$1x10^{-4}$	$2x10^{-5}$	$7x10^{-7}$
0-2 hr.	$5x10^{-3}$	$2x10^{-4}$	$3x10^{-5}$	$9x10^{-7}$
0-8 hr.	$7x10^{-3}$	$3x10^{-4}$	$5x10^{-5}$	$2x10^{-6}$
0-24 hr.	$1x10^{-2}$	$4x10^{-4}$	$7x10^{-5}$	$3x10^{-6}$

Thyroid Dosage, Rem

	Site Boundary		10 Miles	
	Inversion	Unstable Atmosphere	Inversion	Unstable Atmosphere
0-10 min.	$8x10^{-3}$	$3x10^{-4}$	$6x10^{-5}$	$2x10^{-6}$
0-1 hr.	$5x10^{-2}$	$2x10^{-3}$	$4x10^{-4}$	$1x10^{-5}$
0-2 hr.	$1x10^{-1}$	$3x10^{-3}$	$6x10^{-4}$	$2x10^{-5}$
0-8 hr.	$3x10^{-1}$	$8x10^{-3}$	$2x10^{-3}$	$5x10^{-5}$
0-24 hr.	$4x10^{-1}$	$2x10^{-2}$	$3x10^{-3}$	$8x10^{-5}$

Bone Dosage, Rem

	Site Boundary		10 Miles	
	Inversion	Unstable Atmosphere	Inversion	Unstable Atmosphere
0-10 min.	$4x10^{-4}$	$1x10^{-5}$	$3x10^{-6}$	$6x10^{-8}$
0-1 hr.	$2x10^{-3}$	$6x10^{-5}$	$2x10^{-5}$	$4x10^{-7}$
0-2 hr.	$4x10^{-3}$	$2x10^{-4}$	$3x10^{-5}$	$7x10^{-7}$
0-8 hr.	$1x10^{-2}$	$4x10^{-4}$	$8x10^{-5}$	$3x10^{-6}$
0-24 hr.	$2x10^{-2}$	$6x10^{-4}$	$2x10^{-4}$	$4x10^{-6}$

TABLE 58

DOSAGES FROM PRIMARY SYSTEM RUPTURE AND LOSS OF NORMAL COOLING WITH NO BACKFLOW FROM EXTERNAL FISSION PRODUCT TRAPS
(Case C-1)

Whole Body Gamma Dosage from Immersion, Rem

	Site Boundary		10 Miles	
	Inversion	Unstable Atmosphere	Inversion	Unstable Atmosphere
0-10 min.	$3x10^{-4}$	$9x10^{-6}$	$2x10^{-6}$	$6x10^{-8}$
0-1 hr.	$7x10^{-4}$	$3x10^{-5}$	$6x10^{-6}$	$2x10^{-7}$
0-2 hr.	$2x10^{-3}$	$4x10^{-5}$	$8x10^{-6}$	$3x10^{-7}$
0-8 hr.	$5x10^{-2}$	$2x10^{-3}$	$4x10^{-4}$	$1x10^{-5}$
0-24 hr.	$4x10^{-1}$	$2x10^{-2}$	$3x10^{-3}$	$8x10^{-5}$

Thyroid Dosage, Rem

	Site Boundary		10 Miles	
	Inversion	Unstable Atmosphere	Inversion	Unstable Atmosphere
0-10 min.	$2x10^{-3}$	$7x10^{-5}$	$2x10^{-5}$	$4x10^{-7}$
0-1 hr.	$1x10^{-2}$	$4x10^{-4}$	$7x10^{-5}$	$2x10^{-6}$
0-2 hr.	$2x10^{-2}$	$7x10^{-4}$	$1x10^{-4}$	$4x10^{-6}$
0-8 hr.	9	$3x10^{-1}$	$6x10^{-2}$	$2x10^{-3}$
0-24 hr.	100	4	$7x10^{-1}$	$2x10^{-2}$

Bone Dosage, Rem

	Site Boundary		10 Miles	
	Inversion	Unstable Atmosphere	Inversion	Unstable Atmosphere
0-10 min.	$6x10^{-5}$	$2x10^{-6}$	$4x10^{-7}$	$1x10^{-8}$
0-1 hr.	$4x10^{-4}$	$1x10^{-5}$	$2x10^{-6}$	$7x10^{-8}$
0-2 hr.	$6x10^{-4}$	$2x10^{-5}$	$4x10^{-6}$	$2x10^{-7}$
0-8 hr.	$9x10^{-1}$	$3x10^{-2}$	$6x10^{-3}$	$2x10^{-3}$
0-24 hr.	20	$7x10^{-1}$	$2x10^{-1}$	$4x10^{-3}$

TABLE 59

DOSAGES FROM PRIMARY SYSTEM RUPTURE AND LOSS OF NORMAL COOLING WITH BACKFLOW FROM FIRST THREE EXTERNAL FISSION PRODUCT TRAPS (Case C-2)

Whole Body Gamma Dosage From Fission Products Inside Containment, Rem

	1,000 ft.	2,000 ft.	3,000 ft.
0-10 min.	$4x10^{-2}$	$2x10^{-3}$	$3x10^{-4}$
0-1 hr.	$1x10^{-1}$	$6x10^{-3}$	$9x10^{-4}$
0-2 hr.	$2x10^{-1}$	$1x10^{-2}$	$2x10^{-3}$
0-8 hr.	15	1	$2x10^{-2}$
0-24 hr.	120	6	$8x10^{-2}$

Whole Body Gamma Dosage From Immersion, Rem

	Site Boundary		10 Miles	
	Inversion	Unstable Atmosphere	Inversion	Unstable Atmosphere
0-10 min.	$1x10^{-3}$	$3x10^{-5}$	$1x10^{-5}$	$2x10^{-7}$
0-1 hr.	$3x10^{-3}$	$1x10^{-4}$	$2x10^{-5}$	$7x10^{-7}$
0-2 hr.	$5x10^{-3}$	$2x10^{-4}$	$3x10^{-5}$	$9x10^{-7}$
0-8 hr.	$6x10^{-2}$	$2x10^{-3}$	$4x10^{-4}$	$1x10^{-5}$
0-24 hr.	$4x10^{-1}$	$2x10^{-2}$	$3x10^{-3}$	$8x10^{-5}$

Thyroid Dosage, Rem

	Site Boundary		10 Miles	
	Inversion	Unstable Atmosphere	Inversion	Unstable Atmosphere
0-10 min.	$8x10^{-3}$	$3x10^{-4}$	$6x10^{-5}$	$2x10^{-6}$
0-1 hr.	$5x10^{-2}$	$2x10^{-3}$	$4x10^{-4}$	$1x10^{-5}$
0-2 hr.	$1x10^{-1}$	$3x10^{-3}$	$6x10^{-4}$	$2x10^{-5}$
0-8 hr.	9	$3x10^{-1}$	$6x10^{-2}$	$2x10^{-3}$
0-24 hr.	100	4	$7x10^{-1}$	$2x10^{-2}$

TABLE 59 (Contd.)

Bone Dosage, Rem

	Site Boundary		10 Miles	
	Inversion	Unstable Atmosphere	Inversion	Unstable Atmosphere
0-10 min.	$4x10^{-4}$	$1x10^{-5}$	$3x10^{-6}$	$6x10^{-8}$
0-1 hr.	$2x10^{-3}$	$6x10^{-5}$	$2x10^{-5}$	$4x10^{-7}$
0-2 hr.	$4x10^{-3}$	$2x10^{-4}$	$3x10^{-5}$	$7x10^{-7}$
0-8 hr.	$9x10^{-1}$	$3x10^{-2}$	$6x10^{-3}$	$2x10^{-4}$
0-24 hr.	20	$7x10^{-1}$	$2x10^{-1}$	$4x10^{-3}$

TABLE 60

DOSAGES FROM RUPTURE OF FISSION PRODUCT PURGE LINE
(Case D)

Whole Body Gamma Dosages from Immersion, Rem

	Site Boundary		10 Miles	
	Inversion	Unstable Atmosphere	Inversion	Unstable Atmosphere
0-10 min.	$5x10^{-4}$	$2x10^{-5}$	$4x10^{-6}$	$1x10^{-7}$
0-1 hr.	$2x10^{-3}$	$6x10^{-5}$	$1x10^{-5}$	$4x10^{-7}$
0-2 hr.	$3x10^{-3}$	$8x10^{-5}$	$2x10^{-5}$	$5x10^{-7}$
0-8 hr.	$6x10^{-3}$	$2x10^{-4}$	$4x10^{-5}$	$1x10^{-6}$
0-24 hr.	$1x10^{-2}$	$4x10^{-4}$	$7x10^{-5}$	$2x10^{-6}$

Thyroid Dosages, Rem

	Site Boundary		10 Miles	
	Inversion	Unstable Atmosphere	Inversion	Unstable Atmosphere
0-10 min.	$7x10^{-2}$	$2x10^{-3}$	$5x10^{-4}$	$2x10^{-5}$
0-1 hr.	$4x10^{-1}$	$2x10^{-2}$	$3x10^{-3}$	$8x10^{-5}$
0-2 hr.	$8x10^{-1}$	$3x10^{-2}$	$5x10^{-3}$	$2x10^{-4}$
0-8 hr.	3	$1x10^{-1}$	$2x10^{-2}$	$6x10^{-4}$
0-24 hr.	6	$2x10^{-1}$	$4x10^{-2}$	$1x10^{-3}$

TABLE 61

RELEASE OF VOLATILE FISSION PRODUCTS FROM ONE FUEL ELEMENT IN SPENT-FUEL STORAGE POOL*
(Case E)

Whole Body Gamma Dosage from Immersion, Rem

	Site Boundary		10 Miles	
	Inversion	Unstable Atmosphere	Inversion	Unstable Atmosphere
$0-\infty$ (total release)	$9x10^{-2}$	$1.1x10^{-2}$	$6x10^{-4}$	$2x10^{-5}$

*Primarily noble gases, negligible thyroid dose

TABLE 62

RELATIVE ATMOSPHERIC DILUTION FOR ACCIDENTS
(sec/m^3)

Location	Normal Nocturnal Inversion	Normal Unstable Conditions
Pond at boundary	3×10^{-4}	1×10^{-5}
10 Miles up or down Conowingo Pond	2×10^{-6}	6×10^{-8}

TABLE 63

THYROID DOSE FROM INHALATION OF IODINE ISOTOPES

Isotope	Dose per microcurie inhaled, rem
I^{131}	1.49
I^{132}	0.56
I^{133}	0.42
I^{134}	0.026
I^{135}	0.11

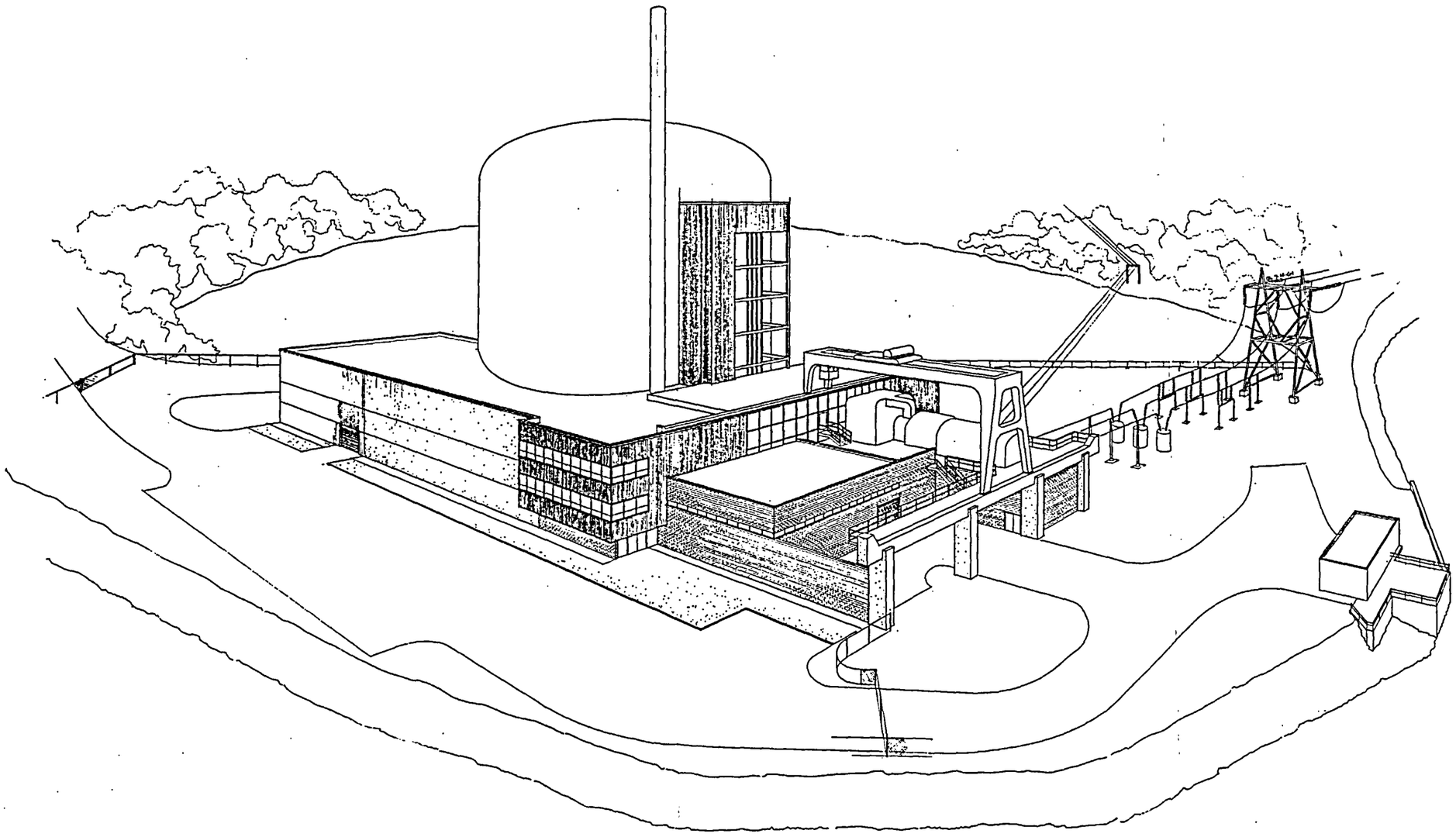

PLANT PERSPECTIVE

PEACH BOTTOM ATOMIC POWER STATION
PHILADELPHIA ELECTRIC COMPANY

FIGURE 1

August, 1961

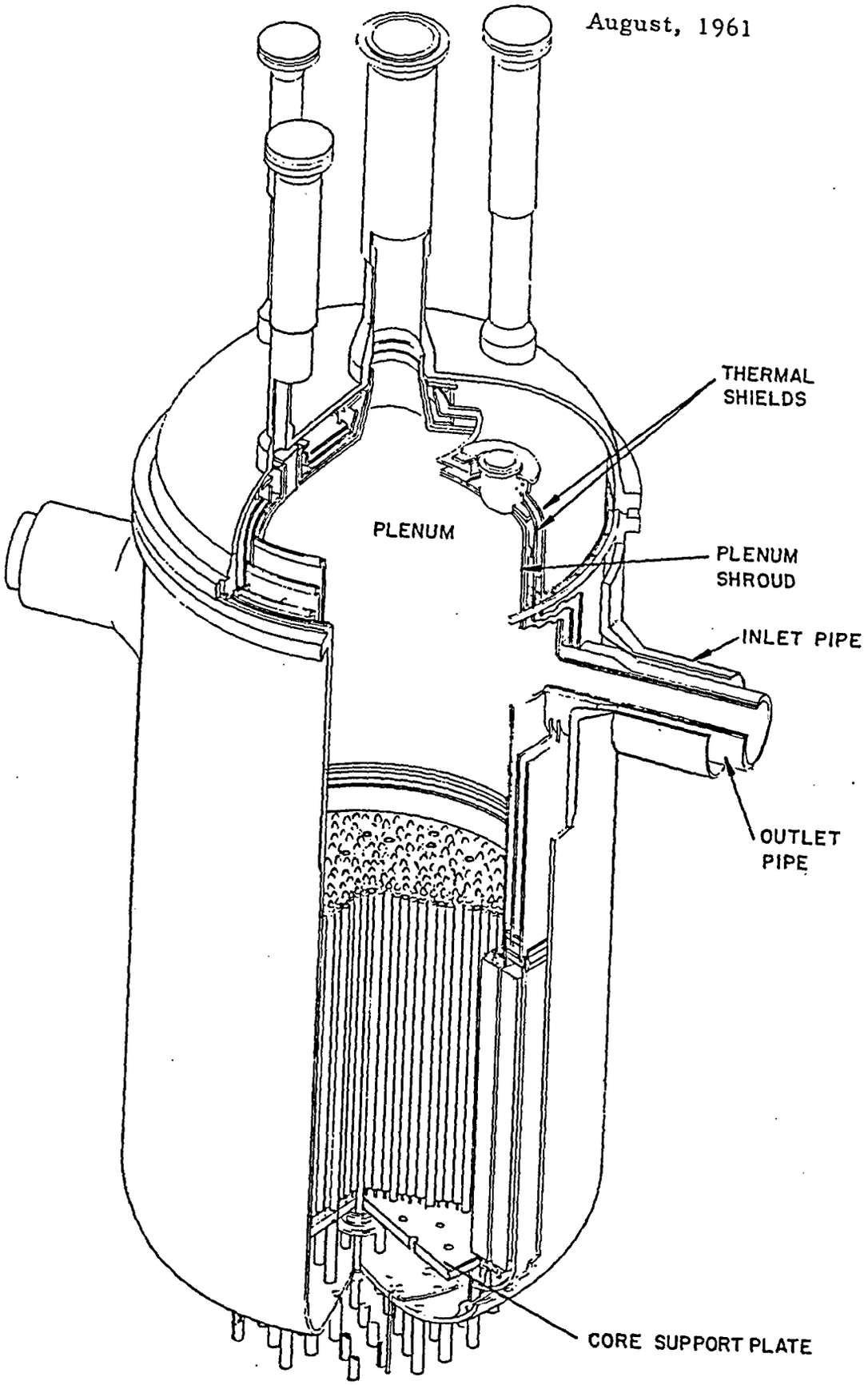

REACTOR CUTAWAY

FIGURE 2

August, 1961

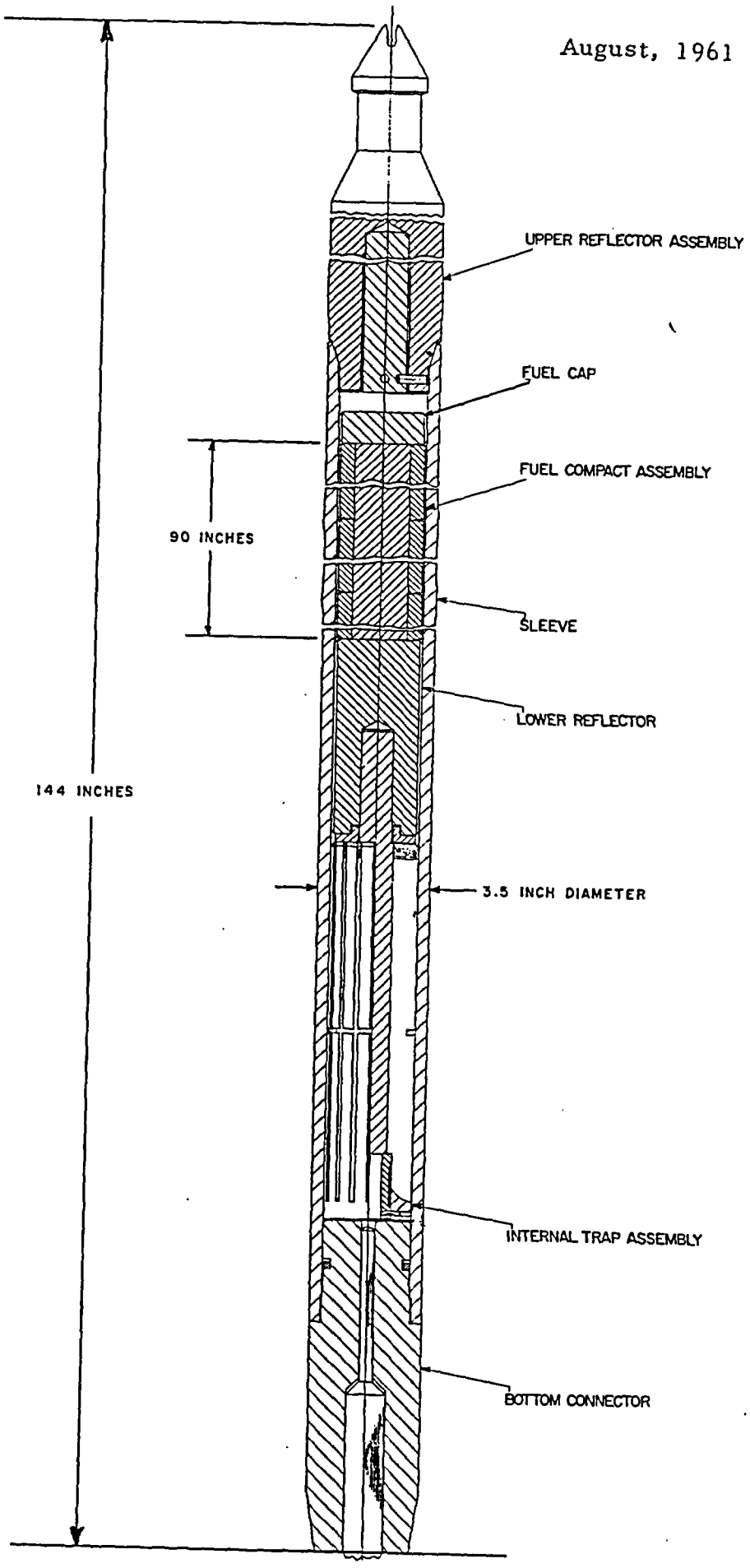

HTGR FUEL ELEMENT

FIGURE 3

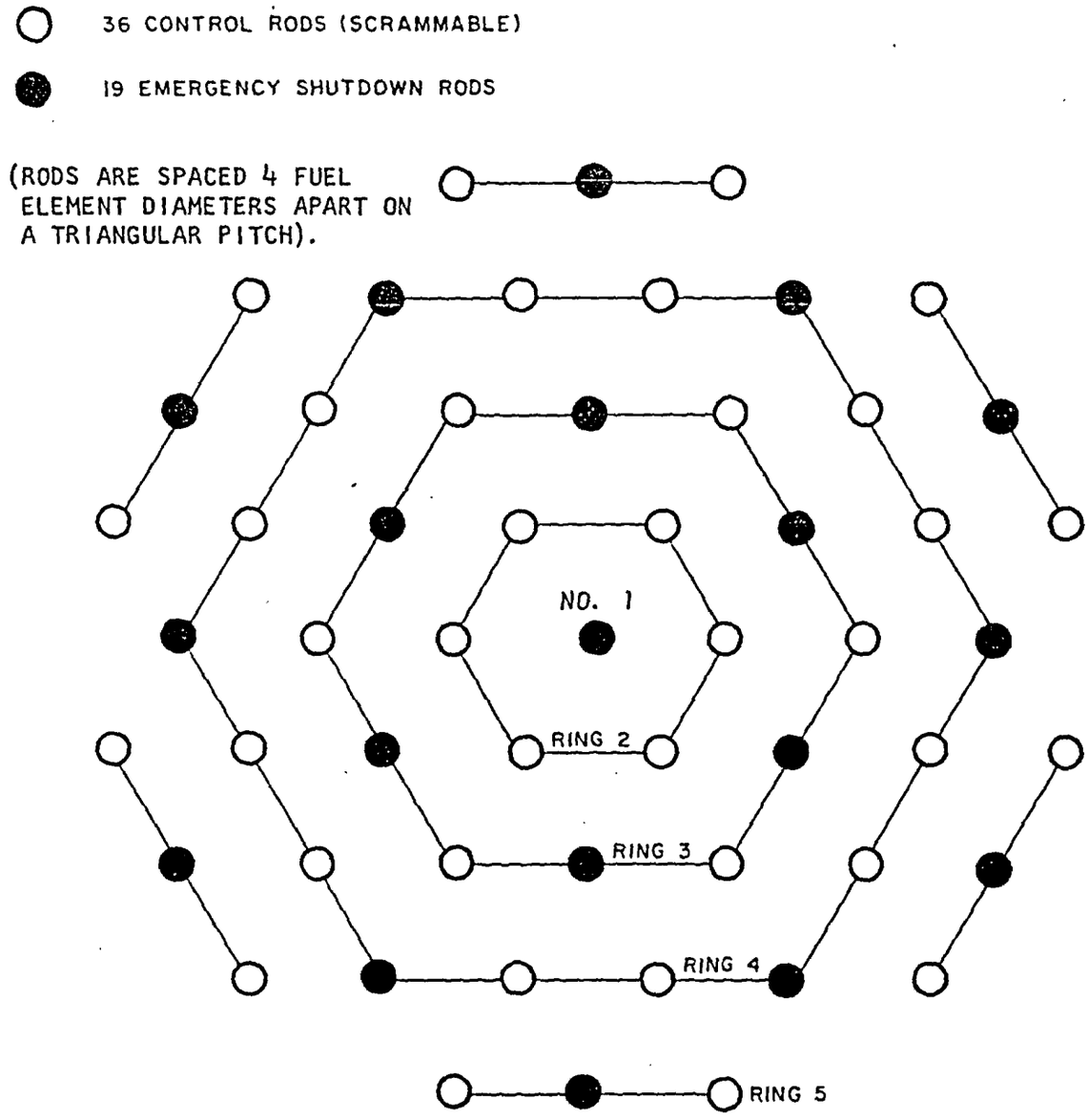

PROPOSED HTGR CONTROL ROD ARRANGEMENT

FIGURE 4

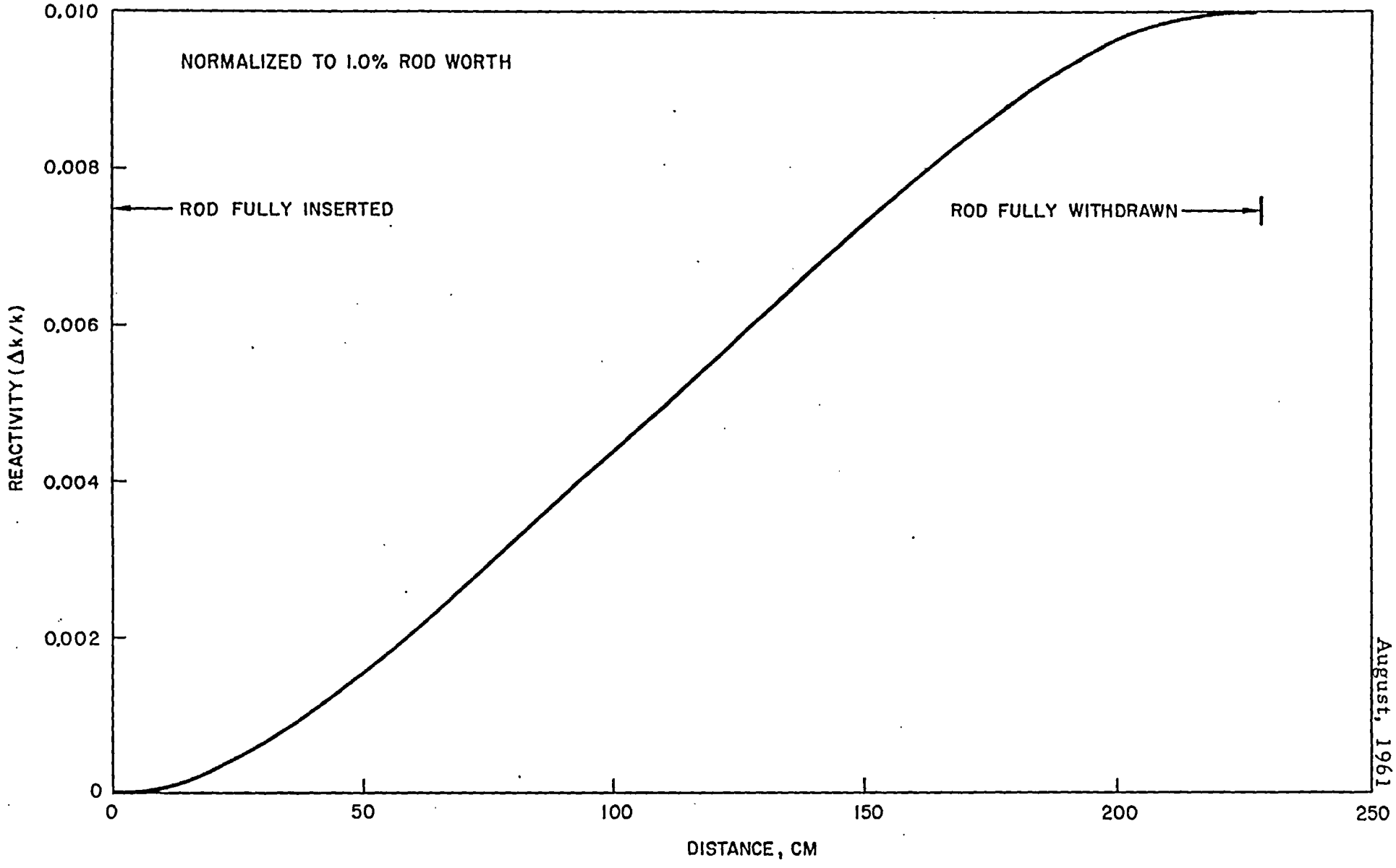

FIGURE 5

REACTIVITY INSERTED BY REMOVAL OF CENTER CONTROL ROD

August, 1961

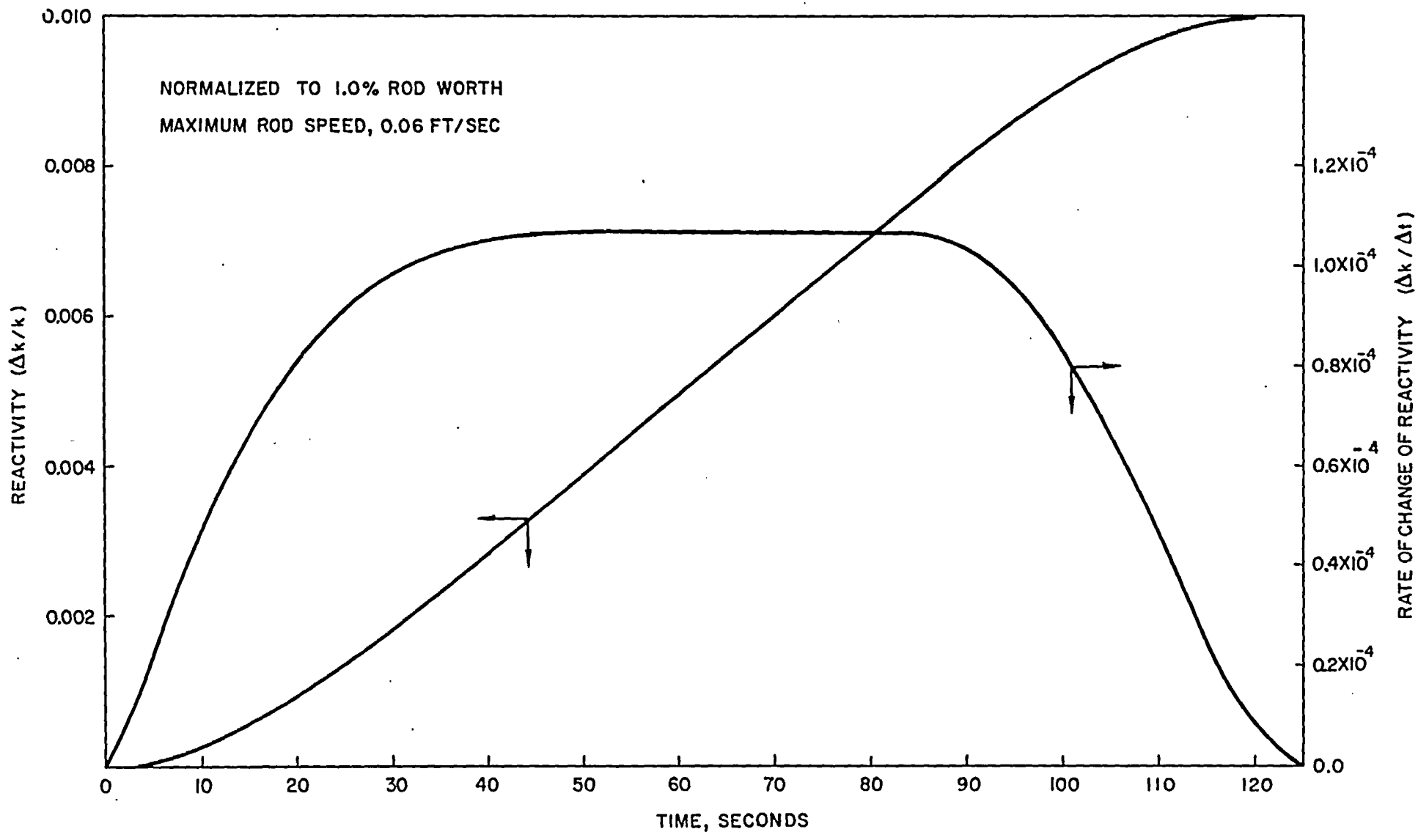

REACTIVITY VS. TIME AND RATE OF CHANGE OF REACTIVITY
VS. TIME FOR WITHDRAWAL OF INNER CONTROL ROD

FIGURE 6

August, 1961

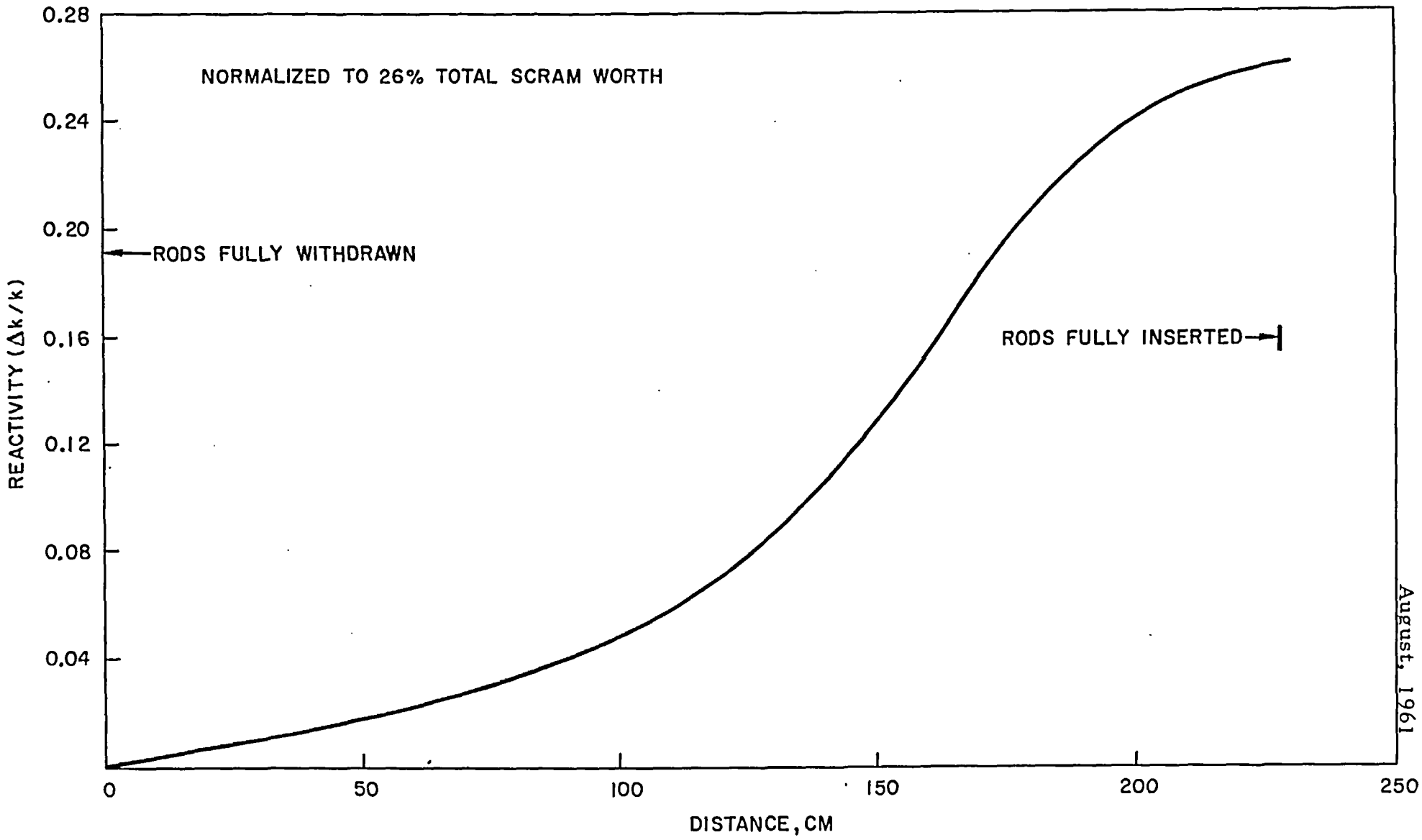

SCRAM REACTIVITY INPUT FOR 36 RODS; 1200°K;
END OF LIFE; XENON AND SAMARIUM PRESENT

August, 1961

FIGURE 7

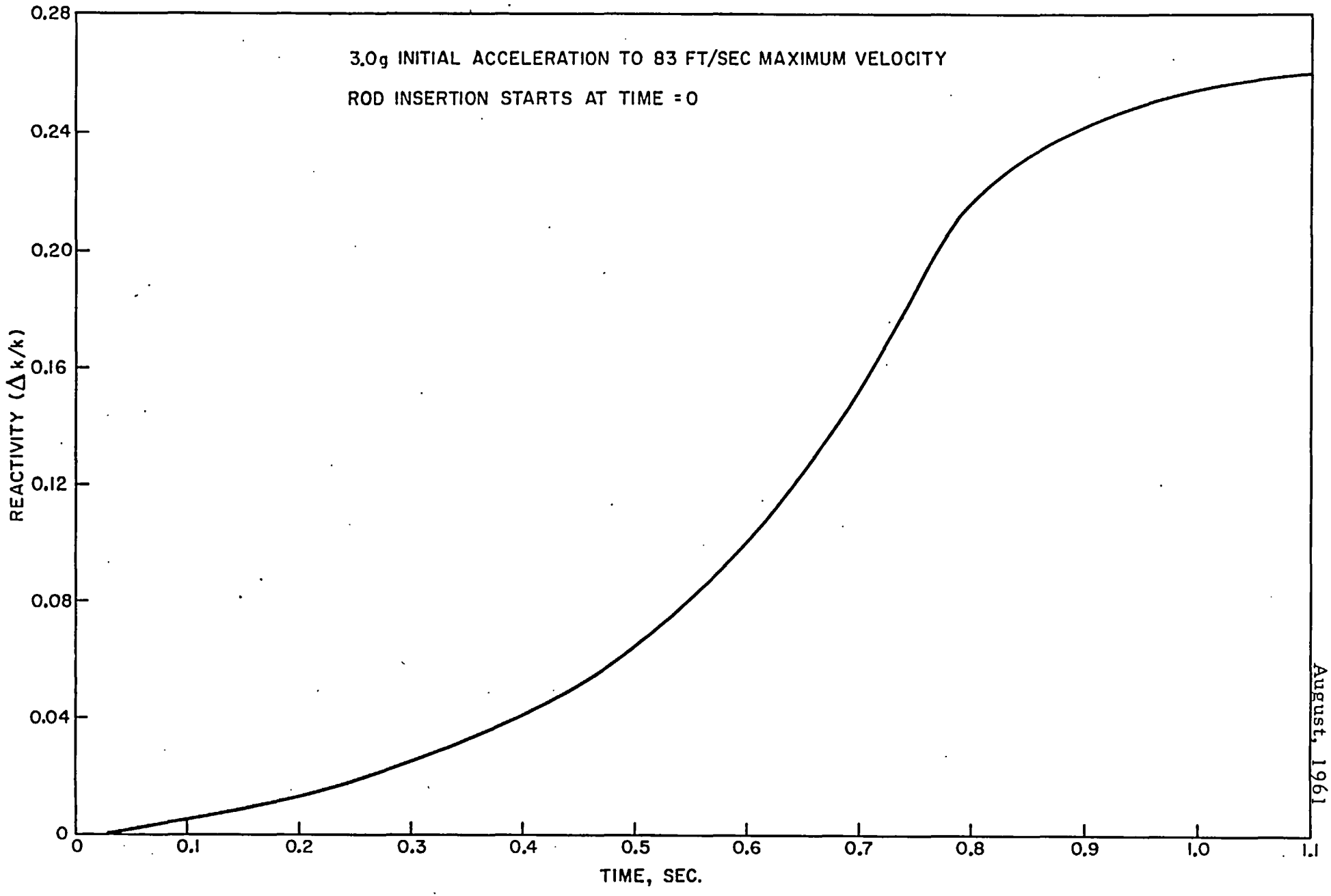

FIGURE 8

SCRAM REACTIVITY VS. TIME FOR 36 ROD SCRAM; END OF LIFE

August, 1961

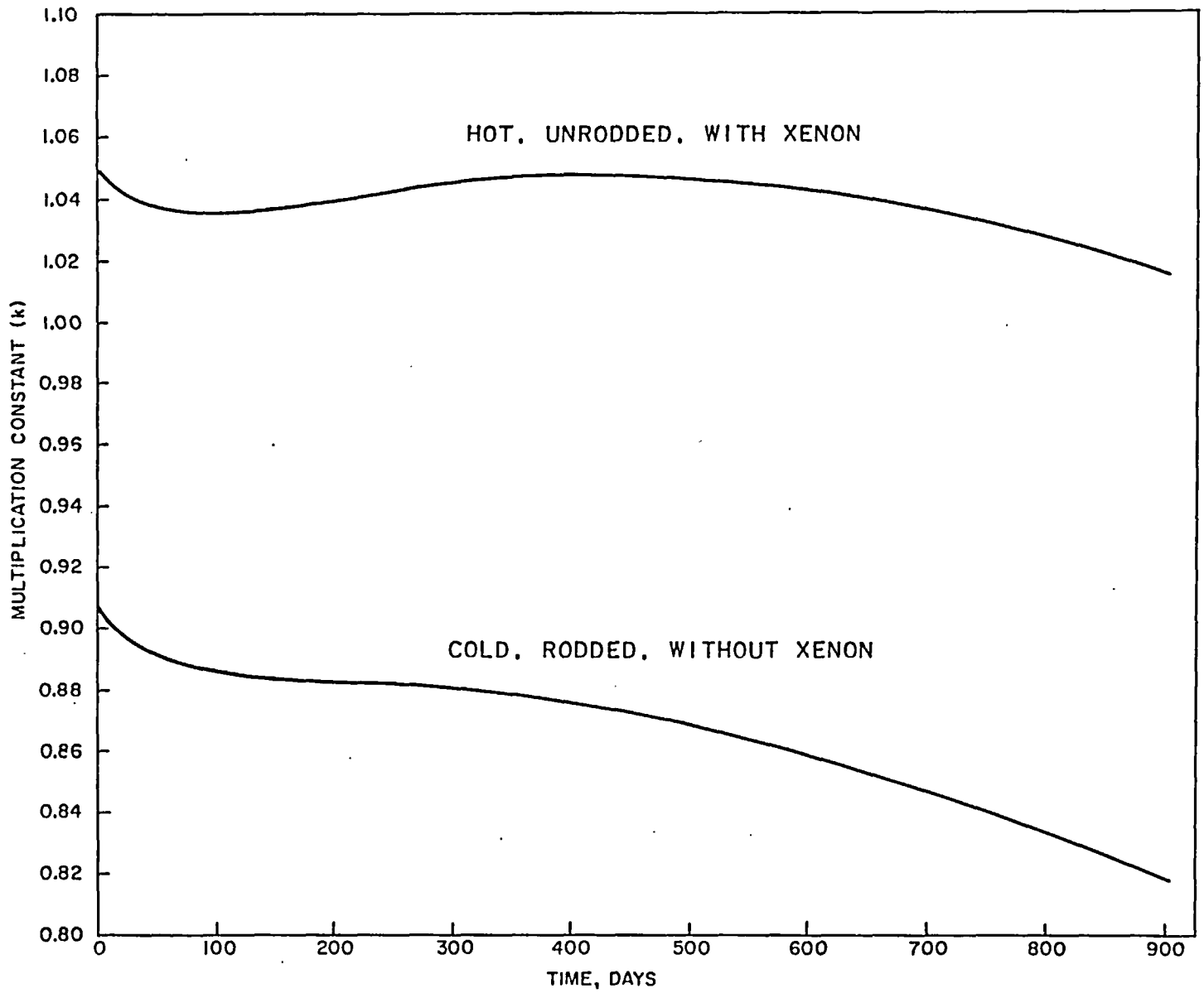

MULTIPLICATION CONSTANT VS. TIME OF OPERATION

FIGURE 9

August, 1961

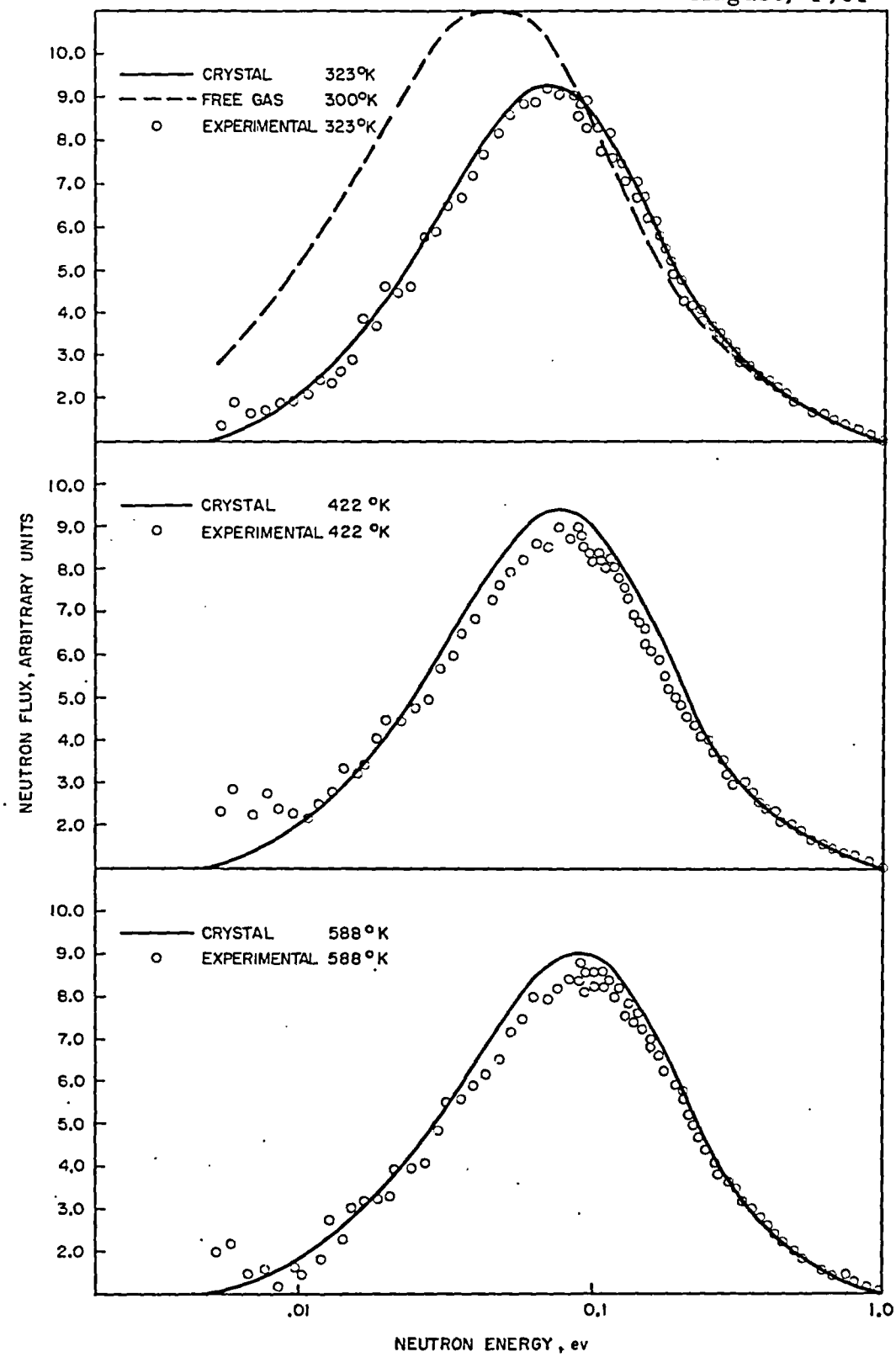

COMPARISON OF VALUES OF THE NEUTRON FLUX IN A POISONED GRAPHITE BLOCK WITH CALCULATED SPECTRA USING A FREE GAS MODEL AND THE PARKS CRYSTAL MODEL

FIGURE 10

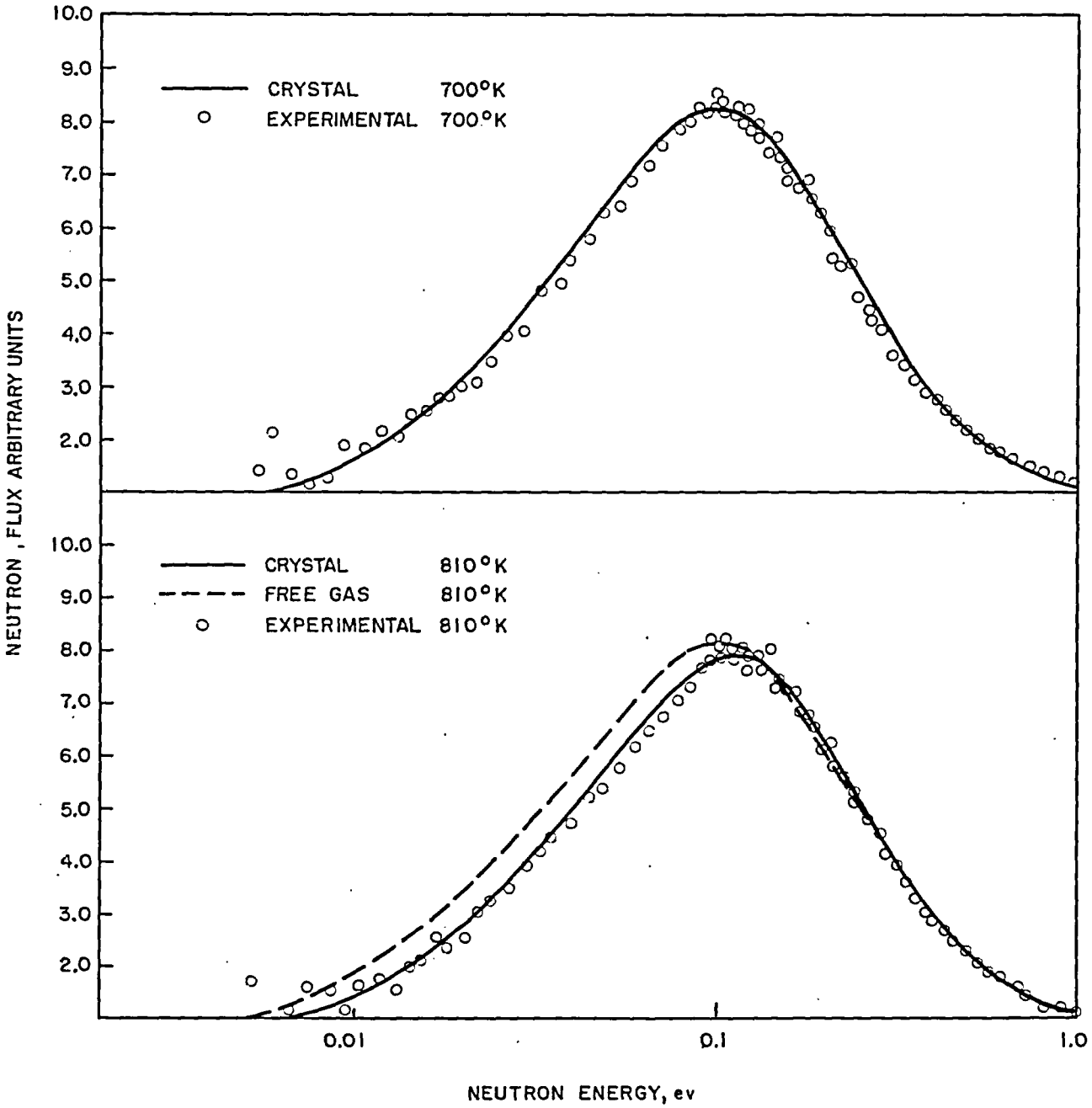

COMPARISON OF VALUES OF THE NEUTRON FLUX IN A POISONED GRAPHITE BLOCK WITH CALCULATED SPECTRA USING A FREE GAS MODEL AND THE PARKS CRYSTAL MODEL

FIGURE 11

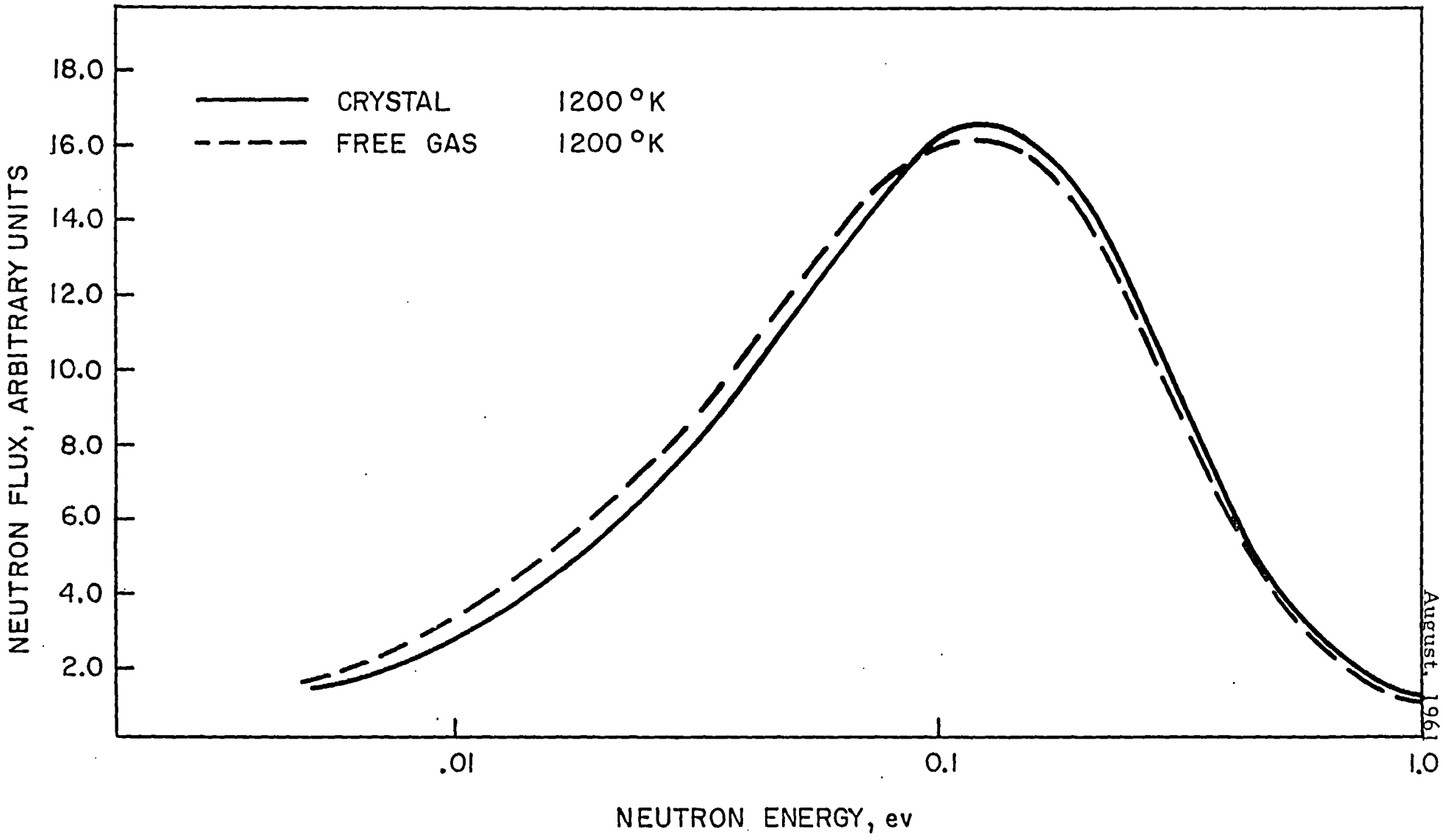

FIGURE 12

COMPARISON OF THE FREE GAS MODEL WITH THE PARKS CRYSTAL MODEL FOR AN HTGR LATTICE

August, 1961

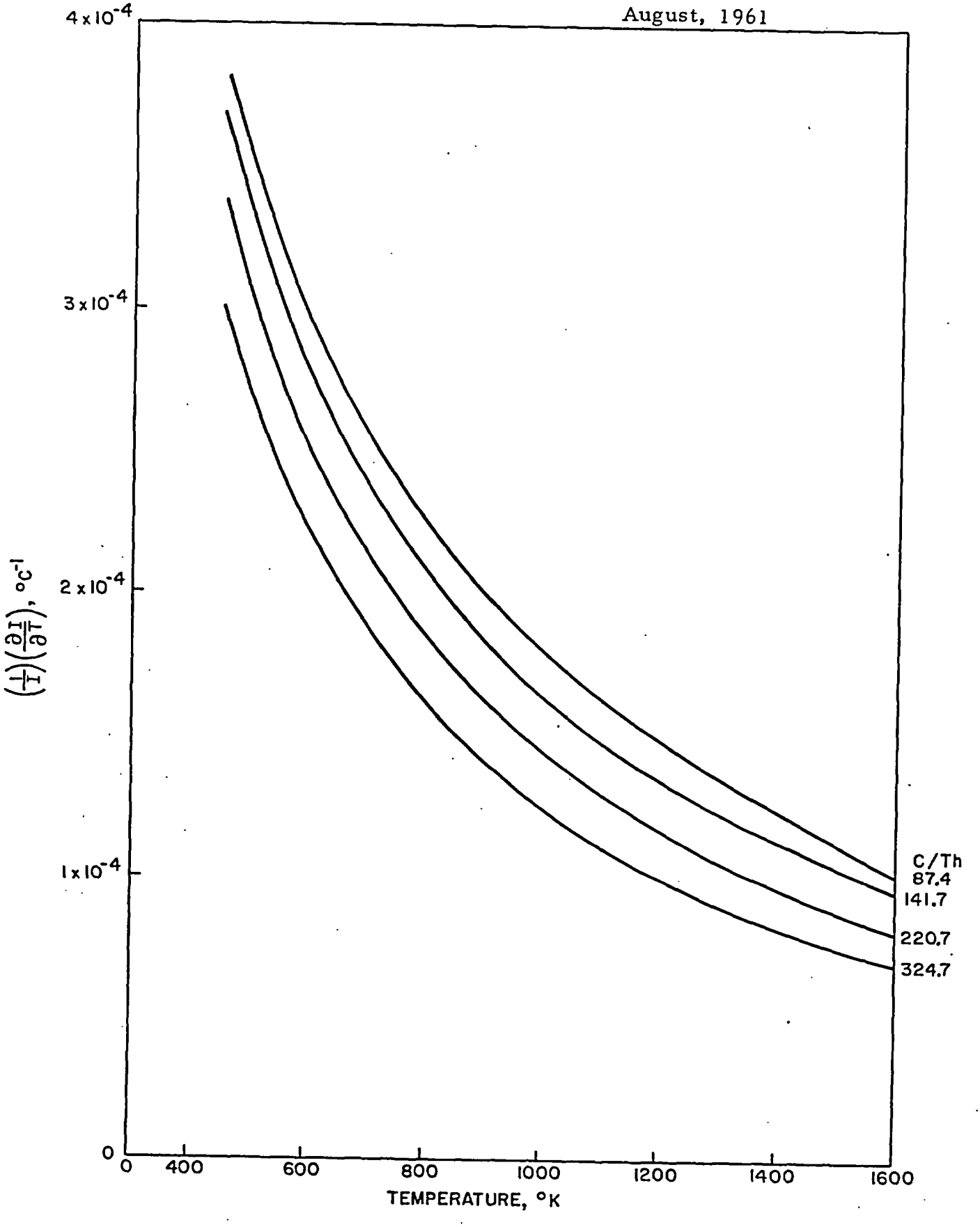

VALUES OF (1/I)(∂I/∂T) VS. TEMPERATURE FOR TH-232

FIGURE 13

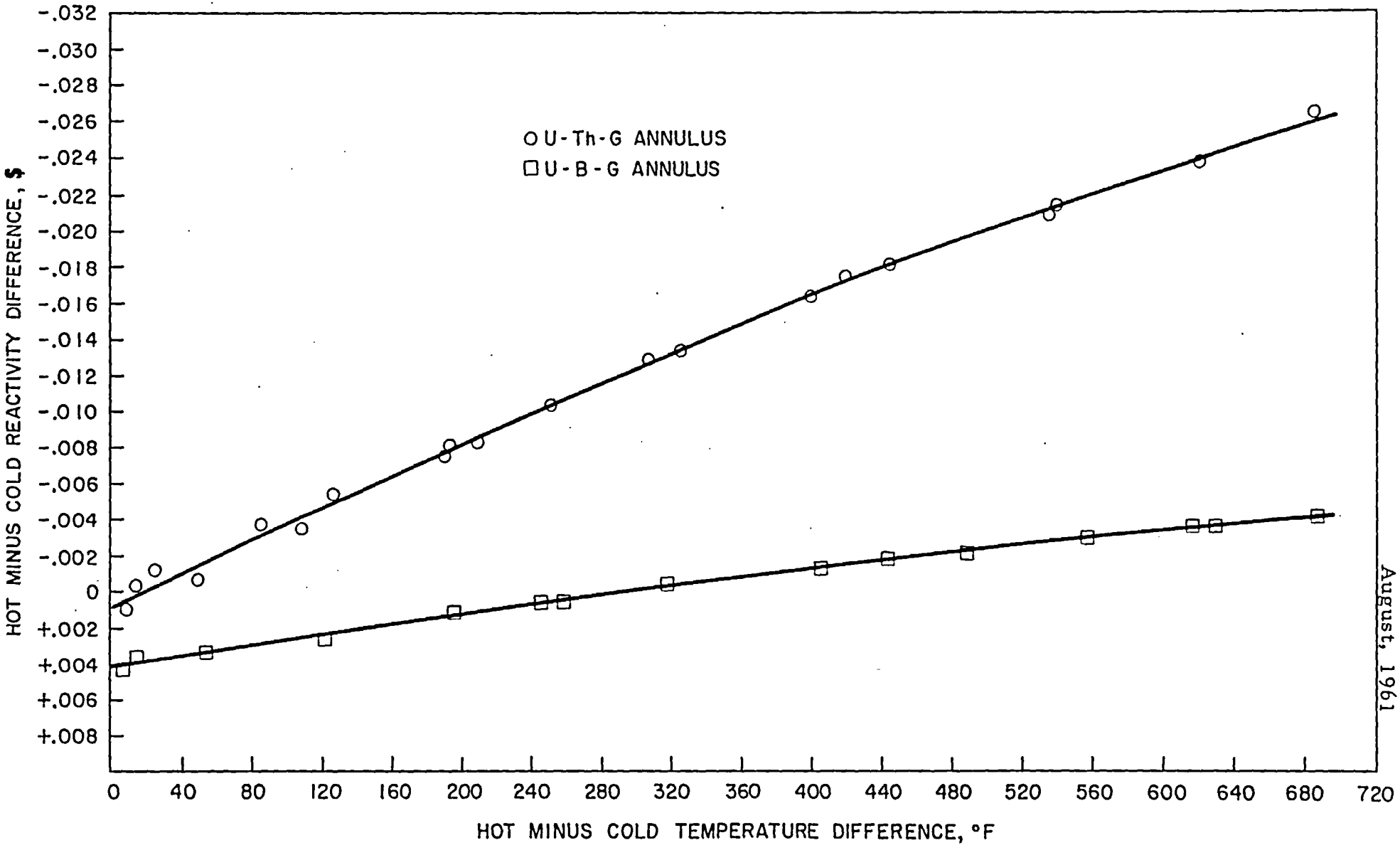

REACTIVITY CHANGE WITH HEATING

August, 1961

FIGURE 14

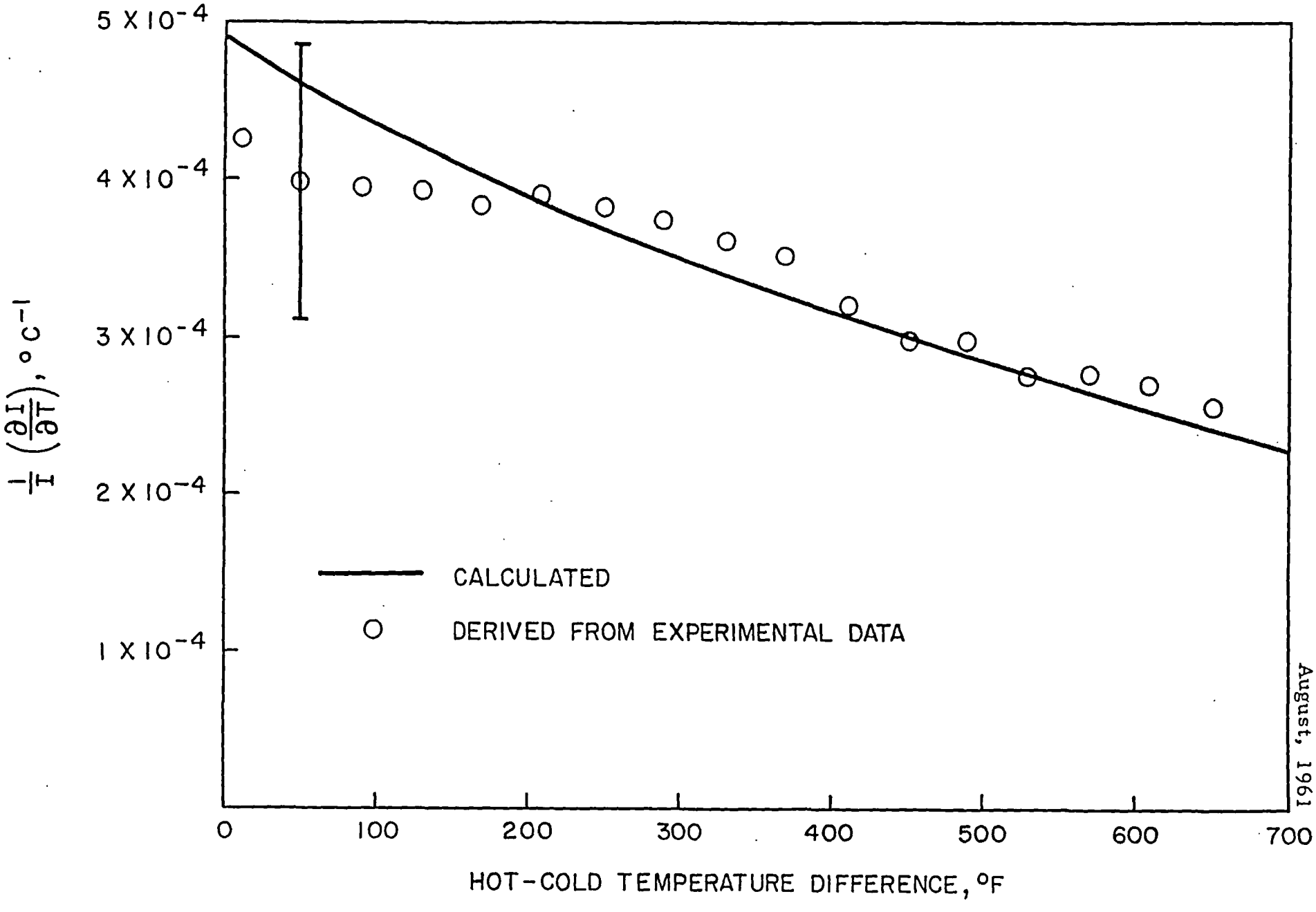

August, 1961

FIGURE 15

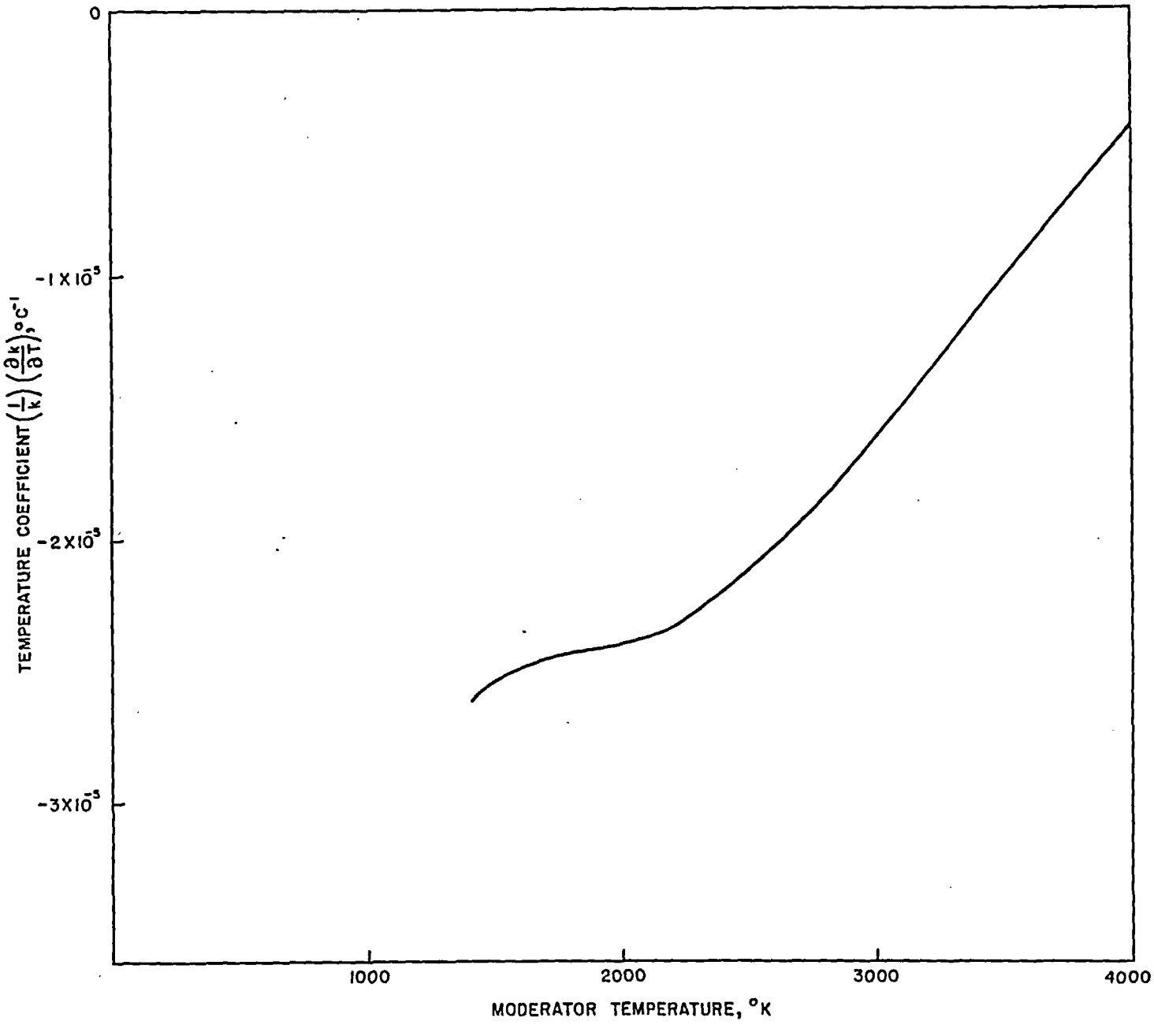

VARIATION OF OVER-ALL TEMPERATURE COEFFICIENT VS. TEMPERATURE
AT END OF LIFE WITH XENON PRESENT

FIGURE 16

August, 1961

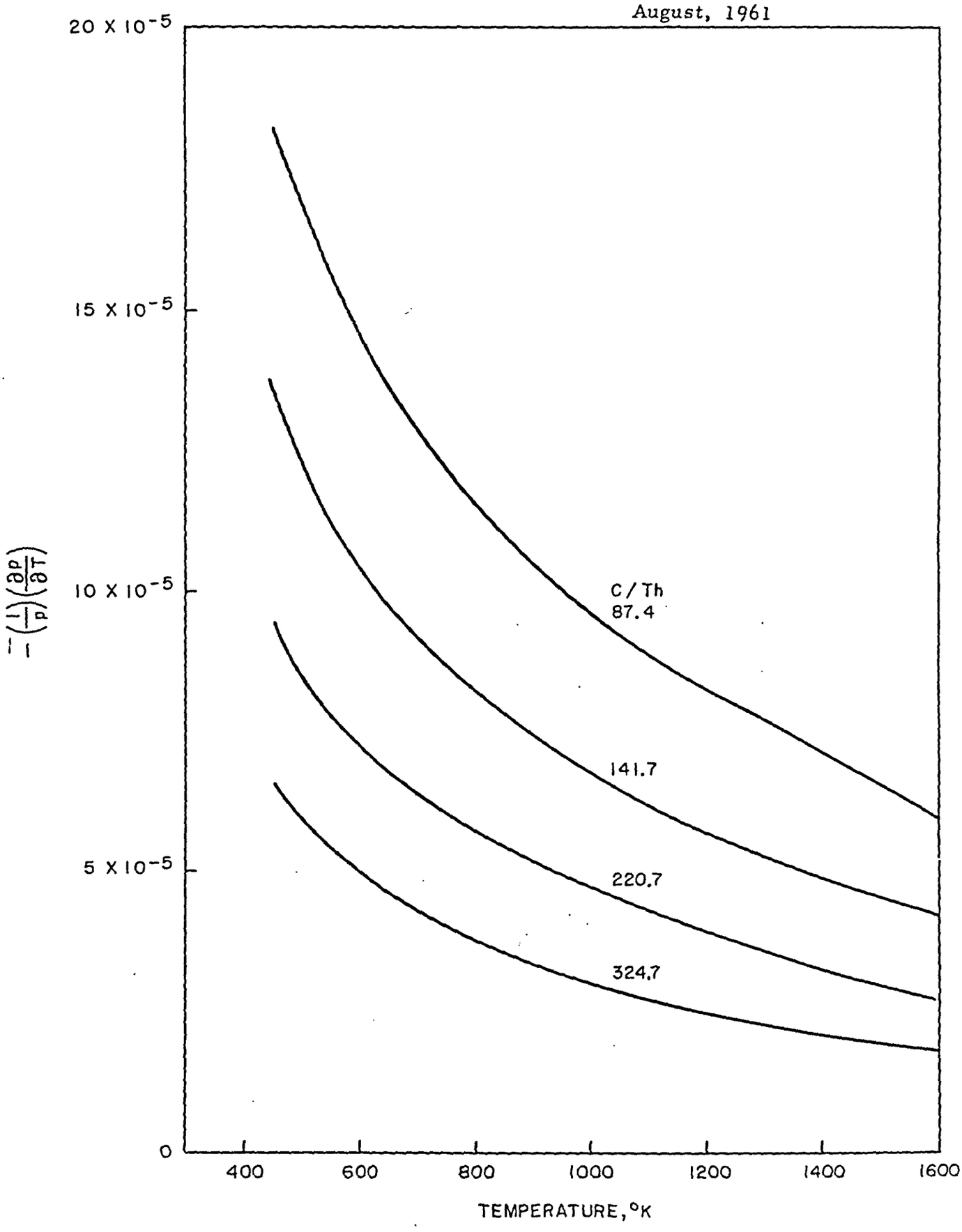

VALUES OF (1/P(∂P/∂T) VS. TEMPERATURE FOR TH-232
AT CARBON-TO-THORIUM RATIOS INDICATED

FIGURE 17

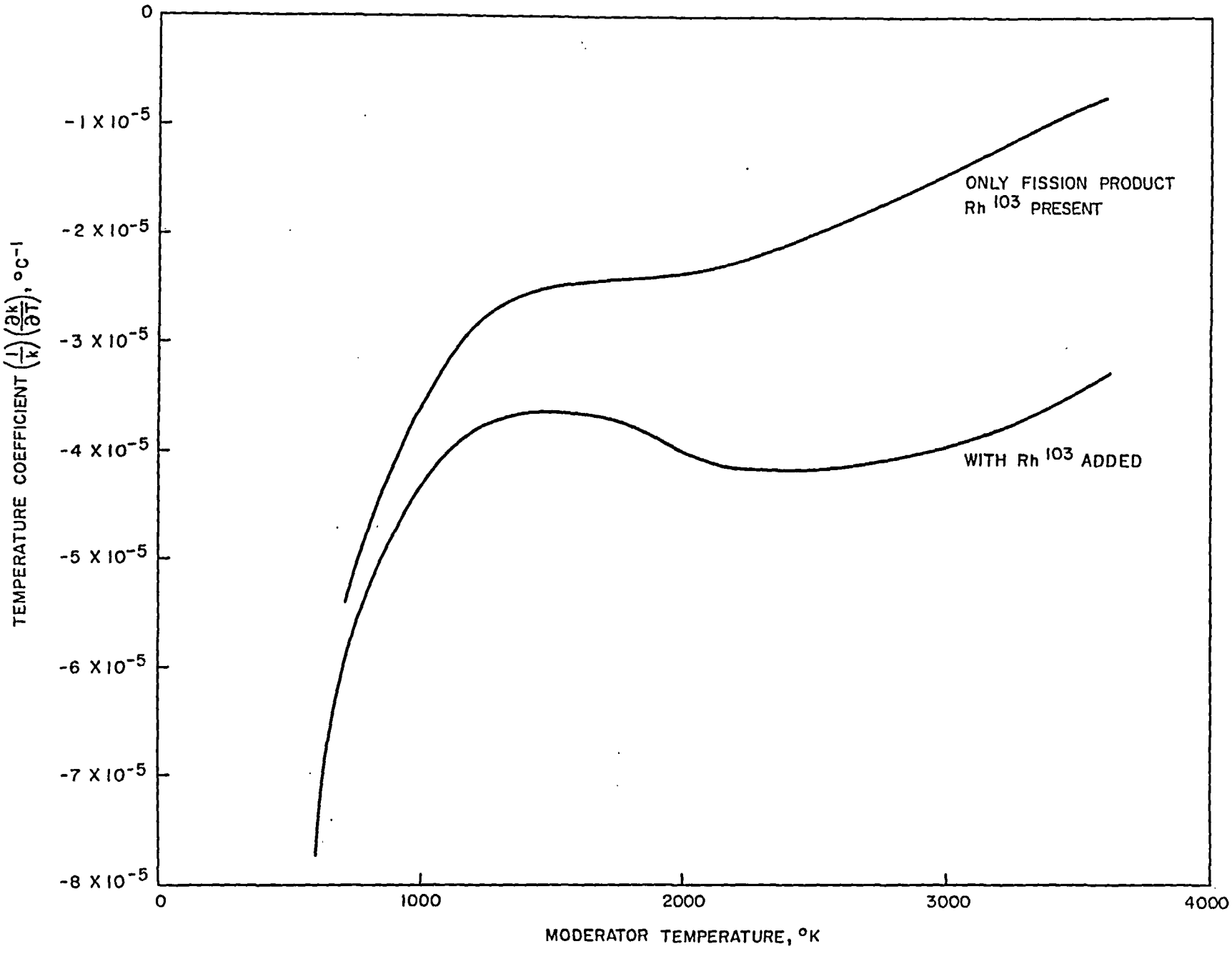

FIGURE 18

VARIATION OF OVER-ALL TEMPERATURE COEFFICIENT
VS. TEMPERATURE AT END OF LIFE

August, 1961

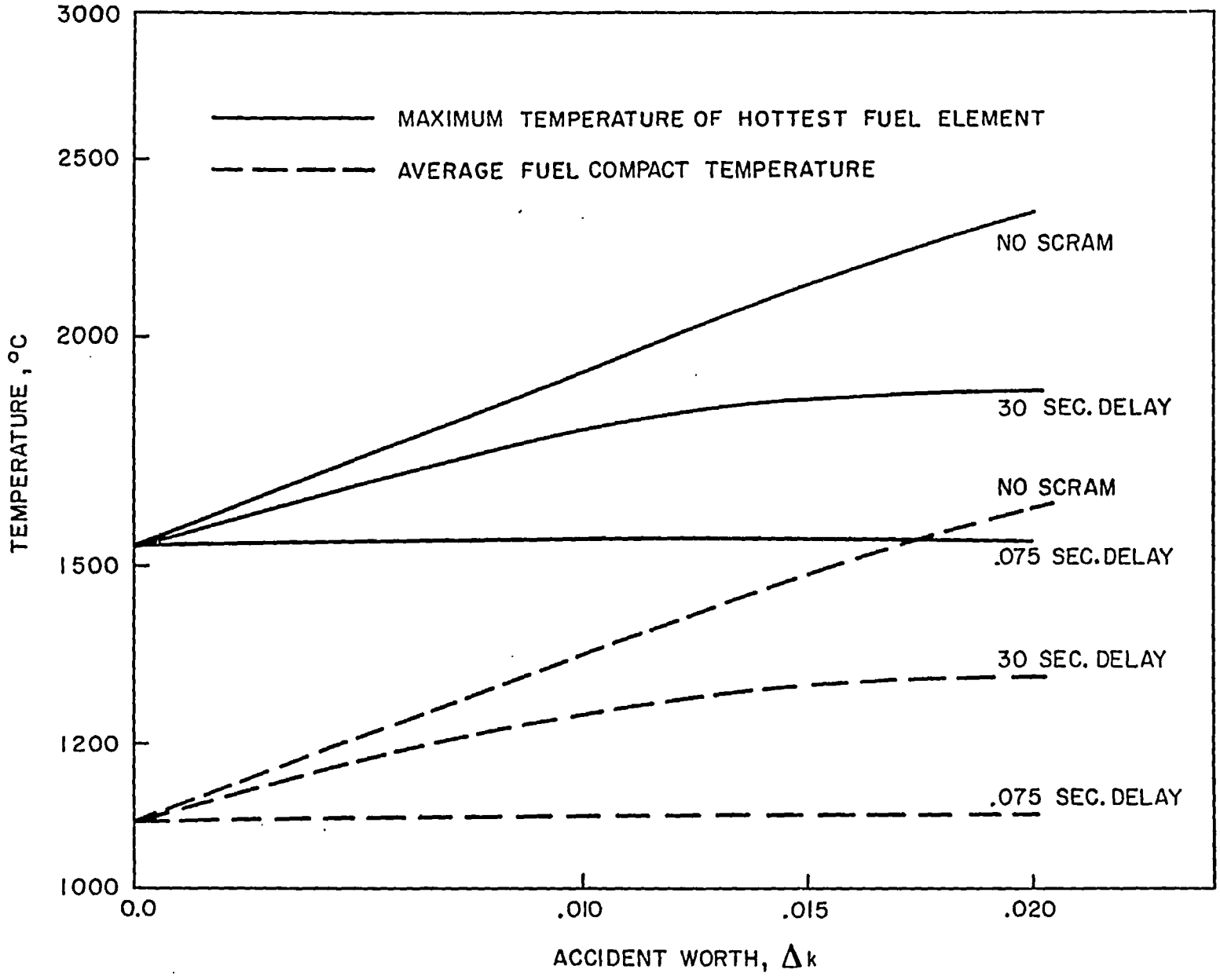

PEAK FUEL COMPACT TEMPERATURES FOLLOWING RAMP INSERTIONS CORRESPONDING TO MAXIMUM ROD REMOVAL RATE (0.06 FT/ SEC) FOR VARIOUS DELAY TIMES: END OF LIFE; NO XENON PRESENT: NORMAL OPERATING POWER. SCRAM AT 140% NORMAL POWER

FIGURE 19

August, 1961

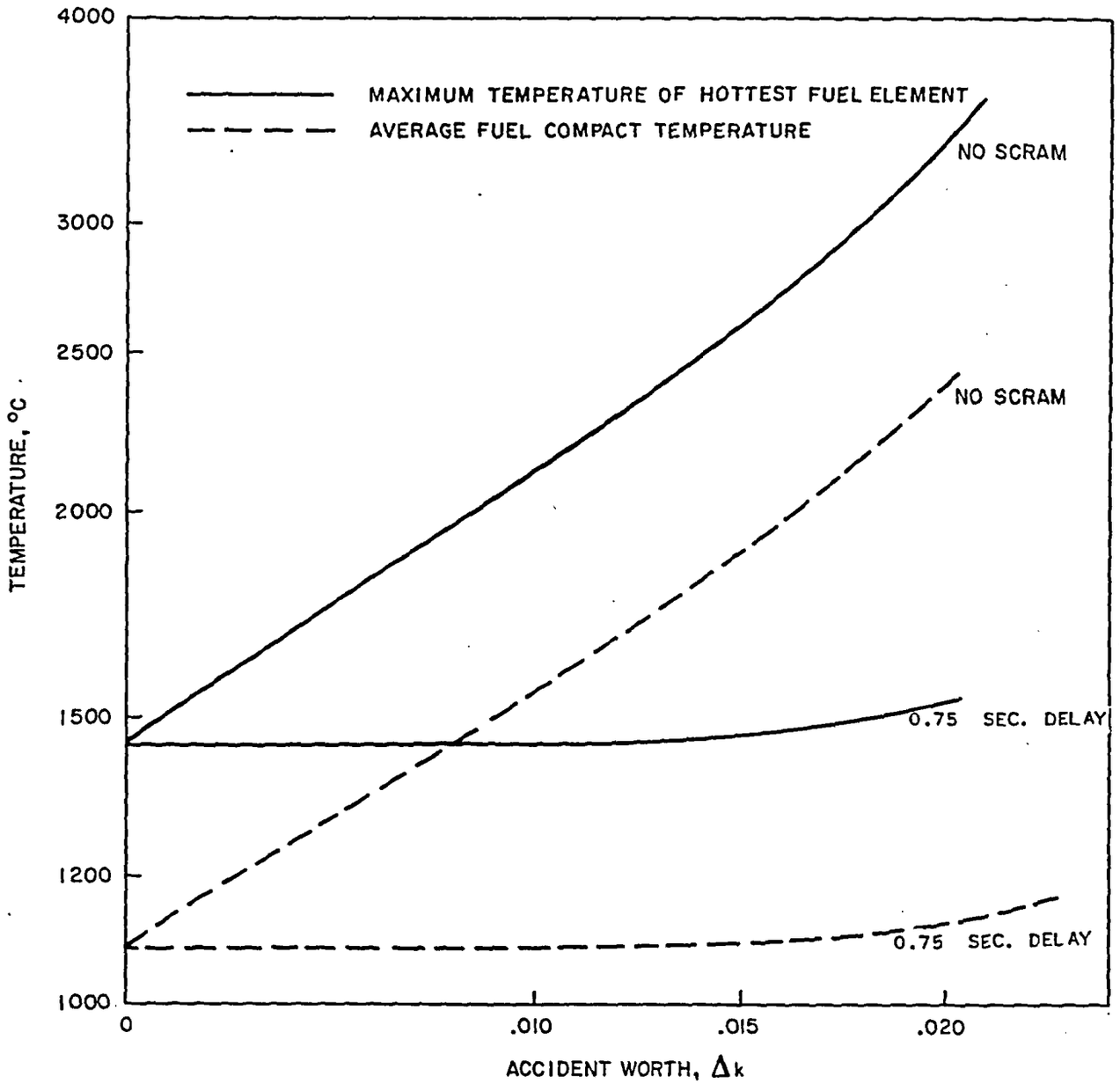

PEAK FUEL COMPACT TEMPERATURES VS. SCRAM DELAY TIME:
1.0g ROD DROP: NORMAL OPERATING POWER:
SCRAM AT 140% NORMAL POWER

FIGURE 20

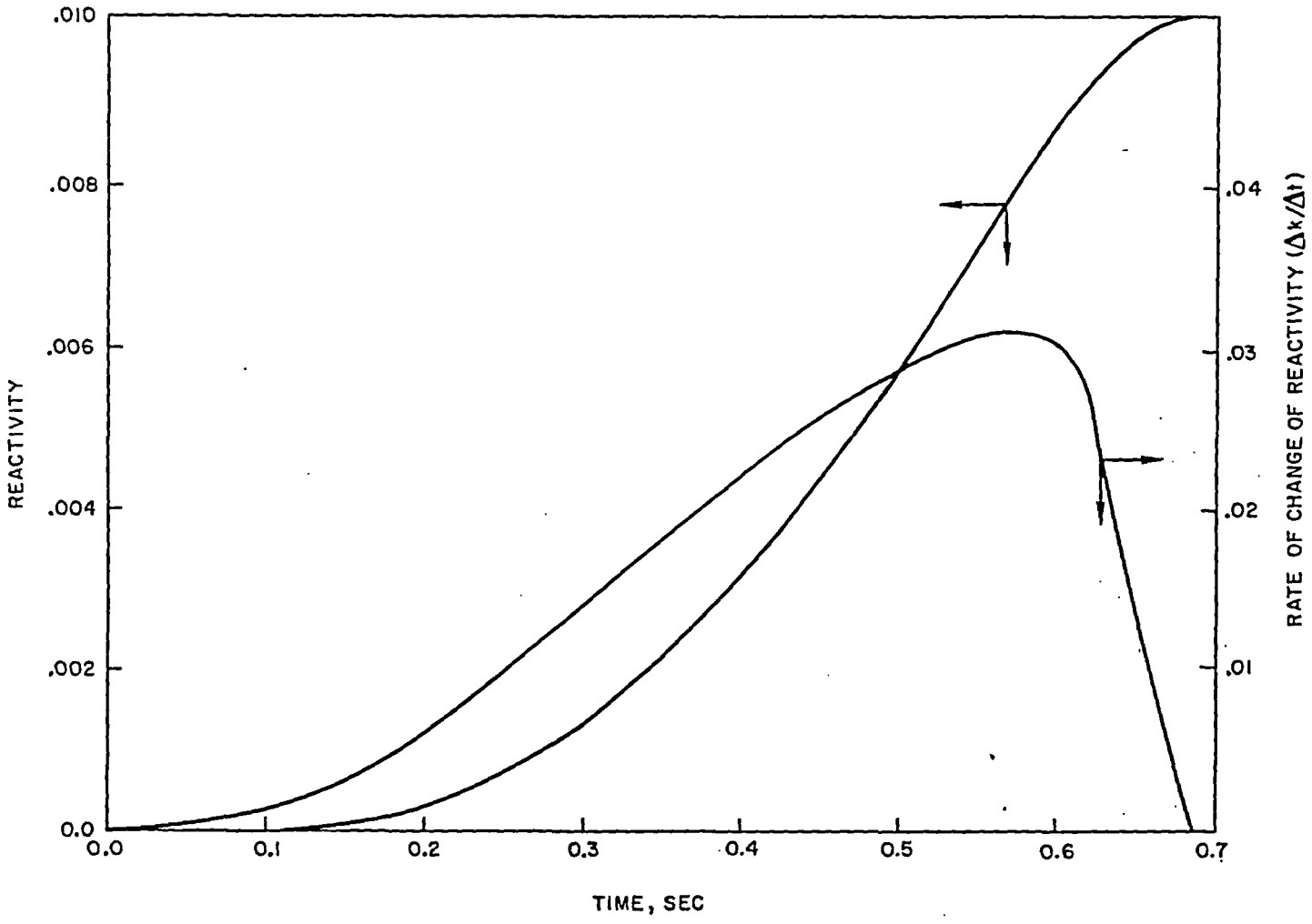

REACTIVITY ADDED BY ROD FALL VS. TIME AND RATE OF CHANGE OF REACTIVITY VS. TIME FOR 1.0g ROD FALL; NORMALIZED TO .01 Δk

FIGURE 21

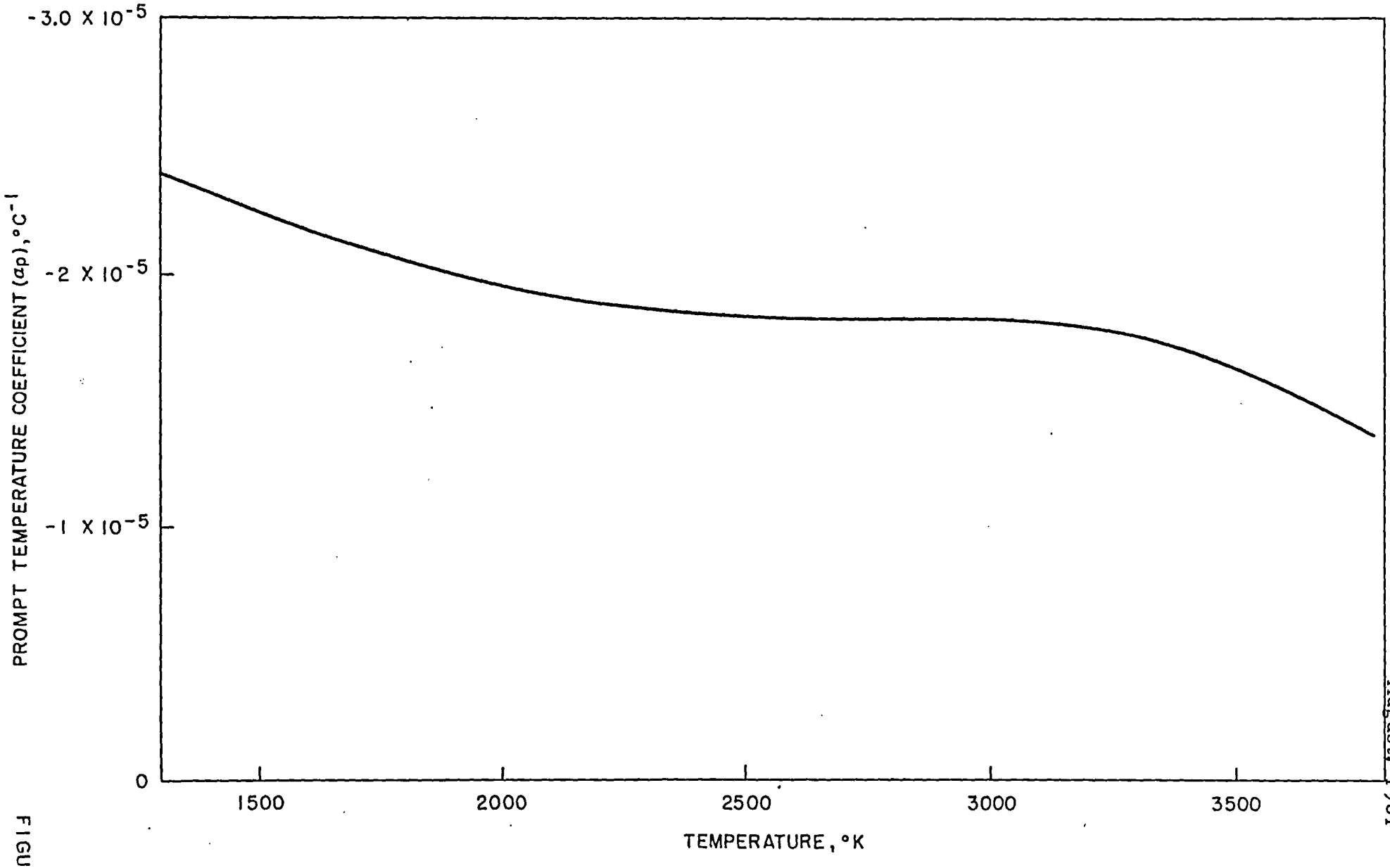

FIGURE 22

PROMPT TEMPERATURE COEFFICIENT AT END OF LIFE:
WITH EQUILIBRIUM XENON AND SAMARIUM AND
ADDED RHODIUM

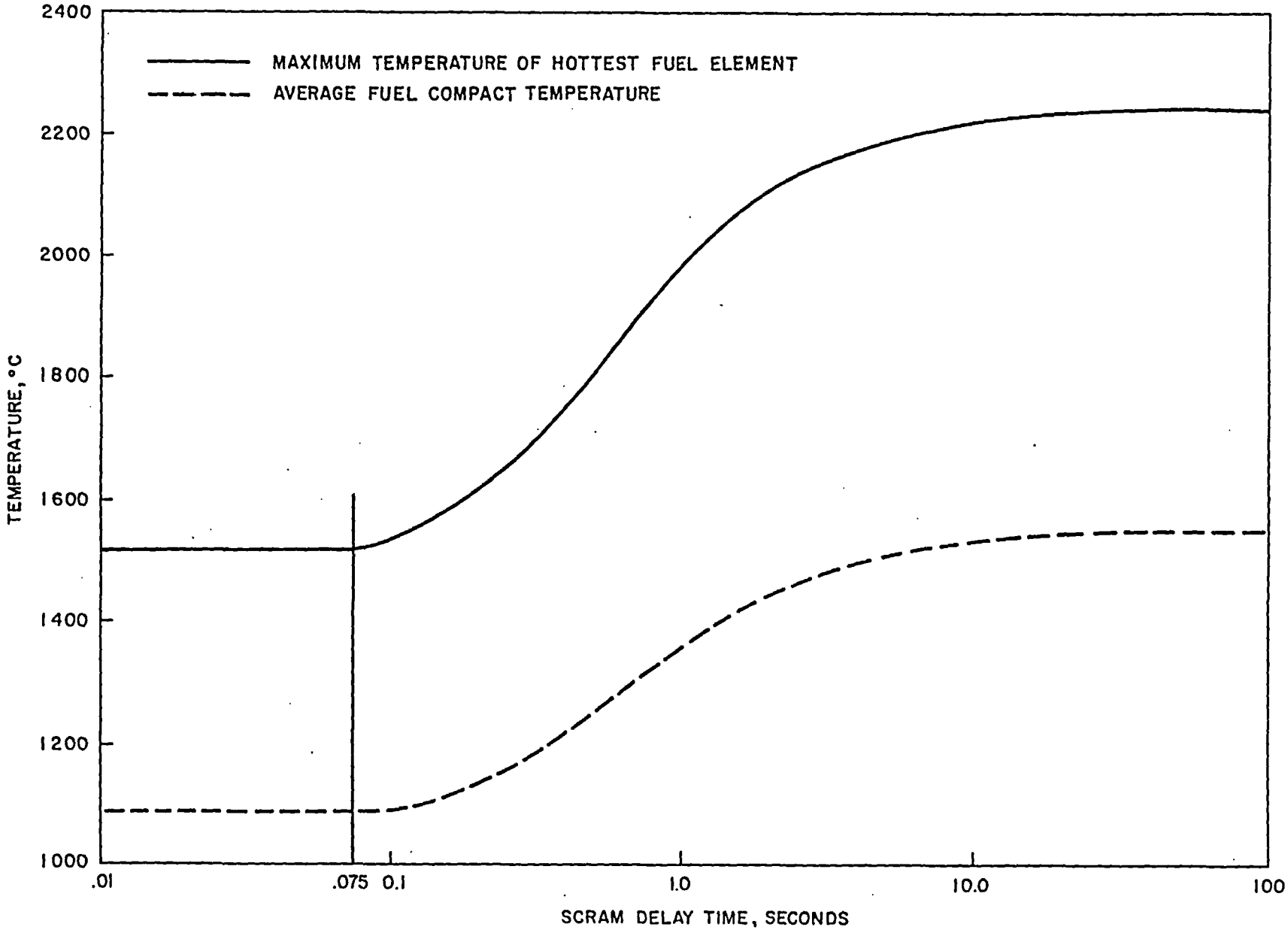

PEAK FUEL COMPACT TEMPERATURES FOLLOWING 1.0g ROD FALL:
END OF LIFE: XENON PRESENT: NORMAL OPERATING POWER.
SCRAM AT 140% NORMAL POWER

FIGURE 23

August, 1961

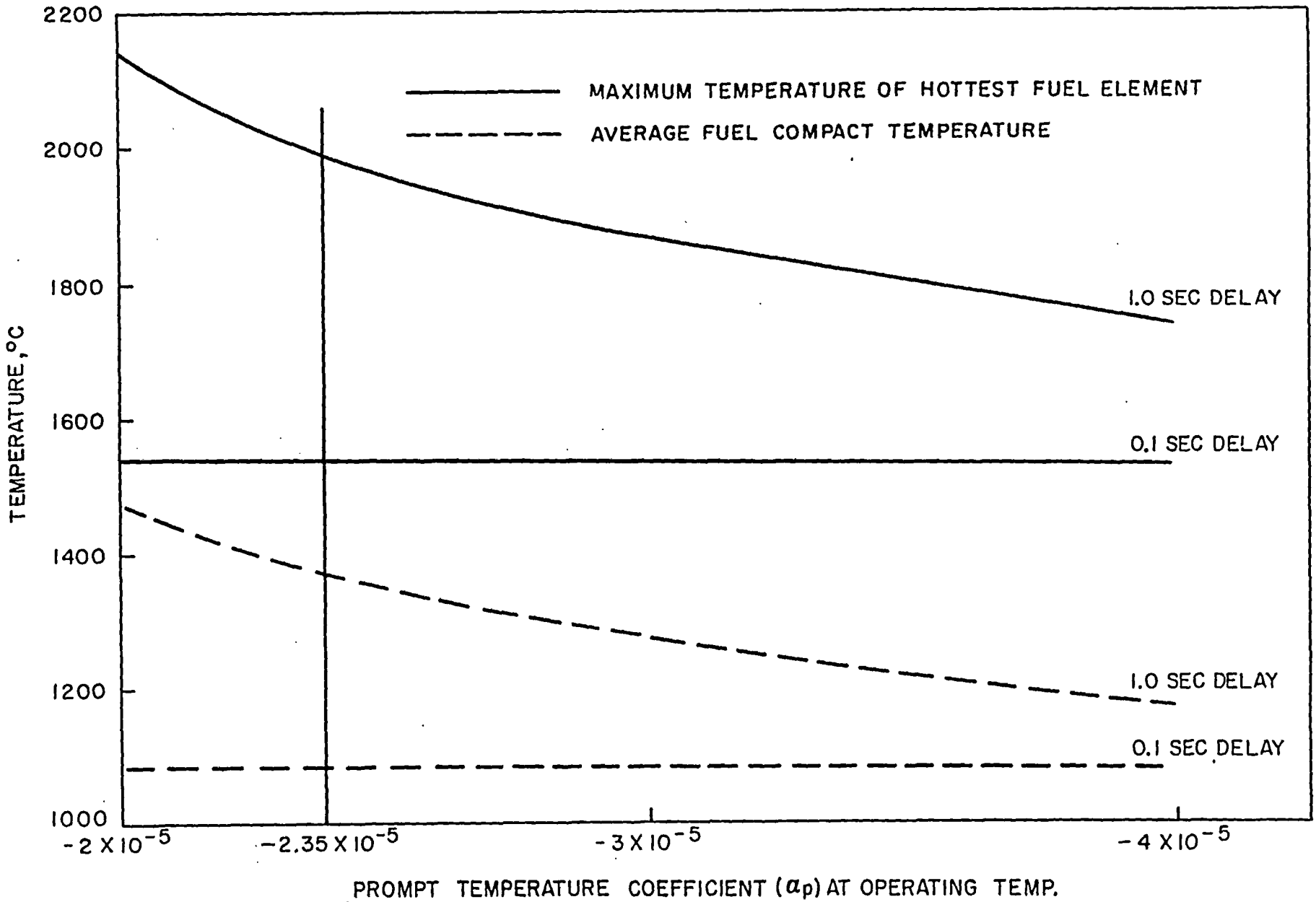

PEAK FUEL COMPACT TEMPERATURES VS. MAGNITUDE OF PROMPT TEMPERATURE COEFFICIENT FOLLOWING 1.0g ROD FALL. NORMAL OPERATING POWER: SCRAM AT 140% NORMAL POWER

FIGURE 24

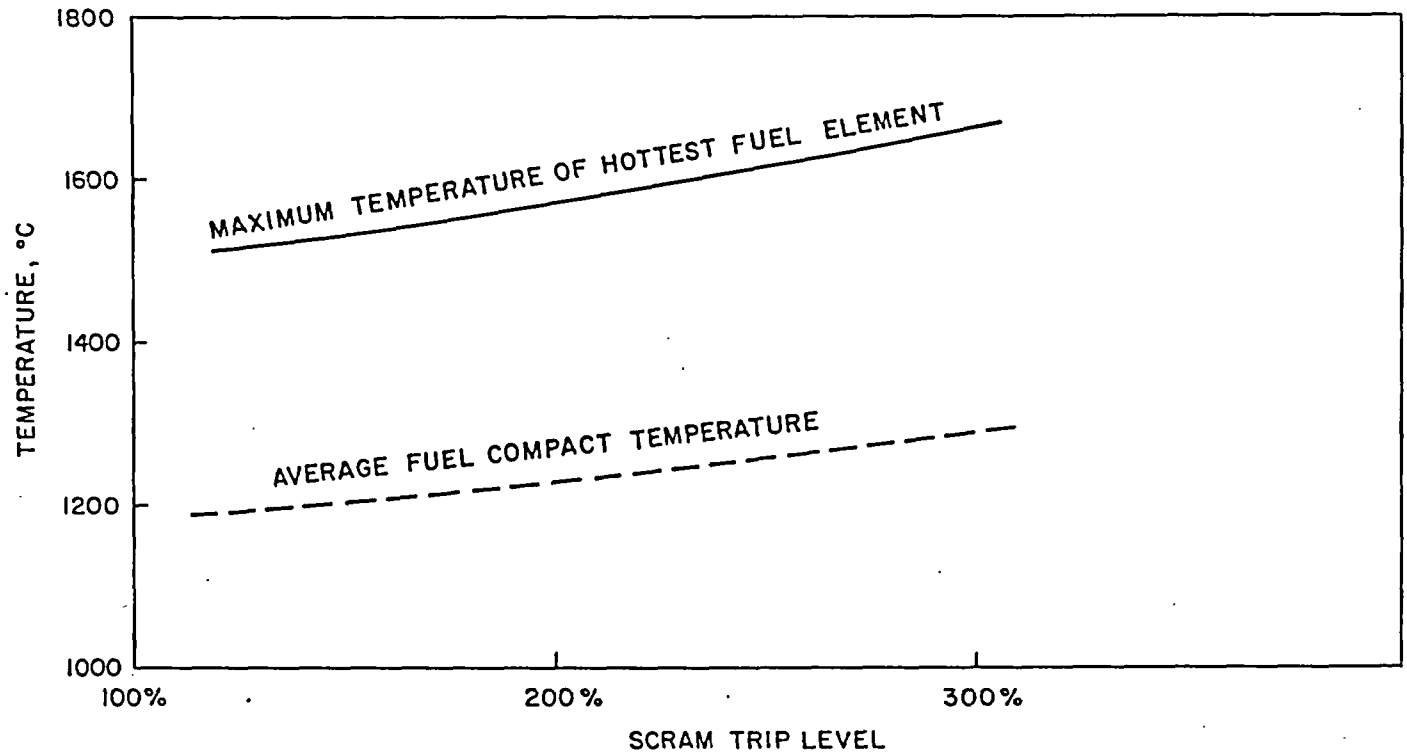

PEAK FUEL COMPACT TEMPERATURES VS. SCRAM TRIP LEVEL
FOR A 1.0g ROD FALL: NORMAL OPERATING POWER

FIGURE 25

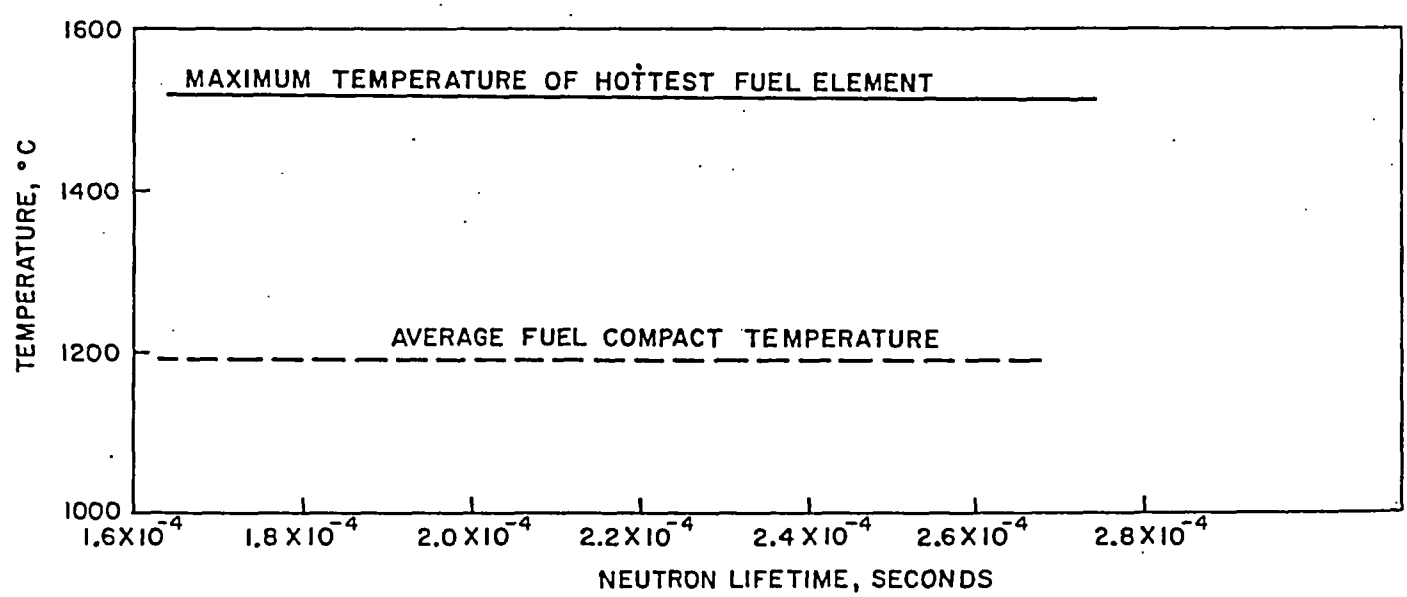

PEAK FUEL COMPACT TEMPERATURES VS. NEUTRON LIFETIME
FOR A 1.0g ROD FALL: NORMAL OPERATING POWER:
SCRAM AT 140% NORMAL POWER

FIGURE 26

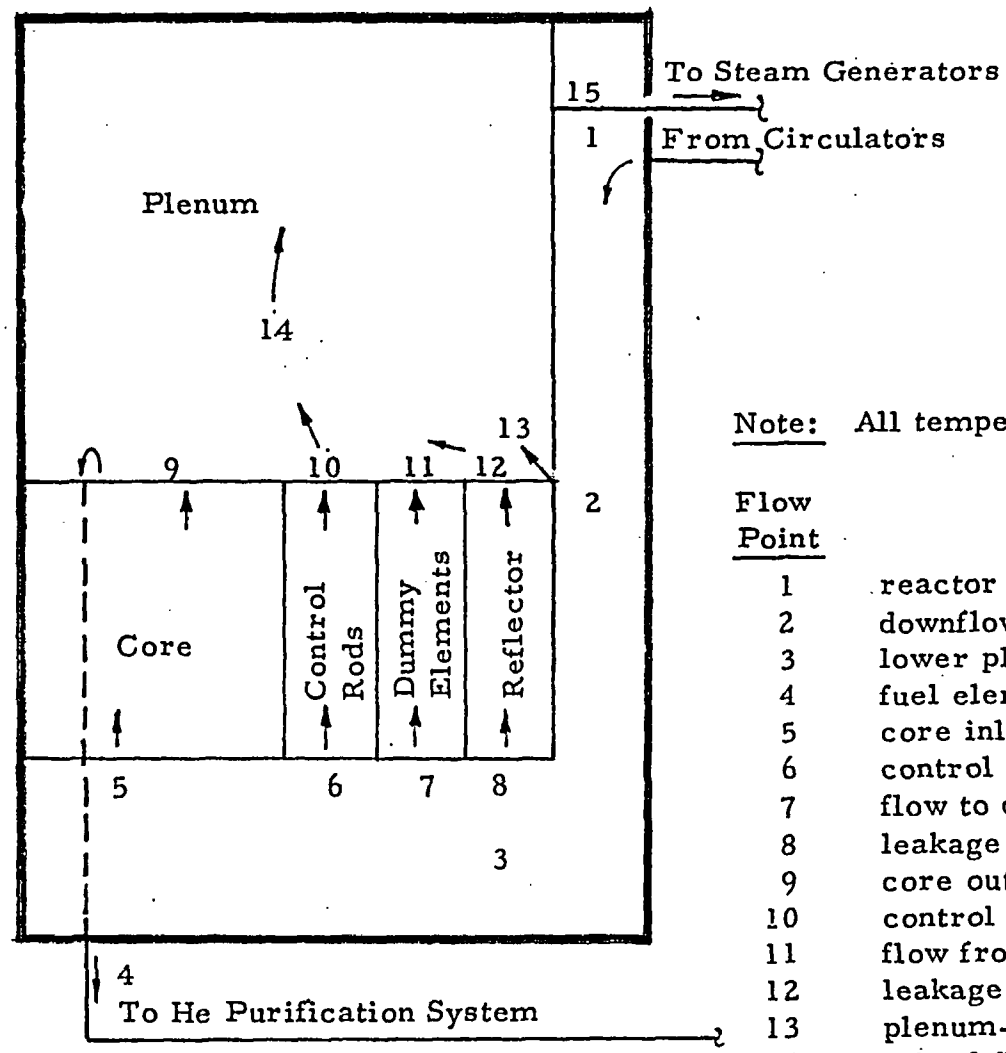

KEY TO FLOW DIAGRAM

Note: All temperatures are rounded off to the nearest integer.

Flow Point	Description	Flow Rate, lb/hr	Temperature oF
1	reactor inlet	440,200	634
2	downflow past reflector	438,600	642
3	lower plenum	438,600	654
4	fuel element purge	1,000	700
5	core inlet	418,450	654
6	control rod coolant inlet	12,250	654
7	flow to dummy elements	4,700	654
8	leakage through reflector, in	3,200	654
9	core outlet	417,450	1380
10	control rod coolant outlet	12,250	850
11	flow from dummy elements	4,700	1200
12	leakage through reflector, out	3,200	1100
13	plenum-to-reflector seal leakage	1,600	642
14	mixed flow above core	439,200	1358
15	reactor outlet	439,200	1354

SIMPLIFIED FLOW DIAGRAM SHOWING REACTOR FLOW PATHS

FIGURE 27

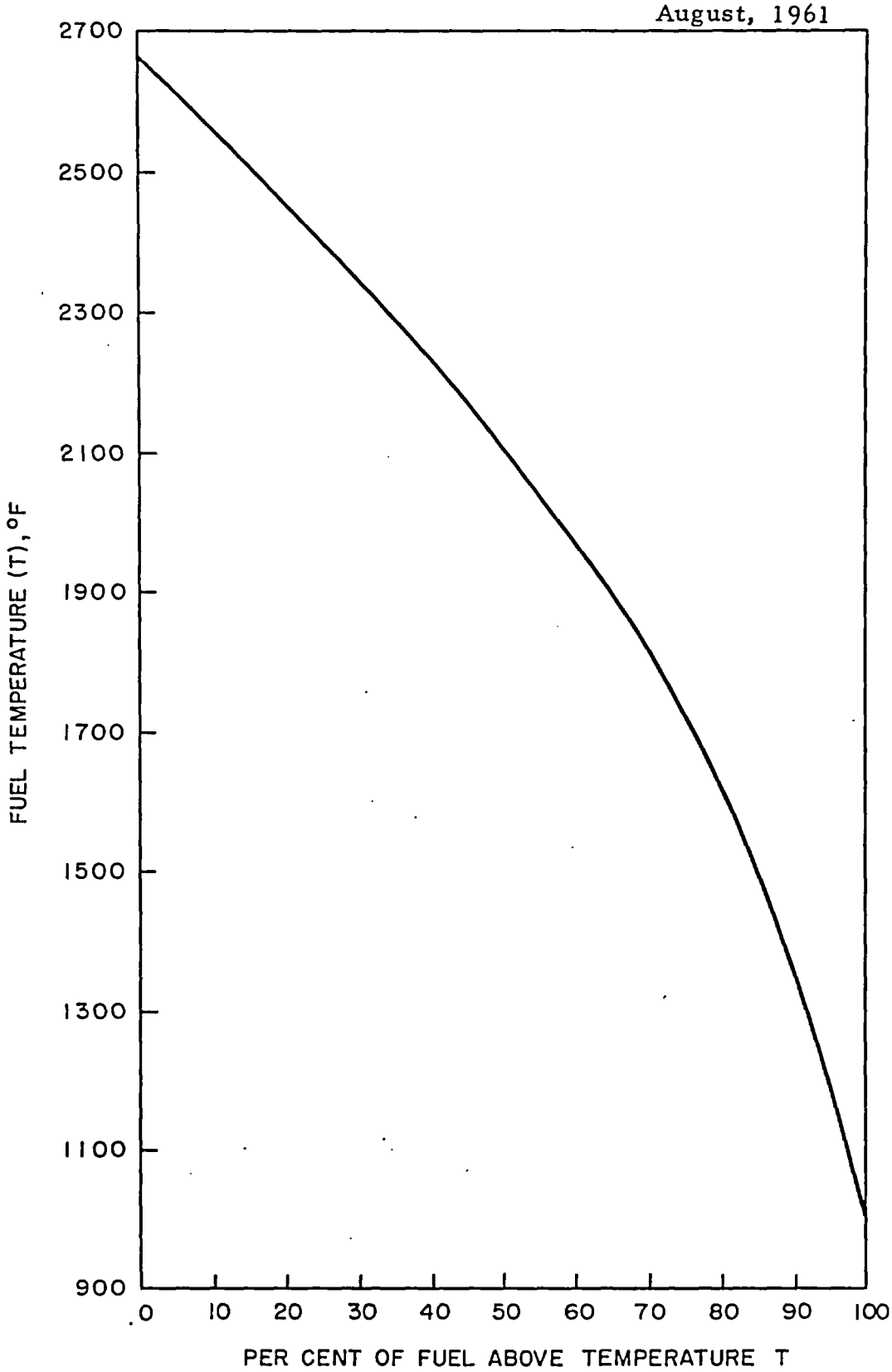

PER CENT OF FUEL COMPACT MATERIAL WHOSE TEMPERATURE IS ABOVE A GIVEN TEMPERATURE T. T IS THE RADIAL AVERAGE TEMPERATURE OF THE FUEL COMPACT

FIGURE 28

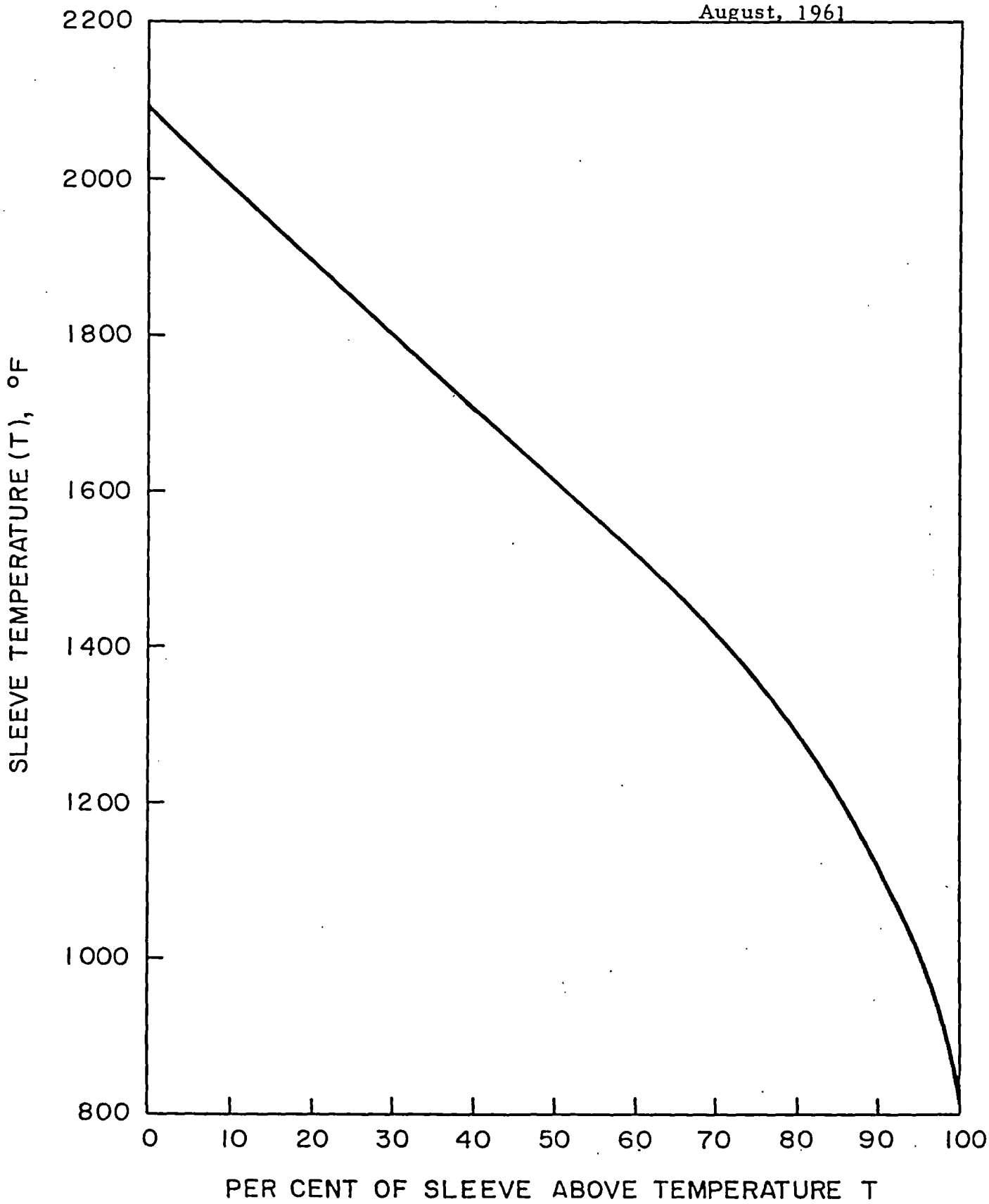

PER CENT OF SLEEVE MATERIAL WHOSE TEMPERATURE IS ABOVE A GIVEN TEMPERATURE T. T IS THE RADIAL AVERAGE TEMPERATURE OF THE SLEEVE

FIGURE 29

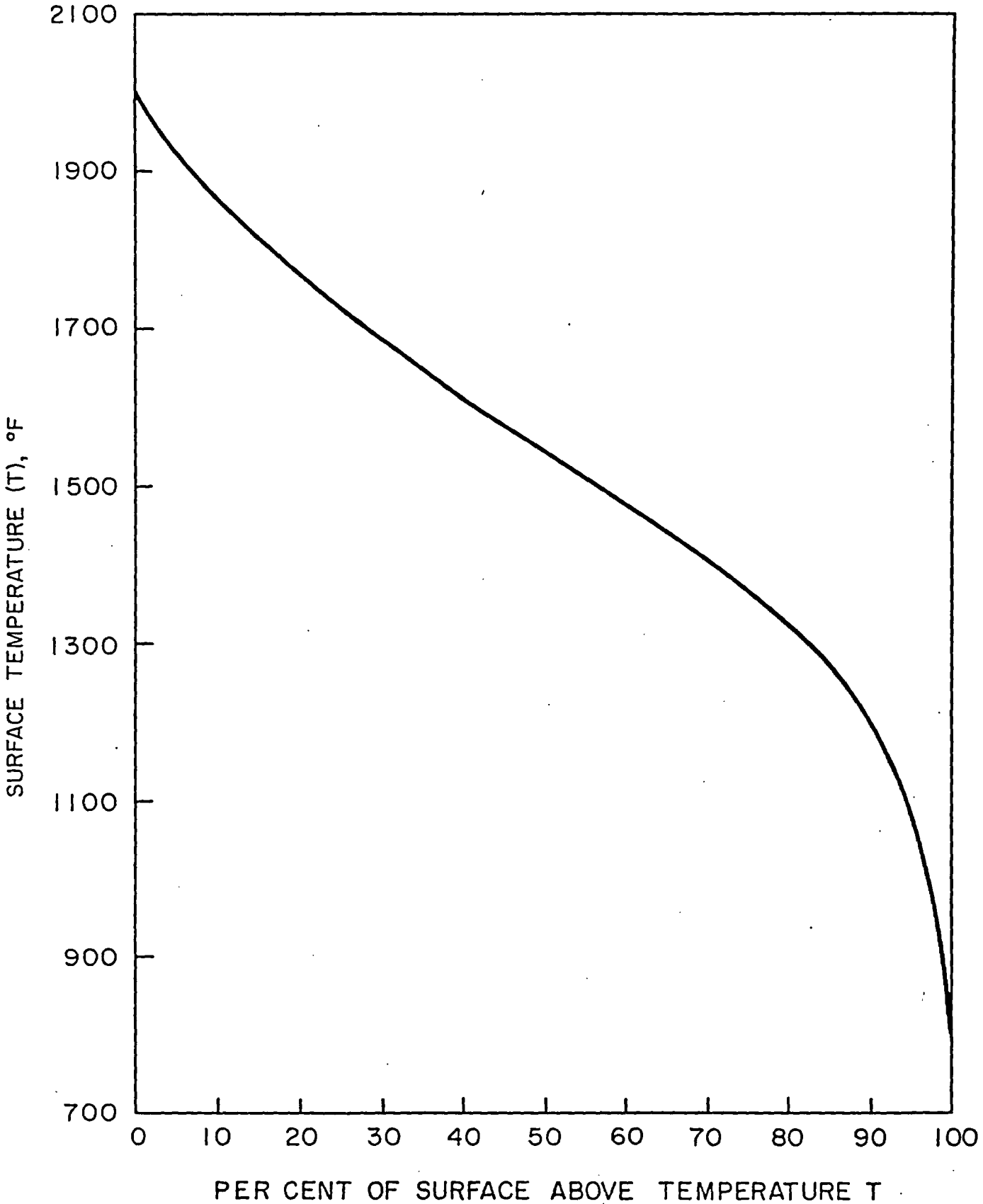

PER CENT OF THE TOTAL FUEL ELEMENT SURFACE AREA WHOSE TEMPERATURE IS ABOVE A GIVEN TEMPERATURE

FIGURE 30

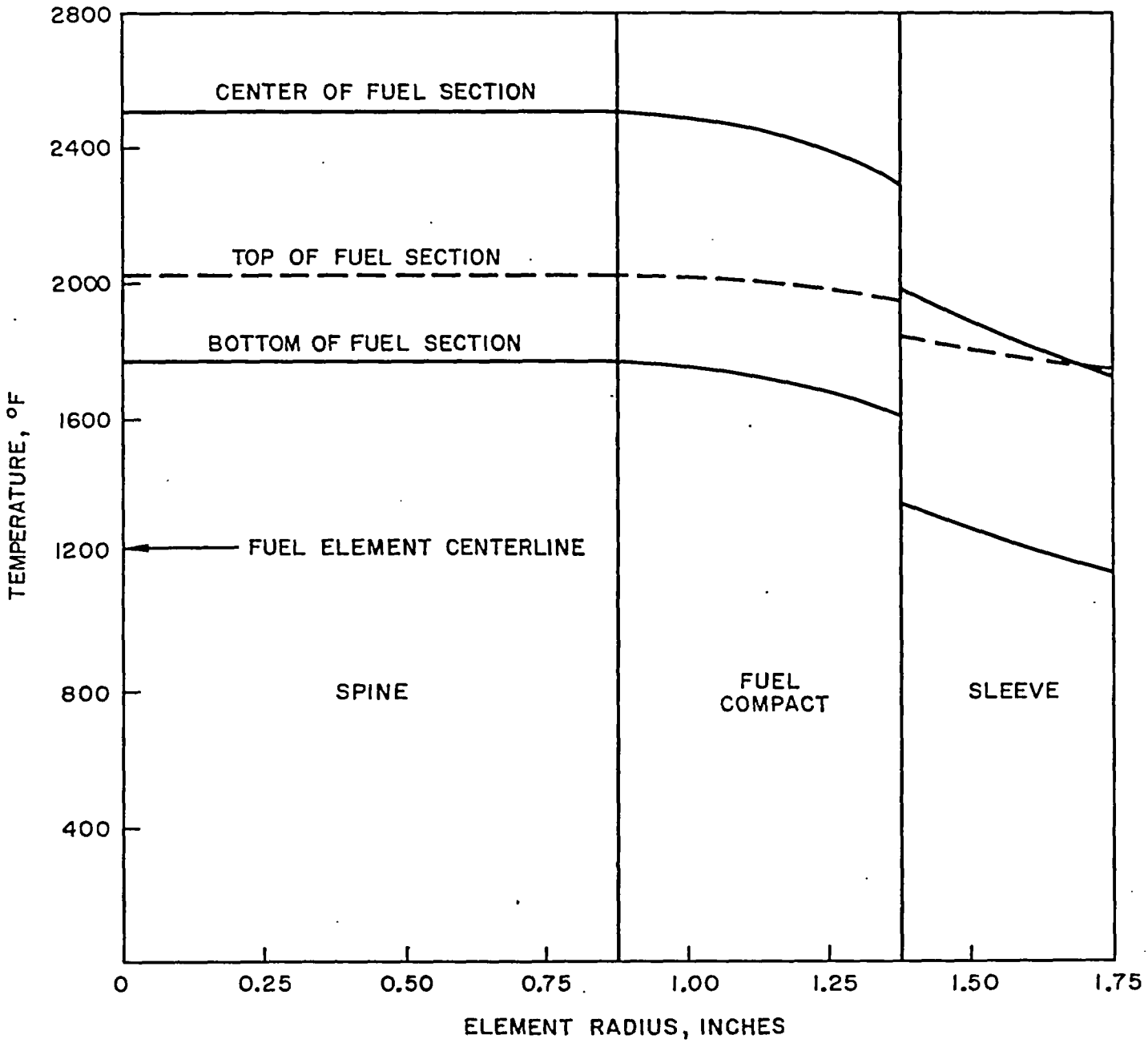

RADIAL TEMPERATURE PROFILES - "AVERAGE" FUEL ELEMENT

FIGURE 31

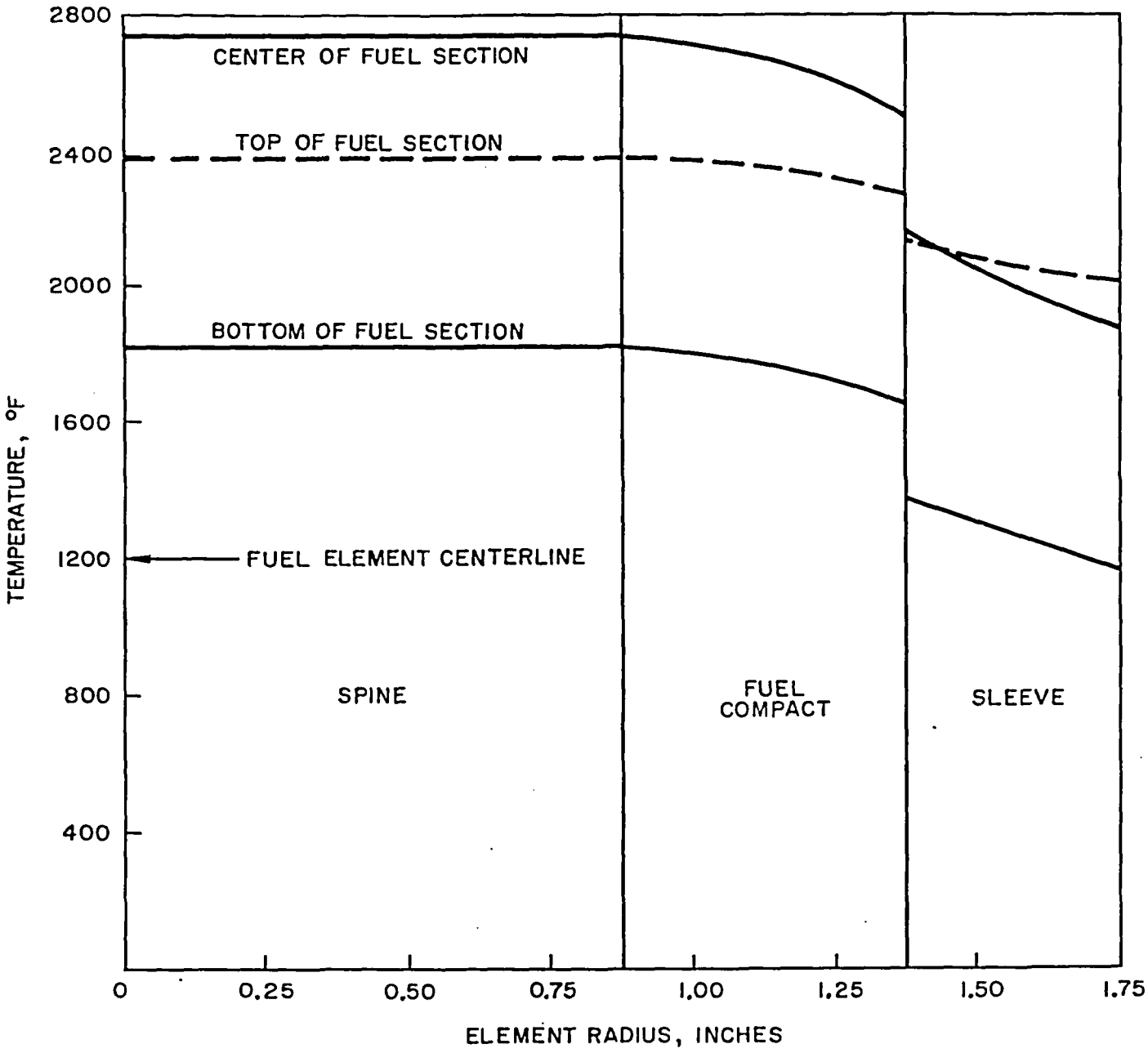

RADIAL TEMPERATURE PROFILES - "HOTTEST" FUEL ELEMENT

FIGURE 32

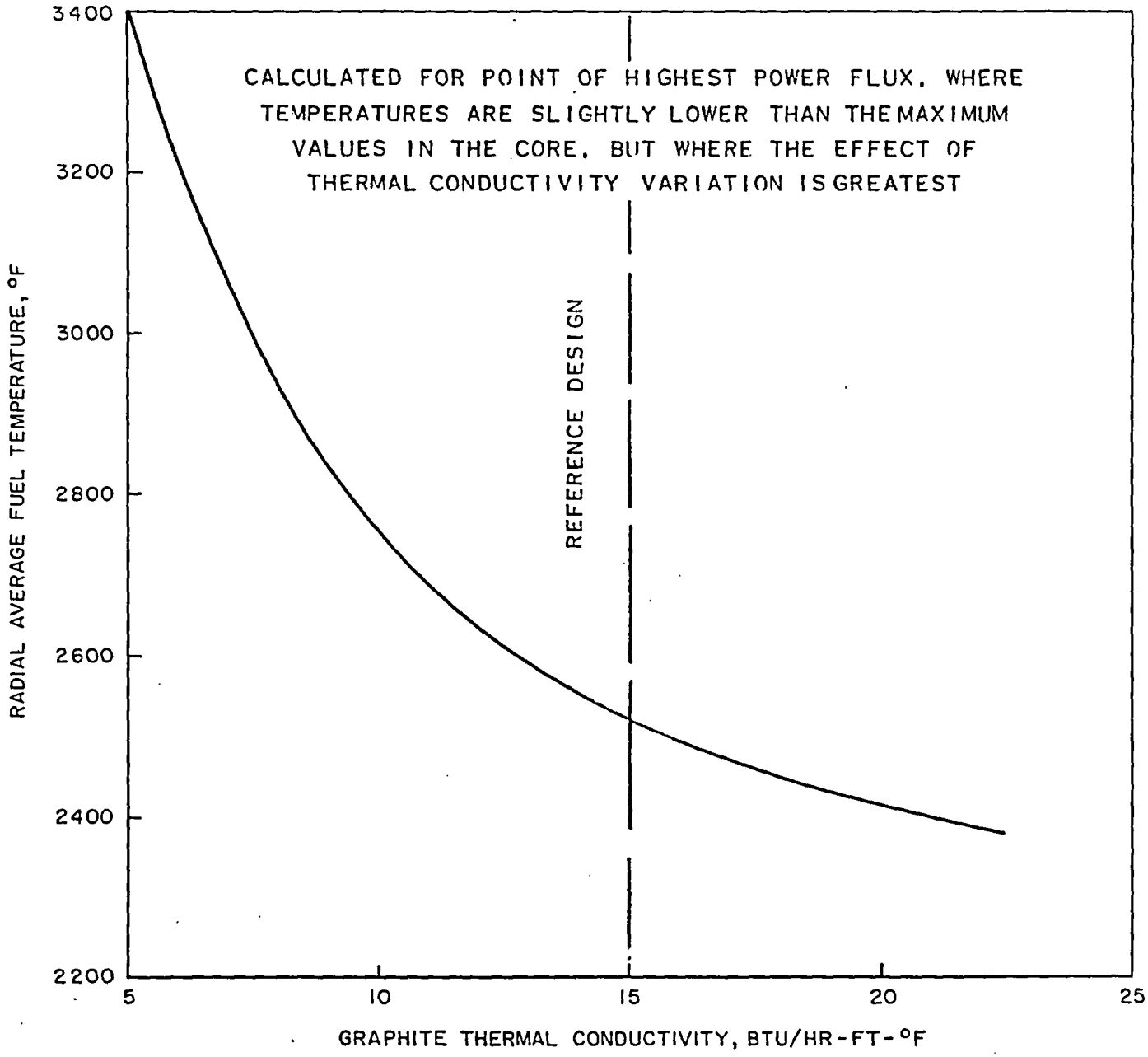

VARIATION IN FUEL TEMPERATURE WITH THERMAL CONDUCTIVITY OF THE SLEEVE AND FUEL MATERIAL.

FIGURE 33

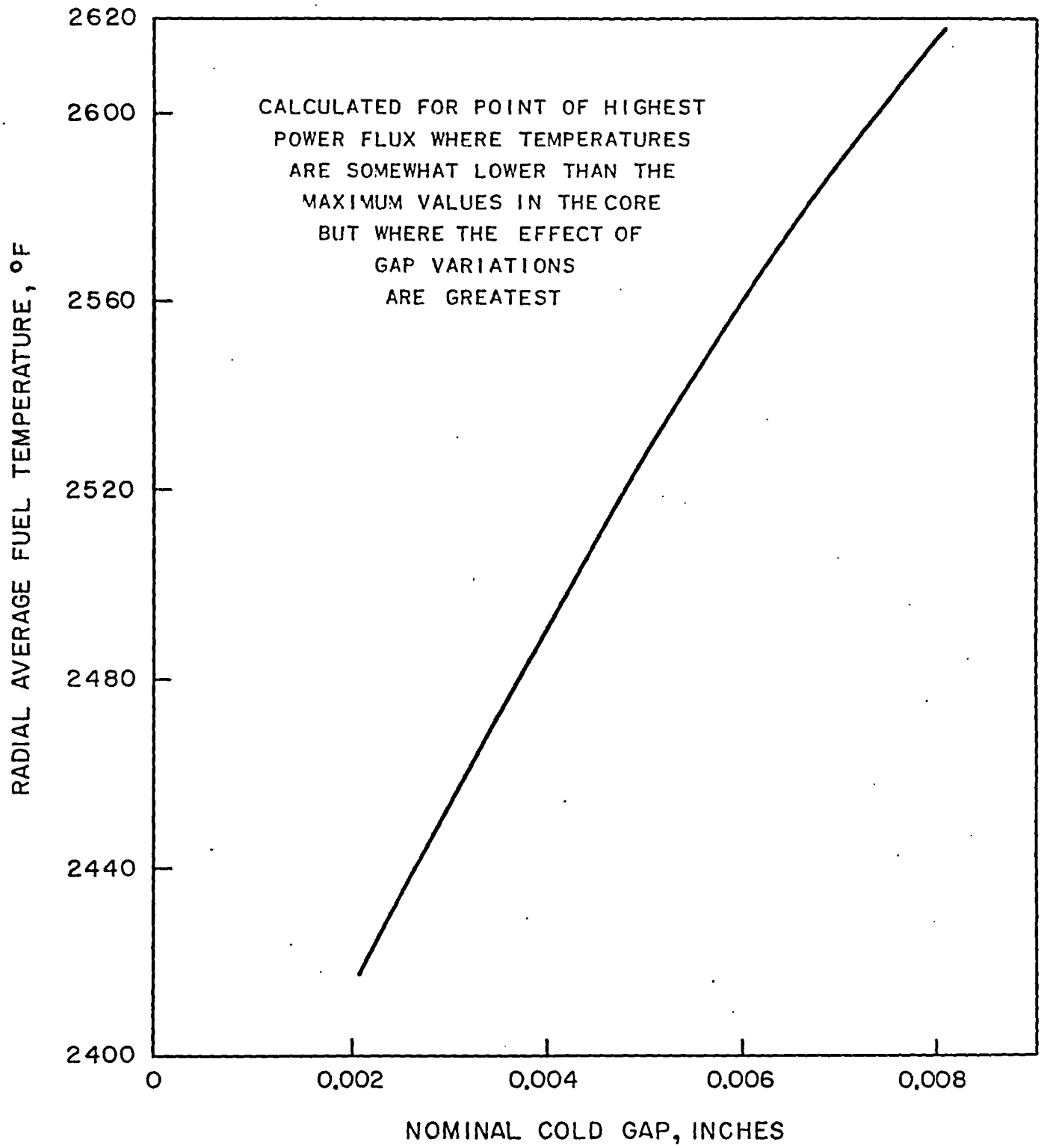

VARIATION IN FUEL TEMPERATURE WITH WIDTH OF GAP BETWEEN COMPACT AND SLEEVE.

FIGURE 34

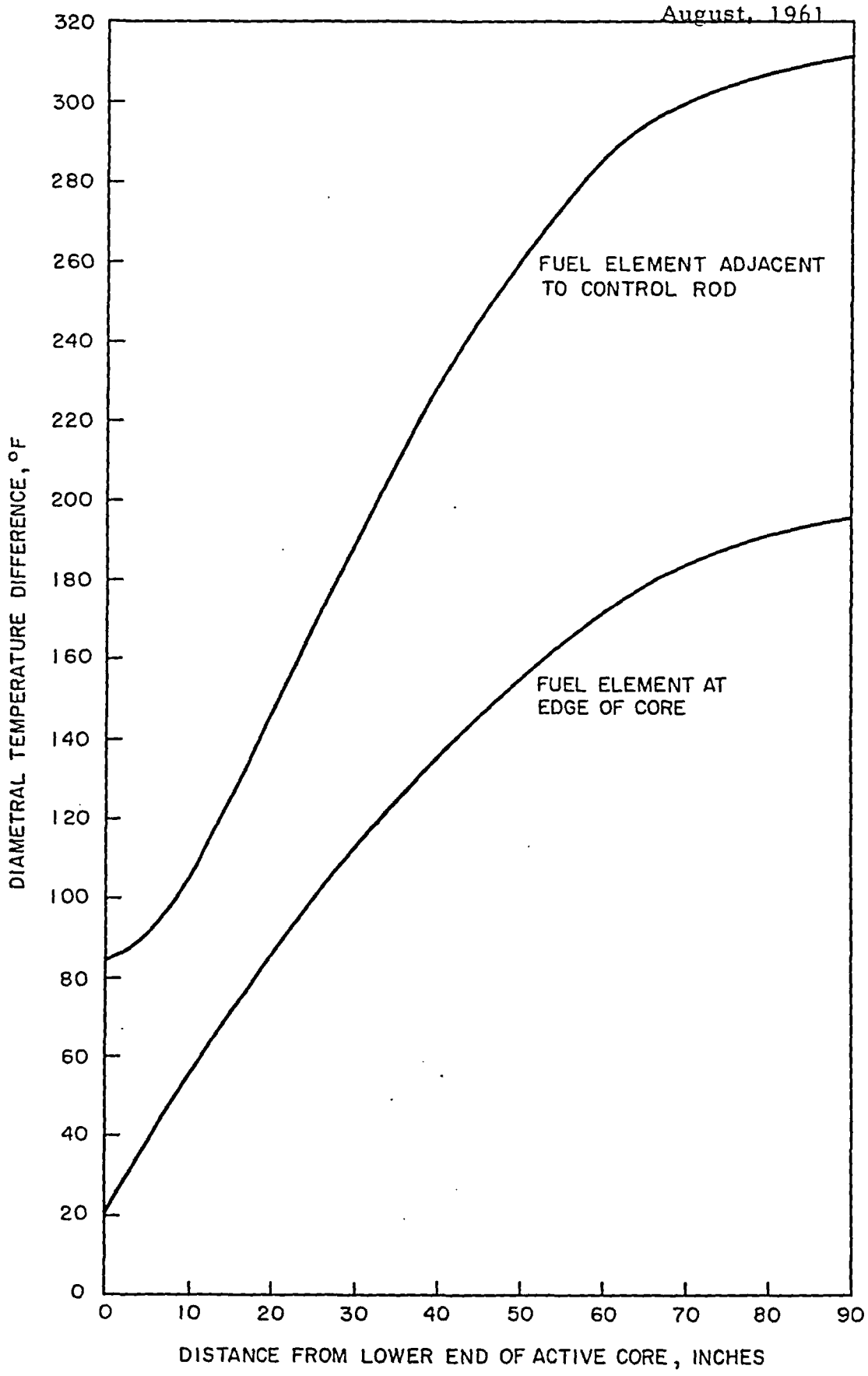

AXIAL VARIATION OF DIAMETRAL TEMPERATURE DIFFERENCE IN A FUEL ELEMENT NEXT TO A FULLY INSERTED CONTROL ROD AND IN A FUEL ELEMENT AT THE EDGE OF THE CORE

FIGURE 35

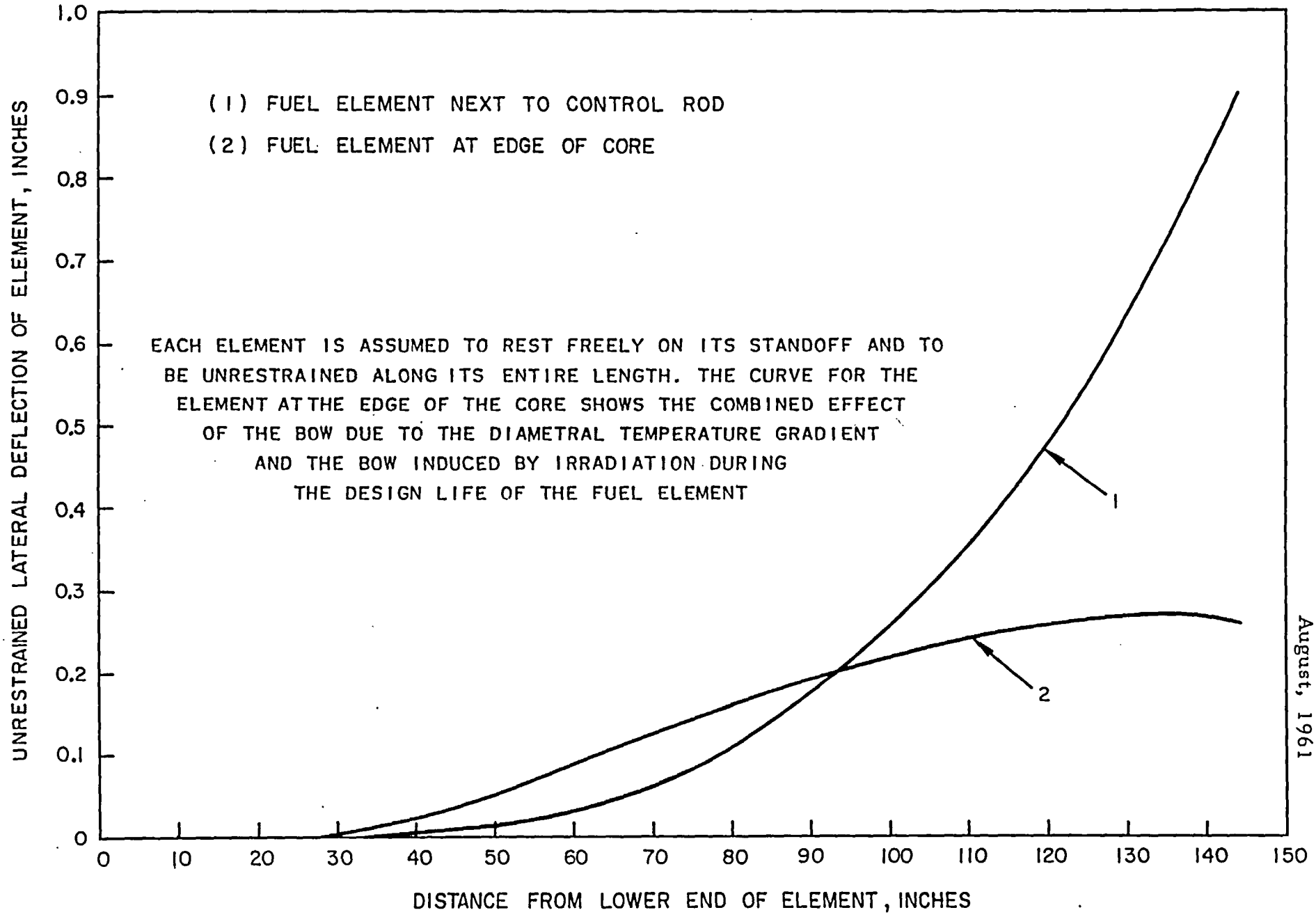

HYPOTHETICAL DEFLECTIONS OF ASYMMETRICALLY HEATED FUEL ELEMENTS.

FIGURE 36

August, 1961

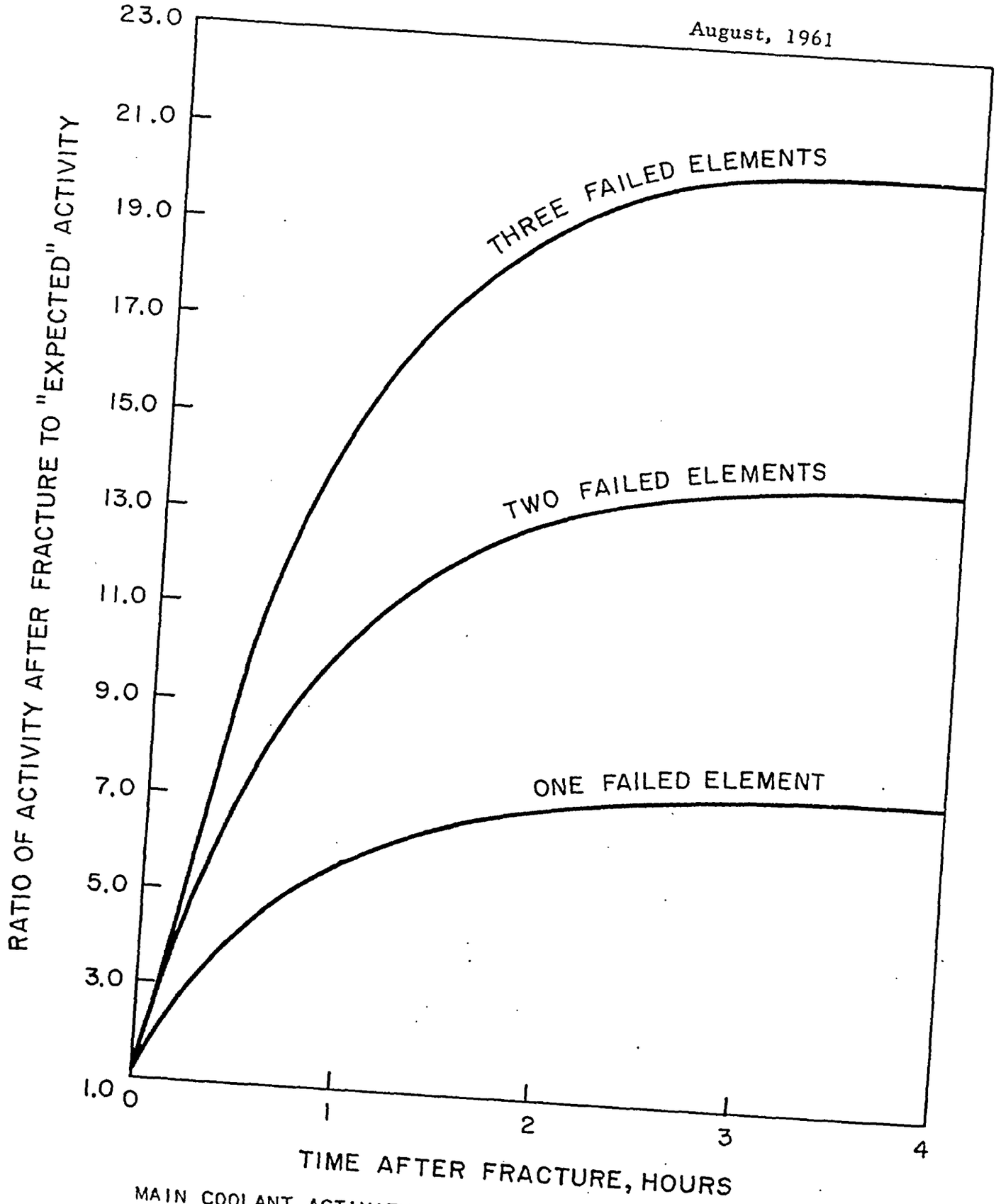

MAIN COOLANT ACTIVITY INCREASE (EXCLUSIVE OF Kr^{85}) VS. TIME FOR CONTINUED REACTOR OPERATION WITH ONE, TWO, OR THREE BADLY FRACTURED FUEL ELEMENTS

FIGURE 37

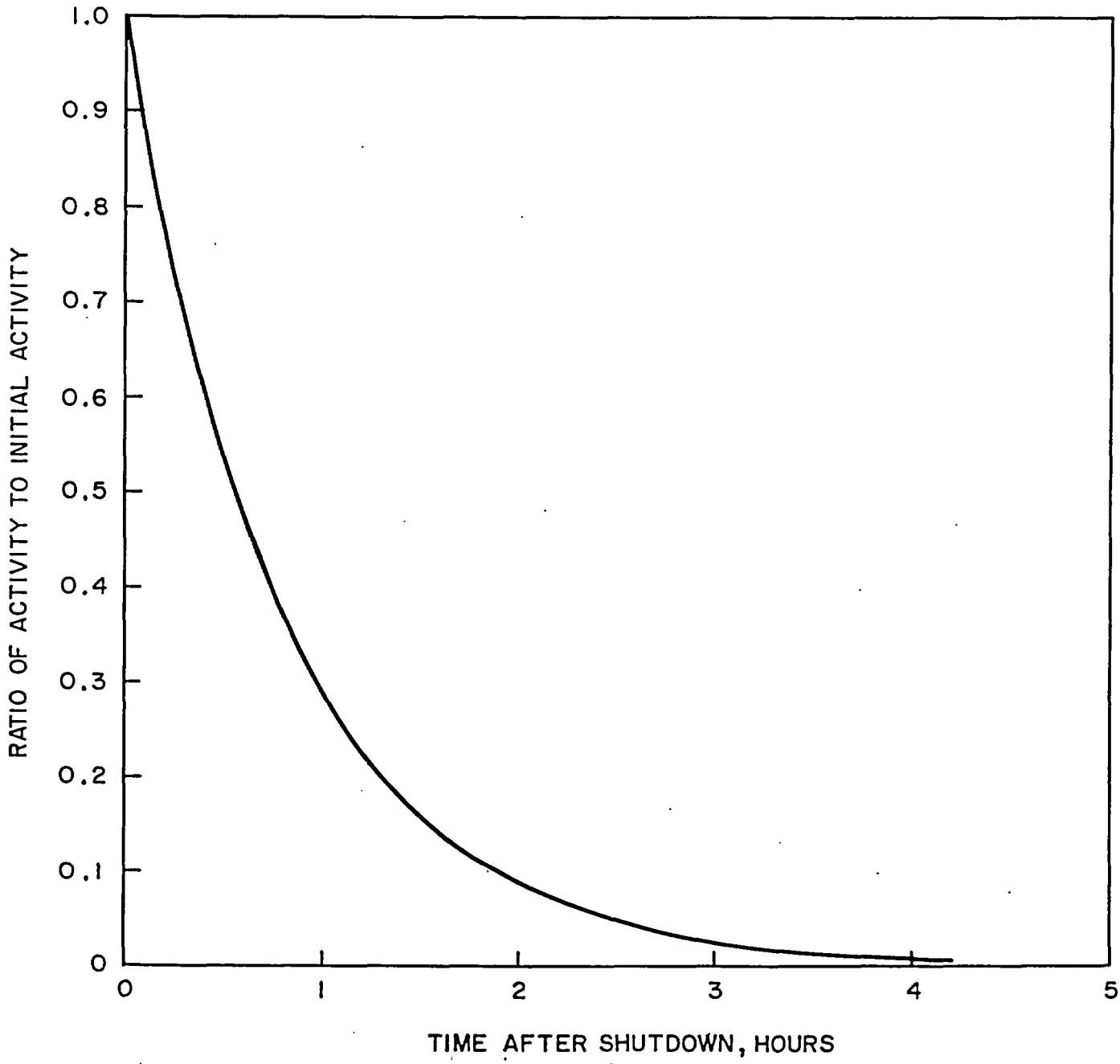

CLEANUP OF MAIN COOLANT ACTIVITY (EXCLUSIVE OF KR^{85})
WITH NO PRODUCTION AND CONTINUED EXTERNAL
TRAP OPERATION

FIGURE 38

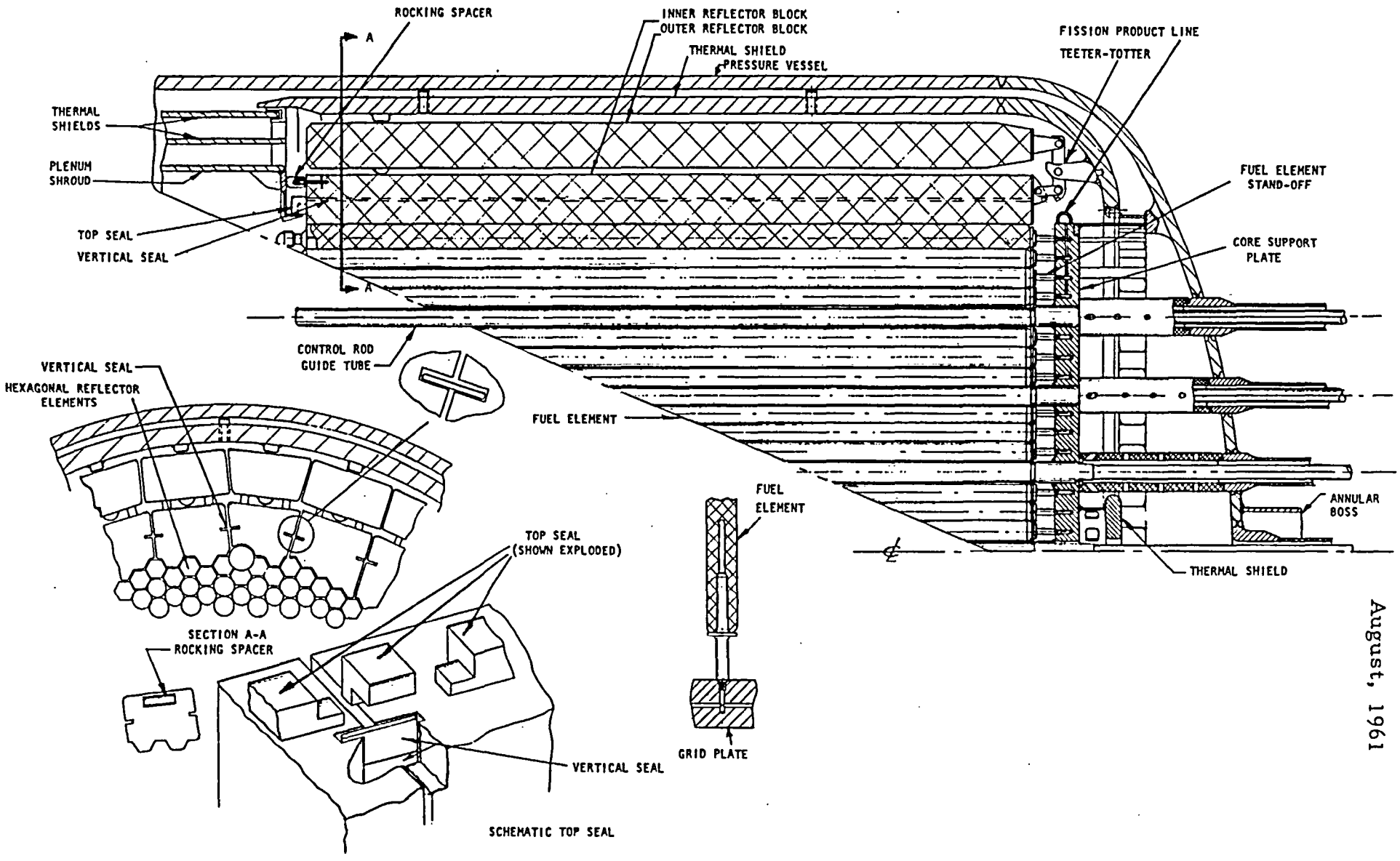

CROSS SECTION OF VESSEL INTERNALS

August, 1961

FIGURE 39

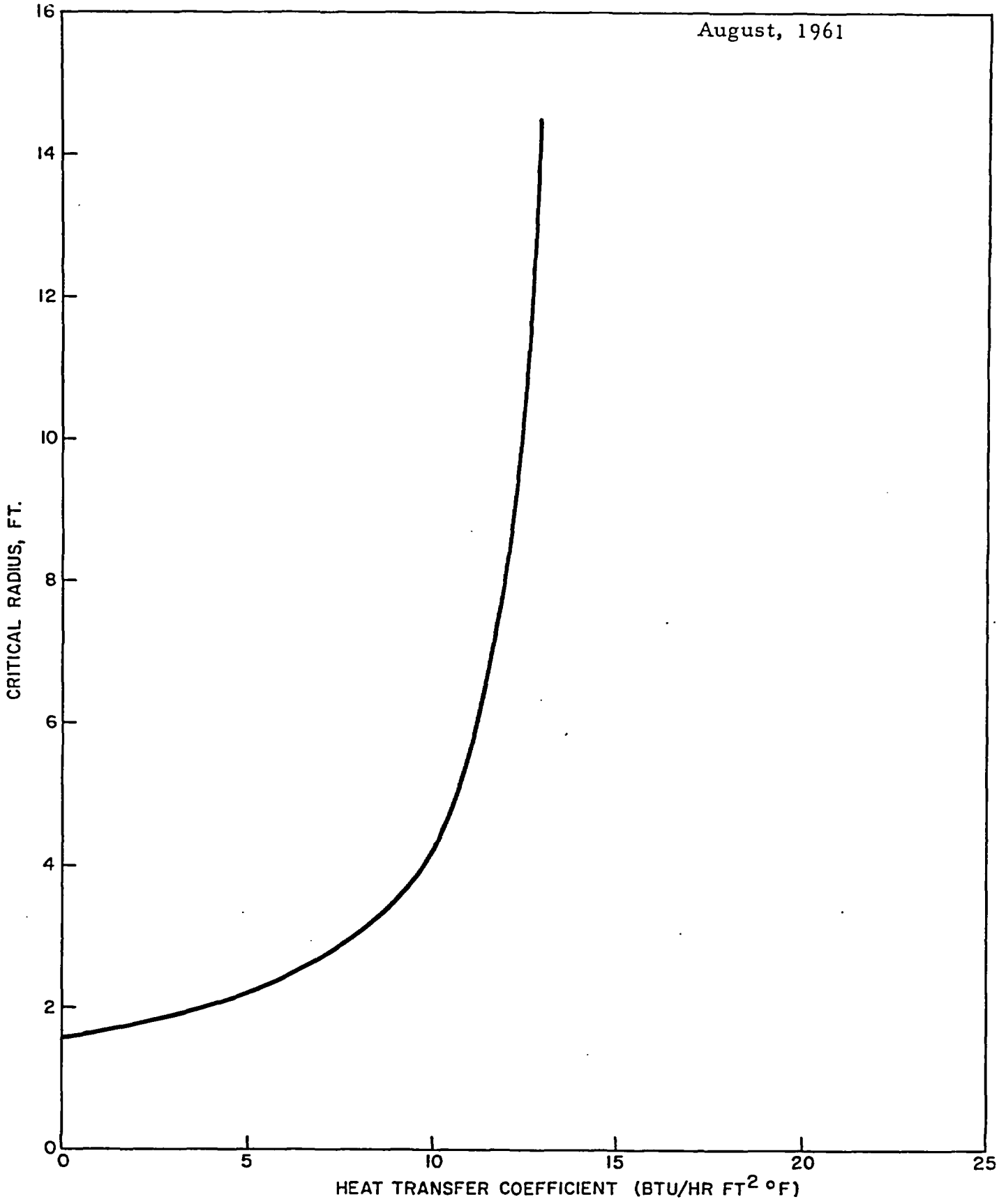

CRITICAL RADIUS OF HOT SPOT VS. HEAT TRANSFER COEFFICIENT
FOR AN ALLOWABLE STRESS OF 8000 PSI

FIGURE 40

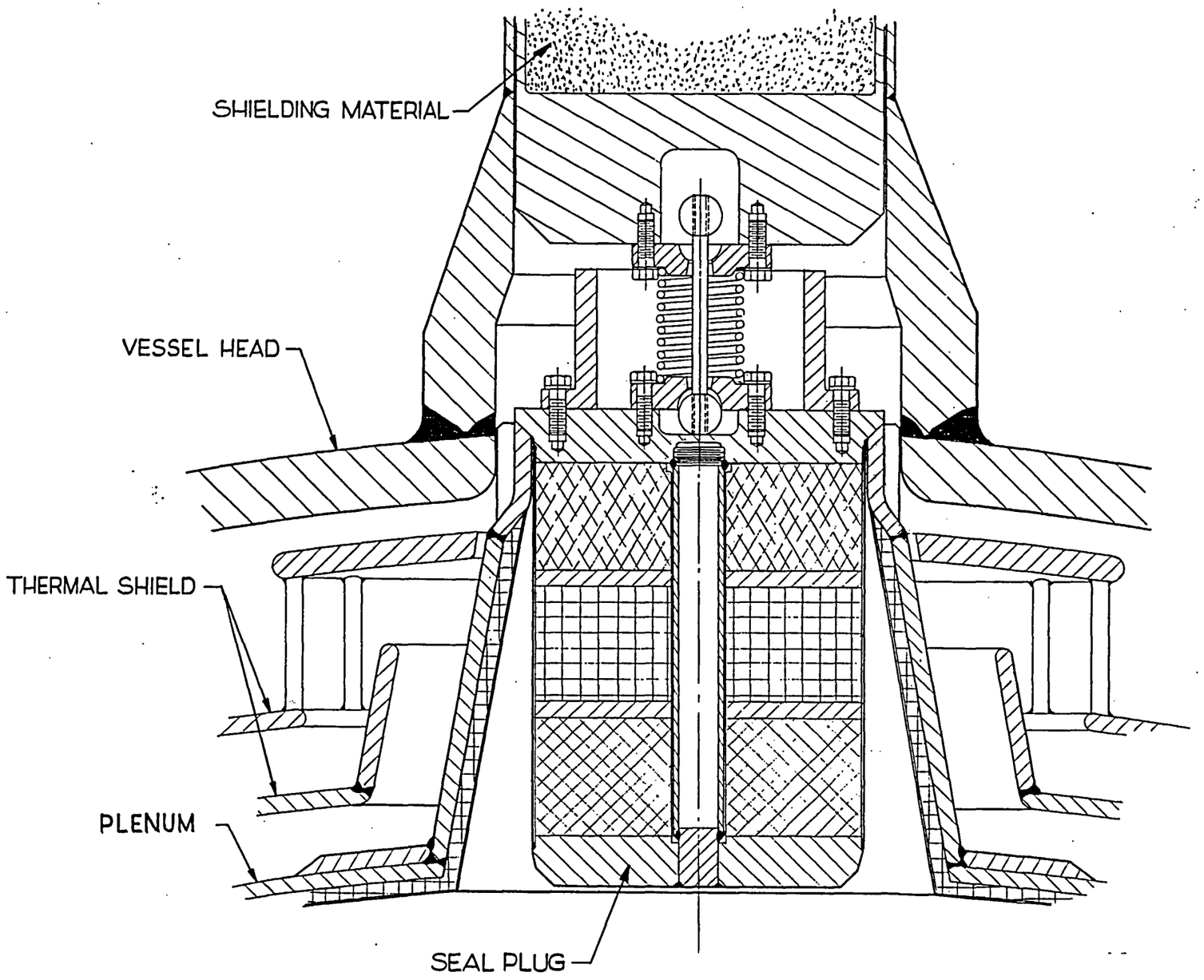

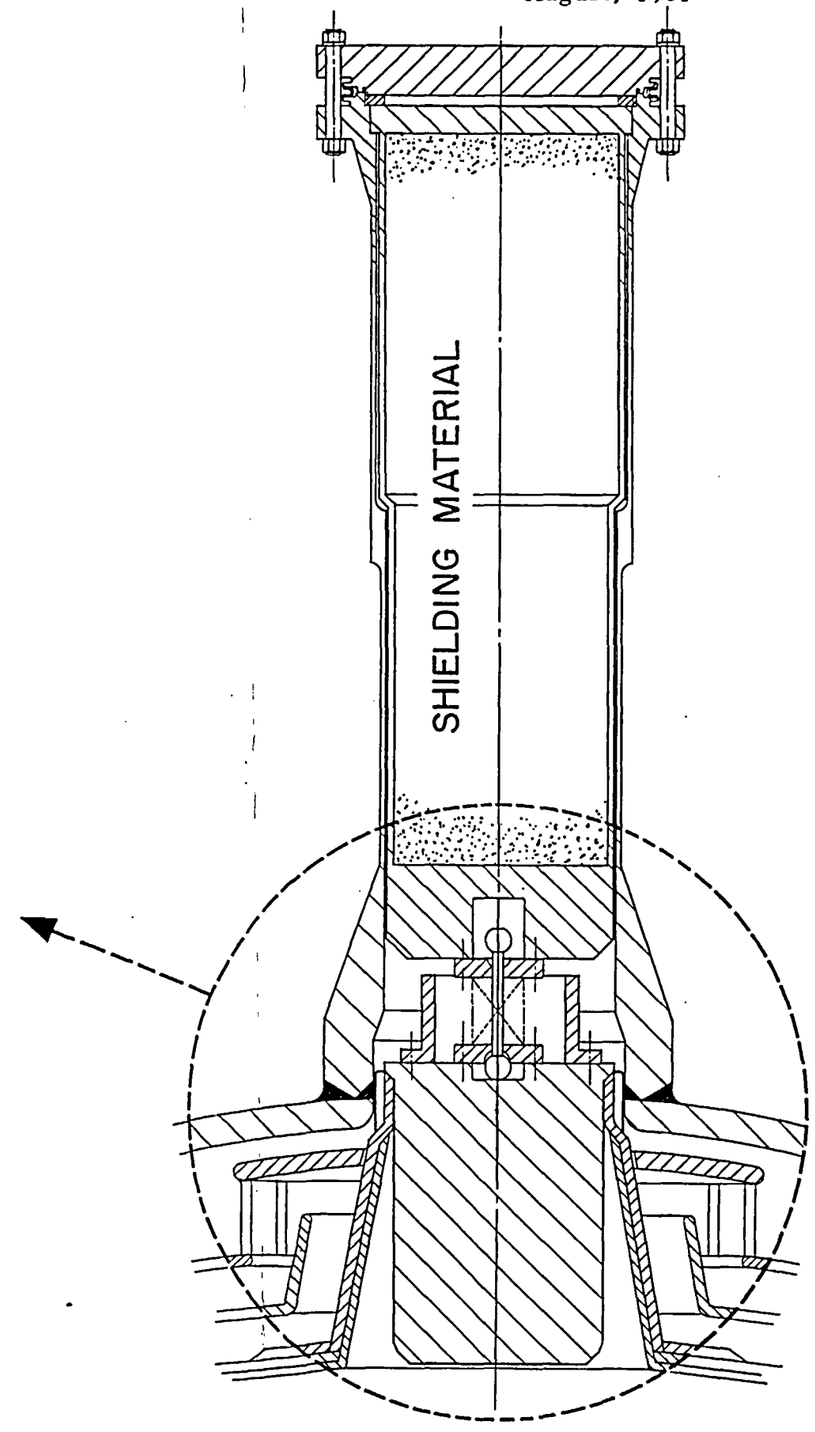

REFUELING NOZZLE AND
REMOVABLE SHIELD PLUG

FIGURE 41

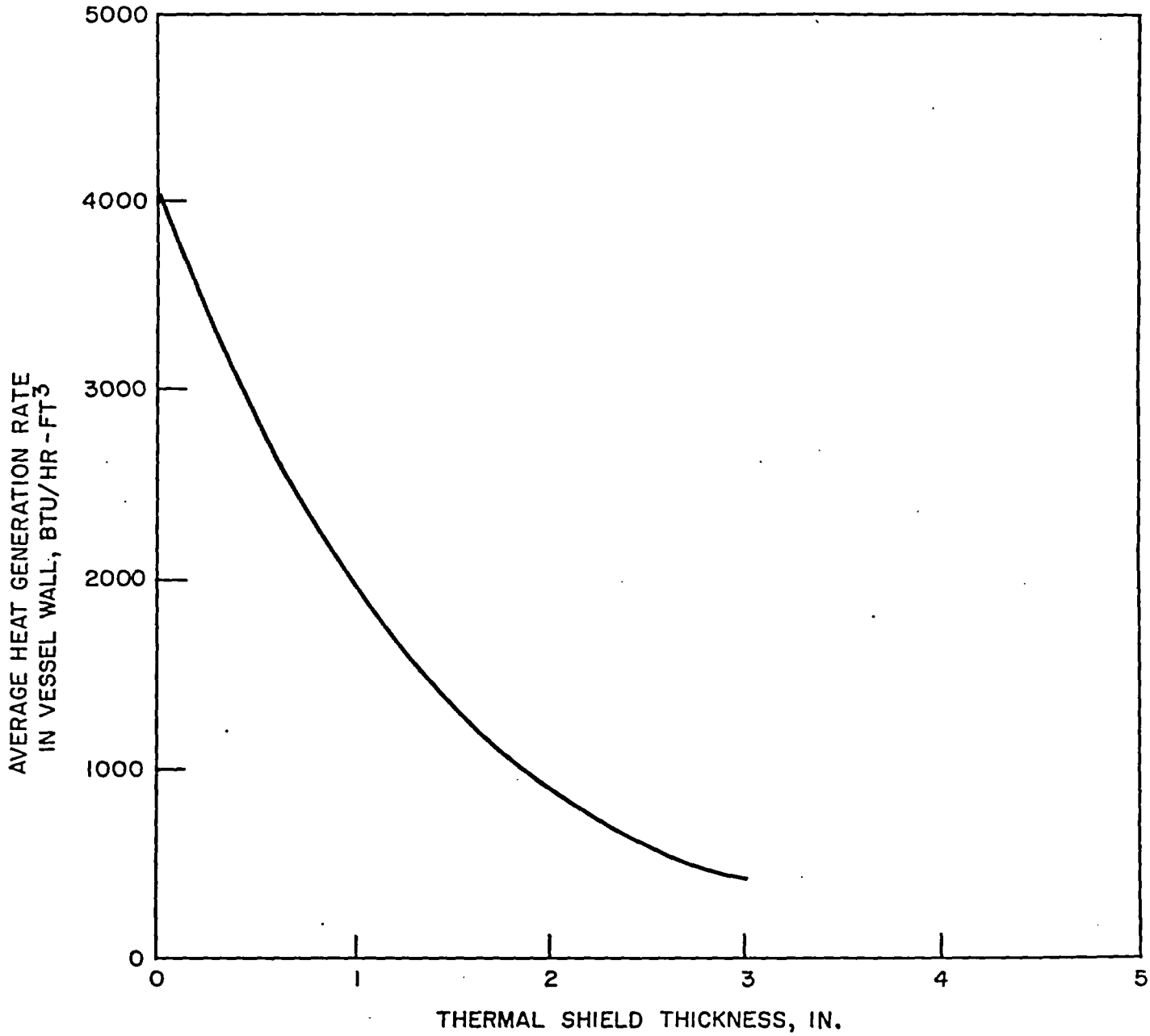

HEAT GENERATION RATES IN REACTOR VESSEL WALL
(WALL THICKNESS 2-1/2")

FIGURE 42

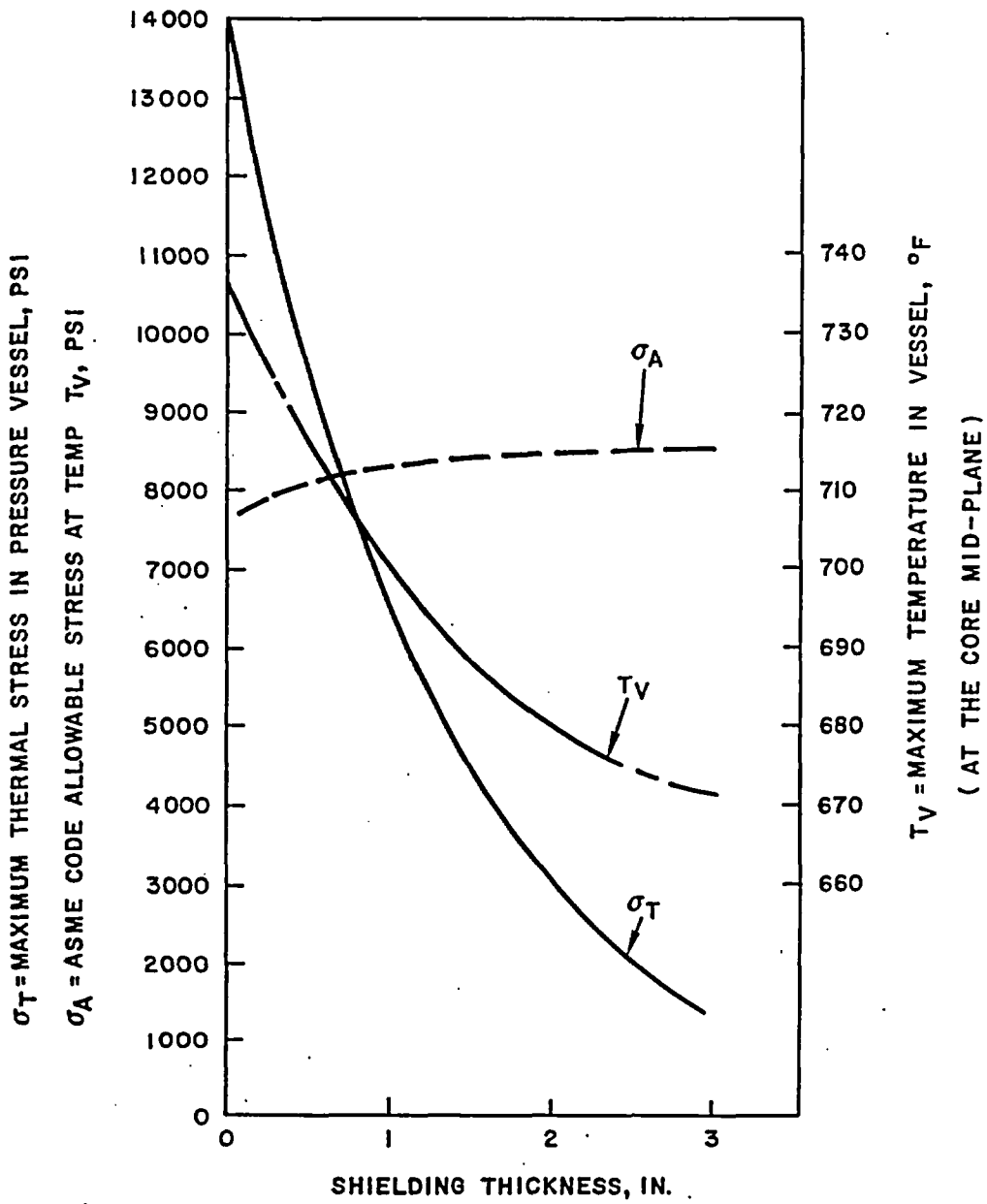

EFFECT OF AMOUNT OF THERMAL SHIELDING ON STRESS AND TEMPERATURE IN PRESSURE VESSEL (2-1/2 INCH WALL. 100% COOLANT FLOW). FOR HEATING RATES GIVEN IN FIGURE 42 AND ADJUSTED FOR PEAK TO AVERAGE OF 1.6

FIGURE 43

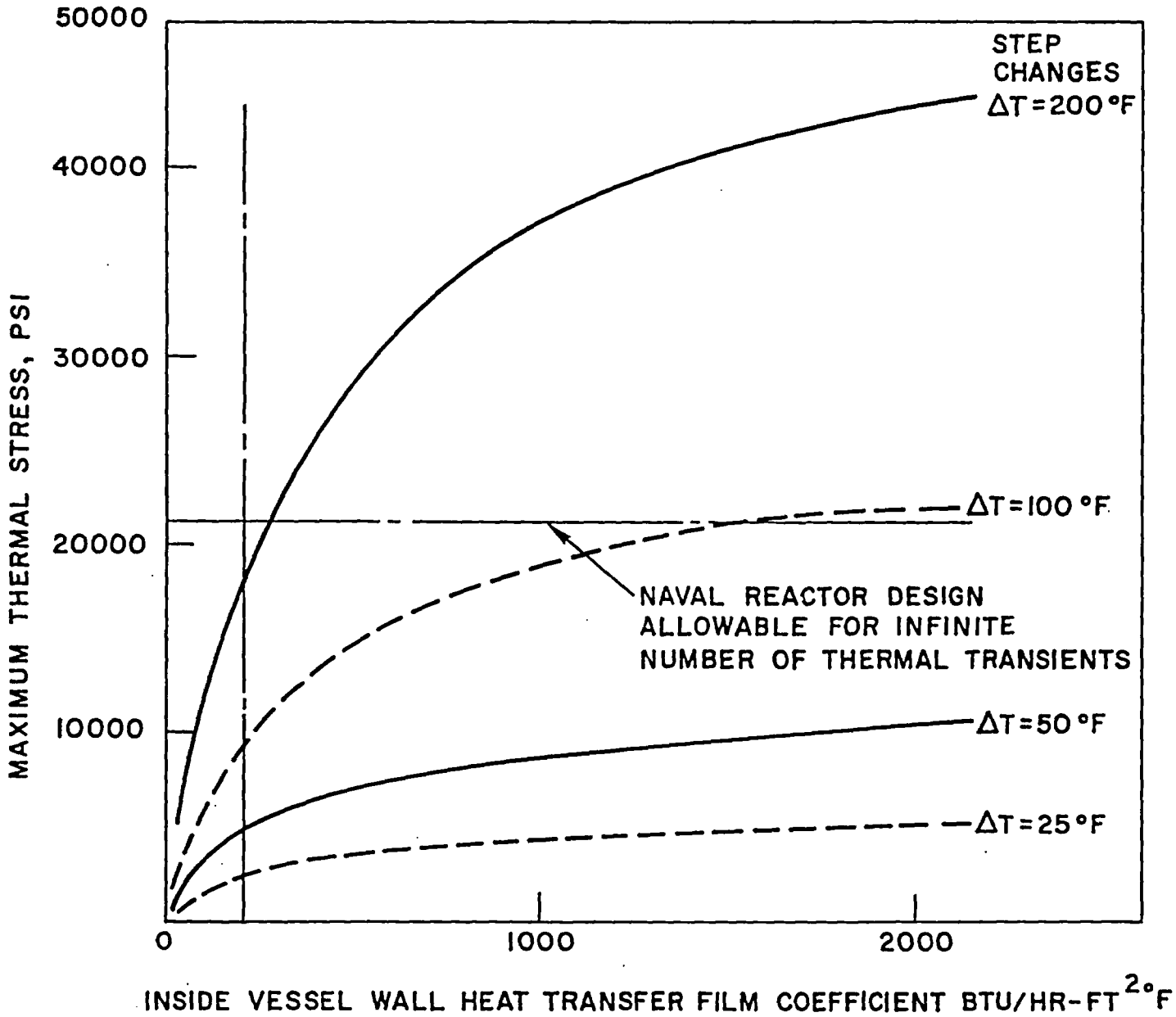

MAXIMUM THERMAL STRESS IN VESSEL WALL DUE TO A STEP CHANGE IN FLUID TEMPERATURE FOR A 2-1/2" WALL OF A212

FIGURE 44

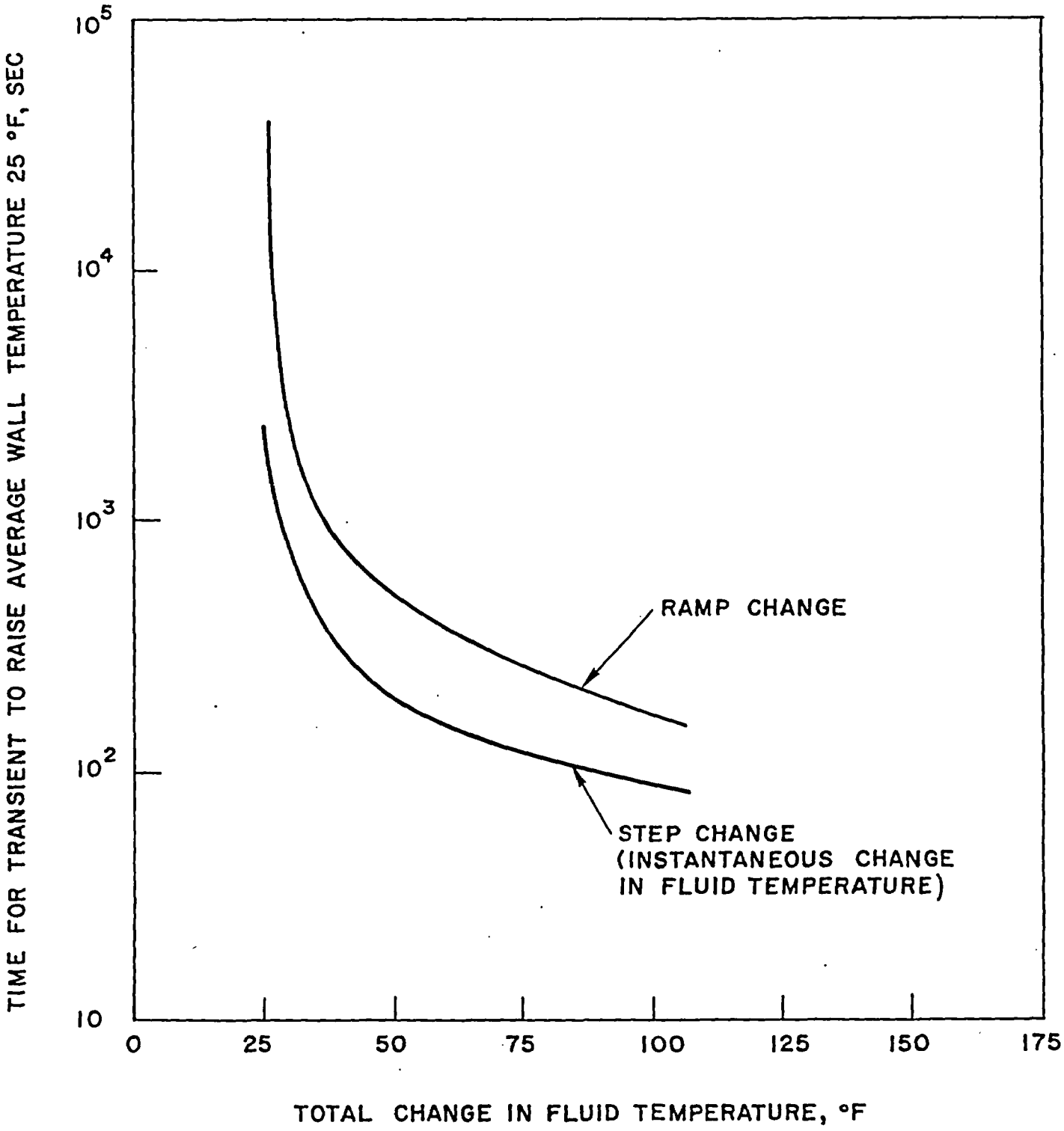

TIME FOR TRANSIENT TO RAISE AVERAGE WALL TEMPERATURE 25°F
FOR 2-1/2" CARBON STEEL WALL AND A HEAT TRANSFER
COEFFICIENT OF 200 BTU/HR-FT^2-°F

FIGURE 45

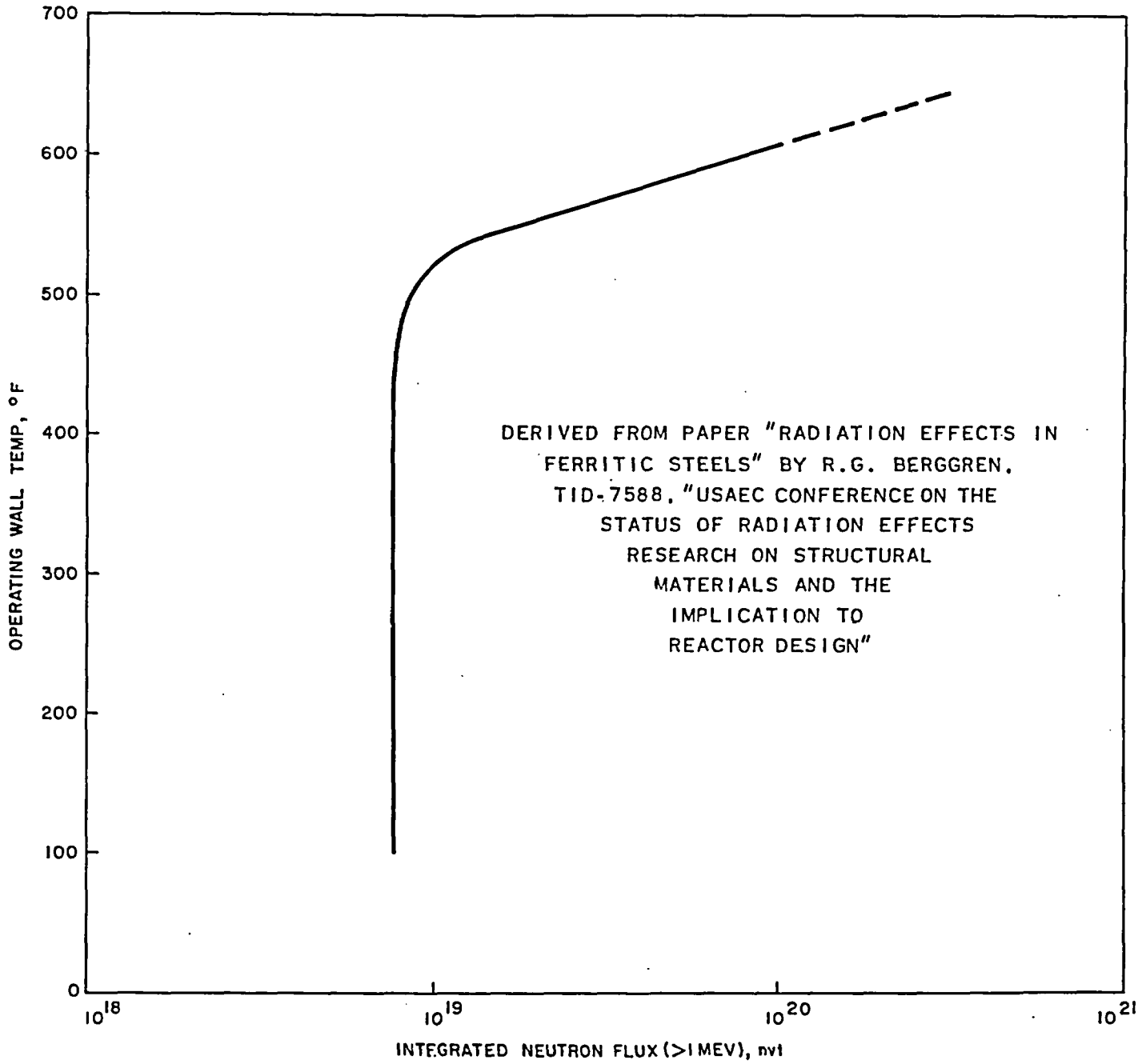

IRRADIATION TEMPERATURE FOR A 100°F RISE IN IMPACT TRANSITION TEMPERATURE VS. NEUTRON DOSE.

FIGURE 46

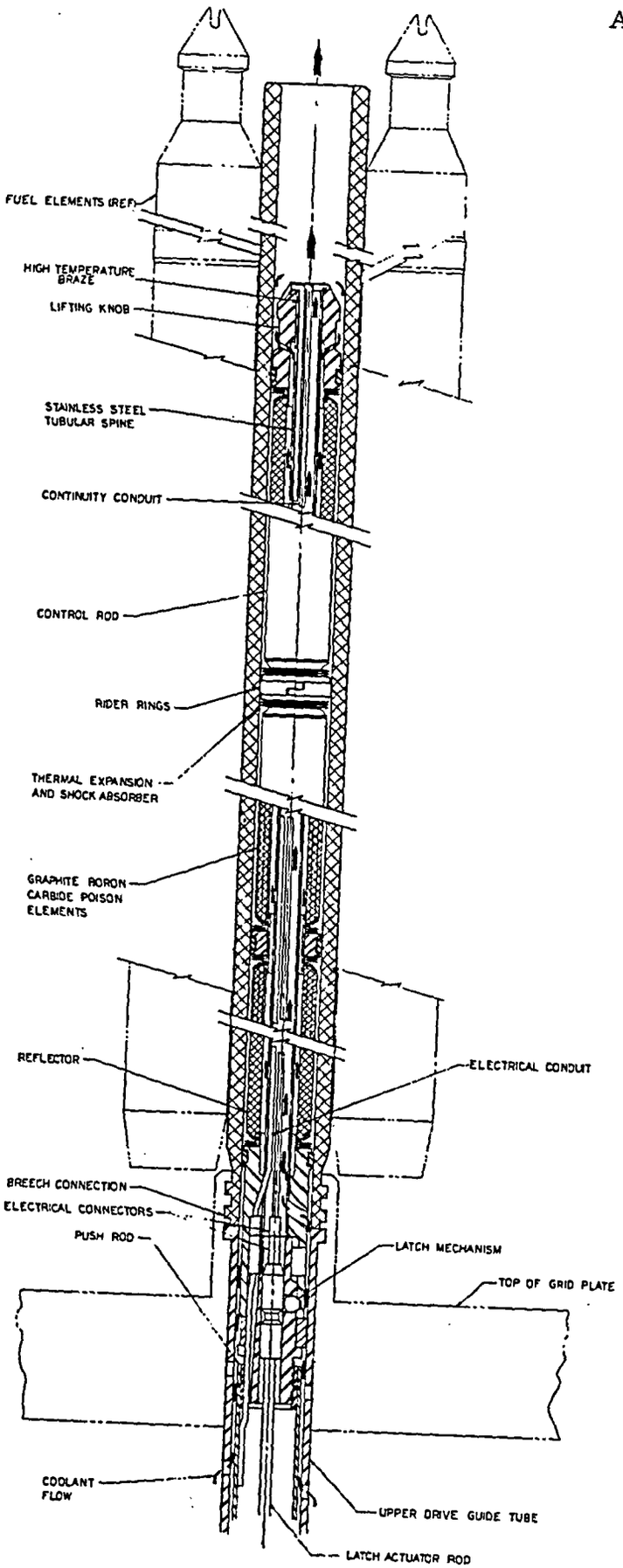

HTGR CONTROL ROD

FIGURE 47

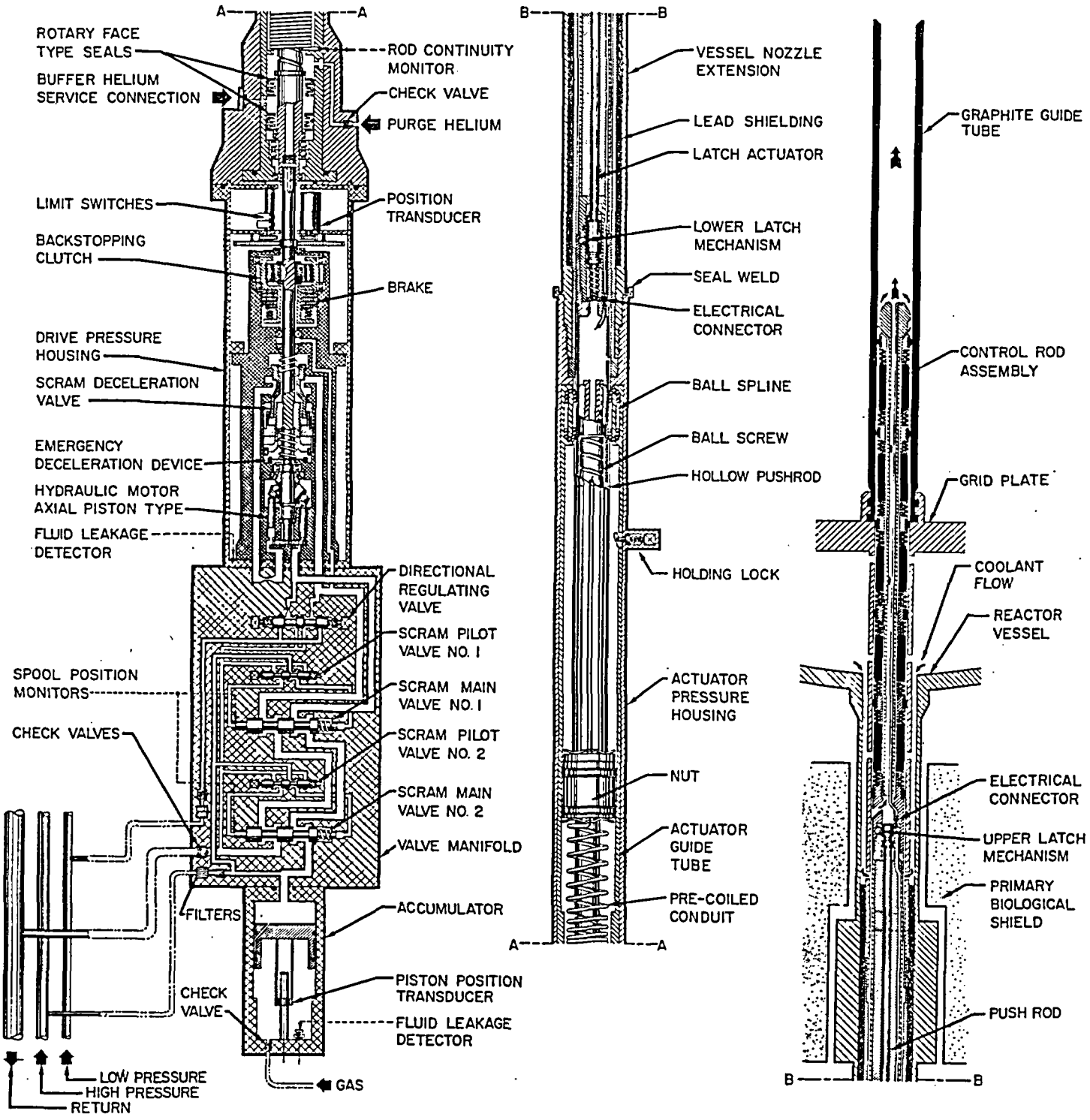

SCHEMATIC OF CONTROL ROD AND DRIVE

FIGURE 48

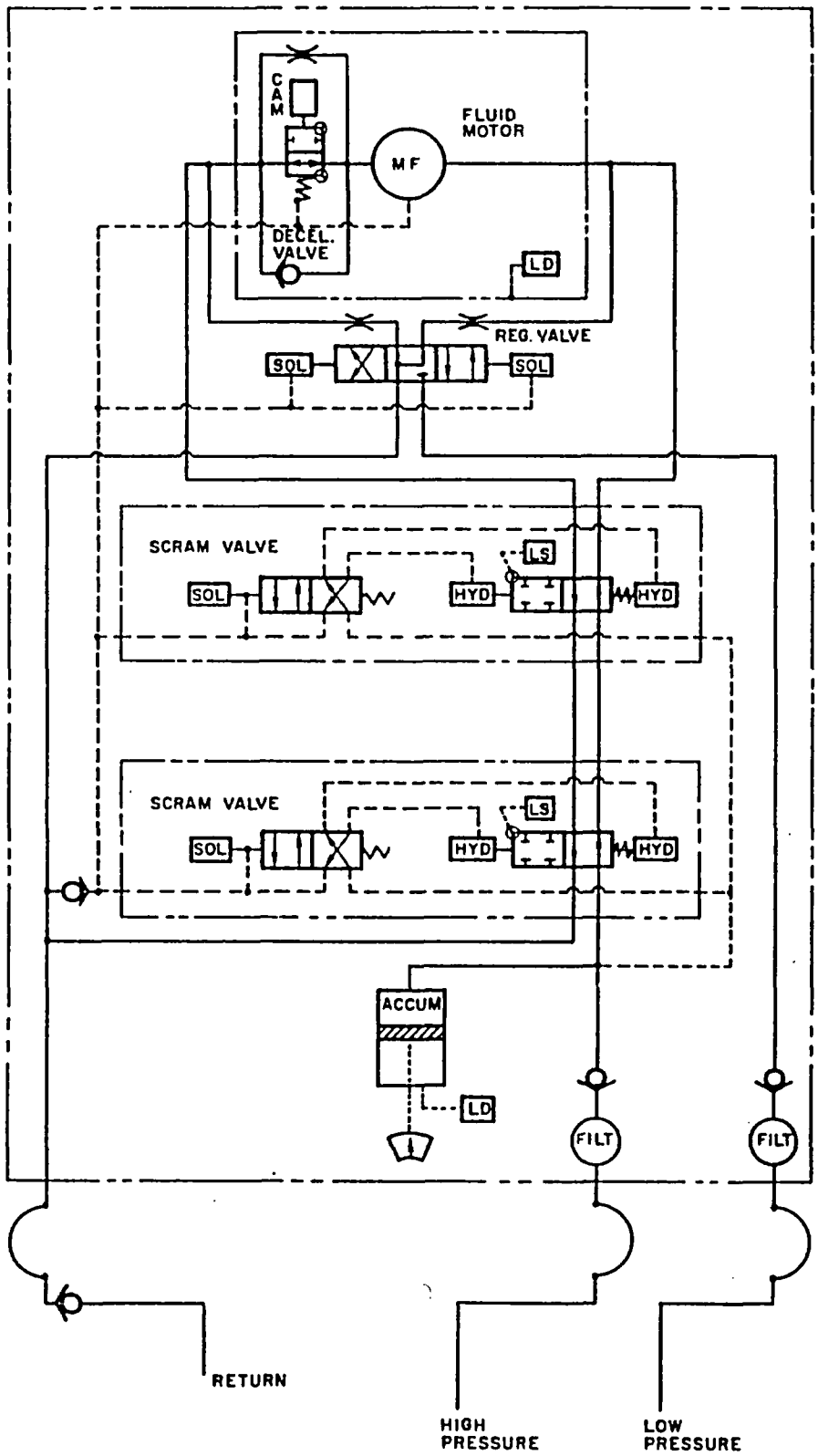

CONTROL ROD DRIVE HYDRAULIC CIRCUIT

FIGURE 49

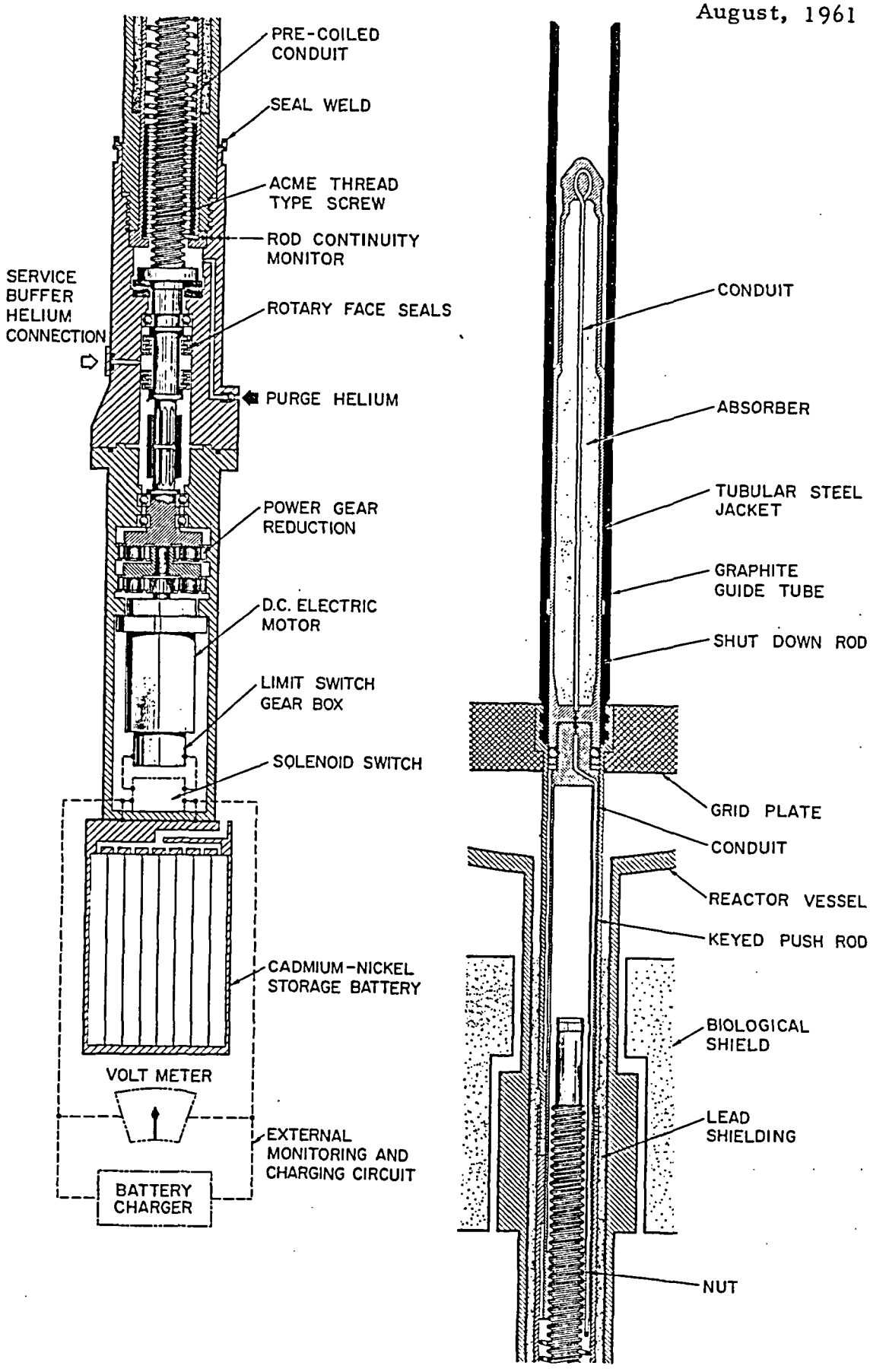

EMERGENCY SHUTDOWN ROD DRIVE

FIGURE 50

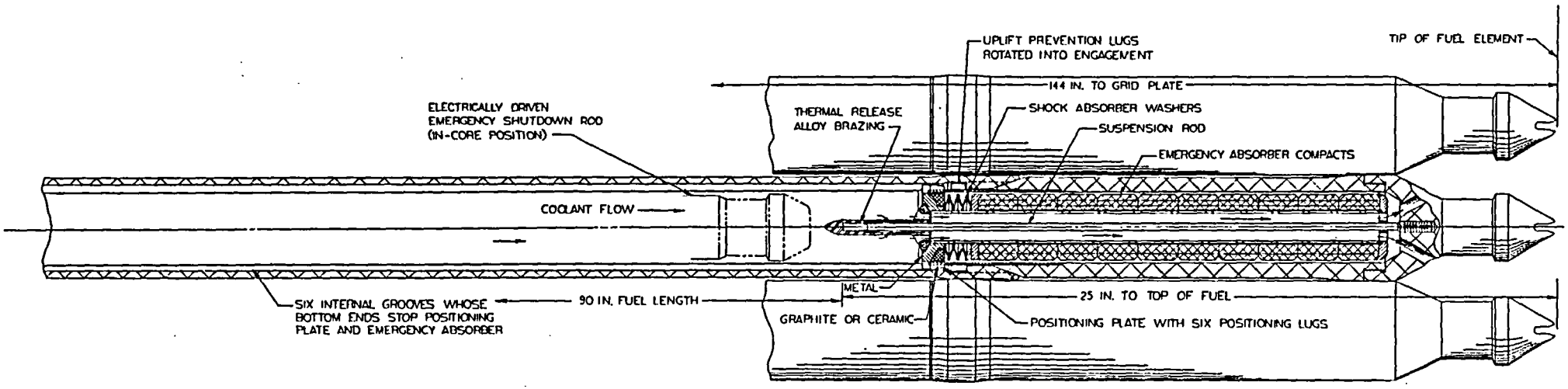

THERMALLY RELEASED EMERGENCY SHUTDOWN ADSORBER AS INSTALLED
IN EMERGENCY SHUTDOWN ROD GUIDE TUBE

FIGURE 51

August, 1961

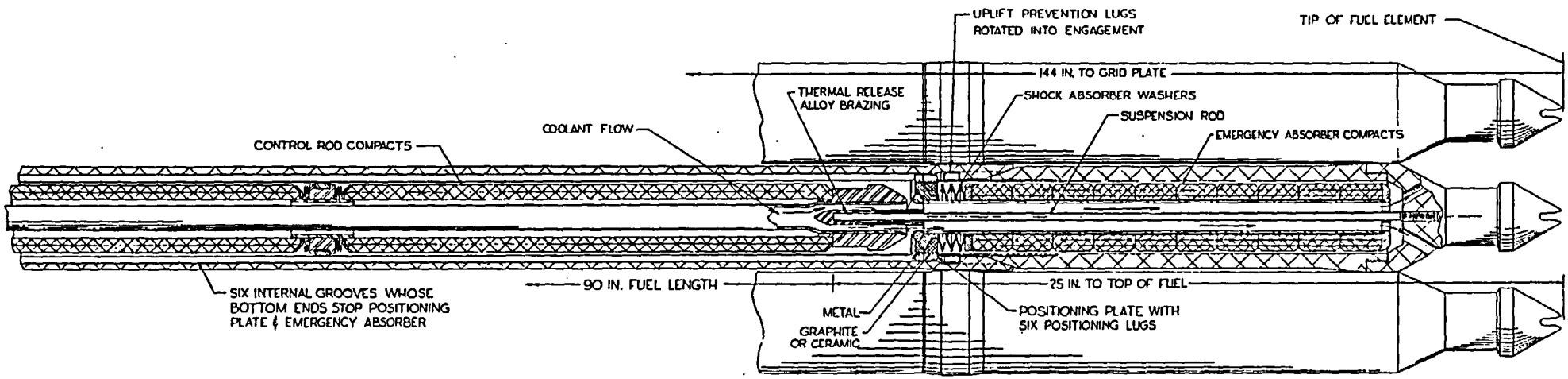

THERMALLY RELEASED EMERGENCY SHUTDOWN ADSORBER AS INSTALLED IN A CONTROL ROD GUIDE TUBE

August, 1961

FIGURE 52

August, 1961

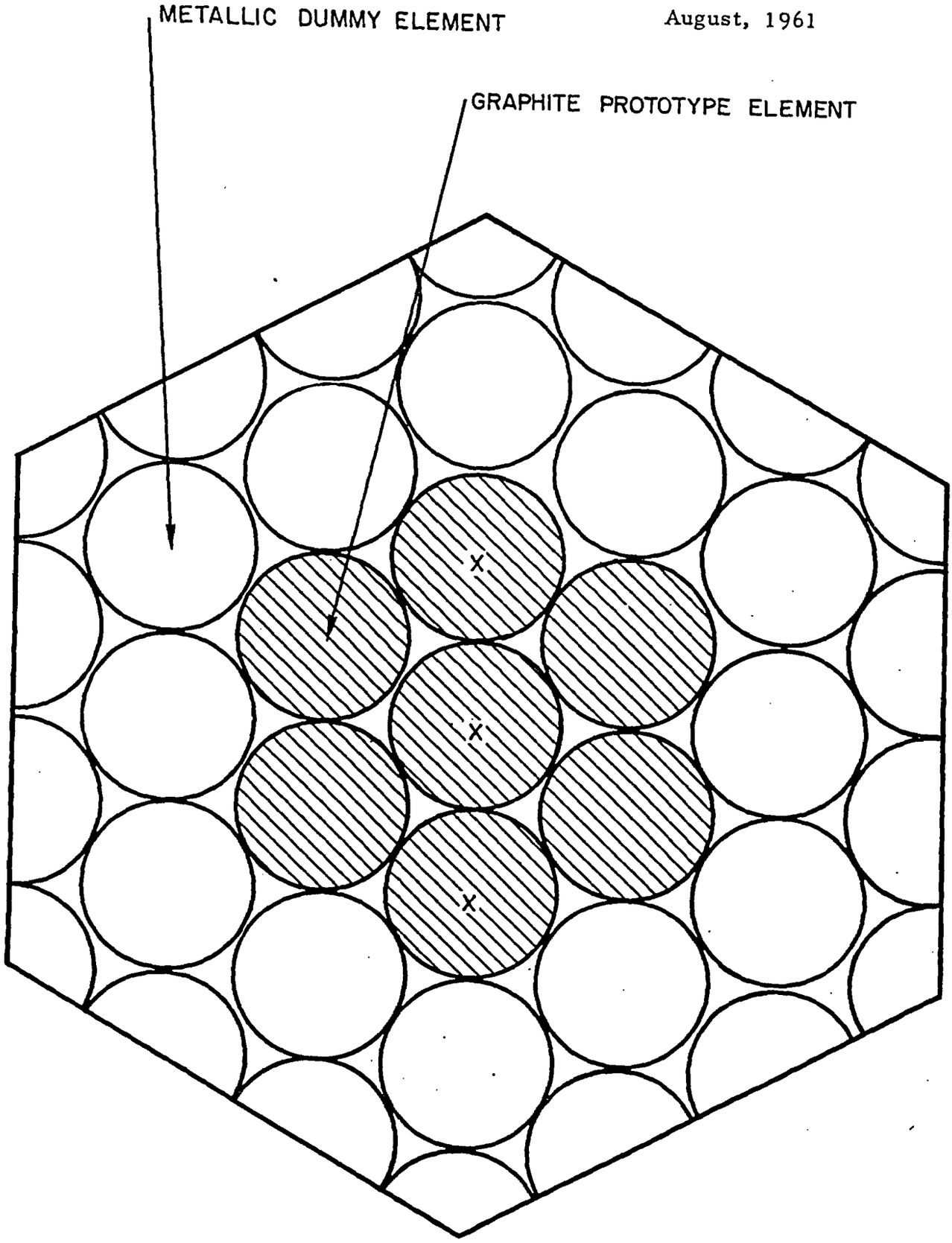

FUEL ELEMENT VIBRATION TEST: CROSS SECTION OF TEST CHAMBER

FIGURE 53

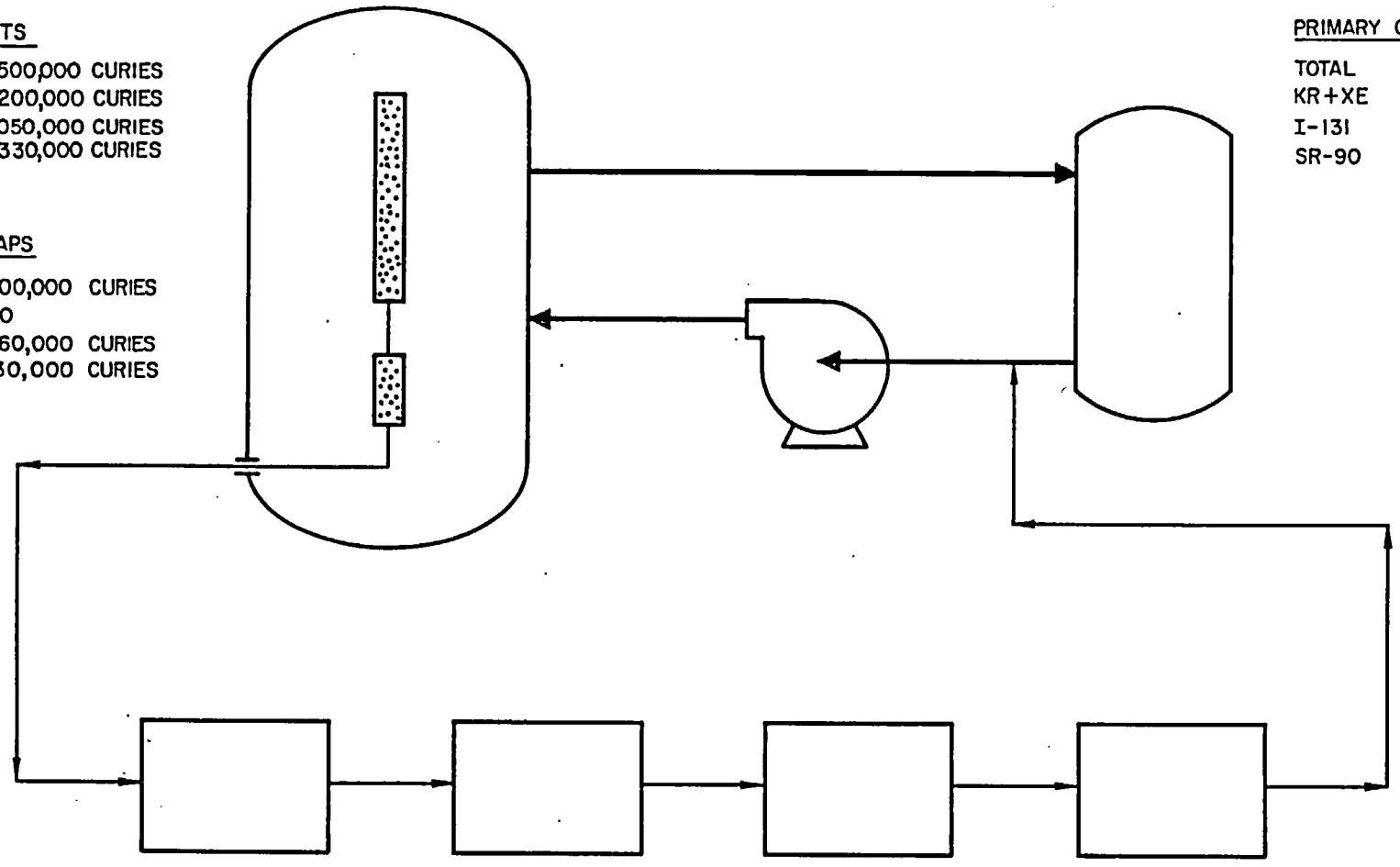

FUEL COMPACTS

TOTAL	427,500,000 CURIES
KR+XE	53,200,000 CURIES
I-131	3,050,000 CURIES
SR-90	330,000 CURIES

INTERNAL TRAPS

TOTAL	33,900,000 CURIES
KR+XE	0
I-131	1,960,000 CURIES
SR-90	330,000 CURIES

PRIMARY COOLANT

TOTAL	4,224 CURIES
KR+XE	633 CURIES
I-131	3.4 CURIES
SR-90	0

CONDENSIBLES TRAP

TOTAL	968,000 CURIES
KR+XE	0
I-131	960,000 CURIES
SR-90	0

WATER-COOLED DELAY BEDS

TOTAL	2,370,000 CURIES
KR+XE	1,640,000 CURIES
I-131	0
SR-90	13,000 CURIES

REFRIGERATED DELAY BEDS

TOTAL	7,890,000 CURIES
KR+XE	7,440,000 CURIES
I-131	0
SR-90	0

LIQUID-NITROGEN-COOLED TRAP

TOTAL	13,900 CURIES
KR+XE	13,900 CURIES
I-131	0
SR-90	0

SUMMARY OF RADIOACTIVITY DISTRIBUTION

DESIGN ACTIVITY LEVELS

August, 1961

FIGURE 54

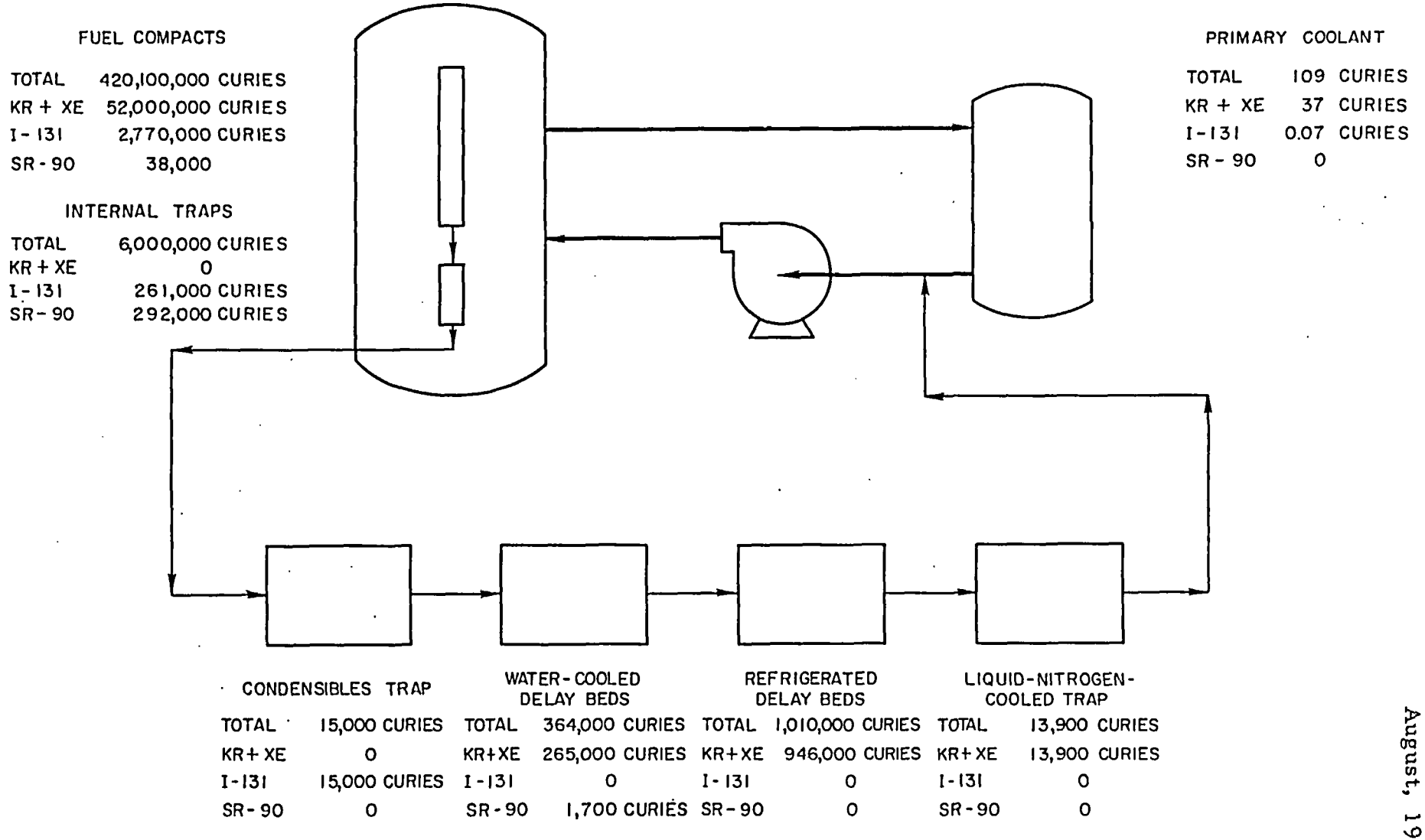

SUMMARY OF RADIOACTIVITY DISTRIBUTION

CALCULATED BEGINNING OF LIFE ACTIVITY LEVELS

BASED ON EXPERIMENTAL RELEASE DATA

FOR COATED PARTICLE FUEL

August, 1961

FIGURE 55

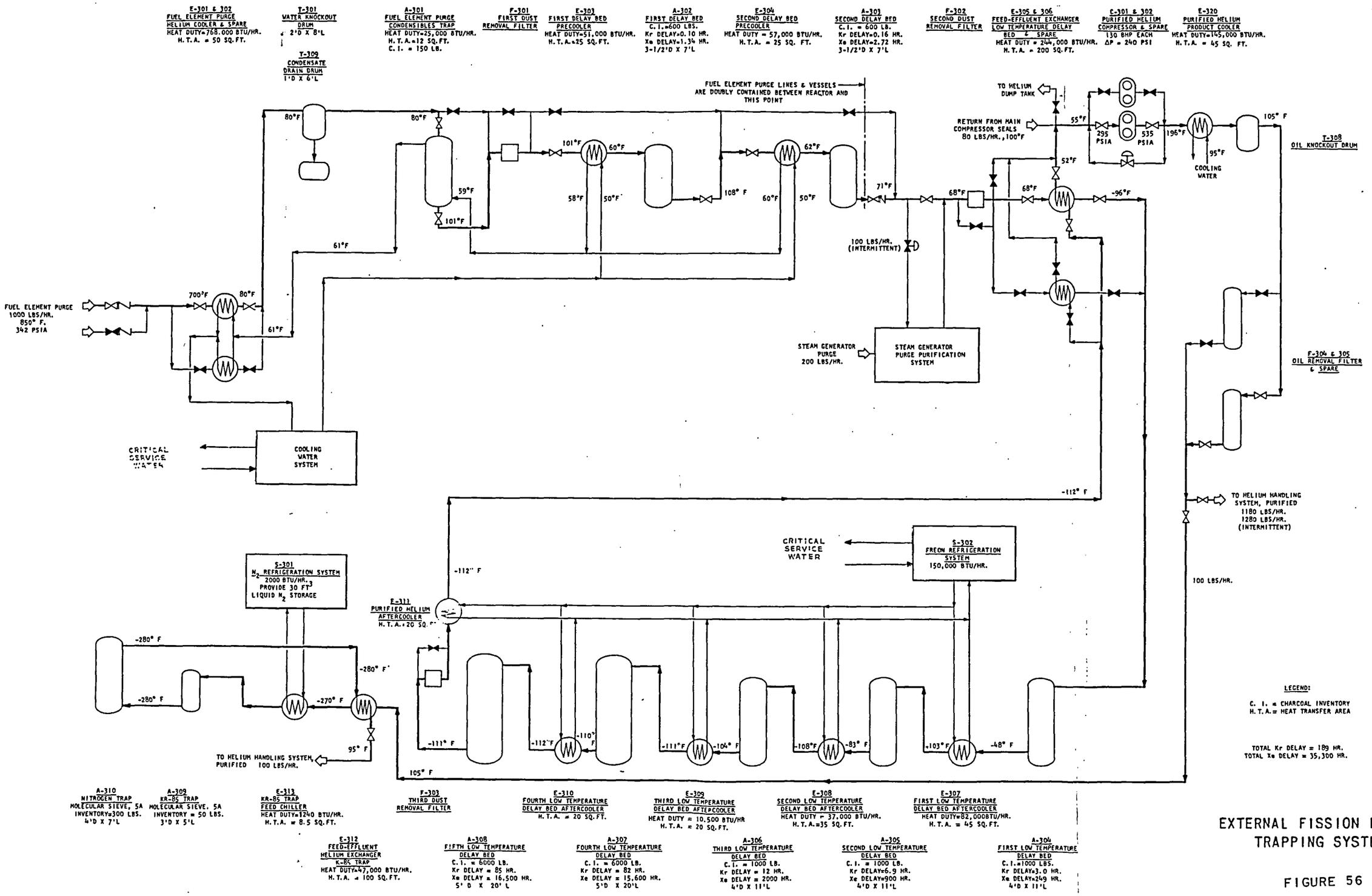

EXTERNAL FISSION PRODUCT TRAPPING SYSTEM

FIGURE 56

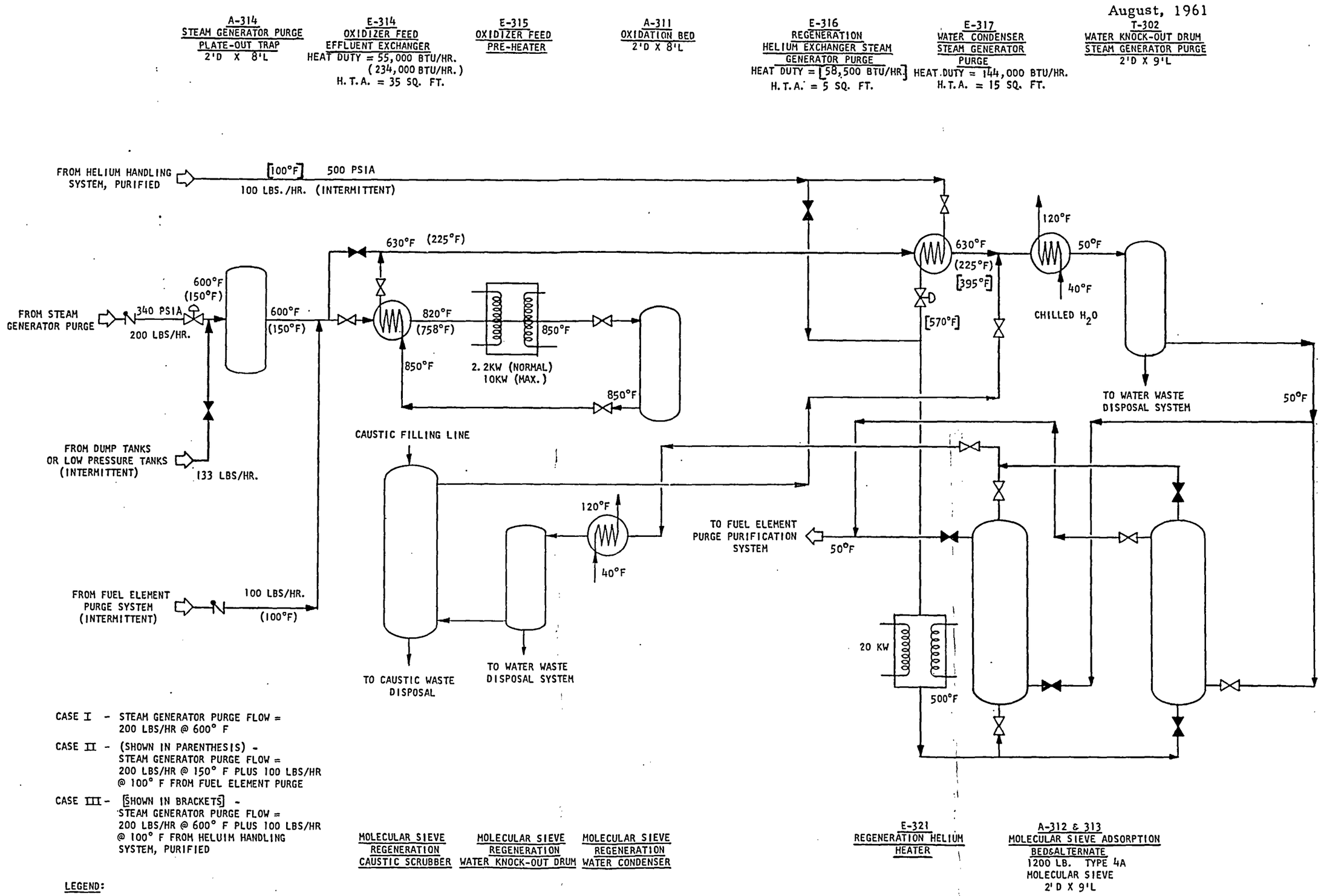

CASE I - STEAM GENERATOR PURGE FLOW = 200 LBS/HR @ 600° F

CASE II - (SHOWN IN PARENTHESIS) - STEAM GENERATOR PURGE FLOW = 200 LBS/HR @ 150° F PLUS 100 LBS/HR @ 100° F FROM FUEL ELEMENT PURGE

CASE III - [SHOWN IN BRACKETS] - STEAM GENERATOR PURGE FLOW = 200 LBS/HR @ 600° F PLUS 100 LBS/HR @ 100° F FROM HELUIM HANDLING SYSTEM, PURIFIED

LEGEND:

H.T.A. = HEAT TRANSFER AREA

STEAM GENERATOR
PURGE PURIFICATION SYSTEM

FIGURE 57

STREAM NO.	1	2	3	4	5	6	7	8	9	10	11	12	13	14	15	16	17	18	19	20	21	22	23	24	25	26	27	28	29	30	31	32	33	34	35	36
LBS/HOUR	439,200	219,600	219,600	219,700	222,100	222,218	219,818	220,050	220,050	440,200	2,400	1,000	870	435	310	155	40	80	200	100	100	200	180,685	15,320	7,660	5,595	0	150,665	506,290	508,355	508,355	182,750	182,750	182,750	6,300	359,700
# SCFM	664,940	328,480	328,780	328,630	332,210	332,390	328,800	329,150	329,150	658,450	3,590	1,496	1,301	651	464	232	60	120	299	150	150	299										60,750	60,750	60,750	2,090	119,410
ACFM	103,530	51,670	51,720	51,110	51,420	51,200	50,860	50,900	51,010	63,260	337	152	43	22	16	8	3	6	28	8	14	28										781	1,584	1,584	55	3,113
GPM @ °F																							424	34	17	12.5	0	517	2,400	2,406						
TEMPERATURE °F	1,358	1,384	1,352	672	672	633	633	632	634	654	633	700	108	105	108	105	105	108	632	105	600	600	428	342	342	342	342	588	604	604	604	604	1,005	1,005	1,005	1,005
PRESSURE PSIA	345.8	345.7	345.3	345.5	343.2	380.0	380.0	349.6	349.1	346.3	350.0	341.8	810	510	510	510	340	340	349.6	810	343	343	~1,800	~1,800	~1,800	~140	~1,800	1,593	1,593	1,613	1,593	1,593	1,559	1,559	1,559	1,559

HEAT GENERATED IN CORE = 112.50 MW(TH)
NUCLEAR HEATING = 2.64
COMPRESSION HEATING = 1.77
TOTAL 117.11 MW(TH)

NET THERMAL EFFICIENCY = $\frac{40}{115.34}$ = 34.7 %

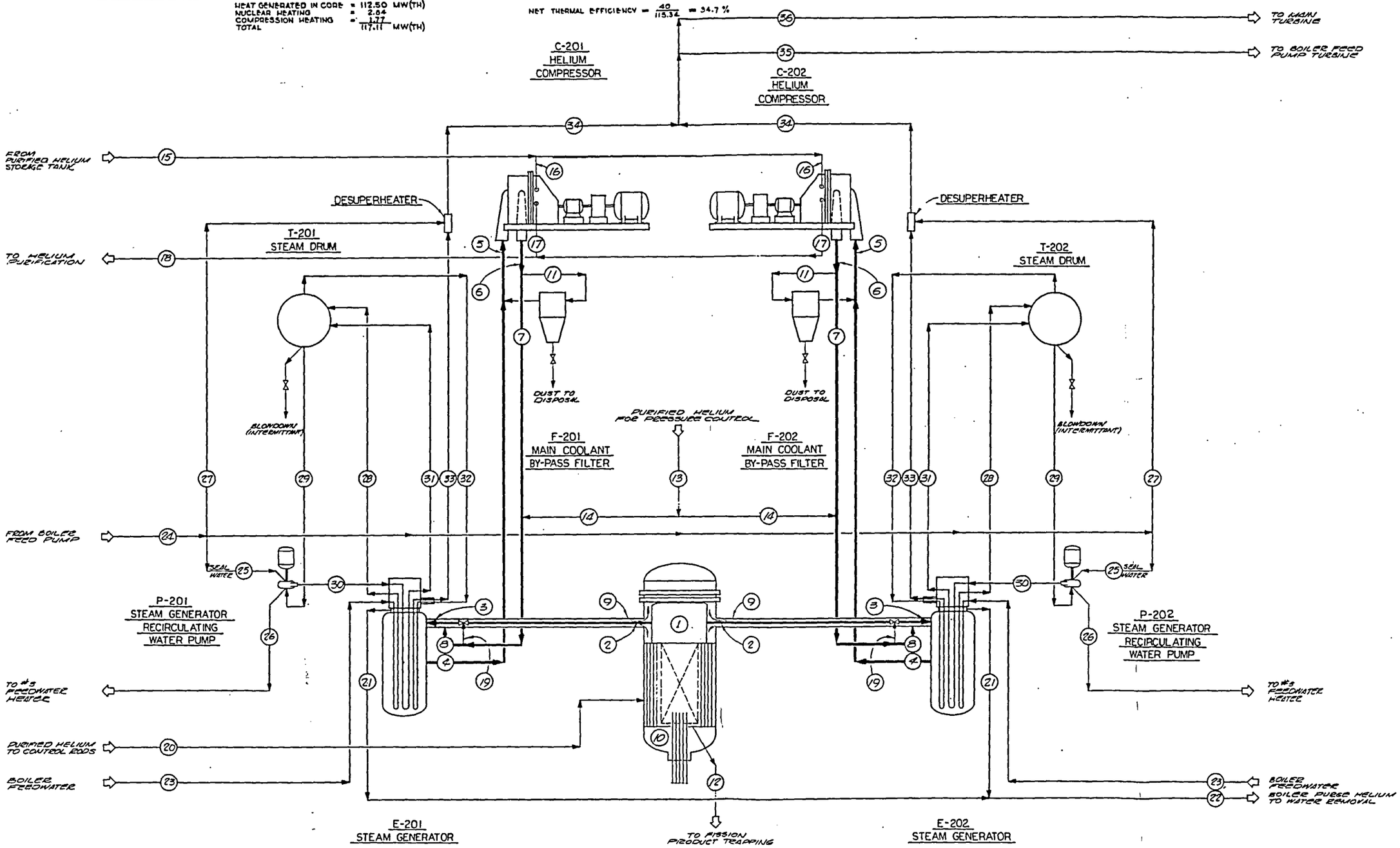

MAIN COOLANT SYSTEM PROCESS FLOW DIAGRAM SHOWING STEADY STATE OPERATING CONDITIONS FOR 100% POWER OUTPUT WITH FOULED AND PLUGGED BOILERS

FIGURE 58

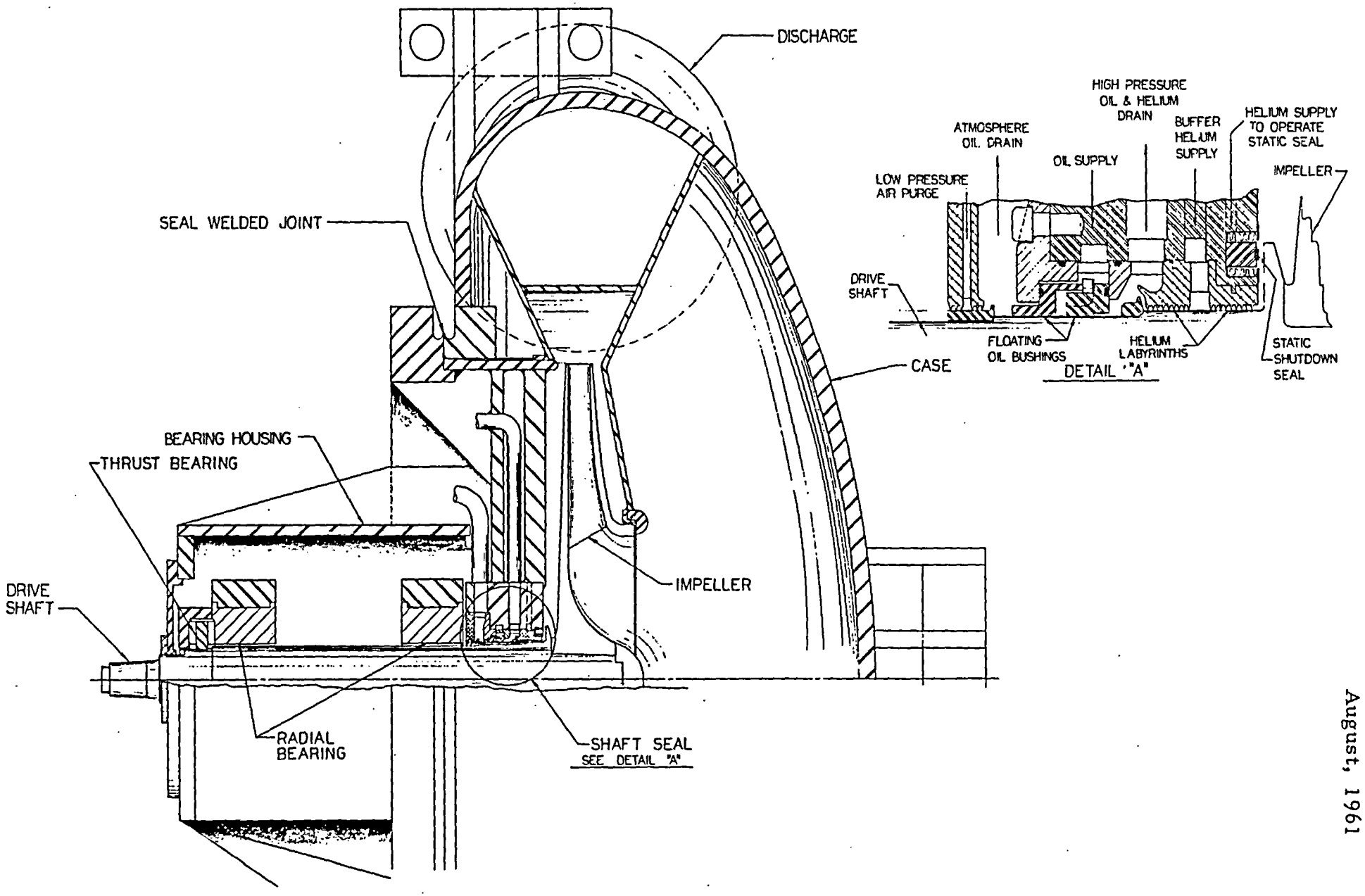

HELIUM COMPRESSOR CROSS SECTION

FIGURE 59

August, 1961

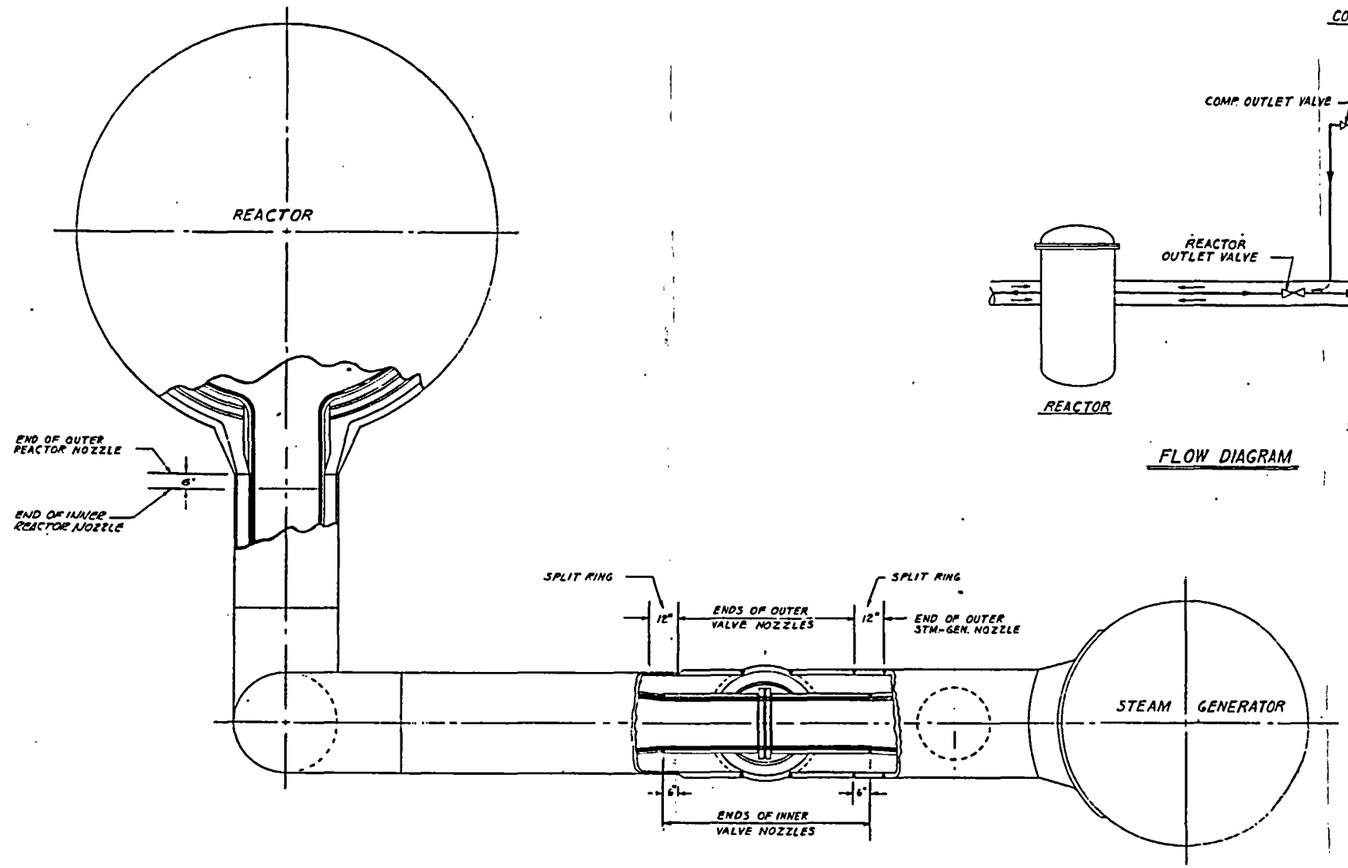

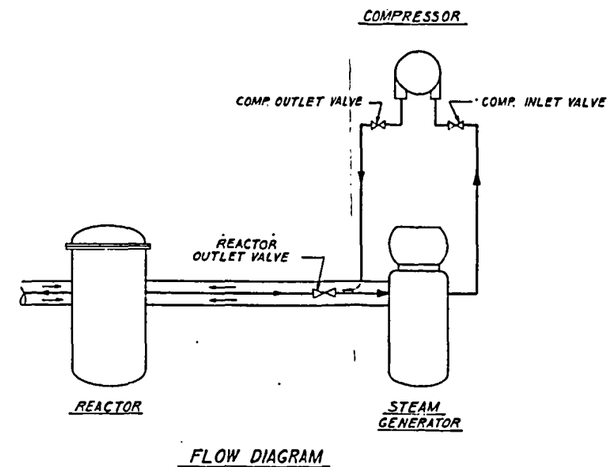

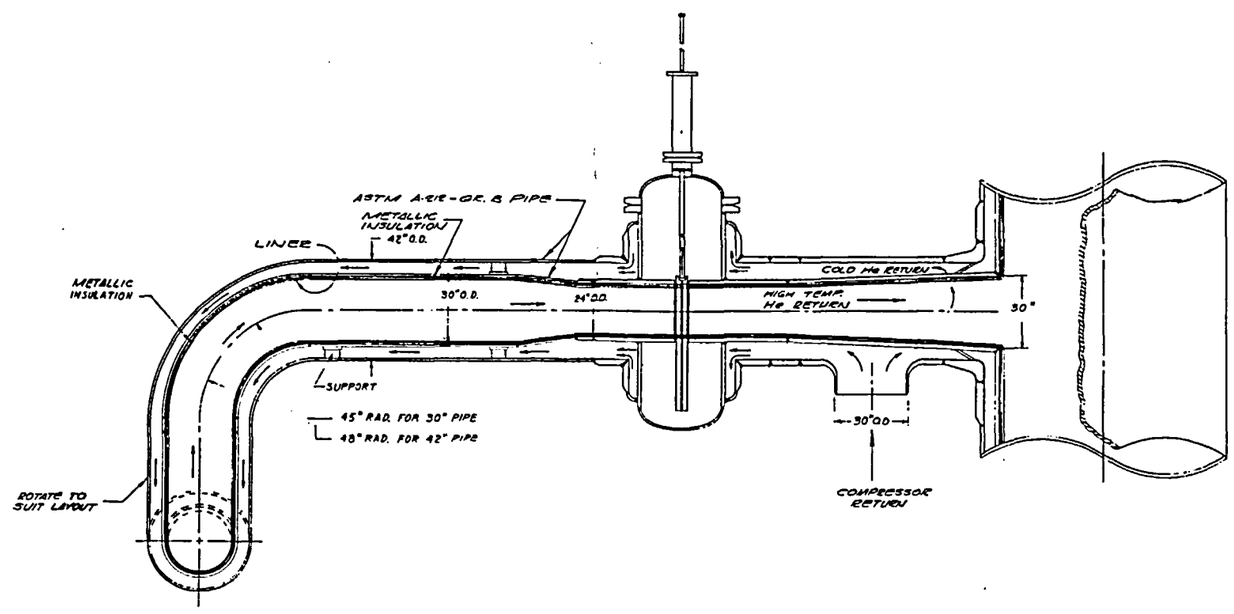

CONCENTRIC PIPE CONSTRUCTION

FIGURE 60

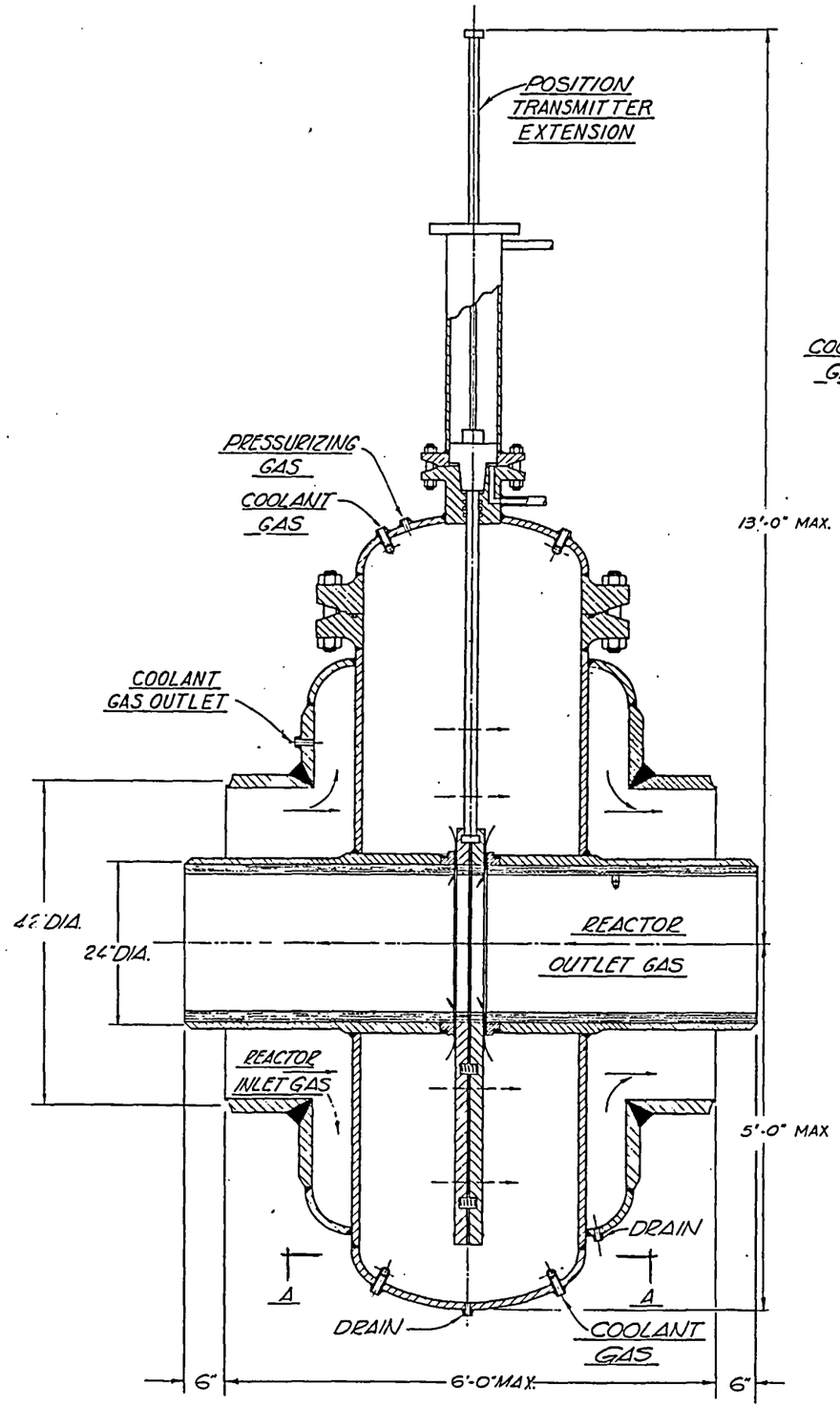

SECTION

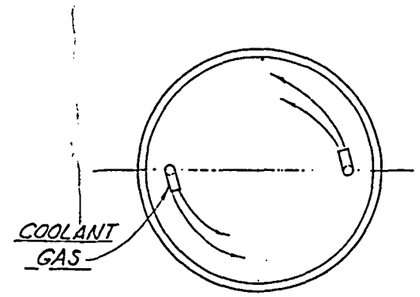

SECTION "A-A"

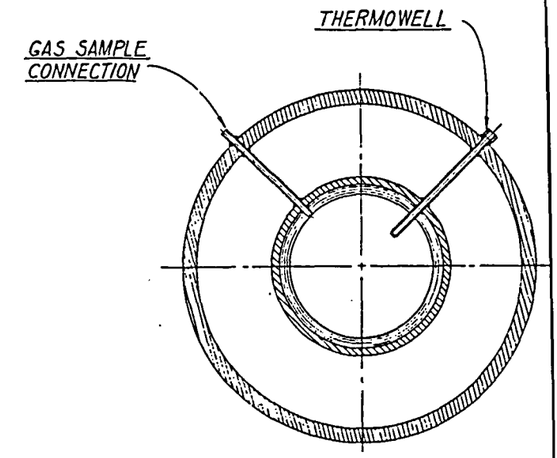

SECTION "B-B"

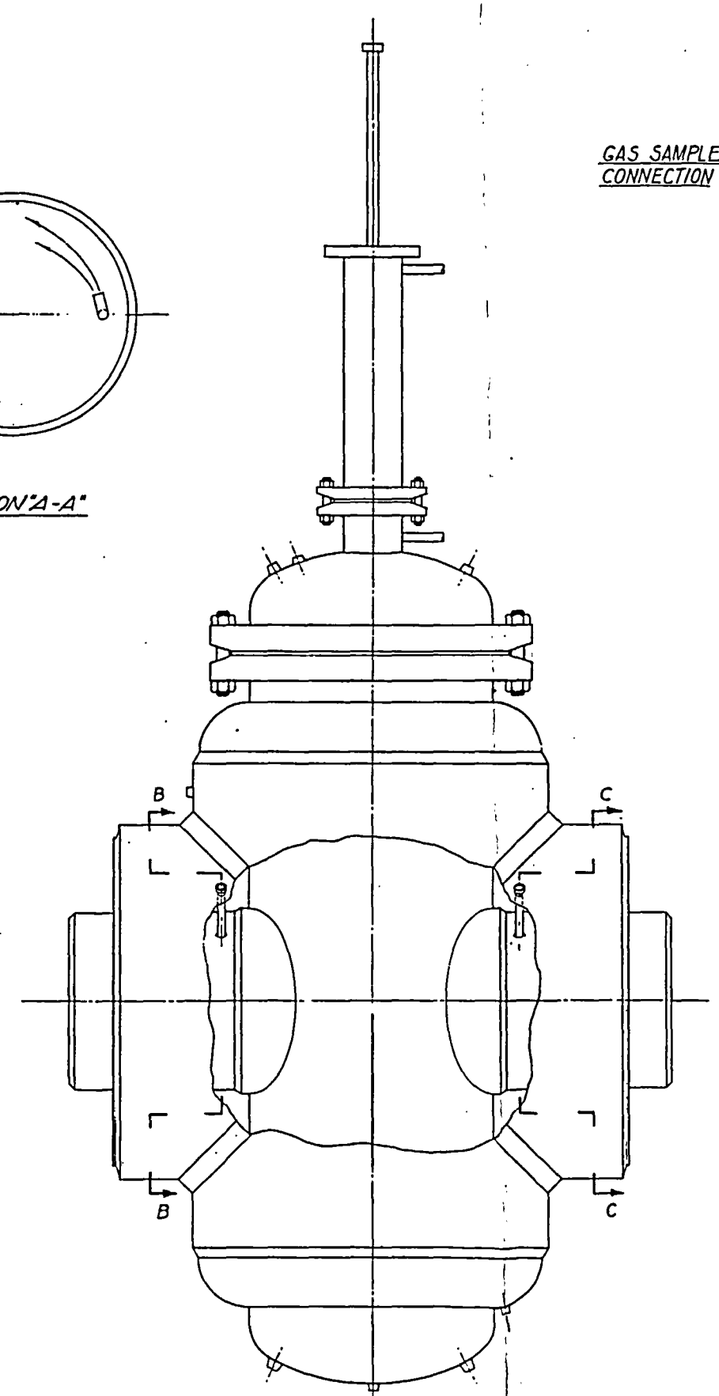

VALVE EXTERIOR

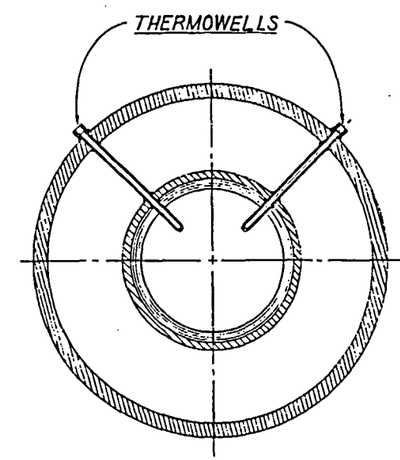

SECTION "C-C"

REACTOR OUTLET VALVE

FIGURE 61

August, 1961

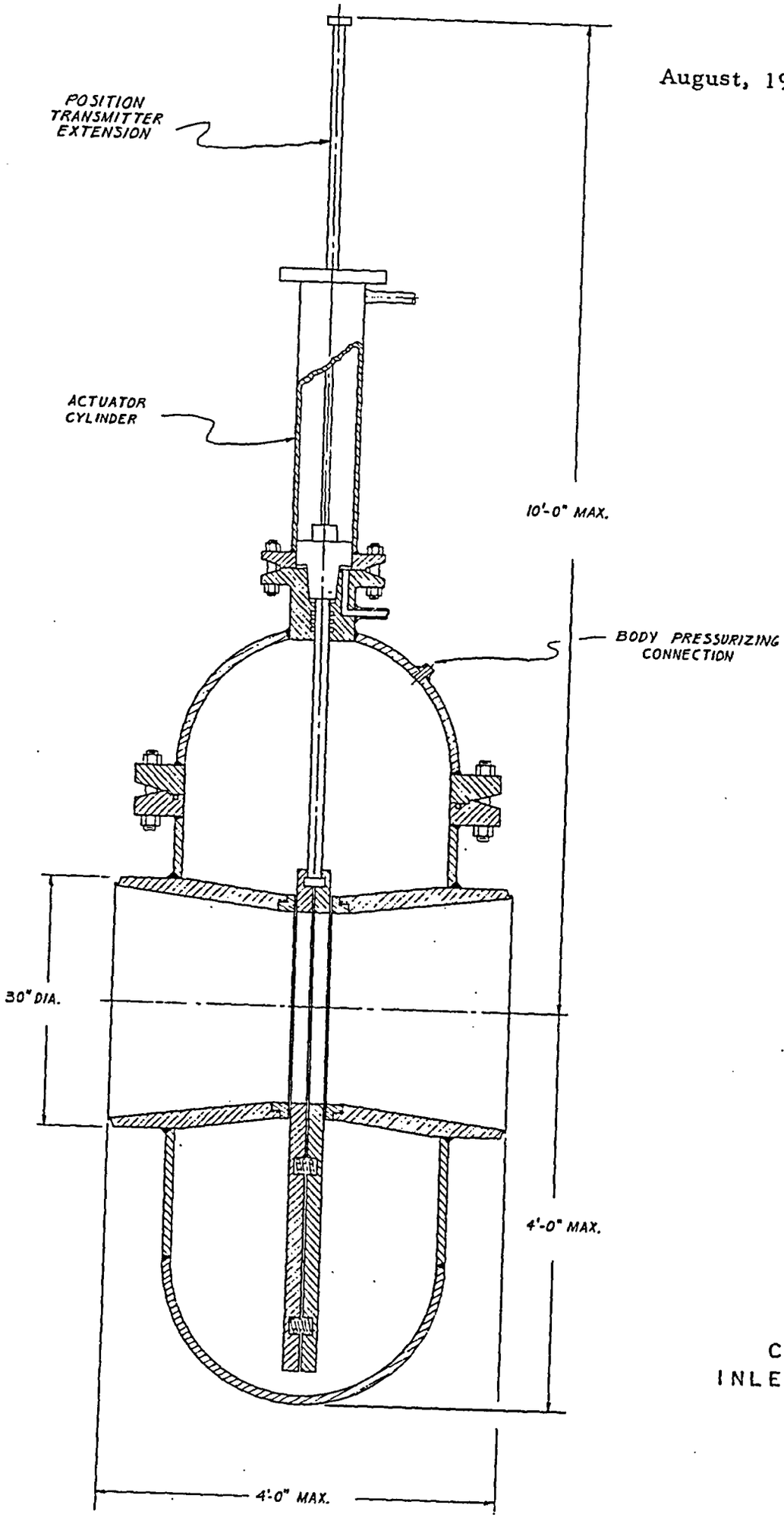

COMPRESSOR INLET AND OUTLET VALVES

FIGURE 62

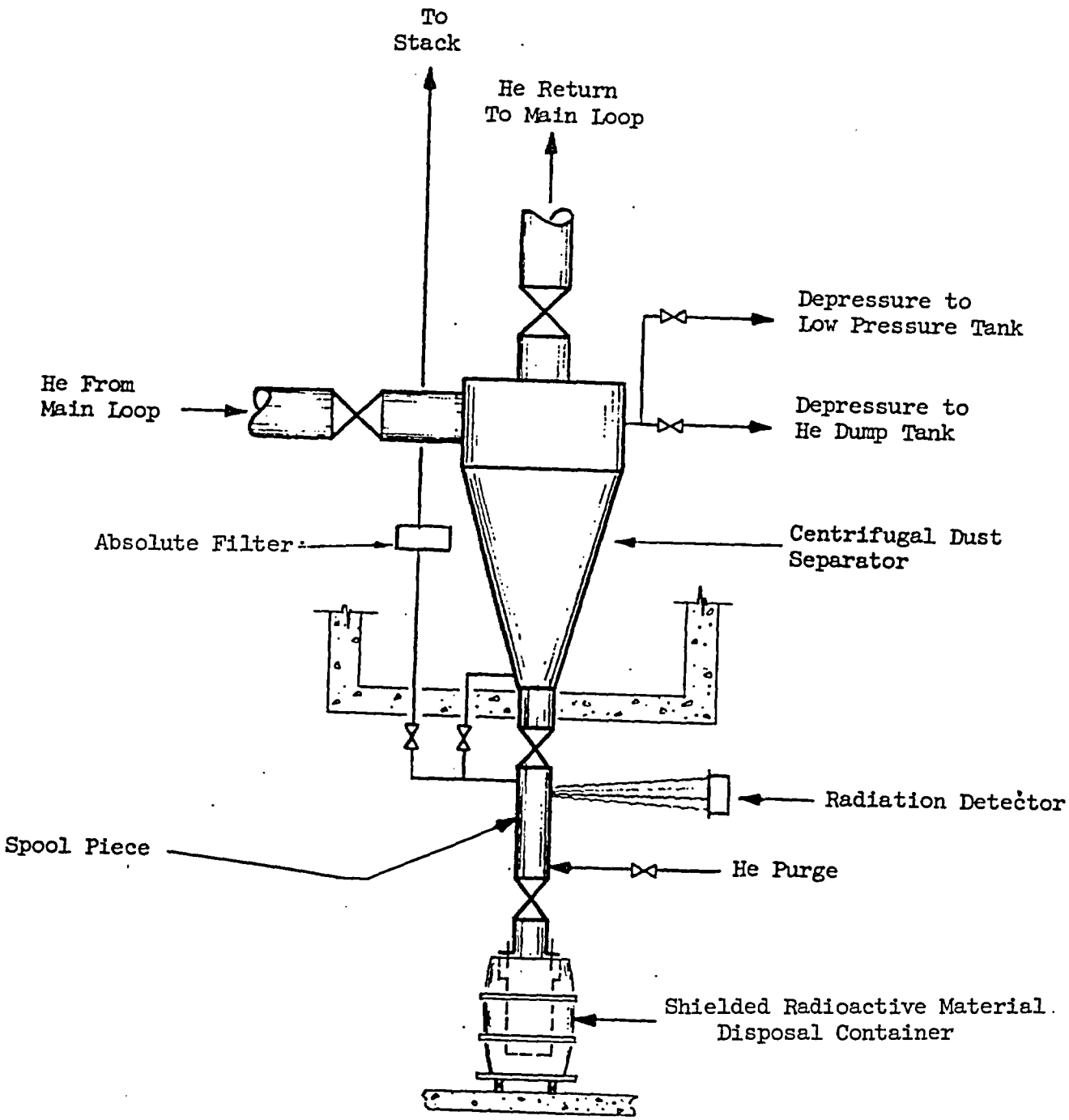

PIPING ARRANGEMENT FOR MAIN COOLANT BYPASS FILTER

FIGURE 63

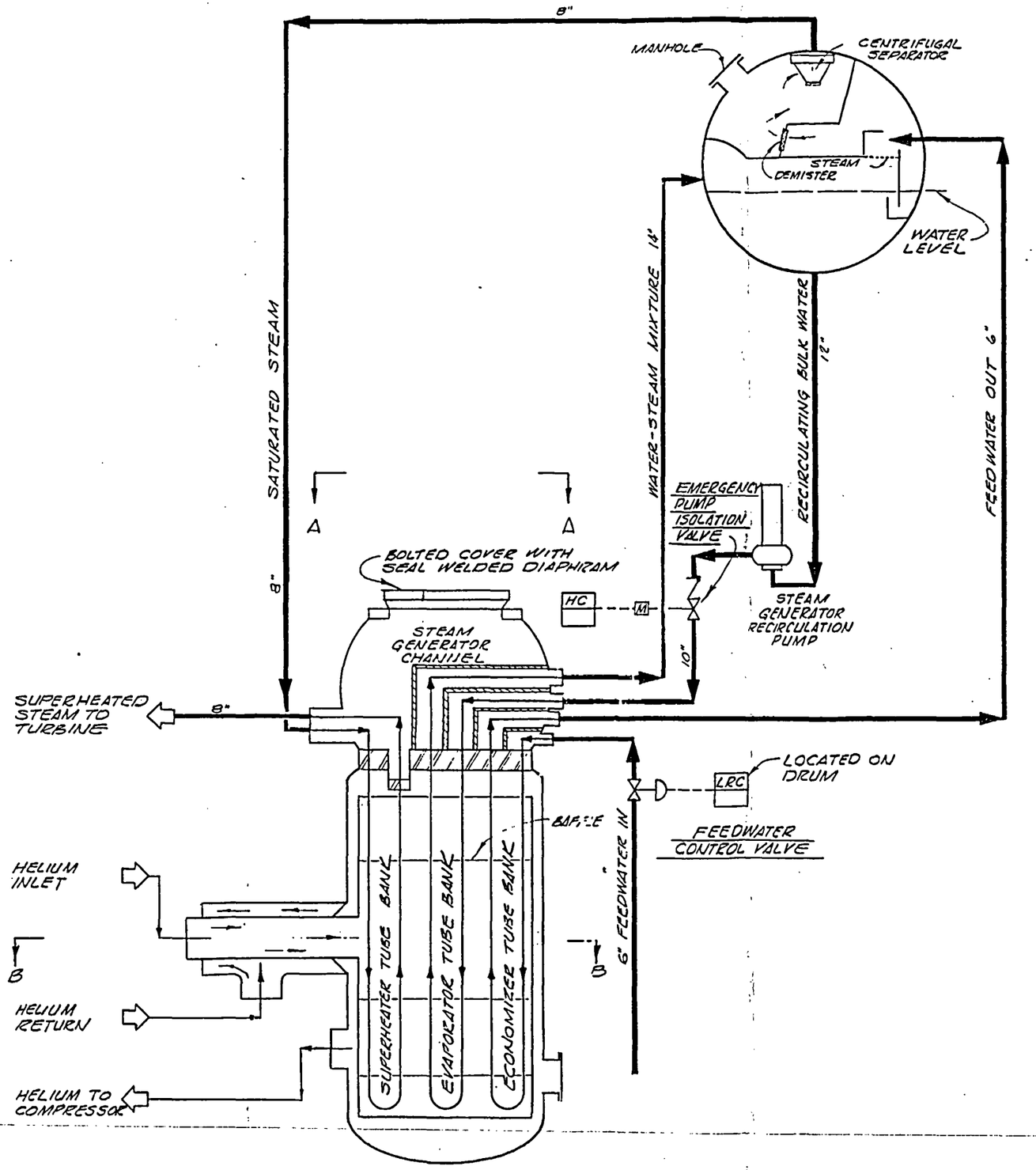

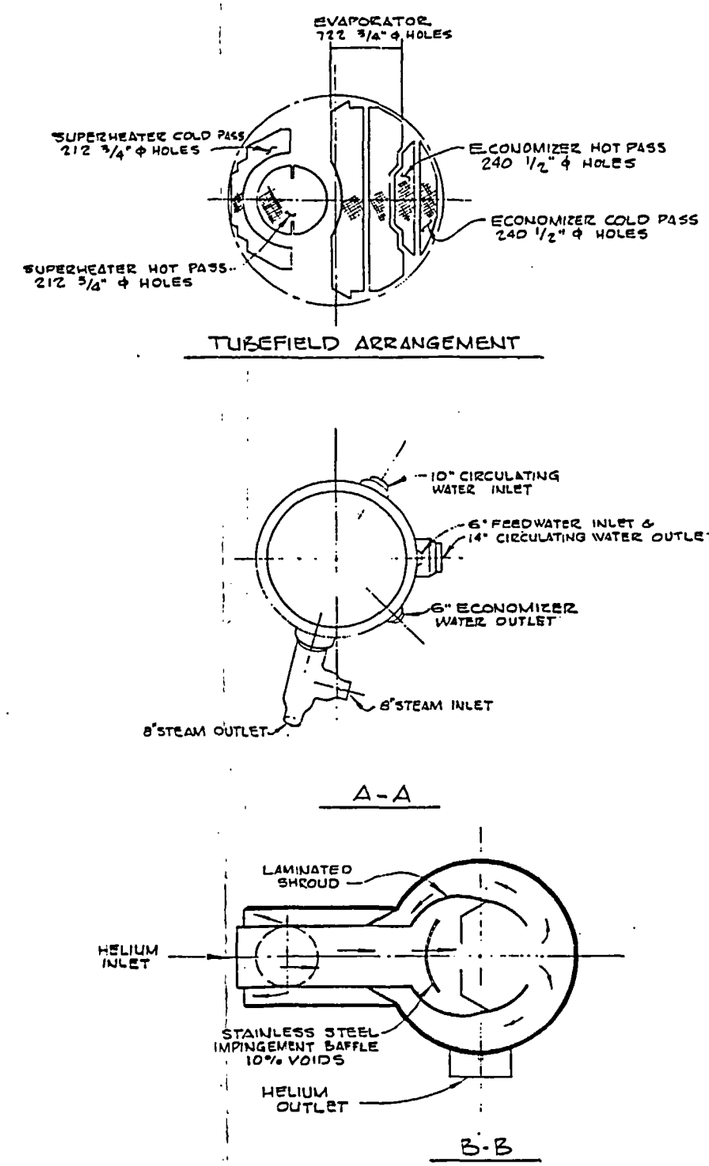

HTGR STEAM GENERATOR CIRCUIT

FIGURE 64

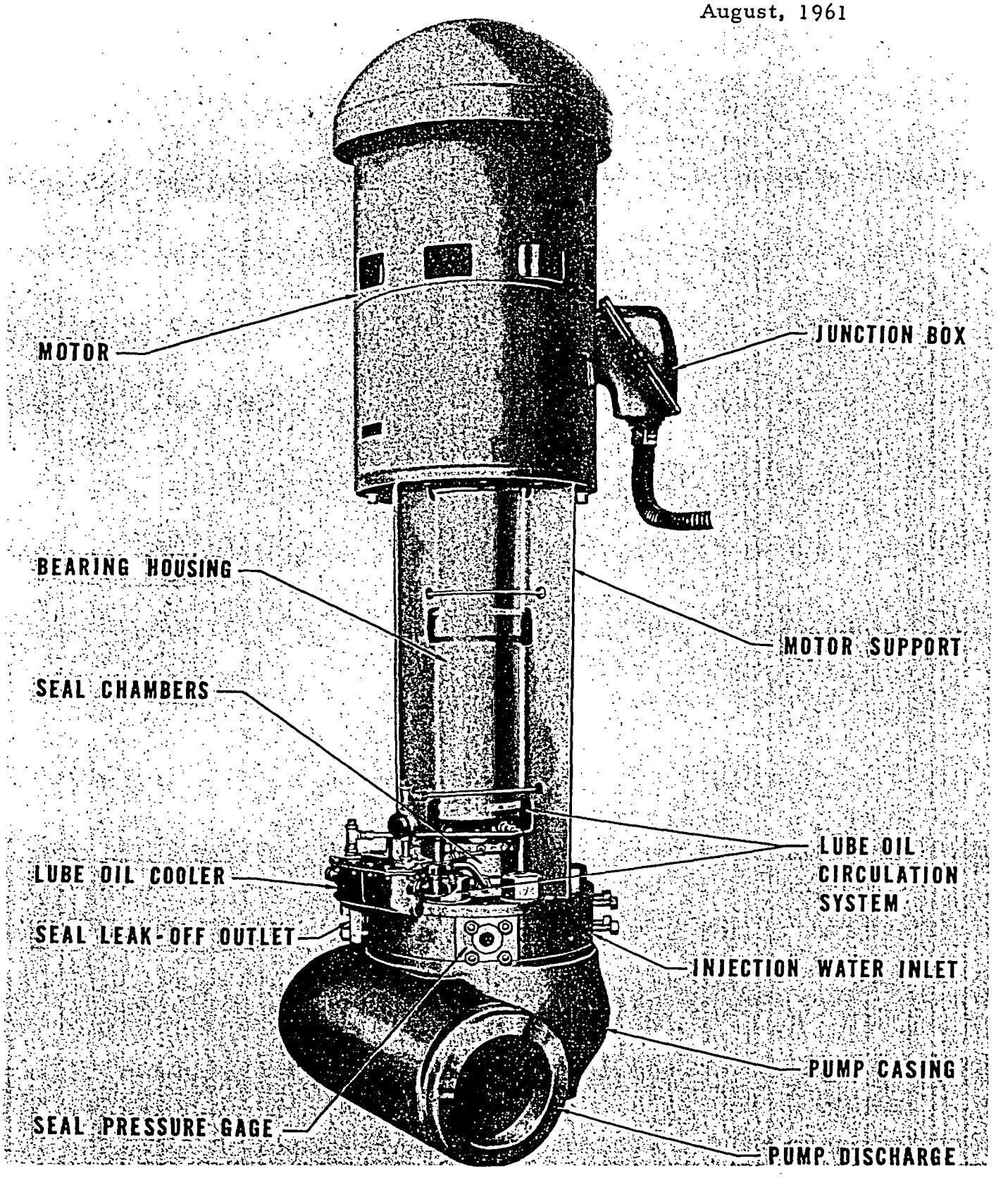

RECIRCULATION PUMP

FIGURE 65

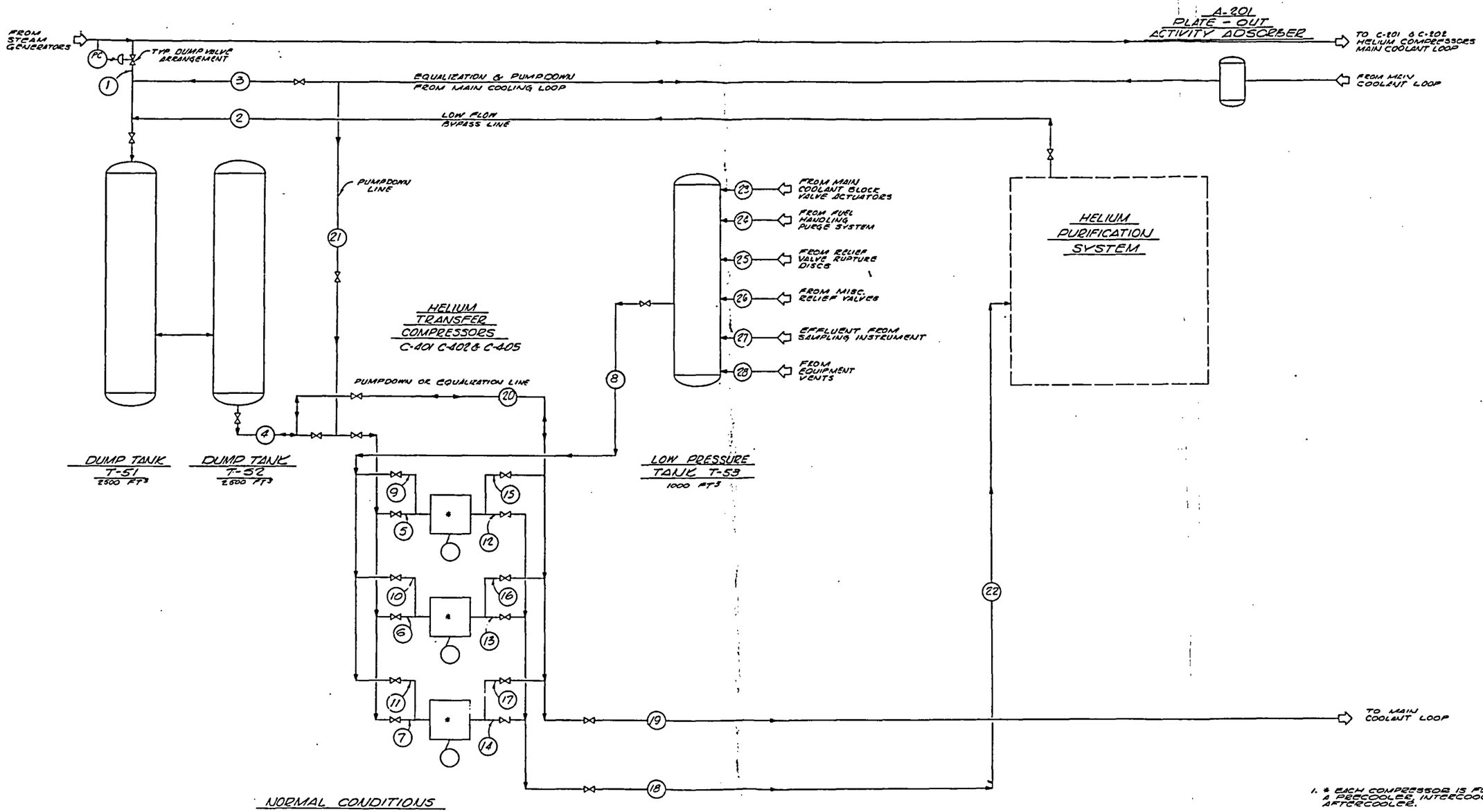

NORMAL CONDITIONS

STREAM NO.	1	2	3	4	5	6	7	8	9	10	11	12	13	14	15	16	17	18	19	20	21	22	23	24	25	26	27	28
MAX. FLOW RATE #/HR	~	0	0	37.5	37.5	0	0	21	0	21	0	0	21	0	37.5	0	0	21	37.5	0	0	21	0	0	0	0	1.5	0
MAX. FLOW RATE SCFM	0	0	0	56.1	56.1	0	0	31.4	0	31.4	0	0	31.4	0	56.1	0	0	31.4	56.1	0	0	31.4	0	0	0	0	2.2	0
MAX. FLOW RATE ACFM	0	0	0	31.4	31.4	0	0	33.7	0	33.7	0	0	1.57	0	2.69	0	0	1.57	2.69	0	0	1.56	0	0	0	0	2.73	0
PRESSURE PSIA	20/30	20/30	20/30	20/30	20/30	17/15	17/15	17/15	20/30	17/15	17/15	355	341	15/17	355	341	17/15	341	355	355	350	340	15/17	15/17	15/17	15/17	15/17	15/17
TEMPERATURE °F	100	100	100	100	100	100	100	100	100	150	100	110	110	100	110	110	100	110	110	100	100	110	100	100	100	100	150	100

1. * EACH COMPRESSOR IS FURNISHED WITH A PRECOOLER, INTERCOOLER, AND AN AFTERCOOLER.
2. STANDARD CONDITIONS @ 14.7 PSIA & 32 °F.
3. NORMAL CONDITIONS SHOW TRANSFER COMPRESSORS AS FOLLOWS:
   a. ONE ON DUMP TANK SERVICE.
   b. ONE ON LOW PRESSURE TANK SERVICE.
   c. ONE ON STANDBY.

NON-PURIFIED HELIUM HANDLING SYSTEM
PROCESS FLOW DIAGRAM

FIGURE 66

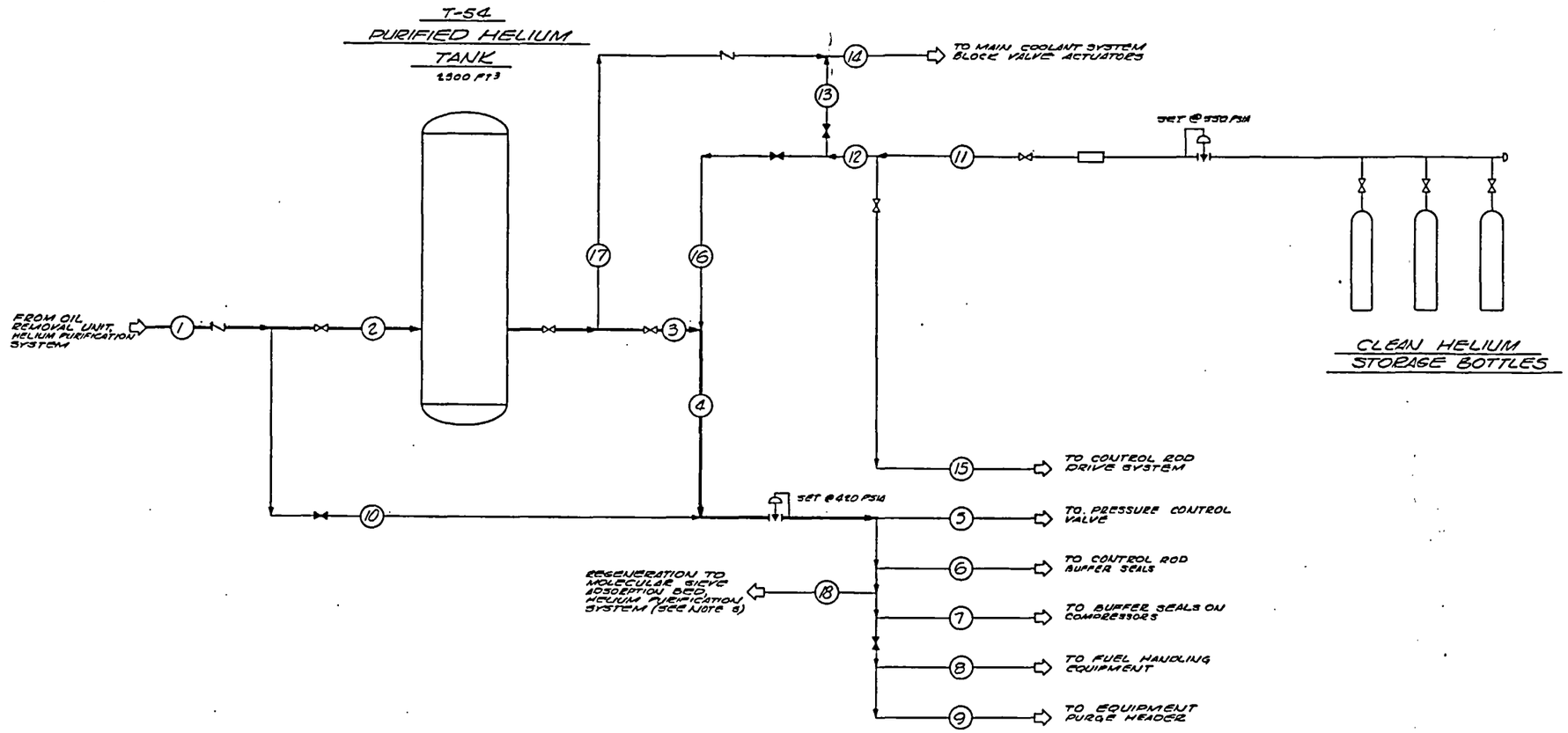

GENERAL NOTES

1. STANDARD CONDITIONS AT 14.7 PSIA & 32 °F.
2. FLOW TO BLOCK VALVE ACTUATORS SHOWN FOR THREE VALVES OPERATING SIMULTANEOUSLY AT TWICE AVERAGE FLOW RATE. EACH OPERATOR WILL REQUIRE APPROXIMATE 0.6 # HELIUM.
3. FLOW FROM CLEAN HELIUM BOTTLES SHOWN AT NOMINAL MAKE-UP RATE.
4. FLOW THRU PRESSURE CONTROL VALVE SHOWN FOR A 3% PER MINUTE LOAD CHANGE.
   a- DECREASING LOAD
   b- INCREASING LOAD
5. MOLECULAR SIEVE REGENERATION FLOW REQUIRED APPROXIMATELY 50% OF THE TIME.

NORMAL CONDITIONS

STREAM NO.	1	2	3	4	5	6	7	8	9	10	11	12	13	14	15	16	17	18
MAT FLOW RATE #/HR	1380	1380	1380	1390	870	100	810	0	0	0	0	0	0	0	0	0	0	100
MAT FLOW RATE SCFM	2320	2320	2320	2320	1302	150	464	0	0	0	0	0	0	0	0	0	0	150
MAT FLOW RATE MOL/HR	72.3	72.3	72.3	72.3	32.8	6.01	18.7	0	0	0	0	0	0	0	0	0	0	6.01
PRESSURE PSIA	320/ABS	320/ABS	320/ABS	320/ABS	460	460	460	460	460	320/ABS	550	550	320/ABS	320/ABS	550	320/ABS	320/ABS	460
TEMPERATURE °F	105	105	105	105	105	105	105	100	100	100	100	100	100	100	100	100	100	105

NOTE 2

14	17
4320	4320
6450	6450
226	226
320/ABS	320/ABS
105	105

NOTE 3

11	12
1000	1000
1495	1495
51.9	51.9
320/ABS	320/ABS
100	100

NOTE 4

"a"	"b"
5	5
1165	775
1741	1160
70	46.6
420	420
105	105

PURIFIED HELIUM HANDLING SYSTEM PROCESS FLOW DIAGRAM

FIGURE 67

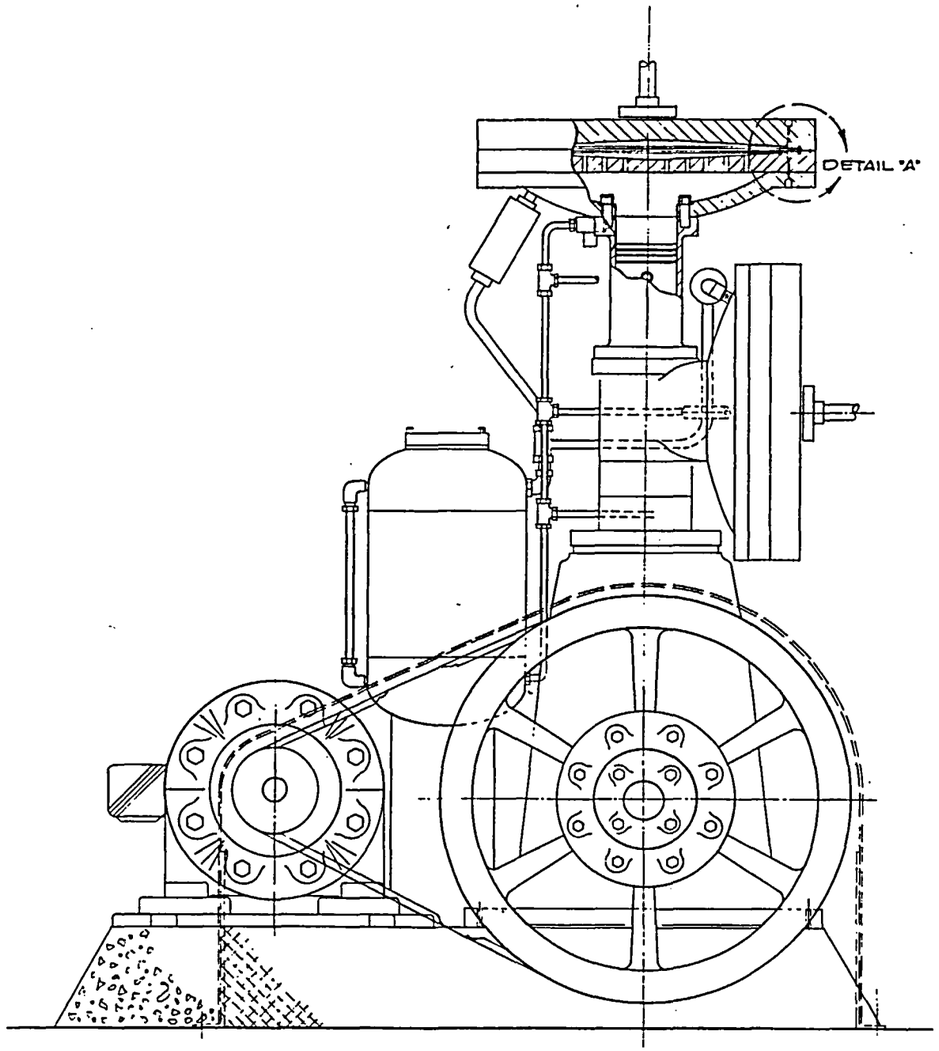

ELEVATION
NO SCALE

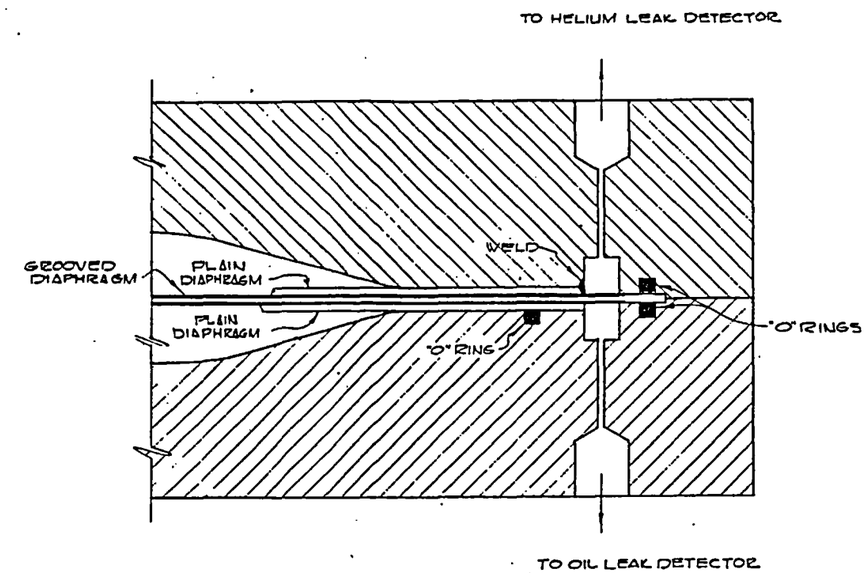

DETAIL "A"
NO SCALE

HELIUM HANDLING SYSTEM TRANSFER COMPRESSOR

FIGURE 68

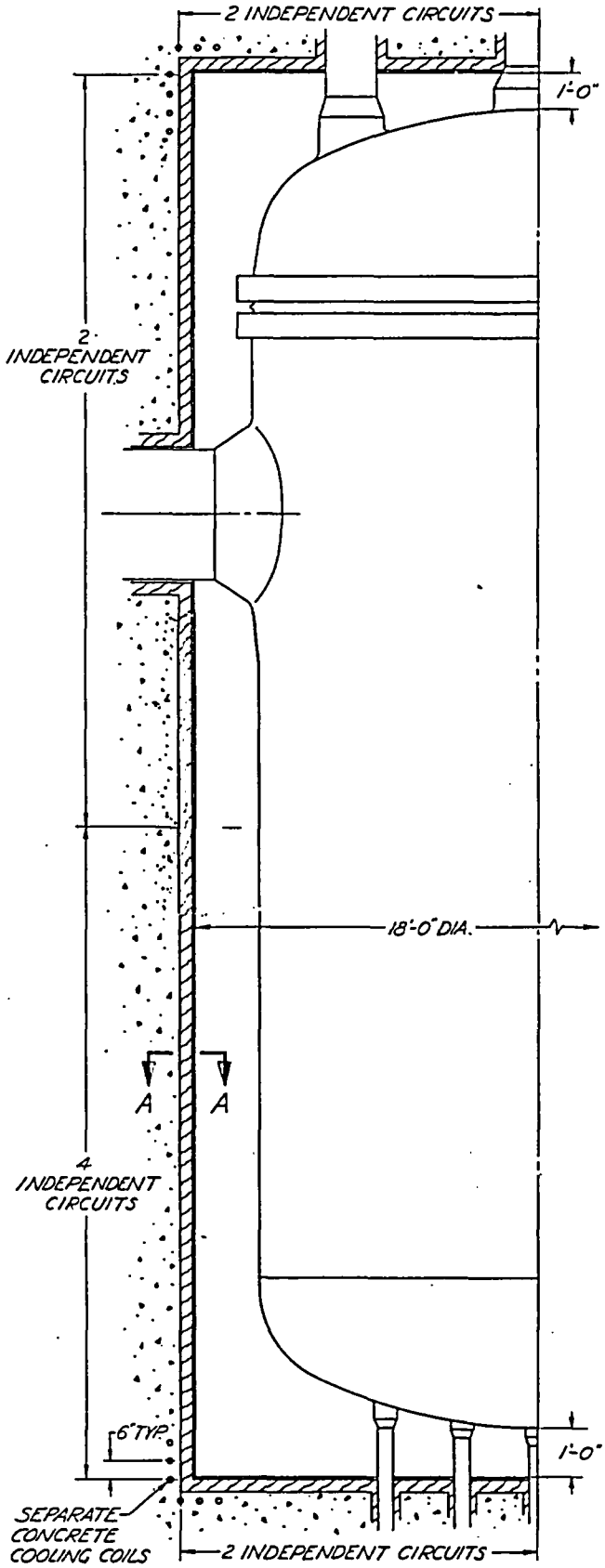

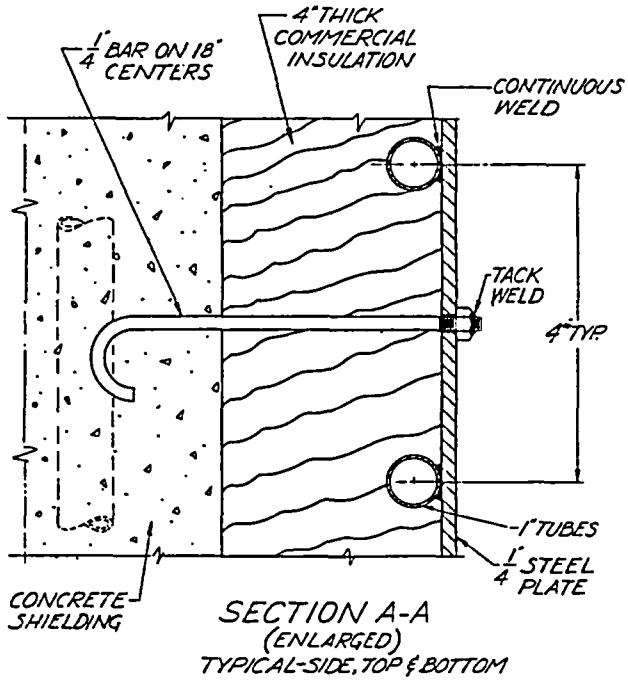

EMERGENCY COOLING COIL SYSTEM

FIGURE 6

August, 1961

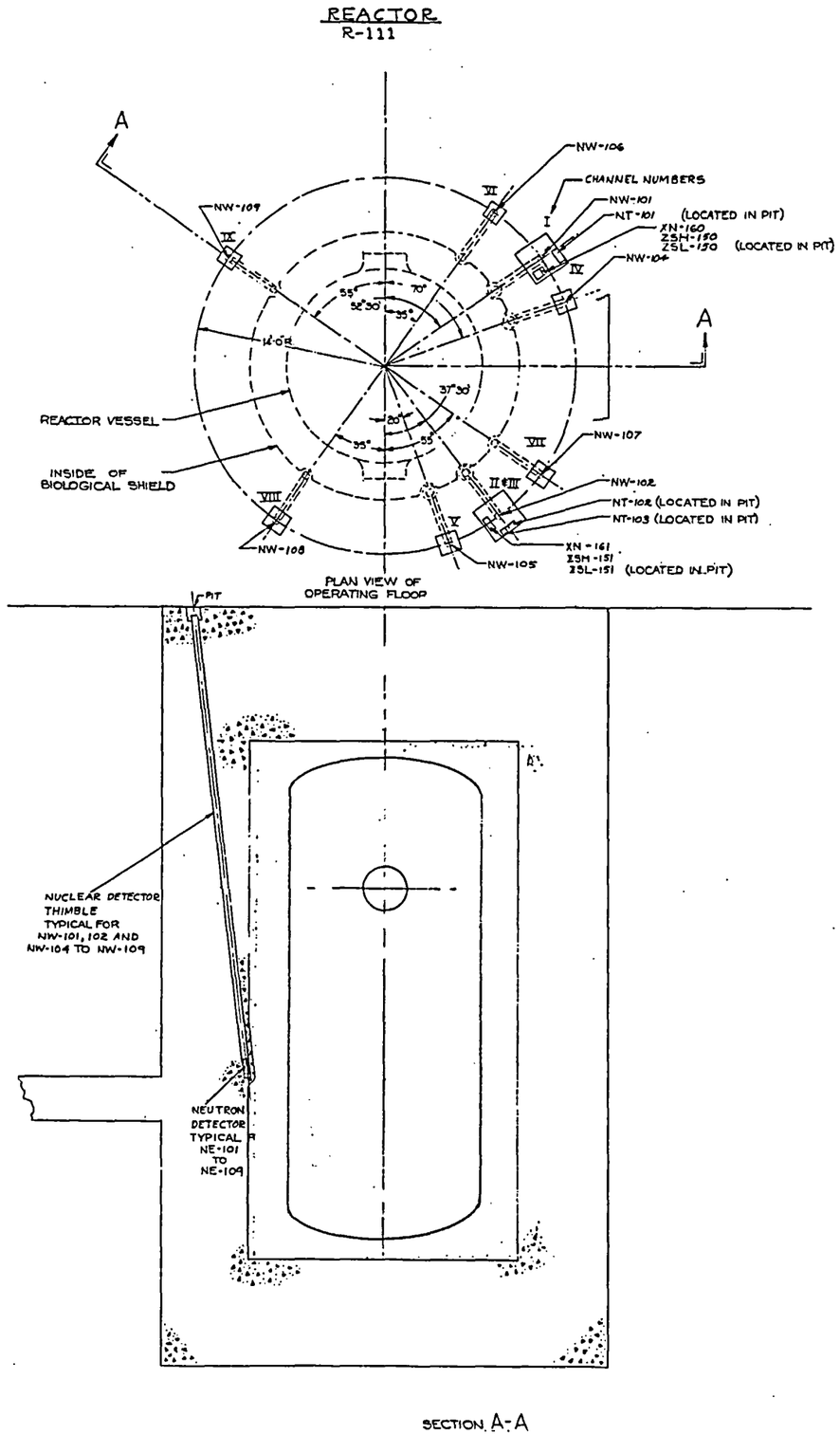

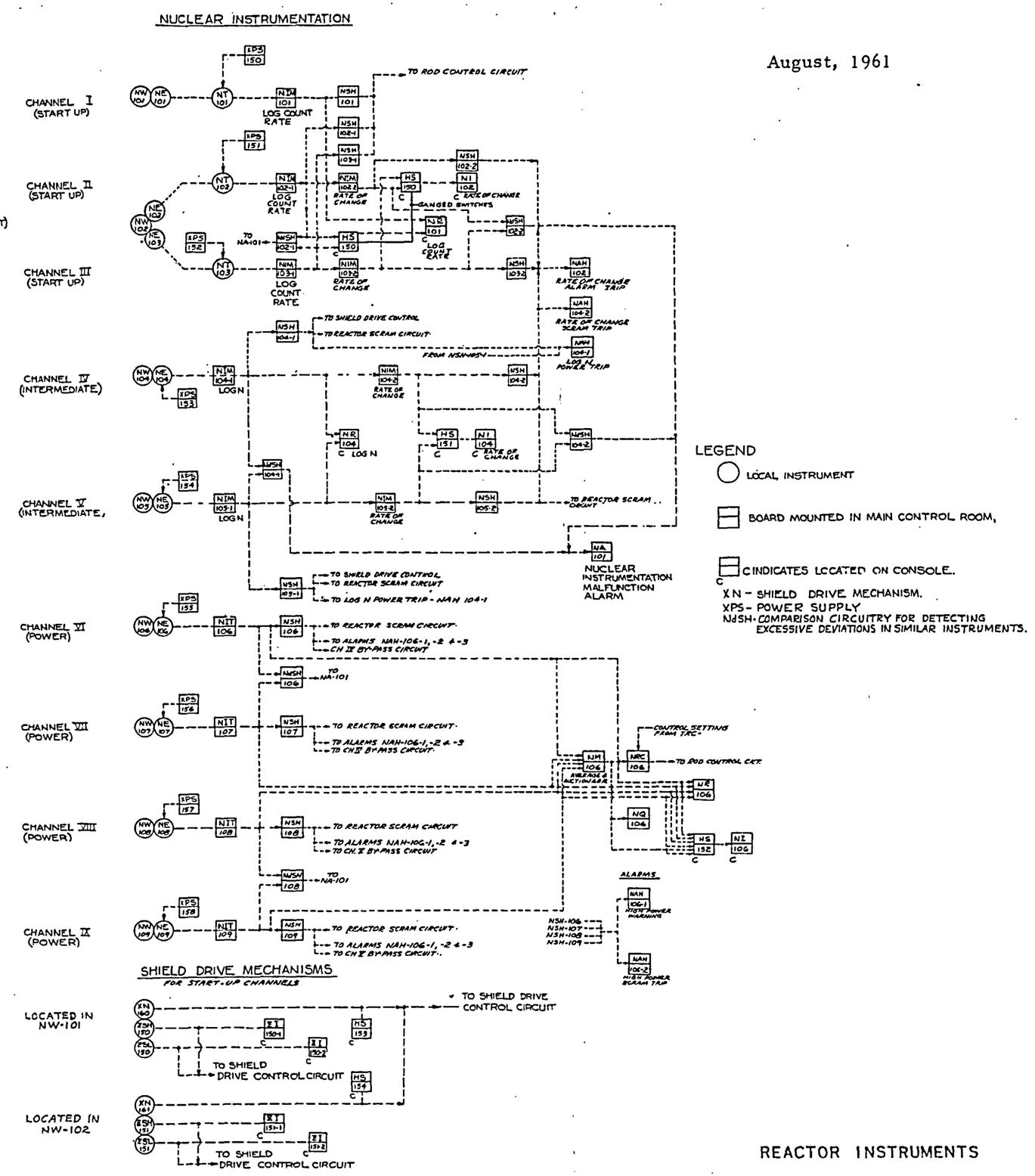

REACTOR INSTRUMENTS

FIGURE 70

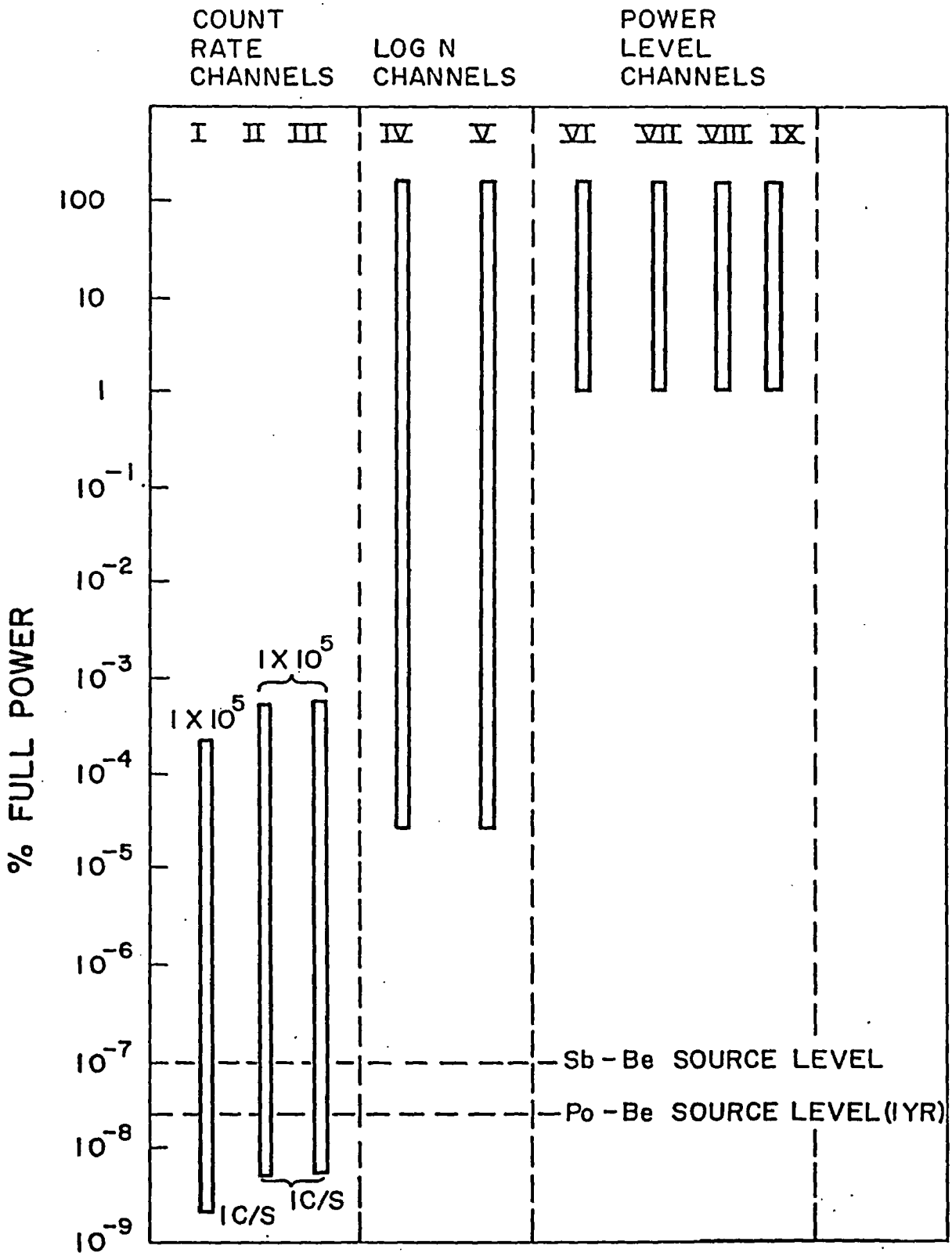

APPROXIMATE HTGR NUCLEAR INSTRUMENT RANGES

FIGURE 71

August, 1961

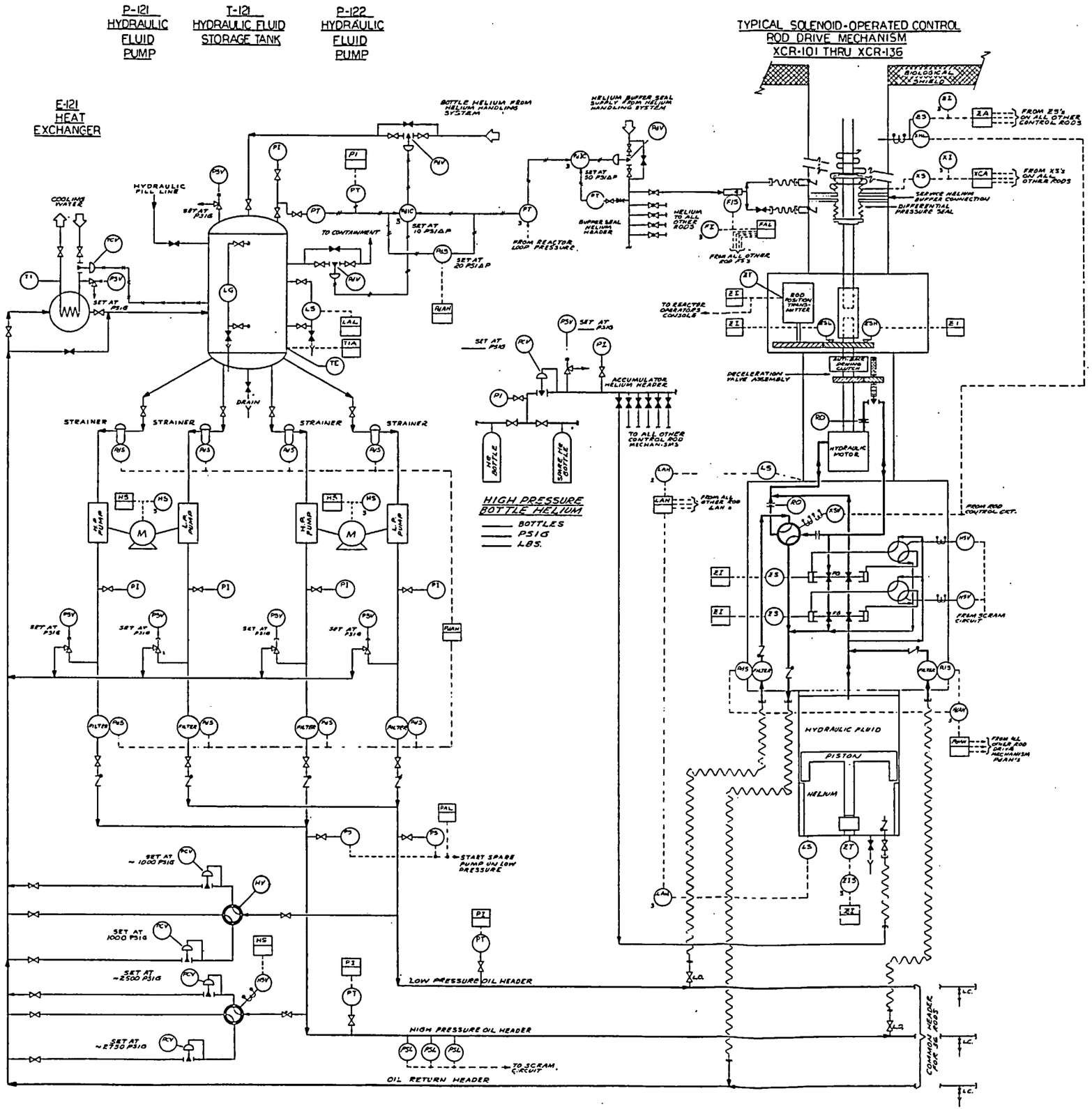

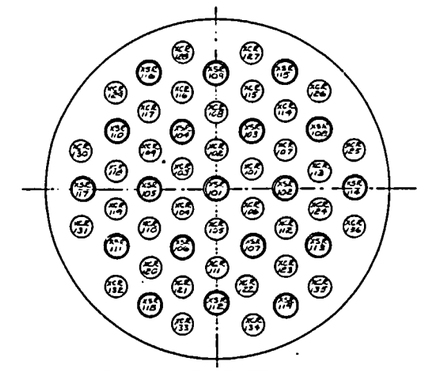

LOCATION OF CONTROL AND EMERGENCY SHUTDOWN RODS IN REACTOR VESSEL, R-111

LEGEND

ALL SYMBOLS ARE STANDARD PER DAMD-1783 EXCEPT AS FOLLOWS:

- XHL - SCRAM HOLDING LOCK
- XSV - SOLENOID CONTROLLED VALVE (ON-OFF)
- INSTRUMENT MOUNTED ON LOCAL ROD DRIVE CONTROL BOARD #3
- XS - ROD CONTINUITY SWITCH
- XCA - ROD CONTINUITY ALARM
- XSR - EMERGENCY SHUTDOWN ROD
- XCR - REACTOR CONTROL ROD
- FLEXIBLE LINE WITH QUICK-CONNECT

NOTES:

1. XSV'S ARE 4 WAY, 3 POSITION VALVES, POSITIONED AS INDICATED BELOW.

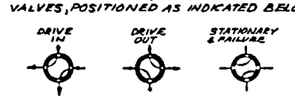

2. ALL VALVES ARE SHOWN IN NORMAL POSITION FOR SYSTEM OPERATION. RODS ARE STATIONARY.
3. ALL INSTRUMENTS ASSOCIATED WITH A PARTICULAR ROD WILL BEAR THE SAME NUMBER AS THAT ROD, ie, 101 THRU 136.

CONTROL ROD DRIVE SYSTEM CONTROL AND INSTRUMENT DIAGRAM

FIGURE 72

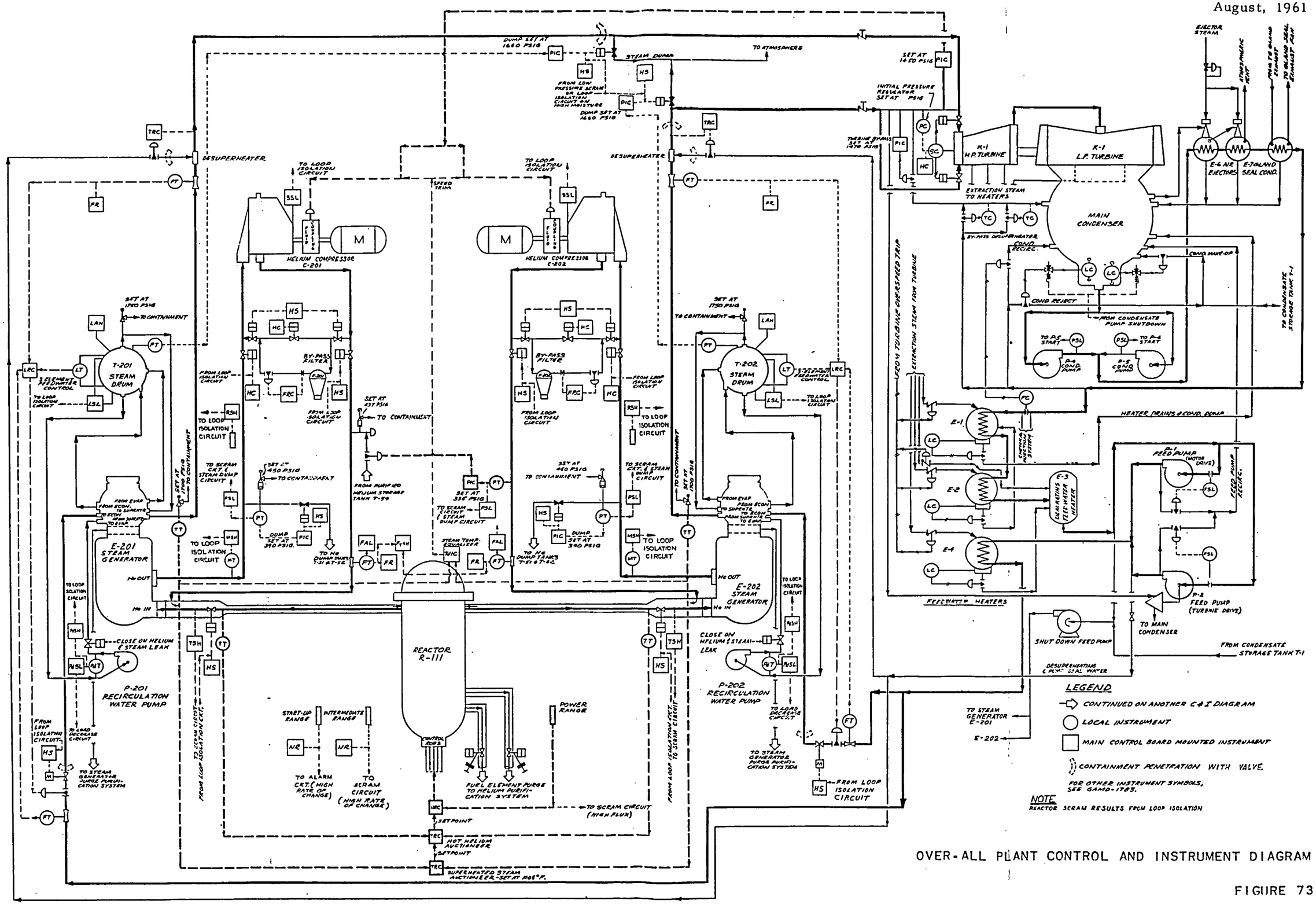

OVER-ALL PLANT CONTROL AND INSTRUMENT DIAGRAM

FIGURE 73

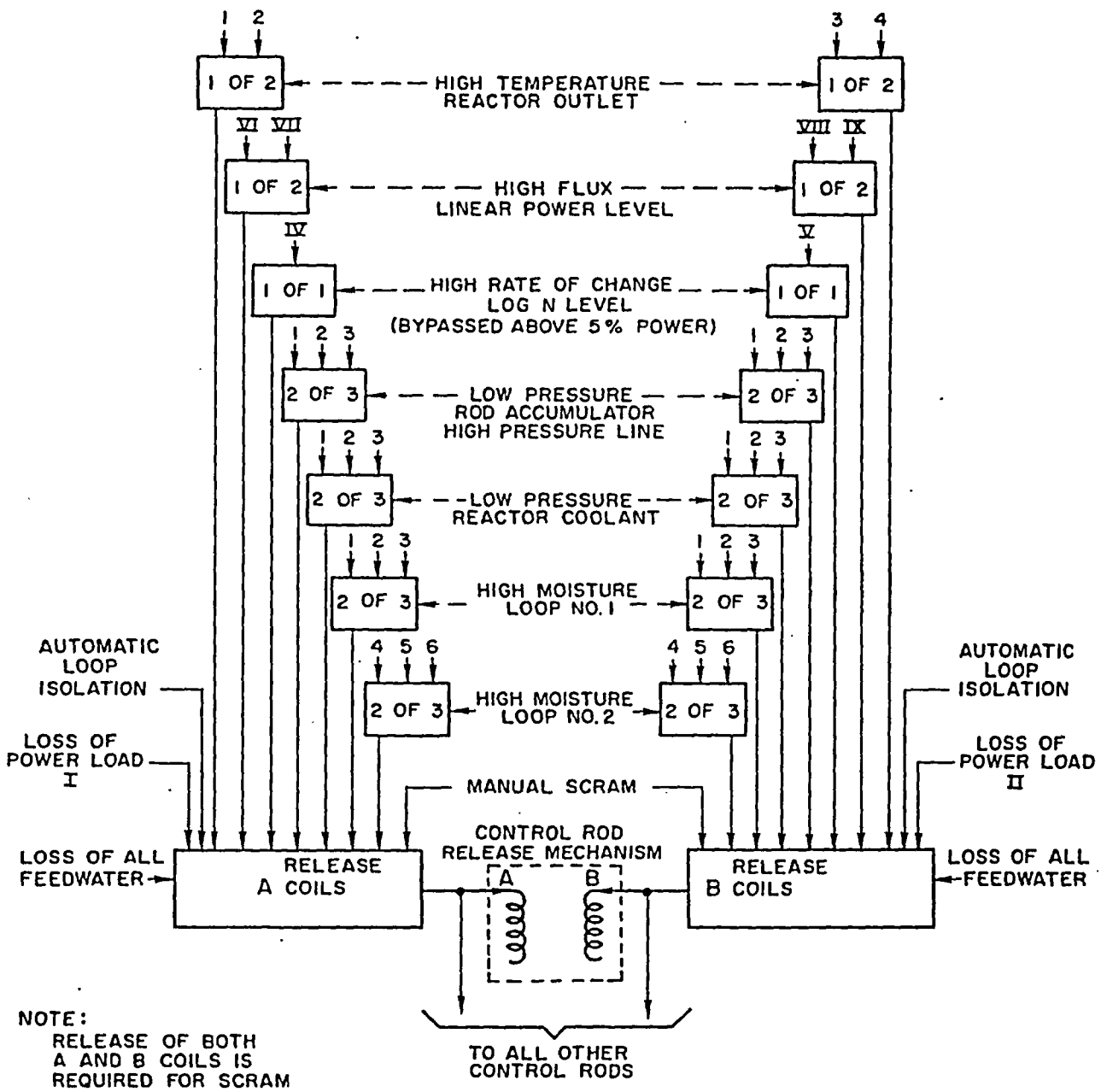

SIMPLIFIED HTGR SCRAM SYSTEM

FIGURE 74

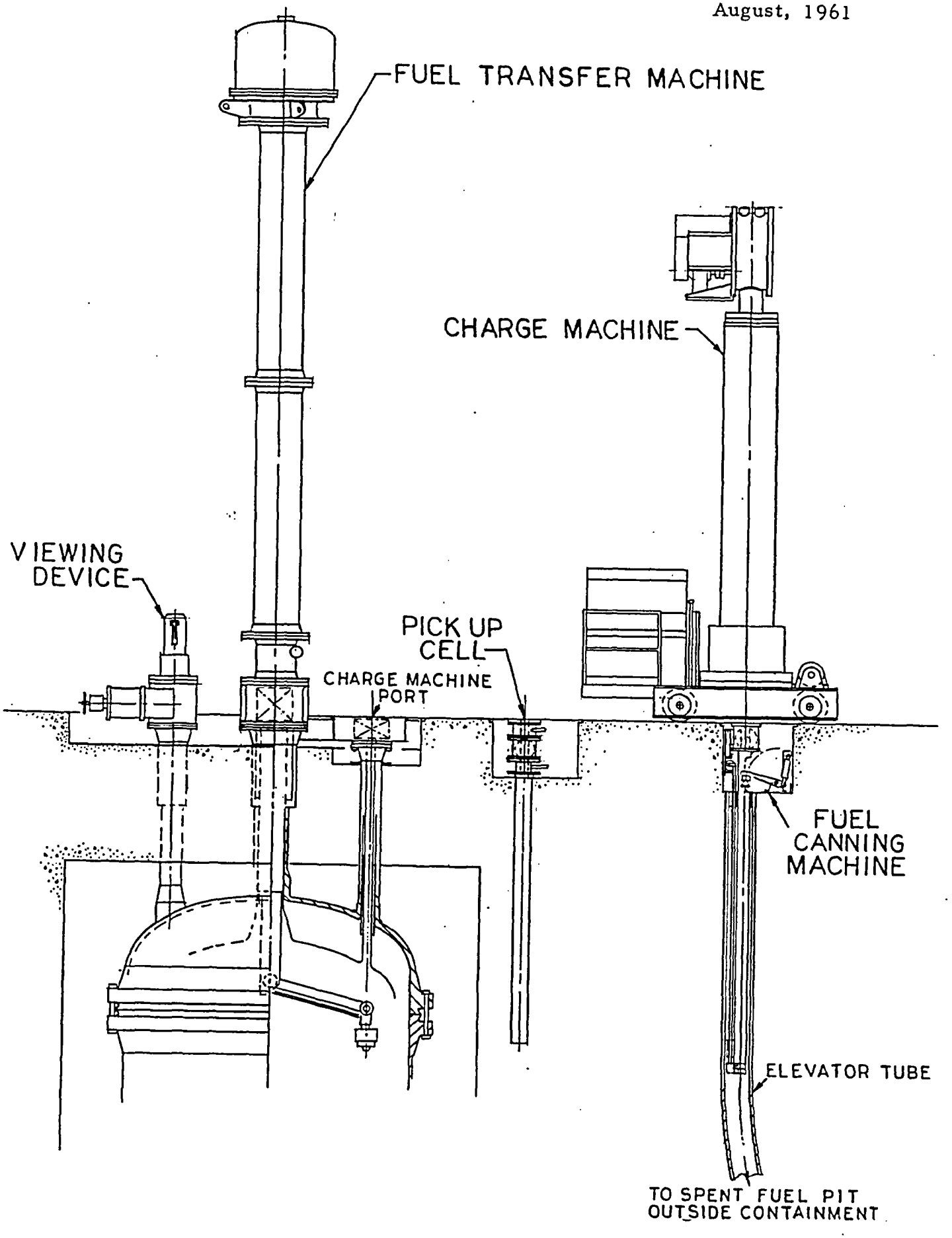

HTGR FUEL HANDLING EQUIPMENT

FIGURE 75

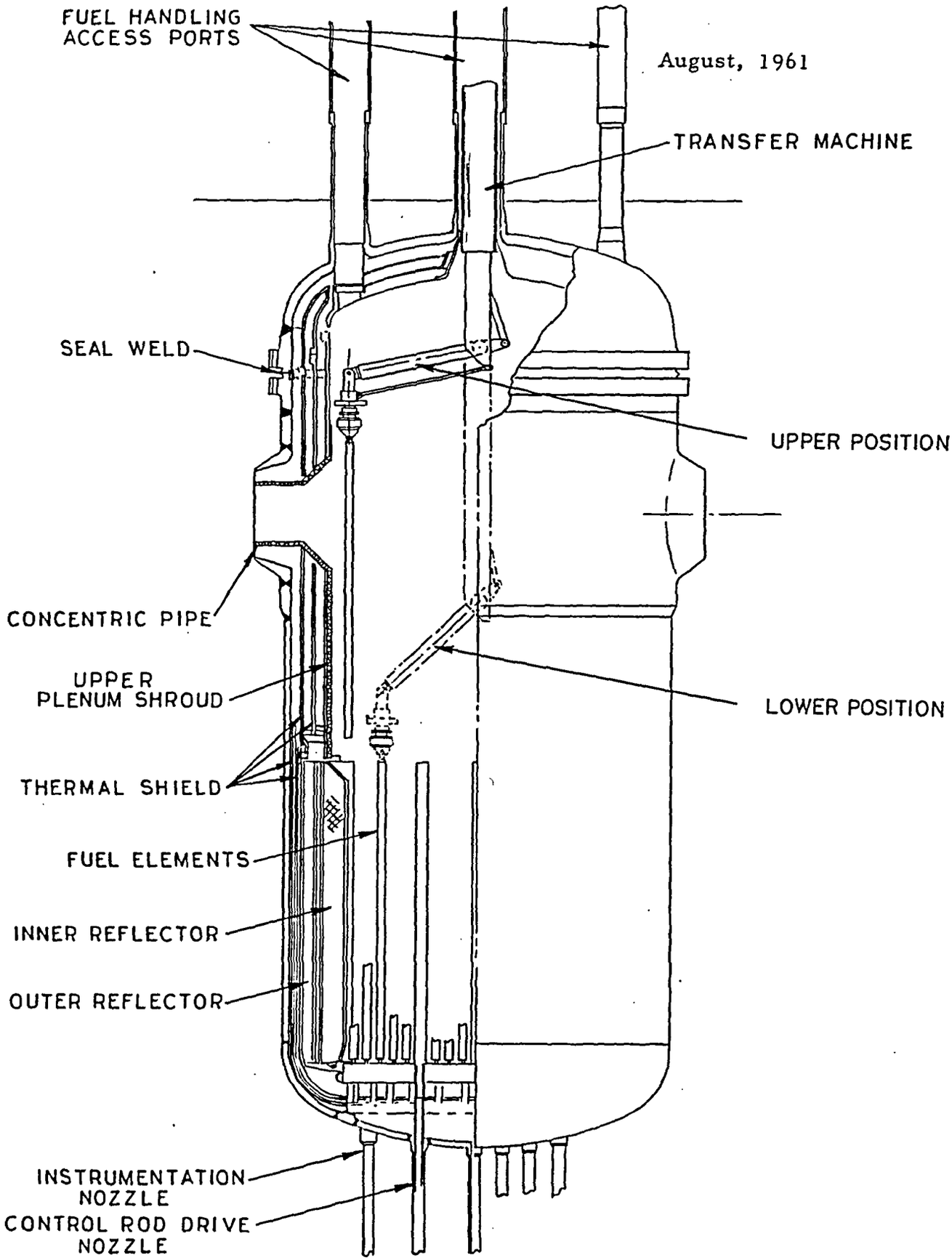

FUEL TRANSFER MACHINE INSIDE PRESSURE VESSEL

FIGURE 76

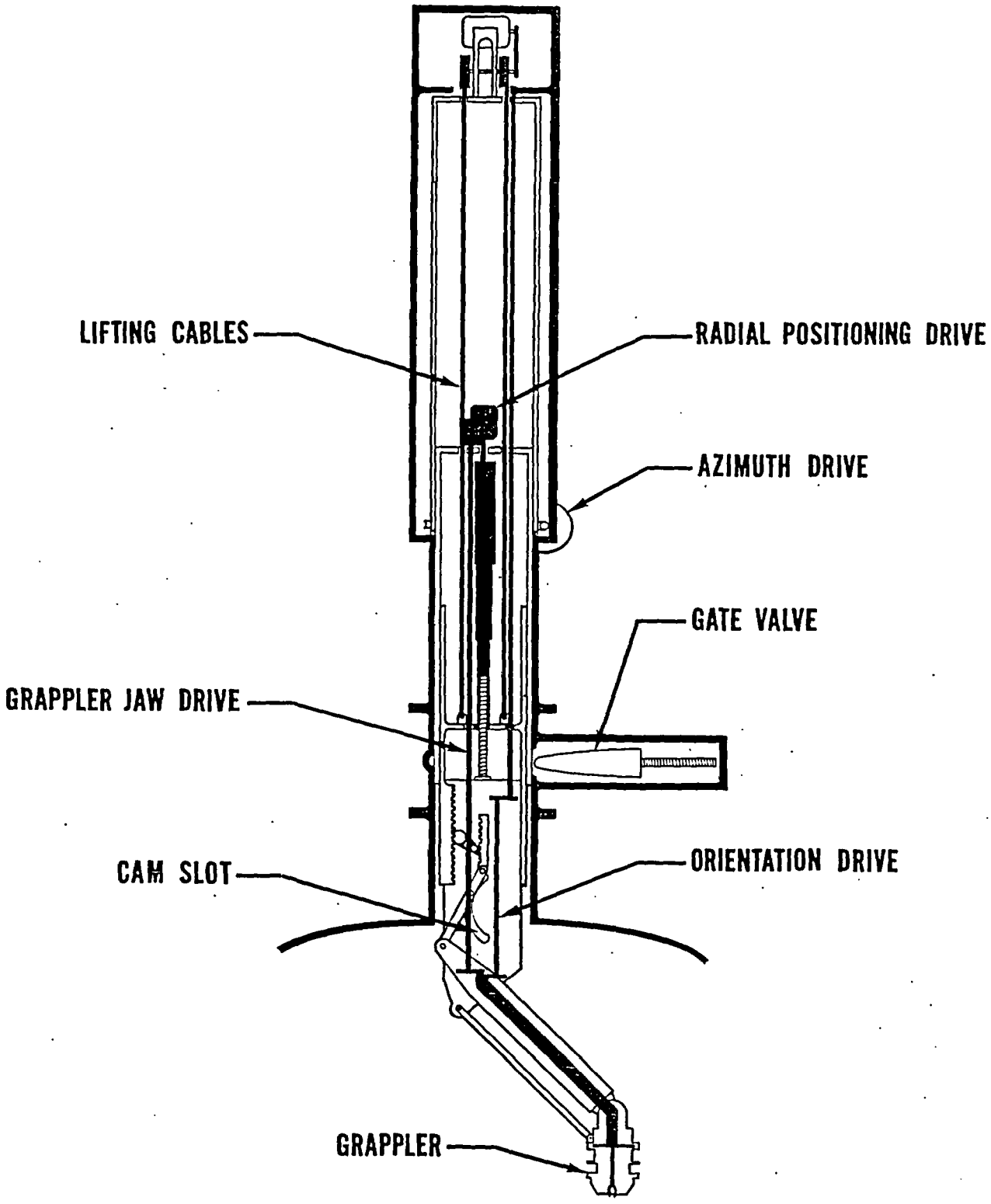

FUEL TRANSFER MACHINE SCHEMATIC

FIGURE 77

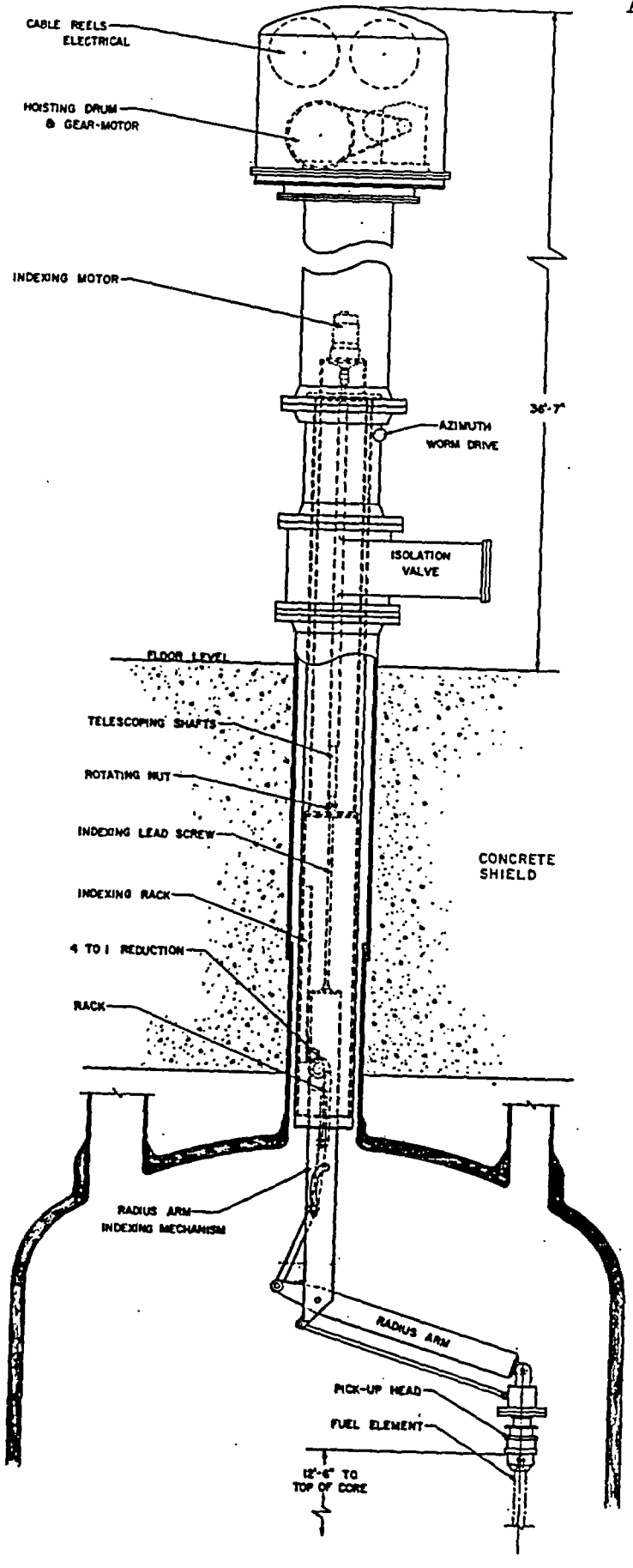

FUEL TRANSFER MACHINE

FIGURE 78

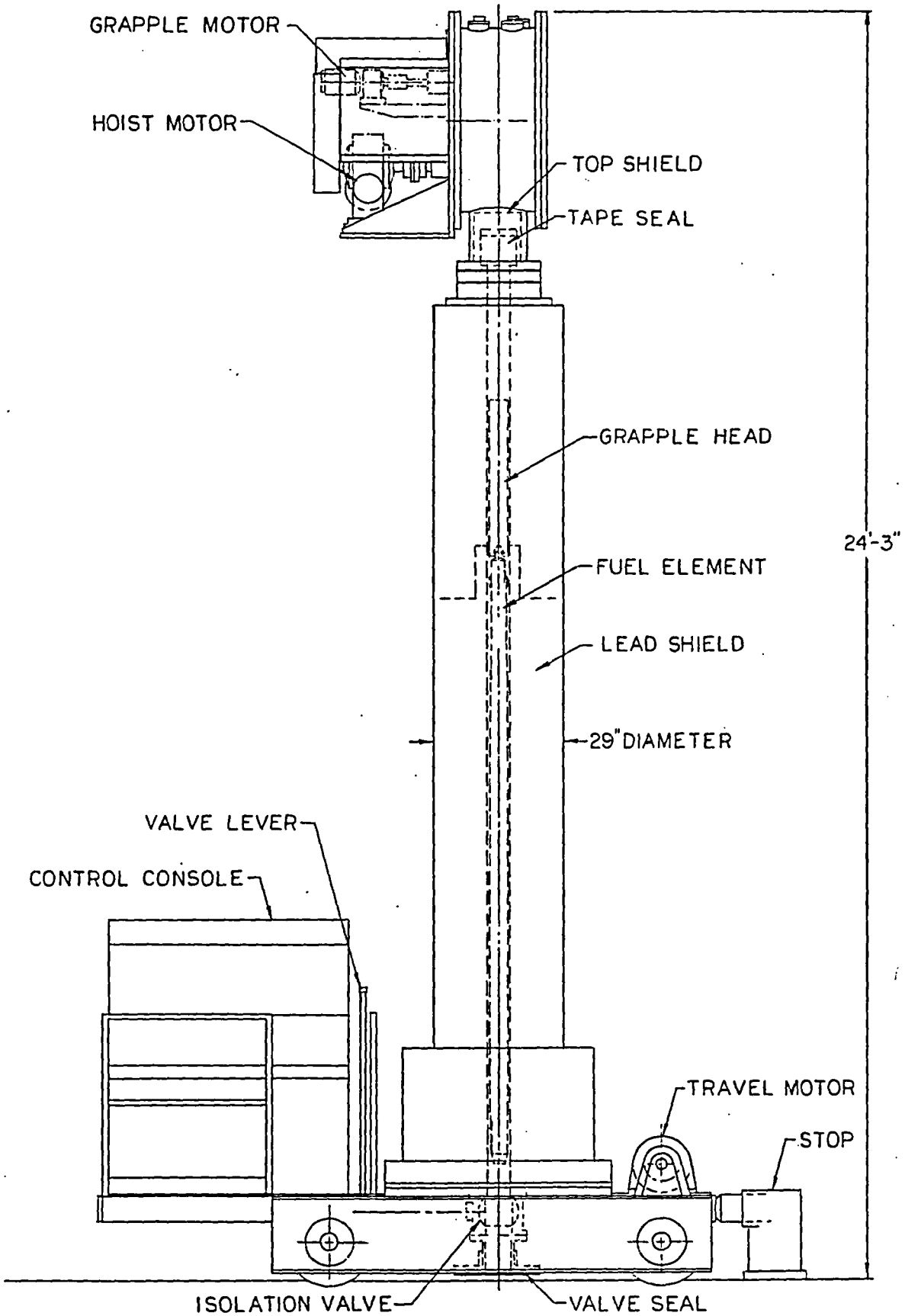

CHARGE MACHINE

FIGURE 79

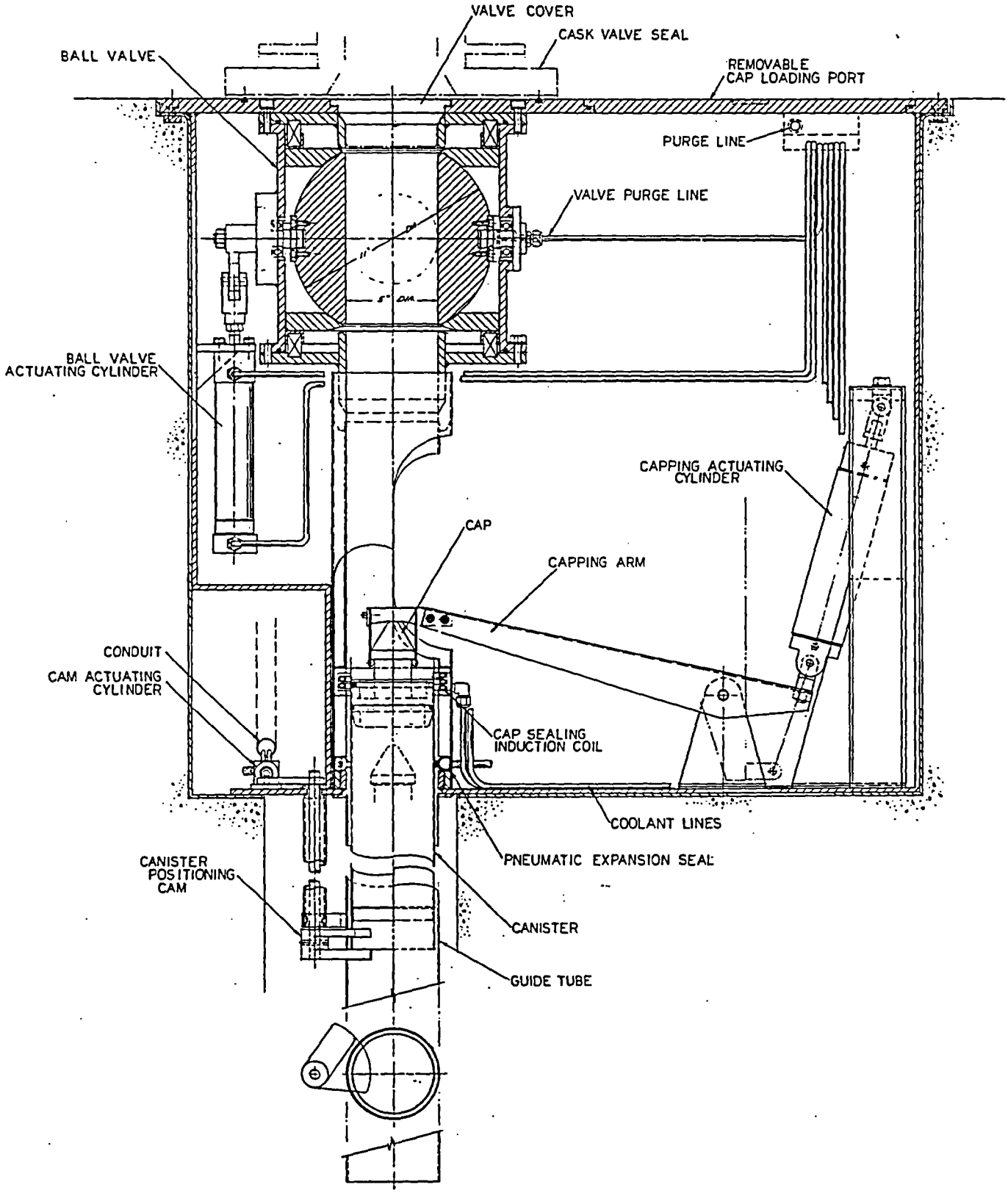

FUEL ELEMENT CANNING MACHINE

FIGURE 80

HANDLING SYSTEM
AUST FILTER
F-131

FUEL HANDLING SYSTEM
OIL REMOVAL TRAP
A-131

FUEL HANDLING SYSTEM
VACUUM PUMP
C-131
C-133

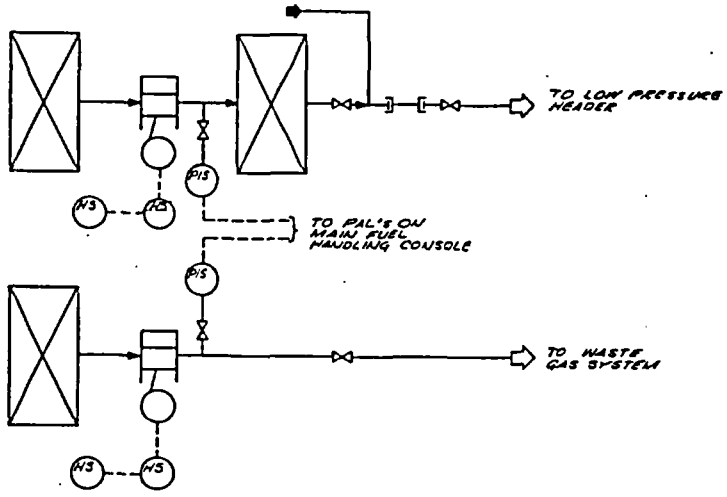

LEGEND

CONTINUED ON ANOTHER SHEET

CONTINUED ON SAME SHEET

XT- HALOGEN DETECTOR

ESH- HALOGEN SWITCH HIGH

FIXED OR VESSEL NOZZLE

ISOLATION VALVE

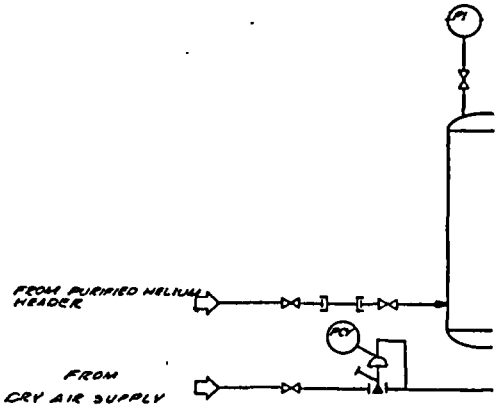

FUEL HAND
HELIUM SI
T-1 L HANDLING PURGE SYSTEM FLOW DIAGRAM

FIGURE 81

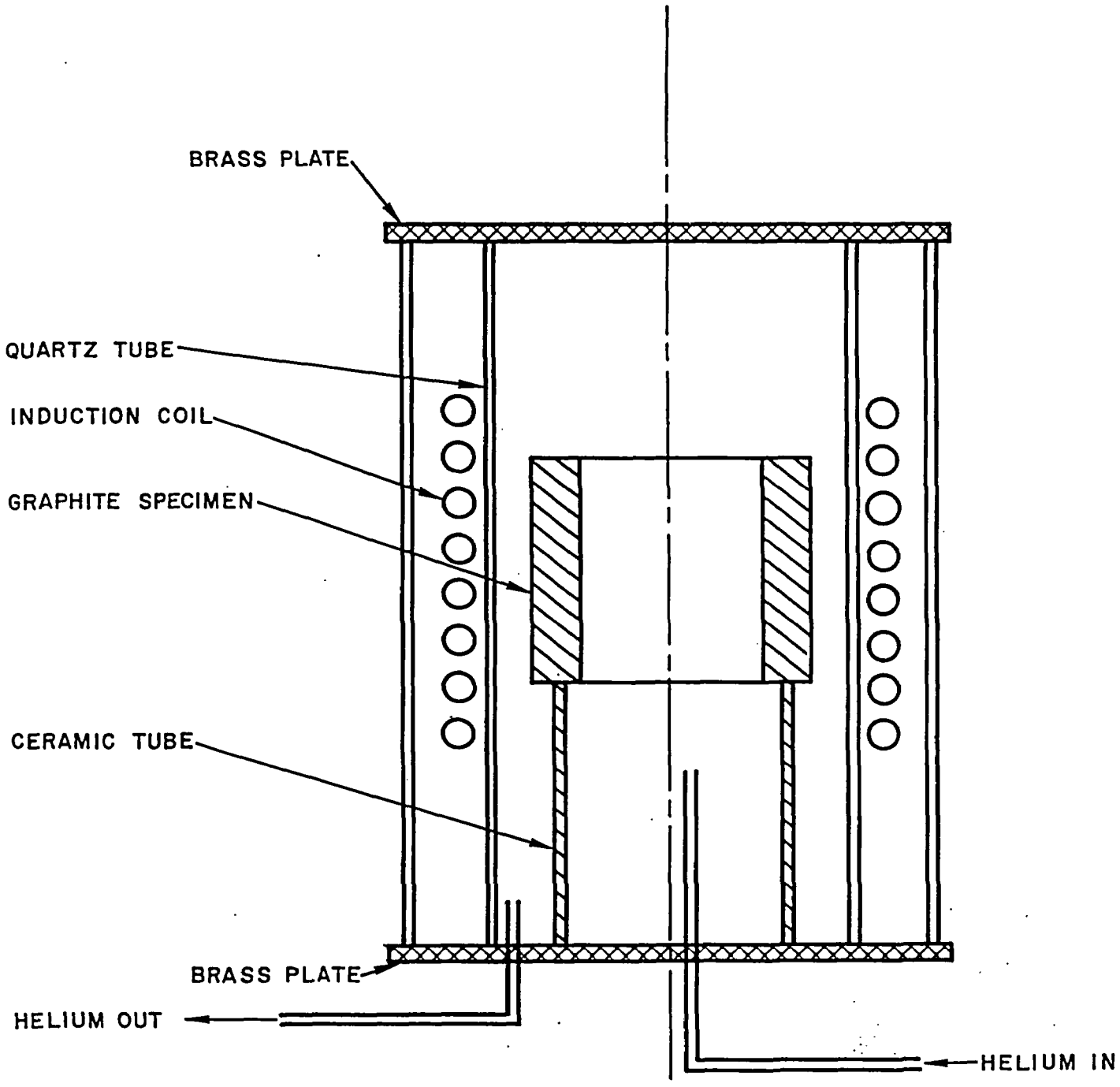

STEAM-GRAPHITE REACTION FURNACE

FIGURE 82

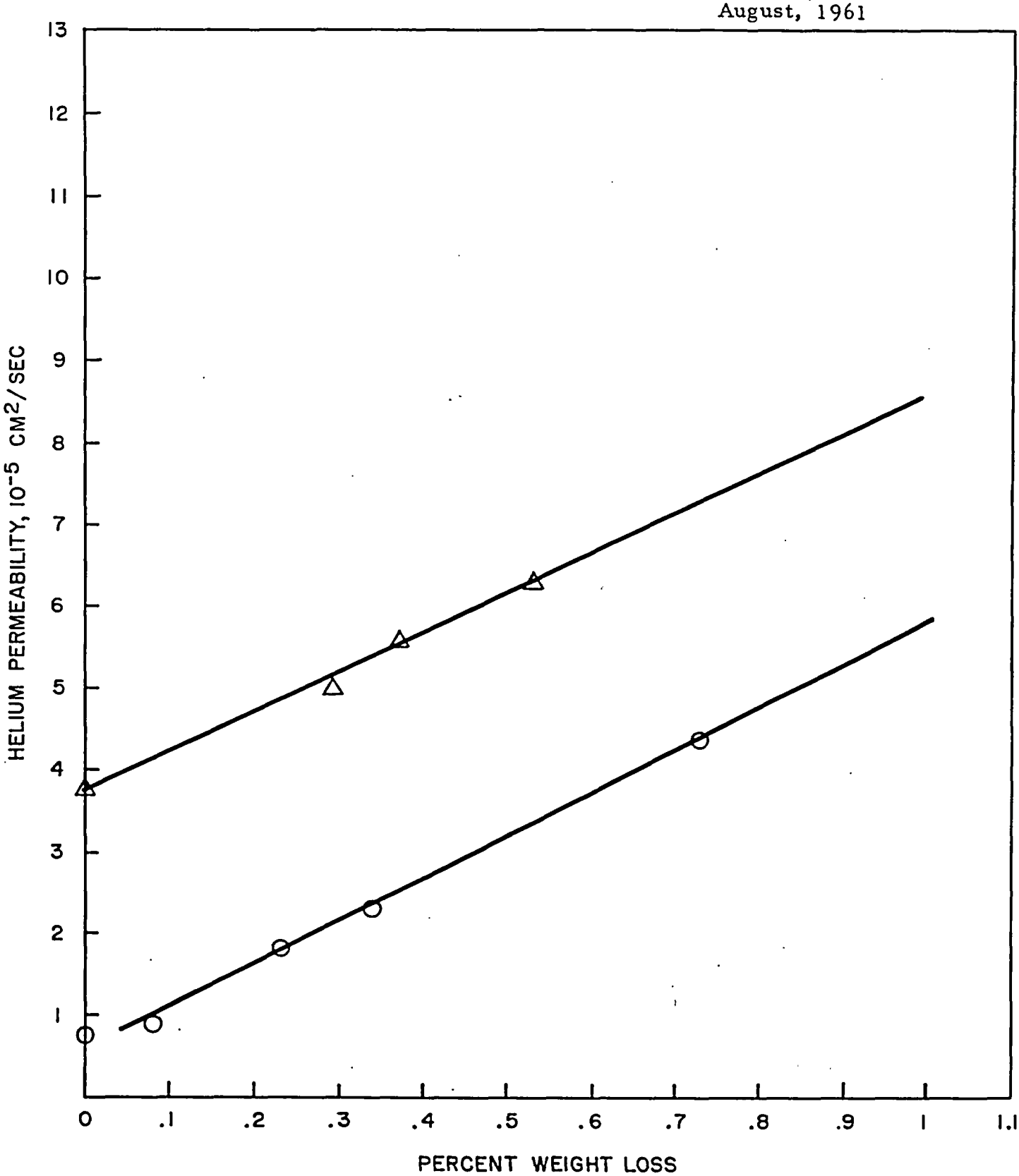

CHANGE IN HELIUM PERMEABILITY VS. CHANGE IN WEIGHT FOR TWO GREAT LAKES CARBON CO. GRAPHITES AFTER EXPOSURE TO HELIUM WITH 3% WATER AT 1000°C; PERMEABILITY MEASURED AT A PRESSURE DIFFERENCE OF 1 ATM

FIGURE 83

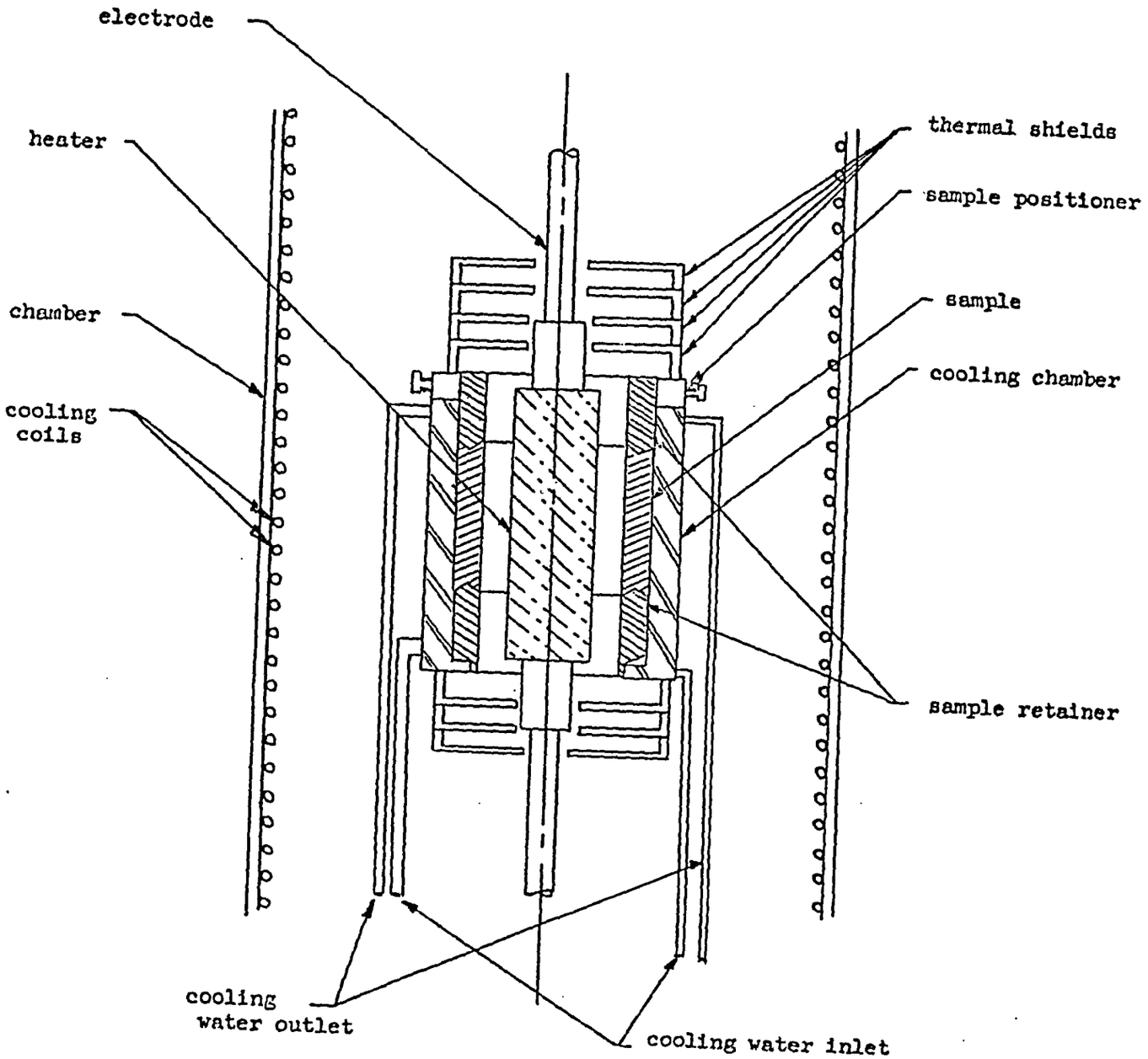

SCHEMATIC OF THERMAL STRESS APPARATUS

FIGURE 84

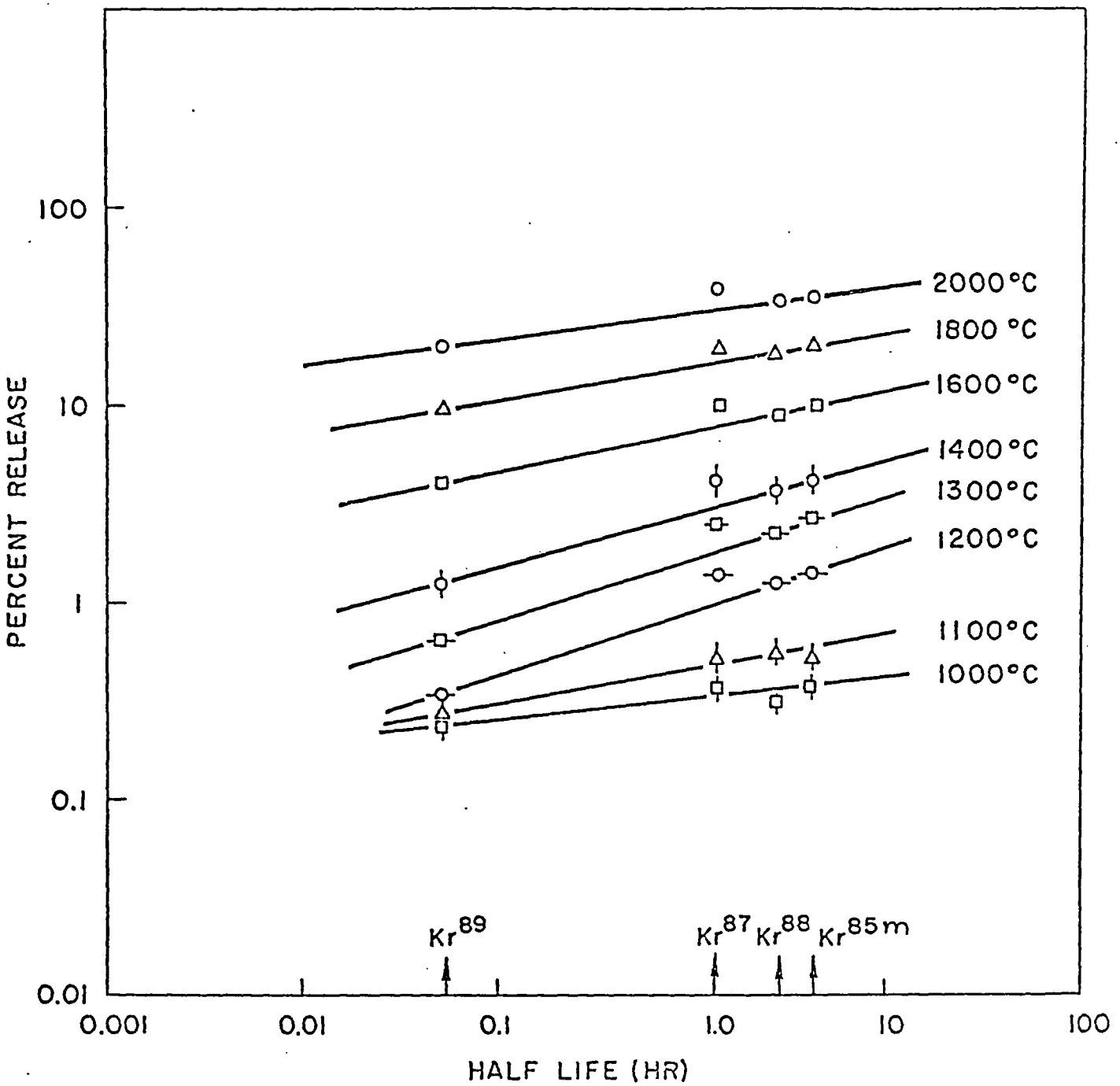

STEADY STATE KR RELEASE, UNCOATED CARBIDE PARTICLE
GRAPHITE MATRIX FUEL BODIES

FIGURE 85

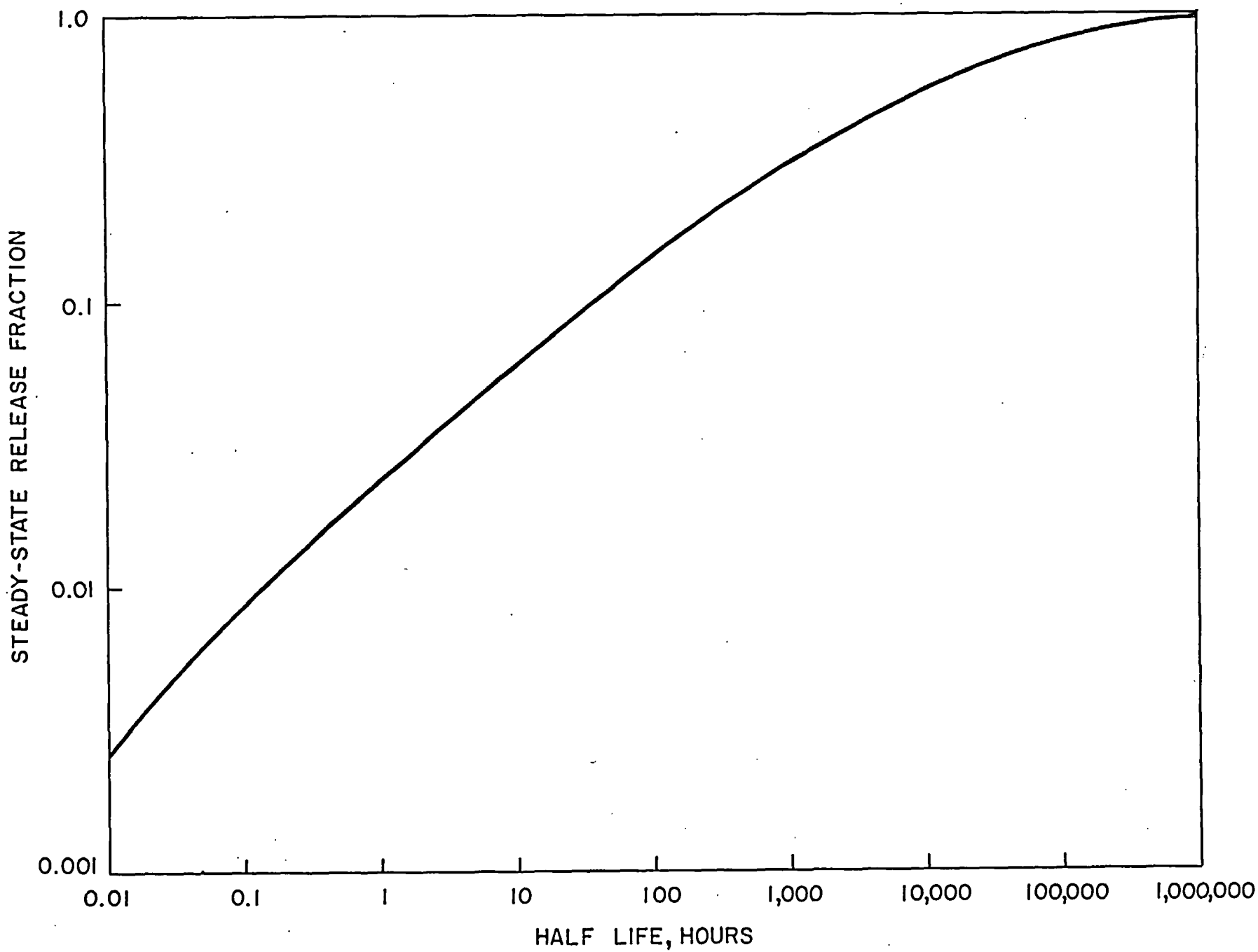

DESIGN BASIS STEADY-STATE RELEASE OF FISSION PRODUCTS FROM UNCOATED FUEL

FIGURE 86

August, 1961

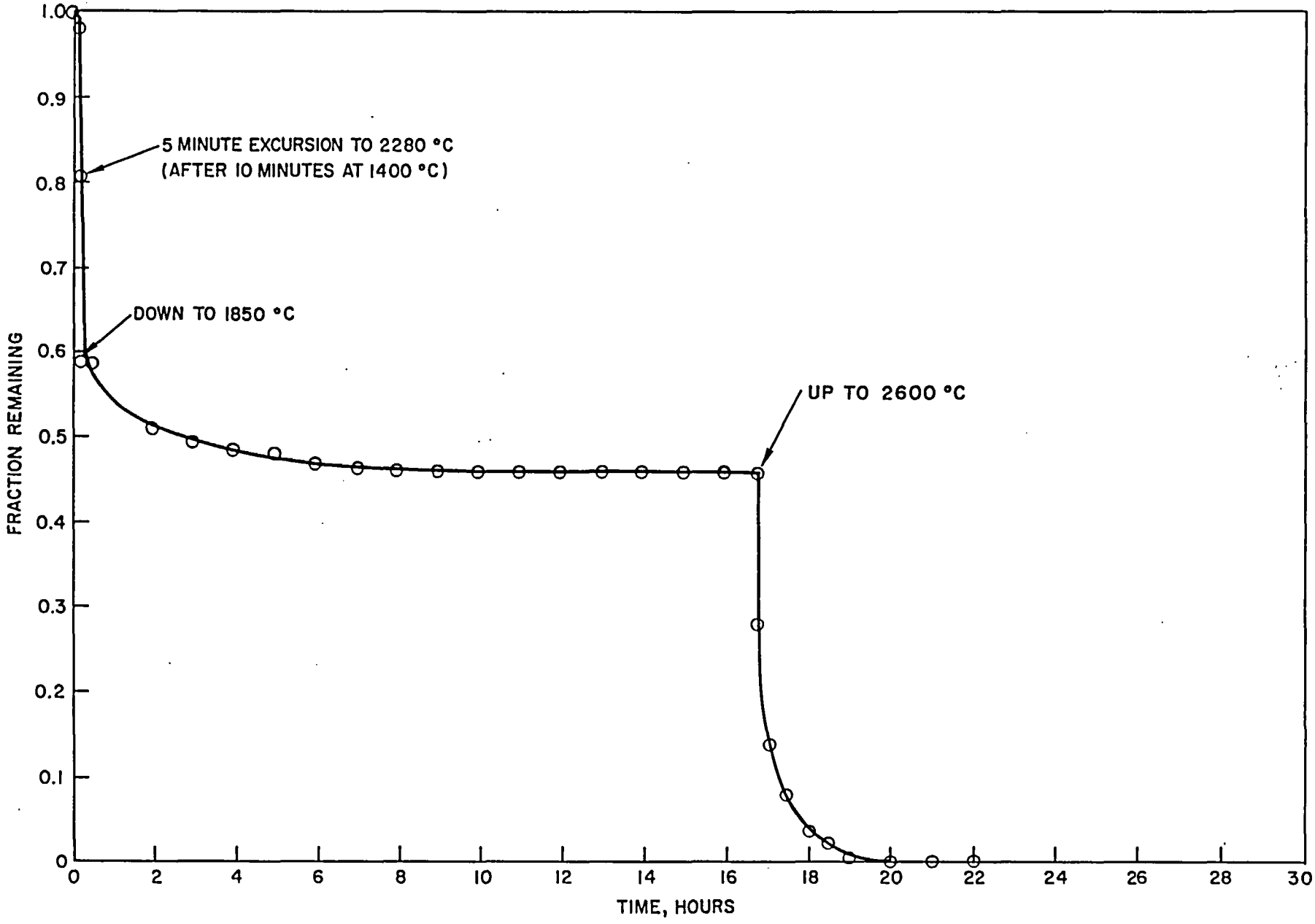

XE-133 RELEASE FROM FUEL COMPACT PREPARED FROM UNCOATED FUEL PARTICLES FOLLOWING A SIMULATED EXCURSION TO 2280°C. $(TH:U)C_2$ 2.19/1.0

FIGURE 87

August, 1961

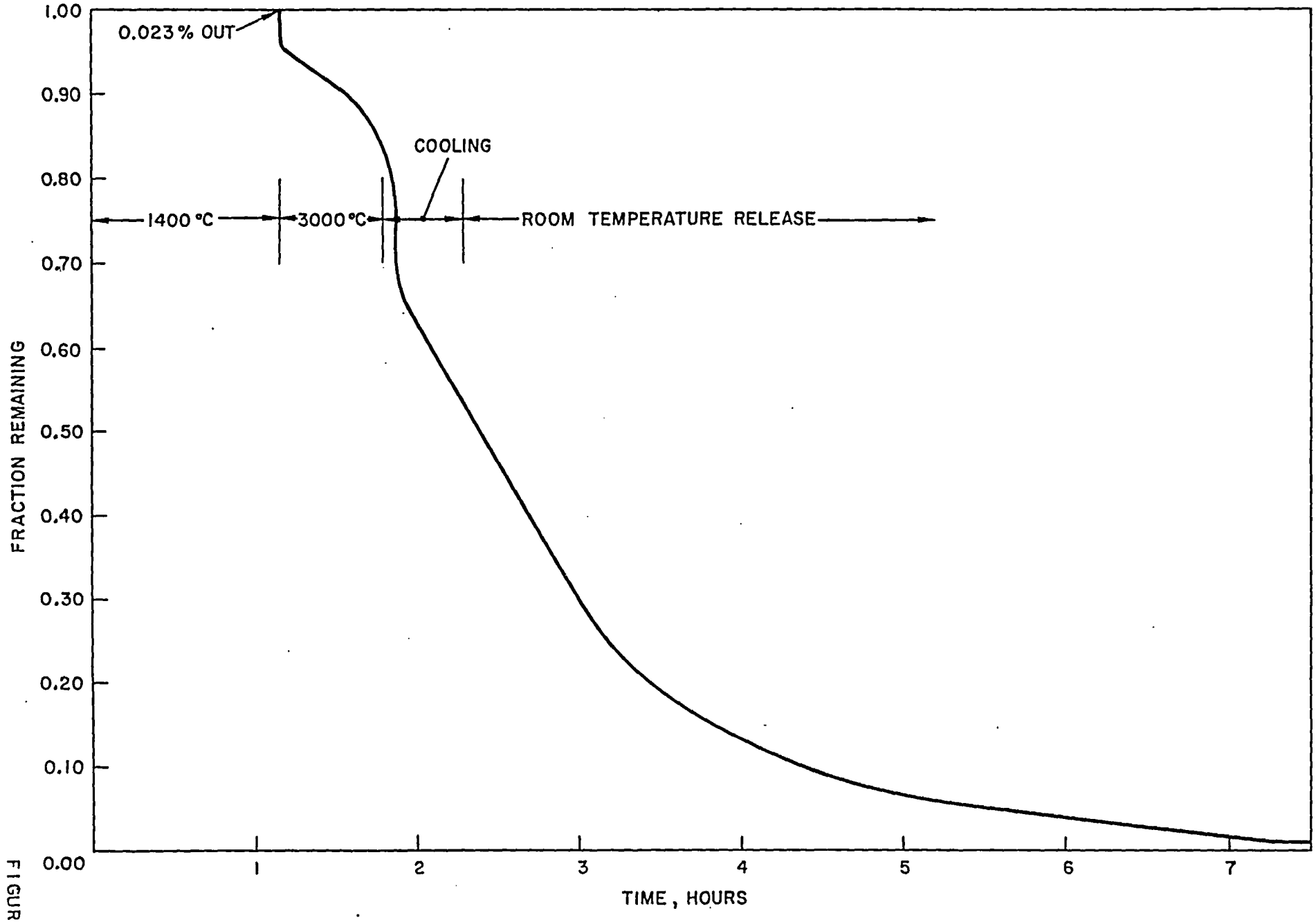

FIGURE 88

XENON-133 RELEASE FROM COATED PARTICLES DUE TO AN EXCURSION TO 3000°C FOR 38 MINUTES

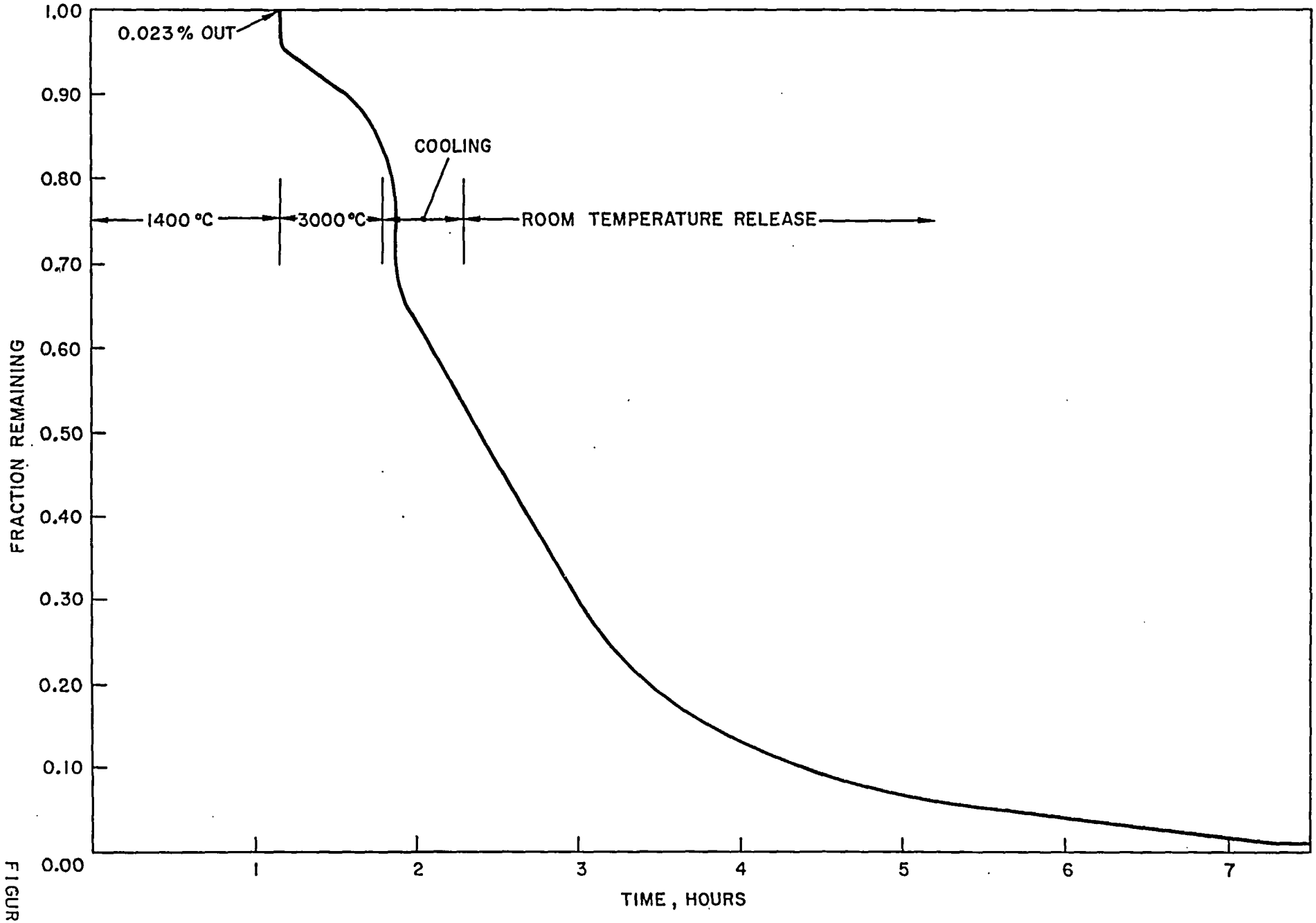

FIGURE 88

XENON-133 RELEASE FROM COATED PARTICLES DUE TO AN EXCURSION TO 3000°C FOR 38 MINUTES

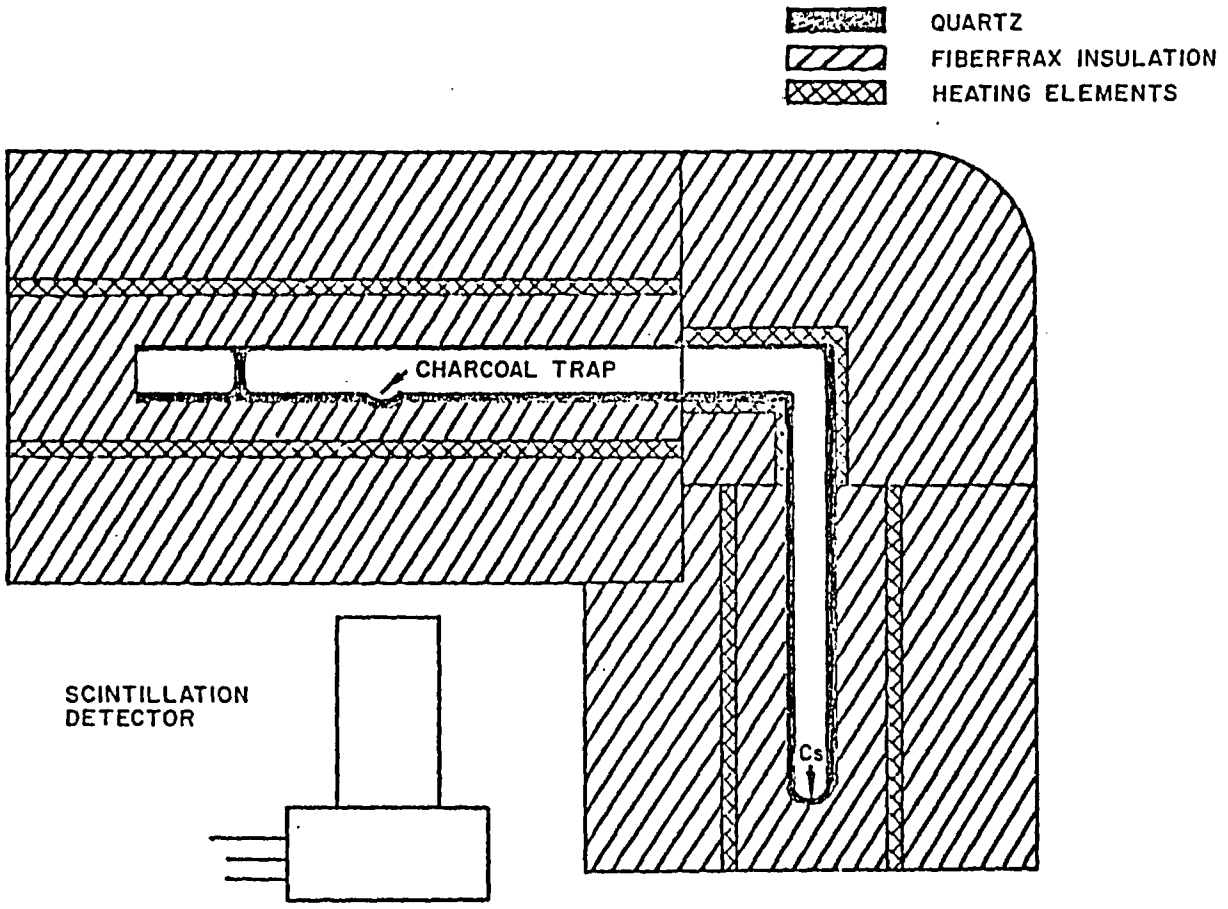

CESIUM SORPTION APPARATUS

FIGURE 89

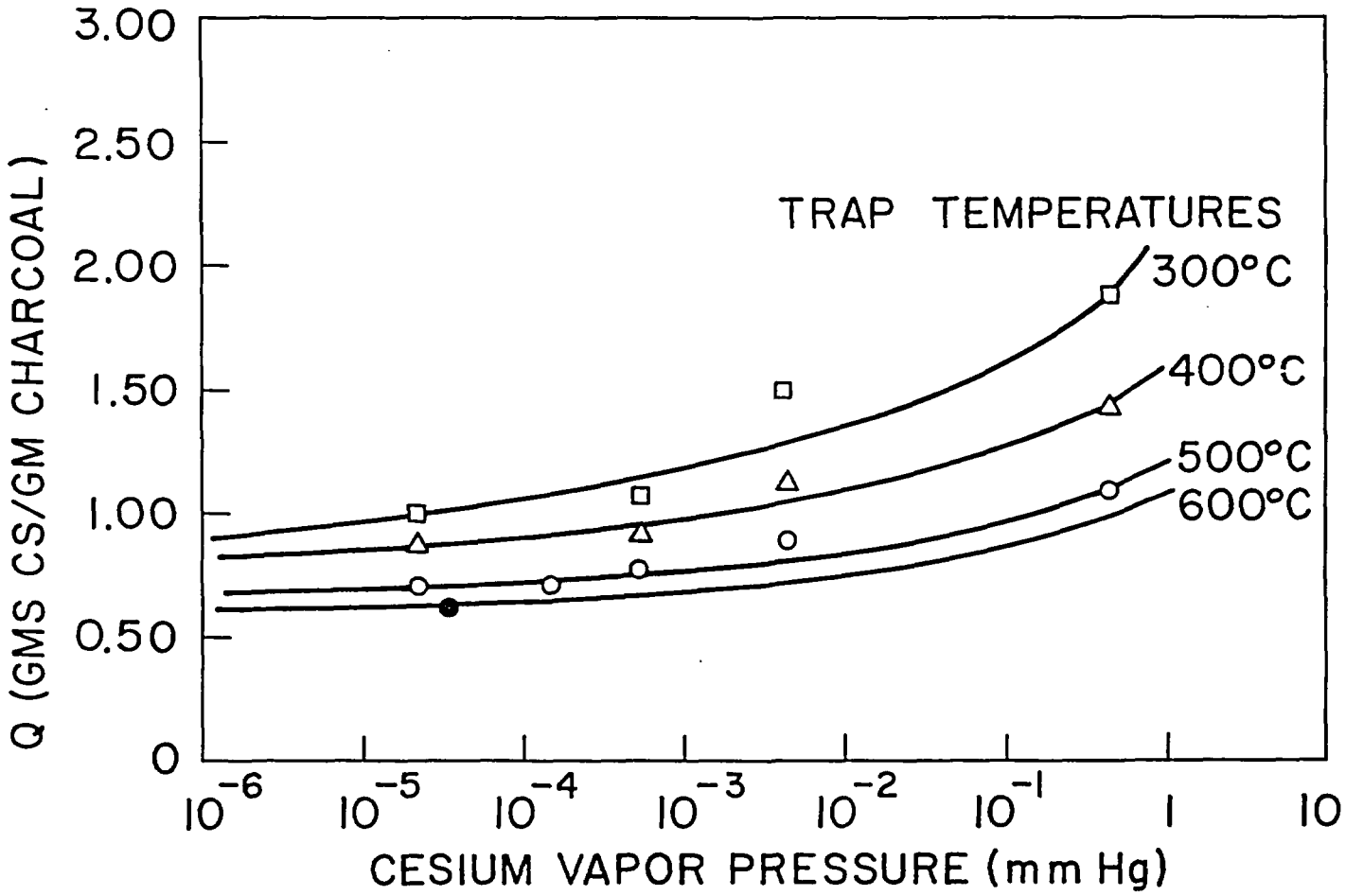

CESIUM SORPTION BY ACTIVATED CHARCOAL (FISCHER CHARCOAL)

FIGURE 90

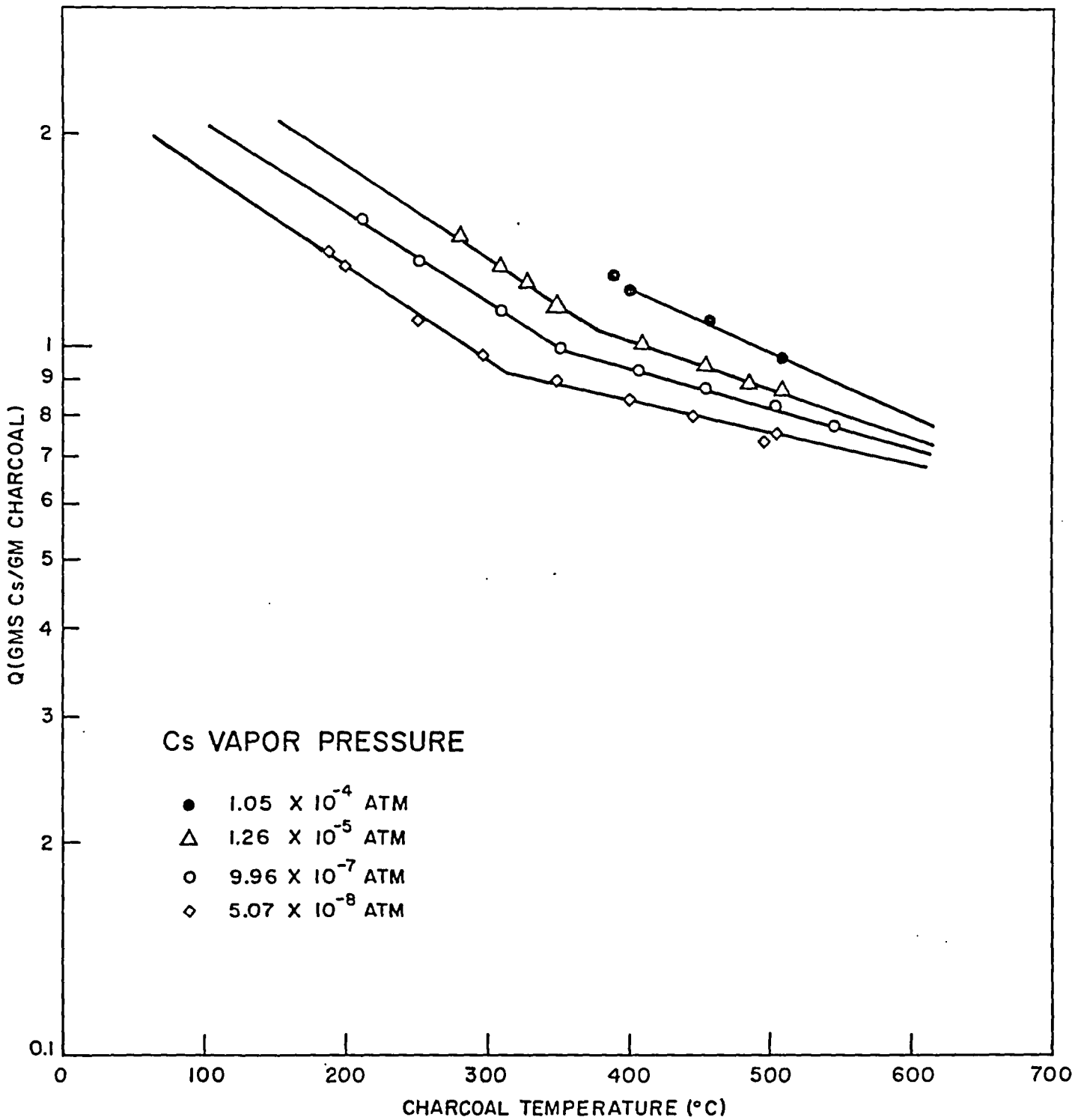

CESIUM SORPTION ON ACTIVATED CHARCOAL (COLUMBIA CHARCOAL)

FIGURE 91

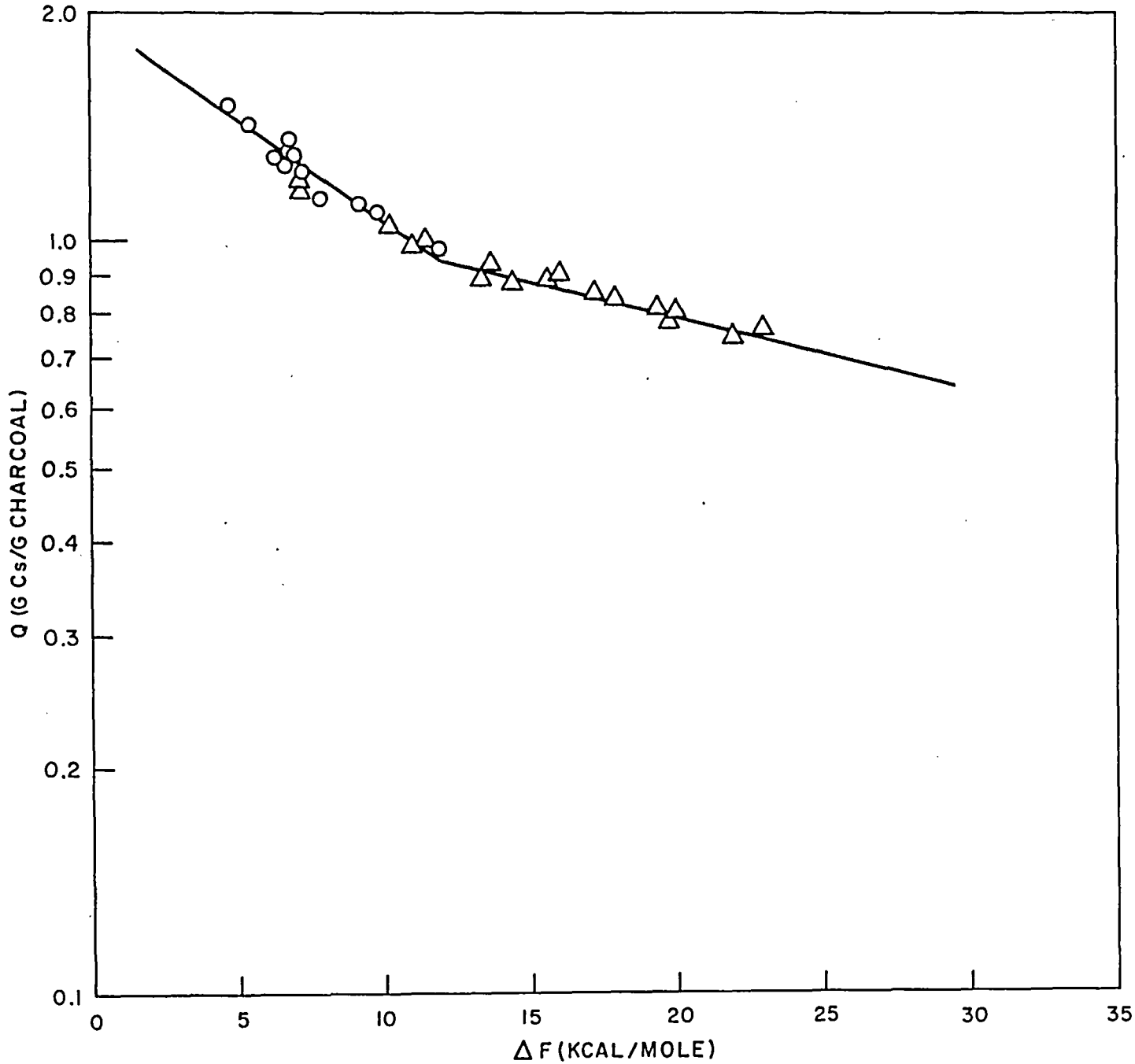

FIGURE 92

FREE ENERGY CHANGE OF SORPTION FOR CESIUM-CHARCOAL SYSTEM

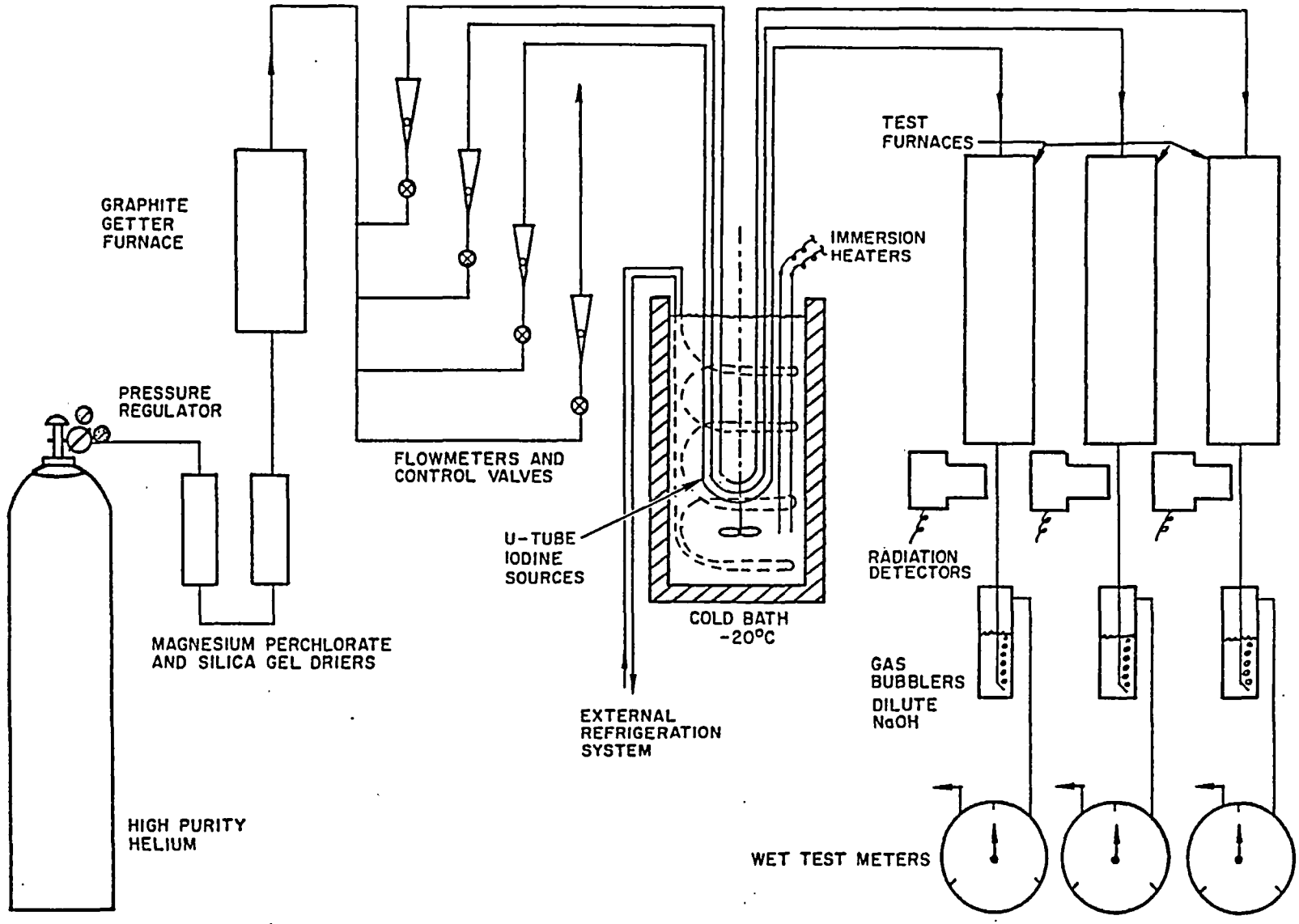

INTERNAL FISSION PRODUCT TRAP EVALUATION SYSTEM

FIGURE 93

August, 1961

TYPICAL SHARP BOUNDARIES OBTAINED IN IODINE AND TELLURIUM VAPOR-HELIUM CHROMATOGRAMS OF TRAPPING REAGENTS.
LEFT 30 WT-% COPPER-CHARCOAL.
RIGHT 35 WT-% SILVER-CHARCOAL

FIGURE 94

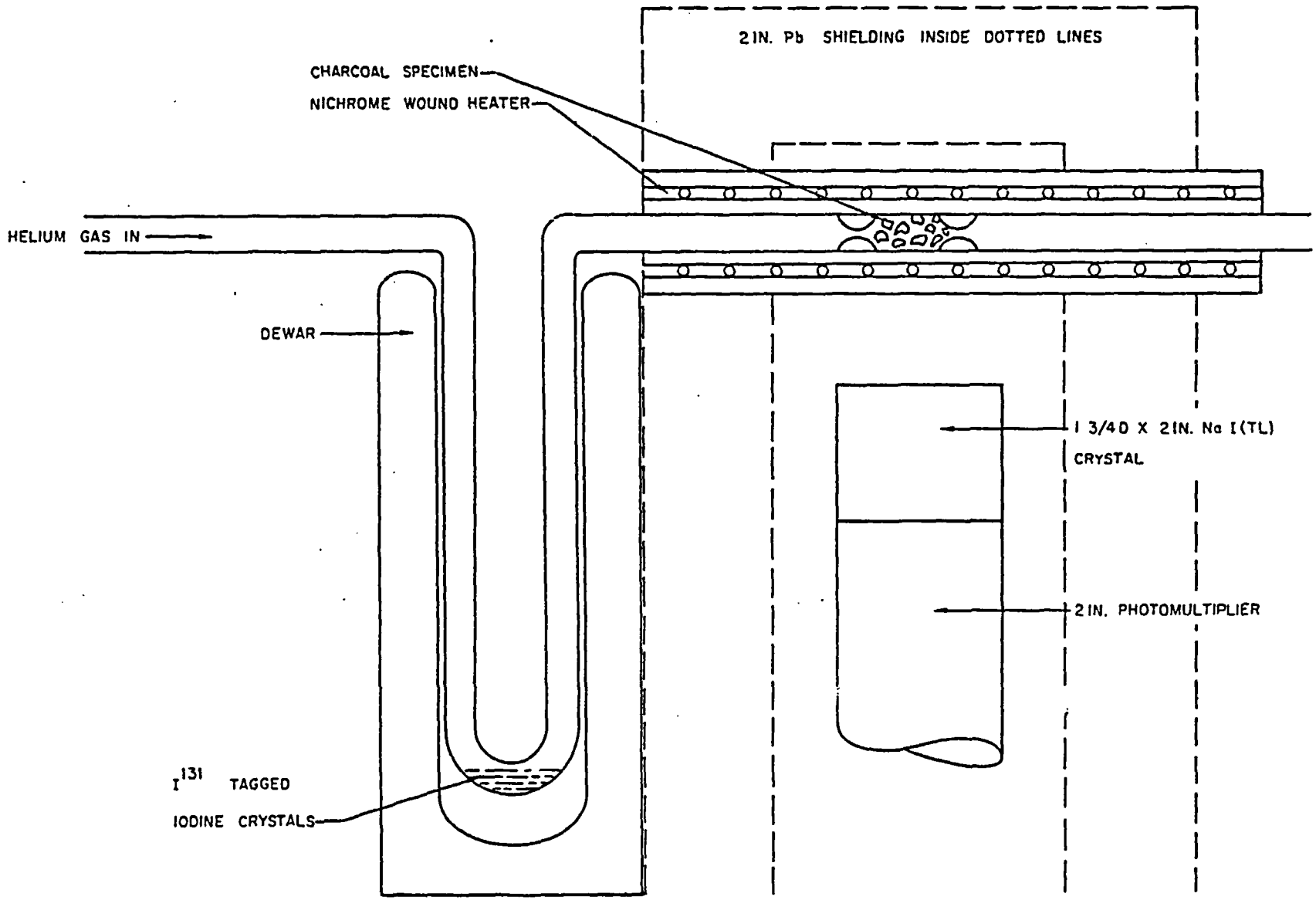

FIGURE 95

DYNAMIC SORPTION APPARATUS

August, 1961

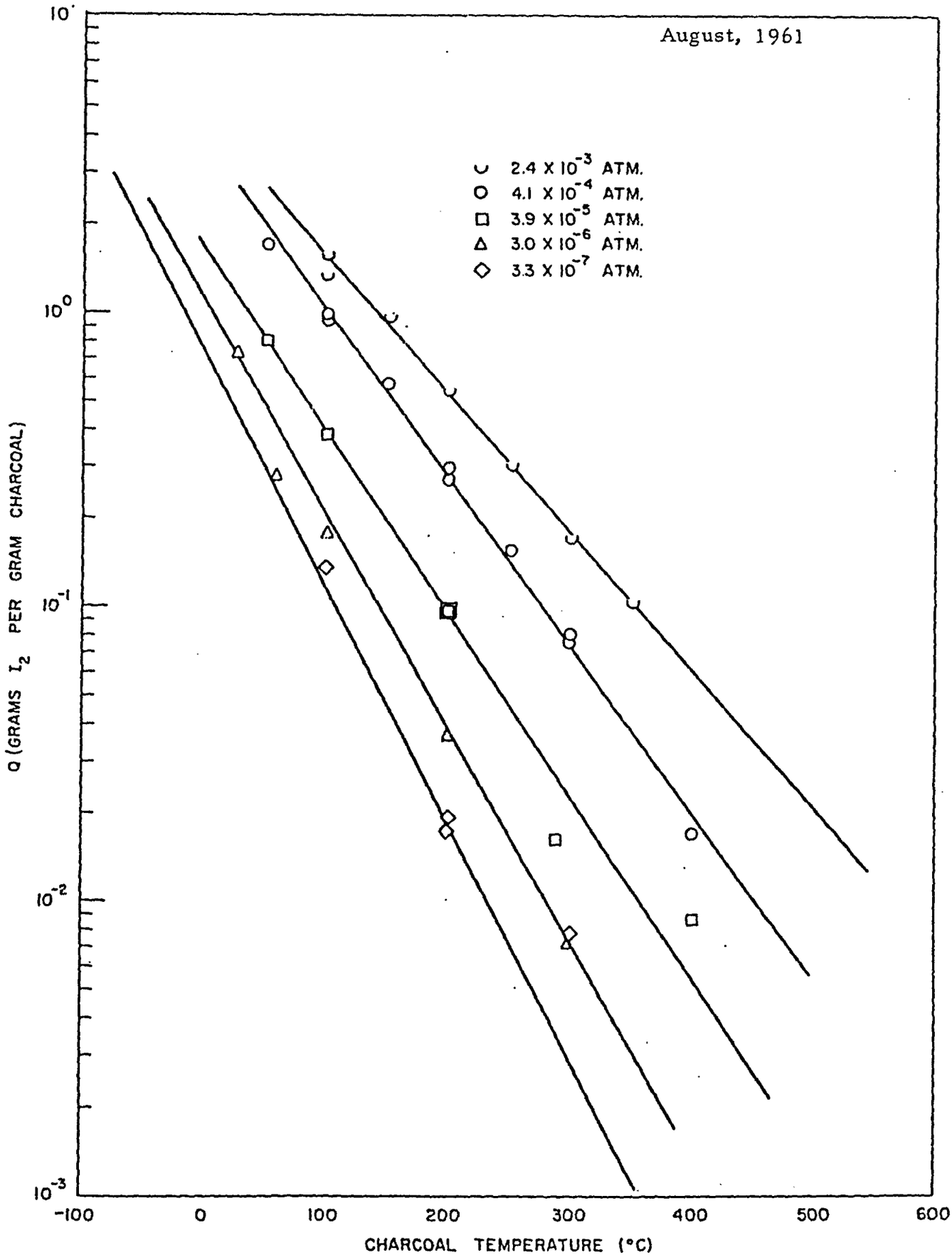

ADSORPTION ISOBARS FOR IODINE ON CHARCOAL

FIGURE 96

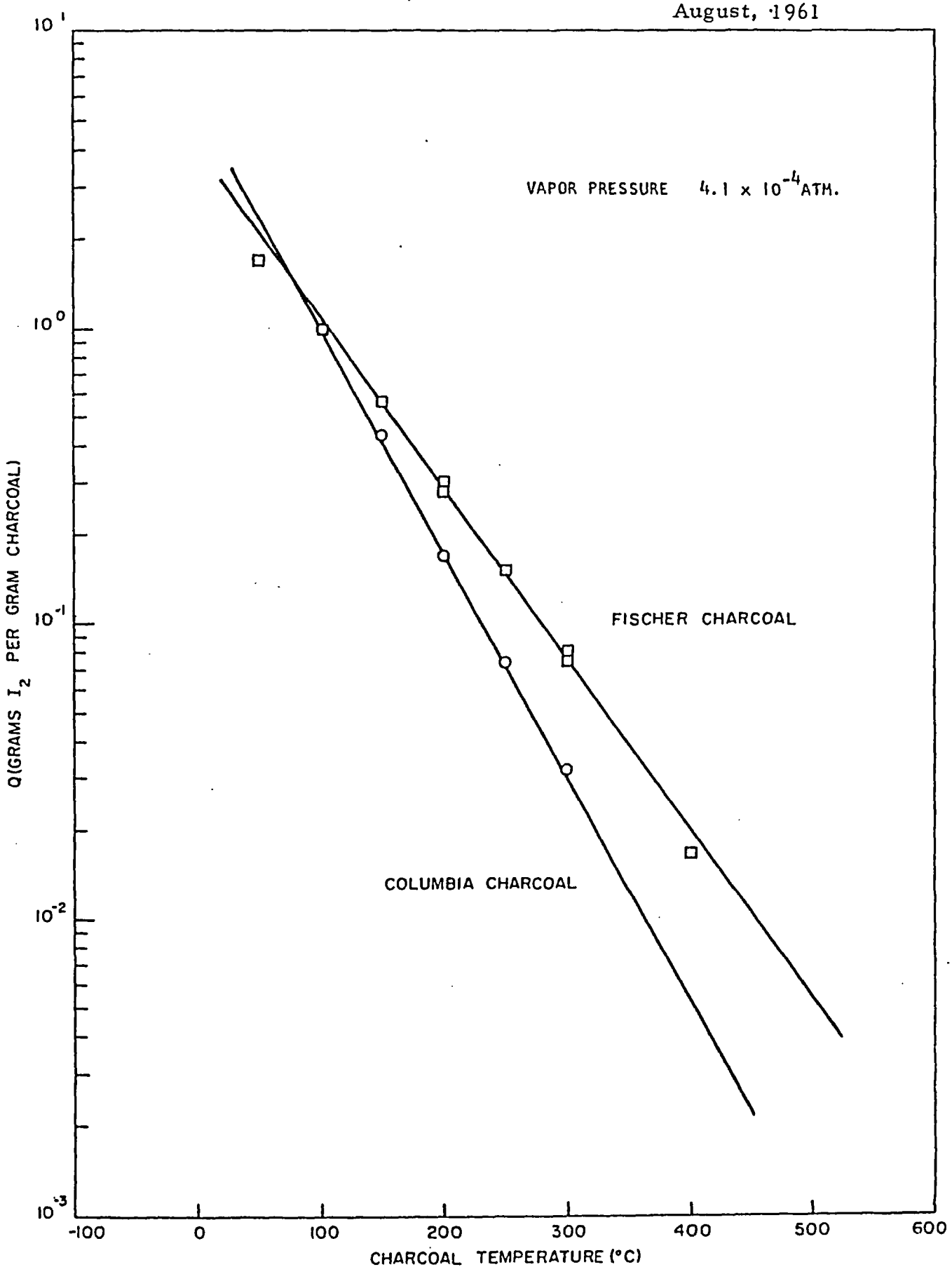

IODINE ADSORPTION ISOBARS ON ACTIVATED CHARCOAL

FIGURE 97

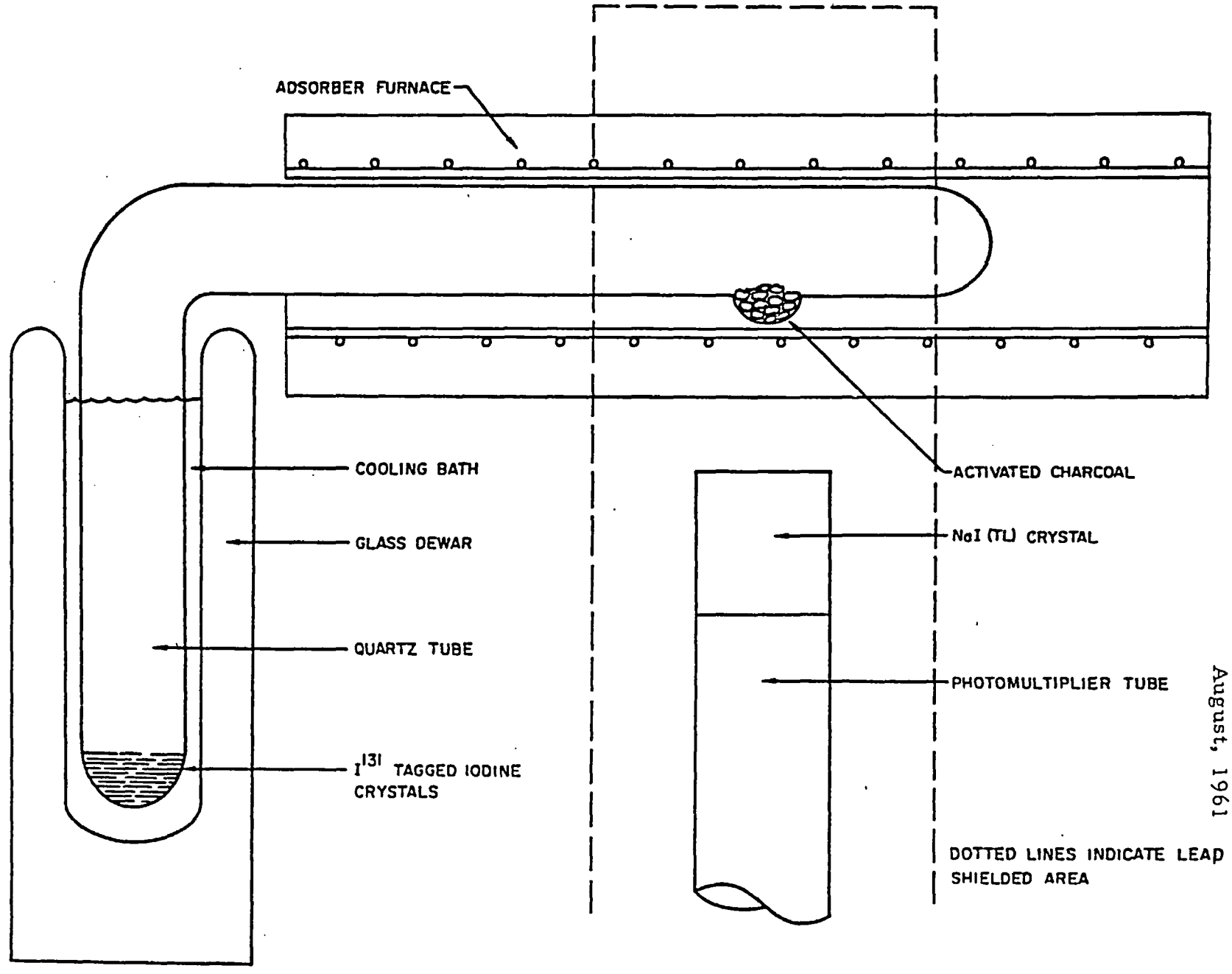

STATIC SORPTION APPARATUS

August, 1961

FIGURE 98

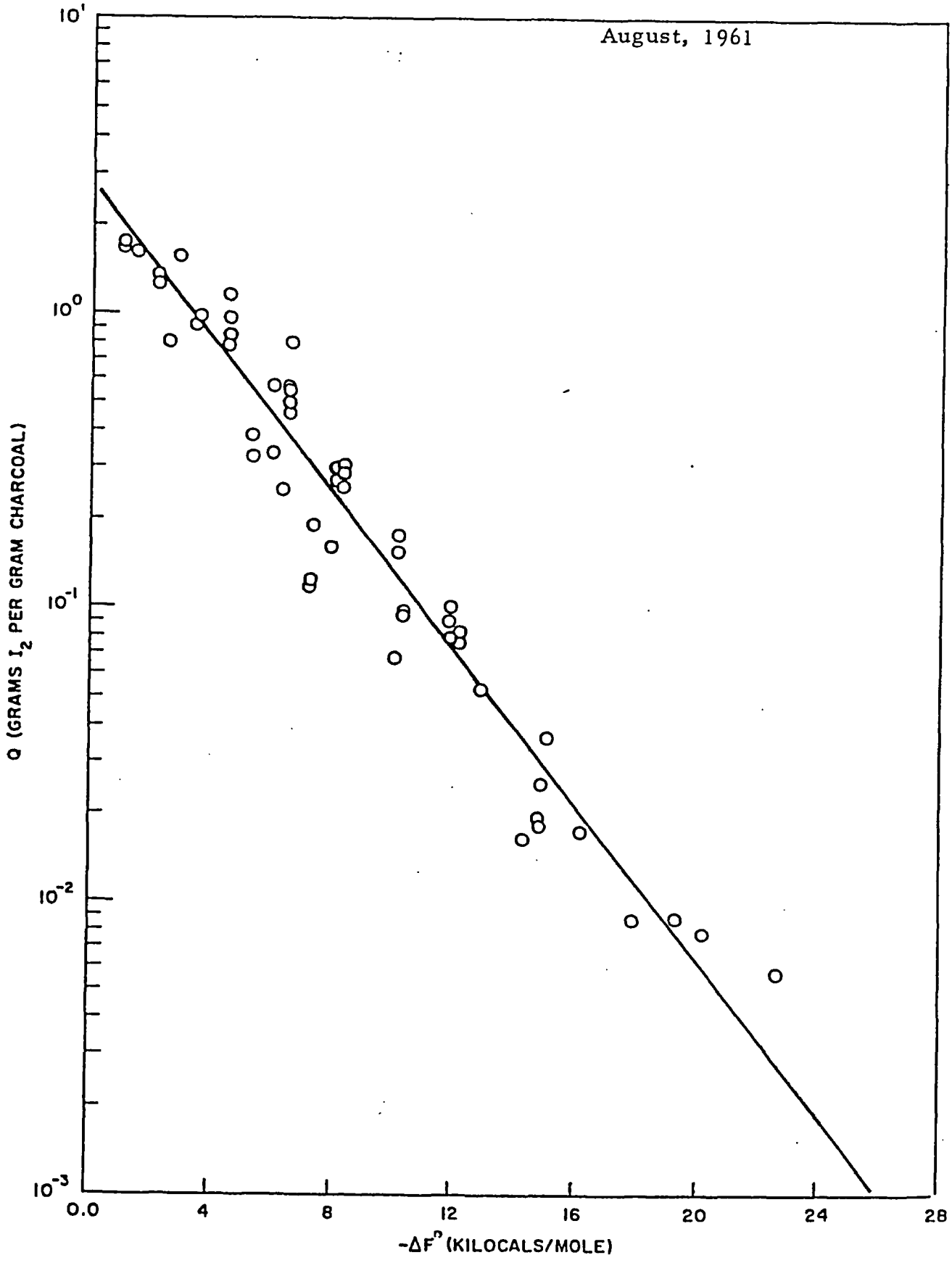

FREE ENERGY OF ADSORPTION FOR IODINE ON CHARCOAL

FIGURE 99

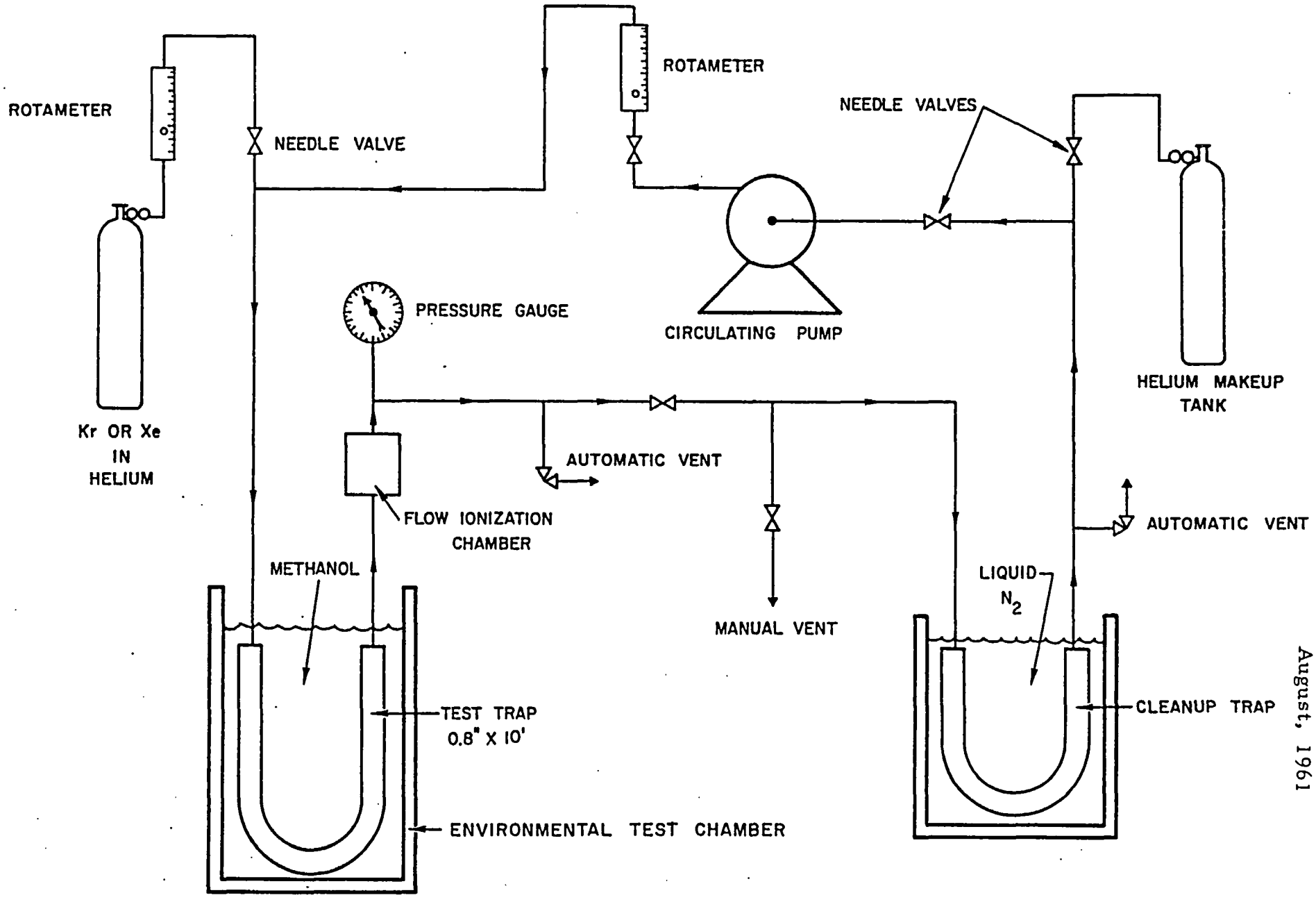

APPARATUS FOR CHARCOAL TRAP ADSORPTION TESTS

FIGURE 100

August, 1961

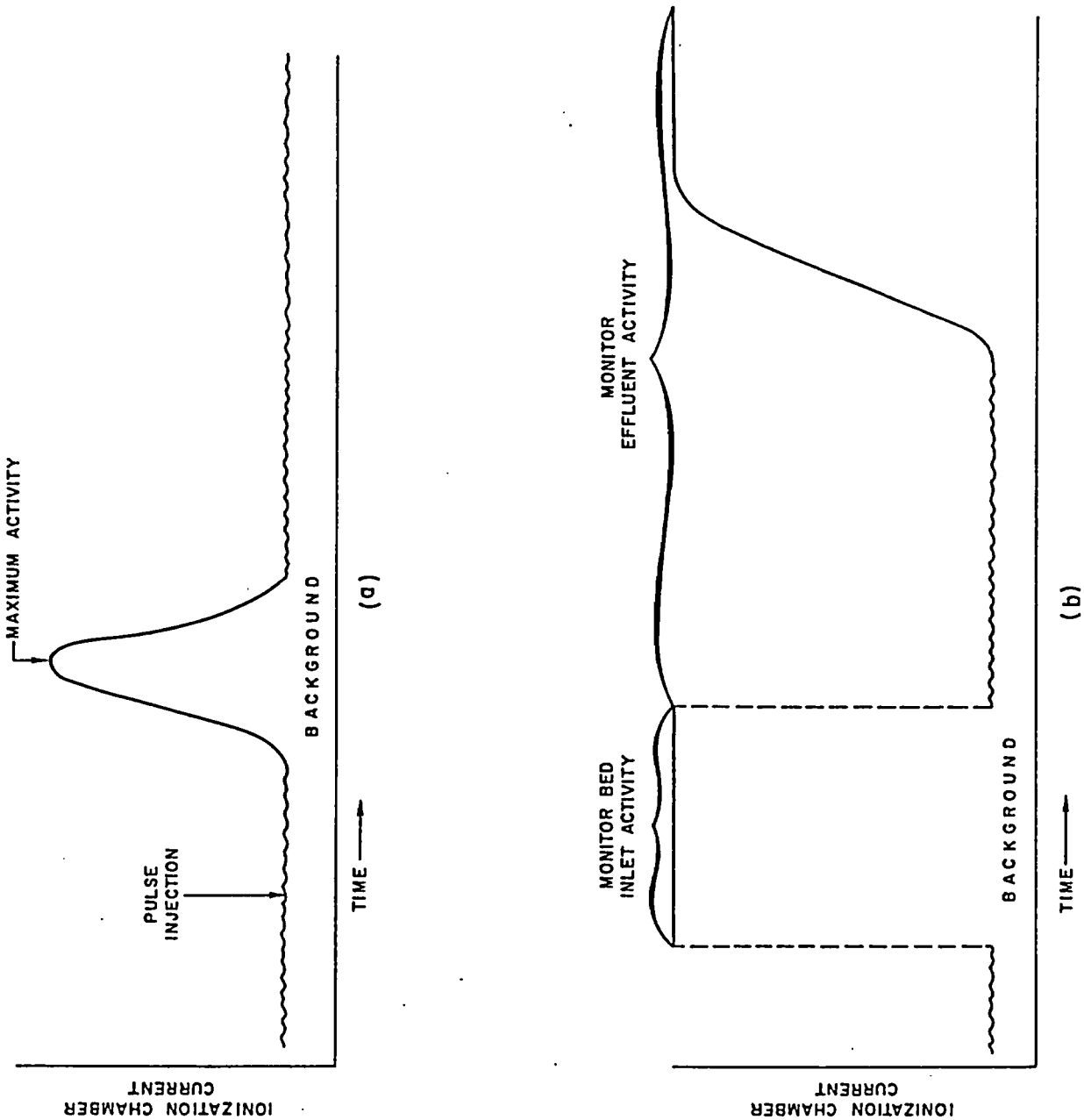

TYPICAL IONIZATION CHAMBER CURRENT TRACES FOR (A) PULSE INJECTION AND (B) CONSTANT RATE INJECTION OF TRACER GAS INTO CHARCOAL TRAP TEST APPARATUS

FIGURE 101

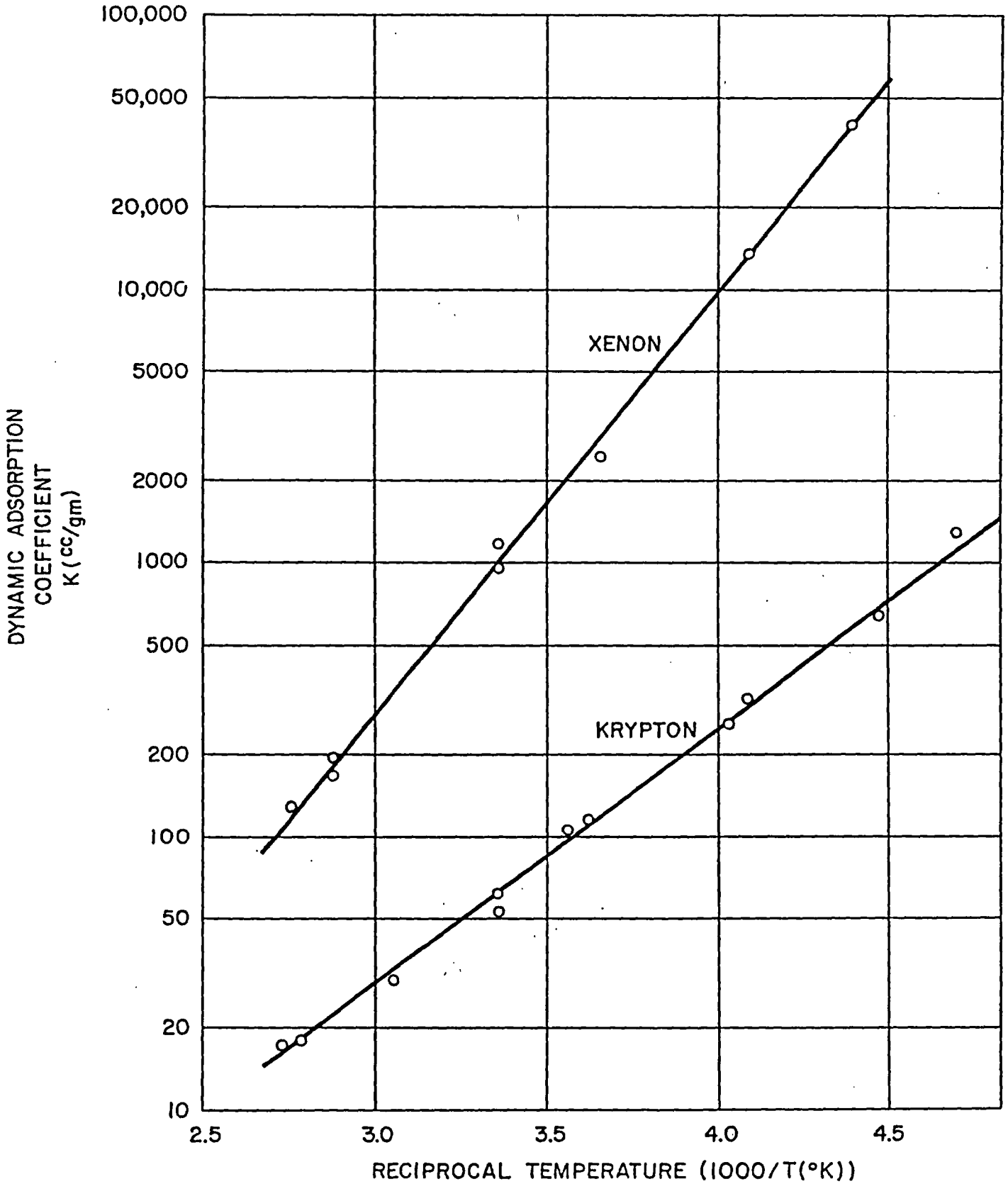

EXPERIMENTAL DYNAMIC ADSORPTION COEFFICIENT VS. RECIPROCAL TEMPERATURE

FIGURE 102

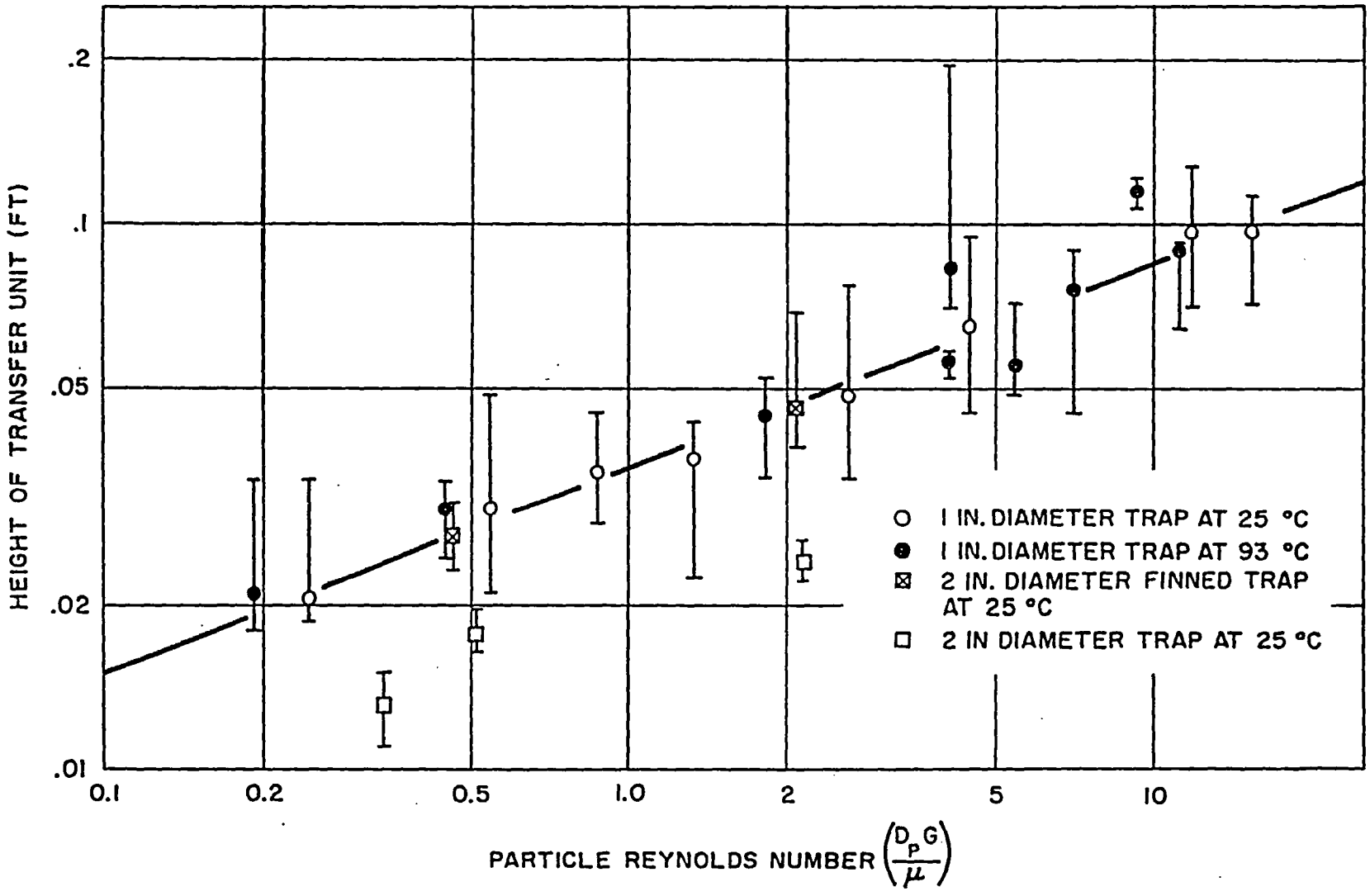

TRANSFER UNIT HEIGHT VS. PARTICLE REYNOLDS NUMBER FOR BARNEBEY-CHENEY 107 6/10 MESH CHARCOAL

FIGURE 103

August, 1961

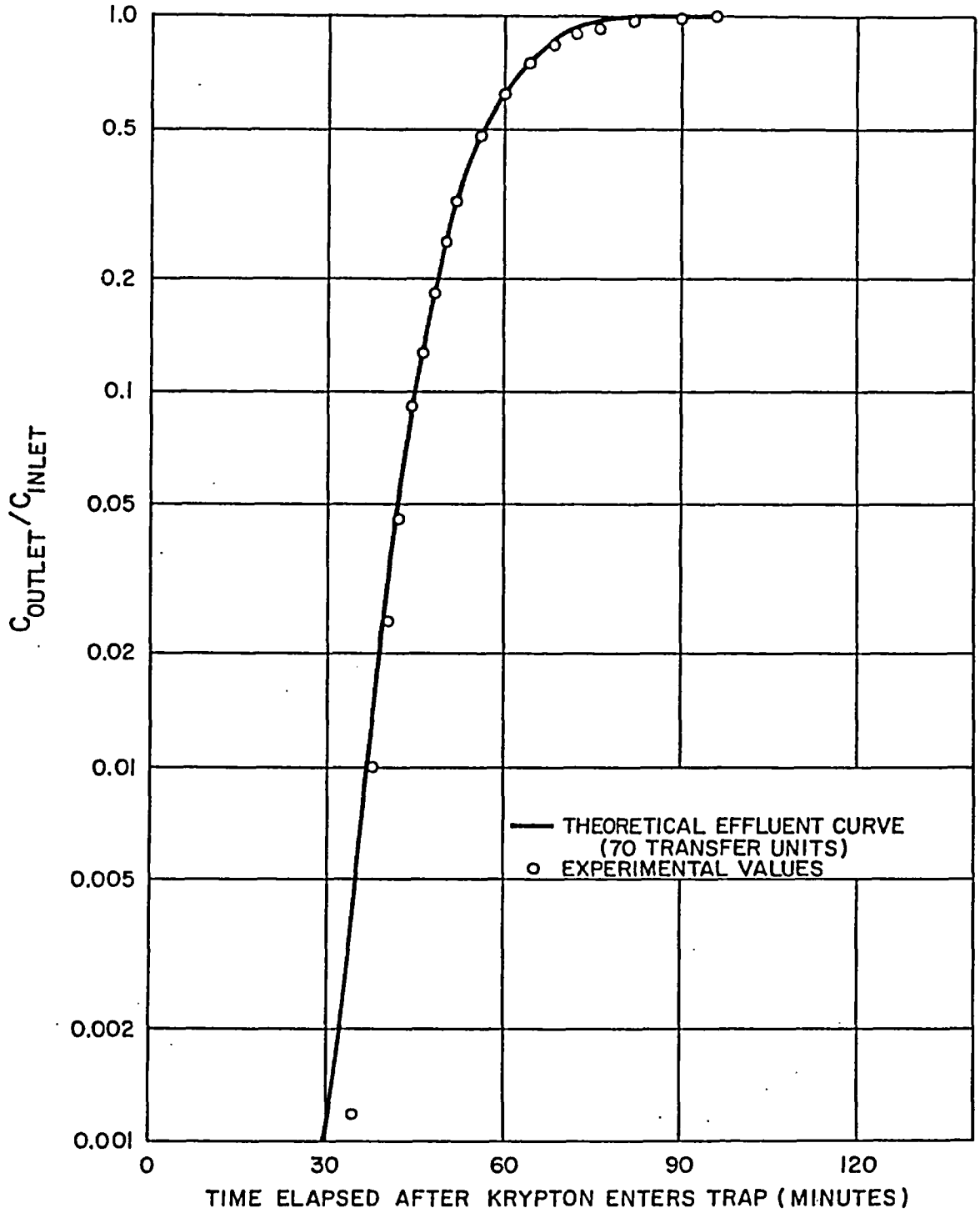

COMPARISON OF A THEORETICAL EFFLUENT CURVE WITH EXPERIMENTAL RESULTS

FIGURE 104

August, 1961

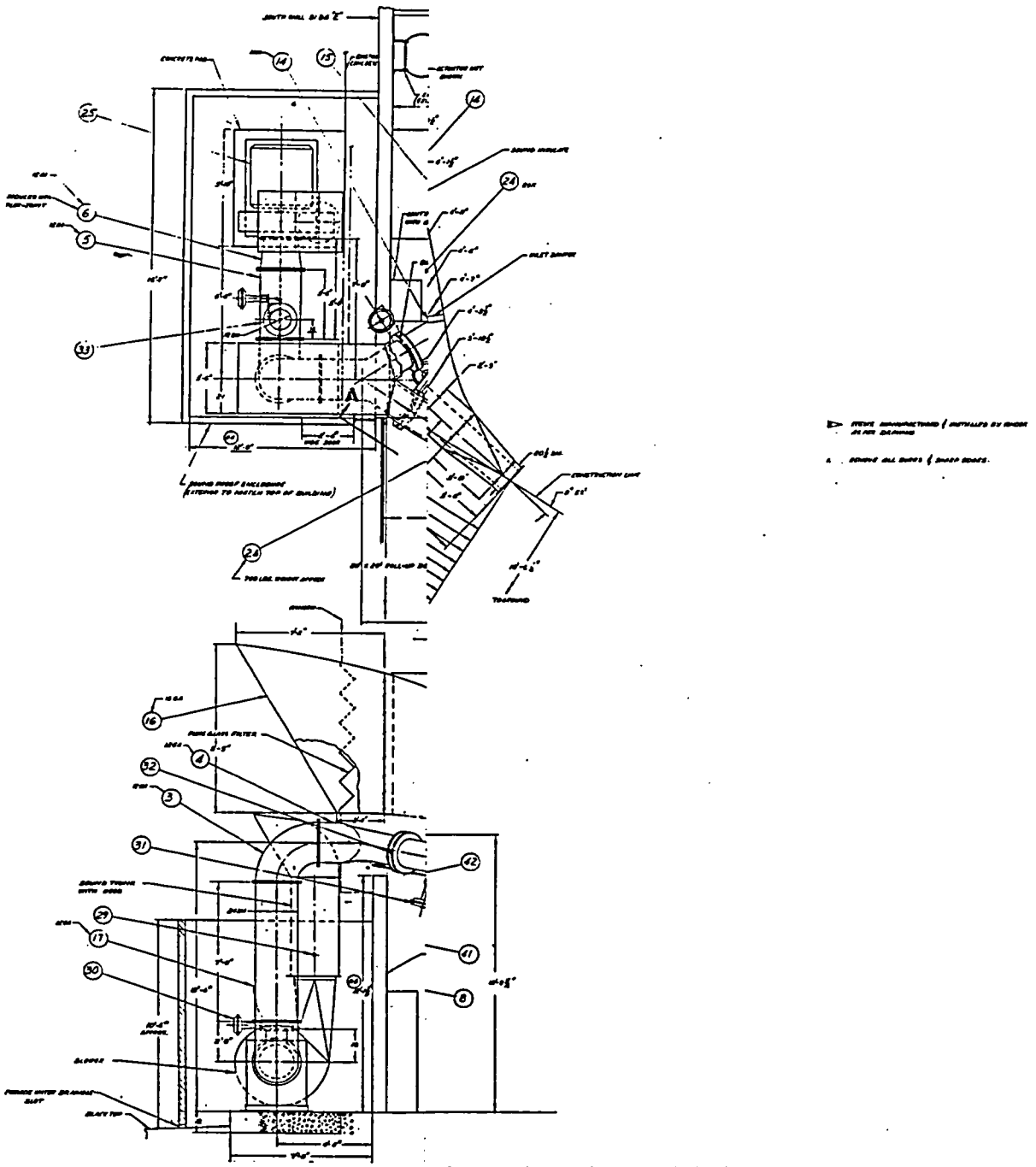

NGEMENT - HALF-LINEAR-SCALE FLOW MODEL

FIGURE 105

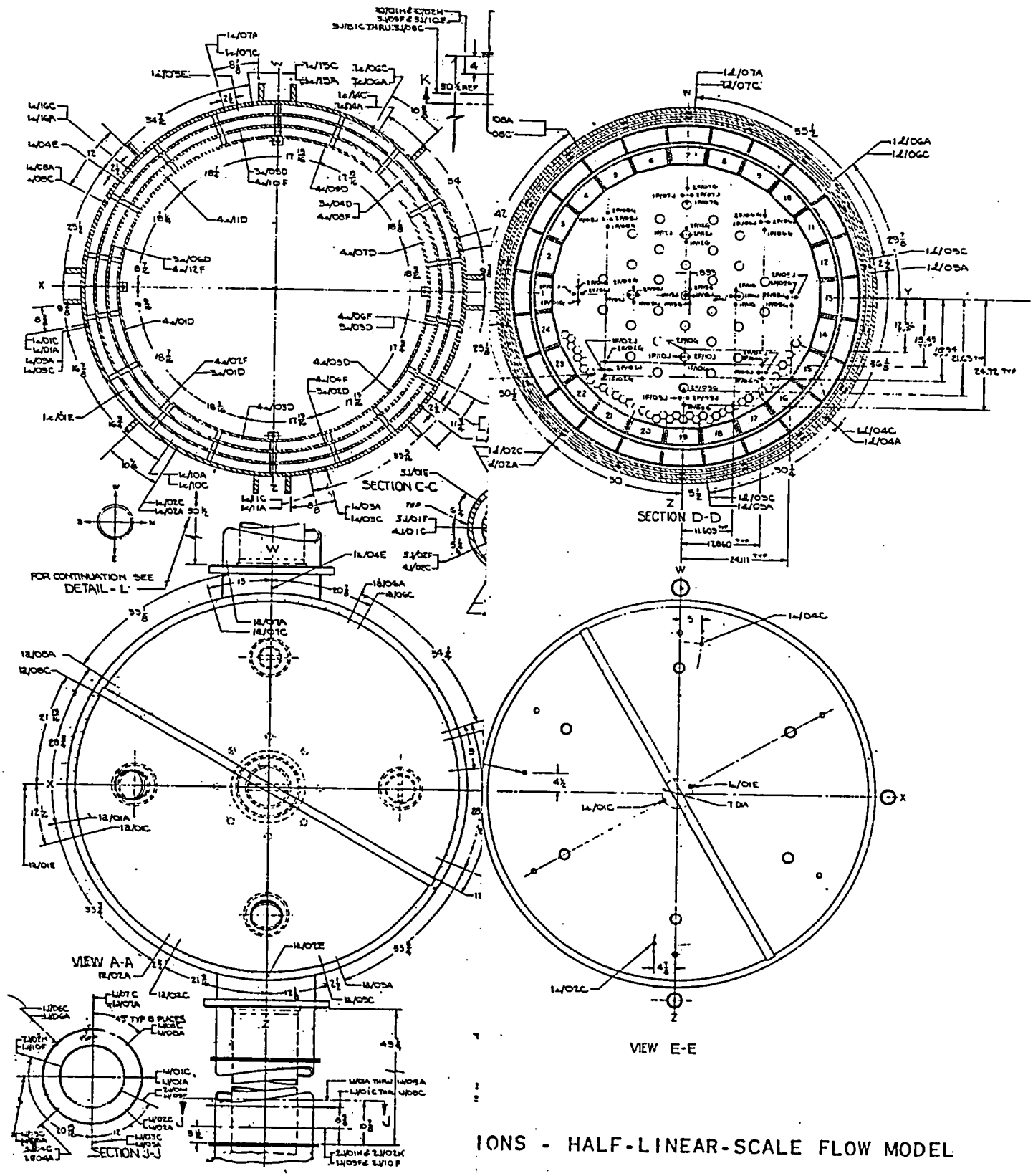

IONS - HALF-LINEAR-SCALE FLOW MODEL

FIGURE 106

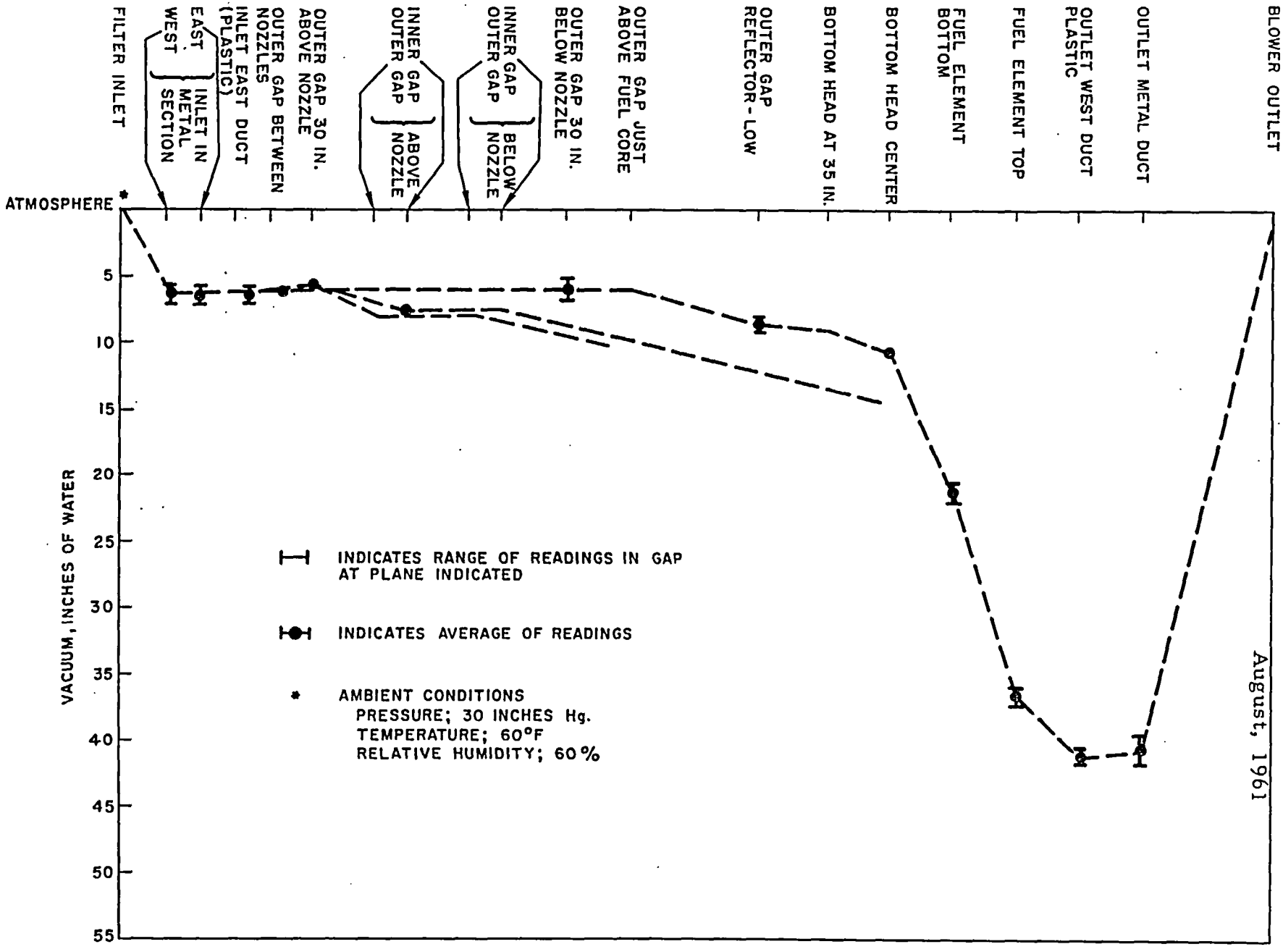

August, 1961

STATIC PRESSURE DISTRIBUTION - HALF-LINEAR-SCALE FLOW MODEL

FIGURE 107

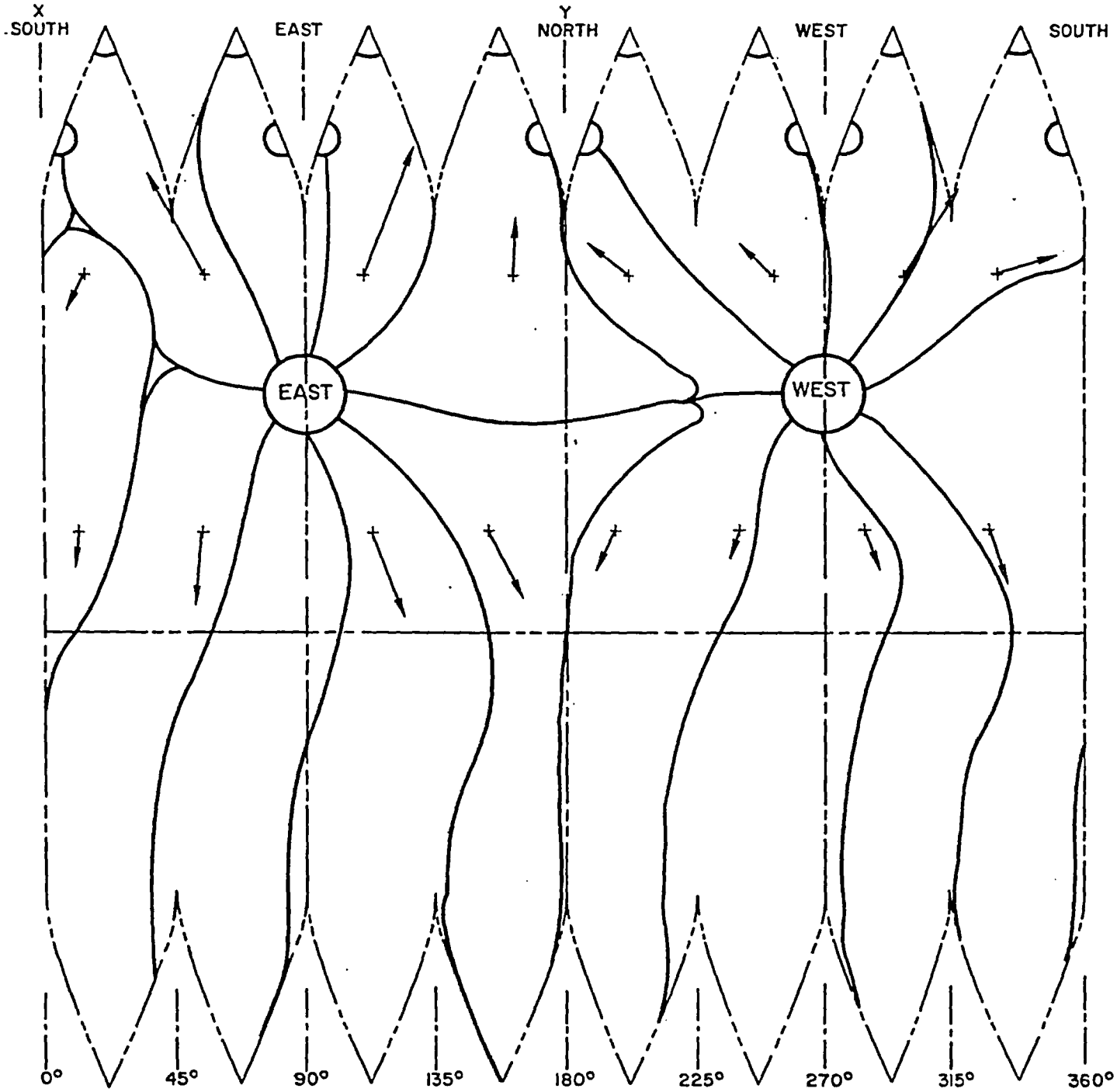

LOCAL VELOCITIES AND PROJECTED REGIONS OF EQUAL MASS FLOW BASED ON THE 16 POINTS SHOWN. DATA OBTAINED IN TESTS OF HALF-LINEAR-SCALE FLOW MODEL WITHOUT INLET STRAIGHTENING VANES AND WITH SPACER BLOCKS ADJACENT TO NOZZLES IN PLACE: BALANCED INLET FLOW

FIGURE 108

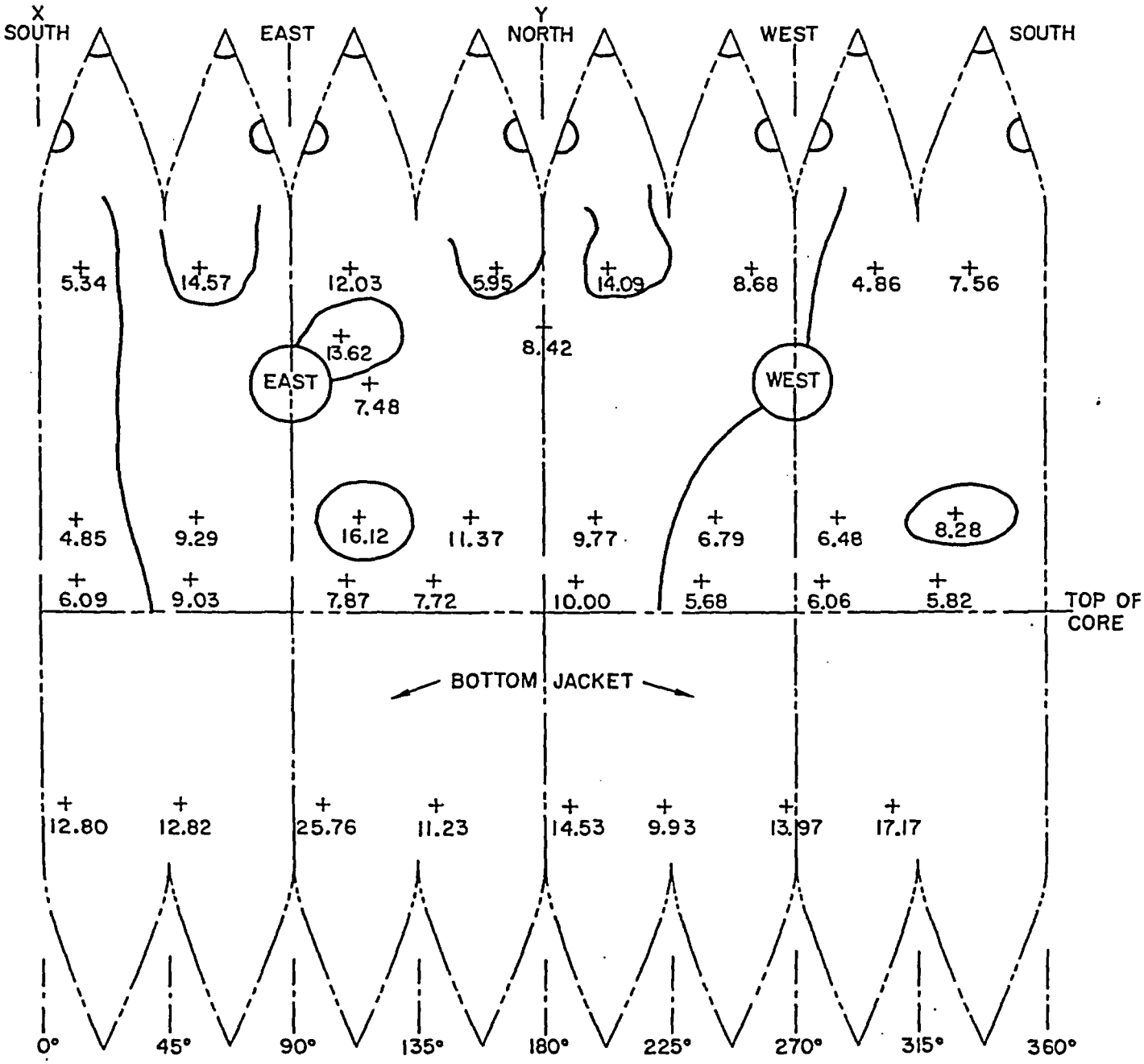

OUTER JACKET HEAT TRANSFER COEFFICIENT FOR AIR IN BTU/HR FT^2·°F. DATA OBTAINED IN TESTS OF HALF-LINEAR-SCALE FLOW MODEL; APPROXIMATELY 1/2 PROTOTYPE REYNOLDS NUMBER

FIGURE 109

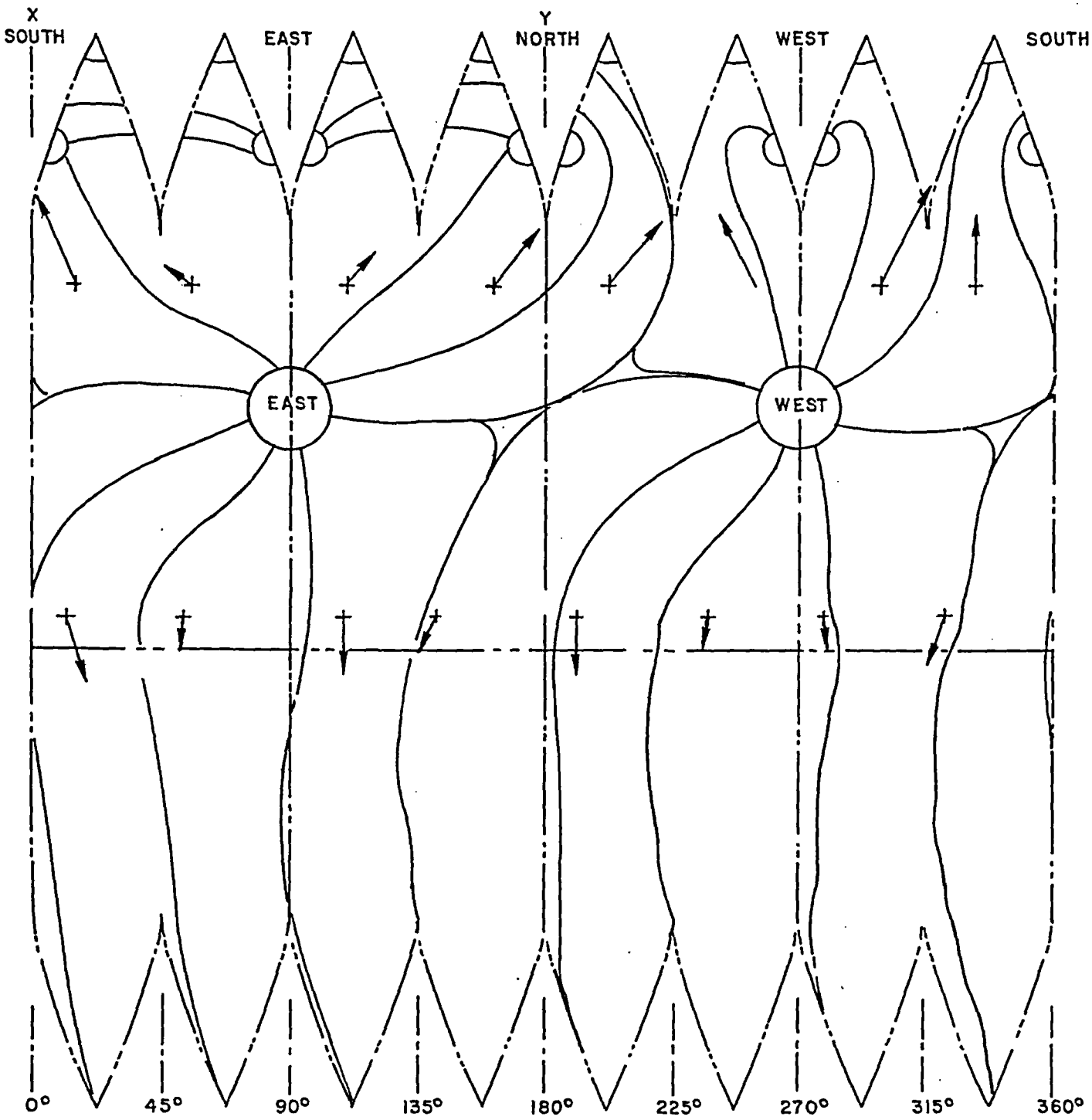

LOCAL VELOCITIES AND PROJECTED REGIONS OF EQUAL MASS FLOW BASED ON THE 16 POINTS SHOWN. DATA OBTAINED IN TESTS OF HALF-LINEAR-SCALE FLOW MODEL WITH INLET STRAIGHTENING VANES INSTALLED AND SPACER BLOCKS ADJACENT TO NOZZLES REMOVED; BALANCE INLET FLOW

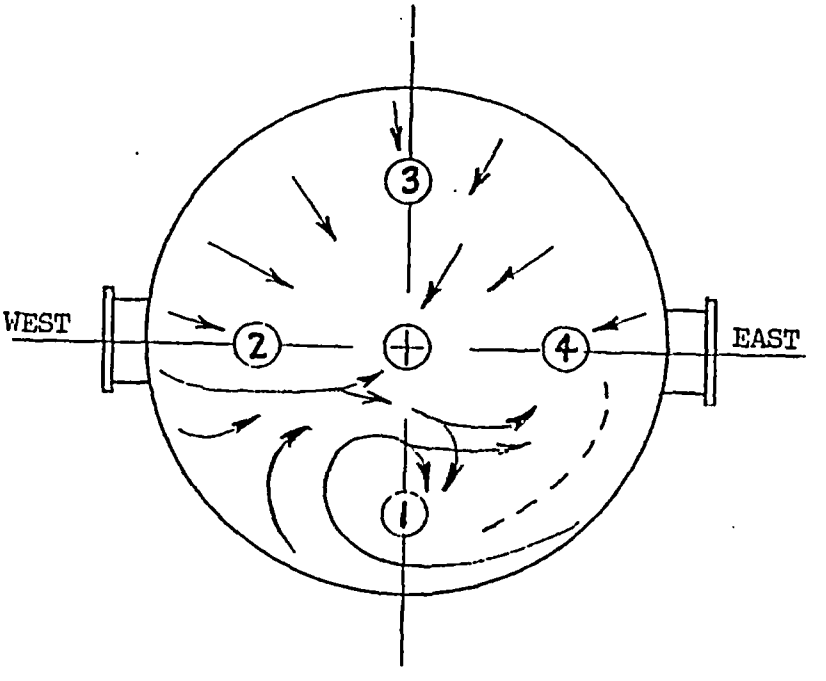

CASE I
Small orifice at positions 2 or 3.

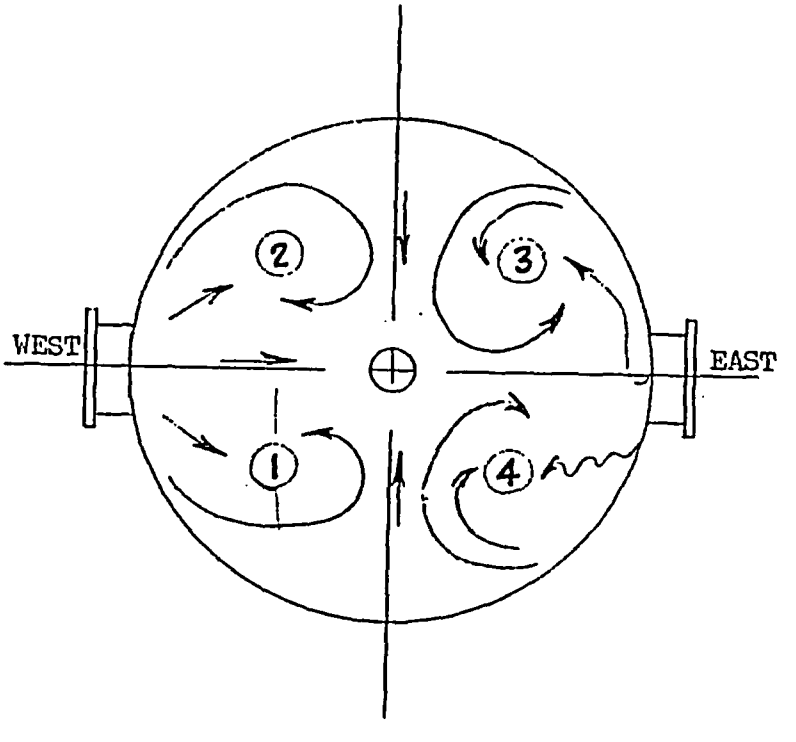

CASE II
Small orifice at positions 1 or 2.

FLOW PATHS IN UPPER HEAD. OUTER GAP FOR DIFFERENT ORIFICE POSITIONS. DATA OBTAINED IN TESTS OF HALF-LINEAR-SCALE FLOW MODEL: UNIFORM FLOW: APPROXIMATELY 30% REYNOLDS NUMBER

FIGURE 111

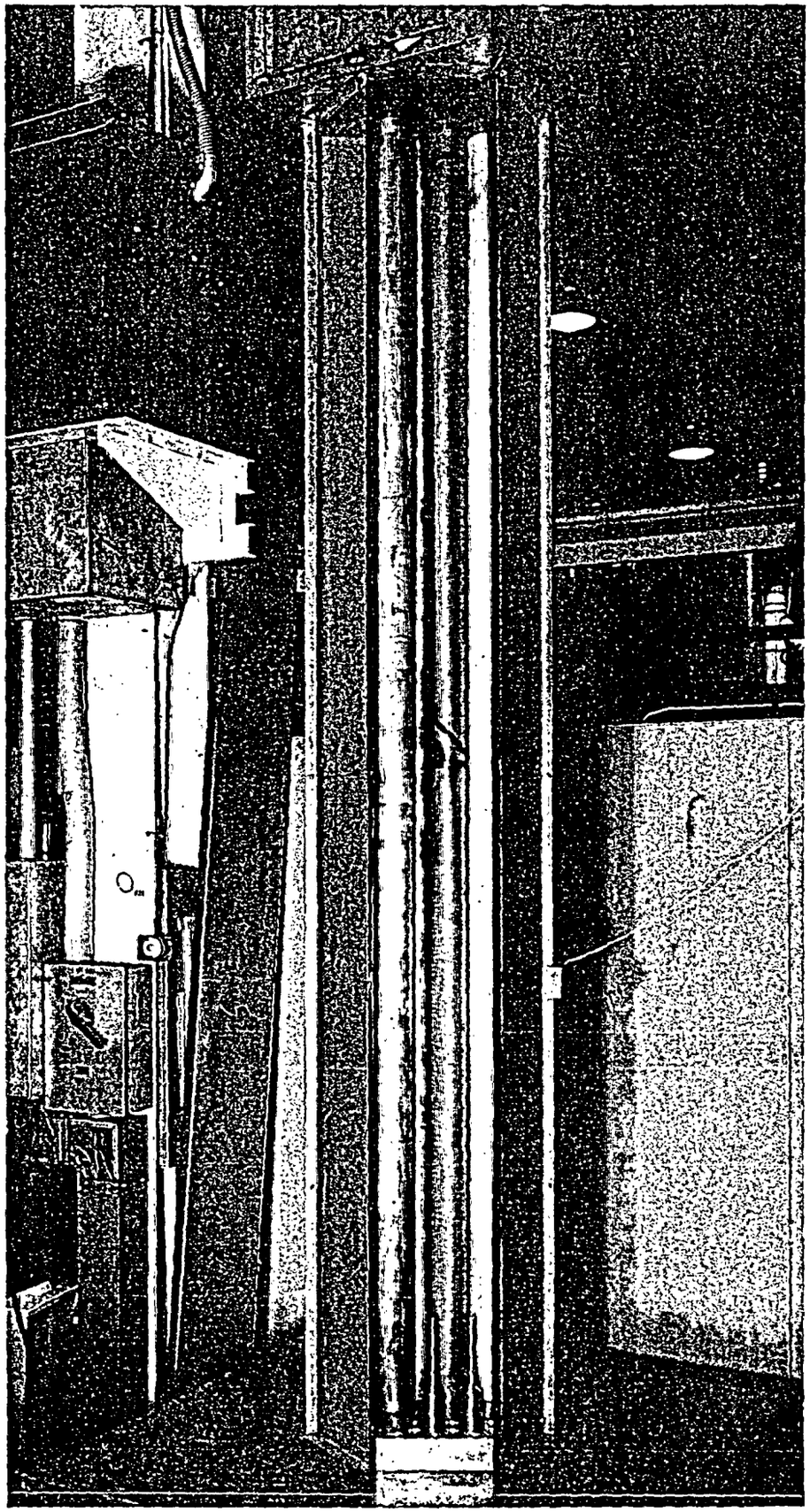

VIEW OF FUEL ELEMENT VIBRATION TEST CHAMBER: ONE SIDE PANEL AND TWO DUMMY ELEMENTS REMOVED

FIGURE 112

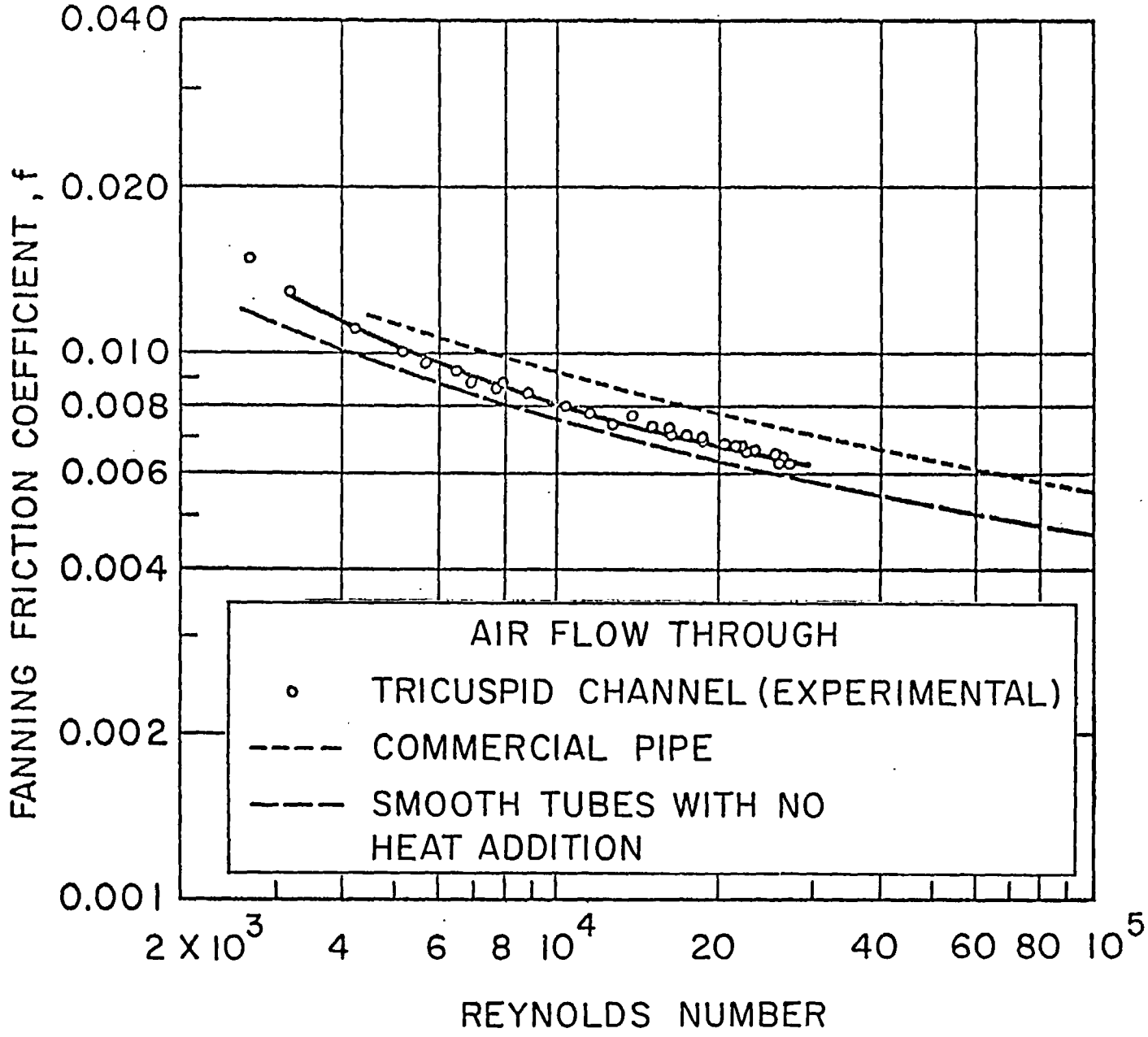

COMPARISON OF FANNING FRICTION FACTORS MEASURED IN FLOW THROUGH TRICUSPID CHANNEL WITH LITERATURE VALUES FOR COMMERCIAL PIPE AND SMOOTH TUBES

FIGURE 113

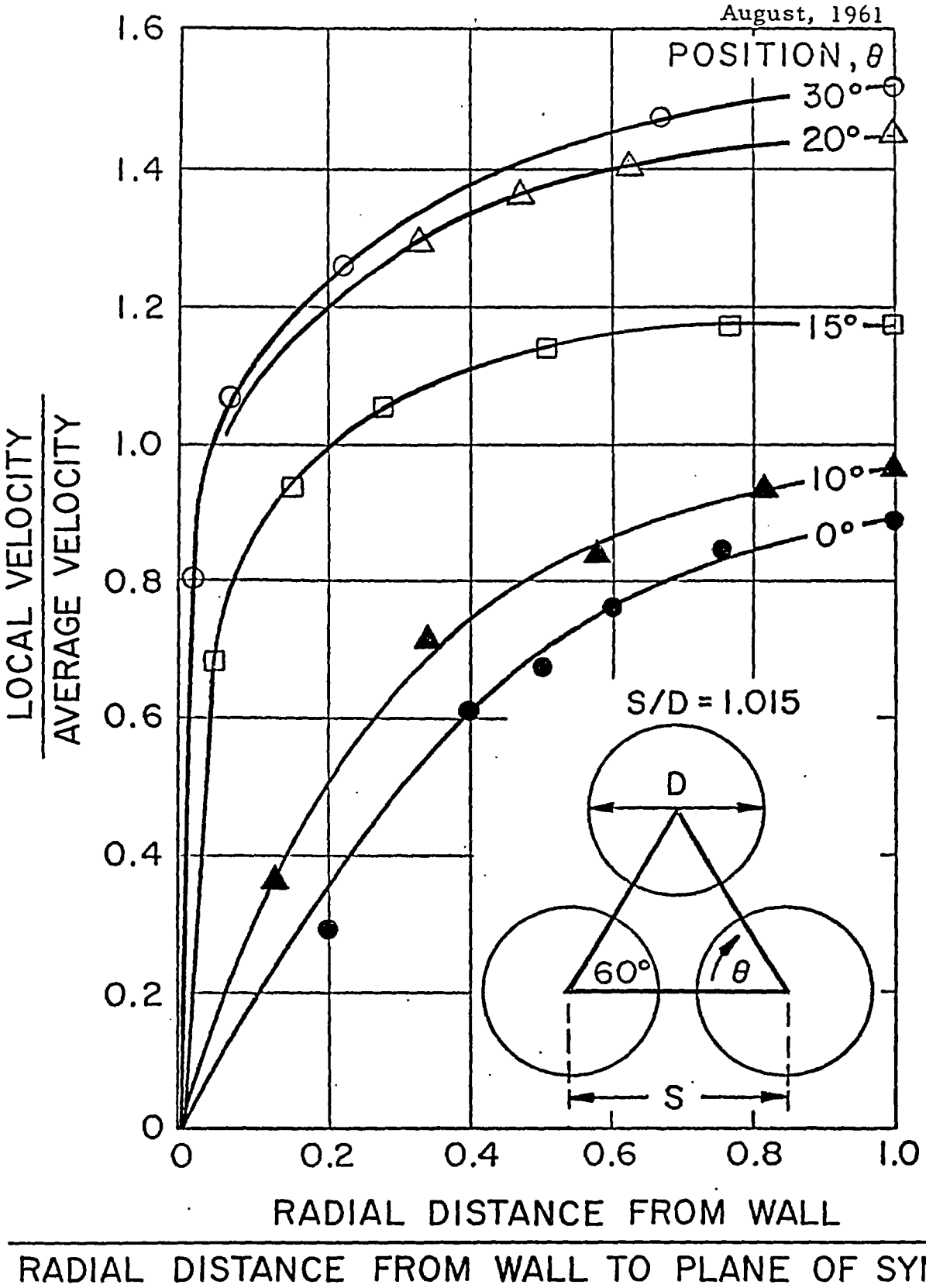

VELOCITY PROFILE FOR TRICUSPID FLOW CHANNELS:
REYNOLDS NUMBER, 20,000

FIGURE 114

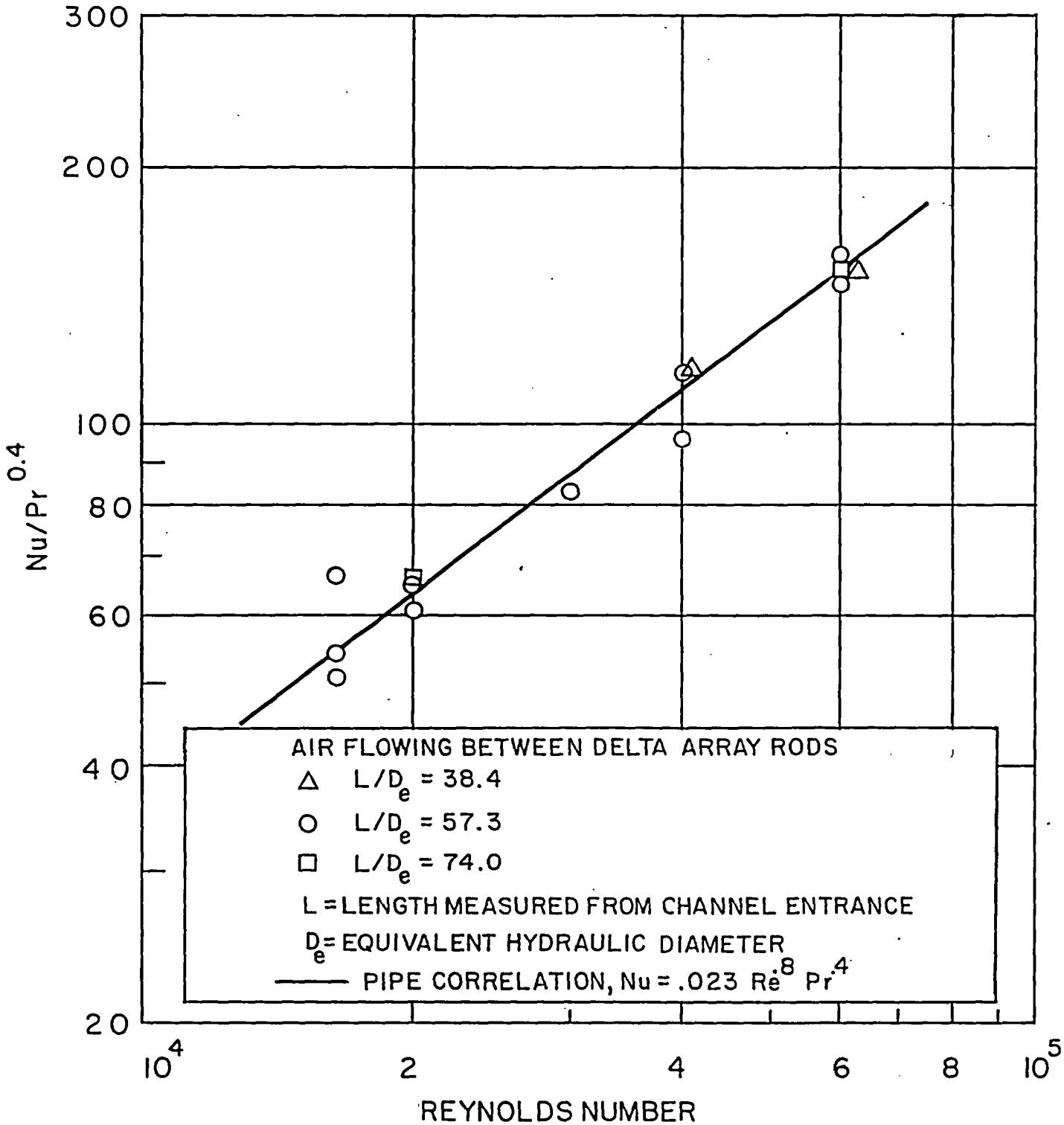

MEASURED OVER-ALL HEAT-TRANSFER RATES FROM THE ROD SURFACE TO AIR AS A FUNCTION OF REYNOLDS NUMBER

FIGURE 115

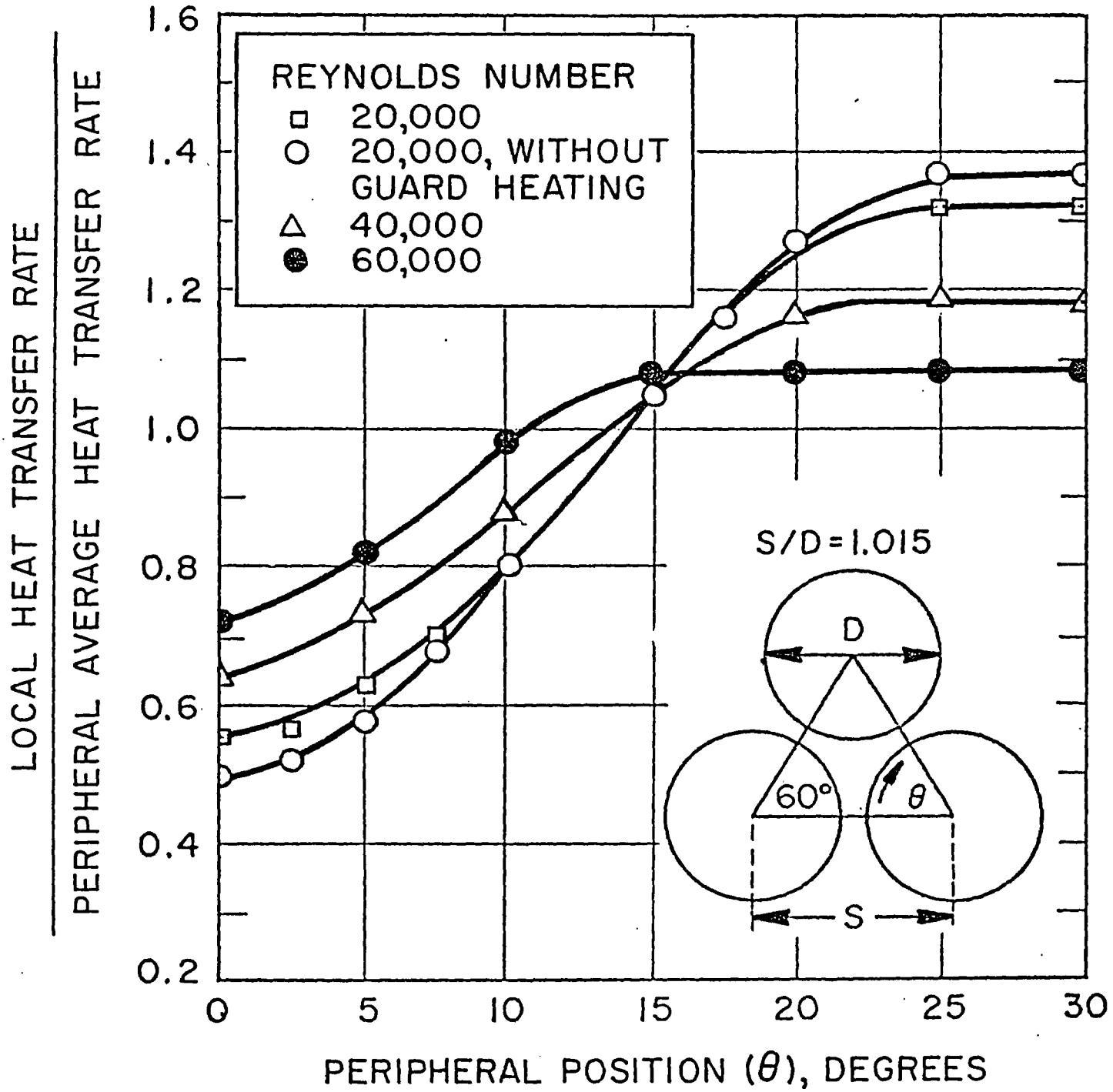

PERIPHERAL VARIATION OF THE MEASURED HEAT TRANSFER RATES

FIGURE 116

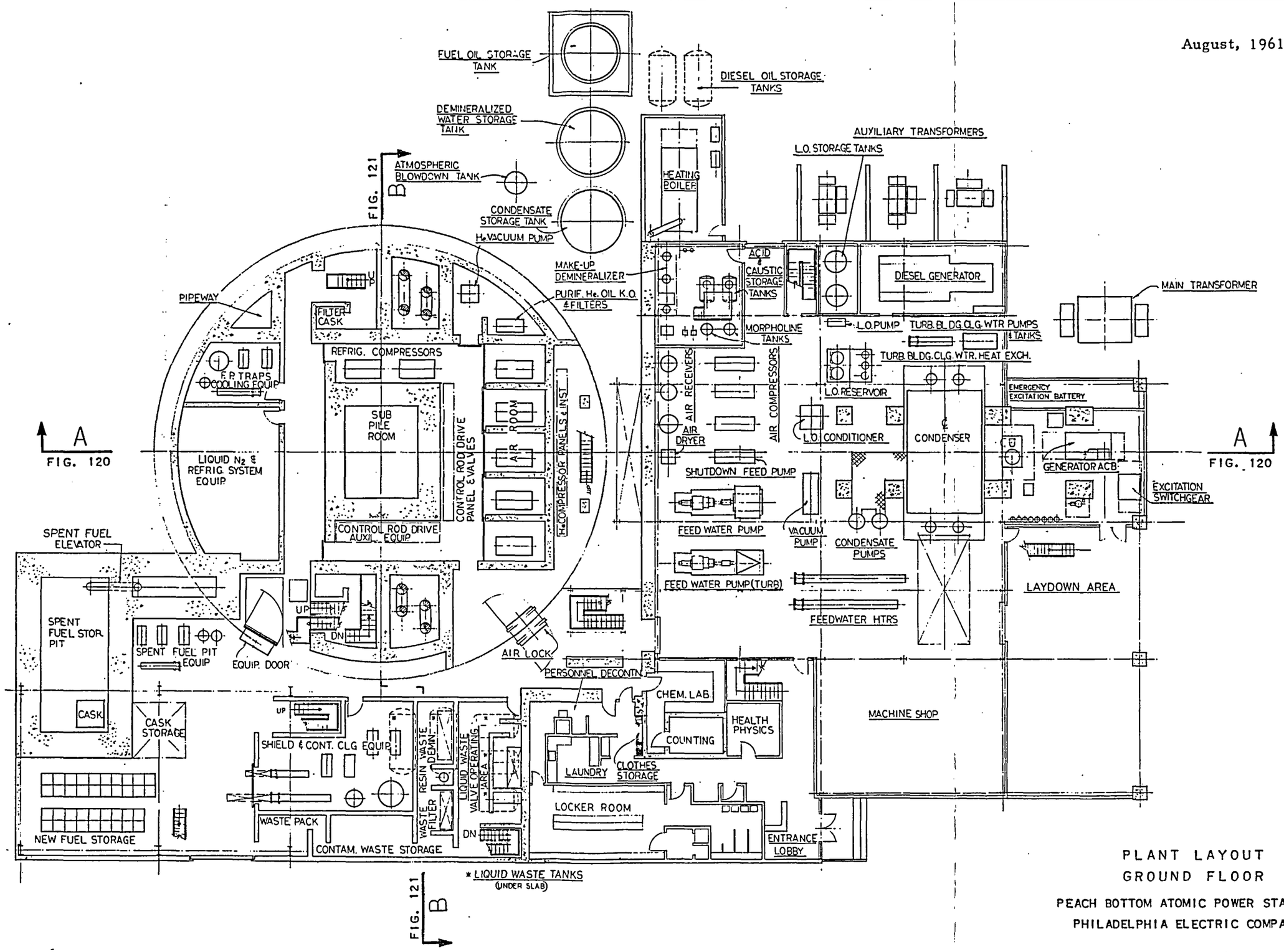

PLANT LAYOUT
GROUND FLOOR

PEACH BOTTOM ATOMIC POWER STATION
PHILADELPHIA ELECTRIC COMPANY

FIGURE 117

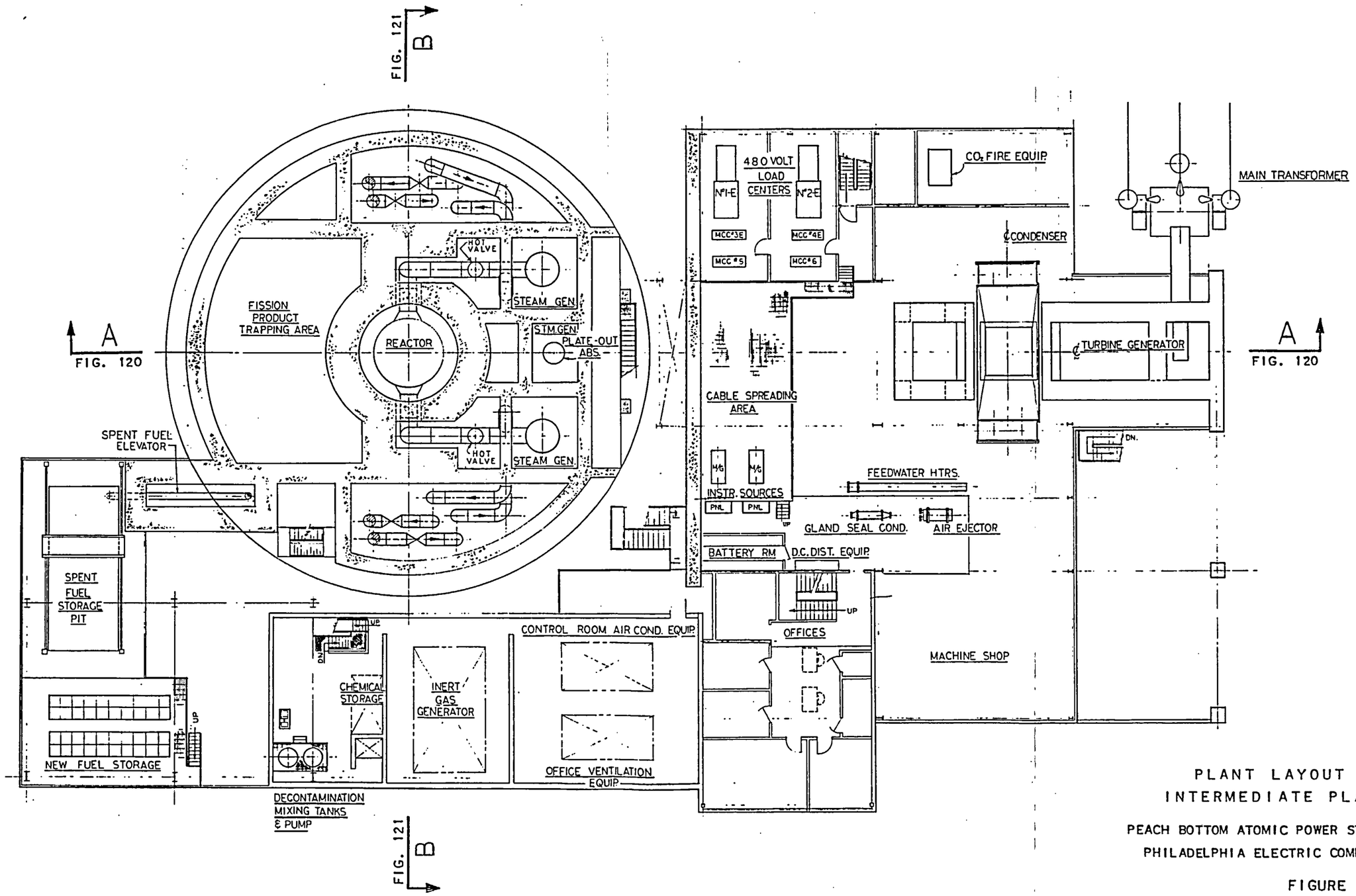

PLANT LAYOUT
INTERMEDIATE PLAN

PEACH BOTTOM ATOMIC POWER STATION
PHILADELPHIA ELECTRIC COMPANY

FIGURE 118

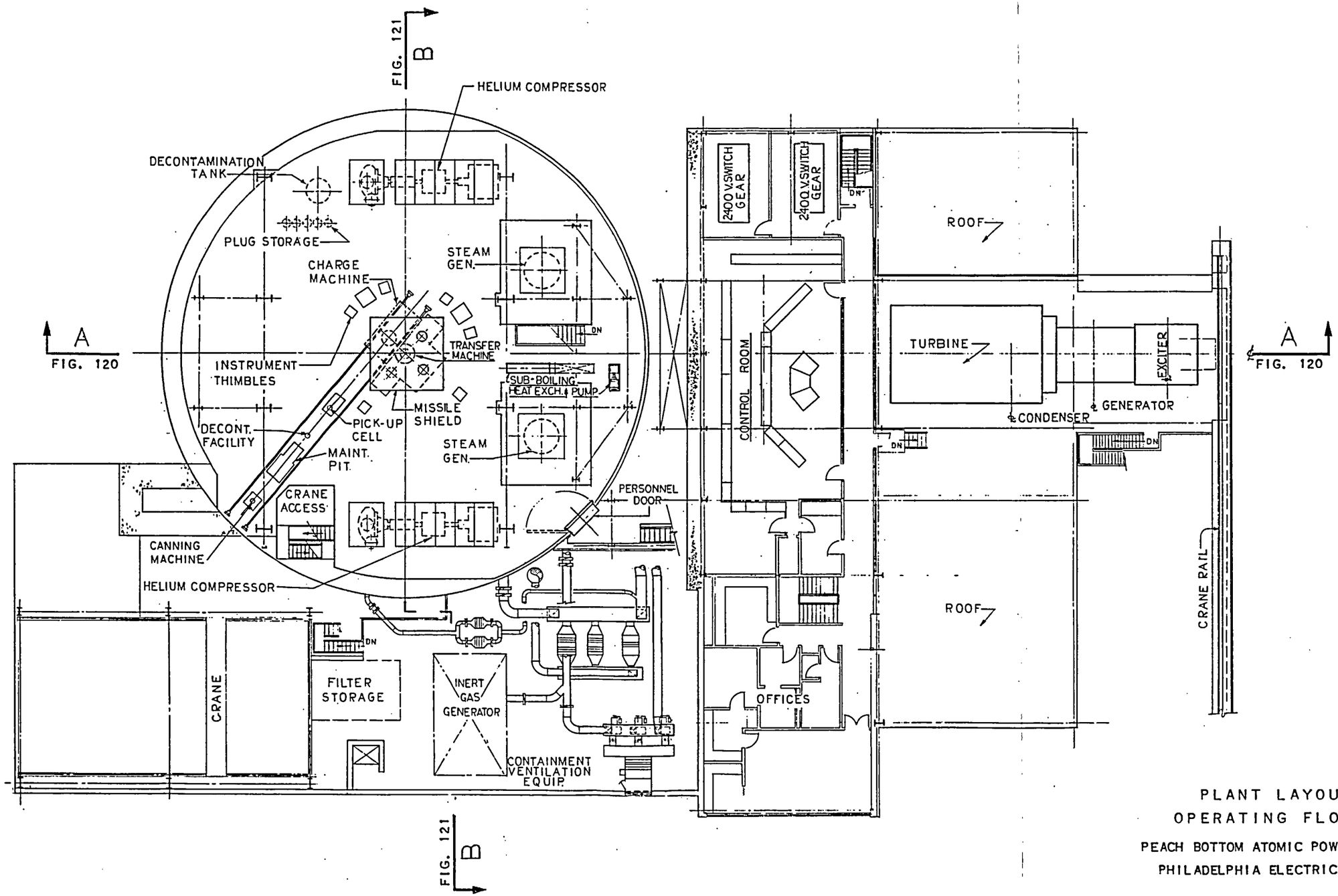

PLANT LAYOUT
OPERATING FLOOR

PEACH BOTTOM ATOMIC POWER STATION
PHILADELPHIA ELECTRIC COMPANY

FIGURE 119

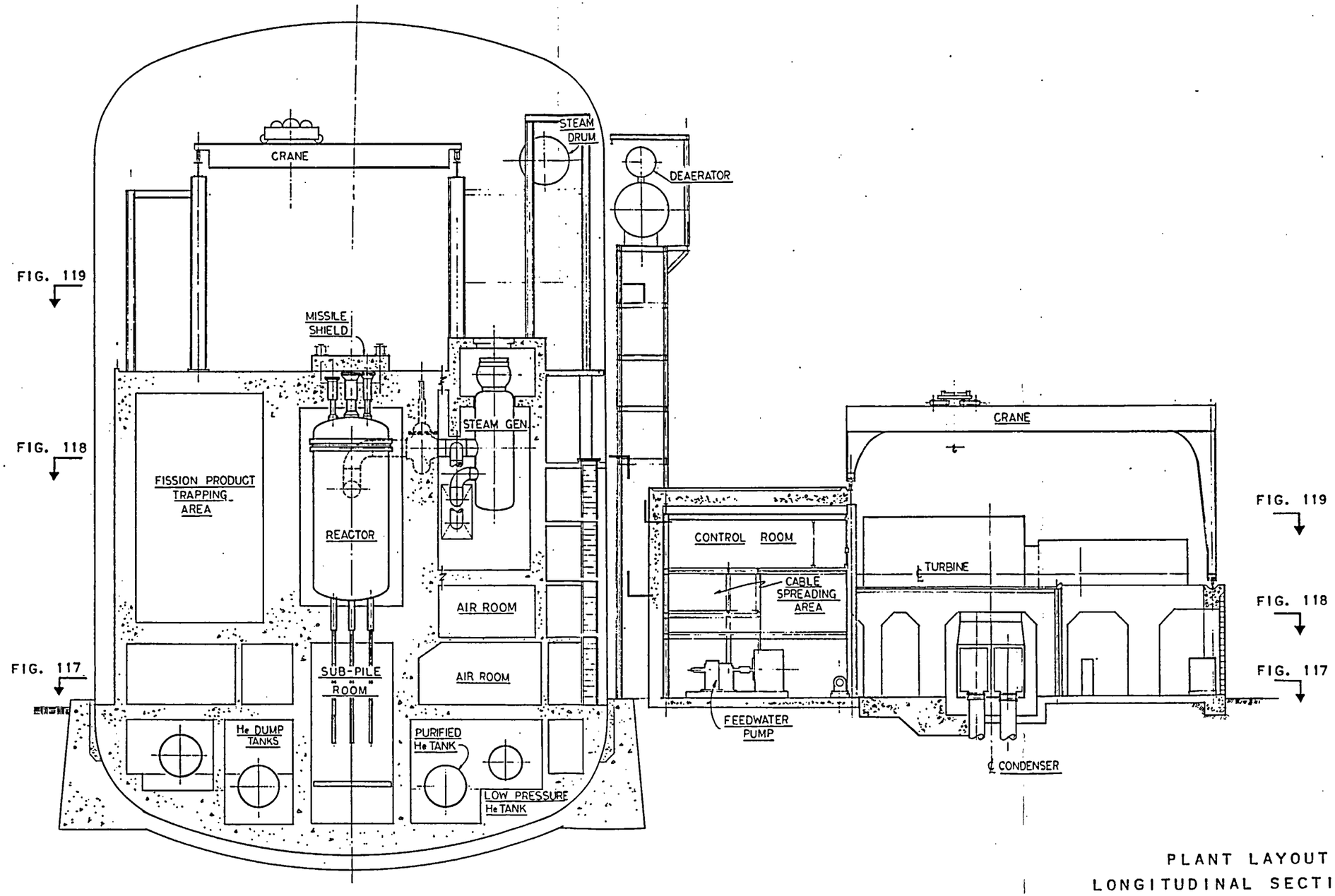

PLANT LAYOUT
LONGITUDINAL SECTION A-A

PEACH BOTTOM ATOMIC POWER STATION
PHILADELPHIA ELECTRIC COMPANY

FIGURE 120

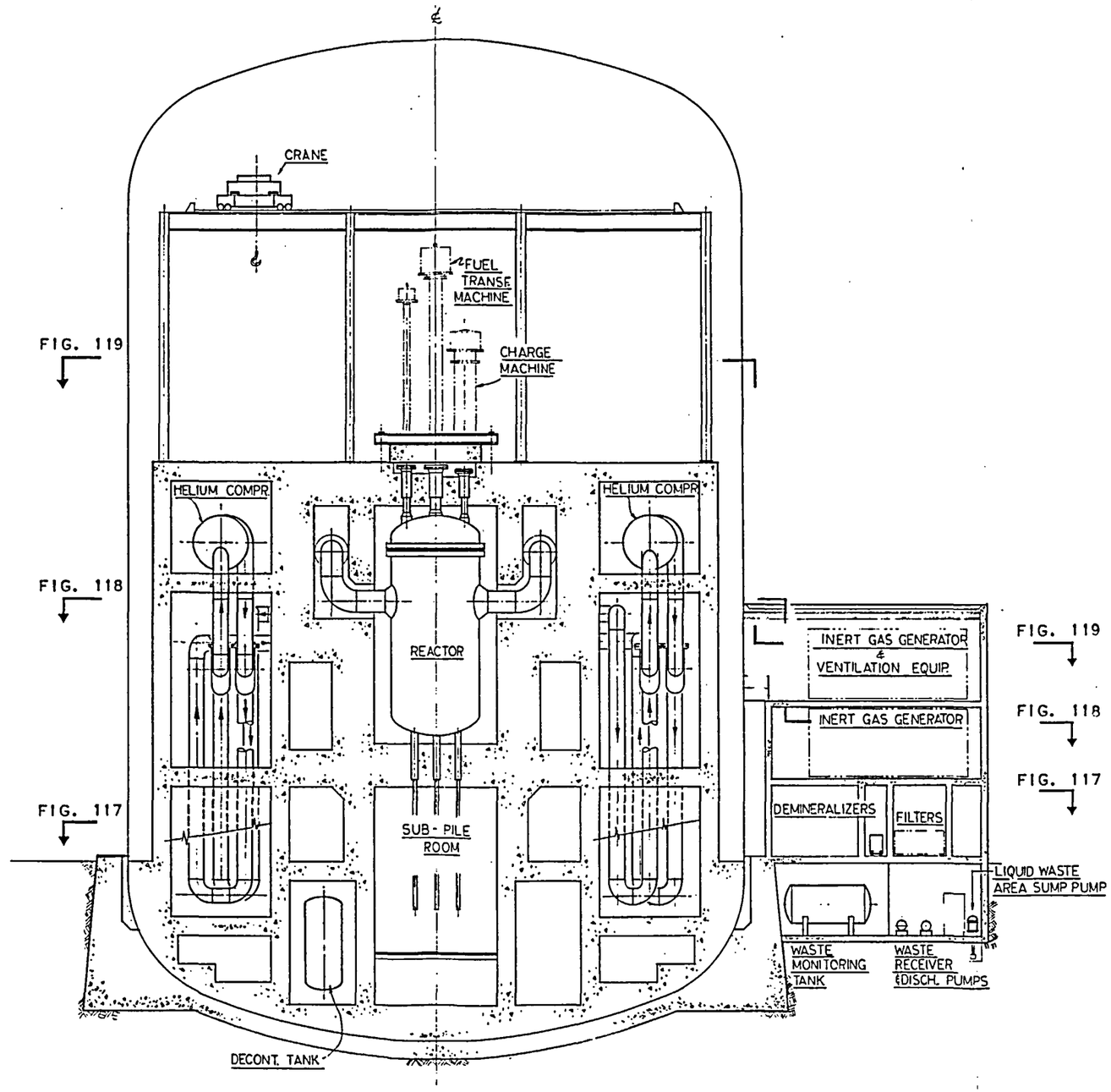

PLANT LAYOUT
CROSS-SECTION B-B
PEACH BOTTOM ATOMIC POWER STATION
PHILADELPHIA ELECTRIC COMPANY

FIGURE 121

August, 1961

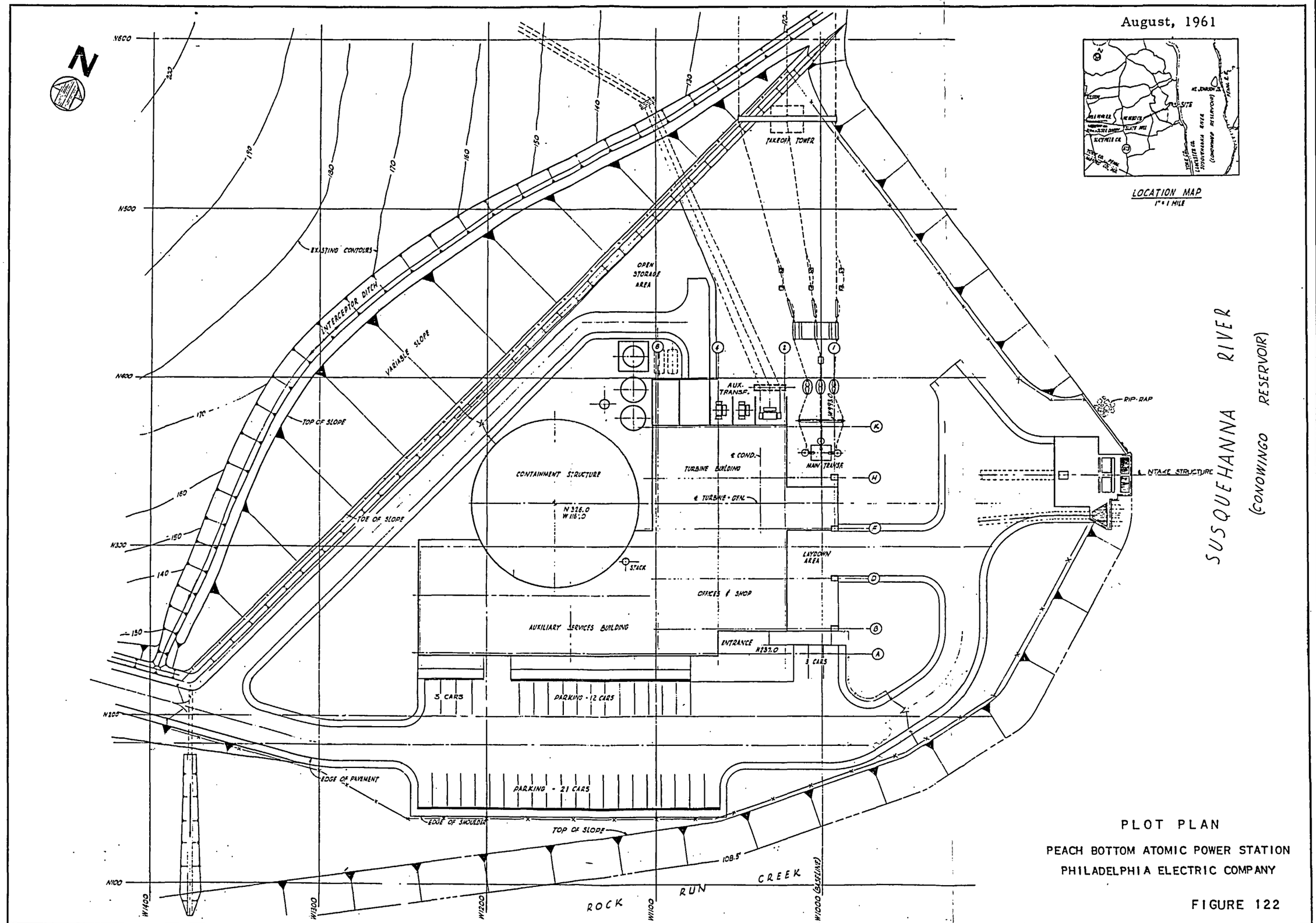

PLOT PLAN

PEACH BOTTOM ATOMIC POWER STATION

PHILADELPHIA ELECTRIC COMPANY

FIGURE 122

August, 1961

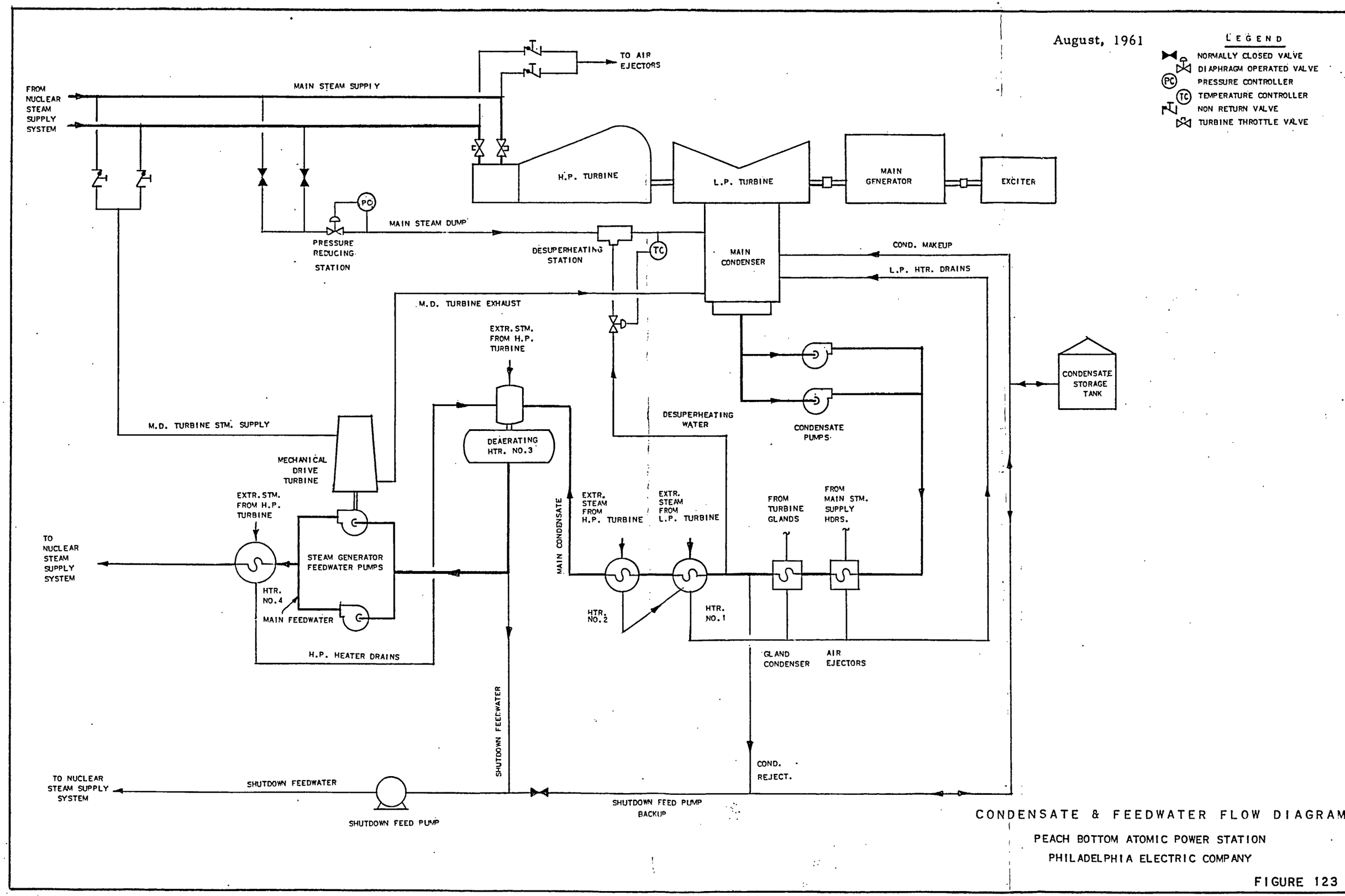

CONDENSATE & FEEDWATER FLOW DIAGRAM

PEACH BOTTOM ATOMIC POWER STATION

PHILADELPHIA ELECTRIC COMPANY

FIGURE 123

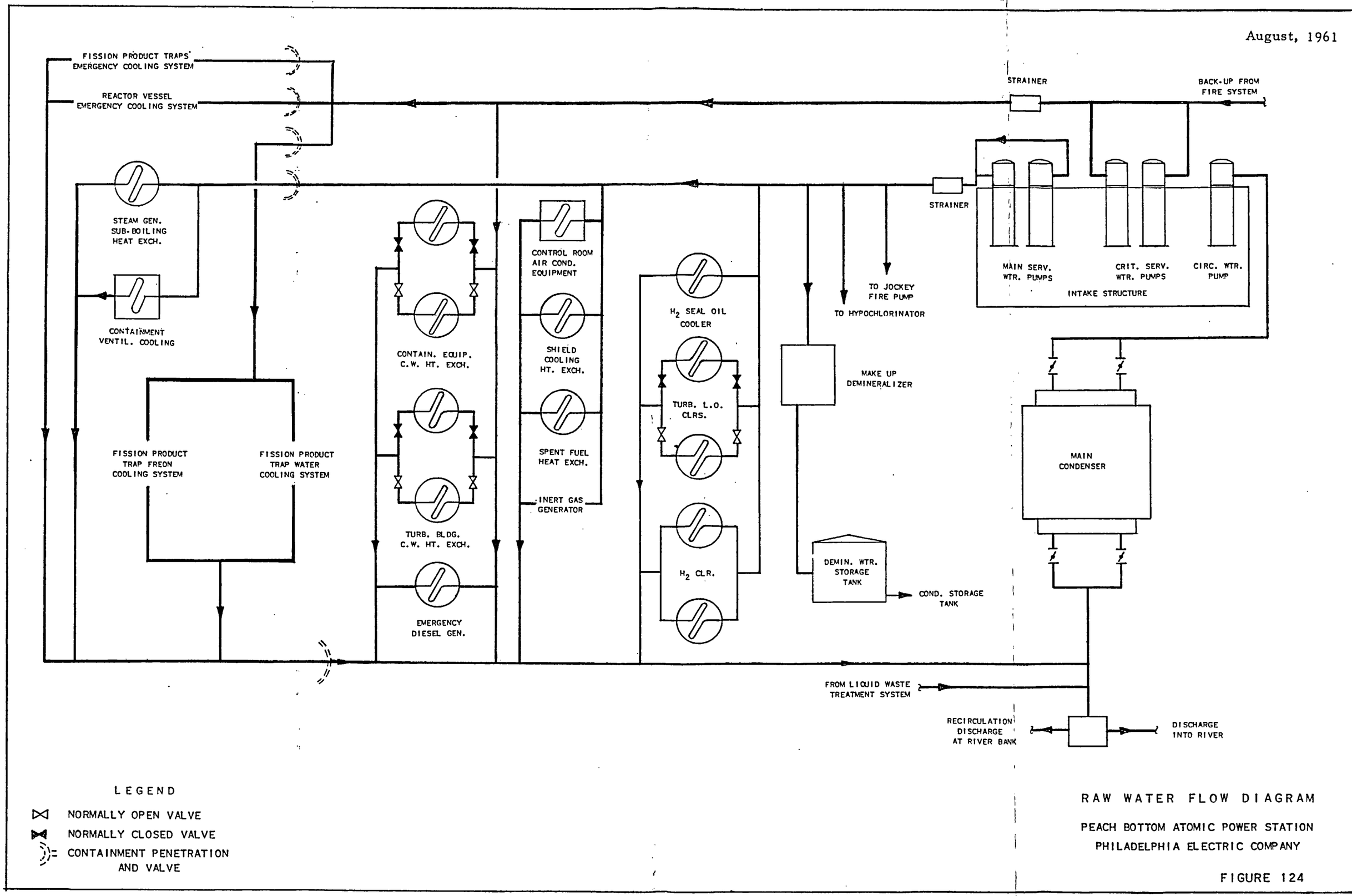

RAW WATER FLOW DIAGRAM

PEACH BOTTOM ATOMIC POWER STATION
PHILADELPHIA ELECTRIC COMPANY

FIGURE 124

August, 1961

LEGEND

NORMALLY OPEN VALVE

NORMALLY CLOSED VALVE

CONTAINMENT PENETRATION AND VALVE

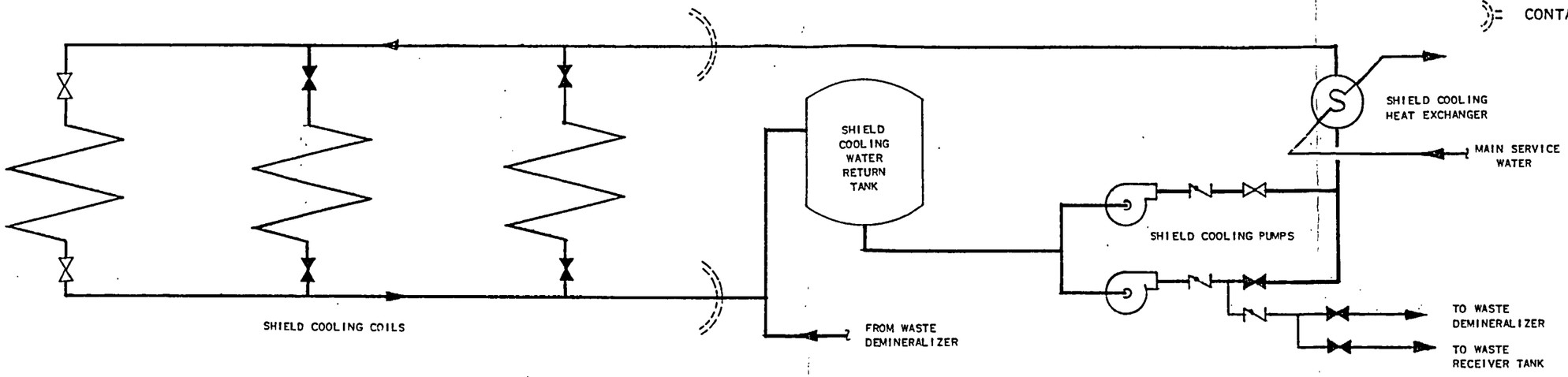

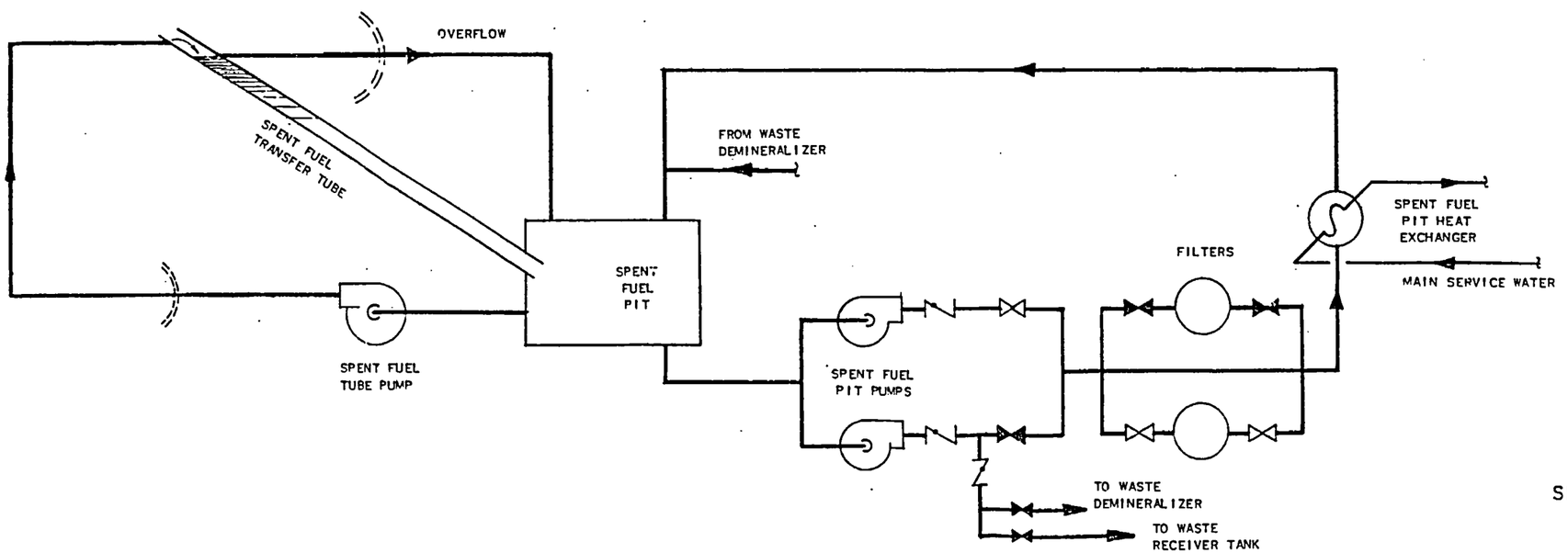

SHIELD COOLING & SPENT FUEL PIT COOLING WATER SYSTEMS

PEACH BOTTOM ATOMIC POWER STATION

PHILADELPHIA ELECTRIC COMPANY

FIGURE 125

August, 1961

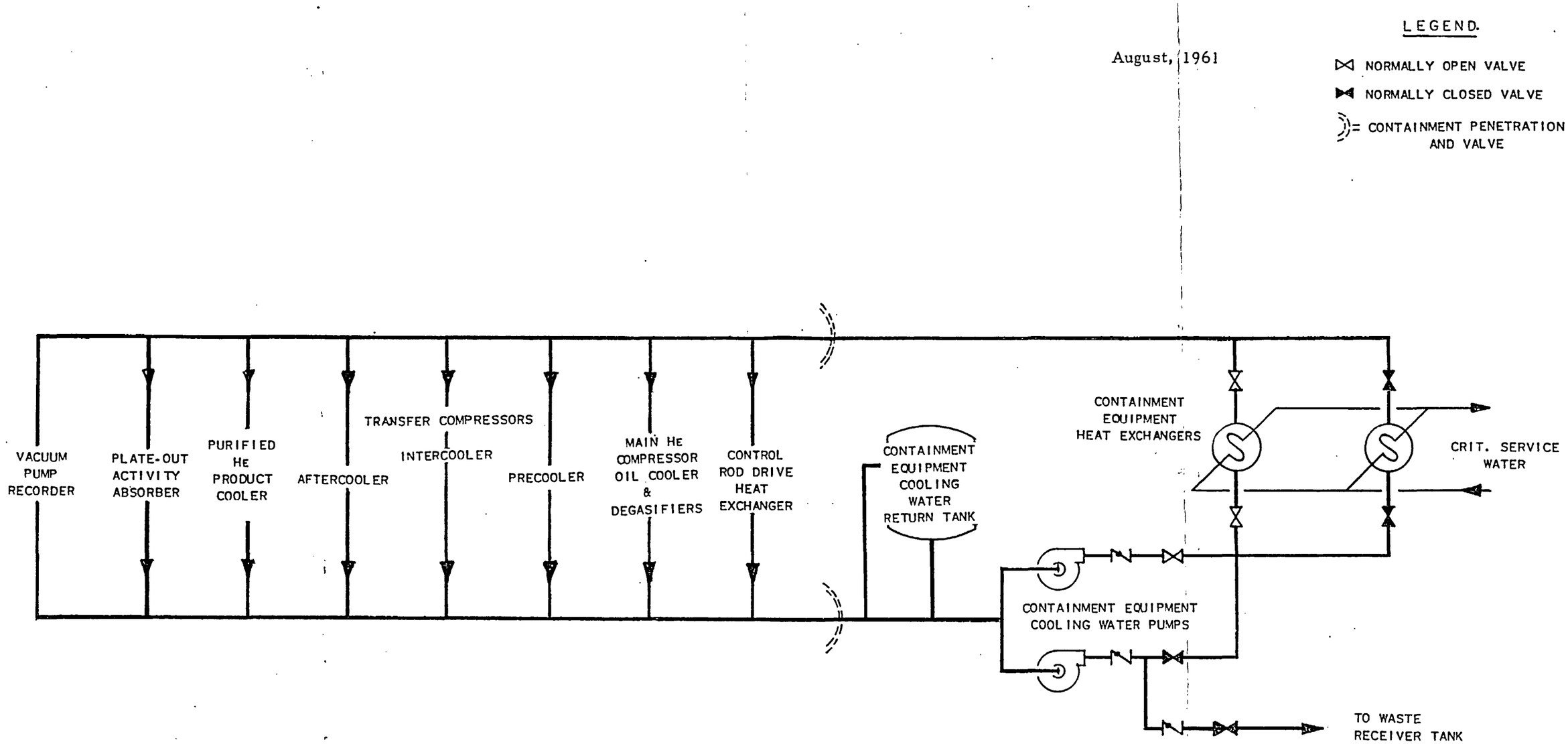

CONTAINMENT EQUIPMENT COOLING WATER SYSTEM

PEACH BOTTOM ATOMIC POWER STATION

PHILADELPHIA ELECTRIC COMPANY

FIGURE 126

August, 1961

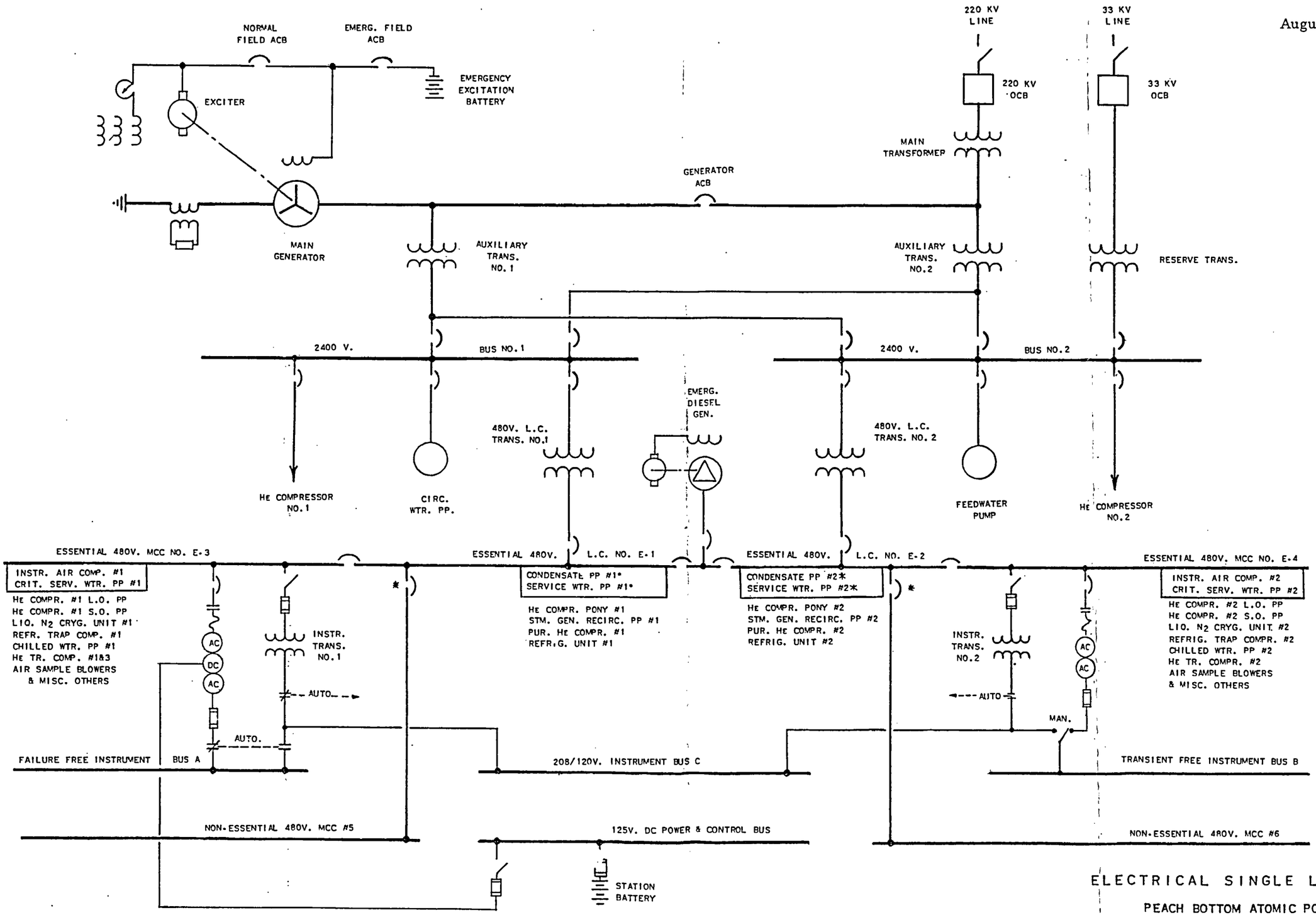

ELECTRICAL SINGLE LINE DIAGRAM

PEACH BOTTOM ATOMIC POWER STATION

PHILADELPHIA ELECTRIC COMPANY

FIGURE 127

* NOTE - LOADS MARKED THUS TRIPPED WHEN SUPPLY IS BY EMERG. DIESEL GEN.

August, 1961

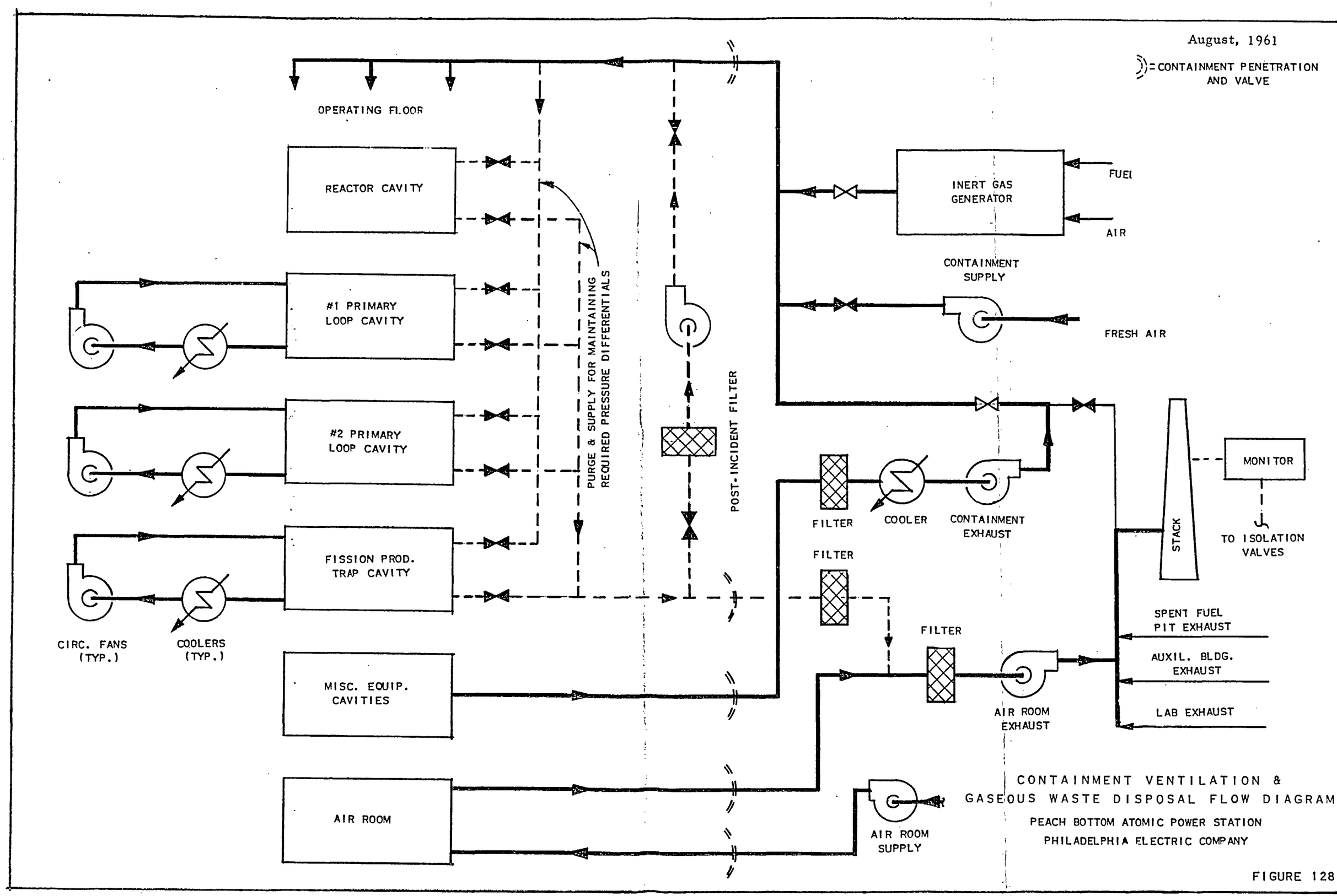

CONTAINMENT VENTILATION & GASEOUS WASTE DISPOSAL FLOW DIAGRAM

PEACH BOTTOM ATOMIC POWER STATION

PHILADELPHIA ELECTRIC COMPANY

FIGURE 128

August, 1961

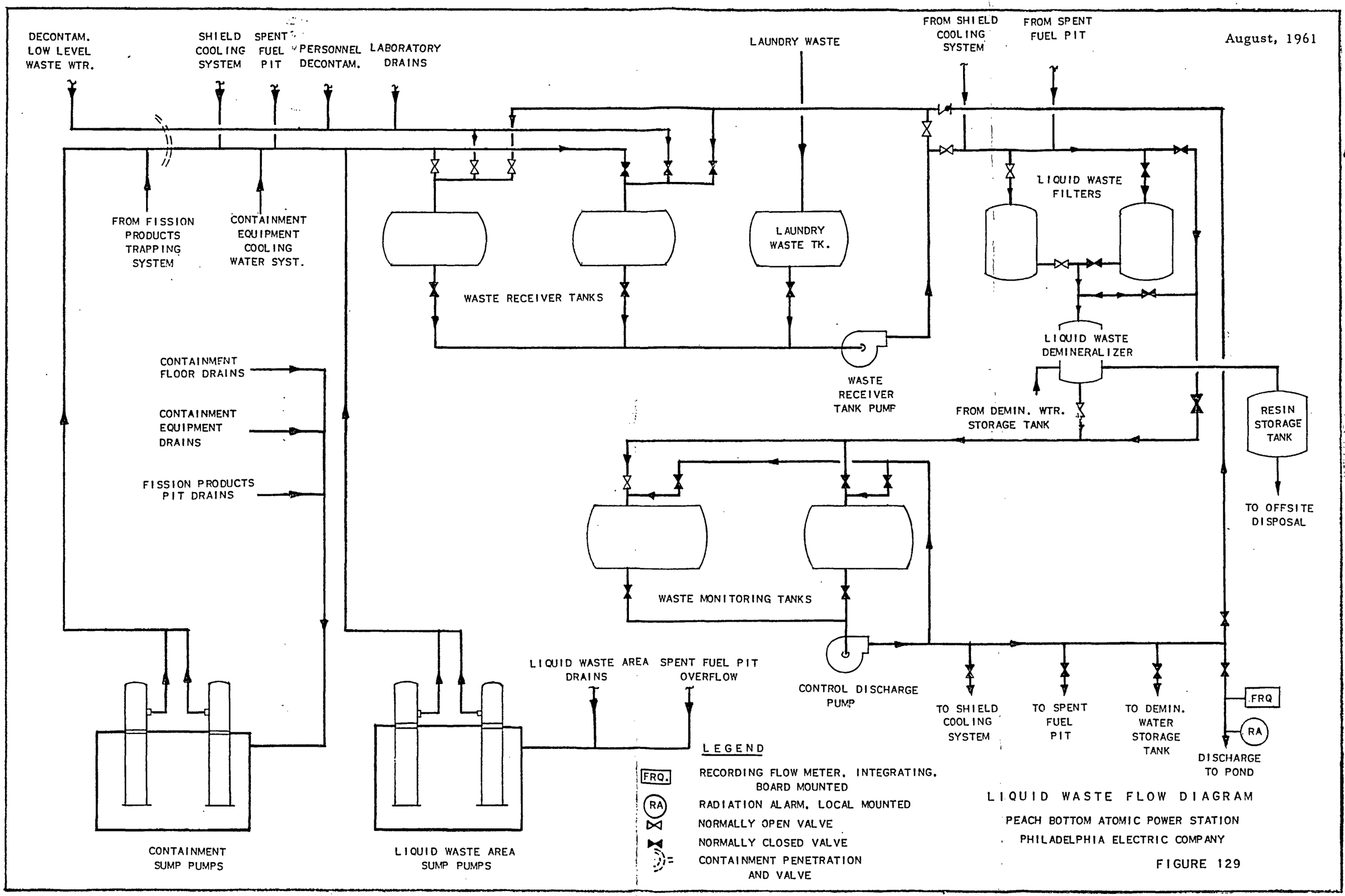

LIQUID WASTE FLOW DIAGRAM

PEACH BOTTOM ATOMIC POWER STATION

PHILADELPHIA ELECTRIC COMPANY

FIGURE 129

August, 1961

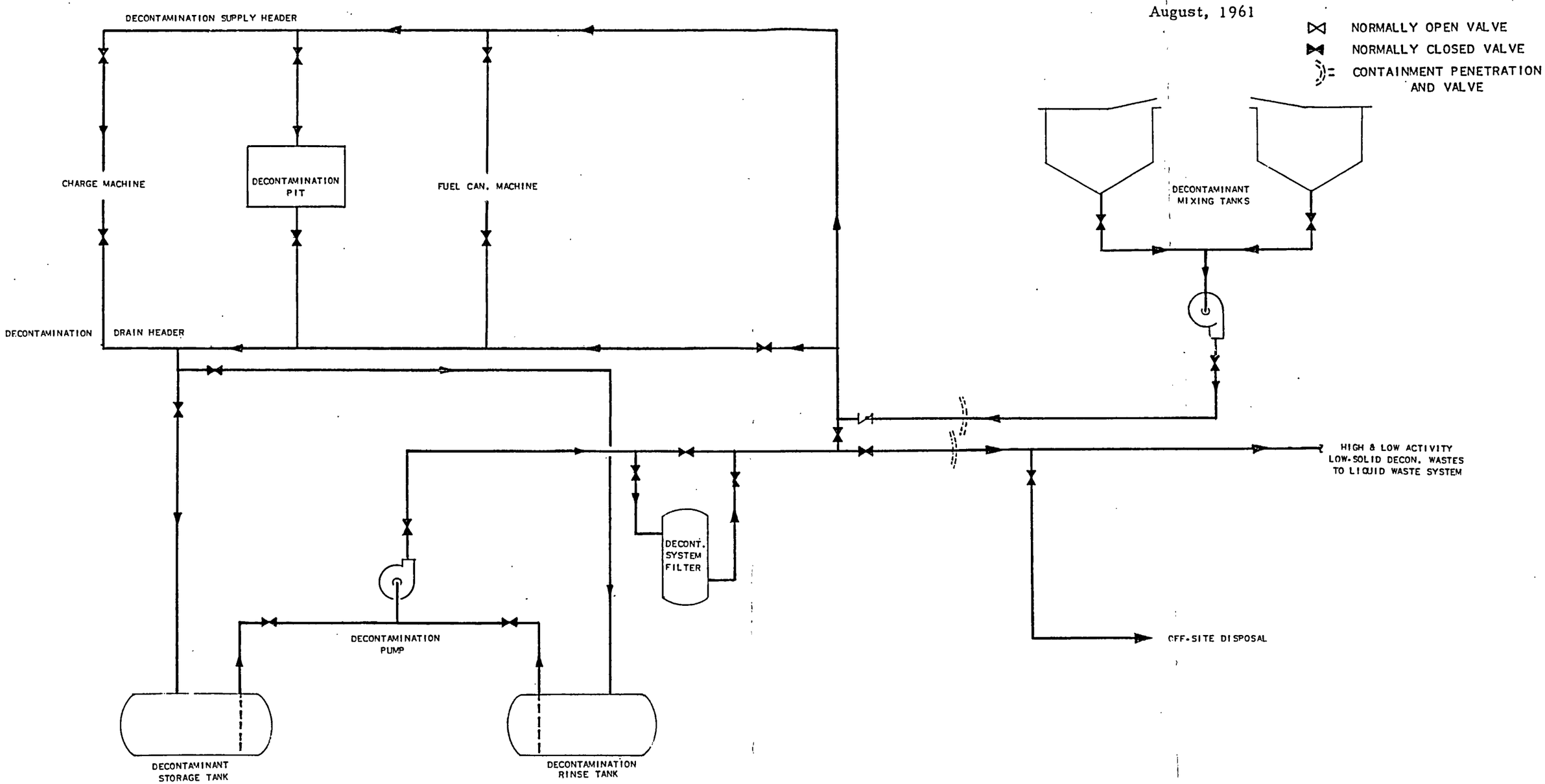

DECONTAMINATION
FLOW DIAGRAM

PEACH BOTTOM ATOMIC POWER STATION
PHILADELPHIA ELECTRIC COMPANY

FIGURE 130

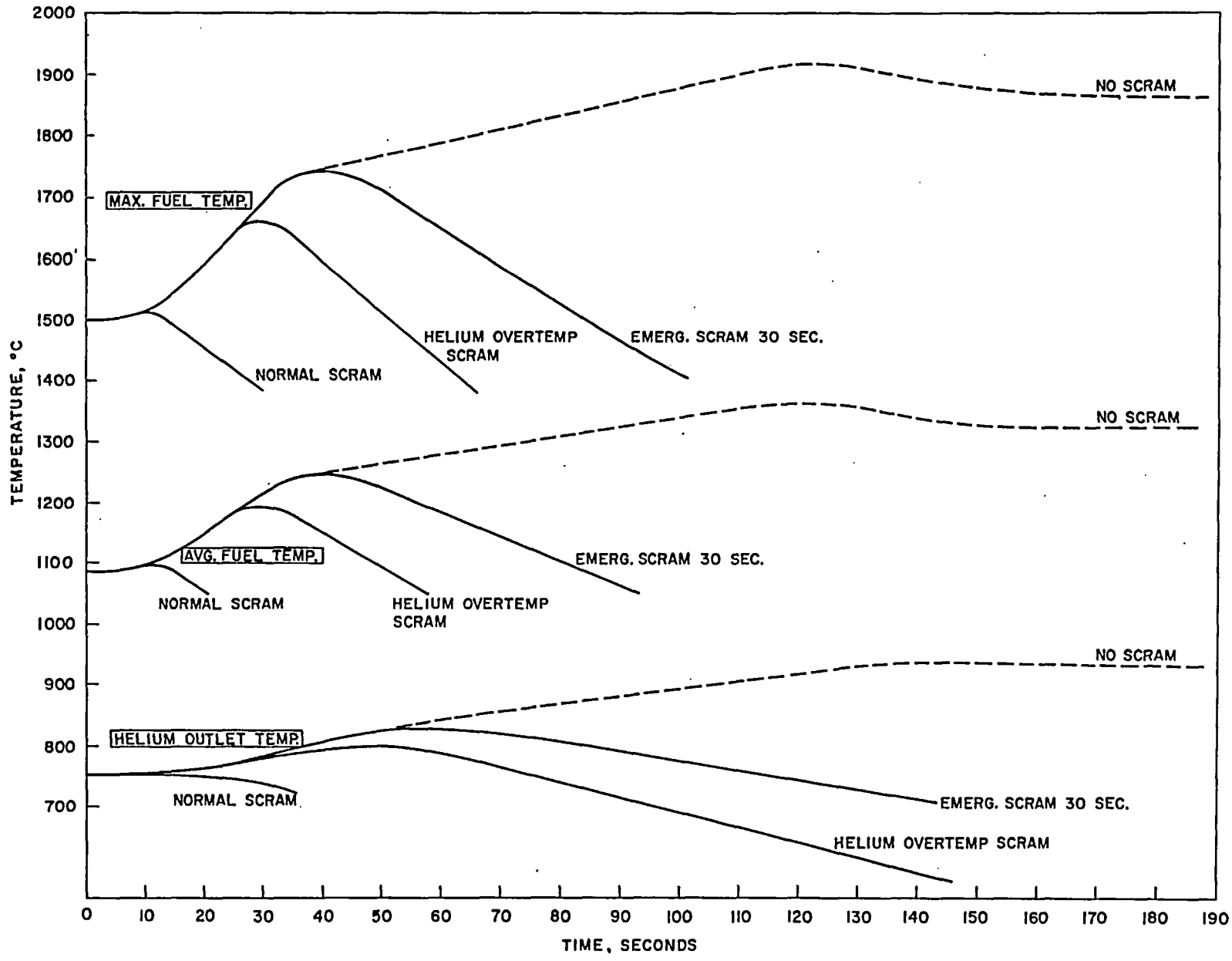

FUEL COMPACT AND HELIUM OUTLET TEMPERATURES FOLLOWING WITHDRAWAL OF ONE CONTROL ROD WORTH 0.01 Δk; NORMAL OPERATING POWER: END OF LIFE: NO XENON PRESENT. NORMAL SCRAM AT 140% NORMAL POWER.

FIGURE 131

August, 1961

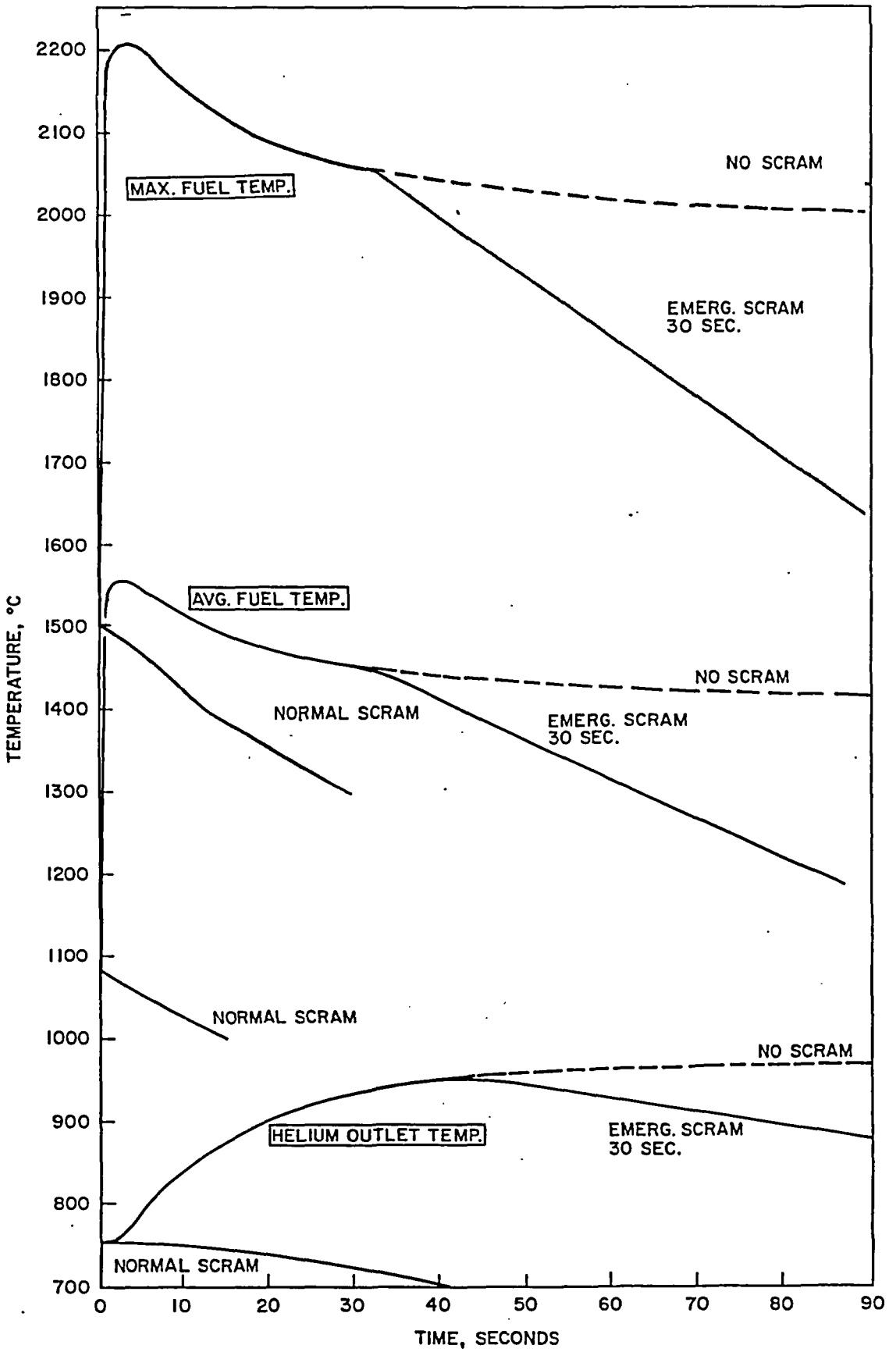

FUEL COMPACT AND HELIUM OUTLET TEMPERATURES FOLLOWING 1.0g ROD FALL (WORTH 0.01Δk); NORMAL OPERATING POWER: END OF LIFE: XENON PRESENT. NORMAL SCRAM AT 140% NORMAL POWER

FIGURE 132

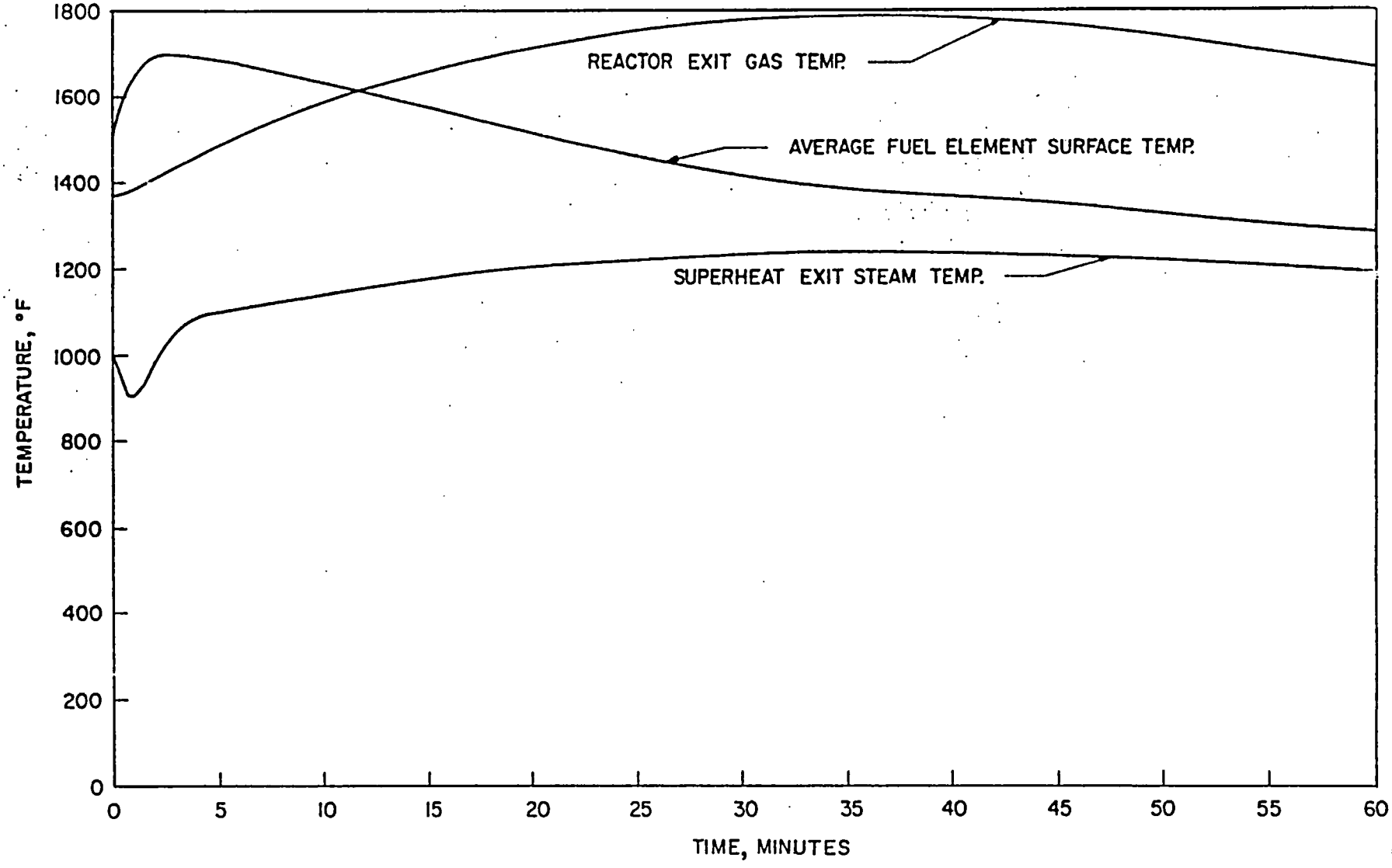

STEAM, COOLANT, AND FUEL TEMPERATURES FOLLOWING INSTANTANEOUS LOSS OF PRESSURE AND ONE HELIUM LOOP ACCOMPANIED BY SCRAM: COOLING WITH THE REMAINING LOOP.

FIGURE 133

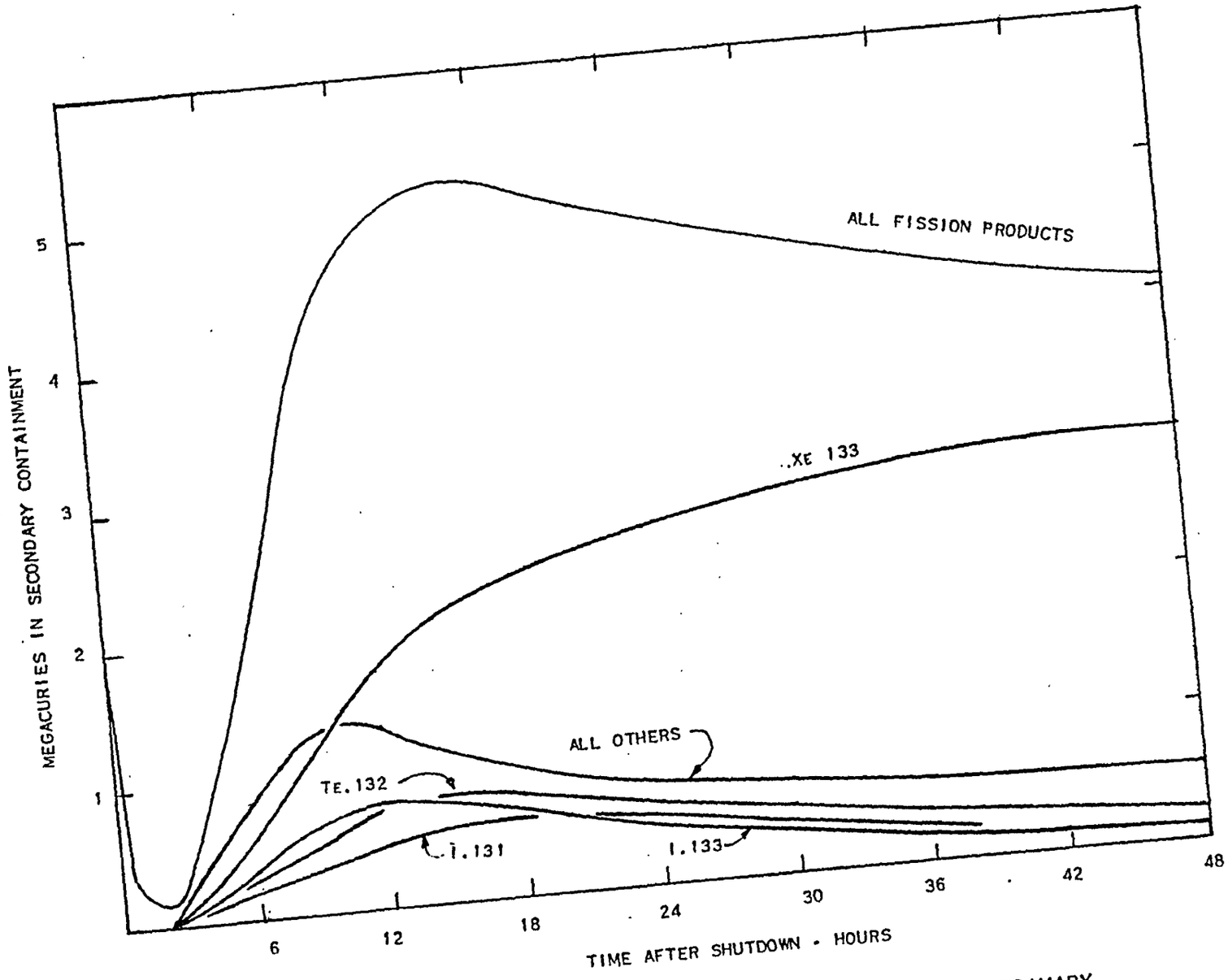

ACTIVITY IN CONTAINMENT DURING EMERGENCY COOLING WITH PRIMARY SYSTEM RUPTURE AND BACKFLOW FROM FIRST THREE FISSION PRODUCT TRAPS

FIGURE 134

August, 1961

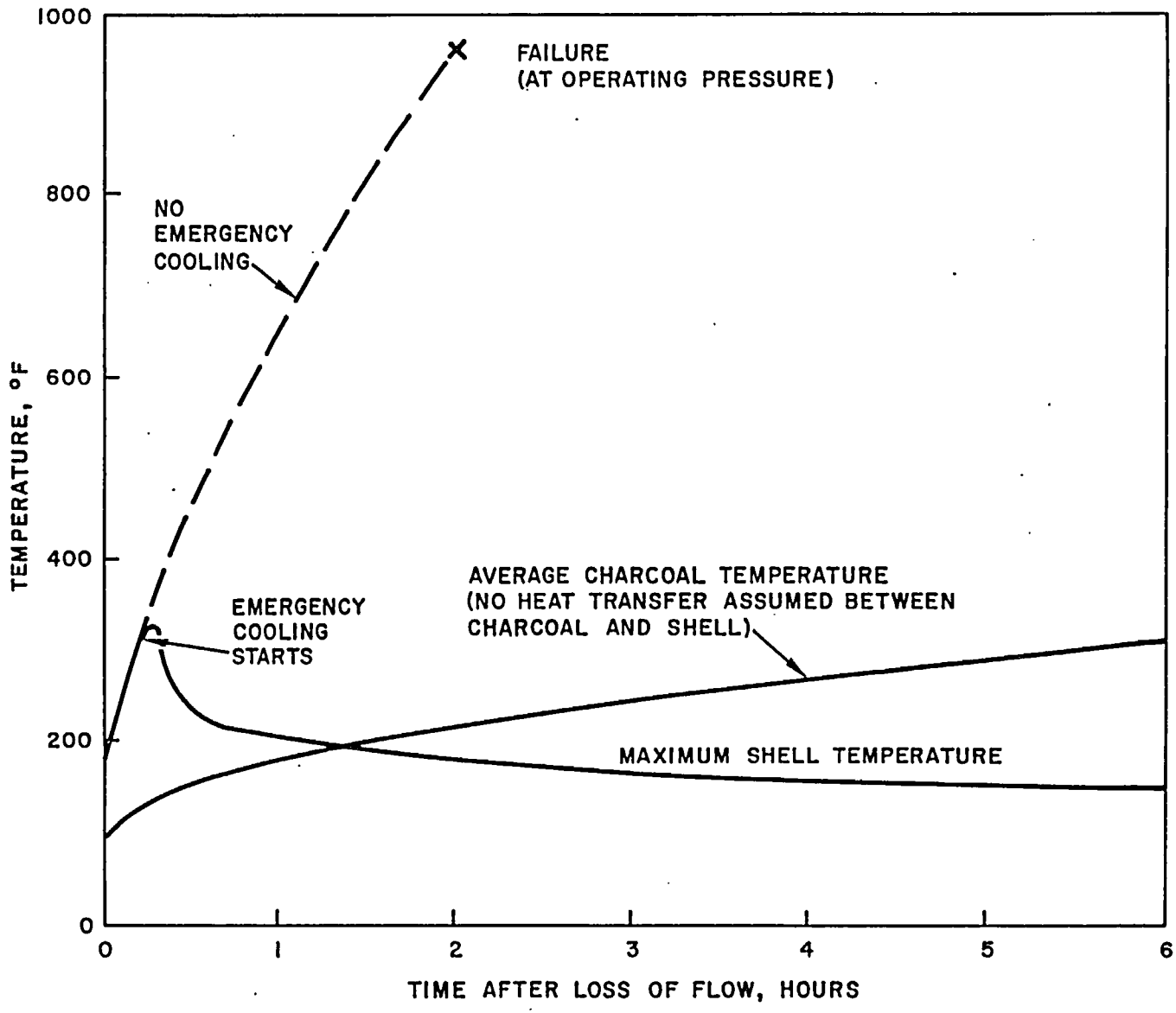

TEMPERATURE RISE IN DELAY BED A-302 FOLLOWING
COMPLETE LOSS OF PURGE FLOW AT TIME = 0

FIGURE 135

August, 1961

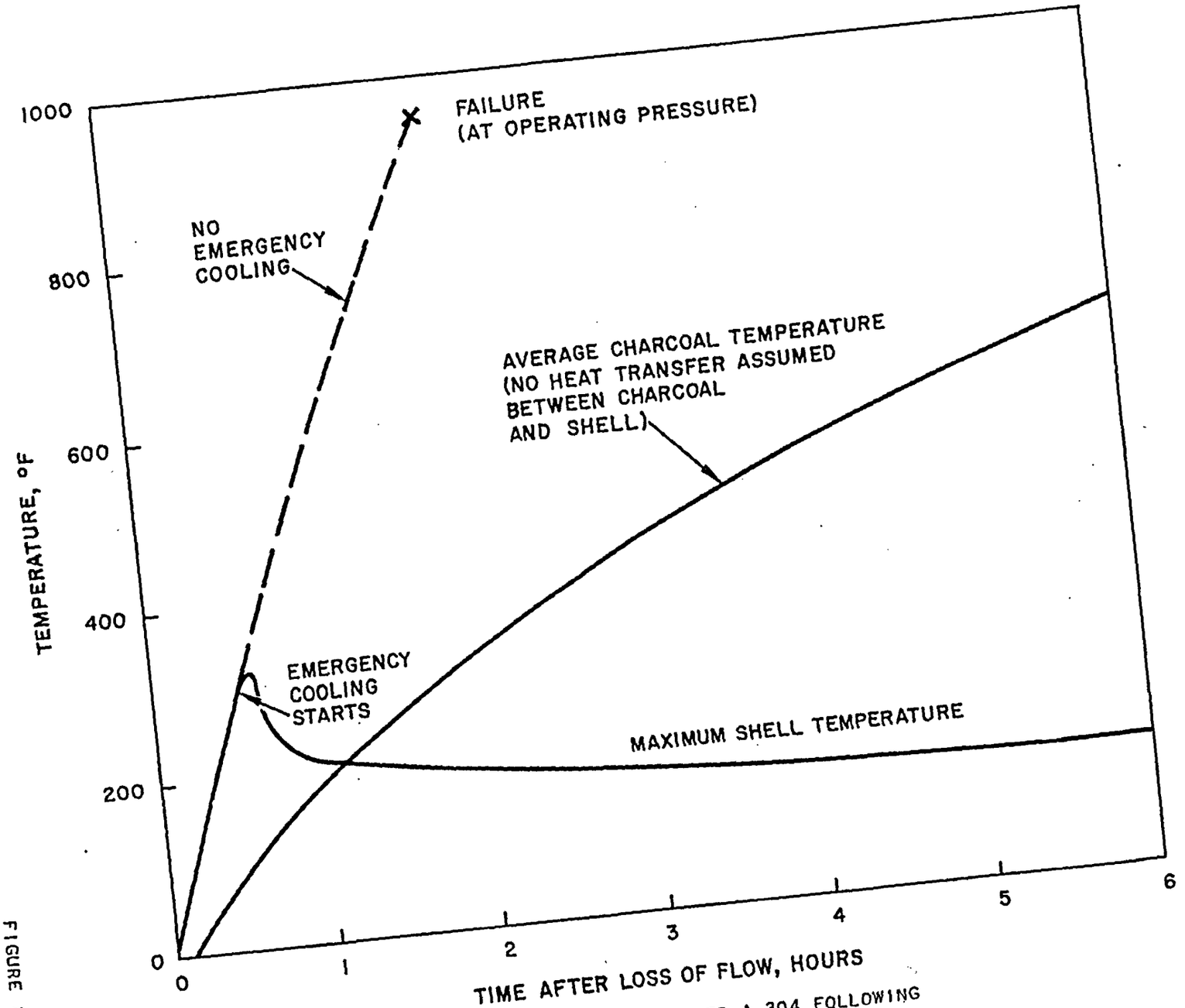

TEMPERATURE RISE IN DELAY BED A-304 FOLLOWING
COMPLETE LOSS OF PURGE FLOW AT TIME = 0

FIGURE 136

August, 1961

APPENDIX B - RADIOACTIVE INVENTORIES

I - HTGR System Activities

This section presents inventories of fission products in the fuel, internal traps, and main coolant.

This includes those fission product isotopes which:

(1) Have half lives greater than 1 minute but less than 10^4 years (33-second Krypton-90, 41-second Xenon-139 and 16-second Xenon-140 are included because they are significant heat producers in the external trap).

(2) Have fission yields greater than 0.1 percent.

TABLE B - 1 Design Activity in Fuel

Fission product inventory in the fuel elements during normal operating conditions is shown assuming the hypothetical design basis of 100 percent retention of the fission products and continuous operation of the plant at 100 percent load factor for 2.4 years, the full core burnup.

TABLE B - 2 Design Activity in Internal Traps

Design activity in internal fission product traps assuming:

(1) Continuous operation of the plant for 2.4 years at 100 percent load factor.

(2) Steady-state experimental release data from uncoated particle fuel bodies, with a factor of 3 applied for conservatism.

TABLE B - 3 Gaseous Activities in the Primary Coolant

a. Calculated Beginning of Life Activity (Calculated BOL)
The activities listed in this column are based on release data from coated fuel particle compacts after burnup equivalent to 50% of fuel element life. All fuel elements are assumed to be operating normally.

b. Design Activity
The activities listed in this column, except for krypton-85, are 20 times the calculated activities based on uncoated fuel particle compacts, or approximately 50 times the Calculated Beginning.

of Life activities based on coated fuel particle compacts. The external traps are specially designed to hold the krypton-85 activity in the coolant to a maximum of 50 curies. The total activity, 4224.6 curies, is designated as the primary system Design Activity, and is the basis for the primary system shielding. The plant may be permitted to operate for periods of some months with this inventory.

c. Maximum Annually Averaged Activity

This activity is the maximum activity averaged over a 12-month period that is expected in the primary system. This level is 1800 curies. Except for krypton-85, the activities of the individual isotopes are in the same proportion as in the Design Activity.

d. Gaseous Activities in the Primary Coolant With Failed Fuel Element Sleeves

To calculate gaseous activity in the primary system with failed fuel elements use the Calculated Beginning of Life Activities (without burst fuel elements) in Table B-3 but multiply all activities except krypton-85 by the following factors for each completely failed fuel element sleeve:

No. of Burst Fuel Elements	Multiplication Factor
0	1.0
1	7.5
2	14.0
3	20.5
Each Additional	Add 6.5

Primary coolant activity of krypton-85 builds up to approximately 25 curies from recycled gas returning from the external traps and is not subject to the multiplication factors above. Design krypton-85 activity is 50 curies.

I. HTGR SYSTEM ACTIVITIES (Cont'd.)

Isotope	TABLE B-1 Activity in Fuel (megacuries)	TABLE B-2 (Sheet 1 of 5) Activity in Internal Traps (megacuries)	TABLE B-3 Coolant Gaseous Activity (curies) Calc. BOL	Design
Se^{81}	0.15	.006	0.12	6.2
Se^{83m}	0.33	.003	-	0.2
Se^{83}	0.23	.012	0.13	6.6
Br^{83}	0.56	.054	0.29	14.6
Kr^{83m}	0.56	-	0.35	17.4
Se^{84}	1.02	.018	0.14	6.8
Br^{84}	1.02	.054	0.72	35.8
Br^{85}	1.35	.024	0.16	8.0
Kr^{85m}	1.35	-	0.53	26.4
Kr^{85}	0.04	-	25.	50.
Kr^{87}	2.59	-	1.40	69.8
Kr^{88}	3.72	-	2.00	100.0
Rb^{88}	3.72	.156	4.00	200.0
Kr^{89}	4.56	-	0.67	33.6
Rb^{89}	4.98	.195	3.83	191.4
Sr^{89}	5.00	4.38	0.03	1.6
Kr^{90}	5.20	-	-	-
Rb^{90}	6.00	.108	0.63	31.6
Sr^{90}	0.33	.33	-	-
Y^{90}	0.33	.33	-	-
Kr^{91}	3.50	-	-	-
Rb^{91}	5.68	.069	0.07	3.4
Sr^{91}	6.05	1.16	1.45	72.4
Y^{91m}	3.63	.696	0.98	48.8
Y^{91}	6.06	1.16	0.01	0.2

I. HTGR SYSTEM ACTIVITIES (Cont'd.)

Isotope	TABLE B-1 Activity in Fuel (megacuries)	TABLE B-2 (Sheet 2 of 5) Activity in Internal Traps (megacuries)	TABLE B-3 Coolant Gaseous Activity (curies) Calculated Design	Design
Sr^{92}	6.27	.657	2.31	115.4
Y^{92}	6.27	.657	1.16	58.0
Sr^{93}	6.60	.198	2.45	122.4
Y^{93}	6.70	.198	0.32	16.2
Sr^{94}	6.13	.054	0.10	5.2
Y^{94}	6.65	.054	0.13	6.6
Zr^{95}	6.45	---	---	---
Nb^{95}	6.45	---	---	---
Zr^{97}	6.14	---	---	---
Nb^{97m}	6.14	---	---	---
Zr^{98}	5.94	---	---	---
Zr^{99}	6.25	---	---	---
Nb^{99}	6.25	---	---	---
Mo^{99}	6.31	---	---	---
Nb^{100}	6.55	---	---	---
Nb^{101}	5.73	---	---	---
Mo^{101}	5.83	---	---	---
Tc^{101}	5.20	---	---	---
Mo^{102}	4.48	---	---	---
Tc^{102}	4.48	---	---	---
Tc^{103}	3.12	---	---	---
Ru^{103}	3.12	---	---	---
Tc^{104}	1.87	---	---	---
Tc^{105}	0.94	---	---	---
Ru^{105}	0.94	---	---	---
Rh^{105}	0.94	---	---	---

I. HTGR SYSTEM ACTIVITIES (Cont'd.)

Isotope	TABLE B-1 Activity In Fuel (megacuries)	TABLE B-2 (Sheet 3 of 5) Activity in Internal Traps (megacuries)	TABLE B-3 Coolant Gaseous Activity (curies) Calc. BOL	Design
Ru^{106}	0.40	---	---	---
Rh^{106}	0.40	---	---	---
Ru^{107}	0.10	---	---	---
Rh^{107}	0.20	---	---	---
Sb^{127}	0.17	.066	0.01	0.4
Te^{127m}	0.04	.040	---	---
Te^{127}	0.17	.081	0.01	0.4
Sn^{128}	0.39	---	---	---
Sb^{128m}	0.37	0.009	0.30	15.2
Sb^{129}	0.83	0.117	0.34	17.2
T^{129m}	0.30	0.261	0.01	0.2
Te^{129}	0.83	0.150	0.36	17.8
Sn^{130}	2.08	---	---	---
Sb^{130}	2.08	0.051	1.71	85.6
Sn^{131}	2.70	---	---	---
Sb^{131}	2.70	0.120	1.55	77.6
Te^{131m}	0.46	0.141	0.06	2.8
Te^{131}	2.68	0.231	2.49	124.2
I^{131}	3.05	1.96	0.07	3.4
Xe^{131m}	0.02	---	0.01	0.2
Sn^{132}	2.91	---	---	---
Sb^{132}	2.91	0.045	0.30	15.0
Te^{132}	4.56	1.68	0.29	14.4
I^{132}	4.56	2.13	0.46	22.8
Sb^{133}	4.16	0.087	0.81	40.4

I. HTGR SYSTEM ACTIVITIES (Cont'd.)

Isotope	TABLE B-1 Activity in Fuel (Megacuries)	TABLE B-2 Activity in Internal Traps (megacuries)	TABLE B-3 Coolant Gaseous Activity (curies) Calc. BOL	Design
	(Sheet 4 of 5)			
Te^{133m}	5.10	0.399	3.49	174.6
Te^{133}	1.83	0.051	4.88	244.0
I^{133}	6.85	2.19	1.14	57.0
Xe^{133m}	0.17	---	0.01	0.2
Xe^{133}	6.85	---	0.07	3.4
Te^{134}	7.18	0.432	4.16	208.0
I^{134}	8.39	0.978	6.68	334.0
I^{135}	6.35	0.954	1.77	88.2
Xe^{135m}	1.90	---	1.33	66.2
Xe^{135}	1.38	---	1.11	55.6
I^{136}	3.12	0.027	0.08	4.0
Xe^{137}	6.25	---	1.21	60.2
Cs^{137}	0.49	0.49	---	---
Ba^{137m}	0.49	0.49	---	---
Xe^{138}	5.67	---	3.00	150.0
Cs^{138}	5.97	0.360	5.44	272.0
Xe^{139}	5.50	---	---	---
Cs^{139}	6.75	0.204	2.78	138.0
Ba^{139}	6.81	0.570	4.88	244.0
Xe^{140}	3.95	---	---	---
Cs^{140}	6.24	0.057	0.06	3.2
Ba^{140}	6.70	3.87	0.15	7.4
La^{140}	6.70	3.87	0.01	0.4
Ba^{141}	6.55	0.276	3.52	176.0
La^{141}	6.66	0.276	0.90	44.8

I. HTGR SYSTEM ACTIVITIES (cont'd)

Isotope	TABLE B-1 Activity in Fuel (megacuries)	TABLE B-2 Activity in Internal Traps (megacuries)	TABLE B-3 Coolant Gaseous Activity (curies) Calc. BOL	Design
	(Sheet 5 of 5)			
Ce^{141}	6.65	0.276	0.01	0.4
Ba^{142}	6.14	0.204	2.78	139.2
La^{142}	6.25	0.204	1.34	67.0
Ce^{143}	6.15	---	---	---
Pr^{143}	6.20	---	---	---
Ce^{144}	5.55	---	---	---
Ce^{145}	4.15	---	---	---
Pr^{145}	4.15	---	---	---
Ce^{146}	3.20	---	---	---
Pr^{146}	3.20	---	---	---
Ce^{147}	2.80	---	---	---
Pr^{147}	2.80	---	---	---
Nd^{147}	2.80	---	---	---
Pm^{147}	1.30	---	---	---
Pr^{148}	1.78	---	---	---
Pm^{149}	1.1	---	---	---
Pm^{151}	0.46	---	---	---
Sm^{151}	0.01	---	---	---
Sm^{153}	0.18	.006	.01	0.6
TOTALS	427.50	33.926	108.57	4224.6

APPENDIX B - RADIOACTIVE INVENTORIES (Cont'd)

II - Activities and Decay Heat Loads in External Fission Product Traps

Distributions of fission product activities and decay heat loads in the external fission product trapping system have been calculated for both Design Activities and Calculated Beginning of Life Activities. The Design Activities in each trap are given in Table B - 4, with the corresponding decay heat loads in Table B - 5. Calculated Beginning of Life Activities and the corresponding decay heat loads are given in Tables B - 6 and B - 7, respectively. Trap designations in these tables are given in Figure 56. Activities not shown in the tables are less than 1 curie, and decay heat loads not shown are less than 1 Btu/hr.

Design Activities are based on fission product release data from uncoated fuel, increased by a safety factor of 3. The internal traps were assumed to give a 7-day holdup of iodine and bromine (compared to the experimentally indicated value of 32 days) but no holdup of krypton and xenon, and to completely retain all other fission products. Calculated Beginning of Life Activities are based on recent fission product release data from in-pile tests of coated-particle fuel. Internal trap performance was assumed the same as in the design case, except that the iodine-bromine holdup was taken as 32 days, as indicated by experiments. The experimental data referred to here are presented in Section II.J. 2.

In calculating the buildup of long-lived isotopes, the operating life for the liquid-nitrogen-cooled trap A-309 (until regenerated or removed) was taken as 6 months. All other traps were assumed to operate for 30 years. Delay of krypton and xenon in the condensibles trap A-301 was assumed zero.

II. ACTIVITIES AND DECAY HEAT LOADS IN EXTERNAL FISSION PRODUCT TRAPS (Cont'd

TABLE B-5 (Sheet 1 of 3)

Decay Heat Loads in External Fission Product Traps Based on Design Activities

	Trap A-301		Trap A-302		Trap A-303	
Isotope	β(Btu/hr)	γ(Btu/hr)	β(Btu/hr)	γ(Btu/hr)	β(Btu/hr)	γ(Btu/hr)
Kr^{83m}	-	-	5	-	7	-
Kr^{85m}	-	-	22	14	34	22
Kr^{85}	-	-	-	-	-	-
Kr^{87}	-	-	379	303	560	447
Kr^{88}	-	-	96	492	147	752
Rb^{88}	-	-	499	259	763	396
Kr^{89}	-	-	1810	3070	587	999
Rb^{89}	-	-	768	3110	250	1010
Sr^{89}	-	-	704	-	229	-
Kr^{90}	-	-	672	-	-	-
Rb^{90}	-	-	340	2630	-	1
Sr^{90}	-	-	40	-	-	-
Y^{90}	-	-	200	-	-	-
I^{131}	3680	7760	-	-	-	-
Xe^{131m}	-	-	-	-	-	-
I^{133}	79	90	-	-	-	-
Xe^{133m}	-	-	6	1	12	2
Xe^{133}	-	-	103	19	208	38
Xe^{135m}	-	-	525	3260	14	87
Xe^{135}	-	-	1410	1070	2450	1860
Xe^{137}	-	-	2630	3240	-	-
Cs^{137}	-	-	210	-	-	-
Ba^{137m}	-	-	70	590	-	-
Xe^{138}	-	-	2810	7610	109	296
Cs^{138}	-	-	5190	10500	202	407
Xe^{139}	-	-	1240	-	-	-
Cs^{139}	-	-	1090	555	-	-
Ba^{139}	-	-	555	277	-	-
Xe^{140}	-	-	236	-	-	-
Cs^{140}	-	-	353	254	-	-
Ba^{140}	-	-	52	34	-	-
La^{140}	-	-	92	444	-	-
TOTALS	3759	7850	22107	37732	5572	6317

ACTIVITIES AND DECAY HEAT LOADS IN EXTERNAL FISSION PRODUCT TRAPS (Cont'd.)

TABLE B-5 (Sheet 2 of 3)

Decay Heat Loads in External Fission Product Traps Based on Design Activities

	Trap A-304		Trap A-305		Trap A-306	
Isotope	β(Btu/hr)	γ(Btu/hr)	β(Btu/hr)	γ(Btu/hr)	β(Btu/hr)	γ(Btu/hr)
Kr^{83m}	84	2	37	1	3	-
Kr^{85m}	516	330	558	357	235	151
Kr^{85}	-	-	1	-	2	-
Kr^{87}	5120	4080	1230	979	31	25
Kr^{88}	1940	9960	1420	7280	293	1500
Rb^{88}	10100	5250	7390	3840	1530	792
Kr^{89}	86	147	-	-	-	-
Rb^{89}	37	149	-	-	-	-
Sr^{89}	34	-	-	-	-	-
Kr^{90}	-	-	-	-	-	-
Rb^{90}	-	-	-	-	-	-
Sr^{90}	-	-	-	-	-	-
Y^{90}	-	-	-	-	-	-
I^{131}	-	-	-	-	-	-
Xe^{131m}	34	2	37	2	5	-
I^{133}	-	-	-	-	-	-
Xe^{133m}	330	61	15	3	-	-
Xe^{133}	10700	1930	4120	747	42	8
Xe^{135m}	-	-	-	-	-	-
Xe^{135}	10700	8130	-	-	-	-
Xe^{137}	-	-	-	-	-	-
Cs^{137}	-	-	-	-	-	-
Ba^{137m}	-	-	-	-	-	-
Xe^{138}	-	-	-	-	-	-
Cs^{138}	-	-	-	-	-	-
Xe^{139}	-	-	-	-	-	-
Cs^{139}	-	-	-	-	-	-
Ba^{139}	-	-	-	-	-	-
Xe^{140}	-	-	-	-	-	-
Cs^{140}	-	-	-	-	-	-
Ba^{140}	-	-	-	-	-	-
La^{140}	-	-	-	-	-	-
TOTALS	39681	30041	14808	13209	2141	2476

ACTIVITIES AND DECAY HEAT LOADS IN EXTERNAL FISSION PRODUCT TRAPS (Cont'd.)

TABLE B-5 (Sheet 3 of 3)

Decay Heat Loads in External Fission Product Traps Based on Design Activities

	Trap A-307		Trap A-308		Trap A-309	
Isotope	β (Btu/hr)	γ (Btu/hr)	β (Btu/hr)	γ (Btu/hr)	β (Btu/hr)	γ (Btu/hr)
Kr^{83m}	-	-	-	-	-	-
Kr^{85m}	46	29	-	-	-	-
Kr^{85}	11	-	11	-	67	1
Kr^{87}	-	-	-	-	-	-
Kr^{88}	18	92	-	-	-	-
Rb^{88}	93	48	-	-	-	-
Kr^{89}	-	-	-	-	-	-
Rb^{89}	-	-	-	-	-	-
Sr^{89}	-	-	-	-	-	-
Kr^{90}	-	-	-	-	-	-
Rb^{90}	-	-	-	-	-	-
Sr^{90}	-	-	-	-	-	-
Y^{90}	-	-	-	-	-	-
I^{131}	-	-	-	-	-	-
Xe^{131m}	-	-	-	-	-	-
I^{133}	-	-	-	-	-	-
Xe^{133m}	-	-	-	-	-	-
Xe^{133}	-	-	-	-	-	-
Xe^{135m}	-	-	-	-	-	-
Xe^{135}	-	-	-	-	-	-
Xe^{137}	-	-	-	-	-	-
Cs^{137}	-	-	-	-	-	-
Ba^{137m}	-	-	-	-	-	-
Xe^{138}	-	-	-	-	-	-
Cs^{138}	-	-	-	-	-	-
Xe^{139}	-	-	-	-	-	-
Cs^{139}	-	-	-	-	-	-
Ba^{139}	-	-	-	-	-	-
Xe^{140}	-	-	-	-	-	-
Cs^{140}	-	-	-	-	-	-
Ba^{140}	-	-	-	-	-	-
La^{140}	-	-	-	-	-	-
TOTALS	168	169	11	0	67	1

II. ACTIVITIES AND DECAY HEAT LOADS IN EXTERNAL FISSION PRODUCT TRAPS (Cont'd.)

TABLE B-6

Calculated Beginning of Life Activities in External Fission Product Traps

Isotope	Trap A-301 (curies)	Trap A-302 (curies)	Trap A-303 (curies)	Trap A-304 (curies)	Trap A-305 (curies)	Trap A-306 (curies)	Trap A-307 (curies)	Trap A-308 (curies)	Trap A-309 (curies
Kr^{83m}	-	1,320	1,490	18,300	1,480	15	-	-	-
Kr^{85m}	-	933	1,100	23,400	10,100	1,480	186	-	-
Kr^{85}	-	4	6	160	300	340	2,270	2,350	13,900
Kr^{87}	-	2,880	3,170	28,100	704	-	-	-	-
Kr^{88}	-	2,530	2,930	48,600	10,100	474	16	-	-
Rb^{88}	-	2,530	2,930	48,600	10,100	474	16	-	-
Kr^{89}	-	9,860	1,270	109	-	-	-	-	-
Rb^{89}	-	9,860	1,270	109	-	-	-	-	-
Sr^{89}	-	9,860	1,270	109	-	-	-	-	-
Kr^{90}	-	3,330	-	-	-	-	-	-	-
Rb^{90}	-	3,330	-	-	-	-	-	-	-
Sr^{90}	-	1,500	-	-	-	-	-	-	-
Y^{90}	-	1,500	-	-	-	-	-	-	-
I^{131}	15,000	-	-	-	-	-	-	-	-
Xe^{131m}	-	21	28	2,750	360	2	-	-	-
Xe^{133m}	-	442	572	11,700	-	-	-	-	-
Xe^{133}	-	9,100	12,100	610,000	6,410	-	-	-	-
Xe^{135m}	-	47,800	23	-	-	-	-	-	-
Xe^{135}	-	52,600	55,300	166,000	-	-	-	-	-
Xe^{137}	-	17,400	-	-	-	-	-	-	-
Cs^{137}	-	7,400	-	-	-	-	-	-	-
Ba^{137m}	-	6,830	-	-	-	-	-	-	-
Xe^{138}	-	33,100	34	-	-	-	-	-	-
Cs^{138}	-	33,100	34	-	-	-	-	-	-
Xe^{139}	-	4,790	-	-	-	-	-	-	-
Cs^{139}	-	4,790	-	-	-	-	-	-	-
Ba^{139}	-	4,790	-	-	-	-	-	-	-
Xe^{140}	-	1,190	-	-	-	-	-	-	-
Cs^{140}	-	1,190	-	-	-	-	-	-	-
Ba^{140}	-	1,190	-	-	-	-	-	-	-
La^{140}	-	1,190	-	-	-	-	-	-	-
TOTALS	15,000	276,360	83,527	957,937	39,554	2,785	2,318	2,350	13,900

II. ACTIVITIES AND DECAY HEAT LOADS IN EXTERNAL FISSION PRODUCT TRAPS (Cont'd.)

TABLE B-7 (Sheet 1 of 3)

Decay Heat Loads in External Fission Product Traps Based on Calculated Beginning of Life Activities

	Trap A-301		Trap A-302		Trap A-303	
Isotope	β(Btu/hr)	γ(Btu/hr)	β(Btu/hr)	γ(Btu/hr)	β(Btu/hr)	γ(Btu/hr)
Kr^{83m}	-	-	1	-	1	-
Kr^{85m}	-	-	5	3	5	4
Kr^{85}	-	-	-	-	-	-
Kr^{87}	-	-	78	62	86	68
Kr^{88}	-	-	21	105	24	121
Rb^{88}	-	-	110	55	125	64
Kr^{89}	-	-	282	477	36	61
Rb^{89}	-	-	120	484	15	62
Sr^{89}	-	-	110	-	14	-
Kr^{90}	-	-	93	-	-	-
Rb^{90}	-	-	47	363	-	-
Sr^{90}	-	-	7	-	-	-
Y^{90}	-	-	32	-	-	-
I^{131}	57	121	-	-	-	-
Xe^{131m}	-	-	-	-	-	-
Xe^{133m}	-	-	2	-	2	-
Xe^{133}	-	-	30	5	39	7
Xe^{135m}	-	-	71	444	-	-
Xe^{135}	-	-	350	266	368	280
Xe^{137}	-	-	349	430	-	-
Cs^{137}	-	-	28	-	-	-
Ba^{137m}	-	-	9	78	-	-
Xe^{138}	-	-	387	1050	-	1
Cs^{138}	-	-	715	1450	1	1
Xe^{139}	-	-	165	-	-	-
Cs^{139}	-	-	145	74	-	-
Ba^{139}	-	-	74	37	-	-
Xe^{140}	-	-	31	-	-	-
Cs^{140}	-	-	47	34	-	-
Ba^{140}	-	-	7	5	-	-
La^{140}	-	-	12	59	-	-
TOTALS	57	121	3328	5481	716	669

II. ACTIVITIES AND DECAY HEAT LOADS IN EXTERNAL FISSION PRODUCT TRAPS (Cont'd.)

TABLE B-7 (Sheet 2 of 3)

Decay Heat Loads in External Fission Product Traps Based on Calculated Beginning of Life Activities

	Trap A-304		Trap A-305		Trap A-306	
Isotope	β(Btu/hr)	γ(Btu/hr)	β(Btu/hr)	γ(Btu/hr)	β(Btu/hr)	γ(Btu/hr)
Kr^{83m}	15	-	1	-	-	-
Kr^{85m}	118	76	51	33	7	5
Kr^{85}	-	-	1	-	2	-
Kr^{87}	762	607	19	15	-	-
Kr^{88}	393	2010	81	417	4	20
Rb^{88}	2050	1060	422	220	21	11
Kr^{89}	3	5	-	-	-	-
Rb^{89}	1	5	-	-	-	-
Sr^{89}	1	-	-	-	-	-
Kr^{90}	-	-	-	-	-	-
Rb^{90}	-	-	-	-	-	-
Sr^{90}	-	-	-	-	-	-
Y^{90}	-	-	-	-	-	-
I^{131}	-	-	-	-	-	-
Xe^{131m}	9	1	1	-	-	-
Xe^{133m}	48	9	-	-	-	-
Xe^{133}	1980	357	21	4	-	-
Xe^{135m}	-	-	-	-	-	-
Xe^{135}	1100	838	-	-	-	-
Xe^{137}	-	-	-	-	-	-
Cs^{137}	-	-	-	-	-	-
Ba^{137m}	-	-	-	-	-	-
Xe^{138}	-	-	-	-	-	-
Cs^{138}	-	-	-	-	-	-
Xe^{139}	-	-	-	-	-	-
Cs^{139}	-	-	-	-	-	-
Ba^{139}	-	-	-	-	-	-
Xe^{140}	-	-	-	-	-	-
Cs^{140}	-	-	-	-	-	-
Ba^{140}	-	-	-	-	-	-
La^{140}	-	-	-	-	-	-
TOTALS	6480	4968	597	689	34	36

II. ACTIVITIES AND DECAY HEAT LOADS IN EXTERNAL FISSION PRODUCT TRAPS (Cont'd.)

TABLE B-7 (Sheet 3 of 3)

Decay Heat Loads in External Fission Product Traps Based on Calculated Beginning of Life Activities

	Trap A-307		Trap A-308		Trap A-309	
Isotope	β(Btu/hr)	γ(Btu/hr)	β(Btu/hr)	γ(Btu/hr)	β(Btu/hr)	γ(Btu/hr)
Kr^{83m}	-	-	-	-	-	-
Kr^{85m}	1	1	-	-	-	-
Kr^{85}	11	-	11	-	67	1
Kr^{87}	-	-	-	-	-	-
Kr^{88}	-	-	-	-	-	-
Rb^{88}	-	-	-	-	-	-
Kr^{89}	-	-	-	-	-	-
Rb^{89}	-	-	-	-	-	-
Sr^{89}	-	-	-	-	-	-
Kr^{90}	-	-	-	-	-	-
Rb^{90}	-	-	-	-	-	-
Sr^{90}	-	-	-	-	-	-
Y^{90}	-	-	-	-	-	-
I^{131}	-	-	-	-	-	-
Xe^{131m}	-	-	-	-	-	-
Xe^{133m}	-	-	-	-	-	-
Xe^{133}	-	-	-	-	-	-
Xe^{135m}	-	-	-	-	-	-
Xe^{135}	-	-	-	-	-	-
Xe^{137}	-	-	-	-	-	-
Cs^{137}	-	-	-	-	-	-
Ba^{137m}	-	-	-	-	-	-
Xe^{138}	-	-	-	-	-	-
Cs^{138}	-	-	-	-	-	-
Xe^{139}	-	-	-	-	-	-
Cs^{139}	-	-	-	-	-	-
Ba^{139}	-	-	-	-	-	-
Xe^{140}	-	-	-	-	-	-
Cs^{140}	-	-	-	-	-	-
Ba^{140}	-	-	-	-	-	-
La^{140}	-	-	-	-	-	-
TOTALS	12	1	11	0	67	1

APPENDIX B - RADIOACTIVE INVENTORIES (Cont'd)

III - FISSION PRODUCTS RELEASED TO THE PLANT CONTAINER AFTER A PRIMARY SYSTEM DUCT RUPTURE

The activities released to the plant container after a primary system duct rupture are given in Table B - 8 for the two cases below.

Purge Line Check Valve Operates

Activities include:

1. Design Primary System Activity.
2. Fission product evolution from the fuel to the purge stream during blowdown.
3. Internal trapping system desorption during blowdown.

Purge Line Check Valve Fails to Operate

Activities include:

1. Design Primary System Activity.
2. Fission product evolution from the fuel to the purge stream during blowdown.
3. Desorption from internal trapping system and first three external traps (A-301, A-302, A-303). Further blowdown is prevented by closure of the check valve and stop valves between A-303 and A-304 during blowdown.

Additional Assumptions:

1. The purge system is assumed to resume operation at the end of the blowdown period. Reverse flow occurs only during the blowdown period.
2. The non-volatile daughter products La, Y and Ce are assumed to remain in the traps.
3. Blowdown occurs over a 100-second period.

FISSION PRODUCTS RELEASED TO THE PLANT CONTAINER AFTER A PRIMARY SYSTEM DUCT RUPTURE

TABLE B-8 (Sheet 1 of 3)

Isotope	Half-life	Purge Line Check Valve Operates (Kilocuries)	Purge Line Check Valve Fails (Kilocuries)
Se^{81}	18m	.43	2.1
Se^{83m}	70s	1.59	2.7
Se^{83}	26m	.52	2.7
Br^{83}	2.3h	.61	3.0
Kr^{83m}	112m	.61	6.6
Se^{84}	3.3m	5.50	16.5
Br^{84}	31.8m	2.43	11.6
Br^{85}	3.0m	7.39	21.9
Kr^{85m}	4.4h	.81	4.8
Kr^{85}	10.3y	.05	.1
Kr^{87}	78m	3.19	18.3
Kr^{88}	2.8h	2.95	16.9
Rb^{88}	17.8m	11.95	53.9
Kr^{89}	3.2m	22.68	73.9
Rb^{89}	15.4m	15.97	75.3
Sr^{89}	50.4d	.06	.4
Kr^{90}	33s	10.17	13.4
Rb^{90}	2.7m	33.33	94.2
Sr^{90}	28y	-	-
Y^{90}	64.3h	-	-
Rb^{91}	68s	26.01	48.0
Sr^{91}	9.7h	2.50	13.4
Y^{91m}	51m	-	-
Y^{91}	58d	-	-
Sr^{92}	2.7h	5.63	30.0
Y^{92}	3.6h	-	-
Sr^{93}	8.2m	27.42	116.0
Y^{93}	10.2h	-	-
Sr^{94}	1.3m	30.10	53.6
Y^{94}	20m	-	-
Sb^{127}	88h	-	-
Te^{127m}	105d	-	.1

FISSION PRODUCTS RELEASED TO THE PLANT CONTAINER AFTER A PRIMARY SYSTEM DUCT RUPTURE (Cont'd)

TABLE B-8 (Sheet 2 of 3)

Isotope	Half-life	Purge Line Check Valve Operates (Kilocuries)	Purge Line Check Valve Fails (Kilocuries)
Te^{127}	9.35h	.06	.4
Sb^{128m}	10m	1.36	5.2
Sb^{129}	4.6h	.53	2.9
Te^{129m}	33d	-	-
Te^{129}	74m	1.13	6.0
Sb^{130}	7.1m	9.06	34.2
Sb^{131}	23.1m	7.01	34.8
Te^{131m}	29h	.09	.5
Te^{131}	24.8m	6.66	33.4
I^{131}	8.05d	.18	.9
Xe^{131m}	12d	-	-
Sb^{132}	2.1m	16.09	40.4
Te^{132}	77h	.49	2.6
I^{132}	2.33h	4.49	24.2
Sb^{133}	4.1m	21.58	72.4
Te^{133m}	53m	8.54	44.6
Te^{133}	2m	9.90	24.3
I^{133}	20.9h	1.77	8.2
Xe^{133m}	2.3d	.03	.1
Xe^{133}	5.27d	.45	2.7
Te^{134}	44m	13.08	68.3
I^{134}	54m	13.83	73.4
I^{135}	6.75h	3.30	17.6
Xe^{135m}	15.3m	5.56	112.4
Xe^{135}	9.13h	2.58	15.1
I^{136}	86s	16.47	28.8
Xe^{137}	3.9m	34.05	109.8
Cs^{137}	30y	-	-
Ba^{137m}	2.57m	-	-
Xe^{138}	17m	15.57	80.2
Cs^{138}	32.2m	13.32	66.2
Xe^{139}	41s	15.00	22.3

FISSION PRODUCTS RELEASED TO THE PLANT CONTAINER AFTER A PRIMARY SYSTEM DUCT RUPTURE (Cont'd)

TABLE B-8 (Sheet 3 of 3)

Isotope	Half-life	Purge Line Check Valve Operates (Kilocuries)	Purge Line Check Valve Fails (Kilocuries)
Cs^{139}	9.5m	25.49	111.5
Ba^{139}	82.9m	8.73	46.1
Xe^{140}	16s	2.19	3.8
Cs^{140}	66s	28.56	50.3
Ba^{140}	12.8d	.28	1.5
La^{140}	40.3h	-	-
Ba^{141}	18m	19.47	44.4
La^{141}	3.8h	-	-
Ce^{141}	32.5d	-	-
Ba^{142}	11m	22.40	100.4
La^{142}	81m	-	-
	TOTALS	541.	1969.3

August, 1961

APPENDIX C

CALCULATIONS OF CORE HEAT-UP FOLLOWING LOSS OF NORMAL COOLING

I SUMMARY

Calculations have been made to determine transient reactor temperatures following a loss of primary coolant circulation accident. It was assumed for the calculations that a complete loss of primary coolant was experienced, that the reactor was scrammed, and that the decay thermal energy was removed by the emergency cooling system. Where simplifying engineering assumptions were necessary, the assumptions made were intentionally conservative in order that the calculated results would be more severe than the actual physical case.

Calculations indicated that the maximum transient core temperature after a loss of coolant circulation accident would be in the neighborhood of 3600 F. This peak would occur at approximately 30 hours after scram. Although damage to the control rods and perhaps the core support plate due to overheating is expected, the emergency cooling system will permit eventual cooling of the reactor and will protect the reactor pressure vessel from the damaging temperatures.

II INTRODUCTION

In the unlikely event of a complete loss of coolant in both main loops the reactor would be scrammed. To protect against the possible damaging results of core overtemperature due to decay heat, an emergency cooling system is provided.

The emergency cooling system is shown in Figure 69. It consists of a cooling water tube bank which surrounds the pressure vessel. The mean cooling water temperature is 150 F. Heat flows from the pressure vessel to the tube bank by convection and radiation, predominantly the latter. For more discussion of this system design, see Section II.F.2 of this report.

III ANALYSIS

a. General Assumptions

The following general assumptions were made for all calculations:

1. A complete loss of coolant circulation accident has occurred.

2. Primary coolant circulation is not restarted.

3. The plant has been operating at a conservatively high thermal power of 124 MW for a three year period immediately prior to the accident.

4. The emergency cooling system provides external cooling to the reactor vessel and is the sole means of reactor heat removal.

5. All decay heat is produced in the core and in the internal traps.

b. Model Description

In solving for the post-accident reactor temperature history, a mathematical model was made by dividing the reactor into nodes. The material within any one node boundary was assumed to be of uniform temperature, and the thermal capacity of this material was placed at the strategically located node point.

As indicated in Figure C-1 the core was divided into 20 nodes starting with the vertical centerline as a reference. The nodes of the first core column are cylindrically shaped. Each succeeding core node column is composed of ring-shaped nodes. The top, inner side and bottom, reflector nodes and the core support plate nodes are similarly shaped. All properties and heat transfer rates were assumed to be symmetrical about the vertical centerline. Surface nodes of the top, bottom and side reflectors radiate independently to the respective opposing surfaces.

The node boundaries for the following reactor parts are not shown: outer side reflector, plenum shroud, core support plate, thermal shields, and pressure vessel. These node boundaries are

placed so as to lump half of the thermal capacitance of each partition at each of its two indicated node points.

The pressure vessel and thermal shields are broken into top, side, and bottom sections as heat was assumed to flow from the core along these three paths.

The treatment of heat flow downward from the core was conservative from the standpoint that it gave conservatively high core support plate temperatures. This was due to two assumptions:

1. Heat flow from the core support plate was assumed not to spread out over the total area of the bottom head but was restricted to a one-dimensional path straight down.

2. No credit was taken for the fin effect which the control rod nozzles would have in cooling the bottom pressure vessel head.

An internal heat source representing the appropriate fraction of total decay power was placed at each core and bottom reflector node point. The bottom reflector heat sources represent the decay power produced in the internal traps at the bottom of each fuel element.

c. Solution

A differential equation was written for each node. The solution of the reactor temperature history was obtained by integrating the 66 simultaneous differential equations (one equation per node) from 0 to 60 hours by use of a PACE operational analog computer. Initial conditions used for this integration are given in Figure C-1. These initial conditions represent normal operating temperatures for the HTGR reactor with single sleeve fuel elements.

IV RESULTS

Reactor temperatures for 20, 40 and 60 hours after scram are given in Figure C-2. Response curves for several strategically located ("key") nodes are given in Figures C-3, C-4, and C-5. The peak core temperature occurs at approximately 30 hours and equals 3600 F. It should be noted that post-accident temperatures of nodes on the surface of the top reflector and nodes above the top reflector were less than respective initial temperatures. For most other nodes the 40 hour temperatures were close to the maximum post-accident temperature. The percentage of core volume exceeding various temperature

levels is plotted versus time after shutdown in Figure C-6. The average core temperature versus time is given in Figure C-7.

Figures C-2 and C-5 show that the transient calculated temperature for the side of the pressure vessel near the core remains at a safe temperature (867 F) after the accident. As an additional safety factor, the reactor will be depressurized during emergency cooling to remove most of the membrane stress from the pressure vessel.

Based on these conservative calculations, the maximum calculated core support plate temperature of 1340 F is somewhat greater than the estimated safe temperature. This calculated peak temperature occurs at some time greater than 60 hours after the accident. It is expected that a more realistic calculation would indicate a considerably lower grid plate temperature. In addition, the use of heat conducting sleeves around the control rods is being considered to improve the heat transfer from the grid plate to the bottom of the vessel.

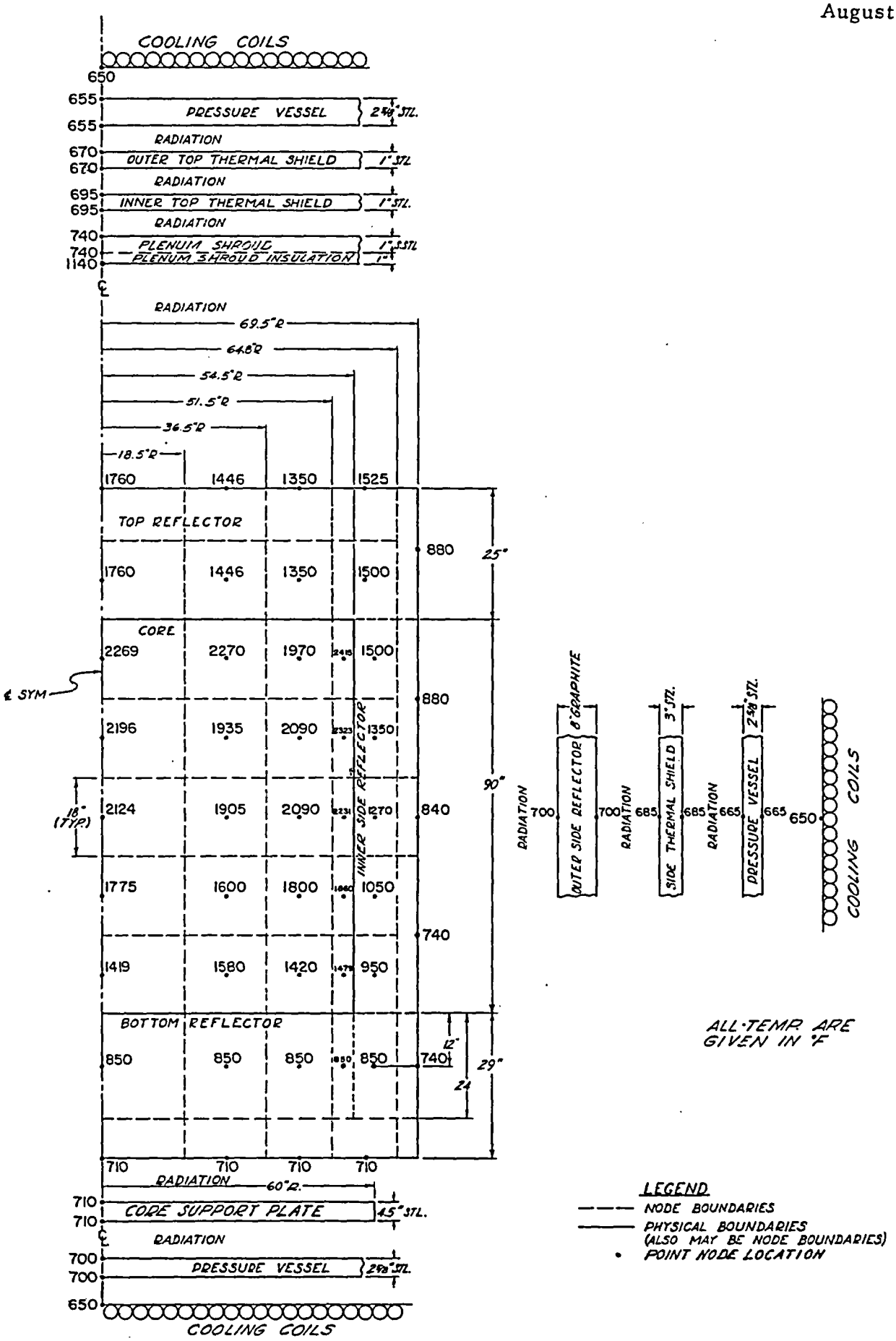

INITIAL REACTOR TEMPERATURES.

FIGURE C-1

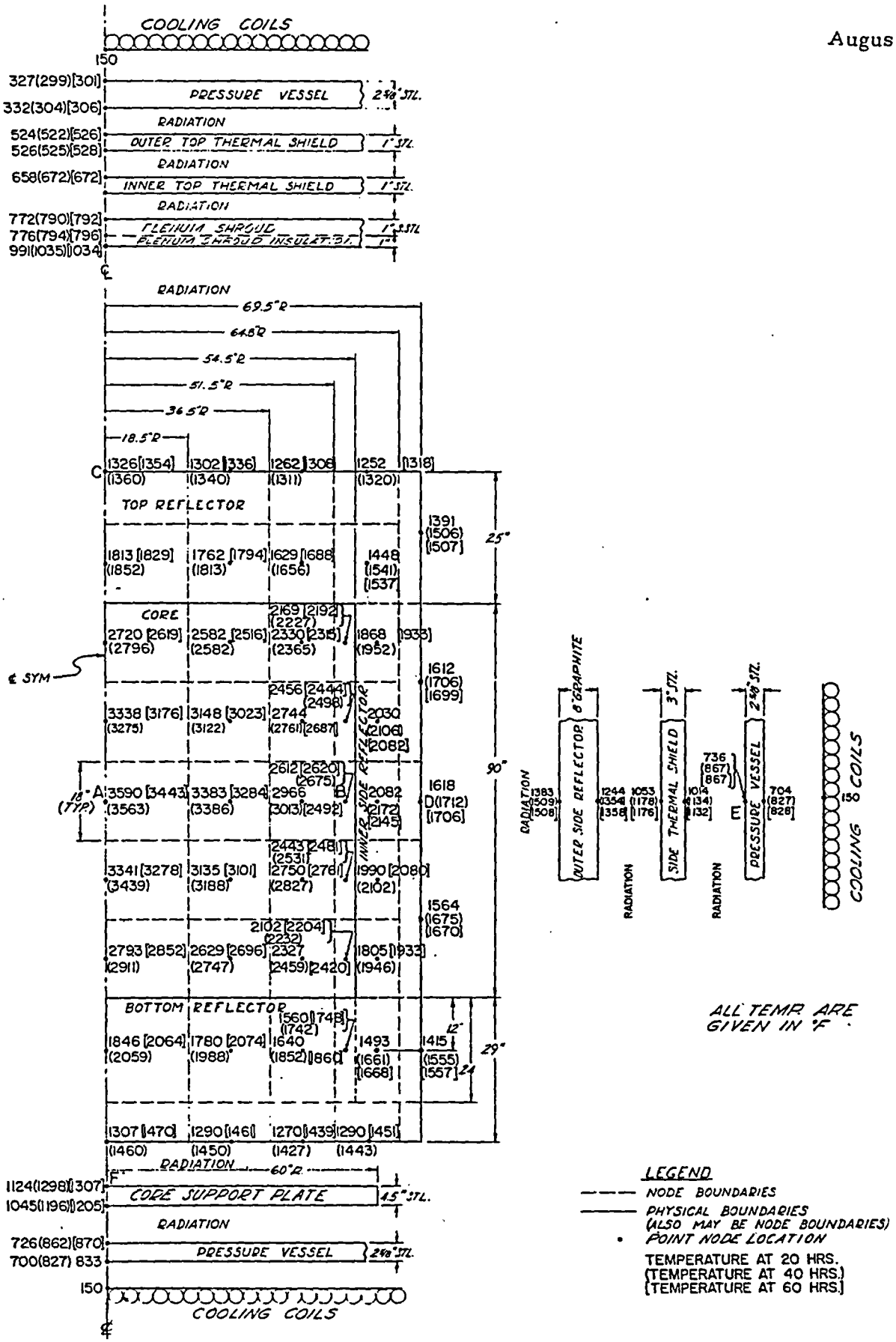

REACTOR TEMPERATURES AFTER LOSS OF COOLANT CIRCULATION ACCIDENT.

FIGURE C-2

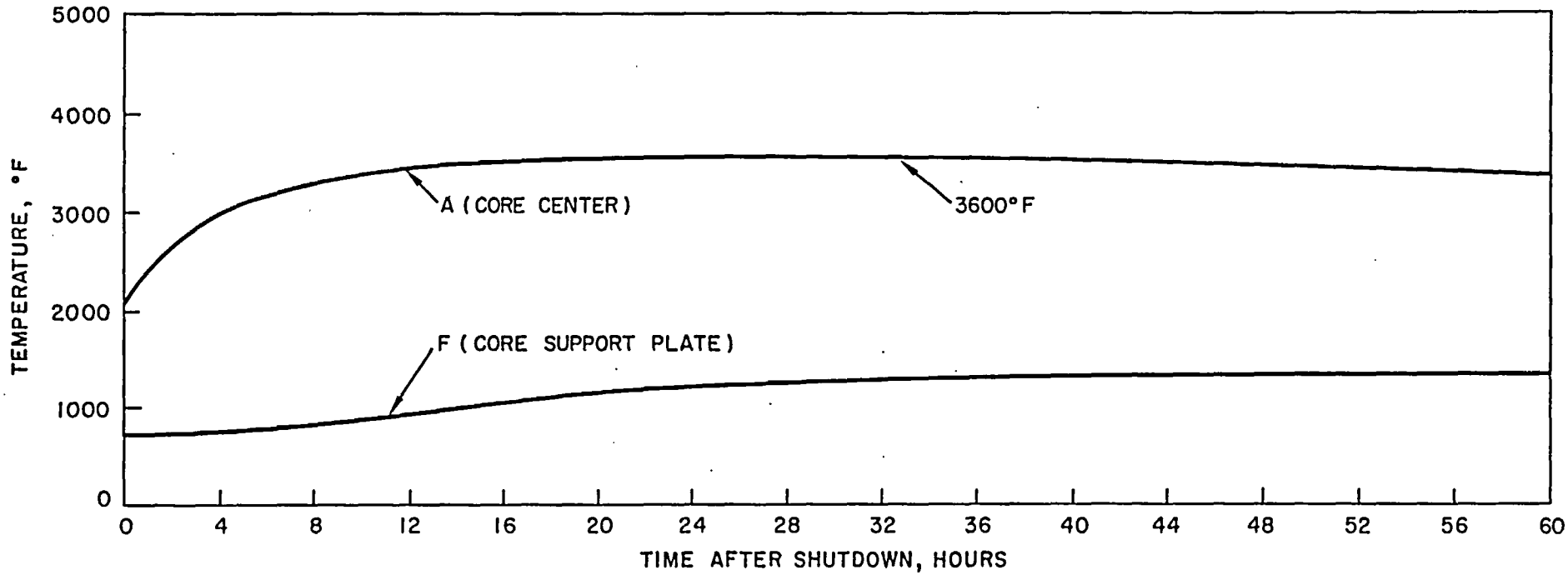

TRANSIENT TEMPERATURE OF KEY NODES AFTER LOSS OF COOLANT CIRCULATION ACCIDENT CONDITION. THE LOCATIONS OF THE NODES ARE SHOWN IN FIGURE C-2

FIGURE C-3

August, 1961

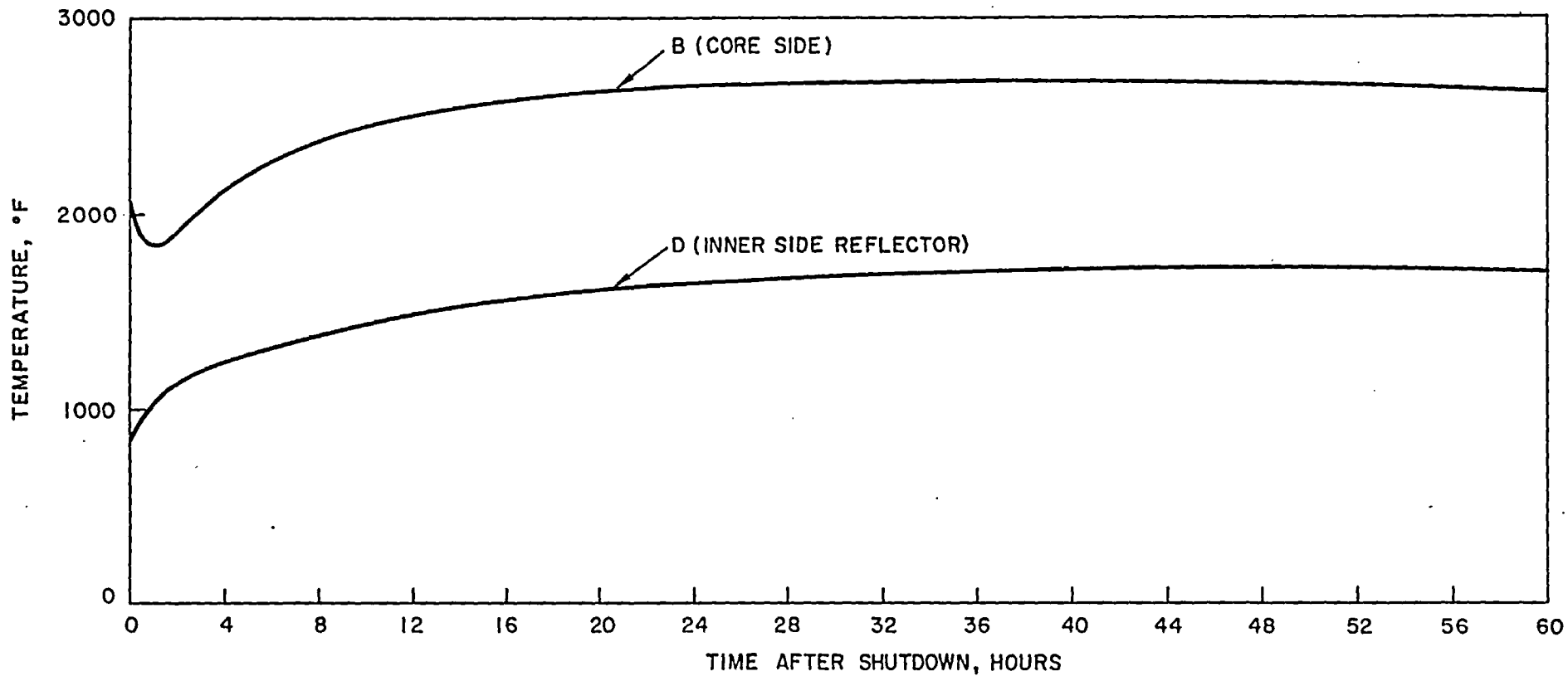

TRANSIENT TEMPERATURE OF KEY NODES AFTER LOSS OF COOLANT CIRCULATION ACCIDENT CONDITION. THE LOCATIONS OF THE NODES ARE SHOWN IN FIGURE C-2

FIGURE C-4

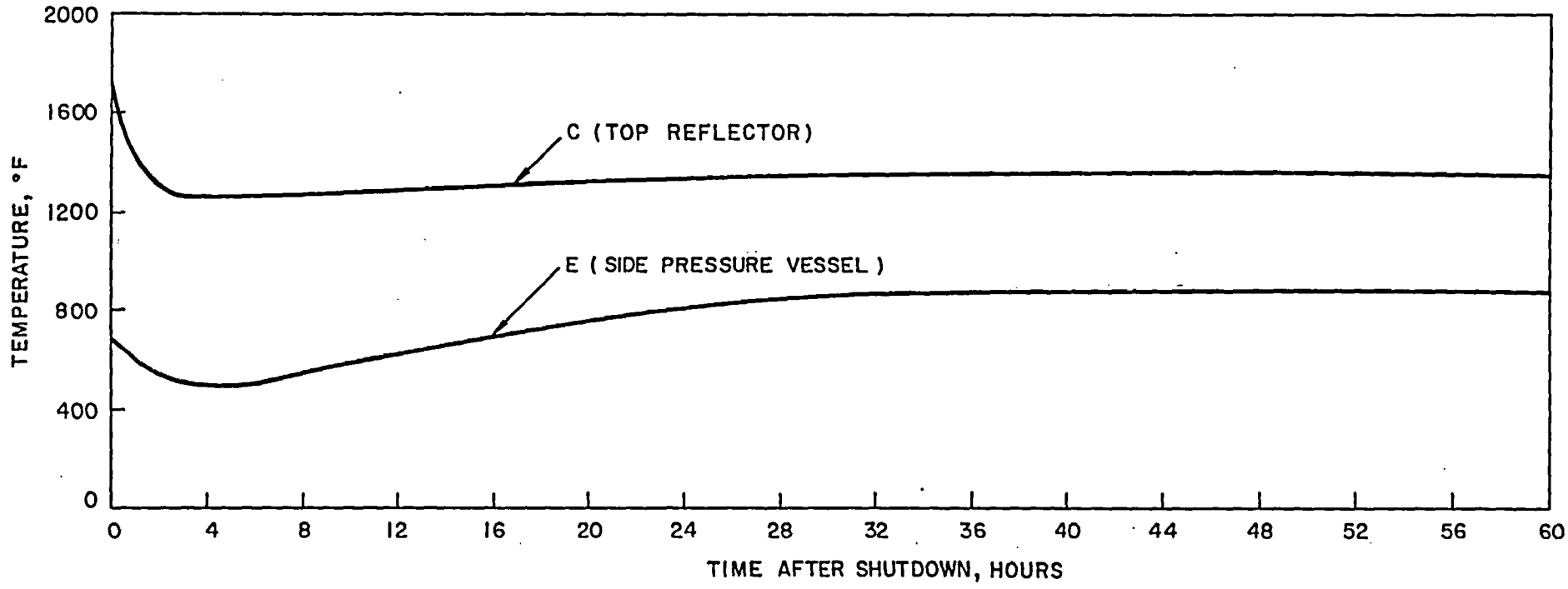

TRANSIENT TEMPERATURE OF KEY NODES AFTER LOSS OF COOLANT CIRCULATION ACCIDENT CONDITION. THE LOCATIONS OF THE NODES ARE SHOWN IN FIGURE C-2

FIGURE C-5

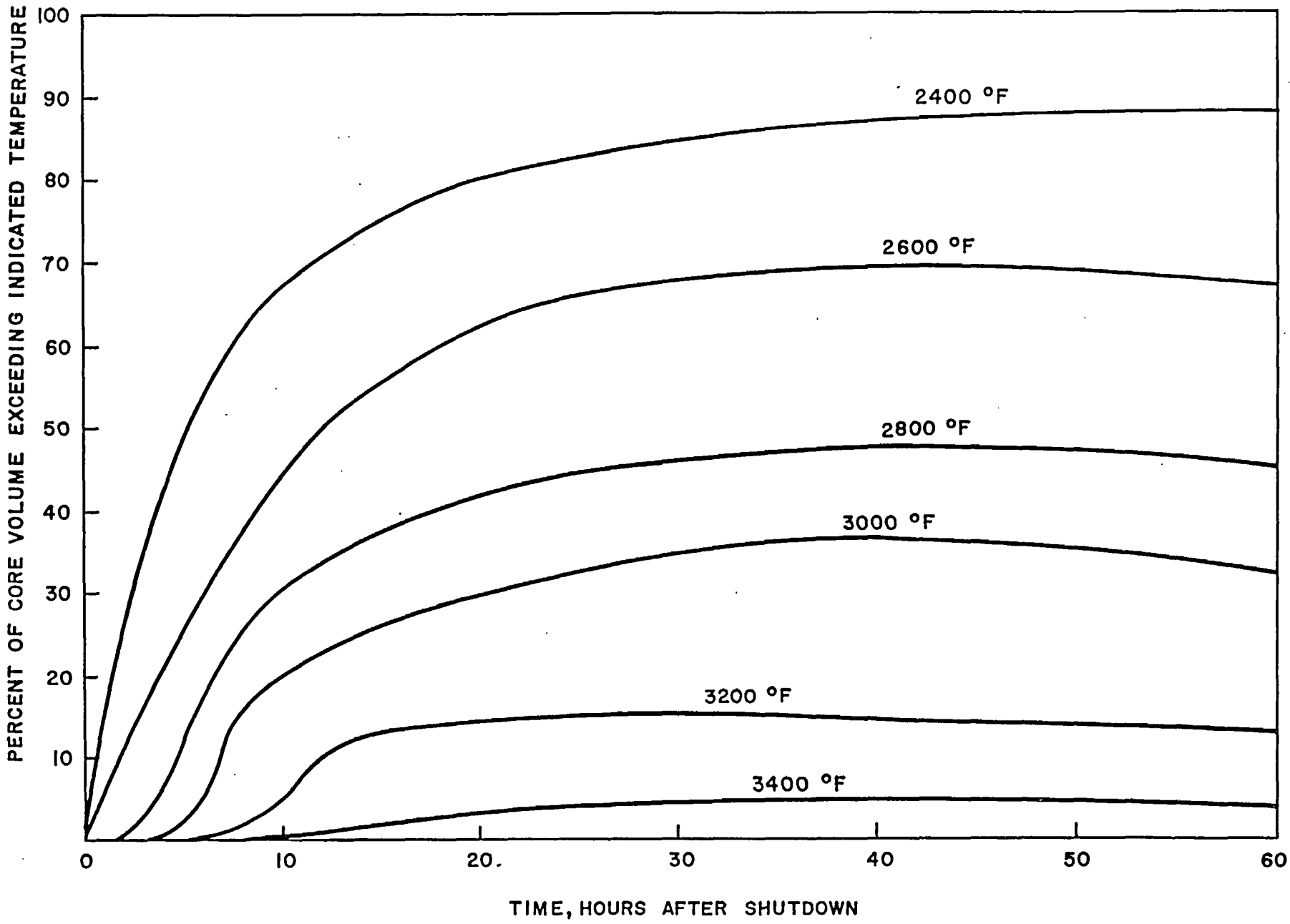

PERCENT OF CORE EXCEEDING VARIOUS TEMPERATURES VS. TIME AFTER SHUTDOWN FOR LOSS OF COOLANT CIRCULATION ACCIDENT.

FIGURE C-6

August, 1961

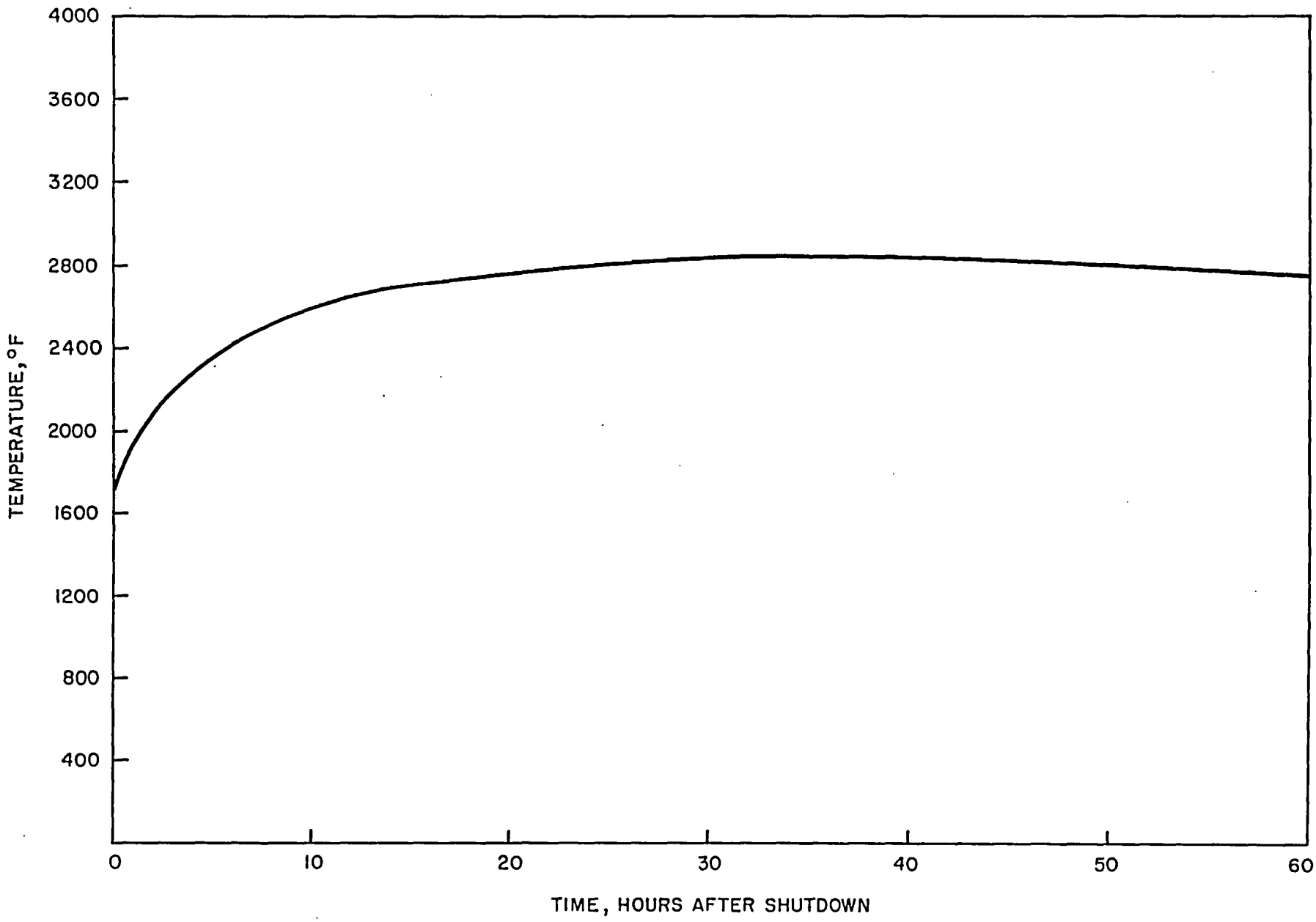

AVERAGE CORE TEMPERATURE VS. TIME AFTER SHUTDOWN:
LOSS OF COOLANT CIRCULATION ACCIDENT.

FIGURE C-7

August, 1961

APPENDIX D

STEAM GENERATOR TUBE RUPTURE CALCULATIONS

I INTRODUCTION

If a number of highly improbable simultaneous accidents occur during operation of the HTGR, a portion of the water inventory of the steam generation system, in the form of steam and/or hydrogen and carbon monoxide, may eventually flow into the secondary containment. The subsequent temperature and pressure of the gas in the secondary containment will depend on the amount, composition, temperature, and rate of entry of the added gas. The secondary containment will be filled during HTGR operation with a reduced oxygen gas except during startup or low power operation.

II PLANT DESIGN AND OPERATING DATA

A. The total inventory of steam and water in each steam generation system, consisting of a steam generator, steam drum, water recirculating pump and associated piping between the feedwater valves and the steam stop-check valves, is approximately 8320 pounds. Closing of the feedwater valves will prohibit additional water from flowing into the steam generator.

B. The HTGR steam generators are designed to limit maximum total flow of steam and water through both ends of a complete tube shear to 10 pounds per second.

C. Three moisture detectors in each loop of the helium coolant system will detect the presence of abnormal quantities of water in the system within five seconds after a steam generator tube has leaked or ruptured.

D. If an abnormal amount of moisture is detected in the helium coolant system and the primary system is intact, the reactor is scrammed and the following actions take place:

1. Within one second after the moisture is detected, the emergency steam generator steam dump valves will open and discharge steam outside the containment vessel. Valves and instrumentation are available to assure that these inventories can be dumped when such action is needed. Steam can be released outside the secondary containment building via the emergency steam dump system at a maximum rate

of 55 pounds per second. This is an initial rate corresponding to a steam drum pressure of 1600 psia; the steam flow will decrease as the steam drum pressure decreases. Steam dump is terminated when the steam pressure is reduced to within 50 psi of the helium pressure in the primary system.

2. Within three seconds after moisture is detected, the hot and cold valves in the helium coolant loop containing the failed steam generator will automatically close isolating the failed generator from the reactor.

3. Within three seconds after the moisture is detected, the feedwater valves close and stop flow of water to the steam generator. Sufficient valves and instrumentation will be provided to assure that the feedwater flow can always be stopped when such action is needed.

E. If, in addition, the primary system is ruptured, the following additional actions take place:

1. The water recirculation valve is closed in one second and the recirculation pump is stopped.

2. The water dump valves are opened. A water dump valve at the steam generator economizer inlet is opened, dumping water to the external blowdown drum until the water pressure is 50 psi above the primary coolant pressure. An additional water dump valve at the recirculation pump discharge is also opened to drain water to a drain tank within the containment and will continue to drain even after the other dump valves are necessarily closed.

F. Some portion of the graphite sleeves of the fuel elements of the HTGR during normal operation are at or above 1500 F, the temperature at which steam and graphite may start to react at significant rates. To determine the effect of the steam-graphite reaction on the secondary containment pressure, 0 and 100 percent reaction of the available steam flowing through the reactor core with the graphite have been assumed.

G. The helium coolant system design provides three pairs of pressure relief valves which discharge to the secondary containment. One pair of valves relieves the portion of the coolant system which is not isolated by the hot and cold valves. These valves open at 452 psia. The portion of each helium coolant loop which can be isolated by the hot and cold valves is relieved by a pair of valves which open at 465 psia. The isolated portions of each coolant loop are also provided with dump

valves which will open at about 405 psia and discharge to the helium dump tanks. The helium dump tanks are pressure-relieved at 515 psia to the secondary containment.

III STEAM GENERATOR TUBE RUPTURE

A. Failed Steam Generator Tube - Primary System Intact

1. Hot and Cold Valves Close, Isolating Reactor from Steam Leak

When an abnormal quantity of moisture is detected in one of the two helium coolant loops, the following actions are taken on the faulty loop: steam generator feedwater flow is stopped, emergency steam dump is started, and the hot and cold valves in the failed coolant loop are closed. Before the hot valve closes (three seconds after moisture is detected, or eight seconds after a tube rupture), up to 10 lb per second or 80 lb of water may be added to the entire helium coolant system. Forty pounds of this water enters that part of the system containing the reactor, accounting for transport time from the leak to the cold valve at the compressor discharge. The 40 lb of steam raise the helium coolant system pressure from the normal operating pressure of 350 psia to 356 psia at 0 percent conversion and to 360 psia at 100 percent conversion. These would be relieved to the helium dump tanks.

After closure of the hot and cold valves in the helium coolant loop containing the failed steam generator, the steam and/or water from the steam generator system will continue to flow into that portion of the helium coolant loop which is isolated from the rest of the system by the hot and cold valves. The steam added to the isolated part of the helium coolant loop will cause loop pressure to rise to 390 psig whereupon dump valves will open and release a mixture of steam and helium to the helium dump tanks. The loop pressure will stay at 390 psig until the pressures of the loop and tanks are equal. The history of steam drum, steam generator shell, and dump tank pressures and of the water inventory of the steam generator, drum, and piping are shown in Figure D-1. To prevent backflow into the steam side of the steam generator of any radioactive material in this isolated portion of the helium coolant loop, emergency steam dumping is stopped when the steam drum pressure approaches within 50 psi of the helium system pressure. The pressure in the generator shell and dump tanks will then equalize as steam continues to flow into the dump tanks. It may be noted in Figure D-1 that the steam drum pressure drops below 465 psia (at about 102 seconds after the tube

rupture); thus the final equilibrium pressure of the steam generator shell, the isolated section of the helium coolant system, and the dump tanks will never reach 465 psia. The isolated section and the dump tanks can therefore contain the steam flowing into them from the steam generation system because the relieving of the isolated section and the dump tanks to the secondary containment begins at 465 psia and 515 psia, respectively.

2. Hot and Cold Valves Do Not Close

If the hot and cold valves do not close and isolate the failed steam generator, steam will flow into the helium coolant system and react to some extent with the hot graphite of the core. Figure D-2 shows the increase in steam generator shell pressure, helium coolant system pressure, and dump tanks pressure as steam flows from a one-tube steam generator rupture into the helium coolant system for the complete range of possible conversion of steam to hydrogen and carbon monoxide. Based on presently available information on the reaction of steam with low permeability graphite, the over-all conversion of the steam passing through the core will be less than 10 percent since the core will be rapidly cooled below the steam-carbon reaction temperature by circulation through the intact steam generator.

The contents of the helium coolant system are not relieved to the secondary containment since the pressure does not build up to the safety valve setting.

B. Simultaneous Rupture of Helium Coolant System and One Steam Generator Tube

1. Hot and Cold Valves Close

If there is a simultaneous rupture of the primary system and a steam generator tube the following action would automatically take place on the loop with the steam generator with the ruptured tube: the boiler feedwater flow is stopped, the hot and cold valves are closed, the emergency steam dumping is started, the recirculating pump is stopped and its discharge valve is closed, and emergency water dump valves are opened (taking 90 seconds to fully open). As in Section A. 1., only about 40 lb. of steam will flow into the helium coolant system before closing of the hot and cold valves which stops the steam flow. Thus, 40 lb. of steam or equivalent hydrogen and carbon monoxide will flow into the secondary containment.

After closure of the hot and cold valves in the helium coolant loop containing the failed steam generator, the steam will continue to flow into the isolated portion of the primary coolant system and out the emergency steam generator dump valve. Steam is dumped until the steam drum pressure drops to within 50 psi of the helium coolant pressure, whereupon the steam dump valves are closed. The water dump continues until the steam drum and helium coolant system pressure become equal.

If the primary system leak were in the "isolated" part of the loop containing the failed steam generator approximately 2200 lb of steam would enter the containment vessel without passing through the core. If the primary system leak is in another part of the system, then most of the steam will remain in the isolated loop and dump tanks.

2. Hot and Cold Valves Do Not Close

If the hot and cold valves do not close and isolate the failed steam generator, part of the steam will flow through the core and react to some extent with the hot graphite. The resultant gases will flow into the secondary containment through the primary system rupture at a temperature of about 660 F. As shown in Figure D-3, the total amount of water and steam that can enter the helium coolant system, including the inventory remaining after the emergency steam and water dump is completed, is 2200 pounds. Approximately 1450 lb of water may remain in the ruptured steam generator after pressures equalize. This water will be vaporized by the sensible heat in the metal of the steam system equipment and pass into the secondary containment via the helium coolant system. However, 100 minutes are needed to completely vaporize the water.

The fraction of the steam which passes through the core enroute to the secondary containment via a primary system rupture depends on the location of the break and the position of the valves. Incidents involving ruptures of the helium system at various points have been considered and there are no plausible accident conditions where more than two-thirds of the steam flow through the steam tube leak, passes through the core, and is converted to hydrogen and carbon monoxide during the 100-minute period of time shown in Figure D-3. For purposes of calculating the containment pressure in Section IV, it has been conservatively assumed that 1100 lb of H_2O passes through the core and reacts completely during the first few minutes, and that all of the 2200 lb eventually reacts with the core graphite.

C. Summary

The above analysis shows that if the helium system remains intact with the rupture of one steam generator tube, there is no release of gases to the secondary containment building.

In the case that the helium system fails simultaneously with the rupture of one steam generator tube and the isolation valve does not operate, 2200 lb of steam are released.

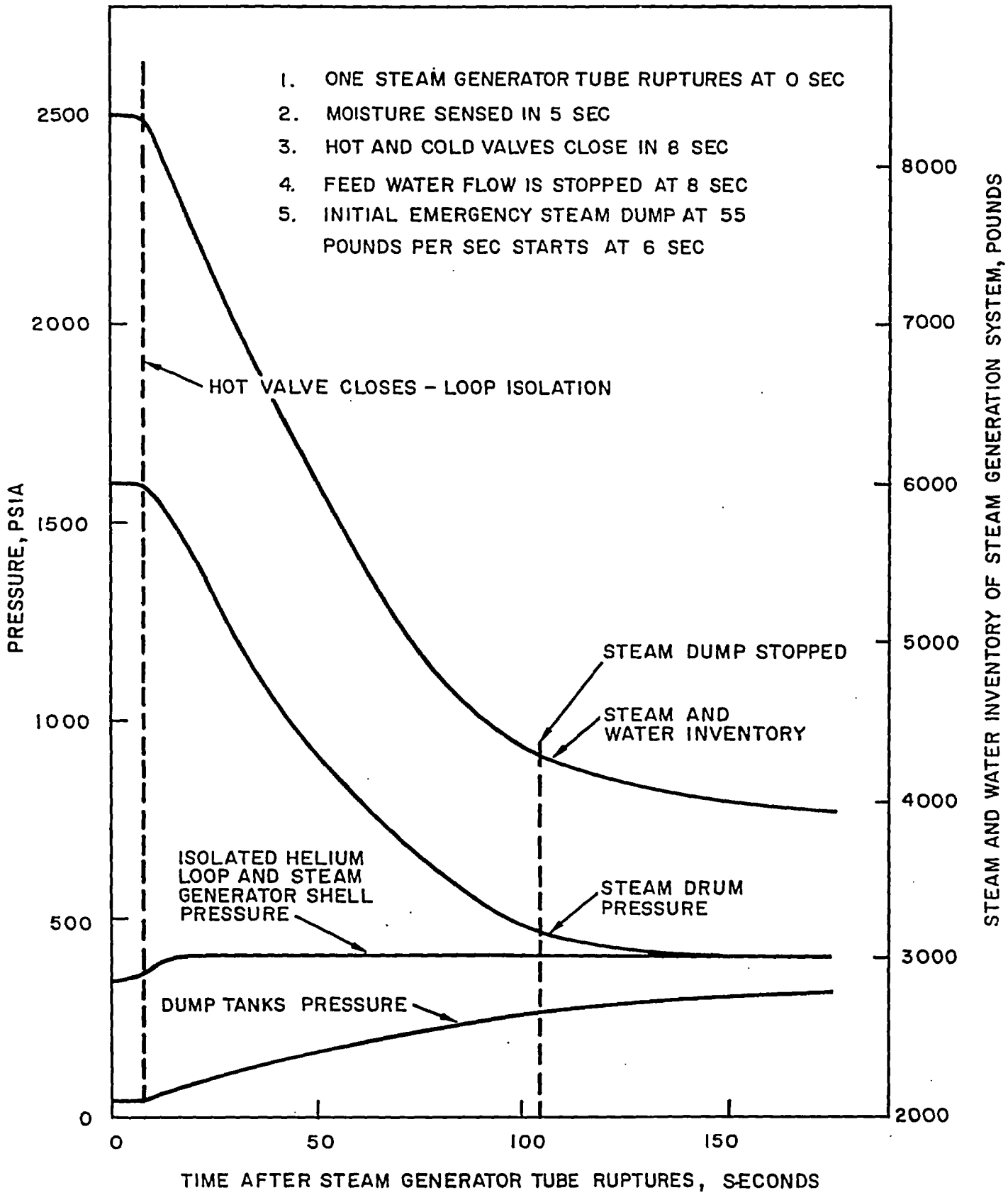

EFFECT OF STEAM ADDITION ON AN ISOLATED HELIUM COOLANT LOOP AND DUMP TANK SYSTEM.

FIG. D-1

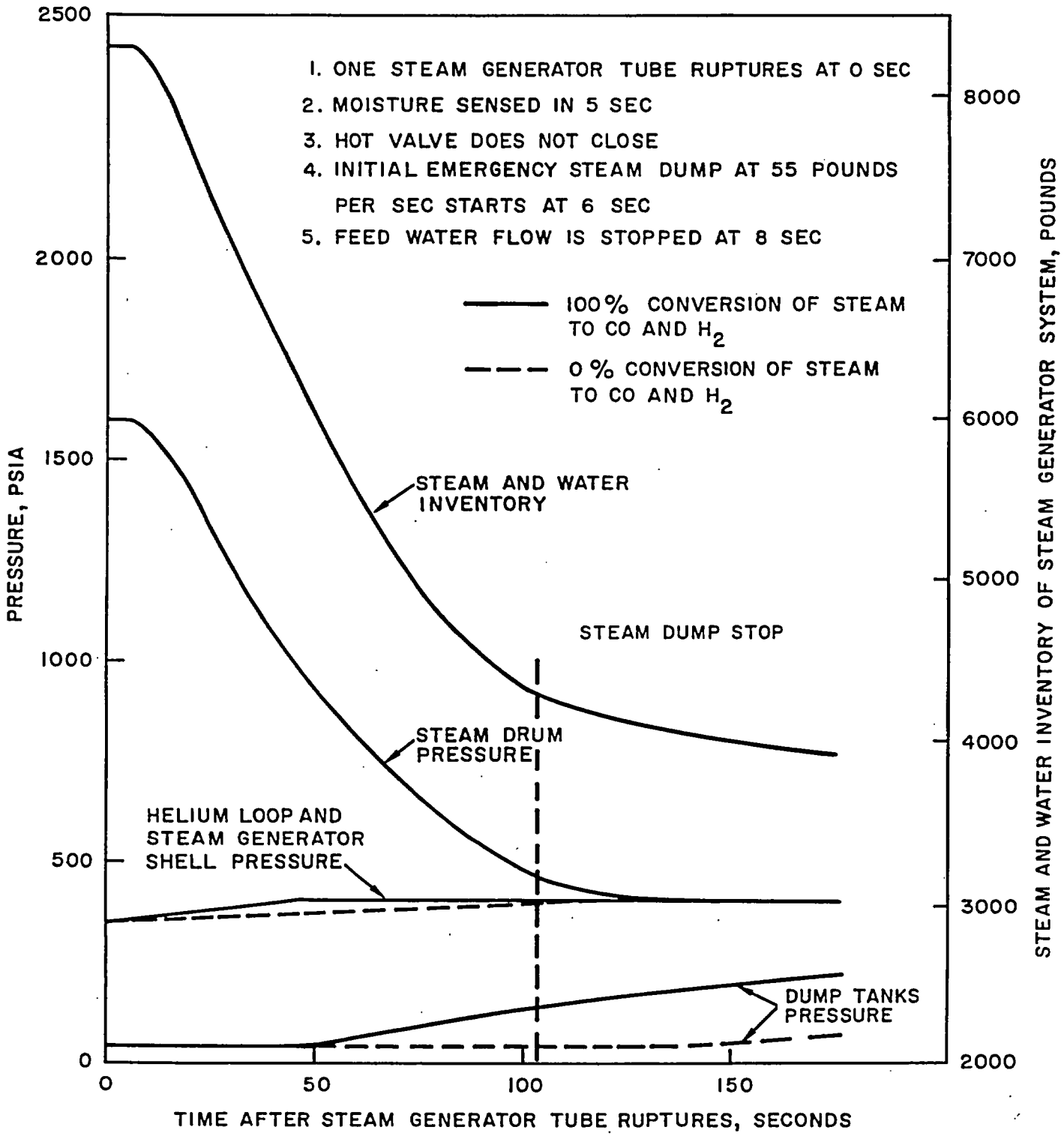

EFFECT OF STEAM ADDITION ON UNISOLATED HELIUM COOLANT LOOP AND DUMP TANK SYSTEM.

FIG. D-2

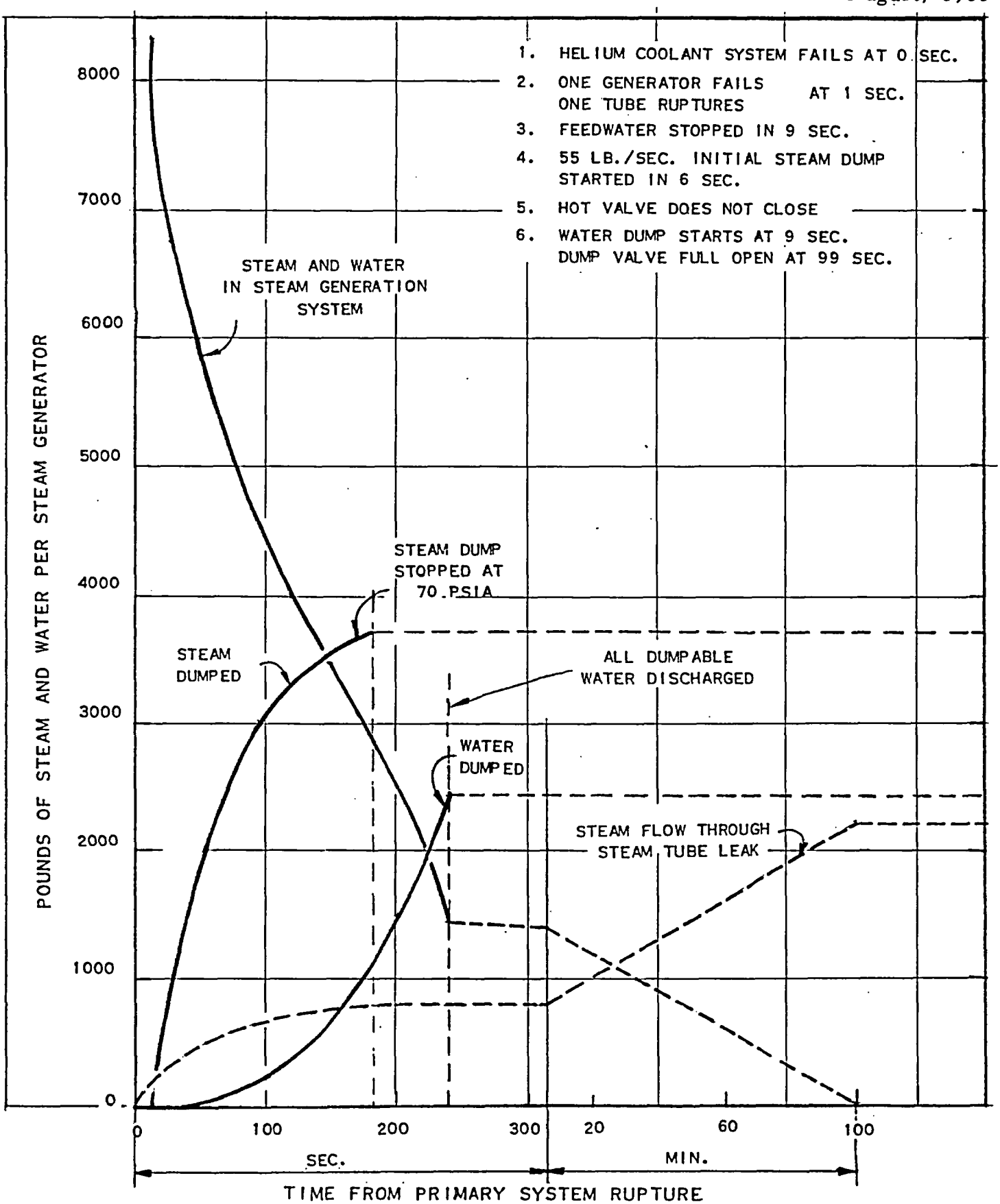

TRANSIENT STEAM AND WATER QUANTITIES FOLLOWING RUPTURE OF HELIUM COOLANT SYSTEM AND ONE STEAM TUBE.

FIGURE D-3

October, 1961

APPENDIX E

REACTOR PRESSURE VESSEL

Table of Contents

			Page
I	DESIGN SPECIFICATIONS		
	A.	Design Criteria, Including Normal and Abnormal Conditions	E - 1
	B.	Codes, Standards, and Failure Criteria	E - 2
	C.	Stress Analysis	E - 5
	D.	Fast Neutron NVT Design Values and Effects	E - 9
II	MANUFACTURING AND FABRICATION SPECIFICATIONS		
	A.	Manufacturing Process Control and Responsibility	E - 10
	B.	Specifications for Each Component of Vessel	E - 20
	C.	Normalizing Procedures	E - 22
	D.	Methods of NDT Determination	E - 23
	E.	NDT Temperature Specifications	E - 24
	F.	Treatment of Material Following Fabrication	E - 24
	G.	Post-Manufacturing Tests to be Conducted	E - 24
III	OPERATIONAL LIMITS		
	A.	Temperature-Pressure Transition Limits	E - 26
	B.	Control of Transition Limits	E - 26
	C.	Coupon Testing	E - 27

October, 1961

APPENDIX E

REACTOR PRESSURE VESSEL

This appendix sets forth design criteria, material considerations, quality control and inspection procedures, and other information relative to the pressure vessel and the pressure vessel support. The reactor pressure vessel was described in Section II. B. 6.

I DESIGN SPECIFICATIONS

A. Design Criteria, Including Normal and Abnormal Conditions

1. Code Design

The HTGR pressure vessel, shown in Figure E-1, will be designed in accordance with Section VIII of the ASME Unfired Pressure Vessel Code for the following conditions:

a. Design Pressure 450 psig
Design Temperature 725 F
No Corrosion Allowance
Gamma Volumetric Heating Rate per Figure E-2

b. Design Pressure 0 psia
Design Temperature 700 F
No Corrosion Allowance
No Gamma Heating

2. Transient Loadings

The reactor pressure vessel will be engineered and designed to resist the loads given below. The transient conditions described start either from shutdown conditions or from steady state operating conditions. During steady state operation, the flow enters the vessel through both nozzles, with equal flow in each nozzle.

The steady state conditions from which the transients start are:

Operating Pressure 335 psig
Coolant flow varies from 170,000 lb/hr to 464,000 lb/hr
Gamma Volumetric Heating Rate Per Figure E-2
Piping Loads Per Figure E-3
Inlet Gas Temperature Per Figure E-4

The following transients will be considered:

(1) Normal operation with control stutter

(2) Load following with variable inlet gas temperature

(3) Startup

(4) Controlled shutdown

(5) Emergency shutdown, including loss of coolant pressure

(6) Steam leak

The details of these transients are shown in Figure E-5.

The permissible number of transients for the above conditions have been analyzed and are discussed in Section I. C. 3. This permissible number in every case exceeds the expected number.

3. Other Design Conditions

In addition to the Code and transient cases, five other cases will be considered. They are:

a. Refueling

b. Search for Broken Fuel Element

c. Annealing of Reactor Vessel up to 850 F

d. Earthquake (0. 1g)

e. Flooded Condition (for future unforeseen field need)

Cases a and e will take into account appropriate loads on the top vessel nozzles.

Case c will take into account reduced coolant pressure and increased piping reactions (as compared with other cases).

A dynamic analysis will be made for the top nozzles for case d.

Case b is identical with normal operation at reduced power except for the load on the top central nozzle.

4. Pressure Vessel Support

The vessel is to be supported on a conical skirt support bolted to a ring attached to the reactor vessel. The support will be designed for the conditions of Sections I. A. 2 and I. A. 3 of this appendix.

The support will be designed to the same standards as the pressure vessel.

The support temperature at full power varies from approximately 650 F at the point of attachment to the vessel down to

approximately 200 F at the point of contact with the foundation. The cool portion of the skirt, if made of carbon steel, would be subject to embrittlement at these low temperatures. For this reason, the cool portion of the support may be made of austenitic stainless steel. In this case, the point at which the stainless steel will join the carbon steel will be at no less than 600 F. This point will be a distance of at least $1.566\sqrt{Rt}$ inches away from the top or bottom flange of the support, where R is the radius of the support at the bimetallic joint and t is the thickness of the support, both in inches.

B. Codes, Standards, and Failure Criteria

1. Design Codes

The pressure vessel will be designed (1) in accordance with the 1959 ASME Code for Unfired Pressure Vessels, Section VIII, (which is applicable in the Commonwealth of Pennsylvania) and the latest code case rulings, including the nuclear rulings and (2), to resist the transient loadings which may occur during its life.

The minimum thickness of a vessel component will be determined by the "Code" design pressure and temperature (see Section I. A. 1), and the appropriate Code formula and allowable stress listed in Section VIII of the 1959 ASME Code for Unfired Pressure Vessels.

2. Detail Engineering Standards

Detail engineering will be guided by "The Tentative Structural Design Basis for Reactor Vessels and Directly Associated Components," dated 1 December 1958, with Addendum dated 27 February 1959, Department of U.S. Navy, Bureau of Ships, with the exceptions of Section 1, paragraphs 3.3.4.1, 3.3.4.2, 3.3.4.3, 6.2.4, 6.4.1. Charts A.3-5 and A. 3-6 and the values for S_{aI}, S_{aII}, and S_{aIII} in Table 5-1 will not be used. Chart A.6-2 has some inconsistencies with the latest published texts and will be investigated before use.

3. Failure Criteria

Detailed stress analysis of the vessel for the conditions listed will be governed by the following failure criteria:

a. Steady State Operation

The maximum shear theory will be used to establish the failure criterion. This states that yielding begins when the maximum shear stress equals the yield stress in shear. The shear yeild stress will be defined as 50 percent of the tensile yield stress used by the ASME Code in determining the allowable stresses in Table UCS-23. The maximum shear stress is represented in terms of the principal stresses by:

$$\tau_{max} = 1/2\ (\sigma_{max} - \sigma_{min})$$

where

τ_{max} = Maximum shear stress

σ_{max} = Maximum principal stress

σ_{min} = Minimum principal stress

In the case of a triaxial stress field where all principal stresses have the same algebraic sign, it is possible that the maximum shear theory will not indicate incipient failure. Consequently, in a triaxial stress field, yielding will be considered to begin when the critical principal stress equals 90 percent of the tensile yield stress.

Steady state thermal stress plus membrane pressure stress will satisfy the ASME Code requirements. The steady state thermal stresses will also be checked for fatigue effects.

b. Thermal Transient Conditions

Section 5 of the "Tentative Structural Design Basis for Reactor Pressure Vessels and Directly Associated Components," revised 1 December 1958, Addendum dated 27 February 1959, Department of U. S. Navy, Bureau of Ships, will be used to establish failure criteria.

For the purpose of analyzing transient stresses, the term one cycle will be taken to mean the initiation and establishment of a new operating condition and the return to the original operating condition. This definition conforms to that given in the "Tentative Structural Design Basis for Reactor Vessels and Directly Associated

Components," dated 1 December 1958, with Addendum dated 27 February 1959, Department of U.S. Navy, Bureau of Ships.

When evaluating fatigue life, the total stress range experienced by the part will be taken into consideration, i.e., the stress due to the + 250 F/hr transient will be added to the stress due to the -150 F/min transient (See Cases 3 and 5 of Figure E-5), rather than the transients being treated separately. One cycle of operating temperature may lead to "two cycles" of stress change.

C. Stress Analysis

1. Determination of Transient Temperature Distributions

Two methods of computation will be used for determining the thermal gradients and values of average temperature in various sections of the vessel. Where the section is uniform, as in the main portion of the shell, the differential equation for one dimensional transient temperature distribution will be solved. For areas of complex heat flow, such as in the nozzles and flange areas, a two-dimensional resistance-capacitance analog will be constructed to give the time-temperature history at various points in the structure. From the values of temperatures obtained from the analogs, the maximum thermal gradients occurring in the vessel will be obtained. Thermal stresses will then be calculated from these temperatures and temperature gradients.

2. Determination of Mechanical and Thermal Stresses

A stress analysis of mechanical and thermal loads on the reactor vessel will be performed in order to ensure adequacy of the design. Critical areas will be investigated to determine that stresses are within design limits and to establish that the permissible number of cycles of application of transient loadings are all beyond the number of cycles expected during the life of the plant. The design limits are given in Section I. B.

A majority of the stress analyses will be performed by breaking the structure to be analyzed into free bodies. The equations representing the behavior of these free bodies will be written into a system of equations representing the composite structure. Solving

this system of equations will give the loads necessary to maintain continuity in the structure. Stresses will then be calculated from the loads obtained from the solution of the equations.

The following sections will be investigated:

a. Lower Vessel Section, Bottom Head with Attachments and Core Support

This section will be analyzed for the effects of internal pressure, dead weight, axisymmetric internal loads, dynamic loads, earthquake loads and thermal transient loads.

b. Thermal Gradient at the Top of Outer Lower Thermal Shield

A thermal discontinuity stress will be present in the shell, even though the thickness is constant, due to an increase in the local coefficient of heat transfer at the top of the outer thermal shield. This area will be investigated for internal pressure, dead weight, axisymmetric internal loads, dynamic loads, earthquake loads, and such thermal loads as are necessary. Methods outlined in "Thermal Stress Techniques in the Nuclear Industry," (Staff of The Franklin Institute Laboratories for Research and Development, Philadelphia, Pennsylvania. Prepared for U.S. Atomic Energy Commission under Contract No. AT(30-1)-2103, Oct. 1960) will be used for evaluating this section.

c. Change in Vessel Shell Thickness

This is the area that joins the 2-1/2 in.-thick shell to the 4-1/2 in.-thick shell. The discontinuity stresses present in this area will be due mainly to different pressure deflections and different transient temperature distribution rates. Other effects to be analyzed in the area are dead weight, dynamic loads, and earthquake loads.

d. Nozzle Stresses and Shell Stresses due to Piping Loads

The junctions of the main coolant piping to the nozzles and the nozzles to the shell will be analyzed for pressure discontinuity stresses, thermal transient stresses, and shell stresses due to the imposed piping loads. The analyses of these nozzles will

use the latest data from hard model and photoelastic testing conducted by the Pressure Vessel Research Committee on Reinforced Openings of the Welding Research Council of the Engineering Foundation.

e. Top Head and Vessel Joint

The top head and flanges will be analyzed by a discontinuity analysis for the effects of internal pressure, dead weight, axisymmetric internal loads, dynamic loads, bolting loads, earthquake loads, and thermal transient effects. The effect of the center nozzle in the top head on the discontinuity stresses in this area is negligible. All top head nozzles will be analyzed as described below. Methods as described in "Thermal Stress Techniques in the Nuclear Industry," (Staff of The Franklin Institute Laboratories for Research and Development, Philadelphia, Pennsylvania. Prepared for U.S. Atomic Energy Commission under Contract No. AT(30-1)-2103, Oct. 1960) will be used. The stresses in the ellipsoid will be computed by numerical integration of the exact thin shell differential equation.

f. Nozzles in Top Head

The nozzles in the top head will be analyzed by a discontinuity analysis for the effects of internal pressure, dead weight, axisymmetric internal loads, dynamic loads, earthquake loads, and steady state and thermal transient effects.

g. Step in the Diameter in Fuel Handling Nozzles

These sections will be analyzed by a discontinuity analysis for the effects of internal pressure, dead weight, axisymmetric internal loads, dynamic loads, and earthquake loads.

h. Blind Flange, Shielding Plug Retainer

This section will be analyzed assuming (1) that the blind flange cover and bolts take the load and (2), that the plug retainer ring takes the load. This area will be investigated for the effects of internal pressure and bolt loads.

i. Effects of Control Rod Housings in the Bottom Head

The effect of a control rod nozzle penetration in

the bottom head will be calculated, treating the nozzle as a single rod in the bottom head. The composite effect of all the nozzles in the bottom head will be evaluated by treating the crown as a perforated member and using equivalent elastic constants. This analysis will be part of the final analysis covered under item I. C. 2. a.

j. Reactor Vessel Support

The reactor vessel support will be analyzed for the effects of the applied load, dead weight, pressure deflection of the vessel, effect on the proximity to other vessel attachments, thermal stresses, dynamic loads and earthquake loads.

3. Effects of Thermal Transients

The various thermal transients considered in the pressure vessel stress analysis are set forth in Figure E-5. It will be noted that Case 1 represents normal operation at power, that Case 2 is a design case for load-following, which is more severe than the base load operation case mentioned in Section II. B. 6. b, and also, that Cases 5 and 6 represent abnormal conditions.

Case 1 of Figure E-5 has been analyzed and it was determined that, since the amplitude of the transient is so small, an infinite number of cycles of application of the Case 1 transient can be withstood.

The most critical region of the vessel from the standpoint of thermal transients is the junction between a coolant inlet nozzle and the thick upper barrel of the vessel (see Figure E-1). Here the vessel material is thickest, the heat transfer coefficient highest, and the rate of change of gas temperature highest. An analysis of this region for the most severe transient, Case 5 of Figure E-5, revealed a transient thermal stress less than the permissible stress for the range 10^5 to 10^6 cycles of application shown in the "Tentative Structural Design Basis for Reactor Pressure Vessels and Directly Associated Components" revised 1 December 1958, with Addendum dated 27 February 1959, Department of US Navy, Bureau of Ships (See paragraph 3 of Section II. B. 6. b). Since all other thermal transients are much less severe than Case 5 and will occur fewer times than 10^5 cycles, further calculation of transient thermal

stresses was unnecessary, since it was already obvious from Case 5 that the vessel could withstand a practically unlimited number of thermal transients. The fundamental reason for this is that local heat transfer coefficients are rather small because the coolant is a gas.

D. Fast Neutron NVT Design Values

The fast neutron flux for two different energy groups has been calculated for 12 planes in the reactor vessel. The two energy groups are neutrons with energy above 1.0 Mev and neutrons with energy above 0.1 Mev. The points calculated are points 1 to 13, shown on Figure E-1.

The fluxes and corresponding doses for 30 years of reactor life at full power and 100 percent load factor for points in the reactor vessel above the top of the core are shown in Figures E-6 and E-7 as a function of iron thickness.

The fast leakage from the top of the core was modified by the results of a Monte Carlo calculation with empty control rod channels. The angular distribution of the neutrons leaving the top reflector determined by these calculations, and the flux distribution in the top reflector determined by the ANGIE Diffusion Code calculations were used to obtain more accurate answers than were possible previously.

The fluxes and corresponding doses for 30 years of reactor life at full power and 100 percent load factor for the lower portion of the reactor vessel are shown in Figures E-8 and E-9 as a function of iron thickness.

The neutron fluxes shown in Figures E-8 and E-9 should not be used for estimating radiation damage to the grid plate, since the fast neutron leakage from the core is predominantly from the coolant channels. The peak flux beneath these channels is approximately 2.7×10^{11} n/cm^2 sec for neutrons with energy above 1.0 Mev and 1.6×10^{12} n/cm^2 sec for neutrons with energy above 0.1 Mev.

II. MANUFACTURING AND FABRICATION SPECIFICATIONS

A. Manufacturing Process Control and Responsibility

1. Fabrication and Inspection Requirements

a. Weld Rod and Welding Wire

All weld rod and welding wire will be positively identified by marking before use and a record of the weld in which it was used will be made and turned over to the General Atomic inspector.

b. Magnetic Particle and Liquid Penetrant Inspection

Magnetic particle and liquid penetrant inspection will be performed in accordance with Sections 5 and 6 of "Military Standard for Non-Destructive Testing Requirements for Metals, Mil. Std. 271A (Ships) 2 January 1959." Zyglo, Magnaflux or dye penetrant methods will be used. All welds will be inspected on all exposed surfaces by the liquid penetrant, Zyglo or magnetic particle inspection methods. Any defects detected by this method will be repaired and the repairs retested until no defect indication is shown by the dye penetrant, Zyglo or magnetic particle test.

c. Radiographic Inspection

Radiographic inspection of all joints will be made in accordance with paragraphs 4.2 to 4.9 of the Military Standard for Non-Destructive Testing Requirements for Metals, Mil. Std. 271A including attachment components, where the radiographic procedure can be used to determine quality of welds. Exceptions to radiographic inspection will have to be authorized by General Atomic.

Any imperfections determined by radiographic examination to be greater than outlined below will be judged unacceptable.

Any type of crack or zone of incomplete fusion or penetration.

Any group of slag inclusions in line that has an aggregate length greater than 1/4 T in a length of 12 T.

Any defects greater than the following:

Parent Metal Thickness (T) (Inches)	Porosity Diameter (Inches)	Slag Inclusions or Cavities (Inches)	No. of Defects per 1" Weld Metal Length	Minimum Permitted Spacing (Inches)
Less than 1/4	10% or 0.012 whichever is smaller	12% or 0.015 whichever is smaller	5	5/32
1/4 to 1/2	0.021	0.025	5	1/8
1/2 to 1	0.041	0.048	5	1/8
1 to 1-1/2	0.060	0.085	4	1/8
1-1/2 to 2	0.075	0.100	3	1/8
Greater than 2	0.075	0.125	3	1/8

Adjoining porosity, adjoining elongated slag inclusions or adjoining cavities will be considered a single defect.

d. Ultrasonic Inspection

Ultrasonic inspection of materials will be made in accordance with Section 7 of "Military Standard for Non-Destructive Testing Requirements for Metals" Mil. Std. 271A, 2 January 1951.

The plates used to fabricate the vessel will be completely ultrasonically inspected at the mill. All plate material requiring ultrasonic testing will be inspected by longitudinal and shear wave techniques. Laminar defects over one square inch in area and transverse defects larger than 3% of the material thickness will not be accepted.

e. Material Performance Testing

In addition to the mill test reports on the material used, the testing outlined in this subsection will be required. Test plates of the heats used and of the thicknesses of plate involved will be subjected to the same processes and procedures used to fabricate the vessel. The test plates will be welded as an extension of the longitudinal seam on the vessel barrels. These test plates will be subjected to the same heat effects as the vessel shell. From these test plates the following specimens will be prepared. Drawings of the locations of the samples with respect to the test plates will be submitted to General Atomic for approval.

Both Charpy V-notch and keyhole tests will be performed for both the welded and non-welded plates. Specimens will be taken so that both longitudinal and transverse properties may be determined. Six Charpy V and six keyhold specimens for each direction will be tested for each barrel in the shell (total 24).

Tensile tests on specimens taken from each barrel will be performed to prove that the tensile properties are at least those required by ASME SA 212 Gr B made to ASME SA 300 specification. Four specimens will be taken longitudinally through the parent metal and four through the weld. Four specimens will be taken transverse through the parent metal and four across the weld. These tests will be performed prior to welding the barrel they represent to the shell assembly.

The following testing will be performed to determine the ductility of the plate material used in the completed vessel. The test specimens will be standard 10 mm Charpy V-notch specimens. The specimens will be taken from the plate used for the weld starting tabs of the long seams. These plates will have the same forming and heat treatment as the material of the barrel. The samples will be taken with the root of the notch of the sample perpendicular to the surface of the plate. The samples will be taken from a point midway between the surface of the plate and the center of the plate. Ten specimens will be taken from each barrel for each of the positions described in this paragraph. Each group of ten specimens will be tested to provide information to make a plot of impact energy versus test temperature for the temperature range of -50 F to + 140 F. The specimens will be taken from the following positions:

Ten specimens from the parent metal. The long dimension of the specimen will be parallel to the direction of rolling.

Ten specimens across the weld. The long dimensions of the specimens will be perpendicular to the long axis of the weld. The notch of the specimen will be in the weld metal.

Ten specimens across the weld. The long dimensions of the specimens will be perpendicular to the long axis of the weld. The notch of the specimen will be in the heat affected zone. No stamping or other identification of material or welds which produces stress raisers will be permitted.

2. Quality Control by the Vessel Supplier

Detailed quality control procedures will be prepared on completion of the detail design of the pressure vessel. The following is a preliminary description of the quality control procedure to be used by the vessel manufacturer.

a. General

All Quality Control Procedures will be approved by the Manager of Quality Control. Although manufacture and assembly

will be performed in various shops, all supervision of the Quality Control Department will report directly to the Manager of Quality Control. The Manager of Quality Control will report directly to the Vice President and General Manager.

b. Receiving Control

All incoming items (purchased) will be inspected in the receiving area. The inspector will check to drawings issued by the Engineering Department. Metallurgical requirements will be checked by the Laboratory, and necessary tests will be performed to insure conformity to specification. Written authority will be given the Manufacturing Department before work is started on raw material or semi-finished parts. Mill test reports will be checked and kept on file in the Materials Test Lab. If a vendor is unable to perform various non-destructive tests, the Receiving Quality Control will dispatch the part or parts to testing departments.

Defective Material Reports will be written for parts deviating from specifications.

c. Machine Shop Control

Inspectors will be assigned to specific areas and will be responsible for "in process inspection." Work will be moved into these areas by following the inspection "call outs" on the process sheets. Complicated parts may have numerous inspection "call outs" on the process sheets. In addition to the above, a roving inspector will check the machine setup and make periodic checks on large and complicated work. Charts and forms will be provided for a record of these checks. Final inspection approval will be noted by an "accepted" ticket attached to the part. A "Defective Material Report" will be written for parts that do not conform to the drawing. Engineering will either give written approval of a part being used "as reported" or issue proper salvage procedures. Quality Control will have the right to over-rule any salvage decision and the right to stop any job in process if it affects safety, life, interchangeability, or performance to specifications.

d. Assembly Shop Control

The Assembly Shop will operate in the same manner as has been outlined in II.A.2.c. with regard to parts machined in this area.

Non-destructive tests will be performed on all weldments as specified in the welding procedure. The welding procedures will be written up to proper specifications by the Welding Engineer. The weld procedure will conform with the ASME code and the description given in Section II.B.3.

Locations of areas where impact tests are to be taken will be recorded and sketches will be made.

Flame cutting, grinding, preheating, welding, back chipping, and stress relieving will be inspected by Quality Control. The inspector will check all weld rod to proper specifications, proper oven drying of flux coating, and area of deposited metal.

All magnetic particle inspection will be performed by Quality Control personnel that have been certified to Mil. Stds. C7701-Mil. Spec. 271A, 1/2/59.

All radiography will be performed according to paragraphs 4.2 to 4.9 of Mil. Std. 271-A. Radiographers will report to the Manager of Quality Control.

e. Deviations

All deviations from drawings and specifications will be reported on Defective Material Reports. The project manager will consult General Atomic for disposition.

Quality Control will have the right to deviate from the specifications only to the extent of additional tests or inspections required to maintain a high quality level.

3. Inspection by General Atomic

a. General

A resident General Atomic inspector will perform inspection in conjunction with or following complete quality control inspection by the vessel supplier. Certain inspection points are indicated below for mandatory participation by the General Atomic inspector; his participation in others listed will be as determined by the level of confidence which is developed in materials, processes and the vessel supplier's inspection. The supplier will be required to give adequate notification to allow participation of the General Atomic inspector in inspection noted as mandatory. If inspection by General Atomic is waived, this notice will be given in writing.

b. Material Inspection

The General Atomic inspector will participate in the inspection of all plate and forgings whether performed at the mill or on receipt at the vessel supplier. He will be responsible for the following:

(1) Mill test certificates will be obtained and the presence of the proper heat numbers, etc., properly marked on all material will be verified.

(2) Ultrasonic Inspection of the plate at the mill will be witnessed. Qualification of the operator, calibration of the equipment, and proper application of techniques will be confirmed and reported. A complete report of all test results will be made including reasons for any rejections and description of any measurable defects which fall within allowable limits. The inspection report will make it possible to identify material and to refer to recorded conditions at a later period in manufacture.

(3) A visual inspection of both sides and all edges of plate will be made prior to fabrication. Any evidences of inclusions, laminations or tears will be reason for intensive application of special inspection techniques to extend knowledge of the apparent defect and verify acceptability or rejection.

(4) Ultrasonic inspection of the top and bottom heads (after forming) will be witnessed at the mill. A close visual and dimensional inspection will be performed with special attention to head thickness to detect any excessive thinning which may have occurred in forming. Furnace charts or process certifications for normalizing, or any other heat treatments performed on the heads, will be obtained at this time.

(5) The ultrasonic and magnetic particle inspection of the head flanges, grid support ring, and head studs will be witnessed.

(6) Compliance with the vessel specification of all other materials used in the vessel will be verified by receipt of certifications and inspection reports from the vessel supplier's quality control department.

c. Certifications and Qualifications

Prior to the start of any fabrication operations on any material, all material certifications, process certifications, laboratory tests, and the like will be reviewed to determine complete compliance. Identification of material for correlation with certificates will be maintained throughout the fabrication process. Any material which cannot be identified to the satisfaction of the General Atomic inspector will be subject to rejection.

Prior to the start of any welding the General Atomic Inspector will review welding procedures and welder qualifications. The General Atomic inspector will be present when procedure qualifications are made and will witness all tests made to determine acceptability of welding procedures. He will also witness the qualification of all welders who will perform work on the vessel unless evidence is presented by the

vessel supplier of valid welder qualification in the exact welding procedure to be used.

The General Atomic inspector will obtain verification of the qualifications of all operators of magnetic particle, ultrasonic and radiographic inspection equipment and of the adequacy of the equipment to be used.

d. Fabrication Surveillance Inspection

(1) General

The following lists the minimum inspection steps required to ensure compliance with the intent of the vessel specification. The General Atomic inspector will perform directly or participate in those steps marked with an asterisk in parenthesis (*). He will participate in others listed or perform additional inspections at his discretion. The sequence of the inspection steps may be changed by the fabrication sequence.

(2) Top Head

Visually and dimensionally inspect the weld preparation of the formed head and of the flange and the location of the five nozzle holes for possible evidence of laminations and as a positive check on head thickness in these areas.

Verify the qualification of the welder who is to do the work.

Verify the welding rod to be used. Require removal of any other welding rod from the immediate work area.

Check to assure compliance with approved weld procedure.

Check preheat.

(*) Inspect fit-up of flange and nozzles to head. Perform interpass inspection and apply additional tests as needed.

(*) Inspect welds by Zyglo, Magnaflux, or dye penetrant.

(*) Radiograph welds, review radiographs, require indicated repairs, and retake before stress relieving.

(*) Check the furnace chart after stress relief to assure proper stress relief cycle. A copy of the chart or a process certification will be obtained by the General Atomic inspector.

Visually inspect head for evidence of distortion.

(*) Perform complete dimensional check of head after final machining and welding of upper nozzle extensions.

(3) Bottom Head

Visually and dimensionally inspect grid support ring after rough machining.

Check fit-up of ring into head. Ensure that location is correct for cleanup on final machining.

Verify weld procedure and welder qualification.

Magnaflux or dye penetrant check ring weld.

(*) Inspect weld preparation and location penetrations for lower nozzle stubs after machining. Check head thickness and material condition at penetrations.

(*) Check fit-up of nozzle stubs.

(*) Magnaflux or dye penetrant check nozzle stub welds.

(*) Radiograph all welds.

(4) Lower Shell Course and Bottom Head Assembly

Inspect weld preparation of lower course plate after machining in the flat. Stamp head number of plate in two places on the weld preparation surface on each long side of plate.

After course is rolled check (a) roundness, (b) diameter, (c) match and gap on longitudinal seam.

Inspect welding of test specimen plates and verify correct material by check of heat numbers or other identification which must be marked in a permanent manner on the material.

(*) Check final fit-up of longitudinal seam, verify welder qualifications, proper welding rod and preheat.

(*) Perform visual interpass inspection of weld. Check interpass heat. Perform Magnaflux or dye penetrant check on intermediate passes where visual inspection indicates need. Check roundness, diameter, and match after welding.

(*) Magnaflux and x-ray weld, review radiographs and require needed repairs, and retake before welding shell course to head.

(*) Check fit-up of shell course to head before machine weld.

(*) Magnaflux and x-ray circumferential weld. Require any needed weld repairs before stress relieving. Check diameter, roundness, and offset.

(*) Check furnace chart for proper stress relief cycle.

(*) Complete dimensional check after boring nozzle stubs and finish machining grid support ring.

(5) Nozzle Girth Course

Inspect weld preparation of vessel top flange and vessel support flange.

Verify the heat numbers for the two plates to make up the girth course. Inspect the weld preparation and stamp the heat numbers in two places on each long edge of each plate. These measures are to preserve positive identification of each plate until its location in the vessel has been fixed by welding to an adjacent part. A sketch or marked-up drawing will be prepared showing heat number of every part of the vessel.

(*) Weld preparation, fit-up, and welding of the nozzle girth course and flanges will be inspected in the same manner as the top head and lower shell course with special attention to roundness and diameter as affected by the two longitudinal welds.

(*) Perform complete dimensional inspection of the girth course after machining inlet nozzle openings. The inspector will take this opportunity to inspect the material closely at the machined openings and will apply special inspection techniques (Magnaflux, dye-check) wherever visual inspection indicates the need for further investigation.

(*). The inlet nozzles and welds will be inspected in the same manner as stated for the top and bottom head nozzles.

(6) Top Vessel Subassembly

Course 3 will be inspected in the same manner as course 1.

The welding of the top vessel subassembly will be inspected as detailed above for similar assemblies.

A complete dimensional check of the top vessel subassembly will be made after machining.

Particular attention will be given to ensure that the lower surface of the support flange is perpendicular to the centerline, and parallel to the lower edge of the assembly and to the upper locating surface of the top vessel flange.

(7) Vessel Final Assembly

(*). Course number 2 will be inspected in the same manner as courses numbers 1 and 3.

(*). Check fit-up of course 2 to the lower assembly and to the top vessel assembly. Pay special attention to offset of courses and to any buildup of tolerances on parallelism of ends of the courses. Avoid angularity between centerlines of courses as well as mismatch at the joint.

(*) Inspect circumferential welds between course 2 and the upper and lower assemblies as described for others. Magnaflux and x-ray before local stress relieving.

(*). Check local stress relief temperature, extent and duration.

(*). Final dimensional and visual inspection of vessel components.

A final dimensional check of the vessel will be made to ensure fit of the internals.

e. Review of Radiographs

The General Atomic Inspector will review all radiographs, including original shots and retakes. The vessel supplier will

be instructed to maintain a record of all x-rays taken and to identify them so that the location of each shot may be recorded on a drawing of the complete vessel. The General Atomic inspector will complete the General Atomic radiograph record form listing results of his review. Any film exhibiting apparent film artifacts which might obscure material defects will be retaken.

f. Acceptance Testing

The General Atomic Inspector will witness all acceptance testing and will verify compliance with all relevant specifications and approved test procedures.

g. Administrative

Inspection reports will be made in memorandum form. All inspection steps will be fully reported as separate work units.

The successful completion of each of the inspection steps listed in this procedure and any additional steps performed will be noted in reports.

The General Atomic inspector will not be authorized to approve any deviations from the approved specifications. All deviations observed will be noted in detail as well as rework methods and results. The inspector will notify the fabricator that the deviating material is not acceptable. The fabricator will be responsible for initiating any requests for deviation approval in accordance with established procedures. The inspector will assist in developing information concerning deviations and will verify the extent of deviations reported by the fabricator.

B. Specifications for Each Component of Vessel

1. Vessel Materials

Carbon Steel Plate for the pressure vessel barrels and heads will be ASME SA212 grade B made to ASME SA300 specifications and manufactured in accordance with fine grain melting practice. The steel will be killed to procure a small grain size. Grain size will be generally ASTM size 6 to 8 but no larger than 5. Charpy impact test specimens required by the ASME SA300 specification will include both longitudinal and transverse specimens as specified in Part 4 of the ASME specification. In addition to the ASME SA 300 Charpy impact tests required, additional tests as described in II.A.1.e. will be performed on plate from all heats used. The vessel barrels and heads will be normalized after hot forming or normalized before cold forming.

The plate will be ultrasonically tested as described in II. A. 1. d.

Carbon Steel Forgings will be ASME SA 105 grade II, made to ASME SA350 LF-1. These forgings will be magnafluxed as described in II. A. 1. b. and will have a fine grain structure. The minimum tensile strength requirement will be that of SA 105 grade II. Forgings will be ultrasonically tested as described in II. A. 1. d.

Studs - Alloy steel ASME SA-193 grade B14. The material will be ultrasonically tested as described in II. A. 1. d., before cutting threads. Thread roots will be ground and checked for cracks by dye penetrant or magnetic particle inspection.

Nuts will be Carbon steel ASME SA-194 grade II.

Washers will be made from a steel capable of being hardened to Rockwell C45.

Stainless Steel Plate (for the vessel support) will be made to ASME SA 167-58 grade 3. Stainless Steel Plate will be ultrasonically tested as described in II. A. 1. d.

Pipe material for nozzles will be ASME SA 333 grade C. The pipe material will be ultrasonically tested as described in II. A. 1. d.

2. Welding Requirements

Controls more restrictive than normally used for unfired pressure vessel fabrication will be used, and certain additional quality control and inspection procedures specified. The ASME Boiler and Pressure Vessel Code Section IX, Welding Qualification, will be used for welding procedure and welder qualification.

No sharp corners or stress raisers will be allowed in this vessel as a result of welding.

Minimum preheating requirements will be 200 F minimum preheat and interpass temperature with EXX15, EXX16 or EXX18 electrodes for welding carbon steel parts, and with AIS E-312 or E-310 for stainless steel to carbon steel joints.

Grinding or machining of all weld joint surfaces will be done before welding to remove any oxides or other material down to clean metal (flame cut edges will not be accepted). All welding on this vessel, whether temporary welding, tack welding or any other welding, will be done according to the requirements of the ASME pressure vessel code and those outlined below. The area of any temporary welding will be inspected with magnaflux or dye penetrant after the temporary weld has been ground smooth with the adjacent plate.

The maximum permissible offset of completed joints will not exceed 5 percent of the plate thickness.

As a final treatment, the vessel will be stress relieved after all welding has been completed except for the stainless steel to carbon steel weld in the support skirt. No repairs by welding will be permitted after stress relief.

In making test plates at least one stop and start per pass will be made near the middle of the test plate. Under paragraph Q-5 of the ASME Code Section IX, all weld procedure and welder qualification tests must be 100 percent radiographed. These radiographs must be acceptable under the restrictive requirements outlined in paragraph II.A.1.c. Each test weld will be evaluated to ensure that the impact properties specified in paragraph UG-84 of Section VIII of the ASME Code at minus 50 F are met.

Any changes in dimensions of weld grooves or other welding changes which may raise a question as to fulfillment of procedure requirements in the mind of the inspector will be requalified if the change is one of the essential variables in the welding specifications.

The vessel supplier will submit to General Atomic complete shop working drawings showing all weld preparation, procedures, materials, and other information which will be used to evaluate the proposed fabrication procedures.

C. Normalizing Procedures

All materials used in the vessel and associated components will be procured from the mill in the normalized condition. Any material hot formed by the fabricator will be normalized after hot forming if the hot forming has reduced the properties below those specified for normalized material.

Normalizing of these low carbon steels will consist of heating to 1650 to 1700 F. The time at temperature will be one hour per inch of plate thickness. Normalizing will be done so that the properties specified in SA-300 for plate and SA-350 for forgings will be met in the treated plate or forgings.

D. Methods of NDT Determination

The Nil Ductility Temperature (NDT) is defined as the temperature below which the steel loses all ability to deform in the presence of a sharp crack. A very close correlation between the NDT as determined by the drop weight test and the Charpy V notch transition temperature corresponding to the 15 ft-lb level for A-212B steel has been established[1,2]. A second standard method of determining the NDT of a material is based on a plot of Charpy V notch impact energy in ft-lb versus temperature. In this case the NDT is taken as the point at which the curve deviates from a straight line at the low energy absorption end of the curve.

A large number of experimental programs for pressure vessels, ships, and nuclear radiation studies have been made, and a number of different methods of determining the impact properties of steel have resulted. In most cases the Charpy V notch test appears to be best from the standpoint of simplicity, reliability, correlation with service failures, and much reported data on steels. Most of the work on the effects of irradiation of steels is based on tests of Charpy V notch specimens, therefore, the monitor specimens for impact property controls for the pressure vessel components were selected to be Charpy V notch specimens. Plots of Charpy V notch energy absorption with respect to test temperature will be made on the steels used for the pressure vessel and associated components. Section II.A.1.e. covers this requirement.

From these plots the NDT for each section of steel can be determined. These curves will become a part of the monitoring system for the pressure vessel.

The forgings used for the control rod nozzles will be tested by determination of the Charpy V notch plot of energy absorption with respect to temperature from a forging which is representative of the working applied to the nozzle and from the same heat as used for obtaining the nozzle material. This plot will then be used to establish the NDT of the nozzle material. As a check of the NDT for each control rod nozzle three Charpy V notch specimens will be taken after final forming of the nozzle. These specimens will be tested and compared with the curve obtained from the test of the representative forging to assure that each nozzle is acceptable.

E. NDT Temperature Specifications

1. Shell Materials

The 212B plate material will be made to ASME SA300 specification, which requires a 15 ft-lb impact strength at -50 F. For additional information on test specimens see II.A.1.e.

2. End Closures

The plate material of the vessel heads will be made to ASME SA300 and the forged material will be made to ASME SA-350-LF1, which has the same impact requirements.

3. Nozzles

All nozzles will be forged and will conform to SA-350-LF1.

F. Treatment of Material Following Fabrication

The vessel will be stress relieved. The barrels, heads, and forgings will be stress relieved prior to final closure seal welding. The final closure seal welds will be locally stress relieved. All stress relief operation will be in accordance with Section VIII Unfired Pressure Vessel Code, 1959, paragraph UCS-56 subparagraph C. Stress relieving will be performed by heating the material to 1200 F and holding at this temperature for 1 hour per inch of material thickness. The cooling rate after completion of the 1200 F hold time will not be more than 100 F per hour down to 600 F; below that temperature normal air cooling will be acceptable.

G. Post-Manufacturing Tests to be Conducted

1. Hydrostatic Test

The unit will be hydrostatically tested after fabrication to a pressure of 750 psig with water at 70 F or the metal transition temperature plus 100 F whichever is higher. The test pressure will be maintained for two hours. This test will be done in the presence of the General Atomic inspector.

At the time of the hydrostatic test, the following instruments will be installed and measurements taken:

a. Biaxial strain gauges at eight points around the circumference of the flange and at the outside of the flange fillet. These will be placed on both the head and the vessel to the satisfaction of General Atomic.

b. Dial gauges mounted in pairs so as to measure the combined flange rotations occurring as a result of the bolting-up operation and also as a result of the application of the hydrostatic pressure.

c. The stud elongations will be measured and recorded to provide information for field bolting-up operation.

2. Helium Leak Tests

Following the hydrostatic test, the vessel will be cleaned and helium leak tested in accordance with the applicable sections of paragraph 8.4 and 8.5 of "Military Standard for Non-Destructive Testing Requirements for Metal" Mil. Std. 271A (Ships) 2 January 1959. Rubber O-ring gaskets will be used to seal off the main flange and fuel handling equipment nozzles.

The pressure vessel will be leak tested when internally pressurized. It will be demonstrated that the total leak rate of the completed vessel is not greater than the equivalent of 10^{-7} lb/hr of helium at 350 psig. The method of test and the pressure level used will be subject to approval by General Atomic. This test will be performed in the presence of the General Atomic inspector.

The pressure vessel will also be checked for leakage under vacuum. The total permissible leak rate of the vessel will be 1.5×10^{-6} lb/hr of helium with an absolute pressure in the vessel of 50 microns of mercury or less with a helium atmosphere surrounding the vessel. This test will be performed in the presence of the General Atomic inspector.

The vessel will have a helium leak test in the field after all internals are installed. This test will be performed to determine the quality of the seal welds. The vessel will be pressurized to 300 psig and the seal weld area bagged.

III OPERATIONAL LIMITS

A. Temperature-Pressure Transition Limits

Initially, no temperature-pressure transition limits will be imposed, i.e., room-temperature pressurization will be permitted. As operation progresses, results will become available from the coupon testing program (Section III. C). If these results indicate the transition temperature of the pressure vessel steel has increased by 100 F, the vessel will be annealed.

During normal operation at power, since the plant is to be operated as a base load station, the temperature of the pressure vessel will be between the limits 600 F and 700 F at all times, except for relatively very short periods at low loads. The helium pressure in the vessel will be limited to 350 psia during normal operation by pressure control valves. These will be backed up by electromatic relief valves, set at 390 psig, which discharge to the helium dump tanks and these are, in turn, backed up by rupture discs designed so that the pressure will not exceed 450 psig, the coolant being discharged to the secondary containment in this case.

B. Control of Transition Limits

Bearing in mind that the total thickness of the thermal shields is 3 inches above the grid plate and 4-1/2 inches below the core, it is seen from Figures E-6 and E-9 that the total fast neutron doses in 30 years at the worst point on the vessel are about 8×10^{18} nvt ($>$1 Mev) and about 2×10^{20} nvt ($>$0.1 Mev). The corresponding doses to the top of the grid plate are about 2×10^{20} nvt and 1.2×10^{21} nvt. The normal operating temperatures of all these regions will be above 600 F during irradiation except for relatively very short periods. The support skirt (outside the vessel, shielded by 7-1/4 inches of steel) will experience doses of 8×10^{16} nvt ($>$1 Mev) and 7×10^{18} nvt ($>$0.1 Mev), at a temperature not very much lower than that of the vessel except where it is made of austenitic steel.

The effect of irradiation on steel is to increase the transition temperature. It has been well established that a very large increase can occur as a result of irradiation to a level of 10^{19} nvt ($>$1 Mev) at

temperatures below 450 F [3, 4, 5, 6]. Information on the effects of irradiation at higher temperatures, between 550 F and 700 F have been reported [7, 8, 9]. A plot of the effect of irradiation on several steels exposed at different temperatures is shown in Figure E-10. It can be noted that the effect of irradiation at 600 F is very small; a shift in transition temperature of about 30 F, for 10^{19} nvt (>1 Mev). From the latest reported data on transition temperature shift caused by irradiation, it would appear that irradiations, when the material is at 550 F or more, would not result in a shift of greater than 100 F for an exposure of 1×10^{19} nvt (>1 Mev). The effects of annealing radiation damage have been studied [10, 11]. From Figure E-11, it can be seen that most of the damage is recovered with a 24 hour anneal at 750 F.

C. Coupon Testing

Four hundred standard ASME 10 mm x 10 mm Charpy V-notch coupon specimens of plate material will be made. Two hundred of the specimens will be taken from across weld joints. The other two hundred specimens will be taken from the parent metal perpendicular to the direction of rolling. The plate for these specimens will be stress relieved at the same time and under the same conditions as the pressure vessel. All samples will be of the same heat as the plate of the barrel adjacent to the reactor core.

All specimens will be taken from a point nearly midway between the plate surface and the center of the plate thickness. For plate three inches or over in thickness, two specimens may be taken from near each midpoint between the center and the outside of the plate. The specimens for weld impact properties will be taken from across the longitudinal weld seam. The specimens for parent metal impact properties will be taken parallel to the vertical axis of the barrels and the direction of rolling of the plate will be indicated.

Two hundred of the specimens will be placed in a radiation field similar to that which the vessel will receive. Batches of specimens will be extracted periodically in units of 10. A curve of energy absorption vs. temperature will be plotted from data obtained by testing the irradiated monitor samples. This curve will be compared with

the curves obtained during fabrication of the vessel to determine any shift in the transition temperature as a result of operation.

The other 200 Charpy V-notch samples will be placed in reflector positions where they will be exposed to a fast neutron flux which is at least a factor of 10 greater than the flux experienced by the pressure vessel, and a little greater than the fast flux experienced by the grid plate. The temperature of these samples will be close to that of the grid plate. As a consequence of these exposure conditions, these samples will be usable for monitoring the transition temperature of the grid plate material, and for obtaining advance information on behavior of the pressure vessel steel. These two hundred samples will be tested and otherwise handled in the same manner as the other 200.

October, 1961

REFERENCES

1. Comparison of Charpy V Notch and Drop-Weight Tests for Structural Steels, by J. H. Gross; American Welding Society Journal, Feb. 1960.

2. Evaluation of the Significance of Charpy Tests, by William S. Pellini; Symposium on Effects of Temperature on the Brittle Behavior of Metals with Particular Reference to Low Temperatures; ASTM Publication No. 158, 1953.

3. Porter, L. F., "Radiation Effects in Steel". Symposium on Materials in Nuclear Application. ASTM Special Technical Publication No. 276, Oct. 1960.

4. Berggren, R. G., "Neutron Irradiation Effects in Steels". London Symposium on Steels for Reactor Pressure Circuits, Dec. 1960.

5. Berggren, R. G., "Radiation Effects in Ferritic Steels". Status of Radiation Effects Research on Structural Materials and the Implications to Reactor Design. USAEC Conf. TID-7588, October 1959.

6. Trudeau, L. P., "Effects of Irradiation on Mechanical Properties of Materials for Reactor Pressure Vessels". USAEC Conf. TID-7588.

7. Alger, J. V. and L. M. Skupien, "Neutron Radiation Embrittlement at 500°F and 650°F of Reactor Pressure Vessel Steels". WAPD-T-913.

8. Hawthorne, J. R. and L. E. Steele, "The Effect of Neutron Irradiation on the Charpy V and Drop Weight Test Transition Temperatures of Various Steels and Weld Metals". USAEC Conf. TID-7588, Oct. 1959 (NRL Report 5479)

9. Steele, L. E. and J. R. Hawthorne, "Effects of Irradiation Temperature on Neutron-Induced Changes in Notch Ductility of Pressure Vessel Steels". NRL Report 5629.

10. Hawthorne, J. R. and L. E. Steele, "Preliminary Observations on the Effectiveness of Heat Treatment for the Recovery of Properties of Irradiated Steels, NRL Report 5582, Feb. 1961.

11. Steele, L. E., Naval Research Laboratory, Discussion of September 12, 1961. (To be published)

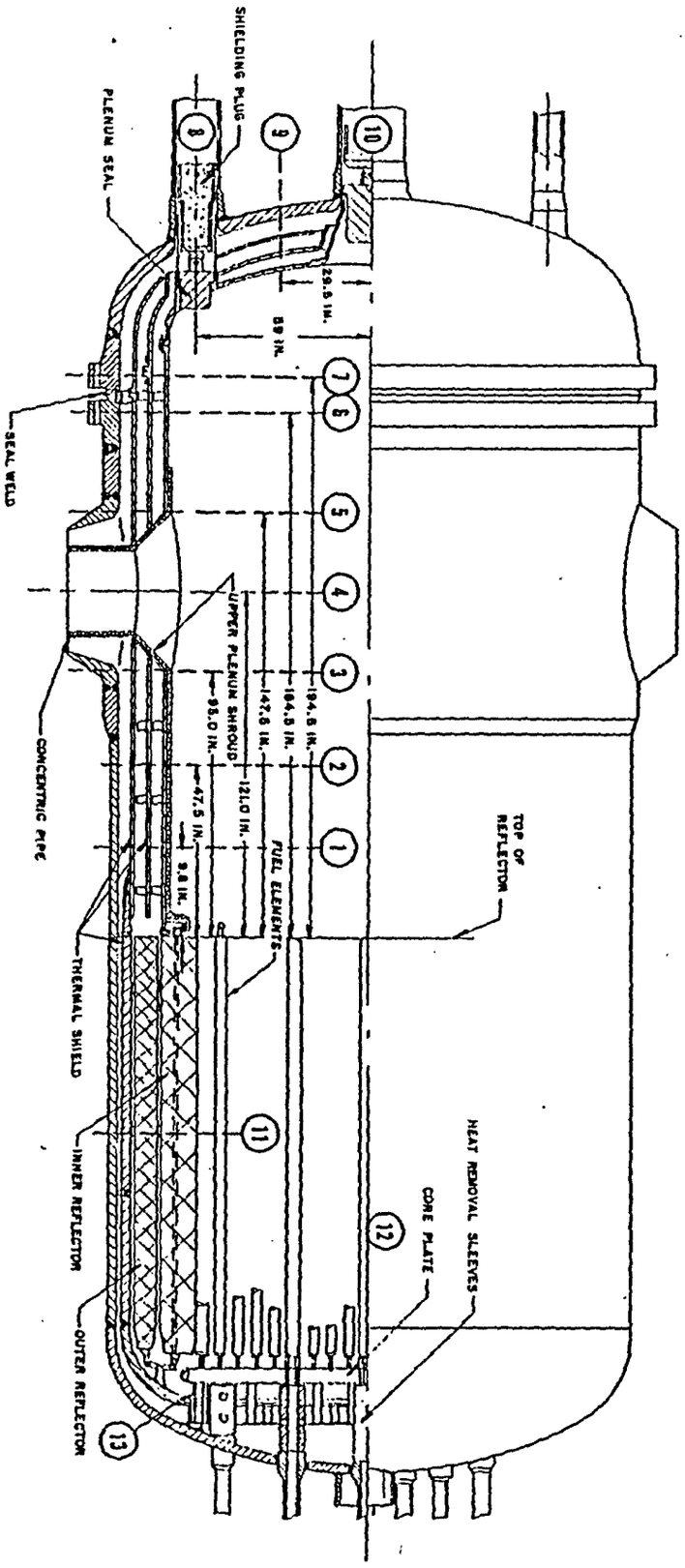

REFERENCE POINTS FOR NUCLEAR HEATING
AND FAST FLUX IN REACTOR PRESSURE VESSEL

FIG. E-1

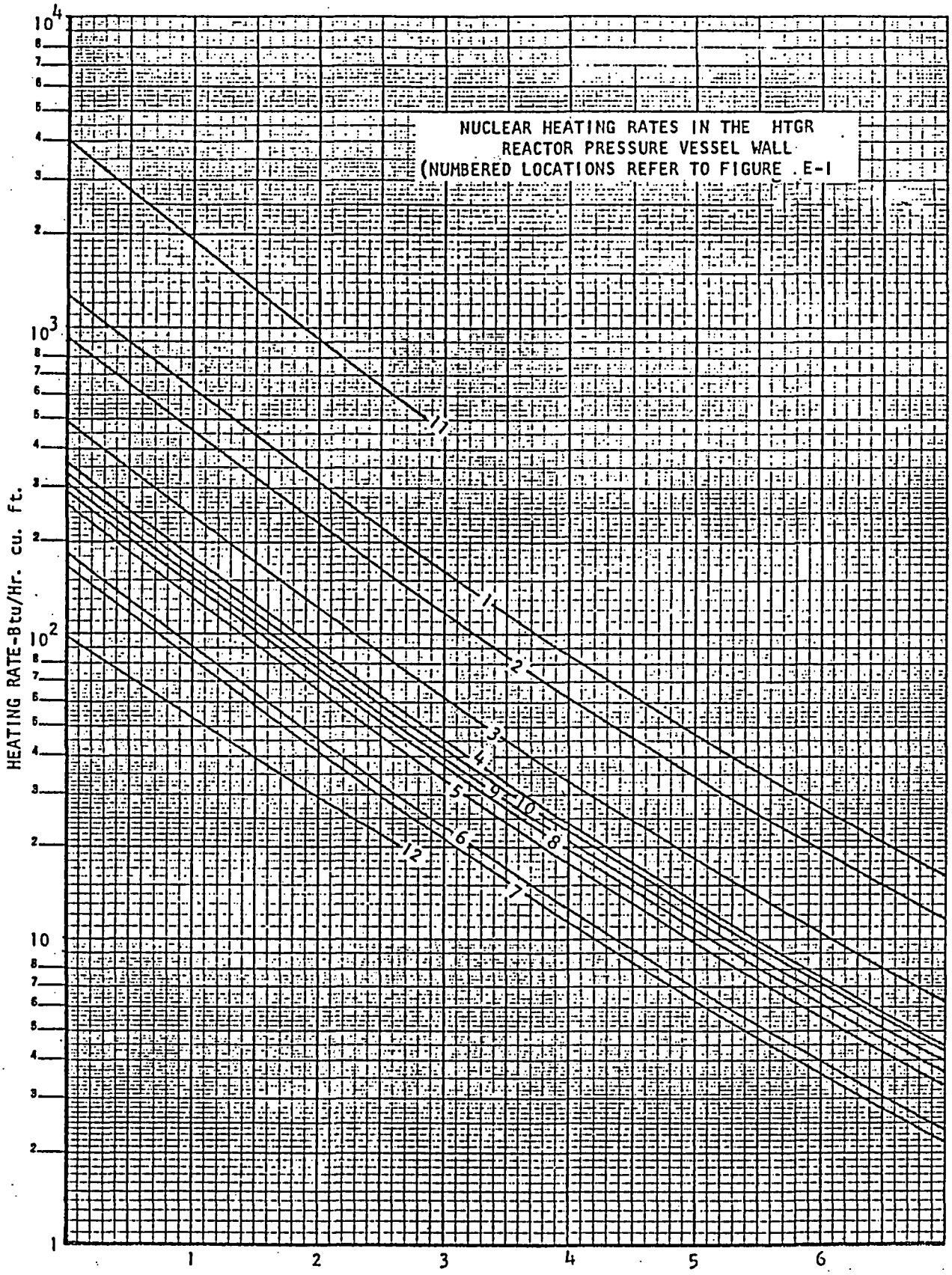
NUCLEAR HEATING RATES IN THE HTGR
REACTOR PRESSURE VESSEL WALL
(NUMBERED LOCATIONS REFER TO FIGURE E-1
HEATING RATE-Btu/Hr. cu. Ft.
DISTANCE FROM INSIDE SURFACE OF PRESSURE VESSEL INCHES
1
2
3
4
5
6
7
8
9
10
11
12

FIG. E-2

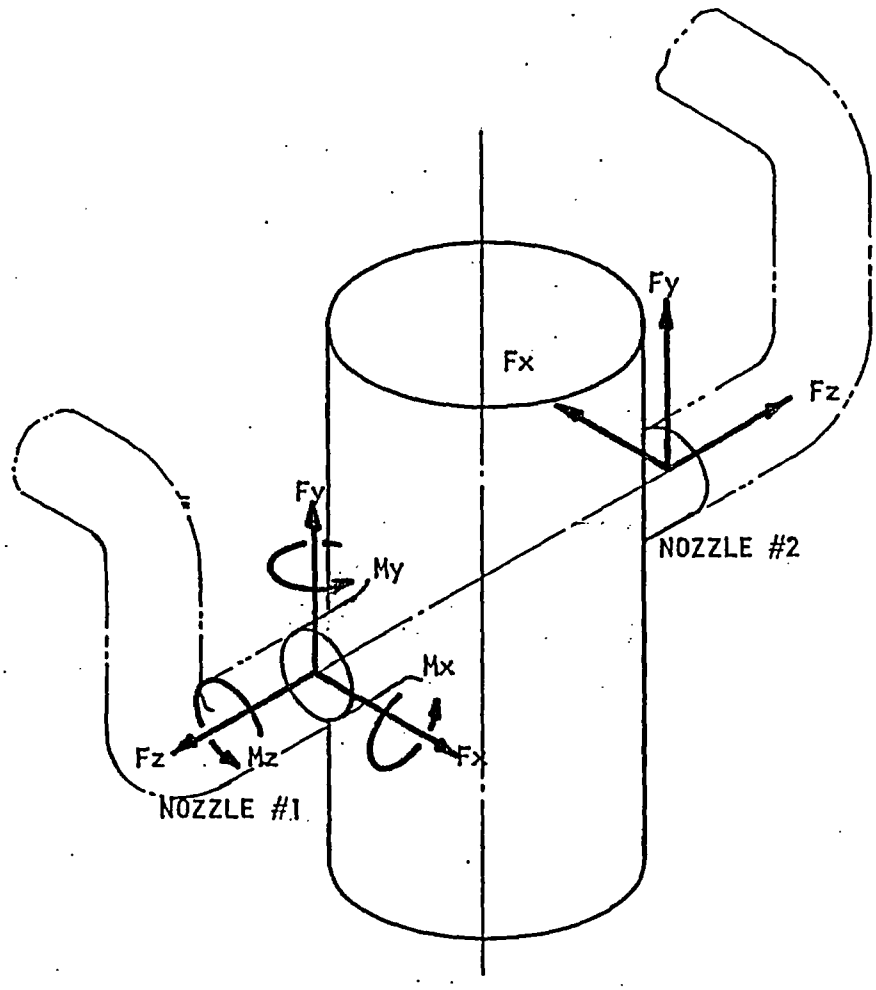

	LOSS OF COOLANT NOZZLE #2 **				STEADY STATE OPERATION
	NOZZLE #1	CASE 1	CASE 2	CASE 3	
Fx	20,366	0	0	-635,000	-2,120 LBS.
Fy	8,730	0	-635,000	0	2,473 LBS.
Fz	10,355	635,000 *	0	0	4,827 LBS.
Mx	72,000	0	5,060,000	0	-35,839 FT. LBS.
My	173,000	0	0	5,060,000	-27,437 FT. LBS.
Mz	88,348	0	0	5,060,000	7,952 FT. LBS.

* ACTS AT CENTER LINE OF PIPE, BUT DOES NOT ACT AS LOAD ON NOZZLE
** EACH CASE ACTS SEPARATELY BUT AT THE SAME TIME AS THE LOADS ON NOZZLE #1 OCCUR.

PIPING LOADS ON INLET NOZZLE

FIG. E-3

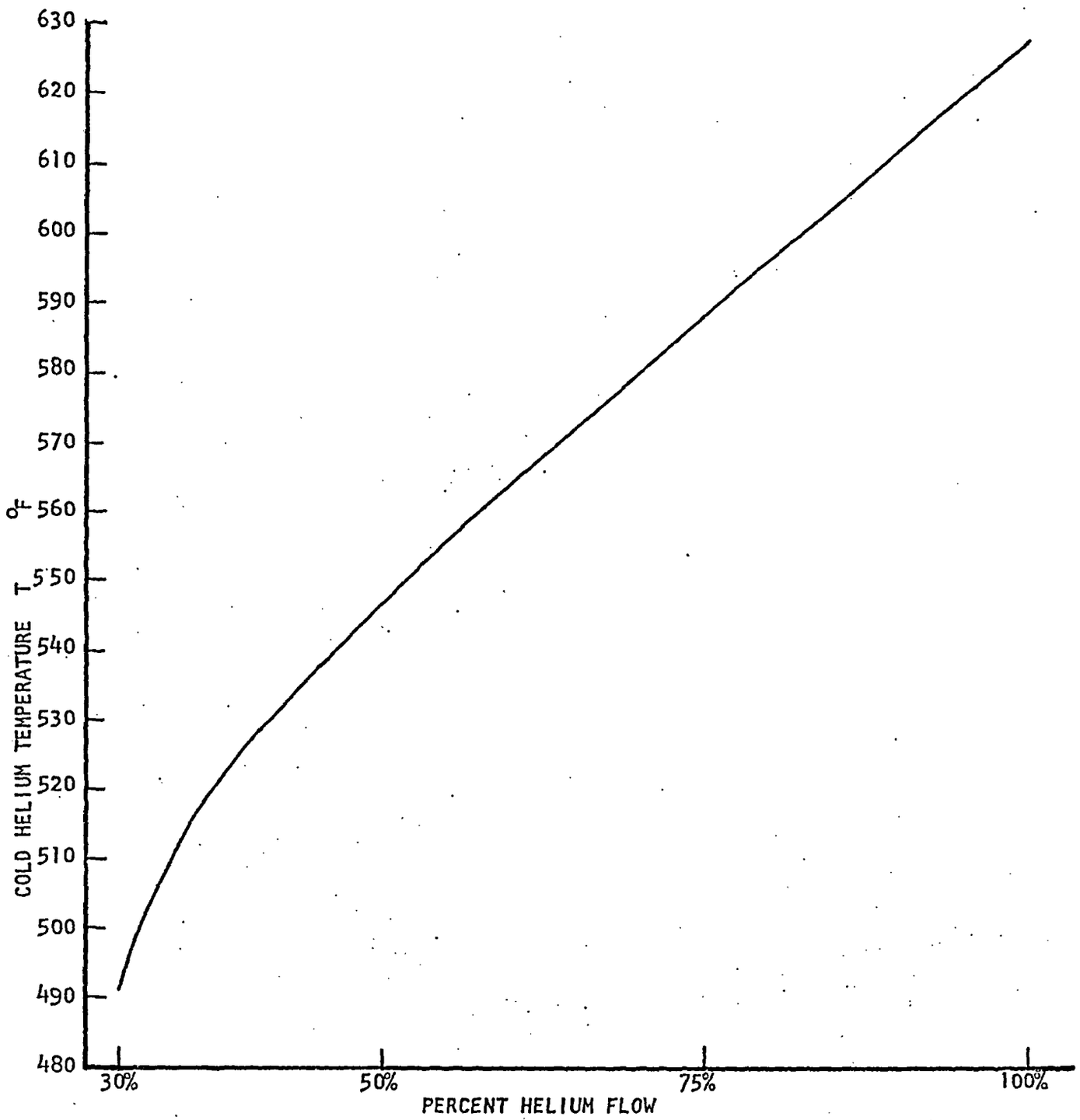

INLET GAS TEMPERATURE

FIG. E-4

Operating Condition	Source of Transient	Amplitude of Temp. Transient of Inlet Gas	Maximum Time Rate of Change of Temperature	Temperature Conditions at Start of Transient	Remarks
1)Normal operation at steady load	Control stutter	± 20 F	± 10 F/min	662 F	
2) Load following with variable inlet gas temperature	Control system response to load-change	450 F to 662 F	± 20 F/min	Any value from 450 F to 662 F	
3) Startup	a. Cold Startup	100 F to 662 F	+ 250 F/hr	100 F	Flow through both nozzles
	b. Hot Startup	250 F to 662 F	+ 40 F/min	250 F	Flow through both nozzles
4) Controlled shutdown after scram	a. Cold	662 F to 100 F	- 40 F/min	662 F	Flow through one nozzle
	b. Hot	662 F to 250 F	- 50 F/min	662 F	Flow through one nozzle
5) Emergency shutdown (Reactor scram or loss of electric power)	Cold shutdown Hot shutdown	662 F to 100 F 662 F to 250 F	- 150 F/min - 150 F/min	662 F 662 F	Covers loss of coolant pressure also
6) Steam Leak	Ruptured Boiler Tube	No change	No change	662 F	Instantaneous rise in pressure and change to flow through one nozzle

SYSTEM TRANSIENTS CONSIDERED

FIG. E-5

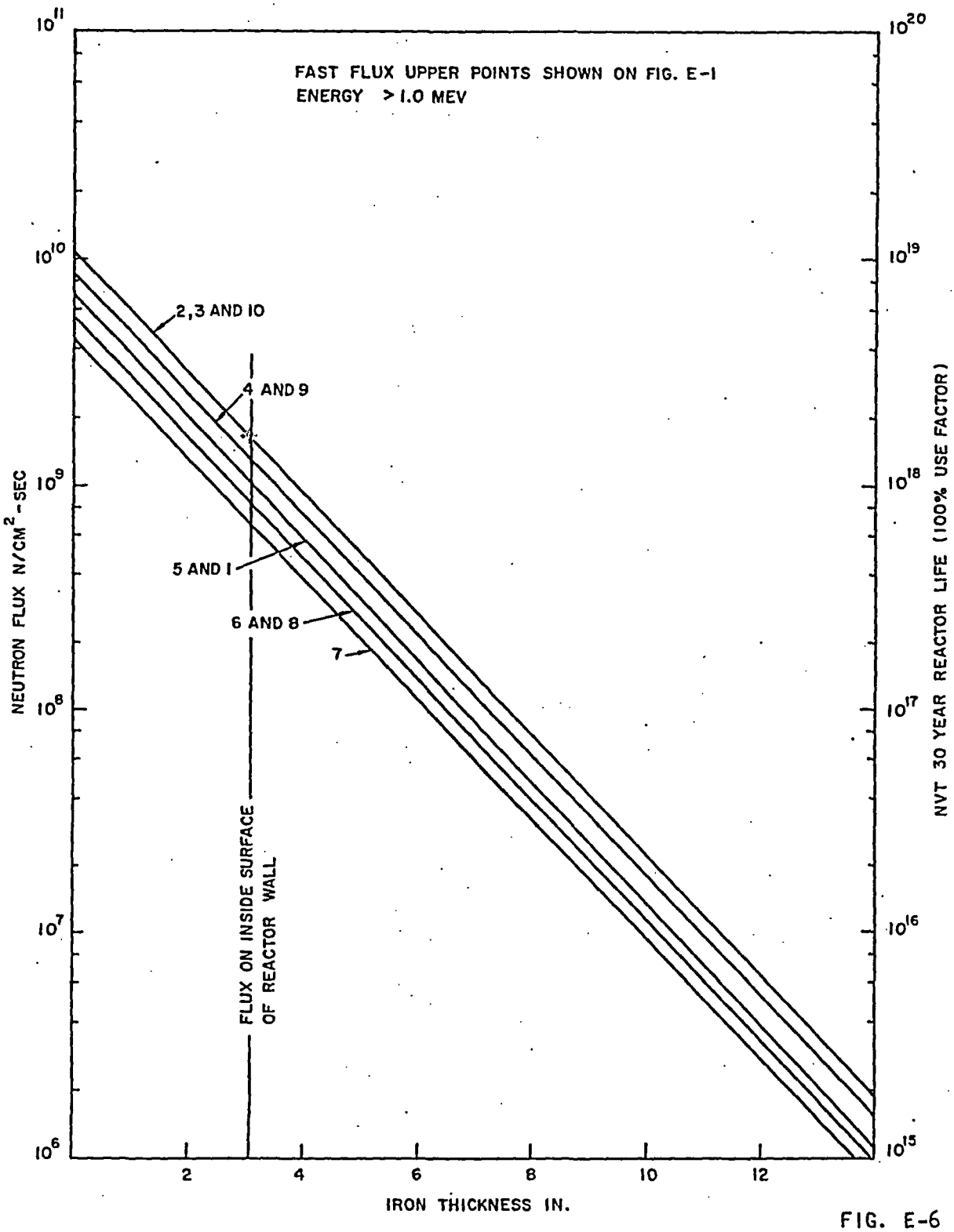
FAST FLUX UPPER POINTS SHOWN ON FIG. E-1
ENERGY > 1.0 MEV
2,3 AND 10
4 AND 9
5 AND 1
6 AND 8
7
FLUX ON INSIDE SURFACE OF REACTOR WALL
NEUTRON FLUX N/CM^2-SEC
NVT 30 YEAR REACTOR LIFE (100% USE FACTOR)
IRON THICKNESS IN.
10^{11}
10^{10}
10^{9}
10^{8}
10^{7}
10^{6}
10^{20}
10^{19}
10^{18}
10^{17}
10^{16}
10^{15}
2
4
6
8
10
12

FIG. E-6

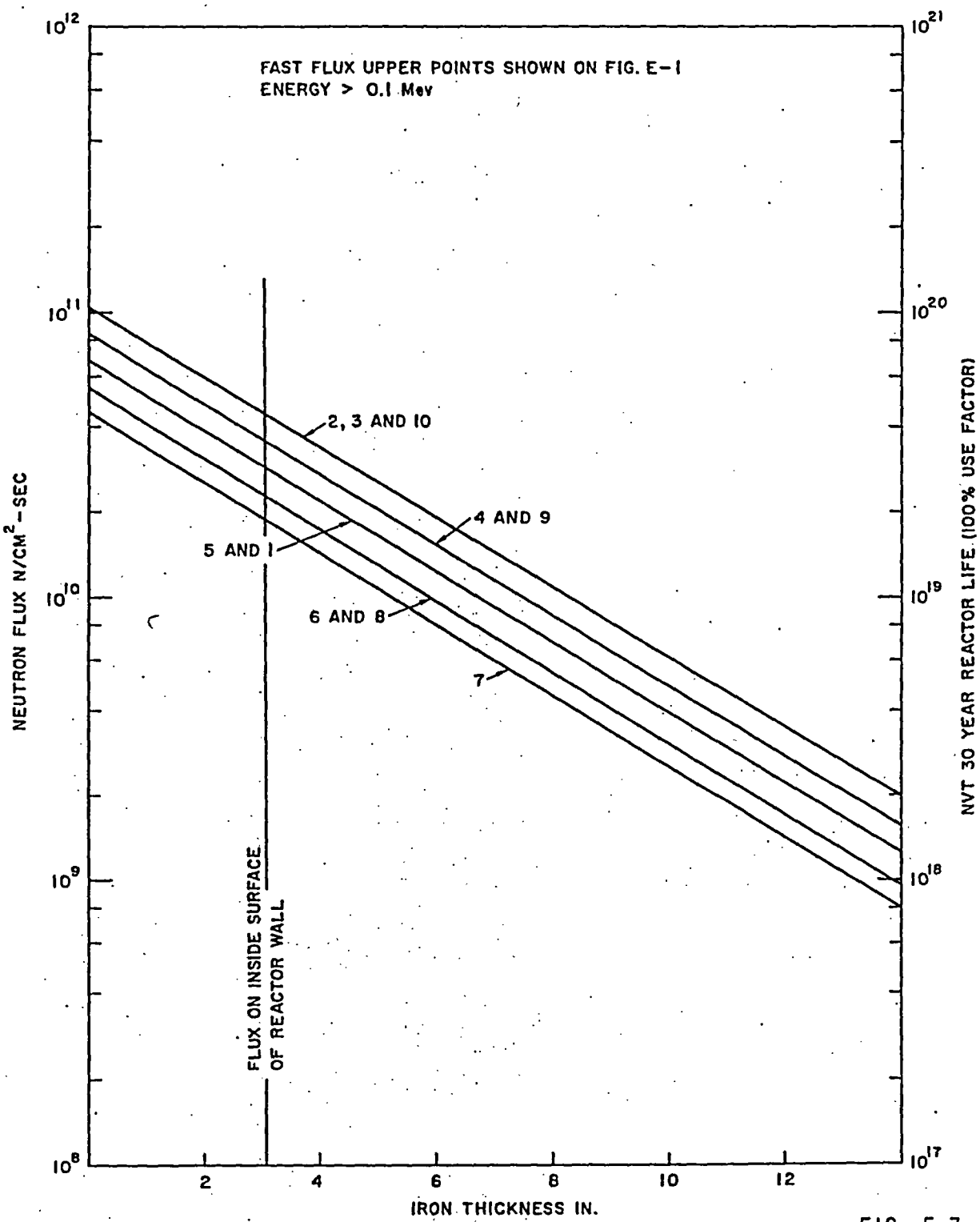
FAST FLUX UPPER POINTS SHOWN ON FIG. E-1
ENERGY > 0.1 Mev
2, 3 AND 10
4 AND 9
5 AND 1
6 AND 8
7
FLUX ON INSIDE SURFACE OF REACTOR WALL
NEUTRON FLUX N/CM²-SEC
NVT 30 YEAR REACTOR LIFE (100% USE FACTOR)
IRON THICKNESS IN.
10¹²
10¹¹
10¹⁰
10⁹
10⁸
10²¹
10²⁰
10¹⁹
10¹⁸
10¹⁷
2
4
6
8
10
12

FIG. E-7

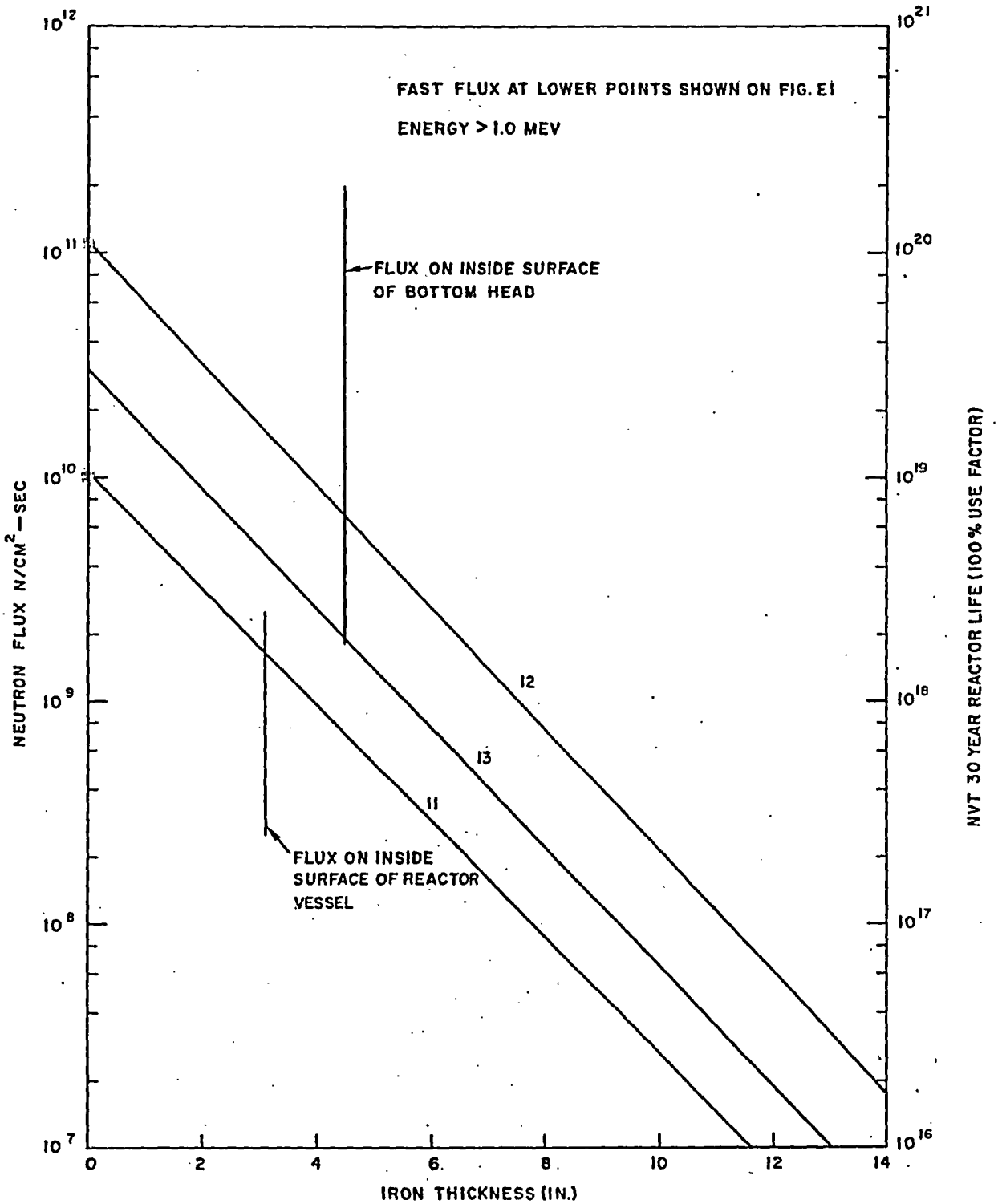
FAST FLUX AT LOWER POINTS SHOWN ON FIG. E1
ENERGY > 1.0 MEV
FLUX ON INSIDE SURFACE OF BOTTOM HEAD
FLUX ON INSIDE SURFACE OF REACTOR VESSEL
12
13
11
NEUTRON FLUX N/CM²—SEC
NVT 30 YEAR REACTOR LIFE (100% USE FACTOR)
IRON THICKNESS (IN.)
10¹²
10¹¹
10¹⁰
10⁹
10⁸
10⁷
10²¹
10²⁰
10¹⁹
10¹⁸
10¹⁷
10¹⁶
0
2
4
6
8
10
12
14

FIG. E-8

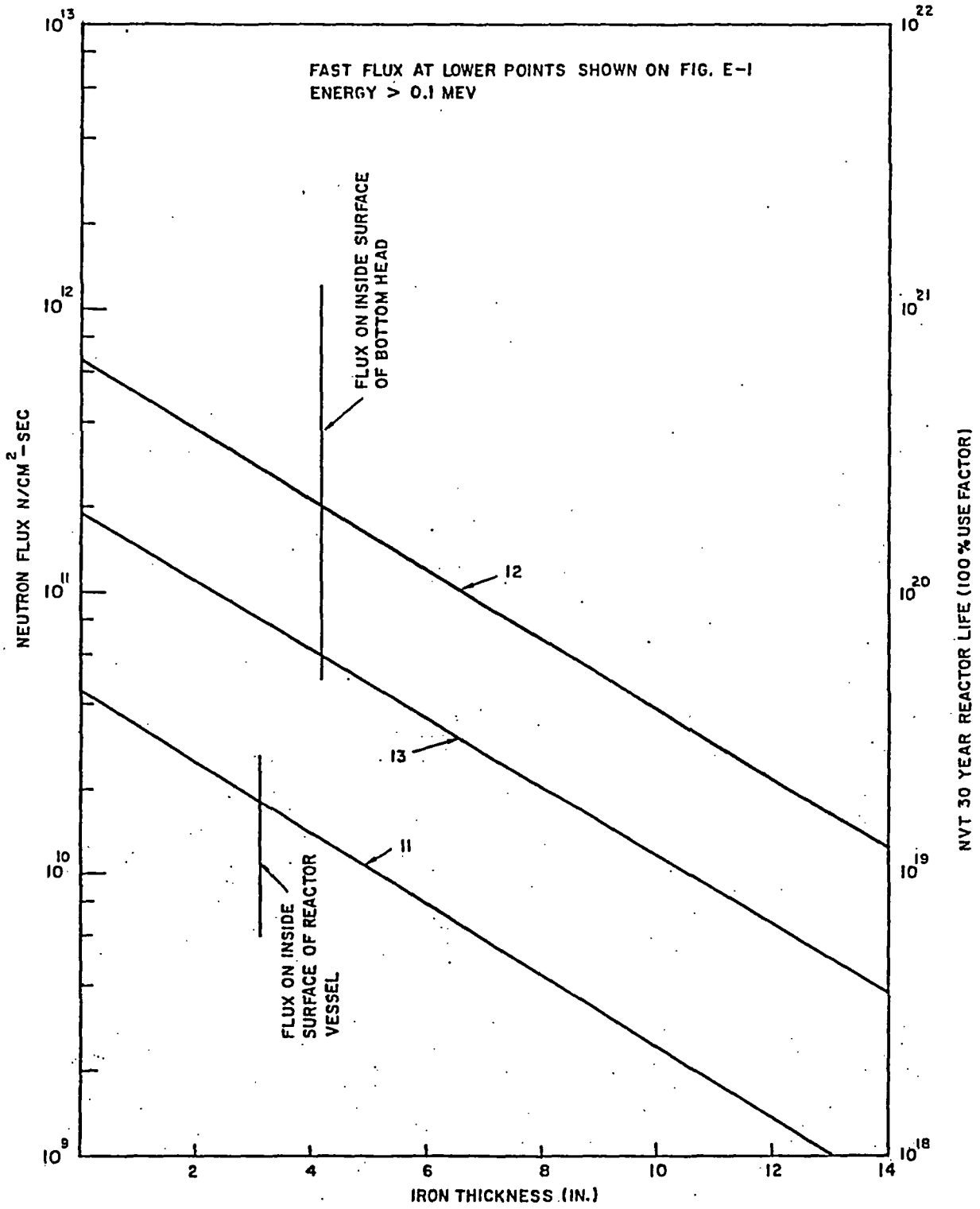
FAST FLUX AT LOWER POINTS SHOWN ON FIG. E-1
ENERGY > 0.1 MEV
FLUX ON INSIDE SURFACE OF BOTTOM HEAD
FLUX ON INSIDE SURFACE OF REACTOR VESSEL
12
13
11
NEUTRON FLUX N/CM^2-SEC
NVT 30 YEAR REACTOR LIFE (100 % USE FACTOR)
IRON THICKNESS (IN.)
10^{13}
10^{12}
10^{11}
10^{10}
10^{9}
10^{22}
10^{21}
10^{20}
10^{19}
10^{18}
2
4
6
8
10
12
14

FIG. E-9

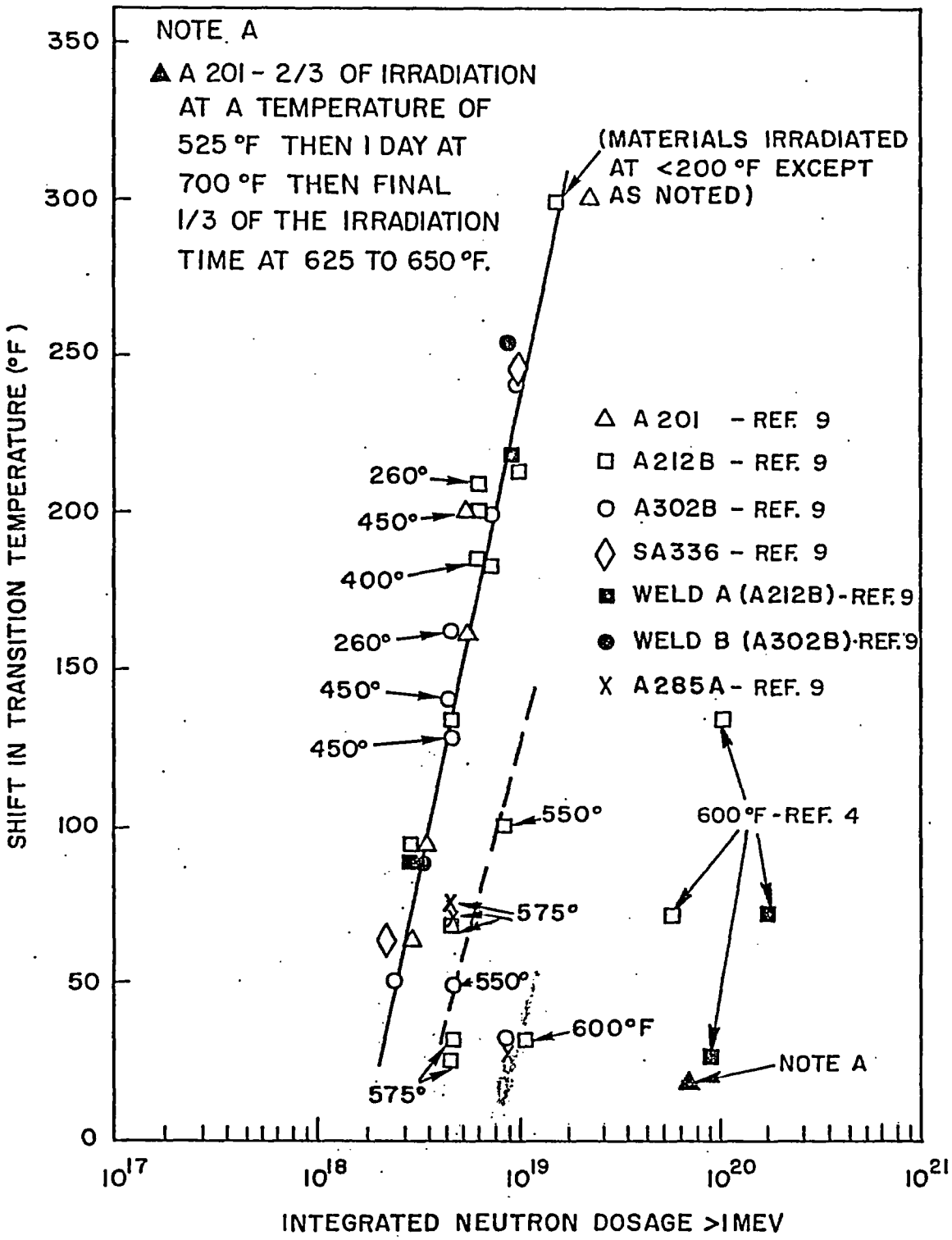

DUCTILE-TO-BRITTLE TRANSITION TEMPERATURE SHIFTS
WITH INTEGRATED NEUTRON DOSAGE AT DIFFERENT IRRADIATION TEMPERATURES

FIG. E-10

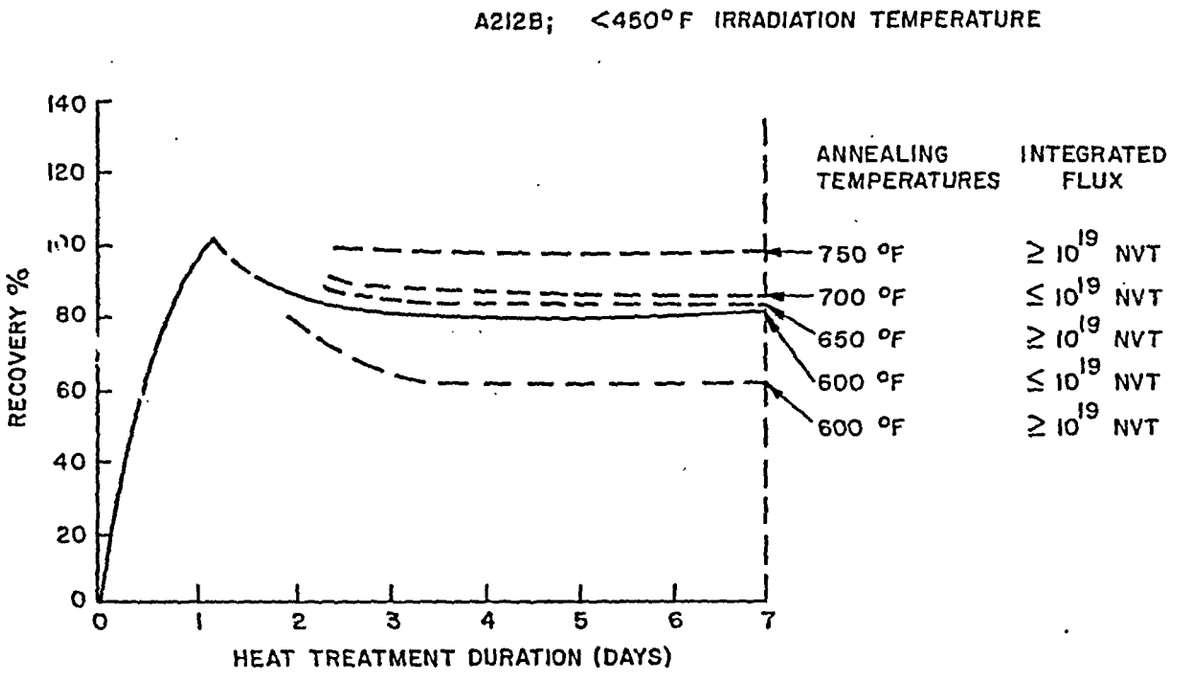

EFFECTS OF ANNEALING
OF STEELS FOLLOWING IRRADIATION

(from reference 11)

FIG. E-11